EVALUATION OF THE SDF METHOD USING A CUSTOMISED DESIGN FLOOD ESTIMATION TOOL

by

OCKERT JACOBUS GERICKE

Thesis presented in fulfilment of the requirements for the degree
Master of Science in Engineering (Civil)
at the Stellenbosch University

Supervisor: Mr Jakobus Andries du Plessis
Faculty of Engineering
Department of Civil Engineering

December 2010

DECLARATION

By submitting this thesis electronically, I declare that the entirety of the work contained therein is my own, original work, that I am the owner of the copyright thereof (unless to the extent explicitly otherwise stated) and that I have not previously in its entirety or in part submitted it for obtaining any qualification.

Signed: ____________

Date: DECEMBER 2010

ABSTRACT

The *primary aim* of this study was to evaluate, calibrate and verify the SDF run-off coefficients at a quaternary catchment level in the C5 secondary drainage region (SDF basin 9) and other selected SDF basins in South Africa by establishing the catchment parameters and SDF/probability distribution-ratios. The probability distribution-ratios were based on the comparison between the flood peaks estimated by the SDF method and statistical analyses of observed flow data. These quaternary run-off coefficients were then compared with the existing regional SDF run-off coefficients, whilst the run-off coefficient adjustment factors as proposed by Van Bladeren (2005) were also evaluated.

It was evident from this study that the calibrated run-off coefficients obtained are spread around those of Alexander (2003), but were generally lower in magnitude. The adjusted run-off coefficients (Van Bladeren, 2005) had a tendency to decrease in magnitude with increasing recurrence interval, whilst some of the adjusted run-off coefficients exceeded unity.

The extent to which the original SDF method overestimated the magnitude and frequency of flood peaks varied form basin to basin, with the SDF/probability distribution-ratios the highest in the Highveld and southern coastal regions with summer convective precipitation. In these regions the flood peak-ratios were occasionally different by up to a factor of 3 or even more. The southern coastal regions with winter orographic/frontal precipitation demonstrated the best flood peak-ratios, varying from 0.78 to 1.63.

The adjusted SDF method results (Van Bladeren, 2005) were only better in 26% of all the basins under consideration when compared to those estimated by the original SDF method. On average, the adjusted SDF/probability distribution-ratios varied between 0.30 and 6.58, which is unacceptable.

The calibrated version of the SDF method proved to be the most accurate in all the basins under consideration.

On average, the calibrated SDF/probability distribution-ratios varied between 0.85 and 1.15, whilst at some basins and individual return periods, less accurate results were evident.

Verification tests were conducted in catchments not considered during the calibration process with a view to establish whether the calibrated run-off coefficients are predictable and to confirm that the method is reliable. The verification results showed that the calibrated/verified SDF method is the most accurate and similar trends were evident in all the basins under consideration. On average, the verified SDF/probability distribution-ratios varied between 0.82 and 1.19, except in SDF basins 6 and 21 where the 5 to 20-year return period flood peaks were overestimated by 41% and 56% respectively, which is still conservative.

The *secondary aim* of this study was to develop a customised, user-friendly Design Flood Estimation Tool (DFET) in a Microsoft Office Excel/Visual Basic for Applications environment in order to assess the use and applicability of the various design flood estimation methods.

The developed DFET will provide designers with a software tool for the rapid investigation and evaluation of alternative design flood estimation methods either at a regional or site specific scale. The focus user group of the application will comprises of engineering technicians, engineering technologist and engineers employed at civil engineering consultants, not necessarily specialists in the field of flood hydrology. The DFET processed all the catchment, meteorological (precipitation) and hydrological (observed flows) data used as input for the various design flood estimation methods.

OPSOMMING

Die *primêre doelwit* van die studie was om die SDF-afloopkoëffisiënte op ‘n kwartinêre opvangsgebiedvlak in die C5-sekondêre dreineringsgebied (SDF-opvangsgebied 9) en ander gekose SDF-opvangsgebiede in Suid-Afrika te evalueer, te kalibreer en te verifieer deur die opvangsgebiedparameters en SDF/waarskynlikheidsverspreiding-verhoudings vas te stel. Dié waarskynlikheidsverspreiding-verhoudings was gebaseer op die vergelyking tussen die vloedpieke soos beraam deur die SDF-metode en statistiese analises van waargenome vloeidata. Dié kwartinêre afloopkoëffisiënte is met die bestaande streeksgebonde SDF-afloopkoëffisiënte vergelyk, terwyl die afloopkoëffisiënt-aanpassingsfaktore soos voorgestel deur Van Bladeren (2005) ook geëvalueer is.

Dit het duidelik uit die studie geblyk dat die gekalibreerde afloopkoëffisiënte verspreid rondom die van Alexander (2003) is, maar in die algemeen laer in omvang. Die aangepaste afloopkoëffisiënte (Van Bladeren, 2005) was geneig om af te neem in grootte met ‘n toename in die herhalingsperiode, terwyl sommige afloopkoëffisiënte ‘n waarde van 1 oorskry het.

Die omvang waartoe die oorspronklike SDF metode die grootte en herhaalperiode van vloedpieke oorskat het, wissel van opvangsgebied tot opvangsgebied, met die SDF/waarskynlikheidsverspreiding-verhoudings die hoogste in die Hoëveld en suidelike kusstreke gekenmerk deur konveksie-somerreënval. In hierdie streke het die vloedpiekverhoudings gereeld verskil tot en met ‘n faktor van 3 of selfs meer. Die suidelike kusstreke met kenmerkende ortografiese/frontale winterreënval het oor die beste vloedpiekverhoudings beskik wat gewissel het tussen 0.78 en 1.63.

Die resultate van die aangepaste SDF-metode (Van Bladeren, 2005) was slegs in 26% van al die opvangsgebiede beter as die beramings van die oorspronklike SDF-metode. Die aangepaste SDF/waarskynlikheidsverspreiding-verhoudings het, met verwysing na gemiddeldes, tussen 0.30 en 6.58 gewissel, wat onaanvaarbaar is.

Die gekalibreerde weergawe van die SDF-metode was die mees akkurate metode in al die opvangsgebiede van belang. Die gekalibreerde SDF/waarskynlikheidsverspreiding-verhoudings het, met verwysing na gemiddeldes, tussen 0.85 en 1.15 gewissel, terwyl die resultate van sommige opvangsgebiede en individuele herhalingsperiodes minder akkuraat was.

Verifikasietoetse is uitgevoer in die opvangsgebiede wat nie tydens die kalibrasieproses gebruik was nie om vas te stel of die gekalibreerde afloopkoëffisiënte voorspelbaar is en om te bevestig dat die metode betroubaar is. Die verifikasieresultate het getoon dat die gekalibreerde/geverifieerde SDF-metode die mees akkurate metode is en dat soortgelyke tendense duidelik was in al die relevante opvangsgebiede. Die geverifieerde SDF/waarskynlikheidsverspreiding-verhoudings het, met verwysing na gemiddeldes, tussen 0.82 en 1.19 gewissel, behalwe in SDF-opvangsgebiede 6 en 21 waar die 5- en 20-jaar herhalingsperiode-vloedpieke onderskeidelik met 41% en 56% oorskat is, wat steeds konserwatief is.

Die *sekondêre doelwit* van die studie was om ‘n gebruikersvriendelike “Design Flood Estimation Tool” (DFET) in ‘n *Microsoft Office Excel/Visual Basic for Applications* omgewing te ontwikkel om die gebruik en toepaslikheid van die verskeie ontwerpvloedberamingsmetodes te bepaal.

Die DFET sal ontwerpers voorsien van ‘n sagtewareprogram om alternatiewe ontwerpvloedberamingsmetodes op streek- of plaaslike skaal te ondersoek en te evalueer. Die fokus-gebruikersgroep vir die toepassing van die program sal bestaan uit ingenieurstegnici, ingenieurstegnoloë en ingenieurs werksaam by raadgewende siviele ingenieurs, nie noodwendig vakkundiges in die veld van hidrologie nie. Die DFET was gebruik om al die opvangsgebied-, meteorologiese (reënval) en hidrologiese (waargenome vloeie) data vir die verskeie ontwerpvloedberamingsmetodes te verwerk.

ACKNOWLEDGEMENTS

I wish to express my gratitude to:

- The Rectorate and relevant functionaries from the Central University of Technology, Free State, for the opportunity of completing this study.
- Mr J.A. du Plessis, my supervisor, for guidance and support given.
- Mr P.F. Rademeyer and Mr D. van der Spuy from the Department of Water Affairs (Directorate Hydrological Services: Flood Studies) for expert and technical assistance in flood hydrology and all relevant hydrological data.
- Prof J.C. Smithers, Head of School of Bioresources Engineering and Environmental Hydrology, University of KwaZulu-Natal, for sharing his expertise on design precipitation estimation in South Africa.
- Mr M. van Dijk, School of Civil and Biosystems Engineering, University of Pretoria, for technical assistance in flood hydrology.
- Mr L. Twyman (Computer Foundation, Arivia) and Dr C.H. Barker (University of the Free State) for technical assistance in compiling all the relevant Geographical Information Systems data.
- Department of Water Affairs for providing the observed streamflow and precipitation data.
- South African Weather Services for providing the daily precipitation data.
- My family and colleagues, for their patience and understanding throughout this study.
- My wife, Berdine, for her love and support.

Acknowledgement above all to my Heavenly Father for setting my feet on a rock and making my steps secure (Ps. 40).

TABLE OF CONTENTS

Page

CHAPTER 5: RESULTS AND DISCUSSIONS

CHAPTER 7: REFERENCES

LIST OF TABLES

LIST OF FIGURES

Page

LIST OF ADDENDA

ADDENDUM A:

SPATIAL GIS DATA OF THE C5 DRAINAGE REGION

ADDENDUM B:

TABULATED RESULTS

ADDENDUM C:

GRAPHICAL PLOT RESULTS

Page

Page

ADDENDUM D:

USER MANUAL: DESIGN FLOOD ESTIMATION TOOL

LIST OF TABLES

LIST OF FIGURES

LIST OF ABBREVIATIONS

AMS	Annual Maximum Series
AMF	Annual Maximum Flood
ARF	Area Reduction Factor
ARM	Alternative Rational method
BI	Bayesian Inference
CAPA	Catchment Parameter method
CDF	Cumulative Distribution Function
CN	Curve Number
CSIR	Council for Scientific and Industrial Research
DADF	Depth-Area-Duration-Frequency
DDF	Depth-Duration-Frequency
DEM	Digital Elevation Model
DFET	Design Flood Estimation Tool
DWA	Department of Water Affairs
DWAF	Department of Water Affairs and Forestry
ER	Ecological Reserve
ESRI	Environmental Systems Research Institute
EV	Extreme Value
EV1	Extreme Value Type 1
EV2	Extreme Value Type 2
EV3	Extreme Value Type 3
FEH	Flood Estimation Handbook
FSC	Full Supply Capacity
GEV	General Extreme Value
GEV/LM	General Extreme Value using Linear Moments
GEV/PWM	General Extreme Value using Probability Weighted Moments
GIS	Geographical Information Systems
GLO	Generalised Logistic
GOF	Goodness-of-Fit
GPD	Generalised Pareto Distribution
HRU	Hydrological Research Unit

IH	Institute of Hydrology
LEV1	Log-Extreme Value Type 1
LM	Linear Moments
LMRD	Linear Moment Ratio Diagram
LN	Log-Normal
LP3	Log-Pearson Type III
LRH	Lag-routed Hydrograph method
MAE	Mean annual evaporation
MAF	Mean annual flood
MAP	Mean annual precipitation
MAR	Mean annual run-off
MIPI	Midgley and Pitman method
ML	Maximum Likelihood
MLM	Method of Linear Moments
MLS	Method of Least-squares
MM	Method of Moments
MML	Method of Maximum Likelihood
MRC	Modder River Catchment
MS-Excel	Microsoft Office Excel
MS-VBA	Microsoft Office Visual Basic for Applications
NASA	National Aeronautics and Space Administration
NERC	Natural Environment Research Council
PDF	Probability Density Function
PDS	Partial Duration Series
PMP	Probable Maximum Precipitation
PRHL	Proportional Reversed Hazard Logistic
PWM	Probable Weighted Moments
RLMA	Regional Linear Moment Algorithm
RLMA&SI	Regional Linear Moment Algorithm and Scale Invariance
RM	Rational method
RMF	Regional Maximum Flood
RRC	Riet River Catchment
SA	South Africa
SANRAL	South African National Roads Agency Limited

SAWB	South African Weather Bureau
SAWS	South African Weather Services
SCS	Soil Conservation Services method
SDF	Standard Design Flood method
SRTM	Shuttle Radar Topography Mission
SSE	Unexplained Sum of Squares
SSR	Explained Sum of Squares
SST	Total Sum of Squares
SUH	Synthetic Unit Hydrograph method
TR	Technical Report
UK	United Kingdom
UK FSR	United Kingdom Flood Studies Report
UOWMA	Upper Orange Water Management Area
USA	United States of America
USGS	United States Geological Survey
US-SCS	United States Soil Conservation Services
WAK	Wakeby distribution
WMAs	Water Management Areas
WRC	Water Research Commission

CHAPTER

1

INTRODUCTION

CHAPTER 1: INTRODUCTION

1.1 BACKGROUND

The estimation of flood events at a given site in a given region is fundamentally important in the planning, design and operation of civil engineering structures (Pegram & Parak, 2004: 377). Hence, flood frequency analysis remains a subject of great importance as a result of the economic and environmental impacts of failures of civil engineering structures (Pilgrim & Cordery, 1993: 9.9).

The failures of civil engineering structures caused by floods in South Africa are largely due to the immense variability in the flood response of catchments to storm precipitation, which is innately variable in its own right. Consequently, flood estimations for design purposes can be expected to display relatively wide confidence bands of uncertainty around all estimates of flood magnitude-frequency relationships, combined with steep increases in flood magnitudes with an increase in return periods (Alexander, 2002a: 2; 2003: 2). These uncertainties indicate that reliable estimates of flood frequency in terms of peak flows and volumes remain a constant challenge in hydrology (Cameron *et al.*, 1999: 169).

The words *estimate* and *uncertainty* introduced in the paragraphs above are used throughout this thesis. *Estimate* emphasises that in hydrology and meteorology, the true values are never known. *Uncertainty* designates *error* in hydrological analyses. Thus, measurement errors in observed data result in hydrological uncertainties, which may or may not be hydrologically meaningful (Alexander, 2001: 459).

In design flood estimation, the practising engineer or hydrologist therefore has to seek for meaningful hydrological results by balancing the demand for *deep scientific analysis* in recognition of the precipitation run-off variability and the demand for *sufficiently optimal analysis* methods, which are accurate, data-parsimonious, low-cost and consistent (Görgens, 1997).

Localised and widespread, severe floods have occurred on several occasions over the last four decades in Southern Africa.

A characteristic of most of the notable floods is that they were preceded by precipitation which lasted several days. The countrywide floods of the period December 1999 through March 2000 were described as the most severe humanitarian disaster experienced on the subcontinent. These periods of flooding were characterised by more than a million people having no access to potable water, hundreds of lives were lost, tens of thousands of people in Mozambique and South Africa were transferred to refugee camps, more than 200 bridges were either destroyed or severely damaged and several thousand kilometres of roads were damaged. The estimated repair cost to the overland communication infrastructure in these areas was estimated to be more than R1 000 million (Alexander, 2002: 2).

According to Cordery and Pilgrim (2000), the demands for improved design flood estimations have not been met with any increased understanding of the fundamental hydrological processes. Despite the collection of a vast amount of meteorological and hydrological data in South Africa as well as elsewhere in the world, there is still no universally applicable method for design flood estimation (Van der Spuy & Rademeyer, 2008: 1.1).

The above-mentioned factors and the lack of updated design flood estimation methods in South Africa since the 1970's, indicate that there is an urgent need to revise existing methods or develop alternative design flood estimation methods by using about 40 years of additional data. The effort in this regard led to the development of a numerically calibrated version of the Rational method (RM), known as the Standard Design Flood (SDF) method which incorporates engineering factors of safety to accommodate the uncertainties in hydrological analyses at a regional level (Alexander, 2002a: 4; 2003: 2).

To conclude, the definition proposed by Roberts (1963) to describe a hydrologist, sketches a good picture of the designer's actual dilemma:

"A Hydrologist is a Scientist who is capable of producing an exact answer from a mass of unreliable basic data, using dubious statistical methods based on guesswork."

1.2 PROBLEM STATEMENT

There are no theoretical criteria that can be applied to determine the most accurate design flood estimation method. The results of the application of all methods are estimates of the unknown true values. Alexander (1990) stated that:

"The first and most important lesson to be learnt is that there is no single calculation method that is better than all other methods under all the wide variety of flood magnitude determination problems that will be encountered in practice. Consequently you will have to apply your own experience and knowledge to your particular problem."

There have been recent claims in the literature published abroad that one method is theoretically more accurate than another based on assumptions that the data are from a statistically homogeneous population (Institute of Hydrology (IH), 1999; as cited in Alexander, 2002: 3). This might be applicable in countries with moderate climates, but not in South Africa, especially due to the extensive variation in climate and exposure to severe, flood-producing meteorological systems.

On the contrary, the results of all statistical methods for determining the flood magnitude-frequency relationship have wide and unquantifiable bands of uncertainty around them, especially due to the assumption that the annual flood peak maxima is the result of a single set of annual, flood-causative mechanisms with only variable magnitudes (Alexander, 2001: 421; 2002: 3).

The hydrological under-design and high failure rates of civil engineering structures exposed to floods in South Africa are due to the misunderstanding of these phenomena. On the other hand, the risk of failure of a structure should not be equated to the probability of occurrence of the flood, irrespective of the indirect economic and social consequences thereof (Alexander, 2001: 541). In the following paragraphs, key problems associated with above-mentioned assumptions or misunderstandings will be highlighted.

Observed data sets of precipitation and streamflow are normally characterised by the presence of high and low outliers. These outliers, especially the maxima, were assumed to have an undesirable influence on the flood magnitude-frequency relationship at a single site. However, these maxima result in floods causing damage (Alexander, 2001: 477).

Outliers more than three to eight times the mean observed annual flood peak are not satisfactorily accommodated by any frequency distribution, whether it is based on untransformed or $\log_{10}$-transformed data. This is evident from the fact that the return period plotting positions (confirmed by other observations) and calculated return periods of these frequency distributions do not correspond (Alexander, 2002: 5, 9). These differences are the source of differing opinions by hydrologists in the past, some describing a flood as a 100-year flood, whilst non-hydrologists argue the question regarding the possibility to have three 100-year floods at a specific site within 20 years.

Additional to the uncertainty around all estimates of flood magnitude-frequency relationships, developmental variables – such as the effects of upstream development, agricultural use, urbanisation, water storage and water abstractions also have an effect on design flood estimation, especially on direct statistical analysis. The extent and nature of these effects due to developmental variables are influenced by the variations in flood magnitude, as well as by the storage state of upstream dams immediately prior to flood events (Alexander, 2002: 9).

Multiple failure probabilities of occurrence associated with flood damage in a region cannot be determined analytically by single site statistical analysis, but must be based on a regional analysis and associated larger degree of engineering judgement (Alexander, 2002: 10). Again, this emphasises the statement made by Alexander (1990). Thus the investigation, evaluation and application of alternative design flood estimation methods either at a regional or site specific scale must be supported by practical experience and knowledge applicable to the particular problem.

The acknowledgement and inclusion of socio-economic, humanitarian and economic considerations in the design process are of great importance. It is also of utmost importance to realise that all design flood estimation methods, except direct statistical analysis at a gauging station, are based on average values derived from a large number of events at a regional level (Alexander, 2002a: 5).

These include average precipitation criteria, average catchment characteristics and average run-off coefficients. Thus, the precipitation run-off relationship at a specific site will only be the same as that produced by direct statistical analysis if the site characteristics and hydrological and meteorological conditions are similar to the average conditions used in the development of the method, but this is unlikely (Alexander, 2002a: 5).

Based on all these factors contributing to the uncertain estimates of flood magnitude-frequency relationships, Alexander (2002a: 4; 2003: 10) recommended that a single method, namely the SDF, must be used in conjunction with the Regional Maximum Flood (RMF) method to estimate the design flood at structures vulnerable to flood damage at a regional level.

In this study, the SDF method will be evaluated by establishing the applicability of the regionalised SDF run-off coefficients both in terms of areal extent and homogenous hydrological catchment responses. The question whether the probabilistic-based approach of the SDF method does have the ability to overcome some of the deficiencies evident in the other techniques used for design flood estimation will thus be investigated and confirmed, alternatively revised at a smaller scale.

1.3 PURPOSE OF STUDY

1.3.1 Research aims

The *primary aim* of this study is to evaluate, calibrate and verify the SDF run-off coefficients at a quaternary catchment level in the C5 secondary drainage region (SDF basin 9) by establishing the catchment parameters and SDF/probability distribution-ratios. The probability distribution-ratios are based on the comparison between the flood peaks estimated by the SDF method and statistical analyses of observed flow data. These quaternary run-off coefficients will then be compared with the existing regional SDF run-off coefficients, whilst the run-off coefficient adjustment factors as proposed by Van Bladeren (2005) will also be evaluated. Only the most suitable probability distributions for flood frequency analyses in South Africa, namely the Log-Normal (LN), Log-Pearson Type III (LP3) and the General Extreme Value (GEV), are to be considered.

Goodness-of-Fit (GOF) statistics will be used to select the most suitable single probability or combined probability distribution (mean values of the logarithms of two or more single distributions).

The *secondary aim* of this study is to develop a customised user-friendly Design Flood Estimation Tool (DFET) in a Microsoft Office Excel (MS-Excel) and/or Visual Basic for Applications (MS-VBA) environment in order to assess the use and applicability of the various design flood estimation methods (deterministic, empirical and statistical). The results obtained will then be compared with the original and calibrated version of the SDF method. These comparisons will establish whether the existing SDF method can meet the designer's requirements of robustness, consistency and sufficient accuracy. It must also be borne in mind that accuracy and robustness are non-commensurate objectives; one can only be achieved at the expense of the other. The question whether any perceived shortcomings of the SDF method at a specific site should be accommodated by applying engineering factors of safety in the design of the structure, and not in attempts to apply other methods of hydrological analysis or further refinement, will also be addressed.

SDF basin 9, comprising of the C5 secondary drainage region, will be used for this evaluation. The tertiary drainage regions of concern are the Riet (C51) and Modder (C52) River catchments consisting of twelve and eleven quaternary catchments respectively.

1.3.2 Hypotheses

It is hypothesised that all floods are the result of the complex interaction of hydrological and meteorological processes, which varies both in time and space scales (Alexander, 2002: 2, 3). Therefore, the flood-producing characteristics within an identified SDF basin are non-homogeneous and necessitate the further evaluation, calibration and verification of the regional run-off coefficients being used in order to represent the hydrological response at a smaller scale or quaternary catchment level. It is also hypothesised that water engineers and other consultants, internationally, in general tend to use only well-known and simplified design flood estimation methods, such as the 154-year old RM (Alexander, 2001: 405; 2002a: 4; SANRAL, 2006: 3.14).

This is due to the complexity and associated graphical procedures of some of the alternative methods, as well as the fact that the evaluation of the relative applicability thereof is time-consuming and there is no guarantee that the uncertainties of flood magnitude-frequency relationships will be satisfactorily accommodated in these alternatives. Thus, the development of the DFET will provide designers with a rapid software tool for the investigation and evaluation of alternative design flood estimation methods either at a regional or site specific scale. The focus user group of the application will comprise of engineering technicians, engineering technologist and engineers employed at civil engineering consultants, not necessarily specialists in the field of flood hydrology.

1.3.3 Specific objectives

To achieve the research aims and investigate the hypotheses, the following specific objectives were identified:

- Evaluate and prepare all hydrological and meteorological data from selected representative flow gauging and weather stations in the C5 secondary drainage region (SDF basin 9).
- Develop Geographical Information Systems (GIS) containing the relevant spatial information of the C5 secondary drainage region.
- Investigate the use of a GIS-based Digital Elevation Model (DEM) as opposed to manual procedures and empirical equations to establish the average catchment slope and catchment centroid.
- Conduct direct statistical analyses of observed annual flood peak maxima at representative flow gauging stations in the quaternary catchments.
- Select daily precipitation stations representative of the meteorological conditions in each quaternary catchment of concern by making use of the design precipitation depths as proposed by Smithers and Schulze (2003).
- Numerically calibrate the run-off coefficients used in the SDF method to fit the results obtained by the direct statistical analyses in order to establish the quaternary SDF run-off coefficients for different return periods.
- Compare the quaternary and existing regional SDF run-off coefficients.
- Evaluate the validity of the run-off coefficient adjustment factors as proposed by Van Bladeren (2005).

- Apply the suite of deterministic, empirical and statistical methods available in the DFET in the selected quaternary catchments.
- Demonstrate the use of the DFET and compare the results obtained to establish whether the probabilistic-based approach of the SDF method does have the ability to overcome some of the deficiencies evident in the other techniques used for design flood estimation in the C5 secondary drainage region.
- Compile a user manual for the DFET.

In order to enhance the understanding of all the results obtained from this study, as well as to illustrate the relevance thereof in a South African context, a selection of the procedures followed to achieve the specific objectives will be implemented randomly in some of the other 29 SDF basins in South Africa. The results (catchment areas and time of concentration) from previous research conducted by Petras and Du Plessis (1987) and Parak and Pegram (2006) will be used as default input parameters for the SDF method. Direct statistical analyses will be conducted at selected flow gauging stations used by the above-mentioned researchers. The results will then be compared with their GEV probability distribution results, although the nature and record length of the observed data sets initially used are unknown. Based on the outcome of this exercise, the most suitable probability distributions will then be used for the numerical calibration of the SDF run-off coefficients at a quaternary catchment level. The calibration results will then be compared with the existing regional SDF run-off coefficients and the validity of the run-off coefficient adjustment factors as proposed by Van Bladeren (2005) will be investigated.

This will clarify the influence of different climatic regions (Highveld as opposed to Mediterranean/southern coastal regions), types of weather systems (summer convective as opposed to winter/all year orographic/frontal precipitation) and precipitation occurrence-frequencies on the depth, area, duration and movement of storm precipitation which in turn influence the magnitude and frequency of floods as estimated by the SDF method.

1.4 THESIS LAYOUT

This thesis describes the evaluation of the design flood estimation methods used in South Africa, with specific reference to the evaluation and calibration of the SDF method at a quaternary catchment level.

Chapter 1 provides some background on the designer's dilemma to optimise design flood estimation methods, whilst taking cognisance of the immense variability in precipitation run-off relationships. The misunderstanding of these relationships results in the under-design and high failure rates of civil engineering structures and thus necessitates the implementation of alternative design flood estimation methods, which incorporates engineering factors of safety. Chapter 1 also covers the purpose, aims, hypotheses and specific objectives of the research project to investigate the problem statement.

Chapter 2 provides a literature review of design flood estimation, with the focus on the development and application of the SDF method. The study area is discussed in detail in Chapter 3.

Chapter 4 describes the development and evaluation of all input data comprising of GIS-based catchment, meteorological and hydrological data, as well as the detailed methodology used in this study.

Chapter 5 presents the results concerning the data development and evaluation, development, application and verification of the DFET, flood frequency analyses and evaluation, calibration and verification of the SDF method.

A comparison of the results as obtained by the various other design flood estimation methods is also included. Chapter 6 presents the conclusions and recommendations based on the results obtained in Chapter 5.

The spatial GIS data of the study area are listed in Addendum A, whilst Addendum B and C present a selection of tabulated and graphical plot results. A complete user manual for the DFET is included in Addendum D.

CHAPTER

2

LITERATURE REVIEW: DESIGN FLOOD ESTIMATION

CHAPTER 2:
LITERATURE REVIEW: DESIGN FLOOD ESTIMATION

2.1 INTRODUCTION

Universally, three basic approaches to design flood estimation are followed, namely the probabilistic (statistical analysis of observed data), deterministic (statistical properties of floods and storm precipitation are assumed to be the same) and empirical (mathematical models fitting available data) methods (Van der Spuy & Rademeyer, 2008: 1.1). In order to allow for the inevitable uncertainty in flood estimations, all three approaches should, where possible, feature in any specific design situation. Flood estimation methodologies also distinguish between small, medium and large catchments, and whether or not observed streamflow records are available in reasonable proximity of the site under investigation (Alexander, 2001: 531 - 536).

The following statement made by Bouvard (1988) emphasises the state of affairs outlined above and verbalises the essence of design flood estimation:

"Judgement is important not only as regards the physical phenomena involved and the interpretations of the results but also, and perhaps more importantly, the applicability of the methods envisaged to the problems addressed."

In light of above statement, the purpose of this chapter is to present a literature review on the physical phenomena (catchment processes, precipitation, developmental and climatological variables) and the theoretical basis of the design precipitation and flood estimation methods currently used in South Africa.

2.2 VARIABLES INFLUENCING FLOOD PEAKS AND VOLUMES

Floods are generated in catchments, physiographically contiguous areas in which run-off, caused by precipitation, drains as streamflow through a single outlet. Storm precipitation is the input. Storm *precipitation losses* occur as the catchment experiences a change in storage while it absorbs (infiltration), retains or attenuates (surface, near-surface and riverbank detention) and lose (evaporation and groundwater seepage) some of the precipitation. The *excess precipitation* that exits the catchment as streamflow is the output, the run-off contributing to flood peaks (Alexander, 1990: 4.3; 2001: 381; Görgens, 1997).

2.2.1 Catchment characteristics and processes

Run-off generated by storm precipitation must be a function of some, or all, of the following general catchment characteristics:

2.2.1.1 Catchment area and shape

In small catchments the relationship between precipitation intensity and the infiltration rate of the soil is predominant, whilst in large catchments the quantity of precipitation relative to the number of impoundments (for water storage) is of great importance. In catchments smaller than 10 km², the peak discharge of small streams is approximately proportionate to the area. In larger catchments, the peak discharge tends to be proportionate to the square root of the area. The movement and intensity of a storm passing over a catchment should also be considered, since using only the size of the catchment could be misleading (Alexander, 2001: 383; Rooseboom *et al.*, 1993: 2.5; SANRAL, 2006: 3.5).

Time and areal distribution of storms, precipitation intensity, density of stream patterns and the critical storm duration are variables which will influence the flood peaks in different shaped catchments of the same area (Alexander, 2001: 381).

2.2.1.2 Average catchment and main watercourse slope

The correlation between the catchment and main watercourse slopes is normally good. Slopes, whether flat or steep, influence the time of concentration and hence the precipitation intensity and resulting flood peaks. The average catchment slope has an influence on the hydrological response of a catchment to run-off (Alexander, 2001: 387). The average catchment slope can be calculated using the following methods:

- <u>Grid method:</u> A grid of at least 50 squares is superimposed over the catchment area. At each grid intersection point, measure the horizontal (shortest) distance between the contour intervals which straddle the grid point along a line that passes through the grid point. The average catchment slope is consequently defined as the average slope perpendicular to the nearest contour line at each grid point. This is presented diagrammatically in Figure 2.1 and shown in Equation 2.1 (Alexander, 2001: 387).

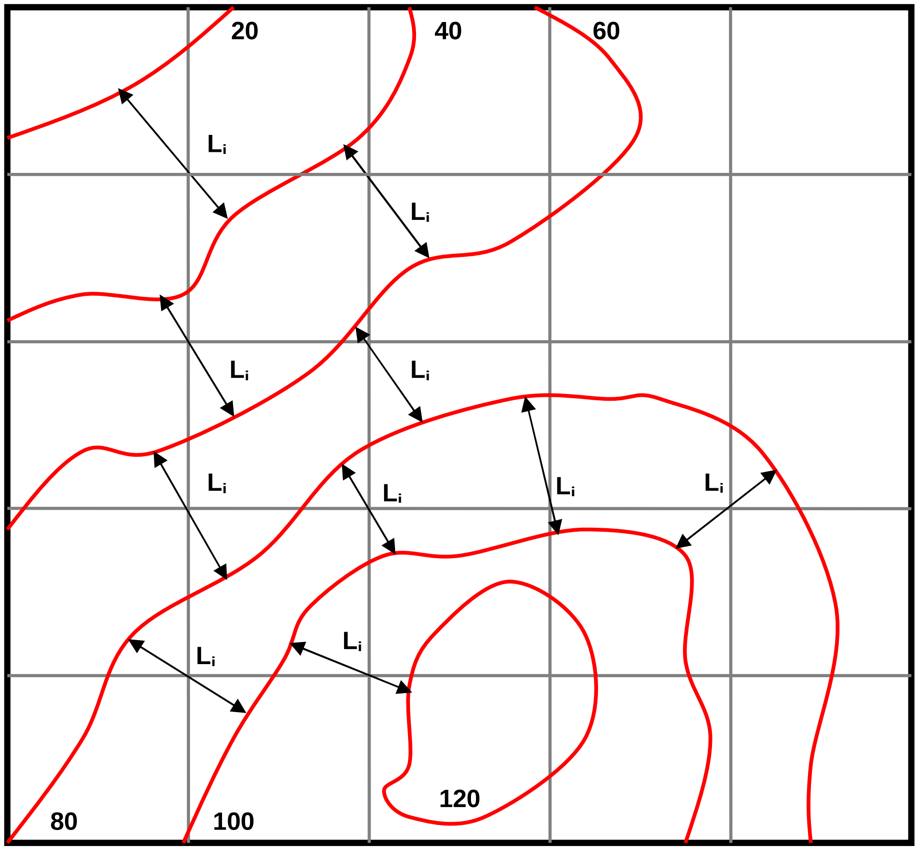

Figure 2.1: Grid method: Average catchment slope (Alexander, 2001: 387)

$$S = \frac{\Delta H}{\sum_{i=1}^{N} \frac{L_i}{N}} \qquad (2.1)$$

Where:

ΔH = Contour interval (m)

L_i = Horisontal distance between consecutive contours (m)

N = Number of grid points

S = Average catchment slope (m/m)

- Empirical equation: According to Schulze *et al*. (1992), the average catchment slope can be determined by making use of the following empirical relationship (Equation 2.2):

$$S = \frac{M \; \Delta H * 10^{-2}}{A} \qquad (2.2)$$

Where:

A	= Catchment area (km²)
ΔH	= Contour interval (m)
M	= Total length of all contour lines within the catchment (m)
S	= Average catchment slope (m/m)

- <u>GIS:</u> Several standard functions are available in ArcGIS™ to determine the average catchment slope and steepness frequency distributions. A slope raster can be generated from a raw DEM based on a cell matrix approach which represents the maximum change in elevation over the distance between the cell and its eight neighbouring cells.

A comparison of the methodology associated with the above-mentioned methods used to determine the average catchment slope is included in Chapter 4, whilst the results are included in Chapter 5.

The main watercourse is a defined flow path along which water will travel the longest time to reach the catchment outlet from a point on or near the catchment boundary. This distance can be measured quite accurately on topographical maps, although the use of standard functions in ArcGIS™ is recommended. The average main watercourse slope can be determined by using the following methods (Alexander, 2001: 385; Van der Spuy & Rademeyer, 2008: 2.2):

- <u>Equal-area method</u>: An average slope line is drawn or positioned in relation to the longitudinal profile of the main watercourse in such a way that the area above (A_1) this line equals the area below (A_2) the line. This relationship is shown in Equation 2.3 and illustrated in Figure 2.2.

$$S_{Avg} = \frac{(H_T - H_B)}{L} \qquad (2.3)$$

Where:

$$A_i = \left(\frac{(H_i + H_{i+1})}{2} - H_B\right)L_i$$

$$H_T = \frac{\left(\sum_{i=1}^{N} A_i * 2\right)}{L} + H_B$$

H_B = Height at catchment outlet (m)

H_i = Specific contour interval height (m)

L = Length of main watercourse (m)

L_i = Distance between two consecutive contours (m)

S_{Avg} = Average main watercourse slope (m/m)

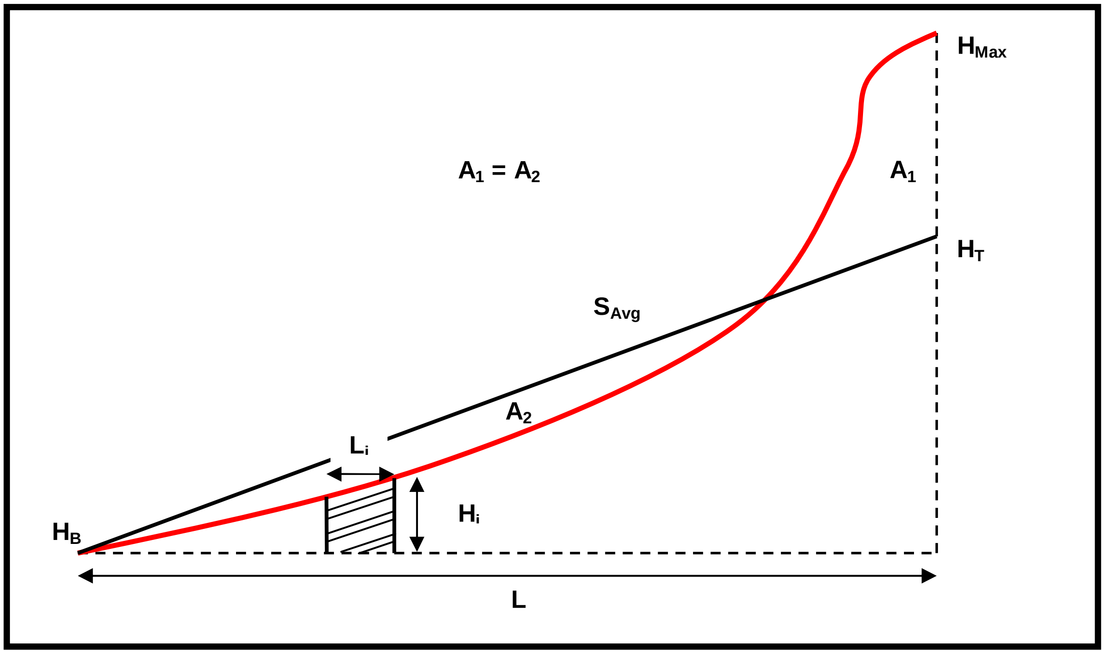

Figure 2.2: Equal-area method (SANRAL, 2006: 3.20)

- <u>10-85 method</u>: This method was developed by the United States Geological Survey (USGS). This relationship is shown in Equation 2.4 and illustrated in Figure 2.3.

$$S_{Avg} = \frac{(H_{0.85L} - H_{0.10L})}{(750L)} \qquad (2.4)$$

Where:

L = Length of main watercourse (m)

$H_{0.85L}$ = Height of main watercourse at length 0.85L

$H_{0.10L}$ = Height of main watercourse at length 0.10L

S_{Avg} = Average main watercourse slope (m/m)

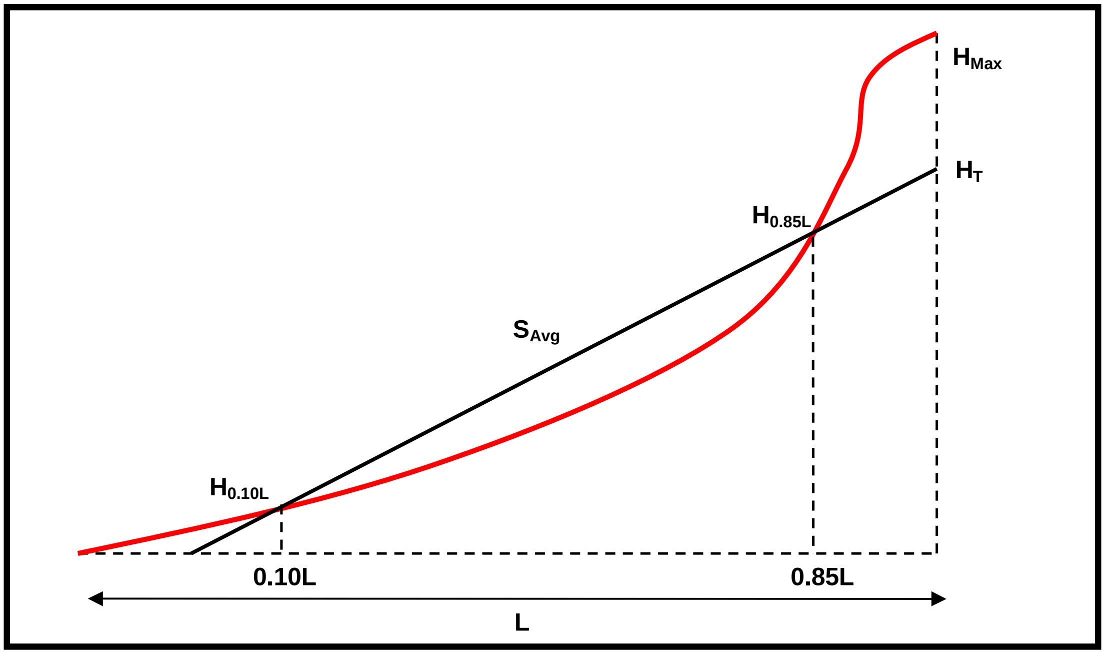

Figure 2.3: 10-85 method (SANRAL, 2006: 3.21)

- Taylor-Schwarz method: According to Van der Spuy and Rademeyer (2008), this method is preferred by the Department of Water Affairs (DWA) and the Natural Environment Research Council (NERC) proposes the use thereof in the United Kingdom (UK) Flood Studies Report (FSR, 1975), due to the more scientifically correct approach of the method. The main watercourse profile is subdivided into sub-reaches of which the velocities are related to the square root of the slope. The index is equivalent to the slope of a uniform channel with the same length as the longest watercourse and an equal travel time. This relationship is shown in Equation 2.5 and illustrated in Figure 2.4.

$$S_{Avg} = \left(\frac{L}{\sum_{i=1}^{N} \frac{L_i}{\sqrt{S_i}}} \right)^2 \qquad (2.5)$$

Where:

L = Length of main watercourse (m)

L_i = Distance between two consecutive contours (m)

S_{Avg} = Average main watercourse slope (m/m)

S_i = Slope between two consecutive contours (m/m)

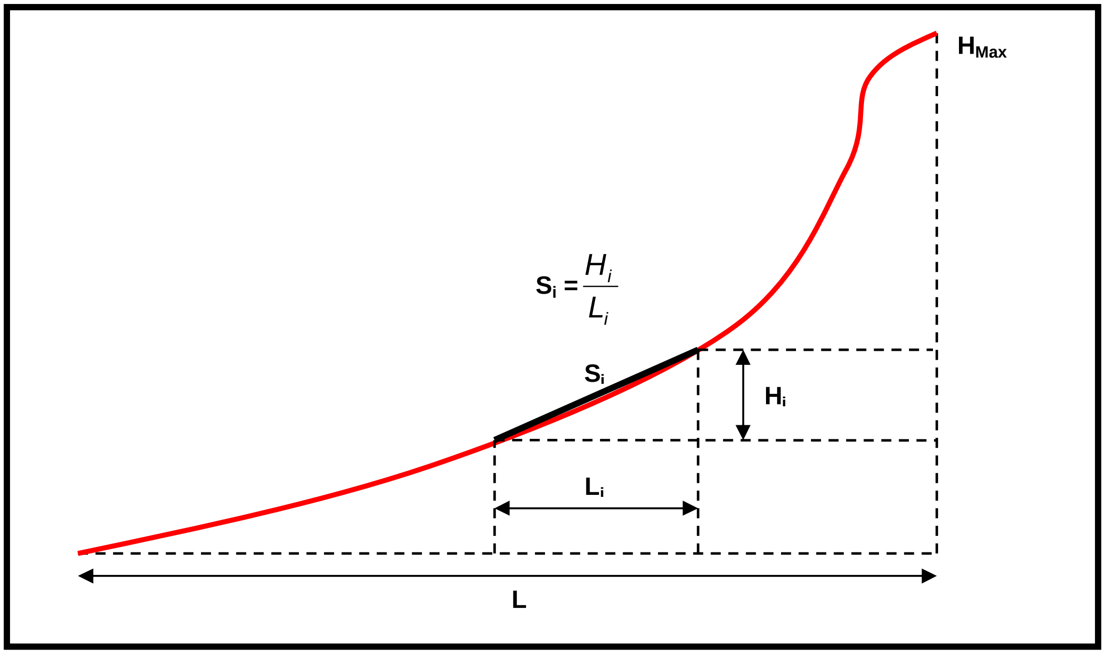

Figure 2.4: Taylor-Schwarz method

2.2.1.3 Drainage density

Drainage density, which can be defined as the proportion of total length of watercourses and the catchment area, can have a marked effect on the run-off rate. A well-drained catchment will have comparatively short concentration times and hence steeper flood-rise hydrographs than a catchment with many surface depressions, marsh ground and minor lakes. The hydraulic effectiveness of a watercourse is of importance, since it affects the flow rate. The meandering of watercourses and marshes outside the riverbanks affects the progress and attenuation of flood peaks (Alexander, 2001: 386).

The following two methods can be used to establish the hierarchical order of watercourses within a catchment (Pegram & Parak, 2004: 389):

- <u>Strahler basin order</u>: An order value of 1 is assigned to the smallest recognisable watercourse (fingertip tributaries). In cases where two watercourses of order *(i)* confluence, a watercourse of order *(i+1)* forms downstream. In cases where watercourses of order *(i)* and *(i+1)* respectively confluence, the watercourse downstream equals the higher order watercourse.

- Shreve stream network magnitude: This technique reflects the number of smallest watercourses (fingertip tributaries) flowing towards the catchment outlet. At the confluence of two watercourses, the resulting order of the downstream watercourse is the sum of the orders of the upstream watercourse(s) feeding it.

2.2.1.4 Soil type and antecedent soil moisture condition

The effect of soil type depends on the volume, duration and intensity of precipitation. The antecedent soil moisture status of a catchment gives an indication of the soil's initial rate of infiltration. Soils are initially dry or more permeable with a resulting higher rate of infiltration, but depletes over a period, since the soil becomes saturated. Most of the effective precipitation and associated run-off are produced after saturation (Alexander, 2001: 388).

2.2.2 Developmental variables

2.2.2.1 Land use

The areal distribution of the main land-use groups within a catchment can play an important role in the distribution of run-off. Land use must be subdivided into pervious and impervious areas and present and future conditions must be taken into account. Urbanised areas have a big influence on flood peaks, especially if impervious areas predominate (SANRAL, 2006: 3.7).

The perception in the past was that urbanisation is normally associated with an increase of 20 to 50% of flood peaks. Although, this is only the case when no attenuation of flood peaks and run-off occur by means of obstructions (walls and fences), ponds, recreational areas, parks and open spaces. During attenuation, large volumes of run-off can be intercepted, thus reducing peak flows by acting as surface water stores while smoothing out the hydrographs, thus resulting in larger flood volumes (SANRAL, 2006: 3.7).

2.2.2.2 Storage and reservoirs

Storage in a catchment occurs as detention storage, i.e. storage in overland and river flows, pans, lakes and marshes. Storage affects the attenuation and translation of flood peaks. Reservoirs intercept large volumes of run-off, thus reducing the peak flows considerably (SANRAL, 2006: 3.8).

2.2.3 Climatological variables

2.2.3.1 Climate

Precipitation distributions vary in South Africa. South Africa's climate ranges from semi-arid to hyper-arid. The mean annual precipitation (MAP) decreases, while evaporation increases westwards and northwards across the southern part of Africa. The overall MAP is 452 mm. Nowhere, except for the few mountain tops in the Drakensberg and South-western Cape does precipitation exceed evaporation. In the area of the lower Orange River evaporation is more than ten times the precipitation. Summer precipitation is normally higher in the north and east, but due to dry high-pressure air masses that persist for long periods, the precipitation is low in the western parts of South Africa (Davies & Day, 1998: 29 -30).

The main effect of climate, however, is on precipitation intensity and duration. Vegetation and soil formations are affected by precipitation and temperature. There is a direct relationship between precipitation intensity and the MAP. Precipitation intensity has a direct bearing on run-off since once the infiltration capacity is exceeded, all the excess precipitation is available and flow to surface watercourses (SANRAL, 2006: 3.8).

2.2.3.2 Precipitation distribution

Run-off depends not only on the amount and intensity of precipitation, but is also affected by the duration, size, uniformity, velocity and direction of a storm passing over a catchment. Point-to-point differences in the area and time distribution of precipitation are dependent on the type of precipitation. Flood-causing storms have durations just long enough to allow run-off from all parts of the catchment to contribute simultaneously to the flood peak, hence the relationship between the critical duration of a storm and the time of concentration (SANRAL, 2006: 3.8).

The time of concentration (Equation 2.6) can be defined as the time required for run-off, as a result of precipitation with a uniform areal and temporal distribution, to contribute to the peak run-off or, in other words, the time required for a water particle to travel from the catchment boundary along the longest watercourse to the catchment outlet (Rooseboom *et al.*, 1993: 2.25; SANRAL, 2006: 3.17).

In determining the time of concentration, overland flow and/or flow in defined watercourses and/or artificial/man-made canals (urban areas) can occur.

$$T_C = T_{C1} + T_{C2} + T_{C3} \qquad (2.6)$$

Where:

T_C = Total time of concentration (hours)

T_{C1} = Time of concentration for overland flow (hours) (Equation 2.7)

T_{C2} = Time of concentration for flow in defined watercourses (hours), (Equations 2.8 and/or 2.9)

T_{C3} = Time of concentration for artificial/man-made canals (hours), (Equation 2.10)

Overland flow occurs in small, relatively flat catchments or in the upper reaches of a catchment where there is no clearly defined watercourse. Run-off occurs in the form of thin layers of water flowing slowly over the ground surface. The Kerby equation (Equation 2.7) is applicable to overland flow conditions (Rooseboom *et al.*, 1993: 2.25; SANRAL, 2006: 3.17).

$$T_{C1} = 0.604\left(\frac{rL}{\sqrt{\frac{H}{1000L}}}\right)^{0.467} \qquad (2.7)$$

Where:

H = Height of most remote point above the catchment outlet (m)

L = Hydraulic length of catchment (km)

r = Roughness coefficient (The standard surface descriptions and associated r-values are included in the DFET)

Channel flow occurs in a defined watercourse. The United States Soil Conservation Services (US-SCS) recommend the use of Equation 2.8, whilst Kirpich (1940) recommends the use of Equation 2.9 to determine the time of concentration in a natural, defined watercourse.

$$T_{C2} = \left(\frac{0.87L^2}{1000S_{Avg}} \right)^{0.385} \quad (2.8)$$

$$T_{C2} = 0.0633\left(\frac{L}{S_{Avg}} \right)^{0.385} \quad (2.9)$$

Where:

L = Length of longest watercourse (km)

S_{Avg} = Average slope (m/m) as determined by Equations 2.3/2.4/2.5

In urban areas or artificial/man-made canals, the time of concentration must be based on the calculated flow velocity according to Chézy or Manning. Permissible velocity ranges, based on the material used, must be adhered to (Rooseboom *et al*., 1993: 2.30; SANRAL, 2006: 3.21).

$$T_{C3} = \left(\frac{L}{3600\bar{v}} \right) \quad (2.10)$$

Where:

L = Length of artificial/man-made canal (m)

$\bar{v}$ = Average velocity (m/s)

2.2.3.3 Precipitation-related variables

Since precipitation is the main driving force behind flood peaks and flood volumes, the following precipitation-related variables are of concern:

Point precipitation:

It is useful to first examine the characteristics of storm precipitation at a single point before engaging the characteristics of spatial or areal precipitation. The point precipitation characteristics which are important in flood estimation are (Görgens, 1997):

- Total depth of precipitation during the storm.
- Duration of the storm.
- Peak intensity.
- Intensity distribution during the duration of the storm.
- Average intensity.

- Time resolution of precipitation information.
- Severity of the storm relative to other storms; the exceedance probability of a particular depth of precipitation for a specific duration.

Areal distribution of precipitation:

The areal distribution of precipitation determines the shape of a hydrograph. Precipitation occurring mainly in the upper reaches of a catchment produces a lower peak at a later point in time, thus resulting in a hydrograph with a longer base length. On the other hand, high intensity precipitation near the catchment outlet results in a rapidly rising and falling hydrograph with a well-defined peak. The distribution coefficient, which is the ratio of maximum point precipitation to the average areal precipitation, can be used as an index for the areal distribution of precipitation (Van der Spuy & Rademeyer, 2008: 3.9).

Time distribution of precipitation:

The time distribution of precipitation in a catchment is important, since precipitation that falls towards the end of a storm will generate more run-off than precipitation with the same intensity at the beginning of a storm. This parameter is significant on small catchments, the hydrograph is characterised by a rising limb followed by a flat peak, while the recession limb can be either concave or convex upwards due to a decreasing or an increasing hyetograph respectively (Alexander, 2001: 277, 333; Van der Spuy & Rademeyer, 2008: 3.10).

In large catchments, the equalising effect makes the hydrograph insensitive to the time distribution of precipitation. In principle, a hyetograph characterised by high intensity precipitation which gradually decreases to zero, produces a hydrograph with a convex rising limb. A hydrograph with an upwards concave rising limb is due to the gradual increase in precipitation from zero to a maximum, followed by no precipitation (Van der Spuy & Rademeyer, 2008: 3.10).

Intensity-duration relationship:

Precipitation intensity will determine the magnitude of a storm or flood, but only a certain proportion of the precipitation will contribute to the actual magnitude of a flood (Alexander, 2001: 277). High intensities of precipitation are associated with a shorter period of duration, thus intensity is inversely proportional to the duration thereof. High intensity precipitation in a short time span will not necessarily generate a higher volume of run-off than a low intensity storm over a longer period (Wilson, 1990: 15 - 16). Intensity and duration are primarily responsible for the severity of a flood, but the magnitude of a flood is not directly proportional to the magnitude of precipitation alone (Alexander, 2001: 279).

2.2.4 Summary

Listed in Table 2.1 is a summary of all the flood-producing mechanisms or variables which can influence both the magnitudes of flood peaks and volume of run-off.

Table 2.1: Summary of flood-producing variables

Variables	Comments
Catchment characteristics	Includes area and shape of catchment, direction of slope with regard to the direction of storm movement, drainage patterns, vegetation and land use.
Catchment processes	Infiltration rate determines the proportion of precipitation that will be available to generate run-off. Storage will play a role in the attenuation of floods, thus reducing the flood peak. River reaches also have an influence on the time distribution of run-off. Pervious and impervious areas and their associated hydrological responses are of importance.
Regional scale processes	Catchment moisture status is predominant; other catchment processes are less dominant. The proportion of precipitation contributing to flood peaks and volume increases.
Precipitation characteristics	The magnitude and frequency of floods are determined by precipitation depth, intensity, area distribution, movement (non-stationarity) and duration of storms. Weather systems and location on the globe will have an influence on the type of precipitation. During short duration storms, the effective precipitation forms a relatively small part of the total precipitation. The opposite, i.e. when the duration is longer, will result in higher flood volumes. In small, impermeable catchments, precipitation intensity is the dominant flood-producing mechanism. In large, permeable catchments, precipitation duration becomes the dominant mechanism.

2.3 REVIEW OF DESIGN PRECIPITATION ESTIMATION

2.3.1 Introduction

Design precipitation, which is a probabilistically-based estimate of precipitation, comprises the precipitation depth and duration associated with a given probability of exceedance or return period. Short and long duration design precipitation estimations can either be based on point or regionalised data. Precipitation durations less than 24 hours are classified as short, whilst long durations typically range from one to seven days (Smithers & Schulze, 2004: 435).

Several regional and national scale studies in South Africa based on short durations and point data were conducted between 1945 and 2001. The studies focusing on long durations and point data were limited to those conducted by the SAWB (South African Weather Bureau) (1956), Schulze (1980), Adamson (1981), Pegram and Adamson (1988) and Smithers and Schulze (2000b). Smithers and Schulze (2000a; 2000b) also used a regionalised approach in an attempt to increase the reliability of the design values at gauged sites, as well as for the estimation of design values at ungauged sites (Smithers & Schulze, 2003: 5).

2.3.2 Single site approach

A single site approach entails that each precipitation station within the catchment of concern needs to be investigated to determine the record length, data quality (errors, missing data and outliers) and topographical position. In order to develop the depth-duration-frequency (DDF) relationship at every single site, the following steps are of importance (Smithers & Schulze, 2000a: 8):

- Selection of the most appropriate data set. This may either be the Annual Maximum Series (AMS) or Partial Duration Series (PDS) with a sufficient record length.
- Selection of the most appropriate probability distribution, a suitable parameter and quantile method.

The above steps are discussed in more detail in the following paragraphs.

Due to a probabilistic analysis that needs to be done on each precipitation station, it is suggested not to use precipitation stations with limited record lengths, since it is impossible to conclusively select a distribution that could consistently provide adequate precipitation frequency estimates for return periods greater than the period of record. On the other hand, small samples may define a distribution which is markedly different to the parent population (Smithers & Schulze, 2000a: 8).

According to Viessman *et al*. (1989), a minimum record length of 10 years is required, whilst Schulze (1984) questioned the significance of the record length on the extreme events recorded and hence the design values. Hogg (1992) demonstrated that even 20 years of data are not stable enough to estimate the 10-year return period event. Hogg (1992) indicated that the assumptions of stationarity and homogeneity of the AMS of precipitation are seldom valid. It is suggested that a regional approach must be used to improve the frequency analysis of extreme precipitation events.

According to Weddepohl (1988), the malfunctioning of precipitation gauges and processing errors are inherent in precipitation data. The spatial density and distribution of precipitation gauges, sporadic precipitation events as opposed to the continuous digitised data in use, length of available records and the presence of outliers are all problems associated with these errors.

In design flood estimation, it is assumed that the critical storm duration equals the time of concentration, thus resulting in the peak run-off draining the catchment. Thus, depending on the time of concentration, the daily precipitation depth used in flood estimations must either be increased or decreased. In order to convert the daily precipitation depth values to independent durations of the same length, conversion factors have to be used. The conversion factors are dependent on the duration in question and various values have been proposed. The factors recommended to convert daily precipitation depths to 24 hour continuous maxima are 1.13 in the United States of America (USA) (Hershfield, 1962), 1.06 in the UK (NERC, 1975), 1.13 (Alexander, 1978) and 1.11 (Adamson, 1981) in South Africa (SA) (Alexander, 2001: 337 - 350; Smithers & Schulze, 2000a: 14).

According to Schulze (1984), the conversion factors vary regionally and variations of up to 20% at some locations were evident. Converting daily precipitation depths to durations longer than one day simply entails the conversion of 1 day to 24 hours, 2 days to 48 hours, etc. and interpolating between the different precipitation depth durations (days) (Van der Spuy & Rademeyer, 2008: 3.3).

The selection of the most suitable probability distribution resembling the probability distribution of the population must be based on the theoretical basis, consistency, acceptance, user-friendliness and applicability thereof. This selection is particularly important when estimating extreme events with return periods greater than the length of record. Equally important is that factors, such as the type of data in use, data stationarity and the method of fitting the distribution should also be considered (Cunnane, 1989; as cited in Smithers & Schulze, 2000a: 14).

The Extreme Value Type I (EV1) distribution has been extensively used in precipitation DDF studies in South Africa since 1963, whilst the use of the integrated GEV distribution is growing in the application of frequency analysis. Van der Spuy and Rademeyer (2008) proposed the use of the LN, LP3, GEV using Method of Moments (GEV/MM) and GEV using Probability Weighted Moments (GEV/PWM) or Linear Moments (GEV/LM) to determine the required design precipitation depths in South Africa. Finally, in order to select the most suitable probability distribution and parameter estimation procedure, GOF tests are also required to evaluate the methods in use. These GOF statistics are discussed in Section 2.4.1.10.

2.3.3 Regional approach

Regional frequency analysis is based on the assumption that the standardised variate distributions of precipitation data are similar at every single site in a region and that the data from various single sites in a region can thus be combined to generate a single regional precipitation frequency curve representative of any site in the specific region with appropriate site-specific scaling. An advantage of this approach is that it can be used to estimate events at ungauged sites where no precipitation data exists (Alexander, 2001: 480; Cunnane, 1989; as cited in Smithers & Schulze, 2003: 24 - 25).

In nearly all practical situations a regional approach is preferred to a single site approach, primarily based on the efficiency and accuracy of the precipitation quantile estimation, both where statistical homogeneity or heterogeneity might exist (Hosking & Wallis, 1997; as cited in Smithers & Schulze, 2003: 5). The large degree of uncertainty introduced in the extrapolation of exceedance probabilities beyond the record length of data can also be reduced by regionalisation, since the observed precipitation at a single site are then related to the hydrological response at a regional scale by making use of an extended or combined record length of data (Smithers & Schulze, 2003: 5).

Regional approaches are well established in frequency analysis and various different techniques are available. Smithers and Schulze (2000a; 2000b) successfully used a regional index-flood type approach based on Linear Moments (LM), termed the Regional Linear Moment Algorithm (RLMA), to estimate short and long duration design precipitation in South Africa.

The RLMA approach to estimate short duration design precipitation (< 24 hours) was based on digitised precipitation data from 172 stations which had at least 10 years of record, while the long duration design precipitation estimates, typically ranging from one to seven days, were based on daily precipitation data from 1 806 stations which had at least 40 years of record. The results obtained from the two above-mentioned studies were inconsistent and are ascribed to the non-concurrent periods of data used, different record lengths, AMS variability and errors in the digitised precipitation data (Smithers & Schulze, 2004: 435).

The sampling variability of the AMS was estimated with three approaches – windows of data extracted from the entire period of record, stochastic modelling, and a bootstrapping technique. The results established that the variation with duration in observed higher order LM is associated with the sampling variability and record length. Based on the fact that the daily precipitation data are more dependable with longer record lengths than the digitised data, the 1-day LM ratios were assumed to be the most reliable estimate of the LM ratios and mean AMS for all durations (Smithers & Schulze, 2003: 22; 2004: 436).

The mean AMS for any duration can be estimated by firstly estimating the mean 1-day AMS at a single site by regional regression, followed by scaling either the mean AMS for durations shorter or longer than one day respectively from the 24-hour and 1-day values. This application of the RLMA in conjunction with a scale invariance approach is referred to as the RLMA&SI approach (Smithers & Schulze, 2003: 6).

The RLMA&SI approach was compared with the single site approach (based on censored LN distributions) used by Adamson (1981) in Technical Report (TR102) at 2 184 daily precipitation stations. The differences between the two approaches were generally less than 20% for return periods less than 50 years, but these differences increased for longer return periods. These differences can be ascribed to the following factors (Smithers & Schulze, 2003: 7):

- The use of longer record lengths and strict data quality control procedures in the RLMA&SI approach.
- The use of different distributions, LN in TR102 as opposed to the GEV in RLMA&SI.
- The LM used in the RLMA&SI approach are not that sensitive or influenced by outliers in data.

Further comparisons between the RLMA&SI approach, the DDF relationships based on Log-EV1 (LEV1) distributions fitted to the AMS as contained in the Hydrological Research Unit (HRU) Report 2/78 (Midgley & Pitman, 1978), the Hershfield equation (Adamson, 1981: 21) and the modified Hershfield equation (Alexander, 2001: 349) for durations less than 24 hours were performed.

The design precipitation estimation results obtained with RLMA&SI and DDF approaches compared well, whilst the modified Hershfield equation generally overestimated the values and there were also inconsistencies between the modified Hershfield equation and the 1-day TR102 data. The functional relationship of the modified Hershfield equation does not seem to accommodate the curvilinear relationship between the design precipitation depth and $\log_{10}$-transformed duration (Smithers & Schulze, 2003: 7).

In conclusion, the RLMA&SI estimates are consistent over the entire range of durations, whereas the other techniques considered are frequently inconsistent for a range of durations. The software program, *Design Rainfall Estimation in South Africa* has been developed in 2003 to facilitate the estimation of design precipitation depths at a spatial resolution of 1-arc minute for any location in South Africa based on the RLMA&SI approach for durations ranging from 5 minutes to 7 days and for return periods of two to 200 years (Smithers & Schulze, 2003: 8; 2004: 443).

2.3.4 Critical storm duration precipitation

Irrespective of whether a single site or regional approach is followed, the design precipitation depth to be used in design flood estimation, especially deterministic methods, must be based on the critical storm duration or time of concentration.

In Section 2.3.2 reference was made to the use of conversion factors to convert the daily precipitation depth values to independent durations of the same length, more specifically, the time of concentration. The following approaches to estimate this unique DDF relationship are included in the DFET developed during this study:

2.3.4.1 DDF relationship based on LEV1 distributions

Midgley and Pitman (1978) developed a DDF co-axial diagram in which the design precipitation is a function of the critical storm duration, regional location (regional factors), probability of exceedance (frequency factors) and MAP. According to Schulze (1984), there are some anomalies in the database used, since the LEV1 distribution estimated physically impossible precipitation values in some cases. Sinske (1982) emphasises the practical difficulties of using the co-axial diagram and on deciding whether a summer/inland or winter/coastal estimate is applicable to the site of concern. Adamson (1981) indicated that storms shorter than two hours in duration are likely to be independent of the MAP.

Least-square regression analyses were used to derive the following relationships from the data used by Midgley and Pitman (1978; as cited in Alexander, 2001: 339):

Precipitation depth (P):

$$P = (I_{w,s})\,(T_C)\,(M_F)\,(F) \tag{2.11}$$

Winter/coastal region (I_w):

$$I_w = \frac{122.8}{(1+4.779T_C)^{0.7372}} \tag{2.12}$$

Summer/inland region (I_s):

$$I_s = \frac{217.8}{(1+4.164T_C)^{0.8832}} \tag{2.13}$$

MAP factor (M_F):

$$M_F = \frac{(18.79+0.17MAP)}{100} \tag{2.14}$$

Where:

F = Frequency factor

$I_{w,s}$ = Precipitation intensity (mm/h)

MAP = Mean annual precipitation (mm)

M_F = MAP factor

P = Precipitation depth (mm)

T_C = Time of concentration (hours)

The frequency factors (F) based on the relationship between the design precipitation depths and various return periods are listed in Table 2.2.

Table 2.2: Frequency factors (Midgley & Pitman, 1978; Alexander, 2001: 340)

Return period (*T*, years)	**Frequency factors (*F*)**
2	0.47
5	0.64
10	0.81
20	1.00
50	1.30
100	1.60
200	1.80

2.3.4.2 DDF relationship based on the SAWS/TR102 precipitation data

The 1-, 2-, 3- and 7-day extreme precipitation depths for return periods of two, five, ten, 20, 50, 100 and 200 years were estimated by Adamson (1981) using approximately 8 000 precipitation stations. A censored LN model based on the PDS was used in this study. According to Adamson (1981), the daily precipitation depth can be converted to a 24-hour precipitation depth by making use of the following relationship:

$$P_{24h} = 1.11 P_{1\text{-}day} \quad (2.15)$$

Where:

P_{24h} = 24-hour Precipitation depth (mm)

$P_{1\text{-}day}$ = 1-day Precipitation depth (mm)

The computed ratios for the T_C (hour) duration storm depth to that of 24 hours for the summer/inland and winter/coastal precipitation regions are listed in Table 2.3.

Table 2.3: Ratio of T_C (hour) storm depth to 24-hour storm depth (Adamson, 1981: 20)

T_C (hours)	Summer/inland region	Winter/coastal region
0.10	0.17	0.14
0.25	0.32	0.23
0.50	0.46	0.32
1	0.60	0.41
2	0.72	0.53
3	0.78	0.60
4	0.82	0.67
5	0.84	0.71
6	0.87	0.75
8	0.90	0.81
10	0.92	0.85
12	0.94	0.89
18	0.98	0.96
24	1.00	1.00

Converting daily precipitation depths to durations longer than one day simply entails the conversion of 1 day to 24 hours, 2 days to 48 hours, etc. and interpolating between the different precipitation depth durations (days) as indicated in Table 2.4.

Table 2.4: Conversion of daily precipitation to hourly precipitation (Van der Spuy & Rademeyer, 2008: 3.3)

Duration		Conversion factor
From (days)	To (hours)	
1	24	1.11
2	48	1.07
3	72	1.05
4	96	1.04
5	120	1.03
7	168	1.02
> 7	> 168	1

2.3.4.3 DDF relationship based on the modified Hershfield equation

Alexander (2001) proposed that the modified Hershfield equation, as shown in Equation 2.16, must be used to calculate the precipitation DDF relationships for durations less than 6 hours. Although, if the time of concentration (T_C) is longer than 6 hours and less than 24 hours, then linear interpolation between Equation 2.16 and the 1-day point precipitation depth from TR102 or the SAWS database must be used. If the time of concentration exceeds 24 hours, then linear interpolation between the *n*-day point precipitation depth values must be used.

$$P = 1.13(0.41 + 0.64\ln T)(-0.11 + 0.27\ln(60T_C))(0.79M^{0.69}R^{0.20}) \qquad (2.16)$$

Where:

M = 2-year Mean of the annual daily maxima precipitation (mm)

P = Precipitation depth (mm)

R = Average number of days per year on which thunder was heard

T = Return period (years)

T_C = Time of concentration (hours)

2.3.4.4 DDF relationship based on the RLMA&SI approach

None of the above-mentioned (Sections 2.3.4.1 - 2.3.4.3) DDF relationships are based on a regional approach. As indicated in Section 2.3.3, RLMA&SI is a regional approach resulting in consistent design precipitation depths over the entire range of durations. The detailed mathematical relationships related to this approach are not included in the DFET, although the results obtained by the Java-based software program, *Design Rainfall Estimation in South Africa* (Smithers & Schulze, 2003; 2004) can be entered by the user into the DFET precipitation database to compare the various approaches. The data management and associated procedural steps to follow, the theoretical basis applicable, as well as the shortcomings or advantages associated with each approach will be highlighted in Chapters 4 and 5, as well as in the DFET User manual contained in Addendum D.

2.3.5 Averaging precipitation depth over area

In the assessment of total quantities of precipitation over large areas, the occurrence of storms and their contribution to single gauging sites are unknown. Therefore, it is necessary to convert many point precipitation depths to provide an average precipitation depth over a certain area. The following three methods may be used for averaging the precipitation depth over an area (Wilson, 1990: 21 - 22):

- Arithmetic mean method (Equation 2.17): This method is defined as the sum of all the point precipitation data divided by the number of precipitation stations within the catchment area. This method is only sufficient when precipitation stations are uniformly distributed, the topography is relatively flat and spatial variations in precipitation are insignificant.

$$\overline{P} = \sum \frac{P_i}{N_i} \qquad (2.17)$$

- Thiessen polygon method (Equation 2.18): This method defines the zone of influence of each precipitation station by drawing lines between pairs of stations, bisecting the lines with perpendiculars. The total area enclosed within the boundary formed by these intersecting perpendiculars has had precipitation of the same amount as the enclosed precipitation station. This method is not suitable for mountainous areas due to orographic influences.

- Isohyetal method (Equation 2.18): This method is based on the interpolation between precipitation stations to produce isohyets or contours of equal precipitation depth. The areal average of the weighted precipitation depths between the isohyets is then used to calculate the average precipitation. This method is possibly the most accurate of the three with an added advantage that the isohyets may be drawn to take into account local effects of climate and uneven topography.

$$\overline{P} = \frac{\sum P_i A_i}{\sum A_i} \qquad (2.18)$$

Where:

A = Area (km²)

N_i = Number of precipitation stations within area

$\overline{P}$ = Average precipitation depth (mm)

P_i = Point precipitation depth (mm)

The design precipitation depth at single sites estimated by all the DDF relationships, except the RLMA&SI approach (Section 2.3.4), can be averaged by making use of either the Thiessen polygon or arithmetic mean method in the DFET. The GIS-integrated application of these methods is discussed in detail in Chapters 4 and 5.

2.3.6 Area reduction factor

Flood-producing storm precipitation is almost never evenly distributed both in time and space over an area. Storms have one or possibly two or more maximum precipitation cores and storm precipitation displays for any given duration, with a sensibly smooth non-linear reduction in average areal values with increasing distance from the maximum precipitation core of the storm. The area reduction factor (ARF) is used to convert point precipitation depth to average areal precipitation for a particular duration and catchment area (Alexander, 2001: 335).

In catchment areas less than 800 km², the ARF is mainly a function of the area and point intensity, since the relationship between precipitation intensity and the infiltration rate of the soil is predominant. In catchment areas up to 30 000 km², the ARF is mainly a function of the area and storm duration, since the quantity of precipitation relative to the number of storage areas is of importance. In both cases, the ARF decreases in value with an increase in area. The ARF is also independent of the return period and geographical location (Alexander, 2001: 335; HRU, 1972: 2.3 - 2.4).

The ARF can be used in two different ways:

Firstly, when the ARF is used for percentage reduction, which relates to the statistics of point and area precipitation, the uniform distribution of precipitation in time and space over a catchment for the duration of the storm is determined, in other words, the average areal precipitation depth. A correction factor should be applied when using the ARF derived in this manner. Secondly, if the ARF relates to the way in which precipitation intensity decreases with distance from the core of a storm in individual events, the average areal precipitation intensity is determined (Alexander, 2001: 357 - 358).

Alexander (2001) recommended that the ARF relationship shown in Equation 2.19 must be used for Southern African conditions where the average precipitation depth over a catchment has to be established from point precipitation statistics.

$$ARF = \left(90000 - 12800\ln A + 9830\ln\left(60T_C\right)\right)^{0.4} \qquad (2.19)$$

Where:

ARF = Area reduction factor (%)

A = Catchment area (km²)

T_C = Time of concentration (hours)

In Equation 2.19 the ARF relationship accommodates severe storm mechanisms producing high intensity precipitation with cell core areas exceeding 10 km^2 and durations exceeding 10 minutes. Estimates of shorter duration precipitation based on extrapolation from longer durations are suspect when viewed in the light of the storm mechanisms which produce high-intensity precipitation for durations less than 10 minutes.

2.3.7 Probable maximum precipitation

Probable maximum precipitation (PMP) can be defined as the greatest depth of precipitation for a given duration that is physically possible over a given size of storm area for a particular location and time of year, thus a critical depth-duration-area precipitation relationship (Alexander, 2001: 361).

The PMP is only an estimate, since the current knowledge of storm mechanisms and their precipitation-producing efficiency is inadequate to permit the precise development of an upper limit to possible floods from hydrological data. Therefore, the depth and rate of precipitation over an area must have an upper limit, based on the assumption that there must be upper limits to the perceptible moisture content of a column of air and the rate of influx of perceptible moisture over an area (Alexander, 2001: 361; Wilson, 1990: 34).

The seasonal variation in PMP is important in the design and operation of various structures and flooding considerations. There are three methods which can be used to determine the PMP (Wilson, 1990: 34 - 36):

- *Empirical methods*, with the maximum expected point precipitation as starting point.
- *Statistical methods*, based on a frequency analysis of the observed data.
- *Meteorological methods*, where precipitation is expressed as the product of available moisture content in the air and air movement due to temperature fluctuations.

In South Africa, meteorologists have not concerned themselves with PMP estimation like most overseas countries. Therefore, the only established PMP estimation procedure for South Africa was developed by the HRU of the University of the Witwatersrand in 1972. Envelope curves, depth-area-duration-frequency (DADF) relationships and PMP versus area curves (based on the maximisation of observed storms) for regions experiencing similar extreme point precipitation in South Africa were developed. These envelope curves, as well as the extreme precipitation regions, need some serious revision, since almost 40 years of additional data are now available. An alternative approach could be to use the 0.001% probability of exceedance precipitation depth as the PMP (Alexander, 2001: 364; HRU, 1972: 2.1 - 2.4).

2.4 REVIEW OF DESIGN FLOOD ESTIMATION METHODS

2.4.1 Statistical methods

2.4.1.1 Introduction

The basic issue in flood hydrology is the estimation of the probable magnitude of future floods based on historical data. Floods are natural events which occur randomly and cannot be established with absolute certainty. However, to quantify the measure of uncertainty, the statistical properties of the historical data, which is most unlikely to be repeated in future, must be examined and applied to estimate the likelihood of floods of given magnitude. The most powerful tool available to hydrologists to investigate these statistical properties is that of statistical analysis. The main objective of statistical analyses is to summarise the data, estimate certain parameters and select an appropriate theoretical distribution with which probabilities can be determined. It is important that every user is well informed of the power and weakness, as well as the nomenclature and approach, associated with each of the basic statistical methodologies available (Alexander, 2001: 421).

2.4.1.2 Properties of data sets

<u>Sources of data</u>:

Observed streamflow data from river and reservoir hydrological gauging stations for each hydrological year (October to September) are primarily available from DWA (Directorate: Hydrology), which is responsible for the acquisition, processing and dissemination of the data. Local authorities, water boards and some universities also provide data in certain regions (SANRAL, 2006: 3.10).

<u>Historical information:</u>

Historical information contains flood peaks which occurred over an extended period of time before or after the continuous measurement of streamflow at a specific site. This information must be incorporated to extend the period of analysis. However, the reliability of historical information should be evaluated by comparing against similar extremes in nearby catchments or with available precipitation information (Pilon *et al.*, 1985; as cited in Alexander, 2001: 460).

Alexander (2001) recommends the use of historically weighted conventional and probability moments to incorporate historical information in data sets. The detailed procedure of historical weighting and conditional probability theory used to calculate the historically weighted variables and evaluating the effect of missing data, zero flows or low outliers and apparent high outliers is included in Addendum D (DFET User manual).

Sources of error:

The sources of error most often encountered in observed data used for statistical analyses are (Alexander, 2001: 474 - 477):

- Missing data: In observed data sets which are characterised by missing data for one or more hydrological years, the record length must be reduced accordingly. In cases where the missing data are only limited to one or more months normally characterised by low flows in a year, the maximum observed in the balance of the months can be used. Otherwise, ignore the whole year if this is not the case.
- Zero flows/low outliers*:* Observed data may contain zero flows and/or low outliers which may be considered to be anomalous values as a result of developmental variables within a catchment. In statistical analysis, anomalous low outliers will reduce the calculated skewness of the data set, resulting in an underestimation of the flood peaks. In addition, zero flows cannot be included in analyses using $\log_{10}$-transformed data, since an error condition will be introduced when the log of zero is calculated. The conditional probability theory (specifying a low threshold value equal to zero or predefined minimum value) can be used to exclude all undesirable low outliers. Thus, the number of observations exceeding this low threshold is expressed as a ratio of the total number of observations used in the analysis, which is the probability of exceedance for future peaks.
- Trends in data*:* Increasing trends are associated with small, urbanised catchments, whilst apparent increasing trends in large catchments are likely due to measurement errors. Severe, widespread precipitation can result in high outliers. Decreasing trends are a result of flood attenuation and translation by upstream dams. Anomalous low results, due to this

storage effect must be removed from the data set to prevent the introduction of a negative curvature into the analyses and an underestimation of the long return period peaks. The use of conventional, statistical-based trend analyses in flood peak series representative of South African conditions is unlikely to be successful, due to the small sample sizes and high degree of variability and skewness.

- <u>Measurement errors</u>*:* Most of the observed streamflow data in South Africa contain years where the flood peaks exceeded the hydraulic capacity of the gauging weir. However, high outliers should not be omitted from data sets unless there is sufficient proof that the measurements were in error. Due to the high natural variability of the flood peaks of South African rivers, even relatively large measurement errors will not have a proportionally large effect on the results of the analyses. In many cases the inclusion of approximate flood peak values (beyond the hydraulic capacity) will produce more reliable results than the omission thereof.
- <u>High outliers</u>*:* These are values that plot at an unusual distance away from the trend of the plotted points when the complete data set is plotted on a probability graph. The influence of high outliers on data quality must be evaluated based on both mathematical and hydrological considerations. In cases where high outliers are the maximum observed flows over an extended period of time, the inclusion thereof as historical information is suggested. Otherwise, retention as part of the continuous record is suggested. There is strong evidence that in South Africa most of the high outliers are a result of rare, severe meteorological phenomena contributing to annual flood peak series being a mixture of two or more statistical populations, each with different sets of parameter values and associated flood peak frequency relationships.

2.4.1.3 Description of data sets

Observed data sets can be described or summarised by using graphical and/or numerical methods. Graphical methods include the use of the following methods to represent both the natural data and/or $\log_{10}$-transformed data (Alexander, 2001: 423; Chow *et al*., 1988: 354; Hirsch *et al*., 1993: 17.5 - 17.7):

- Histograms*:* The flood peaks are plotted on the ordinate and the duration on the abscissa. The arbitrary selection of class durations is a drawback to the use of histograms as statistical tools. If the durations are too long, important information about the distribution of the variables may be lost, whilst short durations are characterised by excessive amount of class-to-class variation which is meaningless.
- Frequency distribution histograms*:* The data are grouped in predefined limit ranges and the number of flood peaks in each range is then determined. The relative frequency of occurrence is obtained by dividing the number of flood peaks in each range with the total number of flood peaks. The flood peak ranges are plotted on the ordinate and the corresponding relative frequencies for each range on the abscissa. A probability density function (PDF) is a mathematical equation which fits a frequency polygon that is drawn through the midpoints of the rows of frequency histograms. The area beneath the PDF must be equal to unity.
- Cumulative distribution graphs: These graphs are also known as quantile plots which portray the quantiles of the distribution of sample data. The sum of the relative frequencies in each range of the frequency distribution histogram is determined and plotted as the cumulative frequency on the ordinate with the flood peak distributions on the abscissa. A cumulative distribution function (CDF) is a mathematical equation which fits a cumulative frequency polygon that is drawn through the midpoints of the rows of cumulative frequency histograms, thus the integral of a PDF. The exceedance probability value of a CDF varies between 0 and 1.

Numerical methods are more often used to describe data, since the use thereof is fairly straightforward and the results can be used to determine probabilities of occurrence. Data are described in terms of central tendency (arithmetic mean, mode and median), dispersion (variance, standard deviation and coefficient of variation), asymmetry (skewness coefficient) and flatness (kurtosis coefficient) (Yevjevich, 1982: 102 - 111). The numerical methods are discussed in detail in Section 2.4.1.10, whilst the use of graphical methods to represent the data is included in Chapter 5 and Addendum C.

2.4.1.4 Annual maximum and Partial duration series

Various opinions regarding the use of the AMS and PDS have been expressed in the literature. The AMS and PDS are normally used to sample observed data for extreme meteorological and hydrological events. The AMS can be defined as the highest instantaneous peak streamflow value in each hydrological year for the period of record. In a 50-year period there would thus be 50 values, representing the highest peak flow in each hydrological year, but not necessarily representing the 50 highest peaks (Chadwick & Morfett, 2004: 313; Schulze, 1995: 21.23). The AMS can be described by Gaussian (LN), GEV (Gumbel, Fréchet and Weibull distributions) and Gamma (LP3) distributions (Madsen *et al.*, 1997: 759 - 769; Stedinger *et al*., 1993: 18.37).

In the PDS, the recorded flood peaks are ranked in a descending order and the number of peaks equal to the number of years of data is then selected for the calculation. This selection procedure entails that some of the annual peaks may be excluded in the series using a threshold exceedance value (Kite, 1988: 4 - 5).

A Generalised Pareto Distribution (GPD) is used to establish this threshold exceedance value, but this value is the most important obstacle in PDS, since it affects the basic assumptions of the method, including homogeneity, arrival times and exceedance magnitudes (Madsen *et al.*, 1997: 759 - 769).

Adamowski (2000) indicated that the threshold value can even hide the presence of different generating processes at different frequencies, thus affecting the uni-modal or multi-modal character of the distribution. A Poisson process for event arrivals is assumed since the frequency (inter-arrival times and number of occurrences) of flood events in a given time period is random, thus more than one flood peak from certain years may be included. An exponential distribution is used to describe the magnitudes of the flood peaks exceeding the threshold value (Madsen *et al.*, 1997: 759 - 769; Stedinger *et al*., 1993: 18.38).

The choice of the threshold value is frequently based on expert judgement, but this involves a great level of subjectivity. Different systematic methods were evaluated for the choice of the threshold value, whereas the selection according to a fixed frequency is often used. The AMS are in general statistically independent, while achieving statistical independence in PDS is more complicated, since the data used must be based only on independent flood peaks and not multiple flood peaks originating from the same storm event. In general, a high threshold value ensures that the events are independent, but can lead to a significant loss of information and increasing uncertainty. On the other hand, a low threshold value can project the events too close in time, thus introducing serial dependence of both frequency and magnitudes, thereby violating the assumption of independence (Madsen *et al.*, 1997: 759 - 769).

According to Adamson (1981), the AMS are preferred to the PDS based on the ease of use, rather than on the theoretical efficiency in characterising extreme value-time series. The maximum likelihood (ML), the MM and the PWM methods can be used to evaluate the performance of the two series in terms of the uncertainty of the *T*-year event estimator. In the case of ML estimation, the PDS are the most efficient *T*-year event estimator. In general, the PDS with MM estimation must be used for negative skewness, the PDS with exponentially distributed exceedance if the skewness coefficient is close to zero, the AMS with MM estimation for moderately positive skewness and the PDS with ML estimation for large positive skewness coefficients. The PDS are preferred for single site quantile estimation, since heavy-tailed distributions and associated negative skewness coefficients are common in hydrology (Madsen *et al.*, 1997: 759 - 769).

The use of PDS in short data records is recommended, since the AMS can result in a considerable loss of information for the estimation of flood probabilities. In addition, the use of PDS overcomes the objection of exclusion of large events that not being the largest event in a specific year. Therefore, if the arrival rate of events is large enough, the PDS design estimates should be more accurate than the AMS (Madsen *et al.*, 1997: 759 - 769; Smithers & Schulze, 2000a: 9).

2.4.1.5 Single site analysis

A single site approach entails that each flow gauging station within the catchment of concern needs to be investigated to determine the record length and data quality. In addition, a selection of the following aspects must be made (Alexander, 2001: 430, 473, 480, 525; Smithers & Schulze, 2000a: 7- 24):

- Suitable probability distribution (LN, LP3, EV1, GEV or Wakeby [WAK]): Schulze (1989) questions whether a suitable probability distribution can be selected, given that the best distribution varies with, *inter alia*, the season, storm type, storm duration and regional differences. The use of PDS with a suitable probability distribution might overcome this problem, since seasonal parameters in PDS can be used to estimate more than one flood-causing event in a season or year.
- Parameter estimation method (MM, ML, PWM or LM): LM estimators are used overseas as a standard procedure for frequency estimation, screening for discordant data and testing clusters for homogeneity. Some caution and criticism of the use of LM is also evident in the literature; Alexander (2001) caution that LM are too robust against outliers and emphasised that both low and high outliers are important characteristics of the flood peak maxima. The suppression of the effect of outliers could result in unrealistic estimates of long return period values. Therefore, further investigation of LM for possible general use in South Africa is necessary.
- The use of either natural or $\log_{10}$-transformed data: In data sets with a high variability about the mean and asymmetrical distribution of flood peaks, the use of $\log_{10}$-transformed data provides more normalised values resulting in a evened out graphical presentation of the results.
- Plotting positions: The graphical evaluation of the adequacy of fitted probability distributions is normally performed by plotting the observed data approximately on a straight line if a postulated distribution was a true distribution from which the observed data were drawn. The most commonly used plotting positions in hydrological analyses are Beard, Blom, Cunnane, Greenwood, Gringorten and Weibull. The various plotting positions are discussed in detail in Section 2.4.1.9.

Schulze (1989) highlights the problems associated with short record observed streamflow data and extrapolation beyond the record length. Typical measurement errors at flow gauging stations, as well as the inconsistency, non-homogeneity and non-stationarity of data, violate the assumptions made when fitting a probability distribution to the data.

The Square root-area method (Equation 2.20) can be used to combine observed streamflow data sets at single sites up- or downstream from one another, thus the flood peaks at one station are adjusted to reflect the flood peaks at the other station. This will result in a longer, more reliable record length, which contributes to improved fitting of probability distributions to data (Van der Spuy & Rademeyer, 2008). However, the time and scale variability of the flood-producing mechanisms in the two or more catchments under consideration must be homogeneous. In addition, the differences in catchment areas must be limited to $\pm$25% (Rademeyer, 2008; Van der Spuy & Rademeyer, 2008: 9.13).

$$Q_{DS} = Q_{US}\left(\frac{\sqrt{A_{DS}}}{\sqrt{A_{US}}}\right) \qquad (2.20)$$

Where:

A_{DS} = Catchment area contributing to downstream gauging station (km²)

A_{US} = Catchment area contributing to upstream gauging station (km²)

Q_{DS} = AMS or PDS at downstream gauging station (m^3/s)

Q_{US} = AMS or PDS at upstream gauging station (m^3/s)

2.4.1.6 Regional analysis

Regional frequency analysis is based on the assumption that the standardised variate distributions of flow data are similar at every single site in a region and that the data from various single sites in a region can thus be combined to generate a single regional flood frequency curve representative of any site in the specific region with appropriate site-specific scaling. Advantages of this approach are that it can be used to estimate events at ungauged sites where no flow data exists and standard estimation errors at gauged sites are reduced (Alexander, 2001: 480; Cunnane, 1989; as cited in Smithers & Schulze, 2003: 24 - 25; Kite, 1988: 201).

Regionalisation in flood frequency analysis entails the identification of homogeneous flood response regions and the selection of an appropriate probability distribution for the selected regions. It is important to note that geographical proximity does not imply hydrological homogeneity. Historical data are pooled in homogeneous regions to obtain improved estimates of the distribution parameters and quantile estimates (Kachroo *et al.*, 2000: 437 - 447).

Hosking and Wallis (1997) identified the following general approaches to regional frequency analysis (Smithers & Schulze, 2000a: 26 - 28):

- <u>Regional shape approach</u>: The mean and standard deviation are estimated from single site statistics and the skewness is based on a regional average of the shape parameters. This approach is preferred to the index-value approach when the distribution of flood events in a region is non-homogeneous; estimation is only focused on the quantiles in the extreme upper tail and/or the single site flow records are fairly long. The regional estimates of L-skewness are still more accurate than the single site estimate.
- <u>Index-value approach</u>: The mean is estimated from single site statistics, whilst the standard deviation and skewness are based on a regional average. The regionalised shape approach estimates the higher order moments more accurately.
- <u>Hierarchical regional approach</u>: The mean is estimated from single site statistics, the standard deviation is based on a sub-regional average and the skewness is based on a regional average representative of all the sub-regions. A disadvantage of this method is that estimated parameters and quantiles may change abruptly between adjacent regions.
- <u>Fractional membership approach</u>: The mean is estimated from single site statistics, whilst the standard deviation and skewness are based on a weighted average of regional estimates. This method does not allow any relaxation of the criteria for homogeneous regions, but does enable a smooth transition between regions.
- <u>Regional influence approach</u>: The mean is estimated from single site statistics, whilst the standard deviation and skewness are based on a

weighted average of regional estimates for stations in a site's region of influence. A disadvantage of the method is that appropriate site characteristics have to be chosen and weights have to be assigned to the characteristics.

- Mapping: The mean is estimated from single site statistics, whilst the standard deviation and skewness are estimated functions of site characteristics of which a map can be constructed and used to estimate the parameters at a particular site. This method is normally applicable when the parameters of a regional frequency analysis vary smoothly.

Numerous respected researchers (Alexander, 1990; 2001; Chow *et al*., 1988; Cunnane, 1989; Hosking & Wallis, 1997; Kite, 1988; Stedinger *et al*., 1993) concluded that in nearly all practical situations a regional approach is preferred to a single site approach, primarily based on the efficiency and accuracy of the flood quantile estimation.

2.4.1.7 Probability distributions

Statistical analyses of observed flow data, using various probability distributions, are based on the following fundamental assumptions (Alexander, 2001: 422):

- Each observation is independent of previous and subsequent observations.
- Observed data are free of measurement errors. These, especially introduced systematic errors, should be tested in all cases where major structures are involved.
- The data are identically distributed, originating from a single parent population, which in turn implies a single type of precipitation-producing meteorological phenomena. Hydrologists should be conscious of the possibility that many of the apparent anomalies in statistical analyses evolve from the mixture of different meteorological phenomena and different states of antecedent conditions that determine the magnitude of flood events.

The most common probability distributions which are used in flood frequency analyses will be discussed in the following paragraphs.

Normal distribution:

The normal distribution was first developed by de Moivre in 1753 (Alexander, 2001: 427). The distribution is widely used in hydrology to describe well-behaved phenomena such as average annual streamflow. This distribution is symmetrical about the mean and is therefore only suitable for data where the skewness coefficient is equal or close to zero. This distribution is applicable if variables are continuous and independent and probabilities are stable. Certain deficiencies (generation of negative flows) can occur when the minima of data sets are examined (Chow *et al*., 1988: 371; Kite, 1988: 45; Stedinger *et al*., 1993: 18.11). The PDF for a random variable (x) is shown in Equation 2.21*:*

$$F(x) = \frac{1}{\sqrt{2\pi s^2}} \exp\left[-\frac{1}{2}\left(\frac{x-\bar{x}}{s} \right)^2 \right] \qquad (2.21)$$

Where:

s = Standard deviation of observed values

x = Observed value

$\bar{x}$ = Mean of observed values

LN distribution:

The LN distribution is a normal distribution using the logarithms of the observed values. The $\log_{10}$-transformation of data tends to reduce positive skewness commonly found in hydrology, since the logarithms have a near symmetrical distribution (Yevjevich, 1982: 134). The PDF for a random variable (x) is shown in Equation 2.22*:*

$$F(x) = \frac{1}{x\sqrt{2\pi s_y^{\,2}}} \exp\left[-\frac{1}{2}\left(\frac{\log(x) - \overline{\log(x)}}{s_y} \right)^2 \right] \qquad (2.22)$$

Where:

N = Total number of observations

s_y = Standard deviation of the logarithms of the observed values

$$\left[\frac{\sum \left(\log(x) - \overline{\log(x)} \right)^2}{N-1} \right]^{0.5}$$

$\overline{\log(x)}$ = Logarithm of the mean of observed values

x = Observed value

Exponential distribution:

An exponential distribution is used to describe the inter-arrival times and magnitudes of the flood peaks exceeding the threshold value in a PDS based on a Poisson process, although this distribution is rarely used directly in hydrological analyses. Normally, the exponential distribution is incorporated in the more complex equations derived from it (Chow *et al*., 1988: 374). This is the simplest of the one-tailed distributions and the PDF is shown in Equation 2.23:

$$F(x) = \lambda e^{-\lambda x} \tag{2.23}$$

Where:

$\lambda = \frac{1}{\bar{x}}$

x = Observed value

$\bar{x}$ = Mean of observed values

Gamma distribution:

This is a strongly skewed distribution with a lower bound at zero and it represents the distribution of the sum of a number of independent exponentially distributed random variables.

The distribution involves the gamma function $\Gamma(\beta)$ based on a factorial series $(\beta - 1)!$ The PDF is shown in Equation 2.24 (Chow *et al*., 1988: 374):

$$F(x) = \frac{\lambda^{\beta} x^{\beta-1} e^{-\lambda x}}{\Gamma(\beta)} \tag{2.24}$$

Where:

$\beta = \frac{\bar{x}^2}{s^2}$

$\lambda = \frac{\bar{x}}{s^2}$

Γ = Gamma function

s = Standard deviation of observed values

x = Observed value

$\bar{x}$ = Mean of observed values

Pearson Type III distribution:

This is a three-parameter Gamma distribution, since a third parameter, the lower bound (mean displayed by a constant from the origin) is introduced. It includes the normal distribution as a special case when the skewness equals zero (Chow *et al*., 1988: 375). The PDF for a random variable (*x*) is shown in Equation 2.25*:*

$$F(x) = \frac{\lambda^{\beta}(x-\varepsilon)^{\beta-1}e^{-\lambda(x-\varepsilon)}}{\Gamma(\beta)} \qquad (2.25)$$

Where:

β = $\left(\frac{2}{g}\right)^2$

g = Skewness coefficient

Γ = Gamma function

λ = $\frac{s}{\sqrt{\beta}}$

ε = Lower bound, $\bar{x} - s\sqrt{\beta}$

s = Standard deviation of observed values

x = Observed value

$\bar{x}$ = Mean of observed values

LP3 distribution:

This is the form in which the Pearson Type III distribution is most commonly used in hydrological analyses and is the distribution of the logarithms of the observed values. It will fit most sets of hydrological data in South Africa and is the standard distribution for frequency analysis in the USA (Chow *et al*., 1988: 375). The PDF for a random variable (*x*) is shown in Equation 2.26*:*

$$F(x) = \frac{\lambda^{\beta}(\log(x)-\varepsilon)^{\beta-1}e^{-\lambda(\log(x)-\varepsilon)}}{x\Gamma(\beta)} \qquad (2.26)$$

Where:

β = $\left(\frac{2}{g(\log(x))}\right)^2$

g = Skewness coefficient

Γ = Gamma function

λ = $\frac{s_y}{\sqrt{\beta}}$

ε = Lower bound, $\overline{\log(x)} - s_y\sqrt{\beta}$

s_y = Standard deviation of the logarithms of the observed values

$\overline{\log(x)}$ = Logarithm of the mean of observed values

x = Observed value

<u>Extreme Value (EV) distributions</u>:

EV distributions are used in cases where the tail of the distribution of hydrological events decays exponentially within the year. The most commonly used EV distributions are (Alexander, 2001: 429, 445):

- *Extreme Value Type 1 (EV1)*: This distribution is also known as the Gumbel distribution and has a constant positive skewness coefficient (g) of 1.13955 or the shape parameter (k) equals zero. The use thereof must be restricted to data with skewness coefficients close to this value. The PDF for a random variable (*x*) is shown in Equation 2.27 (Chow *et al*., 1988: 376)*:*

$$F(x) = \frac{1}{\alpha}\exp\left[-\frac{x-\mu}{\alpha} - \exp\left(-\frac{x-\mu}{\alpha}\right)\right] \quad (2.27)$$

Where:

α = $\frac{\sqrt{6}s}{\pi}$ (scale parameter)

s = Standard deviation of observed values

μ = $\bar{x} - 0.5772\alpha$ (location parameter)

x = Observed value

$\bar{x}$ = Mean of observed values

- *Extreme Value Type 2 (EV2)*: This positively skewed distribution ($g > 1.13955$ and $k < 0$) is also known as the Fréchet distribution. Natural data characterised by an EV2 distribution will have $\log_{10}$-transformed data which are EV1 distributed.
- *Extreme Value Type 3 (EV3):* This negatively skewed distribution is also known as the Weibull distribution. The shape parameter (k) is larger than zero.

GEV distributions:

This is the generalised form of the EV distributions. It is a family of three sub-types of distributions which are classified according to the value of the skewness coefficient (g) or shape parameter (k). This is a flexible distribution and is the distribution recommended for use in the UK (Alexander, 2001: 429). The PDF for a random variable (*x*) is shown in Equation 2.28 (Chow *et al*., 1988: 376)*:*

$$F(x) = \exp\left[-\left(1-k\frac{x-\mu}{\alpha}\right)^{\frac{1}{k}}\right] \qquad (2.28)$$

Where:

α	= Positive scale parameter
k	= Shape parameter
μ	= Location parameter
x	= Observed value

Wakeby distribution:

This distribution is one of the more recently introduced distributions developed by Thomas in 1978 for flood frequency analyses. The distribution has five parameters and is based on PWM estimation, which makes it flexible, but despite this flexibility, there are many hydrological data sets in South Africa that this distribution cannot fit. The PDF for a random variable (*x*) in its inverse form is shown in Equation 2.29 (Alexander, 2001: 430, 452):

$$F(x) = m + a\left(1-(1-x)^{b}\right) - c\left(1-(1-x)^{-d}\right) \qquad (2.29)$$

Where:

a, b, c & d	= Distribution parameters
m	= Location parameter
x	= Observed value

Generalised logistic (GLO) distribution:

According to the Flood Estimation Handbook (FEH), the GLO distribution is recommended as the standard method for flood frequency analysis in the UK and a variant of the Method of Linear Moments (MLM) are used for the parameter estimation. The PDF for a random variable (*x*) is shown in Equation 2.30 (Kjeldsen & Jones, 2004: 183 - 184):

$$F(x) = \frac{e^{-\frac{x-\mu}{\alpha}}}{\alpha\left(1+e^{-\frac{x-\mu}{\alpha}}\right)^2} \qquad (2.30)$$

Where:

α = Scale parameter

μ = Location parameter

x = Observed value

Two generalisations of the logistic distribution are available, the skew logistic and proportional reversed hazard logistic (PRHL) distribution. These generalisations have location, scale and skewness parameters, can either be positively or negatively skewed, and with a PDF which is uni-modal and log-concave in nature. The distribution function, hazard function and different moments of the skew logistic distribution cannot be obtained in explicit forms and are therefore difficult to use in practice, whilst the PRHL distribution has distribution and hazard functions with explicit forms and the moments can be expressed in terms of digamma and polygamma functions (Gupta & Kundu, 2007: 3 537 - 3 547).

According to Van der Spuy and Rademeyer (2008), the LN, LP3 and GEV distributions are the most suitable probability distributions for flood frequency analyses in South Africa. As mentioned previously, in the USA the LP3 distribution is accepted as being the most general and most objective of their top three distributions, hence the recommendation for general use. The UK FSR (NERC, 1975) gives preference to the GEV distribution, whilst the Institute of Hydrology (IH) recommends the use of the GLO distribution based on LM estimators in the UK. Van der Spuy and Rademeyer (2008) indicated that numerous flood frequency studies at DWA confirmed that these distributions are or can be applicable to South African conditions. Although, they emphasised that, similar to all other methods, probability distributions have limitations and should never be applied without applying one's mind to the problem.

All the above-mentioned distributions based on MM estimation (except the Gamma distribution) and the GLO distributions based on LM/PWM estimation are included in the DFET and were evaluated during this study.

2.4.1.8 Parameter estimation methods

The fitting of a probability distribution to a data set provides a compact and smoothed representation of the frequency distribution revealed by the limited data available and enables the systematic extrapolation to frequencies beyond the data set range. The parameter estimation methods available for fitting probability distributions are as follows (Chow *et al*., 1988: 363 - 365; Kite, 1988: 28 - 33; Stedinger *et al*., 1993: 18.7 - 10; Yevjevich, 1982: 172 - 177):

- Method of Moments (MM): This method was developed by Pearson in 1902, who argued that good parameter estimates of a probability distribution have PDF moments about the origin which are equal to the corresponding moments of the observed data. These moments are functions of the mean and the dispersion about the mean value to the second and third order moments. The second moment is known as the standard deviation and is used as a measure of variability. The third moment is known as the skewness coefficient, which is indicative of the skewness of data. This method is easy to apply, simple to use and limited to only three parameters (mean, standard deviation and skewness). The higher the moment order, the greater the sensitivity to both high and low values in a data set being analysed. Hydrological variables are normally more or less asymmetrical, thus estimations using MM will always represent a small or large loss of efficiency in estimation.

- Method of Maximum Likelihood (MML): This method was developed by Fischer in 1922, who reasoned that the best parameter value of a probability distribution maximises the likelihood or joint probability of occurrence of the observed data. Estimates by the MML are asymptotically unbiased and are based on the mean, standard deviation and skewness of the observed data. This method is the most theoretically correct method of fitting probability distributions, having the least average error in large samples.

In some probability distributions, analytical solutions are not always possible and the estimation must then be based on a numerically maximised log-likelihood function.

- Method of Linear Moments (MLM): LM estimators are similar to ordinary product moments, but LM and PWM can additionally be used to summarise theoretical probability distributions and observed samples, thus resulting in parameter estimation, interval estimation and hypothesis testing. In order to estimate the variance and skewness of a sample, LM, which are linear combinations of ranked observations, do not require squaring and cubing of the observations as in the case of ordinary product moments and are therefore less biased. LM estimators are easy to apply, almost as efficient as MML, but more reasonable and reliable as MM, especially in small samples and lend itself to regional analysis.

- Method of Least-squares (MLS): This method consists of fitting a theoretical function to an empirical distribution. The sum of squares of all deviations of observed points from the fitted function is minimised. In other words, the sum of squared residuals has its least value where a residual is the difference between an observed value and an estimated value. The MLS is only efficient when the deviations are normally or at least symmetrically distributed, the population variance of the deviations must be independent of the magnitude of the observed values and the population variance along the least-squares line must be constant.

Since the MLS, expressed in terms of the coefficient of determination (r^2), and the Chi-square statistic will be extensively used during this study, a simple example illustrating the concepts related to the MLS is contained in Table 2.5 and shown by the scatter plot in Figure 2.5.

An example illustrating the Chi-square statistic and associated contingency tables is included in Section 2.4.1.10.

Table 2.5: Example: Method of Least-squares

A	B	C	D	E	F	G
1	1.5	2.0	1.506	4.901	0.244	2.958
2	4.8	5.8	5.053	1.776	0.559	4.326
3	2.7	2.4	2.796	0.854	0.157	1.742
4	1.0	1.2	0.969	7.569	0.053	6.350
5	8.1	8.6	8.599	23.807	0.000	23.814
6	3.8	3.6	3.978	0.067	0.143	0.014
7	3.2	2.7	3.333	0.150	0.401	1.040
8	4.7	5.5	4.945	1.501	0.308	3.168
9	3.8	3.2	3.978	0.067	0.605	0.270
10	2.0	2.2	2.043	2.811	0.025	2.310
			Total	**43.502**	**2.494**	**45.996**

Where:

[A] Row identifier or number

[B] Observed value (x_i,)

[C] Estimated value (y_i)

[D] Predicted value from the least-squares line of y on x ($\overline{\overline{y}}_i = b\, x_i + a$)

[E] Total variability in the estimated values accounted for by the linear relationship between x and y $\left(\overline{\overline{yi}} - \overline{y}\right)^2$

[F] Dispersion of the estimated values about the least-squares line $\left(y_i - \overline{\overline{y}}_i\right)^2$

[G] Dispersion of the estimated values about their mean $\left(y_i - \overline{y}_i\right)^2$

a Base constant (y-intercept)

b Slope

The sum total of columns $E_{1\text{ - }10}$, $F_{1\text{ - }10}$ and $G_{1\text{ - }10}$ is representative of the explained sum of squares (*SSR*), unexplained sum of squares (*SSE*) and the total sum of squares (*SST*) respectively. The objective function is to maximise the ratio of *SSR:SST* to unity (1) by minimising the difference between the observed and estimated values. This ratio is also representative of the coefficient of determination (r^2), which equals 0.946. The r^2-value based on Equation 2.40 is shown in Figure 2.5 and confirms the applicability of the *SSR:SST*-ratio test.

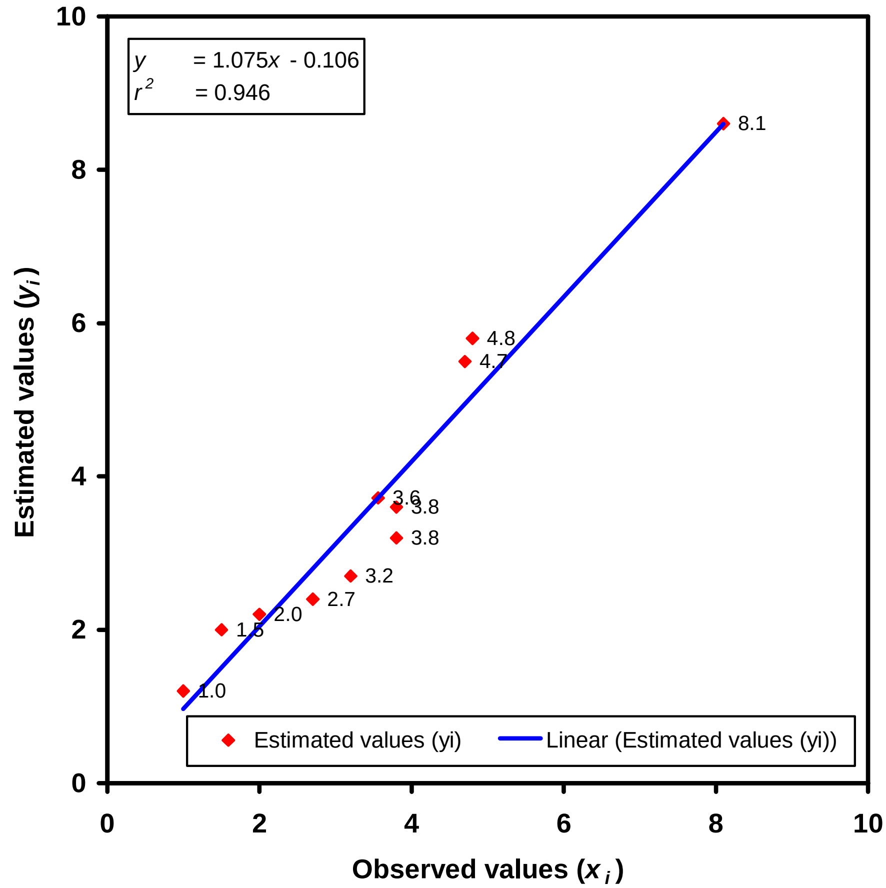

Figure 2.5: Scatter plot: Method of Least-squares

- <u>Graphical method:</u> This method consists of fitting a function visually through a set of coordinate pairs on a graph. In order to estimate the *x*-number of parameters, *x*-number of points must be selected on the curve, resulting in *x*-number equations to solve. The general objective in graphical estimation is to reduce the CDF to a linear relationship by adjusting the horizontal scale of the graph. The horizontal scale can be linearised by expressing the exceedance probabilities or corresponding return periods in units of standard deviations. The most useful graphical representations have linear horizontal scales (units of standard deviations), but calibrated in exceedance or non-exceedance probabilities. The Normal and EV1 distributions are commonly used to determine these probabilities. The vertical scale is normally a logarithmic scale.

- Bayesian Inference (BI): This method combines prior information and regional hydrological information with the likelihood function for available data and allows explicit modelling of uncertainty in parameters.

- Non-parametric methods: These methods estimate frequency relationships, based on the assumption that flood events are not drawn from a particular family of distributions. These methods are robust, but less efficient than parametric methods and are rarely used in practice.

In ascending order of efficiency, the above-mentioned parameter estimation methods, except the BI and non-parametric methods, may be listed as graphical, MLS, MM, MLM and MML. To offset its greater efficiency, however, the MML is more difficult to apply than the MLM. All these methods will, within limits, estimate the parameters of a distribution from a particular data sample. As mentioned previously, the sample may or may not be typical of the underlying population and use of the sample estimates of parameters may distort the results (Kite, 1988: 32).

2.4.1.9 Plotting positions

In order to evaluate the fitting of a probability distribution to hydrological data, the observed data must be ranked in a descending order of magnitude; the plotting position must be determined and then accordingly plotted on probability paper or on a plotting scale which linearises the PDF. The plotted data are then fitted with a straight line for interpolation and extrapolation purposes. Plotting position refers to the probability value or return period assigned to each data point to be plotted (Chow *et al*., 1988: 395 - 396).

Numerous methods, mostly empirical, have been proposed for the determination of plotting positions. The fact that the return period varies with record length is approached in practice by defining a plotting position for the frequency of occurrence. The plotting position is generally based on the assumed position of the sample estimate of the frequency within a population distribution of frequencies (Chow *et al*., 1988: 395 - 396).

The Weibull formula is commonly used to determine plotting positions. It is based on the assumption that if (*n)*-values are distributed uniformly between 0% and 100% probability, then there must be (*n + 1)* intervals, (*n - 1*) intervals between the data points and two (2) intervals at the ends. The Weibull formula is shown in Equation 2.31 (Chow *et al*., 1988: 396, SANRAL, 2006: 3A.6)*:*

$$T = \frac{n+a}{m-b} \qquad (2.31)$$

Where:

- a = Constant (Table 2.6)
- b = Constant (Table 2.6)
- m = Number, in descending order, of the ranked events (peak flows)
- n = Number of observations/record length (years)
- T = Return period (years)

Cunnane (1978) studied the various available plotting position methods using unbiasedness criteria and minimum variance criteria. An unbiased plotting method for equally sized samples is defined as the average of the plotted points for each value of *m* falling on the theoretical distribution line. A minimum variance plotting method minimises the variance of the plotted points about the theoretical line. It was established that Equation 2.31 is biased and plots the largest values of a sample at too small return periods. The findings of this study, based on above-mentioned criteria, indicated that different plotting position methods are applicable to different probability distributions (Chow *et al*., 1988: 396). The results are listed in Table 2.6.

Table 2.6: Common plotting position methods (SANRAL, 2006: 3A.6)

Method		Plotting position	Probability distribution
Beard	(1962)	a = 0.40 and b = 0.30	Pearson 3
Blom	(1958)	a = 0.25 and b = 0.375	Normal
Cunnane	(1978)	a = 0.20 and b = 0.40	General purpose
Greenwood	(1979)	a = 0.00 and b = 0.35	GEV, Wakeby
Gringorten	(1963)	a = 0.12 and b = 0.44	EV1, GEV and Exponential
Weibull	(1939)	a = 1.00 and b = 0.00	Normal and Pearson 3

2.4.1.10 Goodness-of-Fit statistics

The visual comparison of theoretical probability distribution results against observed data, based on an assumed plotting position, can be subjective. Statistical model performance measures are therefore used to evaluate a theoretical probability distribution's performance against certain predetermined statistical criteria of GOF in the reproduction of observed data (Schulze, 1995: 21.1). According to Roberts (1987), these GOF criteria are objective mathematical functions, which express the most desirable characteristics between a model's estimated output and the observed data. Willmott (1982) and Schulze (1995) indicated that the range of GOF statistics applicable to hydrological analyses falls into three major categories, namely conservation, regression and descriptive statistics.

In flood frequency analyses, GOF criteria provide insight as to whether the lack of fit is due to sample variability, or whether the distribution model and data are significantly different. Generally, GOF tests will identify more than one distribution which is statistically acceptable and are more valuable in identifying which distributions appear to be inconsistent with the data. GOF tests can be categorised as descriptive or predictive statistical tests. Descriptive statistical tests seek the best fitting distribution from theoretical distributions based on visual inspections, Chi-squared tests, skewness and moment-diagrams, numerical indices of agreement based on probability plots, regional pooling of data and behaviour analysis. Predictive statistical tests evaluate how well candidate distributions can estimate quantiles when the population distribution is not identical (Smithers & Schulze, 2000a: 21, 78; Stedinger *et al.*, 1993: 18.27).

In the listed equations used for conservation, regression and/or descriptive statistics, the following symbols are applicable:

a = Base constant (y-intercept)
b = Slope
c_v = Coefficient of variation
E_c = Coefficient of efficiency
g = Skewness coefficient

k = Kurtosis coefficient

N = Total number of observations (sample size)

s = Standard deviation of observed values

x = Observed values

$\bar{x}$ = Mean of observed values

y = Estimated values

$\bar{y}$ = Mean of estimated values

$\bar{\bar{y}}$ = Predicted value from the least-squares line of y on x

Conservation statistics:

The following statistical parameters are of concern (Schulze, 1995: 21.8 - 11):

Arithmetic mean: This is a measure of central tendency of the data and is determined by adding all the values and dividing the sum by the total number of observations.

$$\bar{x} = \frac{\sum x}{N} \qquad (2.32)$$

Mode: The value that appears the largest number of times in a data set.

Median: The value of a random variable at which values above and below it are equally possible, thus the value of random variability at which the cumulative frequency is 0.5.

Standard deviation: The standard deviation gives an indication of the spread of values about the mean. The smaller the standard deviations, the more densely most of the values are spaced about the mean.

$$s = \left[\frac{\sum\left(x - \bar{x}\right)^2}{N - 1}\right]^{0.5} \qquad (2.33)$$

Coefficient of variation: A non-dimensional measure of the relative dispersion that is independent of the unit of measure.

$$c_v = \frac{s}{\overline{x}} \qquad (2.34)$$

Skewness coefficient: This coefficient is a measure of asymmetry of data about the arithmetic mean. A skewness of zero is associated with data that are distributed symmetrically. A positive value indicates that the upper tail of the distribution curve is longer than the lower tail and vice versa for a negative value.

$$g = \left(\frac{N}{(N-1)(N-2)}\right)\left(\frac{\sum\left(x-\overline{x}\right)^3}{s^3}\right) \qquad (2.35)$$

Kurtosis coefficient: This coefficient is a non-dimensional quantity which measures the peakedness or flatness of a distribution. It is normally not used in single site analysis, since the sample size (number of observations) is too small for reliable estimates, but can be useful in regional analysis.

$$k = \frac{N(N+1)\sum\left(x-\overline{x}\right)^4}{s^4(N-1)(N-2)(N-3)} - \frac{3(N-1)^2}{(N-2)(N-3)} \qquad (2.36)$$

Root-Mean-Square-Error (RMSE): This statistic defines the actual size of error produced by a model. It does not indicate the source and type of error. The objective is to minimise the *RMSE* to zero.

$$RMSE = \sqrt{\frac{\sum(x-y)^2}{N}} \qquad (2.37)$$

<u>Regression statistics:</u>

A linear regression model is based on two variables, the independent (observed, *x*) and dependent (estimated, *y*) variables. Linear regression by using the MLS technique can be used to determine if values estimated by a probability distribution are comparable with the observed values. The following statistical parameters are of concern (Schulze, 1995: 21.12 - 16):

Slope: It is the slope (*b*) of the least-squares regression line. This line denotes the relative change of estimated to observed trends. The objective is to attain a slope as closely as possible to unity (1). Slope values greater than unity (>1) indicate overestimation at the upper end of the estimated values. Slope values less than unity (<1) indicate underestimation.

$$b = \frac{\sum xy - \sum x \sum y}{N\sum x^2 - \left(\sum x\right)^2} \qquad (2.38)$$

Base constant (y-intercept): This is the point where the line crosses the *y*-axis. A positive *y*-intercept indicates overestimation of low values, while a negative *y*-intercept indicates underestimation of low values. The objective is to minimise the base constant (*y*-intercept) to zero.

$$a = \frac{\sum y - b\sum x}{N} \qquad (2.39)$$

Coefficient of determination: It measures the degree of association between the estimated values (*y*) and the predicted values $\left(\bar{\bar{y}}\right)$ as predicted by the MLS model. The objective is to maximise the coefficient of determination to unity (1). High r^2-values indicate a good degree of association.

$$r^2 = \frac{\sum\left(y-\bar{y}\right)^2 - \sum\left(y-\bar{\bar{y}}\right)^2}{\sum\left(y-\bar{y}\right)^2} \qquad (2.40)$$

Coefficient of efficiency: This coefficient measures the degree of association between observed and estimated values. It can be used to quantify or indicate model bias by determining the difference between the coefficients of determination and efficiency. It is identical to the coefficient of determination, except that the predicted estimated values replace the observed values. The objective is to maximise the coefficient of efficiency to the value of the coefficient of determination.

$$E_c = \frac{\sum\left(y-\bar{y}\right)^2 - \sum\left(y-x\right)^2}{\sum\left(y-\bar{y}\right)^2} \qquad (2.41)$$

Descriptive statistics:

Chi-square test: This independence test is used to establish how well a hypothesised probability distribution fits and reflects an observed data set. This test evaluates the *null hypothesis (H_0),* which assumes that the observed sample is drawn from the hypothesised distribution. Hypothesis tests provide a theoretical convention for measuring the strength of statistical evidence and do not provide proof of the characteristics of a sample population (Chow *et al*., 1988: 367; Hirsch *et al*., 1993: 17.11 - 14).

If the computed Chi-square statistic is a low value, then the observed data and estimated values are close and the distribution is a good fit to the data with an indication of independence. This test can thus be used to determine whether two or more nominal variables are related or not. The random variable χ^2 whose sampling distribution is approximated by a Chi-square distribution is shown in Equation 2.42 (Chow *et al*., 1988: 367):

$$\chi^2 = \sum_{i=1}^{m} \frac{(x_i - y_i)^2}{y_i} \qquad (2.42)$$

Where:

χ^2 = Chi-square statistic

m = Number of intervals

x_i = Observed data

y_i = Expected estimated value

In order to describe the Chi-square test, the χ^2 probability distribution must be defined. A random variable $\chi_v{}^2$ has a Chi-square distribution with *v degrees of freedom* if it is the sum of the squares of *v* independent standard normal random variables *(z_i)*. However, the square of a single standard normal random variable has a Chi-square distribution with 1 degree of freedom (Chow *et al*., 1988: 368).

$$\chi_v{}^2 = \sum_{i=1}^{v} z_i{}^2 \qquad (2.43)$$

The *degree of freedom* *(v)* is a function of the number of intervals *(m)* and parameters *(p)* used to fit a proposed distribution and is shown in Equation 2.44*:*

$$v = m - p - 1 \qquad (2.44)$$

Various criteria can be used to determine the sample size *(N)* and number of intervals *(m).* The sample size should be large enough that no expected frequency is less than unity, whilst not more than 20% of the expected frequencies is less than five (Milton & Arnold, 1986: 525).

The number of intervals chosen should have equal probabilities under the hypothesised distribution. D'Agostino and Stephens (1986) established that the number of equal probable intervals can be determined by making use of Equation 2.45*:*

$$m = 1.88N^{0.4} \qquad (2.45)$$

A confidence level, expressed as $1-\alpha$ (α = significance level) is chosen for the test. Normally a confidence level of 95% is used. A good fit leads to the acceptance of the *null hypothesis*, whereas a poor fit leads to its rejection. In other words, the hypothesis is rejected if χ^2 in (Equation 2.42) is larger than the limiting critical value ($\chi^2_{v,1-\alpha}$). This critical value is determined from the $\chi_v^{\ 2}$ distribution with *v* degrees of freedom, since the critical value has a cumulative probability of $1-\alpha$ (Chow *et al*., 1988: 368).

The often used critical values for Chi-square distributions are listed in Table 2.7, whilst Equation 2.46 provides an approximation of the critical value.

Table 2.7: Critical Chi-squared distribution values (Hirsch *et al*., 1993: 17.17)

Degrees of freedom (*v*)	**Confidence levels ($1-\alpha$)**				
	0.9	**0.95**	**0.975**	**0.99**	**0.995**
1	2.71	3.84	5.02	6.64	7.88
2	4.60	5.99	7.38	9.21	10.60
3	6.35	7.82	9.35	11.34	12.84
4	7.78	9.49	11.14	13.28	14.86
5	9.24	11.07	12.83	15.09	16.75
7	12.02	14.07	16.01	18.48	20.28
10	15.99	18.31	20.48	23.21	25.19
15	22.31	25.00	27.49	30.58	32.80
20	28.41	31.41	34.13	37.57	40.00
30	40.26	43.77	46.98	50.89	53.67

$$\chi^2_{v,1-\alpha} = 0.5\left((1-\alpha) + \sqrt{2v-1}\right)^2 \qquad (2.46)$$

The confidence level of a statistical hypothesis test is the probability of obtaining a value of the Chi-square statistic that is equal to or greater in magnitude than the observed test statistic, if the *null hypothesis* is true. Thus, the *null hypothesis* is rejected if the confidence level is smaller or equal to the significance level. Small confidence level values suggest that the *null hypothesis* is unlikely to be true. A confidence level value close to zero indicate that the *null hypothesis* must be rejected and typically that a difference is likely to exist. Large confidence level values closer to 1 imply that there is no detectable difference for the sample size used (Chow et al., 1988: 368, 371; Kite, 1988: 184; Yevjevich, 1982: 224 - 226).

The degree of association between a hypothesised probability distribution and an observed data set can be measured by using the contingency coefficient (*C*) shown in Equation 2.47:

$$C = \sqrt{\frac{\chi^2}{(N+\chi^2)}} \qquad (2.47)$$

Where:

C = Contingency coefficient

N = Total number of observations (sample size)

χ^2 = Chi-square statistic

The objective is to maximise the contingency coefficient (C) to the value of the theoretical maximum contingency coefficient (C_{Max}) as shown in Equation 2.48a or 2.48b. Equation 2.48a is used when the data set is divided into a number of equal probable intervals, whilst Equation 2.48b is used when the sample size is used as the number of equal probable intervals. Small differences between C and C_{Max} are indicative of a good degree of association.

$$C_{Max} = \sqrt{\frac{m-1}{m}} \qquad (2.48a)$$

or

$$C_{Max} = \sqrt{\frac{N-1}{N}} \qquad (2.48b)$$

In Section 2.4.1.8 the MLS technique was illustrated and the extensive use thereof along with the Chi-square statistic in this study was emphasised. A simple example illustrating the use of Equations 2.42 and 2.46 based on the concept of contingency tables is included in Table 2.8, after which a short explanation follows. A confidence level of 95% was used in this example.

Table 2.8: Example: Chi-square statistics

A	B	C	D	E	F
1	158	172.467	330.467	163.362	0.176
2	162.177	182.552	344.729	170.412	0.398
3	187.838	192.812	380.649	188.169	0.001
4	208	203.265	411.265	203.304	0.108
5	210	213.931	423.931	209.565	0.001
6	217	224.830	441.830	218.413	0.009
7	230	235.981	465.981	230.352	0.001
8	240.186	247.407	487.593	241.035	0.003
9	260	259.132	519.132	256.626	0.044
10	281	271.180	552.180	272.963	0.237
11	**2 154.201**	**2 203.555**	**4 357.756**	**2 154.201**	**0.978**

Where:

[A] Row identifier or number

[B] Observed data (x_i)

[C] Predicted value from the fitting of a probability distribution to observed hydrological data

[D] Row totals, $[B_i] + [C_i]$

[E] Expected estimated value (y_i), $\frac{[D_i * B11]}{[D11]}$

[F] Chi-square statistic, $\frac{([B]-[E])^2}{[E]}$ (Equation 2.42)

Table 2.8 consists of margin totals, which are used to establish the expected estimated values. The margin totals comprise of row (1 - 11) and column variables (B and C) which are representative of the observed data (column B) and probability distribution values (column C). Thus, for each probability of exceedance or return period, the sum of the observed data (B_i) and probability distribution value (C_i) provides the row totals (D_i). The sum of all the different individual column variables (observed data, probability distribution value and row total) provides the column totals (B11, C11 and D11). The expected estimated values (column E) are calculated as the ratio of the product of row and column totals (D_i * B11) to the grand total, where the grand total either equals the sum of the row or column totals (D11). Take note that the sum of the observed data (B11) must always be equal to the sum of the expected estimated values (E11).

The degrees of freedom equal a value of nine (9), since the number of rows (B1 to B10 and C1 to C10) and columns (B and C) are larger than one (1).Thus, the (rows - 1)(columns - 1) is equal to the degrees of freedom. Equation 2.46 resulted in a limiting critical value of 12.87 for the Chi-square distribution. If this value is compared with the limiting critical value contained in Table 2.7, it is evident that the validity of Equation 2.46 is questionable, since it must be 16.90 (interpolation between 14.07 (v= 7) and 18.31 (v = 10)).

Based on the results, it was decided to evaluate the validity of Equation 2.46 in Chapter 5. However, the Chi-square statistic (F11 = 0.978) is smaller than the limiting critical value and therefore the *null hypothesis* can be accepted and the confidence level value of 0.99 implies that there is no detectable difference for the sample size used.

2.4.2 Deterministic methods

2.4.2.1 Conceptual framework of deterministic methods

Deterministic methods endeavour to estimate the expected result (run-off) from causative factors (precipitation), based on the assumption that the frequency of the estimated run-off and the input precipitation is equal, while being influenced by catchment representative inputs and model parameters. In simplistic terms, the *T*-year recurrence interval precipitation will produce the *T*-year flood, if the catchment is at average condition. Thus, the task concerns transforming excess precipitation for the *T*-year design storm into *T*-year flood run-off. This assumption considers the probabilistic nature of precipitation, but the probabilistic behaviour of other inputs and parameters is ignored (Alexander, 2001: 401; Görgens, 1997).

According to the rules of joint probability (mean equals median), this concept is somewhat anomalous. Thus, ignoring the direct implications of joint probability, deterministic methods assume that the catchment would definitely (100% probability) be at its average state when it produces the design flood. Taking into consideration the vast complexity and spatial and temporal variability of catchment processes and their driving forces, it is not surprising that only relatively simple deterministic methods representing the real world processes are recognised and used in design flood practice. The typical sequence of operations associated to a lesser or greater extent with all deterministic methods are as follows (Görgens, 1997):

- Determine the critical storm duration or time of concentration.
- Estimate the point precipitation depth.
- Convert point to areal precipitation and distribute it over duration.
- Determine critical catchment characteristics based on average conditions.
- Apply storm loss-related coefficients to areal precipitation.
- Convert excess areal storm precipitation to flood peak/volume/hydrograph.

The deterministic methods generally used in South Africa are discussed shortly in Sections 2.4.2.2 - 2.5, whilst the SDF method is discussed in detail in Section 2.5. The calculation procedures associated with each method are included in Addendum D (DFET User manual).

2.4.2.2 Rational and alternative Rational methods

The RM was developed in Ireland by Mulvaney in 1855 and it is still the most commonly used method in the world, whilst the alternative Rational method (ARM) is an adaption of the RM. These methods estimate the *T*-year flood peak based on *T*-year average precipitation intensity for durations equal to the critical storm duration or time of concentration. Storm losses are represented by a run-off coefficient expressed as a function of MAP, slope, permeability, land use, vegetation and urbanisation within a catchment. Return period adjustment factors are used to decrease the run-off coefficient for events with return periods less than 50 years (Alexander, 2001: 406 - 407; SANRAL, 2006: 3.4).

Precipitation depth is an important input parameter. The precipitation depth used in the RM is based on the DDF relationship proposed by Midgley and Pitman (1978) (see Section 2.3.4.1 above). The ARM uses the recalibrated, modified Hershfield equation (Equation 2.16) as proposed by Alexander (2001) (see Section 2.3.4.3 above) for storm durations up to six hours and the TR102 values (Adamson, 1981) for durations one to seven days. It is generally recommended that these methods should only be applied to catchments smaller than 15 km²; however, experienced users applied these methods successfully in larger catchments. These methods can only estimate the flood peaks and empirical hydrographs. The following assumptions are relevant when applying these methods (SANRAL, 2006: 3.14):

- Precipitation has a uniform area and time distribution.
- Peak run-off occurs at the end of the critical storm duration.
- Run-off coefficients remain constant throughout the duration of the storm.
- The frequency of the peak run-off and precipitation intensity is the same.

Pilgrim and Cordery (1993: 9.17 - 18) identified the following weaknesses associated with these two methods:

- The level of judgement required to determine the most realistic run-off coefficient is largely subjective.
- The variability of the coefficients between different hydrological regimes in the same catchment is not accommodated.

- The estimation of catchment response time is subjected to regional differences in the time of concentration and cannot be based only on measured catchment characteristics.
- The assumption of uniform precipitation intensity and the exclusion of temporary storage limit the use in urban and small rural catchments.

Hence, the use of a probabilistic as opposed to a deterministic approach to determine the run-off coefficients is recommended in the literature (Alexander, 2001: 408; Parak & Pegram, 2006: 163; Pilgrim & Cordery, 1993: 9.18 - 20). In Australia, the probabilistic approach of the RM in catchments up to 250 km² resulted in more acceptable results without any variation in the probabilistic run-off coefficients with catchment characteristics (Pilgrim & Cordery, 1993: 9.18).

2.4.2.3 Soil Conservation Services method

The Soil Conservation Services (SCS) method has been widely used internationally for the estimation of the flood peak, volume and hydrograph shapes (empirical hydrographs) for rural and suburban catchments smaller than 10 km² and slopes less than 30%. This method takes into account most factors that affect run-off, including the quantity, time distribution of precipitation, storm duration, land use, soil types, antecedent soil moisture conditions and the catchment size and characteristics. It estimates the *T*-year flood hydrograph based on the *T*-year 24-hour precipitation, using a typical unit volume run-off hydrograph of triangular shape, with storm losses as a function of a Curve Number (CN). The CN is based on the land use, vegetation and taxonomic and/or binomial classification of soils within a catchment (Rooseboom *et al.*, 1993: 2.35; Schulze *et al.*, 1992: 4 - 10).

The method was systematically adapted for Southern African use from the late 1970's up to 1992 by Schulze *et al*. (1992). It was established that the adapted SCS method estimates of flood peaks in five catchments of the southern Cape region, with average areas of about 80 km^2, compare favourably with probabilistic estimates. The SCS method is not as sensitive as the RM to user inputs and is recommended for design flood estimation on a considerable range of land use and catchment size categories.

However, the procedures used to estimate the time of concentration, lag-time and the most representative CN are largely subjective and can result in inconsistencies (Schulze *et al*., 1992).

According to Pilgrim and Cordery (1993), the SCS method performed poorly in the USA and Australia. This poor performance could be ascribed to the influence of assumed antecedent moisture conditions and the variation in vegetation densities on the results. In addition, there was little agreement between the conventional and probabilistic derived curve numbers, since the results were influenced both by the method used to estimate the lag-time and return period. In conclusion, to confirm the accuracy and validity of the SCS method, it must be compared with the results obtained from direct statistical analysis in the region in which it is applied.

2.4.2.4 Synthetic unit hydrograph method

The Synthetic unit hydrograph (SUH) method is used to estimate the *T*-year flood hydrograph based on the *T*-year precipitation for the critical storm duration, using a typical unit volume storm run-off hydrograph with storm losses based on regional trends in catchments between 15 and 5 000 km^2. The SUH method provides reliable results, but some natural variability in the hydrological occurrences is lost through the broad regional divisions and the averaged form of the hydrographs (HRU, 1972: 2.6 - 10; SANRAL, 2006: 3.4).

The HRU (1972) derived unit hydrographs from observed data at 96 hydrological gauging stations in South Africa. These derived unit hydrographs and analyses were updated by Bauer and Midgley (1974). The observed data from only 92 hydrological gauging stations with catchment areas ranging from 21 to 22 163 km^2 were used in this analysis. Nine veld-type regions with similar catchment and precipitation characteristics were identified in South Africa and dimensionless synthetic unit hydrographs were derived for each region. The number of catchments represented in each region ranged from five to 18. A co-axial diagram to estimate the average storm losses in the nine veld-type regions was also developed (Alexander, 2001; HRU, 1972).

In the SUH method, precipitation of a specific intensity and duration is applied on the dimensionless one hour unit hydrograph of an identified region, resulting in the derivation of a series of different hydrographs for various precipitation storm durations. The peak run-off and volume can then be derived from this series of hydrographs (Alexander, 2001; HRU, 1972).

Cullis *et al.* (2007) reviewed the SUH method by comparing the unit hydrograph-based design flood estimates with the direct statistical analyses using the LP3 and GEV/PWM distributions at 40 gauged catchments for return periods ranging from two to 100 years. The catchments were grouped according to the nine veld-type regions and co-axial diagram groups A (Veld-type region 2), B (Veld-type regions 4, 5, 6 and 7) and C (Veld-type regions 1, 3, 8 and 9) as proposed by the HRU (1972). In general it was found that the SUH method produced higher design flood peak estimates than the direct statistical analysis for veld-type region groups B and C, whilst group A compared well.

2.4.2.5 Lag-routed hydrograph method

Bauer and Midgley (1974) developed a simple-to-apply method of design flood estimation in South Africa, known as the Lag-routed or Direct run-off hydrograph method which is based on the results of the SUH method. The Lag-routed hydrograph (LRH) method is used to estimate the *T*-year flood hydrograph based on the *T*-year precipitation for the critical storm duration. Inherently, the method is based on the assumption that direct run-off from a catchment can be conveniently simulated by Muskingum routing if the inflow is assumed as excess precipitation and that outflow is run-off with the catchment storage represented by one or more reservoir-type storages. Thus, the run-off is subjected to a time lag and due to the temporary storage in the system, the run-off is released at a rate less than the precipitation input. Precipitation distribution over time is the driving mechanism of this method. The precipitation distribution is expressed as the effective precipitation divided into time segments, and each segment is sequentially routed through the system. The shape of the hydrograph is determined by the precipitation distribution over time and the time of concentration. This method can be used in catchment areas up to 10 000 km², provided the catchment shape is not too unusual (Alexander, 2001: 416 - 418).

Bauer and Midgley (1974) established that the Muskingum storage constant (K) is primarily dependent on the catchment area and vegetation cover, but relatively independent of the catchment shape. In addition, the storage constant (K) and weighing constant (x) used in this routing technique were determined by analysing the standard unit hydrographs developed by Pullen (1969, as cited in Alexander, 2001: 417). These K-values were then regionalised based on the nine veld-type regions used in the SUH method. According to Van der Spuy and Rademeyer (2008: 4.18), the K-values can also be expressed as 60% of the critical storm duration (time of concentration) based on experience and engineering judgement, which explains why Bauer and Midgley (1974) caution users that the decisions regarding the K-values to be adopted should be attempted with engineering judgement.

In conclusion and based on above-mentioned aspects, the LRH and SUH methods are not independent methods and the LRH method cannot be used as an independent check of the more time-consuming SUH method.

2.4.3 Empirical methods

2.4.3.1 Introduction

Empirical methods are based on regional parameters derived from the comparisons between historical peak flows and other catchment characteristics. These methods are therefore likely to be less accurate than statistical or deterministic methods. The reliability of these methods depends largely on the realistic delineation of areas with homogeneous hydrological responses and flood-producing characteristics. Empirical methods are only applicable to medium and large catchments (SANRAL, 2006: 3.42). There exists a need to improve or replace these methods, since there are almost 40 years of additional data available which can be utilised to improve them. The criteria for this evaluation and improvement should be based on the following (Van der Spuy & Rademeyer, 2008: 5.1):

- Theoretical soundness, but by definition empirical methods normally do not meet this.
- Simple and robust application.
- General acceptability to practising engineers and hydrologists.

The empirical methods generally used in South Africa are discussed shortly in Sections 2.4.3.2 - 4 below, whilst the calculation procedures associated with each method are included in Addendum D (DFET User manual).

2.4.3.2 Midgley and Pitman method

The Midgley and Pitman (MIPI) method can be described as an empirical-probabilistic method which is an improved version of the earlier method proposed by Roberts (Alexander, 2001: 481). The Roberts method was improved by the MIPI method through the frequency analyses of the AMS at 83 hydrological gauging stations in South Africa. A LEV1 distribution instead of the Hazen distribution was used to derive the distribution constant (K_T), since the latter distribution assumes that the variance and skewness for all the South African rivers are similar. The catchment coefficient (C) was also regionalised, resulting in a regional-catchment-distribution constant (K_{RP}) which is linked to seven homogeneous flood regions in South Africa. Thus, the MIPI method is only a function of the catchment area and regional-catchment-distribution constant (K_{RP}) (Alexander, 2001: 482; SANRAL, 2006: 3.42 - 43).

A weakness in the method was, however, highlighted. Research showed that although the LEV1 distribution has a sounder theoretical basis, it is less satisfactory than the Hazen, LN and LP3 distributions (Alexander, 2001: 482). Adamson (1978) also indicated that the LEV1 distribution is less satisfactory than most other distributions, especially for long return periods. However, the method is simple to apply and experience has shown that it regularly produces acceptable design flood estimations. It is therefore a useful method to compare with other design flood estimation methods and is suitable for rural catchments larger than 100 km² (SANRAL, 2006: 3.42).

Midgley and Pitman (1971; as cited in SANRAL, 2006: 3.43) also developed an empirical-deterministic method to estimate flood peaks for return periods less than or equal to 100 years in catchments larger than 100 km². As opposed to the MIPI method, this method is a function of the MAP, catchment area, regional-catchment constant (K_T), hydraulic length of the catchment, average slope of the main watercourse and the distance to the catchment centroid (L_C).

This method usually yields results which are comparable to those of the SUH method (SANRAL, 2006, 3.43).

2.4.3.3 Catchment Parameter method

The Catchment Parameter (CAPA) method was developed by McPherson in 1983 and originates from an investigation conducted in South Africa on methods for estimating the mean annual and two-year return period floods with a 50% probability of exceedance. Statistical analyses of the flood peaks revealed that it is preferable to use the mean annual flood (MAF) instead of the two-year flood. The correlation between the MAF and various catchment characteristics was also investigated and gave rise to the basis of the CAPA method. McPherson (1983) identified ten catchment characteristics which were likely to have an influence on the MAF. The preliminary analysis of the investigation showed that four characteristics (MAP, area, average catchment slope and shape parameter) were possibly more influential than the other six. The area was found to be the most significant of the four characteristics (Van der Spuy & Rademeyer, 2008: 5.3 - 4). Pegram and Parak (2004) also noted that a strong relationship exists between the MAF and the catchment area.

DWA (Hydrology, Flood Studies) investigated and developed to a degree regional flood frequency growth curves for the CAPA method by means of statistical analyses of the AMS for return periods ranging from five to 100 years. Kovács (1988) allocated upper limits to these curves based on a predefined maximum flood peak, which will be discussed in Section 2.4.3.4.

2.4.3.4 Regional Maximum Flood

The RMF is an empirically derived upper limit flood peak that can reasonably be expected at a given site. The RMF is only a function of the catchment area and location within a hydrologically homogeneous region. The RMF used the Francou-Rodier method (1967, as cited in Alexander, 2001: 501) to define the upper limit flood peak envelope curves. The primary assumption of the Francou-Rodier method is that the magnitude of a flood is not only dependent on the precipitation retention characteristics of a catchment (area and slope), but also on factors such as possible limits on extreme precipitation.

These extreme precipitation limits can be expected to be controlled by regionally dominant weather systems, while average catchment slope would also be regionally coherent. It was thus established that regional upper limits to extreme flood peaks, as well as regional relationships between area and extreme flood peaks, are plausible. Kovács (1988) delimited eight hydrologically homogeneous regions (Kovács regions) and developed associated regional envelope curves with flood, transitional and storm zones based on a joint consideration of the regional K-values, maximum observed 3-day precipitation, catchment characteristics and 519 observed flood peaks.

A disadvantage of the RMF method is that it does not clearly embody a design flood, in other words, a return period cannot easily be associated with the estimated flood peak. Kovács (1988) estimates the return period to be greater than 200 years. However, Görgens (2002, as cited in Parak, 2007: 11) indicated that Kovács' method of determining the return periods was too simplistic and recommended that the 50-, 100- and 200-year ratios must be factored down by 0.7, 0.8 and 0.9 respectively. This implies that the RMF peaks have return periods that are actually much larger than 200 years, as opposed to the original estimation of Kovács and can be seen as a conservative approach to the upper limit flood estimates.

2.5 STANDARD DESIGN FLOOD METHOD

2.5.1 Introduction

In Chapter 1 it was indicated that design flood estimations display relatively wide confidence bands of uncertainty around all estimates of flood magnitude-frequency relationships. Therefore, in South Africa, the philosophy in design flood estimation is to select the most appropriate method from a suite of deterministic, empirical and statistical methods in order to achieve some degree of certainty.

However, Alexander (2002a: 2; 2002b: 26; 2003: 2) indicated that these uncertainties cannot be satisfactorily accommodated and necessitate a new, single approach to the estimation of the design flood.

The use of the simple, but robust, SDF method in conjunction with the RMF was proposed for the design of most structures vulnerable to flood damage in South Africa. Thus, by implication, the designer does not have to evaluate the relative applicability of alternative design flood estimation methods and is rather encouraged to use engineering factors of safety to accommodate these uncertainties in hydrological analyses (Alexander, 2002b: 29; 2003: 2).

2.5.2 Development

2.5.2.1 Review of available methods

The different design flood estimation methods currently in use, namely statistical, deterministic and empirical methods were reviewed in order to select a suitable method which can be used as the basis for the SDF method (Alexander, 2003: 4). In order to review the suitability of these methods, an extensive study and reprocessing of hydrological and meteorological data were required. This included the use and analyses of the following data (Alexander, 2002a; 2002b: 27):

- Hydrological characteristics from 137 representative catchments in South Africa, varying from less than 10 km^2 to 38 500 km^2 in size (Petras & Du Plessis, 1987).
- Upgraded and extended AMF data from 152 hydrological gauging stations up to October 2000 (DWAF).
- Daily precipitation statistics from TR102 (Adamson, 1981).
- Daily precipitation and other meteorological data (SAWS).
- Digitised short duration precipitation statistics (Smithers & Schulze, 2000a).
- Updated monthly district precipitation data (Dyson & Van Heerden, 2001).
- Properties of widespread severe precipitation (Alexander, 2001).

Direct statistical analyses of the AMS at above-mentioned 152 hydrological gauging stations were conducted. The adverse effects of low outliers were neutralised by using increased values coinciding with the corresponding LN distribution values. Although, the data sets were not adjusted to accommodate the critically important high outliers. The LP3 distribution based on MM estimators was used for the calibration and verification of the SDF method (Alexander, 2002a: 8; 2002b: 27).

2.5.2.2 Regionalisation

The identification of representative, homogeneous flood-producing regions, which followed the boundaries of the drainage regions as depicted by DWA, was a major component in the development of the SDF method. These regions are referred to as SDF basins to avoid confusion with the SAWS precipitation districts and DWA drainage regions. A total of 29 SDF basins were identified (Alexander, 2002a; 2002b; 2003). At least one hydrological gauging station and one representative daily precipitation station was selected for each of the 29 basins from the 2 400 sites in TR102 (Adamson, 1981). The selection of precipitation stations was based on the criterion of representativeness of meteorological conditions, not necessarily of average conditions, since the properties of widespread precipitation events as opposed to point precipitation are of interest. The location of the SDF basins is shown in Figure 2.6.

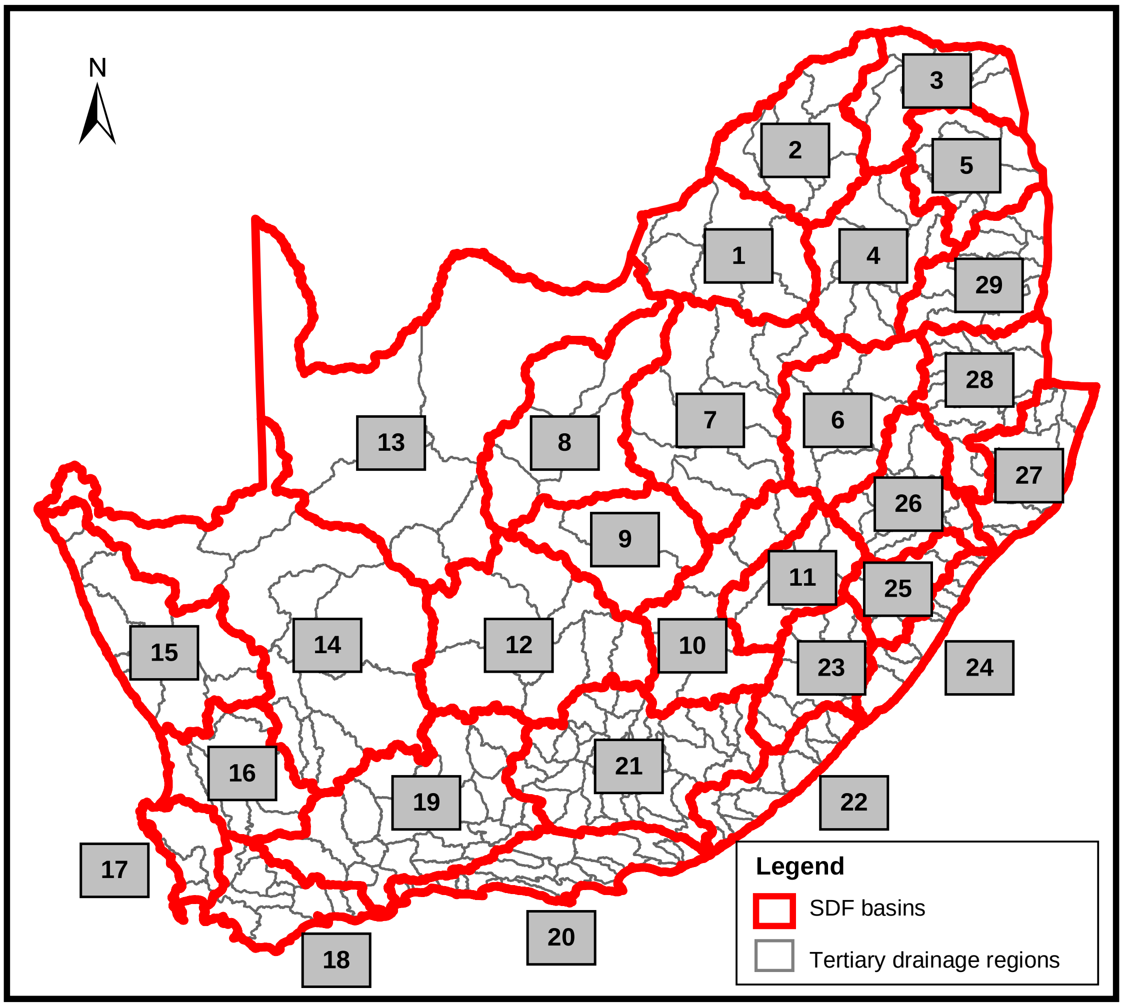

Figure 2.6: SDF basins: Regional map (Alexander, 2003: 14)

2.5.2.3 Calibration

The results of the above-mentioned review (Section 2.5.2.1) indicated that the RM should be used as the basis for the development of the SDF method. In the conventional RM the run-off coefficients are determined by allocating numerical values to the catchment characteristics, whilst the SDF method is based on calibrated, regionalised run-off coefficients established by regional statistical analysis of observed data and an associated probability of exceedance (Alexander, 2002a: 9).

The calibration procedure can be summarised as follows (Alexander, 2002a: 9):

- Direct statistical analyses of observed annual flood peak maxima at selected representative flow gauging stations located in the 29 basins.
- Selection of daily precipitation stations representative of the meteorological conditions in each basin by using the TR102 precipitation data.
- Application of the RM in the various basins.
- Numerical calibration of the catchment related run-off coefficients used in the RM to fit the results obtained by the LP3 distribution of the AMS in order to establish the regionalised SDF run-off coefficients for the two- and 100-year return periods. This procedure was repeated during a second round of analyses in order to improve the two- and 100-year run-off coefficients (C_2 and C_{100}).

2.5.2.4 Verification

The numerically calibrated run-off coefficients were verified at 124 hydrological gauging stations within the different basins. The 29 SDF basins were grouped into eight larger climatic regions, namely the northern interior, central interior, arid areas, South-western Cape, southern midlands, eastern midlands, coastal areas and Lowveld. The final calibrated C_2 and C_{100} run-off coefficients produced design flood estimates that exceeded the LP3 distribution values by 60% on average. Only nine of the 84 stations used for the final analysis had estimated values less than the LP3 distribution values for the two- and 100-year return periods (Alexander, 2002a: 9; 2002b: 27 - 28).

In addition, the 50-year return period flood at 110 hydrological gauging stations was also used for the verification of the SDF method. The verification results indicated that the average value of the SDF/LP3-ratio for all the stations is 2.1 (overestimation of 110%) and only 14 hydrological gauging stations have ratios less than one (Alexander, 2003: 9).

Alexander (2002a: 9) argued that estimates between 50% and 200% of the LP3 distribution values are well within the range of other uncertainties inherent in all design flood estimation procedures and this conservatism is intended to obviate the need for designers to undertake sophisticated hydrological analyses.

Van Bladeren (2005) undertook a verification study at a limited number of sites to demonstrate whether the SDF method is sufficiently robust to be considered as a default method to estimate design floods. The results indicated that the SDF method tends to overestimate floods in basins 1 - 5, 8, 9, 12, 13, 22 and 23, underestimate floods in basins 6, 11, 14, 24 and 28, and with acceptable or reasonable results in basins 7, 10, 15, 16, 18, 20, 21 and 26. These large variations in results indicate that the SDF method has not been thoroughly tested and calibrated throughout the various different climatic regions in South Africa.

Van Bladeren (2005) proposed that the method in its current format needs to be adjusted by an adjustment factor. This adjustment factor is a function of the MAP, catchment area and other catchment characteristics (soils, dolomites, location and orientation of the catchment).

2.5.3 Model parameters

The SDF method is criticised as being too simple and that the introduction of additional parameters are required to improve the reliability of the method. Although, the introduction of each additional parameter is associated with a range of uncertainty, thus resulting in an increased band of uncertainty around the model output, instead of a decrease. There are many examples of conceptually simple, three-parameter hydrological and hydraulic models that are successfully used in international practice. Higher order hydrological models have failed in the past due to the curse of dimensionality and lack of parsimonious parameters (Alexander, 2002b: 28).

The following model parameters are required as input data for the SDF method (Alexander, 2002a: 9 - 10):

- Size of the catchment (km²).
- Length of main watercourse (km).
- Average slope of main watercourse based on the 10-85 method.
- Daily precipitation data (TR102) at a precipitation station representative of the meteorological conditions in the basin of concern.

2.5.4 Design hydrograph

The run-off volume is greater than the proportionate part of the excessive storm precipitation which contributes to run-off during the time of concentration, thus there is no unique relationship between the flood peak and the flood volume. The standard SDF design hydrograph has a fixed triangular shape. The duration of the rising limb equals the time of concentration, whilst the duration of the descending limb is equal to twice the time of concentration. The effective time-base length of the hydrograph is thus three times the time of concentration. The peak run-off will occur after the time of concentration; this assumption is conservative and sufficiently accurate for most applications (Alexander, 2002a: 10; 2002b: 28).

2.5.5 Planning and design objectives

The SDF method is intended to replace the previously recommended RM and SUH method. The basic philosophy of the SDF method is based on a planning and design objective. The planning objectives of the SDF method are based on cost-optimising procedures in the case of minor structures where public safety is not at risk. The different initial costs versus benefits and consequences of failure scenarios must be compared, taking into consideration the risk of failure for each scenario as well as how all these considerations vary with the magnitude of the design flood. Thus, the objective is not only to specify a return period for the design flood, but the use of engineering factors of safety to accommodate any uncertainties in the hydrological analyses is proposed. The design objective of the SDF method is to estimate conservative and realistic design floods based on a regional analysis approach. In cases where public safety is at risk, the planning and design objectives should be the same as that applied to other civil engineering structures (Alexander, 2002b: 28 - 29; 2003: 6 - 7).

However, Görgens (2002, as cited in Parak, 2007: 15 - 16) indicated that although the cost and design implications associated with an intentional over-design of a minor structure (bridge or culvert) are relatively negligible, by contrast it is not acceptable for dam spillway design, since the cost of the spillway is a significant component of the dam's total cost. An average overestimate of 200% might render some projects infeasible. The SDF method should be seen as a conservative approach similar to that of the RMF method.

2.5.5.1 Advantages

The following advantages are associated with the SDF method (Alexander, 2002a: 4):

- *Simplicity:* The method is easy to understand by users with little theoretical knowledge of flood hydrology and is amenable to hand calculation.
- *Consistency:* The method provides the same answer when applied by different users and the subjective assessment of input parameter values is not required.
- *Robustness:* The method can be applied to any catchment, of any size from 5 km^2 to 40 000 km^2, anywhere in South Africa by practitioners with the minimum of hydrological expertise.
- *Accuracy:* The method provides answers that are compatible with all other uncertainties in its application.

2.5.5.2 Disadvantages

The following disadvantages are associated with the SDF method (Alexander, 2003; Van Bladeren, 2005: 40 - 41):

- The method is only applicable to South Africa.
- The method has not been thoroughly tested and calibrated throughout the various different climatic regions in South Africa. Limited studies indicated that the method is inconsistent, either over- or underestimating floods in the various basins and climatic regions.
- The flood-producing characteristics within an identified SDF basin are non-homogeneous and necessitate the further evaluation, calibration and

verification of the regional run-off coefficients being used in order to represent the hydrological response at a smaller scale or catchment level.

- The method does contain components that need to be updated in future, i.e. observed river flow and precipitation data. The current observed flow data are only up until the year 2000, whilst the precipitation data in TR102 were last updated in 1981.
- The method in its current format needs to be adjusted by an adjustment factor, which is a function of the MAP, catchment area and other catchment characteristics (soils, dolomites, location and orientation of the catchment).

2.5.6 Application and calculation procedure

The estimation of design floods rely to a certain degree on personal experience and judgement and therefore it is inevitable that there will be differences of opinion on the merits of the SDF method when compared with alternative methods. The SDF procedure in conjunction with the RMF method for estimating the design flood is conservative and solidly based on many decades of research and practical experience in South Africa. Alexander (2003: 11) maintains that: *"Claims that another method is superior based on theoretical considerations should be treated with caution and any departure from the SDF method should be fully motivated."*

The SDF calculation procedure is as follows (Alexander, 2002b: 29 - 30):

- Identify the SDF basin in which the catchment of concern is located from Figure 2.6.
- Identify the site and demarcate the catchment boundary.
- Determine the catchment area (km^2).
- Identify the main watercourse on the map from the site to the catchment boundary.
- Determine the length of the main watercourse (km).
- Apply the 10-85 method, Equation 2.4 in Section 2.2.1.2 to determine the average slope of the main watercourse.
- Apply Equation 2.8 in Section 2.2.3.2 to determine the time of concentration (T_C) in hours.

- Determine the point precipitation depth by using Equation 2.16 in Section 2.3.4.3 for storm durations up to six hours and the TR102 values (Adamson, 1981) for durations of one to seven days.
- Multiply the point precipitation depth with the ARF, (see Equation 2.19, Section 2.3.6) to determine the average precipitation over the catchment for the required return period. The corresponding average precipitation intensity (mm/h) is obtained by dividing this value with T_C.
- The above steps are the standard procedure used in the conventional RM. The numerically calibrated run-off coefficients C_2 (2-year return period) and C_{100} (100-year return period) are used instead of the catchment related run-off coefficients.

  Large C_2 and C_{100} pair values indicate that a larger proportion of the representative precipitation contributes to the flood peak. Large proportional differences between C_2 and C_{100} confirm that the antecedent soil moisture status of a catchment introduces additional variability into the precipitation run-off process.

- The run-off coefficients for the range of return periods (years) or exceedance probabilities (%) are derived by applying the return period factors *(Y_T)* in Table 2.9 to the relationship in Equation 2.49:

$$C_T = \frac{C_2}{100} + \left(\frac{Y_T}{2.33}\right)\left(\frac{C_{100}}{100} - \frac{C_2}{100}\right) \qquad (2.49)$$

  The return period factor is the inverse of the standard normal cumulative distribution, with a mean of zero and a standard deviation of 1, in other words the LN standard variate. The value of 2.33 in Equation 2.49 is the LN standard variate of the 100-year return period or exceedance probability of 1%.

- Determine the flood peak *(Q_T, m^3/s)* for the required return period as follows:

$$Q_T = 0.278 C_T I_T A \qquad (2.50)$$

Where:

A = Catchment area (km²)

C_T = Run-off coefficient

I_T = Average precipitation intensity (mm/h)

Table 2.9: Return period factors (Alexander, 2003: 13)

Return period (*T*, years)	2	5	10	20	50	100	200
Return period factor (Y_T)	0	0.84	1.28	1.64	2.05	2.33	2.58

The representative percentage run-off coefficients C_2 and C_{100} and additional information required for the SDF calculation procedure are listed in Table 2.10.

The statistical properties of the daily precipitation data from TR102 (Adamson, 1981) at the representative precipitation station for each of the 29 SDF basins are listed in Table 2.11.

Table 2.10: Information required for the SDF calculation procedure (Alexander, 2003: 15)

SDF basin	Station number	Station name	*M* (mm)	*R* (days)	C_2 (%)	C_{100} (%)	MAP (mm)	MAE (mm)
1	0546204W	Struan	56	30	10	40	549	1 800
2	0675125W	Autoriteit	62	44	5	30	452	1 900
3	0760324W	Siloam	64	28	5	40	472	1 700
4	0553351W	Waterval	58	20	10	50	627	1 600
5	0680059W	Leydsdorp	78	10	15	70	625	1 700
6	0369030W	Sylvan	51	54	15	60	668	1 500
7	0328726W	Olivine	49	39	15	60	507	1 700
8	0322071W	Daniëlskuil	47	39	5	20	377	2 100
9	0258452W	Jacobsdal	43	47	15	60	376	1 800
10	0233049W	Wonderboom	54	55	10	50	560	1 600
11	0236521W	Mashai	39	66	40	80	429	1 400
12	0143258W	Scheurfontein	39	52	5	30	288	2 100
13	0284361W	Wilgenhoutsdrif	40	55	5	15	270	2 600
14	0110385W	Middelpos	25	13	10	30	143	2 400
15	0157874W	Garies	22	11	5	20	130	2 100
16	0160807W	Loeriesfontein	28	11	10	40	212	1 900
17	0084558W	Elandspoort	45	1	40	80	498	1 500
18	0022113W	La Motte	59	4	30	60	812	1 400
19	0069483W	Letjiesbos	34	16	10	35	165	2 200
20	0034762W	Uitenhage	53	12	15	60	475	1 600
21	0076884W	Albertvale	45	23	10	35	457	1 700
22	0080569W	Umzoniana	84	26	15	60	821	1 200
23	0180439W	Insizwa	60	45	10	80	890	1 200
24	0240269W	Newlands	76	15	15	80	912	1 200
25	0239138W	Whitson	55	9	10	80	829	1 200
26	0336283W	Nqutu	61	17	15	50	760	1 500
27	0339415W	Hill Farm	85	17	30	80	893	1 400
28	0483193W	Maliba Ranch	75	54	15	60	740	1 400
29	0556088W	Mayfern	66	11	15	50	737	1 600

Where:

M = 2-year Mean of the annual daily maxima precipitation

R = Average number of days per year on which thunder was heard

MAE = Mean annual evaporation using a Symons evaporation pan

Table 2.11: Statistical properties of TR102 precipitation data (Adamson, 1981)

SDF basin	Station number	Latitude	Longitude	Record length	MAP (mm)	Duration (days)	Maxima for return periods (years)						
							2	5	10	20	50	100	200
1	0546204W	25.24	26.07	48	549	1	56	80	99	119	150	177	206
						2	71	105	132	161	205	243	286
						3	105	117	146	177	224	263	308
						7	132	154	196	242	310	369	435
2	0675125W	23.35	28.05	45	452	1	62	93	117	145	187	223	264
						2	74	111	140	173	222	265	313
						3	80	122	156	193	250	300	355
						7	94	144	183	225	289	344	405
3	0760324W	22.54	30.11	46	472	1	64	95	119	146	187	222	262
						2	76	112	142	174	221	263	309
						3	84	129	165	205	266	319	378
						7	103	165	215	271	356	432	517
4	0553351W	25.21	29.42	51	627	1	58	76	89	102	122	138	155
						2	69	90	106	123	146	165	185
						3	76	99	115	132	156	175	195
						7	98	131	154	178	211	238	266
5	0680059W	23.59	30.22	45	377	1	78	116	146	181	233	279	331
						2	99	156	203	257	341	416	503
						3	105	165	215	271	358	435	524
						7	135	225	301	389	528	653	798
6	0369030W	28.00	29.01	44	376	1	51	65	74	84	97	108	120
						2	64	85	99	113	133	149	166
						3	74	98	116	134	160	181	204
						7	92	121	142	164	193	217	242
7	0328726W	28.06	26.55	45	507	1	49	68	82	96	118	137	157
						2	62	87	107	128	158	184	213
						3	68	94	115	136	167	193	221
						7	84	118	144	172	211	243	279
8	0322071W	28.11	23.33	61	377	1	47	69	86	104	132	156	183
						2	60	91	116	144	187	224	267
						3	65	100	128	160	208	250	297
						7	79	126	164	207	272	329	393
9	0258452W	29.08	24.46	86	376	1	43	61	75	91	114	133	155
						2	54	78	98	119	151	179	210
						3	59	87	109	134	171	203	238
						7	70	104	131	160	203	240	280
10	0233049W	29.49	27.02	66	560	1	54	73	88	103	124	143	162
						2	66	88	105	122	146	166	188
						3	75	102	123	144	175	200	227
						7	97	140	172	206	256	298	343
11	0236521W	29.41	28.48	45	429	1	39	53	64	75	92	106	122
						2	47	65	79	93	113	130	149
						3	53	73	88	104	127	147	167
						7	69	97	118	141	173	199	228
12	0143258W	31.18	24.09	64	288	1	39	54	66	79	97	112	129
						2	47	67	82	99	123	143	165
						3	51	75	93	113	143	168	195
						7	62	92	116	141	179	218	245
13	0284361W	28.31	21.43	40	270	1	40	59	73	90	115	135	159
						2	49	75	97	120	157	188	224
						3	52	82	106	133	175	212	250
						7	62	99	129	163	213	257	301
14	0110385W	31.55	20.13	65	143	1	25	38	50	62	82	99	118
						2	30	49	65	84	113	139	170
						3	31	51	68	88	119	147	179
						7	34	57	76	98	131	161	196
15	0157874W	30.34	18.00	63	130	1	22	32	39	46	57	66	76
						2	26	37	46	55	69	80	93
						3	27	40	50	61	78	92	107
						7	30	45	57	70	88	104	122
16	0160807W	30.57	19.27	47	212	1	28	39	48	57	70	81	93
						2	35	48	58	69	84	97	110
						3	37	51	63	74	91	105	120
						7	43	60	73	85	104	118	134
17	0084558W	32.18	18.49	51	498	1	45	59	69	80	96	108	122
						2	60	83	101	119	146	169	193
						3	68	96	118	141	174	202	234
						7	86	126	157	190	240	281	328

Table 2.11: Statistical properties of TR102 precipitation data (Adamson, 1981) (Continued)

SDF basin	Station number	Latitude	Longitude	Record length	MAP (mm)	Duration (days)	Maxima for return periods (years)						
							2	5	10	20	50	100	200
18	0022113W	33.53	19.04	58	812	1	59	77	91	105	125	142	160
						2	82	111	134	158	193	223	254
						3	93	129	155	184	225	260	297
						7	126	183	227	275	345	405	471
19	0069483W	32.33	22.17	62	165	1	34	55	72	92	124	152	185
						2	38	64	87	112	153	190	233
						3	40	68	93	121	166	206	254
						7	45	79	110	145	202	254	315
20	0034762W	33.42	25.26	61	475	1	53	80	103	129	170	206	248
						2	65	102	132	167	221	269	325
						3	70	110	144	182	242	296	358
						7	82	131	171	217	287	350	422
21	0076884W	32.44	26.00	73	457	1	45	64	80	97	123	145	170
						2	56	82	102	126	161	191	225
						3	60	86	107	130	165	194	227
						7	71	104	130	158	199	234	273
22	0080569W	32.59	27.49	57	821	1	84	134	178	229	312	389	480
						2	109	182	248	326	455	576	721
						3	121	205	280	371	521	661	830
						7	140	227	302	385	523	661	830
23	0180439W	30.49	29.15	63	890	1	60	80	95	111	135	154	175
						2	76	102	121	140	169	193	218
						3	85	113	134	156	187	212	240
						7	108	141	165	189	222	249	277
24	0240269W	29.59	30.39	58	912	1	76	114	145	181	235	284	340
						2	95	142	181	224	290	348	415
						3	105	154	192	235	298	354	415
						7	126	179	219	262	325	378	436
25	0239138W	29.48	30.05	42	829	1	55	71	83	95	113	127	143
						2	71	94	111	129	155	176	199
						3	80	108	129	150	181	207	235
						7	104	138	162	187	221	250	279
26	0336283W	28.13	30.40	52	760	1	61	84	102	121	150	175	202
						2	76	105	128	152	187	217	250
						3	84	117	141	168	205	237	272
						7	108	151	182	215	263	302	345
27	0339415W	28.25	32.14	56	893	1	85	130	167	210	278	339	410
						2	107	167	218	277	369	453	550
						3	119	188	246	314	420	517	628
						7	143	223	290	364	480	581	698
28	0483193W	26.13	31.37	40	740	1	75	104	127	151	187	218	252
						2	89	126	154	185	230	268	310
						3	99	142	175	212	265	311	361
						7	122	171	209	248	305	353	405
29	0556088W	25.28	31.03	46	737	1	66	93	113	135	168	196	227
						2	78	108	130	154	189	218	250
						3	89	125	153	183	227	265	306
						7	113	159	194	232	286	331	380

CHAPTER

3

STUDY AREA

CHAPTER 3: STUDY AREA

This chapter is intended to provide a brief overview on the location, climate, topography, geology, land use, vegetation and water resources of the study area (SDF basin 9). The overview serves as background and the various data sets presented will be used as basic input data for the development and evaluation of all the GIS-based catchment data in Chapter 4.

3.1 LOCATION

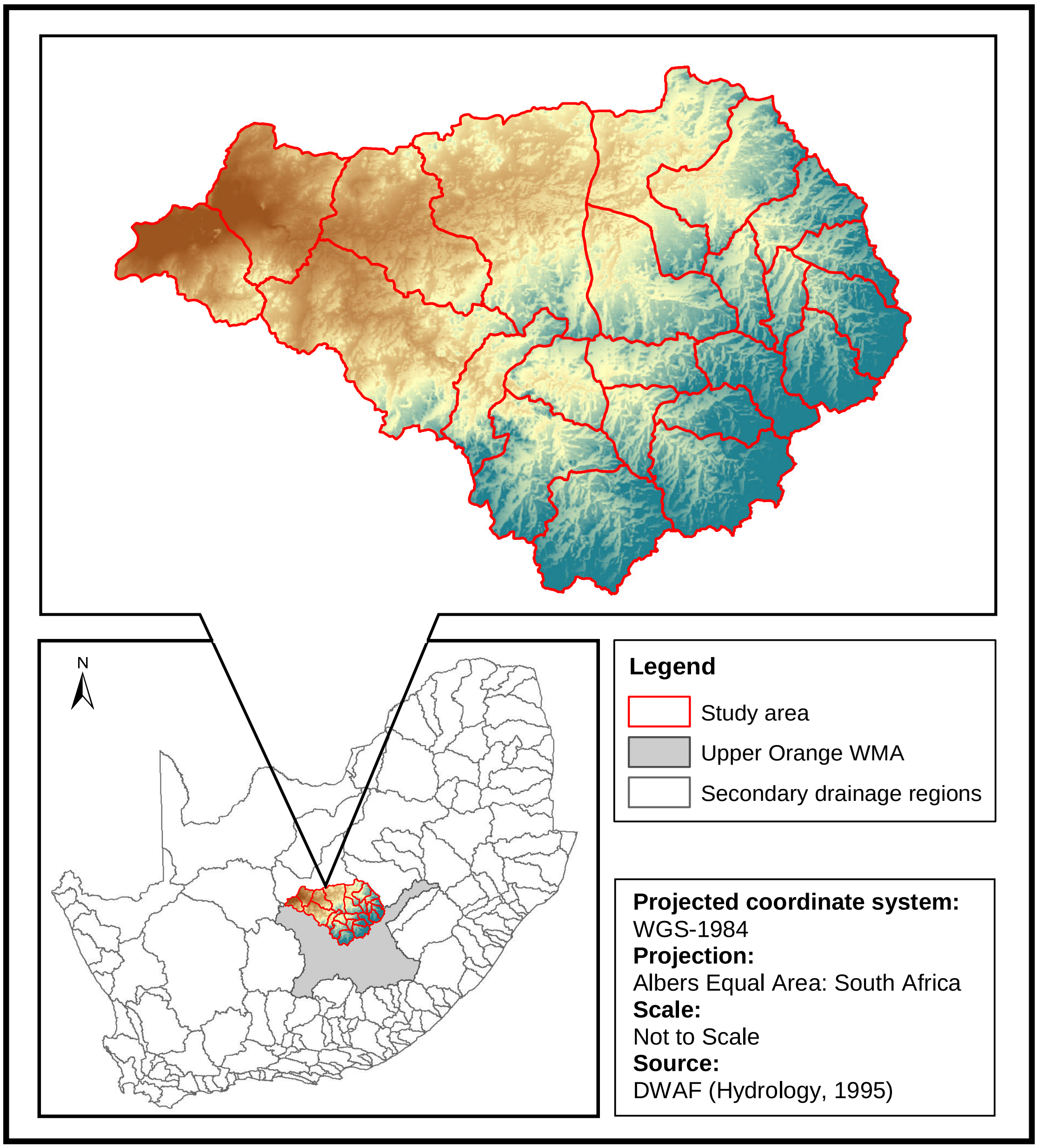

Figure 3.1: Study area (C5 drainage region/SDF basin 9)

The study area covers 34 795 km^2 between 28°25' and 30°17' South and 23°49' and 27°00' East and comprises of the C5 secondary drainage region, which consists of the tertiary Riet River and Modder River catchments (Figure 3.1). The study area forms part of one of the 19 Water Management Areas (WMAs) in South Africa, the Upper Orange Water Management Area (UOWMA) (DWAF, 2004: 1.1; Midgley *et al.*, 1994).

The UOWMA extends over parts of the Free State as well as the Eastern and Northern Cape provinces. Although, the largest part of the study area is located in the southern-central part of the Free State Province, whilst the lesser part is located in the Northern Cape Province (DWAF, 2004: 1.1, 2.2). The spatial GIS data of the study area are illustrated in Addendum A, Plates 1 - 6, which are representative of Sections 3.2 and 3.4 to 3.8.

3.2 DRAINAGE REGION DELINEATION

The basin under consideration is SDF basin 9, which follows the boundary of the C5 secondary drainage region. The tertiary drainage regions of concern are the C51 (Riet River Catchment (RRC)) and C52 (Modder River Catchment (MRC)) covering an area of 17 435 km² and 17 360 km² respectively. The RRC consists of twelve quaternary catchments, whilst there are eleven within the MRC (Midgley *et al.*, 1994: 8.3). The details of the quaternary catchments are listed in Table 3.1.

Table 3.1: Quaternary catchments within SDF basin 9 (DWAF, 1995)

Quaternary catchment description	Area (km²)	%-Distribution
C51A	675.1	1.9
C51B	1 691.2	4.9
C51C	623.9	1.8
C51D	921.6	2.6
C51E	806.0	2.3
C51F	876.1	2.5
C51G	1 834.5	5.3
C51H	1 780.8	5.1
C51J	1 050.8	3.0
C51K	3 627.8	10.4
C51L	2 029.2	5.8
C51M	1 517.6	4.4

Table 3.1: Quaternary catchments within SDF basin 9 (DWAF, 1995) (Continued)

Quaternary catchment description	Area (km²)	%-Distribution
C52A	936.7	2.7
C52B	949.3	2.7
C52C	600.3	1.7
C52D	471.3	1.4
C52E	897.1	2.6
C52F	687.8	2.0
C52G	1 788.5	5.1
C52H	2 372.8	6.8
C52J	1 922.3	5.5
C52K	4 330.5	12.4
C52L	2 403.8	6.9
Total	**34 794.8**	**100**

3.3 CLIMATE

The climate of central South Africa is moderate to hot in summer with an average minimum and maximum temperature of 12°C and 30°C respectively. In winter the average minimum is 3°C with an average maximum of 18°C. The MAP is 424 mm, but it is variable and unpredictable. The MAP ranges from 275 mm in the west (northwest of Koffiefontein) to 685 mm in the east (southeast of Thaba Nchu). The rainy season starts early September and ends mid-April with a dry winter. The MAE varies from 1 600 mm where the Modder River originates at Dewetsdorp to 2 200 mm, just downstream of the confluence of the Modder and Riet Rivers at Ritchie. Evaporation therefore increases from east to west as opposed to the precipitation which decreases from east to west (Midgley *et al*., 1994: 8.3).

3.4 TOPOGRAPHY

The topography is gentle and water tends to pool easily, thus influencing the attenuation and translation of floods and high flows. The mean altitude above sea level in the study area varies between 997 m and 2 122 m, whilst the average quaternary catchment slopes vary between 2.4% and 5.5%. The slope frequency distribution of the study area based on the reclassified Shuttle Radar Topography Mission (SRTM) elevation data for Southern Africa at 90-metre resolution (NASA, 2002) is summarised in Table 3.2.

Table 3.2: Slope frequency distribution of SDF basin 9

Slope classification (%)	Area (km²)	%-Distribution
0 - 3	21 920.7	63
3 - 10	10 786.4	31
10 - 30	1 739.7	5
> 30	348.0	1
Total:	**34 794.8**	**100**

3.5 GEOLOGICAL DATA

The area is geologically stable and relatively uniform consisting mainly of rocks of the Karoo Sequence with shale interspersed in places with dolerite dykes and sheets. Outcrops of the Beaufort Formation belonging to the Karoo Sequence are typical in some parts of the study area, consisting of Intercalated Arenaceous (sandstone) and Argillaceous (mudstone) strata in the west (DWAF, 1999). The characteristic lithology of the study area is summarised in Table 3.3.

Table 3.3: Lithology of SDF basin 9 (Council of Geosciences, 1995)

Lithology	Area (km²)	%-Distribution
Andesite and a combination of sedimentary and extrusive rock types	556.7	1.6
Mudstone and sandstone intruded by dolerite dykes and sheets	13 883.1	39.9
Shale intruded by dolerite dykes and sheets	18 406.5	52.9
Tillite with subordinate sandstone, mudstone and shale, which are intruded by dolerite dykes and sheets	1 948.5	5.6
Total	**34 794.8**	**100**

3.6 SOIL CLASSIFICATION

The soil texture classes vary from moderate to deep sandy clayey and sandy clayey loam in the exceptionally flat central part of the study area, whilst the western part is characterised by a light texture of sandy loamy sand (DWAF, 1999; WRC, 1995). This could be due to the large amounts of sediment which are transported into the area by westerly winds. At least four distinct soil forms and their six associated soil series were identified in the study area. A summary thereof is listed in Table 3.4.

Table 3.4: Soil classification of SDF basin 9 (Midgley *et al.*, 1994; WRC, 1995)

Soil form	Soil series	Area (km²)	%-Distribution
Clovelley	Makuya	9 498.9	27.3
Hutton	Shorrocks	8 072.4	23.2
Hutton	Mangano/Shorrocks	974.3	2.8
Sterkspruit	Swaerskloof	10 786.4	31.0
Vals River	Lindley	5 462.8	15.7
	Total	**34 794.8**	**100**

3.7 LAND USE AND VEGETATION

The study area can be classified as a rural catchment, since 99.1% thereof is characterised by rural areas, whilst only 0.7% is characterised by urbanisation and associated activities. The natural vegetation in the rural areas is dominated by Grassland of the interior plateau, False Karoo and Karoo. Cultivated land is representative of the largest human-induced vegetation alterations in the rural areas, whilst residential and suburban areas dominate the urban areas. The waterbodies (storage reservoirs, farm dams, pans and river reaches) represent only 0.2% (73 km²) of the total area. The land use and vegetation data are based on the National Landcover Database up until the year 2000 as processed by the Council for Scientific and Industrial Research (CSIR), Environmentek. The rural and urban land-use components are listed in Tables 3.5 and 3.6 respectively.

Table 3.5: Rural component: Land use (CSIR, 2001)

Land-use description	Area (km²)	%-Distribution
Bare rock and soil	234.9	0.68
Cultivated land (Commercial dry-land)	2 509.2	7.28
Cultivated land (Commercial irrigation)	1 028.6	2.98
Cultivated land (Subsistence dry-land)	201.4	0.58
Cultivated land (Subsistence irrigation)	46.6	0.14
Degraded shrubland and low fynbos	128.9	0.37
Degraded thickets and bushland	1.9	0.01
Forest and woodland (Eucalyptus, mixed and Pine plantations)	24.3	0.07
Improved natural grassland	447	1.30
Mines and quarries (Mine tailings and waste dumps)	29.9	0.09
Mines and quarries (Surface-based and underground mining)	20.2	0.06
Shrubland and low fynbos	6 902.9	20.02
Smallholdings and grassland	153.2	0.44
Smallholdings, thickets and bushland	6.8	0.02
Thickets, bushland, bush clumps and high fynbos	3 196.2	9.27
Unimproved natural grassland	18 746.7	54.38
Wetlands	793.8	2.30
Total	**34 472.5**	**100**

Table 3.6: Urban component: Land use (CSIR, 2001)

Land-use description	Area (km²)	%-Distribution
Commercial and mercantile	2.2	0.88
Commercial, education, health and information technology	10.1	4.05
Flats and hostels	1.4	0.56
Formal suburban areas	75	30.08
Heavy industrial and transport areas	6.2	2.49
Light industrial and transport areas	26	10.43
Residential (Houses)	48.6	19.49
Residential and formal townships	45.1	18.09
Residential and informal squatter camps	14.1	5.66
Residential and informal townships	20.6	8.26
Total	**249.3**	**100**

The reclassification and grouping of these land uses and vegetation are discussed in Chapter 4, since pre-defined land-use categories are used in the application of the ARM, RM and SCS method.

3.8 RIVER NETWORK AND WATER RESOURCES

3.8.1 River network and storage dams

The Modder and Riet Rivers are the main river reaches in the study area and discharge into the Orange-Vaal River drainage system (Seaman *et al.*, 2001: 16). The Modder River originates in the southern extremity of the C52A quaternary catchment in the vicinity of the town, Dewetsdorp at an altitude of 1 530 m above sea level, after which it flows in a northerly direction and then turns to the northwest just upstream of the Krugersdrift Dam. The river flows in a westerly direction downstream of the Krugersdrift Dam, up until it confluences with the Riet River at Ritchie, approximately 1 110 m above sea level. The total length of the Modder River is about 376 km. The main tributaries that drain into the Modder River are the Klein-Modder River, Doring, Ganna, Kaal, Koranna, Koring, Krom, Matjies, Os, Renoster, Sepane and Stinkhoutspruite (DWAF, 1995; Midgley *et al.*, 1994: 5.5; NASA, 2002).

The Riet River originates in the south-western extremity of the C51B quaternary catchment at an altitude of 1 613 m above sea level, after which it flows in a north-westerly direction for a total distance of 439 km until it discharges into the Orange-Vaal River drainage system at an altitude of 997 m above sea level. The main tributaries that drain into the Riet River are the Fourie, Kromellenboog, Ospoort and Ruigtespruite (DWAF, 1995; NASA, 2002).

The Modder and Riet Rivers were traditionally, like most inland rivers in South Africa, seasonal rivers, but due to the construction of significant storage dams, these rivers now resemble permanent rivers. However, the dams' levels can drop to 30% of the full supply capacity (FSC) during the dry season and the flow in the lower reaches is basically stagnant in winter, except for the controlled releases of water for irrigation purposes downstream. The details of the major storage dams are listed in Table 3.7.

Table 3.7: Major storage dams in SDF basin 9 (Midgley *et al.*, 1994: 5.5)

Dam description	Surface area (km²)	Storage capacity ($10^6 m^3$)
C5R001 (Tierpoort Dam)	9.1	34.6
C5R002 (Kalkfontein Dam)	45.5	323.7
C5R003 (Rustfontein Dam)	11.6	72.2
C5R004 (Krugersdrift Dam)	18.5	73.4
C5R005 (Groothoek Dam)	2.5	13.2
C5R007 (Mockes Dam)	0.1	6

3.8.2 Mean annual run-off

The MRC and RRC have a natural mean annual run-off (MAR) of 185.6 and 212.5 x $10^6 m^3$ respectively. The MAR of the study area forms 8.6% of the total MAR in the UOWMA. According to Midgley *et al*. (1994), originates most of the natural MAR (95%) in the MRC upstream of the Krugersdrift Dam, which might be ascribed to the sound dendritic drainage patterns in this area. Downstream of the Krugersdrift Dam the river flows through an area with shallow slopes where numerous pans and surface depressions are found. These pans are filled after typical convective, high-intensity storms during the summer months, but they hardly ever overflow, therefore contributing little (5%) run-off into the Modder River at the confluence with the Riet River. In the RRC most of the natural MAR (64%) originates in quaternary catchments C51B, D, G and H, with characteristic dendritic drainage patterns flowing towards the Kalkfontein and Tierpoort dams. Downstream of these dams, the Riet River flows through an area characterised by shallow slopes and surface depressions (Midgley *et al*., 1994: 8.3).

3.8.3 Inter-basin transfers

Inter-basin transfers within the UOWMA include the transfer from the Caledon River (Welbedacht and Knellpoort dams) to the Modder River (Rustfontein and Mockes dams) to support Bloemfontein, Botshabelo, Thaba Nchu and other towns or informal settlements. Water is also transferred from Vanderkloof Dam via the Orange Riet Canal to supply mainly irrigation in the study area. In addition, water is also transferred from Welbedacht Dam to Bloemfontein through the Welbedacht-Bloemfontein transfer pipeline, to which several of the small users are also connected, and from Knellpoort to Rustfontein Dam through the Novo Transfer Scheme. The Rustfontein and Mockes dams are part of the water supply system and are located in the MRC upstream of Krugersdrift Dam (DWAF, 2004: 2.14).

CHAPTER

4

METHODOLOGY AND DATA DEVELOPMENT

CHAPTER 4: METHODOLOGY and DATA DEVELOPMENT

This chapter serves as the introduction to the methodology and data development procedures followed during this study. The methodology presented here is based on the comprehensive literature review done in Chapter 2. The development and evaluation of all input data comprising of GIS-based catchment, meteorological and hydrological data are dealt with in the first three sections of this chapter. The focus in the catchment and meteorological data sections (4.1 and 4.2) is on the use of GIS applications in the ArcGIS^{TM} environment for the purpose of catchment parameter and precipitation analyses. The process of obtaining, scrutinising and processing observed streamflow data from DWA hydrological gauging stations is discussed in Section 4.3, whilst issues related to the typical data quality problems encountered, are highlighted.

Section 4.4 describes the development of the DFET in a MS-Excel and/or MS-VBA environment, with the focus on the integral part of automation and functionality to ensure the successful implementation of the various design flood estimation methods. The flood frequency analyses conducted in the study area (SDF basin 9) are discussed in Section 4.5, whilst the exact calculation procedures used are reflected in Addendum D. The methodology used to evaluate, calibrate and verify the SDF method at a quaternary catchment level is discussed in detail in Section 4.6. The last section presents the methodology used to assess all the results, with the focus on the use of regression and descriptive statistics.

4.1 CATCHMENT AND GIS DATA

4.1.1 Projections and data development

All the relevant GIS and catchment related data were obtained from DWA (Directorate: Spatial and Land Information Management), who is responsible for the acquisition, processing and digitising of the data. These data sets are normally presented as geographical coordinate systems, in other words, the position of a geographical location on the earth's surface is described by using spherical measures of latitude and longitude (in degrees) from the centre of the earth to a point on the earth's surface.

These geographical input data sets need to be transformed to a projected coordinate system, which portrays the curved surface of the earth on a flat surface, during which the distance, area, shape, direction or a combination thereof might be distorted.

The Africa Albers-Equal Area projected coordinate system with modification was used during this study, since it is best suited for land masses extending in an east-to-west orientation (as in the case of the study area), rather than those lying north to south. This conic projection uses two standard parallels to reduce some of the distortion of a projection with one standard parallel. Although neither shape nor linear scale is truly correct, the distortion of these properties is minimised in the region between the standard parallels. All areas are proportional to the same areas on the earth, whilst distances are most accurate in the middle latitudes. The standard parallels were established by using the *One-sixth rule* by determining the range in latitude (degrees) north to south divided by six. The first standard parallel is positioned at one-sixth the range above the southern boundary and the second standard parallel minus one-sixth the range below the northern boundary. These modifications are listed in Table 4.1 (ESRI, 2006).

Table 4.1: Modified Albers-Equal Area projection for South Africa (ESRI, 2006)

Parameter description	Modified (original) value
False Easting	0 (0)
False Northing	0 (0)
Central Meridian	24 (25)
Standard parallel 1	-18 (20)
Standard parallel 2	-32 (-23)
Latitude of origin	0 (0)
Linear unit	Metre

The specific GIS data feature classes (points, lines and/or polygons) applicable to the study area were extracted and created from the original GIS data sets by using *Extract (Clip)* in the *Analysis Tools* extension of ArcCatalog. The *Clip* function cuts out a piece of one feature class using one or more of the features in another feature class as a *cookie cutter*. The secondary drainage region polygon was used as the clip feature class, since the clip feature class must be a polygon. The data extraction was followed by data projection and transformation, editing of attribute tables and recalculation of geometry.

All the results related to the development of the catchment and GIS data are listed and discussed in Chapter 5, whilst the spatial GIS data of the study area are illustrated in Addendum A, Plates 1 - 6.

4.1.2 Digital Elevation Model

The SRTM elevation data for Southern Africa at 90-metre resolution (NASA, 2002) was extracted, projected and transformed for the study area and used as the DEM. The DEM contains all other raster information for the determination of area, length and slope, as well as for catchment analyses. The DEM is shown in Addendum A, Plate 2.

An alternative DEM was also generated by making use of point elevation and/or contour data as the input features. The *Topo to Raster* function in the *Spatial Analyst Tools (Interpolation)* extension was used to generate rasters for the DEM interpolation process. The input features (contours or point elevations) were selected, the *Output Surface Raster* was specified and *Tolerance 1* was set to a value of 10, which is equal to half the contour interval, or set to 0, if point elevations are predominately used. The *Output Cell Size*, which specifies the output raster cell size, was then selected. A smaller cell size increases the amount of cells in the raster matrix with both an increased accuracy and computing time. A trade-off between time and accuracy was used in selecting the output cell size.

4.1.3 Average catchment slope and centroid

The average catchment slope of the study area, as well as of individual quaternary catchments, was calculated by using the following methods:

- <u>Grid method</u>: The *Create Vector Grid* function in the *Hawth's Analysis Tools (Sampling)* extension was used to superimpose a grid over the catchment areas. Shape files containing the polylines as feature type were created in ArcGIS^{TM} to represent the horisontal distances measured at each grid intersection point between two consecutive contours. The attribute table of each shape file was edited and the length of each polyline was determined by making use of the *Calculate Geometry* function. These attribute tables can then be exported to MS-Excel for further computations and used as input data for the DFET.

- Empirical equation: The *Sum Line Lengths in Polygons* function in the *Hawth's Analysis Tools* extension was used to calculate the total length of all contour lines (*M*) within each catchment, after which it was used as an input variable for Equation 2.2, Chapter 2. The other input variables, area (*A*) and the contour interval (ΔH) were obtained from the relevant developed feature classes of the study area.
- GIS: A slope raster was generated from the DEM based on a cell matrix approach, which represents the maximum change in elevation over the distance between the cell and its eight neighbouring cells, thus the maximum average slope for each cell. The *Zonal Statistics as Table* function in the *Spatial Analyst Tools (Zonal)* extension was applied on the slope raster to generate a summary table containing the statistical information about the input data or raster for a defined zone within the data frame, thus the average slope for each catchment. The slope raster was converted to a feature class (polygons) and reclassified into four slope frequency distribution classes as required by the deterministic methods (ARM, RM and SCS) to establish the surface slope coefficients associated with different MAP ranges. The conversion was done by using the *Raster to Polygon* function in the *Conversion Tools* extension of *ArcToolbox*, whilst the *Reclassify* function in the *Spatial Analyst Tools (Reclass) extension* was used for the reclassification.

These above-mentioned input parameters are included in the DFET and the user can select the most appropriate method to be used as input data in all the design flood estimation methods.

The centroid of each catchment under consideration was determined by either making use of the *Mean Center* function in the *Spatial Statistics Tools (Measuring Geographical Distributions)* extension or *Generate Polygon Centroid Points* function in the *Hawth's Analysis Tools (Vector Editing)* extension. Only the input polygon feature class representative of each catchment has to be selected to result in a point output feature class and associated attribute table representative of the average *x, y* coordinates of the geometric centroid of each catchment.

The length of the identified main watercourse in each catchment to a point opposite the identified centroid within the catchment was established by using the *Measure* function in ArcMap. This measured length represents the distance along the main watercourse between the outlet and the point closest to the centroid of the catchment.

4.1.4 Length and average slope of main watercourses

The main watercourse in each catchment was manually identified in ArcMap. A new shape file containing polyline feature classes representative of the identified main watercourse was created by making use of the *Trace Tool* in the *Edit Toolbar*. Each identified main watercourse was traced using the polyline feature classes of the 20 m-interval contour shape file as the specified offset or point of intersection, resulting in chainage distances between two consecutive contours. The attribute table of each shape file was then edited by using the *Add Field* function to include the reduced heights of the contour intervals and the length of each polyline was determined by making use of the *Calculate Geometry* function.

These attribute tables can then be exported to MS-Excel for further computations and used as input data for the DFET. The determination of the average slope of the main watercourses in the DFET is based on the Equal-area, 10-85 and Taylor-Schwarz methods (Equations 2.3, 2.4 and 2.5, Chapter 2). The user can select the most appropriate method to be used as input data in all the design flood estimation methods, whilst the results of each method are plotted on the longitudinal profile.

4.1.5 Soil classification

None of the identified soil forms and their associated soil series present in the study area (Section 3.6, Chapter 3) display similar characteristics, especially in terms of the infiltration and permeability rate. Therefore, the binomial soil classification system was used to assign these soil forms/series to hydrological soil groups or intermediate hydrological soil groups (A/B, B/C and C/D) as proposed by Schulze *et al*. (1992):

- <u>Group A:</u> Final infiltration rate ± 25 mm/h and permeability rate larger than 7.6 mm/h.

- Group B: Final infiltration rate ± 13 mm/h and permeability rate between 3.8 and 7.6 mm/h.
- Group C: Final infiltration rate ± 6 mm/h and permeability rate between 1.3 and 3.8 mm/h.
- Group D: Final infiltration rate ± 3 mm/h and permeability rate less than 1.3 mm/h.

The attribute table of the soil data shape file applicable to the study area was edited by using the *Add Field* function to include the hydrological soil groups and their associated areas, after which each area was determined by making use of the *Calculate Geometry* function. The *Extract (Clip)* function in the *Analysis Tools* extension of ArcCatalog was used in the same manner as before (refer to Section 4.1.1) to extract and create soil feature classes (shape files) at a quaternary catchment level or even smaller scale, if applicable. The area of each hydrological soil group, expressed as a percentage of the total area under consideration, can then be used as input data for the deterministic methods (ARM, RM and SCS) in the DFET to establish the permeability coefficients associated with different MAP ranges and the CN-values respectively.

4.1.6 Land use and vegetation

4.1.6.1 Reclassification and grouping of land use and vegetation

The land use and vegetation data of the study area, which are based on the National Landcover Database (CSIR, 2001), were reclassified and grouped according to the standard classification of land use in the urban and vegetation in the rural components used in the deterministic methods (ARM, RM and SCS). These classifications are used to determine weighted urban and rural run-off coefficients. The urban run-off coefficients are only based on land use, whilst the rural run-off coefficients are based on land use and vegetation associated with different MAP ranges.

The attribute table of the Landcover data shape file applicable to the study area was edited by using the *Add Field* function to include a description column containing the above-mentioned pre-defined standard classes. A total of twelve pre-defined standard classes were identified in the study area.

The *Summarize* function was then used to generate a summary table based on the unique values (pre-defined standard classes) from a specified field (description column). The sum of the area field was selected to be included in the summary statistics, which resulted in the automatic addition of an output field named *Sum of Area*. The shape field is ignored when the attributes of a layer are summarised. The *Dissolve* function in the *Data Management Tools (Generalisation)* extension in ArcCatalog works like *Summarize*, except it also processes the features in the shape field.

4.1.6.2 Homogeneous veld-type regions

The *Regions with Generalised Veld-types in South Africa* map contained in the Drainage Manual (SANRAL, 2006: 3.27) was added to the study area project in ArcMap as picture file. Pyramids were created for the picture file and then the *Georeferencing* toolbar was used to define the location using map coordinates and assign a coordinate system. The *Auto Adjust* function was used to add four *Control Points*, which are used to move and orientate the picture file in such a way that it overlays the polygon feature class representative of South Africa perfectly. The *Update Georeferencing* function was used to make the changes permanent.

A new shape file containing polygon feature classes representing the homogeneous veld-type regions was created by making use of the *Sketch Tool* in the *Edit Toolbar*. The different veld-type regions were digitised and the attribute table was then edited by using the *Add Field* function to include the veld-type region descriptions and their associated areas, after which each area was determined by making use of the *Calculate Geometry* function. The *Extract (Clip)* function in the *Analysis Tools* extension of ArcCatalog was used in the same manner as before (refer to Section 4.1.1) to extract and create veld-type region feature classes (shape files) at a quaternary catchment level or even smaller scale, if applicable.

4.1.6.3 Kovács flood regions

The same procedure as described in Section 4.1.6.2, was followed to create a shape file containing polygon feature classes representative of the maximum flood peak regions as illustrated by the *Maximum Flood Peak Regions in Southern Africa (Kovács)* map in the Drainage Manual (SANRAL, 2006: 3.48).

4.2 METEOROLOGICAL DATA

4.2.1 Precipitation database

Two precipitation databases, which are based on the SAWS and TR102 data, are included in the DFET. The SAWS database consists of design precipitation depths for durations ranging from one to seven days and for return periods two to 200 years. This database is also used in the software program, *Design Rainfall Estimation in South Africa* as developed by Smithers and Schulze (2003). The TR102 database consists of design precipitation depths for durations of one, two, three and seven days and also for return periods ranging from two to 200 years.

The precipitation data used for the evaluation, calibration and verification of the SDF method at a quaternary catchment level were only based on the SAWS database as opposed to the original SDF method which is based on the TR102 data. The TR102 precipitation database (1981) has ± 20 years less data available and is limited to 1 946 stations as opposed to the 3 946 SAWS precipitation stations with data up to the year 2002. The selection of a single precipitation station to be used in the SDF method in each quaternary catchment under consideration, was based on the following criteria:

- <u>Average meteorological conditions</u>*:* The MAP and design precipitation depths associated with return periods ranging from two to 200 years of the selected station must have a high degree of association with the MAP and design precipitation depths as obtained by the Thiessen polygon method using the total number of precipitation stations within the catchment(s) under consideration.

- <u>Record length</u>*:* A minimum record length of 50 years was used in order to enable the conclusive selection of a distribution that could consistently provide adequate precipitation frequency estimates for return periods greater than the period of record. Although, in some of the catchments used to evaluate the SDF method in a South African context, shorter records (minimum of 40 years) were used due to the limited number of suitable precipitation stations available.

The flood frequency analyses (deterministic and empirical methods) conducted in the study area were also only based on the SAWS precipitation data. Again, the argument is that the ± 20 years of additional data might be more representative of the probable nature of future events.

4.2.2 Averaging of precipitation depths

The arithmetic mean and/or Thiessen polygon methods were used to convert the point precipitation depths at 185 precipitation stations to an average precipitation depth over the study area. The same procedure was also followed in the 12 catchments used for the flood frequency analyses, as well as in the 29 catchments randomly selected to evaluate the SDF method in a South African context.

The *Areal Rain* extension in ArcView 3.2a was used to generate Thiessen polygons representative of the averaged precipitation depths for a particular area (catchment) from point's precipitation measurements. The boundary of the resultant Thiessen polygons was selected in each case either by the applicable quaternary catchments (polygon feature classes) or buffered group of precipitation stations (point feature classes). The latter option provides an alternative that allows the user to include precipitation stations located outside the catchment boundary. The precipitation station number field in the attribute table of the point feature class (precipitation stations) was used to identify points and precipitation. The attribute table is then automatically updated; fields (Thiessen area, total area, weighted area, Thiessen and areal precipitation) are added with the geometry (area) being calculated.

These attribute tables can then be exported to MS-Excel for further computations and used as input data for the DFET. The determination of the MAP and average precipitation depths associated with various return periods in the DFET are based on the arithmetic mean or Thiessen polygon methods (Equations 2.17 and 2.18, Chapter 2). The user can select the most appropriate method and database to be used as input data in all the design flood estimation methods.

4.2.3 Critical storm duration precipitation

The critical storm duration precipitation depths used in this study, were based on the following approaches used in the various design flood estimation methods:

- DDF relationship based on LEV1 distributions developed by Midgley and Pitman (RM, SUH and LRH methods).
- DDF relationship based on the 24-hour SAWS daily precipitation data (SCS method).
- DDF relationship based on the modified Hershfield equation and/or SAWS daily precipitation data (ARM and SDF method).
- DDF relationship based on the RLMA&SI approach (results obtained from Parak and Pegram (2006) were compared with the design precipitation depths used in the evaluation and calibration of the SDF method).

The critical storm duration was determined by using the US-SCS equation (Section 2.2.3.2, Chapter 2), which represents the time of concentration in natural, defined watercourse.

4.2.4 Area reduction factors

The ARF in each catchment under consideration, in other words the conversion of point precipitation depths or intensities to average areal precipitation depths or intensities, was establish by using Equation 2.19 (see Section 2.3.6, Chapter 2). The validity of this equation was assessed by plotting the time of concentration within each catchment under consideration against the catchment area, after which it was superimposed on both an ARF curve based on Equation 2.19 and an ARF diagram as published in the FSR (NERC, 1975).

4.2.5 Days of thunder per year

The average number of days per year on which thunder was heard (R), is based on the climate data as published in the SAWB publication WB42 (SAWB, 1992) and the generalised map contained in Alexander (2001: 346). There are 280 precipitation stations with associated R-values in WB42, thus representing only ± 7% of the total number of precipitation stations available in the SAWS database as used in the DFET.

The above-mentioned isohyetal map and data contained in WB42 were used to establish *R*-values for the remaining 3 666 precipitation stations by means of linear interpolation. The 280 stations used were also allocated to the two types of 24-hour storm distributions used in the SCS method. The Type 1 distribution applies to coastal areas with winter precipitation or precipitation throughout the year, whilst Type 2 applies to inland areas characterised by convection activity. This was done by superimposing the *Area distribution of storm types in South Africa* map over the *SAWS precipitation station reference grid* map (SANRAL, 2006: 3.24).

The *R* and the 2-year mean of the annual daily maxima precipitation (*M*) values were then plotted against one another to establish whether there exists any direct relationship which can be used to express the *R*-values in terms of the *M*-values (Refer to Section 5.2.5, Chapter 5). The anticipated results will thus exclude the degree of uncertainty associated with the selection of default *R*-values based on location only.

4.3 HYDROLOGICAL DATA

4.3.1 Observed streamflow

4.3.1.1 Hydrological gauging stations

Observed streamflow data were obtained from DWA reservoir and/or river hydrological gauging stations within the study area, as well as at selected locations in the rest of South Africa for the evaluation of the design flood estimation methods, with specific reference to the SDF method. Only the AMS of each gauging station under consideration was used during this study. The theoretical concepts associated with the AMS were highlighted in Section 2.4.1.4, Chapter 2.

In the case of river gauging stations, the AMS of each station was obtained from the DWA website (www.dwa.gov.za/hydrology/dwaapp2/) using the *Dams, Flows & Floods* link, followed by *Access Data* and selecting *Monthly Peaks*. Each data set was then exported to MS-Excel, after which the data were transposed into the correct format to be used as input for the DFET.

In the case of reservoir gauging stations (dams), the complete primary data time series were used as input data for the *Level Route* program used by the DWA (Flood Studies). The primary data series consist of water level, capacity-area, rating (uncontrolled spillways) and outflow (controlled spillways) data. Numerical methods are used to generate a continuous fit of the primary data, thus any time interval in question can be investigated and as a result the AMS for the period under consideration are generated. All these AMS were generated by the DWA (Flood Studies). As in the case of river gauging stations, each AMS data set was then also exported to MS-Excel and used as input for the DFET.

4.3.1.2 Data quality

The quality of the observed streamflow and AMS varied from catchment to catchment. The record length of all the observed data sets which were characterised by missing data for one or more hydrological years was reduced accordingly. Although, in cases where the missing data were only limited to one or more months characterised by low flows in a year, the maximum observed in the balance of the months was used. In addition, zero flows were excluded from the analyses using $\log_{10}$-transformed data, otherwise an error condition would have been introduced.

Most of the observed streamflow data were also characterised by flood peaks that exceeded the hydraulic capacity of the gauging weir. In most of the cases there was no sufficient proof that the measurements were in error and therefore the high outliers were retained as part of the continuous record, but adapted to allow for the overtopping of the structure. Although, in cases where the high outliers were the maximum observed flows over an extended period of time, these maximum observed flows were included as historical information.

In cases where the observed streamflow data seemed unreliable due to short record lengths, the Square root-area method (Equation 2.20, Chapter 2) was used to combine or extend observed streamflow data sets at single sites up- or downstream from one another.

4.4 DESIGN FLOOD ESTIMATION TOOL

4.4.1 Development and application

The DFET was developed and programmed by using MS-VBA 6.5 with MS-Excel (2007) as the operating environment. A workbook named DFET_Excel2007 was created in MS-Excel, followed by the development of each worksheet containing the layout and procedures associated with the various design flood estimation methods. All the basic procedures were automated using standard programming functions in MS-Excel.

The integral part of automation depends on the development of a VBA project comprising of a set of modules. Each module contains a macro consisting of a set of declarations followed by procedures or methods acting on objects (*Forms* toolbar controls). These toolbar controls were placed on the series of developed forms/worksheets. Macros were then recorded and assigned to each toolbar control. Each worksheet has its own set of recognised properties, methods and events. The controls can be used to receive user input, display output and trigger event procedures. Both interactive (responsive to user actions) and static (accessible only through code) controls were used in the DFET.

The following *Forms* toolbar controls with associated macros were included in the DFET:

- Button: Runs a macro when activated by the user.
- Check box: Enables the user to select or exclude single or multiple options.
- Combo box*:* Provides the user with a drop-down list box. The item that is selected in the list box appears in the text box in the applicable worksheet.
- Group box: Groups related controls, such as option buttons/check boxes.
- Option button*:* Enables the user to select one of a group of options contained in a group box.
- Spinner*:* Enables the user to increase or decrease a specific value/range.

The developed DFET was used to process all the catchment (average catchment slope, catchment centroid, length and average slope of main watercourses, soil classification and land use/vegetation), meteorological (precipitation) and hydrological (observed flows, AMS and PDS) data to be used as input for the various design flood estimation methods. The following design flood estimation methods are included in the DFET:

- Deterministic methods*:* ARM, RM, LRH, SCS, SDF and SUH methods.
- Empirical methods*:* CAPA, MIPI and RMF methods.
- Statistical methods*:* N/MM, GEV/MM, LN/MM, LEV1/MM, LP3/MM and GLO (LM/PWM) probability distributions/parameter estimation methods based on either the AMS or PDS.

Both the data development and application phases of the DFET are characterised by a full graphical interface, enabling the printing/plotting of worksheets and graphs. All the results are summarised in the DFET *Summary Report.*

4.5 FLOOD FREQUENCY ANALYSIS

4.5.1 Direct statistical analyses

Direct statistical analyses were conducted at each hydrological gauging station in order to summarise the hydrological data, estimate parameters and select appropriate theoretical probability distributions. The hydrological data were summarised by ranking the AMS in a descending order of magnitude; a process which is automated in the DFET.

The Cunnane plotting position based on the Weibull formula was used to assign a probability to the plotted data points. The parameter estimation was largely based on MM estimation, although the usefulness of LM/PWM estimation to fit probability distributions was also investigated. The statistical properties (mean, standard deviation, skewness and coefficient of variation) of each AMS (normal and $\log_{10}$-transformed) were calculated by using the DFET after which the most suitable probability distribution was selected. This selection was based on the statistical properties, visual inspection of the plotted data and GOF statistics.

Several of the AMS data sets were characterised by short, insufficient record lengths which made it impossible to conclusively select a probability distribution that could consistently provide flood frequency estimates for return periods greater than the period of record. In order to overcome this limitation, the mean values of the logarithms of two or more probability distributions with or without high estimated peak flows were used as the most suitable probability distribution.

4.5.2 Deterministic methods

The DFET was used to process all the catchment (average catchment slope, catchment centroid, length and average slope of main watercourses, soil classification and land use/vegetation) and meteorological (averaged areal design precipitation depths and critical storm durations) data to be used as input for the various deterministic methods. The standard procedure and techniques associated with each deterministic method were used by default, whilst taking cognisance of the limitations and intended application of each method. The exact calculation procedures used are reflected in Addendum D (DFET User manual).

The following deterministic methods were evaluated in the study area:

- ARM, RM, LRH, SCS, SDF and SUH methods.

In addition, the SDF method was also evaluated in other catchments in the rest of South Africa. Refer to Section 4.6 for more detail.

4.5.3 Empirical methods

The developed regional parameters (Homogeneous veld-type and Kovács flood parameters), as discussed in Section 4.1.6, were entered in the DFET, after which the standard procedure and techniques associated with each empirical method were used by default. Again, the limitations and intended application of each method were taken into consideration. The exact calculation procedures used are also reflected in Addendum D (DFET User manual).

The following empirical methods were evaluated in the study area:

- CAPA, MIPI and RMF methods.

4.6 EVALUATION AND CALIBRATION OF THE SDF METHOD

4.6.1 Input data requirements

In order to evaluate, calibrate and verify the original and adapted probabilistic SDF method and associated calibrated run-off coefficients at a quaternary catchment level, the following procedures were followed to prepare and manipulate all the input data:

- Selection of a daily precipitation station with a sufficiently long record length representative of the average meteorological conditions in each quaternary catchment under consideration. The design precipitation depths for the corresponding times of concentration were based on the precipitation database (Smithers & Schulze, 2003) as included in the DFET. Both the MAP and design precipitation depths (various storm durations) at the single selected precipitation station were compared with the Thiessen polygon averaged MAP and design precipitation depths of all the precipitation stations within the quaternary catchment(s) under consideration. None of the stations used had a record length shorter than 50 years.
- Direct statistical analyses of the AMS at a representative flow gauging station in each quaternary catchment under consideration to determine the design values of flood peaks for a range of return periods (refer to Sections 4.5.1 and 5.5.1, Chapter 5). Apart from the total of 36 catchments that were evaluated (12 within the study area), an additional eight catchments of which the direct statistical analyses results are based on the GEV/MM distribution, were also used. The GEV/MM distribution results were obtained from previous research conducted by Parak and Pegram (2006).
- All the other required input parameters (average main watercourse slope, time of concentration, design precipitation depths and intensities and ARFs) were determined in a similar fashion as for the original SDF method.

Refer to Section 2.5.6, Chapter 2, for the application and calculation procedures associated with the SDF method.

4.6.2 Evaluation and calibration of run-off coefficients

The numerical calibration of the run-off coefficients used in the SDF method followed the direct statistical analyses and selection of a single precipitation station in each quaternary catchment. The purpose of the calibration was to fit the results obtained by the direct statistical analyses, thus establishing the SDF/probability distribution-ratios and adapted quaternary SDF run-off coefficients for return periods, ranging from two to 200 years, to produce results comparable to those obtained with the statistical analysis.

This was accomplished by determining the C_2 (2-year return period) and C_{100} (100-year return period) run-off coefficients in Equation 2.49, Chapter 2, in such a way that the calibrated run-off coefficients (C_T) for a range of return periods resulted in the best fit between the design values of flood peaks based on the direct statistical analysis and the SDF method. These coefficients (C_2 and C_{100}) were changed manually until an appropriate fit with the statistical data was achieved. The ratio between the original C_2 and C_{100} coefficients was, however, kept constant to enable this calibration, after which values of C_T were coaxially plotted with the regional SDF run-off coefficients from Alexander (2003) against the return period.

This comparison was followed by investigating the validity of the run-off coefficient adjustment factors as proposed by Van Bladeren (2005).

Thus, for the purposes of calibration, 19 of the 29 SDF basins in South Africa were evaluated. Five catchments within the study area (SDF basin 9) were evaluated. The SDF basins evaluated are basins 1, 2, 4 - 11, 16 - 18, 21 - 23, 26, 28 and 29. These catchments ranged in size from 126 km² to 33 277 km². In all the SDF basins, except the study area, the catchment areas and time of concentration were based on research previously conducted by Petras and Du Plessis (1987) and Parak and Pegram (2006). This was then used as default input parameters for the SDF method.

4.6.3 Verification of calibrated run-off coefficients

The verification exercise was necessary to test whether the calibrated run-off coefficients behaved in the probabilistic manner for which they were designed for: The estimation of design floods of magnitudes equivalent to those derived from direct statistical analysis of AMS at a specific gauging site and associated catchment area. Thus, verification tests are necessary to convey confidence that the method works as expected. In order to verify the C_T - values achieved during calibration, it was necessary to find some physical or regional descriptors on which to relate the run-off coefficients to enable the use and extension of the calibrated run-off coefficients to ungauged catchments. Several regional descriptors, such as MAP, average catchment slope and land-use distribution, were taken into consideration in combination with the C_T - values to establish whether any relationship existed on which to regress the run-off coefficients.

In other words, for the purposes of verification, 16 catchments which were not used in the calibration exercise and for which the AMS were available, were selected based on the fact that their physical and regional descriptors are similar, resulting in homogeneous hydrological responses. These catchments ranged in size from 26 km² to 23 067 km², with eight catchments within the study area (SDF basin 9) and eight other catchments within SDF basins 6 - 7, 9, 10, 18 and 21.

4.7 ASSESSMENT OF RESULTS: METHODOLOGY

4.7.1 Direct statistical analyses

Regression (coefficient of determination) and descriptive (Chi-square) statistics were used to evaluate the GOF of the fitted probability distributions. However, the validity of Equation 2.46, Chapter 2, which can be used to determine the limiting critical value at confidence levels ranging from 90% to 99.5%, was first evaluated. This was done by comparing the critical values obtained with Equation 2.46 with the critical values listed in Table 2.7, Chapter 2. The degrees of freedom and critical values at different confidence levels as listed in Table 2.7 (obtained from Hirsch *et al*., 1993: 17.17) were then plotted against one another to establish whether there exists any direct relationship which can be used to express the critical values in terms of the degrees of freedom.

The coefficient of determination (r^2) calculations were based on the complete record length, in other words, the ranked observed data points with an associated probability or return period were compared with the theoretical probability distributions.

The Chi-square statistics were evaluated by making use of the concept of contingency tables, consisting of margin totals, which are used to establish the expected estimated values. The margin totals comprise of row and column variables, which are representative of the observed data and probability distribution values.

Thus, for each probability of exceedance or return period, the sum of the observed data point and probability distribution value (row variables) was determined to provide the row totals. The sum of all the different individual column variables (observed data, probability distribution value and row total) was also determined to provide the column totals. The expected estimated values were then calculated as the ratio of the product of row totals and column totals to the grand total, where the grand total either equals the sum of the row or column totals.

4.7.2 Deterministic methods

Regressive statistics were used to evaluate the GOF between the deterministic methods and the fitted probability distributions based on the direct statistical analysis (Section 4.7.1) in each catchment under consideration.

4.7.3 Empirical methods

The procedure discussed in Section 4.7.2 was also used to evaluate the GOF between the empirical methods and the direct statistical analyses.

4.7.4 SDF method

The procedure discussed in Section 4.7.2 was also used to evaluate the GOF between the original, adjusted and calibrated versions of the SDF method and the direct statistical analyses.

CHAPTER

5

RESULTS AND DISCUSSIONS

EVALUATION OF THE SDF METHOD USING A CUSTOMISED DESIGN FLOOD ESTIMATION TOOL

CHAPTER 5: RESULTS AND DISCUSSIONS

In the light of the discussion of the methodology in Chapter 4, this chapter will provide the results and an interpretation of the results. The catchment data and various GIS-based input parameter results from the developed DEM will be discussed first. This will be followed by an in-depth evaluation of the meteorological data (Section 5.2) applicable to the study area (SDF basin 9). This section focuses on the selection criteria used to identify the single precipitation stations used in the evaluation of the SDF method, whilst the Thiessen polygon averaged precipitation depths are used to perform a comparative study. The various DDF relationships to estimate the critical storm duration precipitation, as discussed in Chapter 4, will also be compared, whilst the relationship between the catchment area and time of concentration will be investigated to possibly improve the existing ARFs in use.

Section 5.3 provides all the information related to the hydrological data to be used in the direct statistical analyses. In Section 5.4 reference is made to the DFET developed in MS-Excel/VBA, although the schematic layout and application guidelines are included in Addendum D (DFET User manual).

The flood frequency analysis results based on the direct statistical analyses as well as the deterministic and empirical methods are included in Section 5.5. The evaluation, calibration and verification results of the SDF method are presented and discussed in detail in Section 5.6. The focus will be on the evaluation and calibration of the run-off coefficients at a quaternary catchment level. This calibration exercise is followed by the comparison of the design flood peaks based on both the original, adjusted (Van Bladeren, 2005) and calibrated run-off coefficients. In order to establish whether these calibrated run-off coefficients and associated flood peaks behave in the probabilistic manner for which they were designed for, verification tests will be conducted. In the last section, the relationship between the limiting critical values and degrees of freedom used in the Chi-square statistic will be investigated, after which the assessment/comparison of all the flood frequency analysis results by utilising regression and descriptive statistics will follow.

5.1 CATCHMENT AND GIS DATA

5.1.1 Projections and data development

The developed catchment and spatial GIS data of the study area (SDF basin 9) are illustrated in Addendum A. The following Plates are included:

- Plate 1: Drainage regions of the study area
- Plate 2: Topography (DEM) of the study area
- Plate 3*:* Geological data of the study area
- Plate 4*:* Soil classification of the study area
- Plate 5*:* Land use and vegetation of the study area
- Plate 6*:* River network and water resources of the study area

5.1.2 Digital Elevation Model

A summary of the results representative of the main characteristics of the developed DEM of the study area (SDF basin 9) is listed in Table 5.1, whilst the frequency distribution of the altitude above sea level classes is summarised in Table 5.2. Figure 5.1 is illustrative of the histogram with the count (number based on 100 columns) of input pixel values on the ordinate and the input pixel values (altitude above sea level) on the abscissa, illustrating the class-to-class variation in reduced heights.

Table 5.1: Main characteristics of the developed DEM

Description	Value
Count (number) of input pixel values	68 770 241
Cell size (x, y)	22.5, 22.5
Minimum altitude above sea level (m)	997
Maximum altitude above sea level (m)	2 122
Mean altitude above sea level (m)	1 321.3
Standard deviation (s)	128.9

Table 5.2: Altitude above sea level frequency distribution

Altitude above sea level class (m)	Area (km²)	%-Distribution
997 – 1 200	6 592.6	18.9
1 200 – 1 400	18 443.2	53
1 400 – 1 600	9 273.2	26.7
1 600 –1 800	474.1	1.4
1 800 – 2 122	11.8	0.03
Total	**34 794.8**	**100**

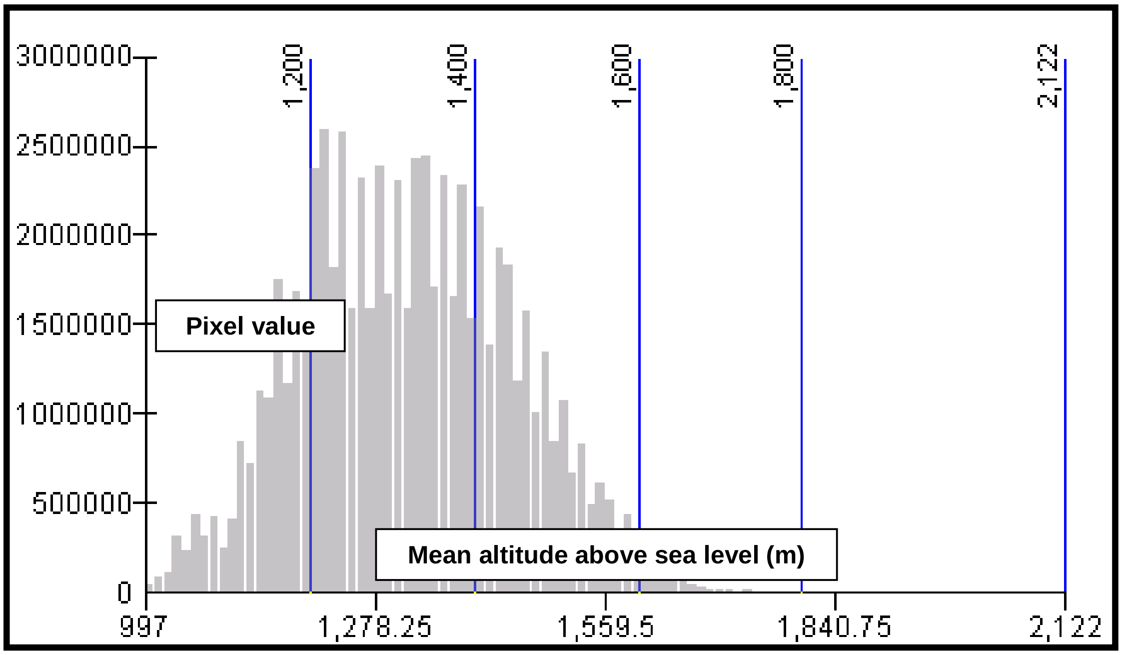

Figure 5.1: Histogram: Mean altitude above sea level classes

The class-to-class variation and frequency distribution of the altitude above sea level classes indicate that the topography is relatively flat and that flood peaks will be attenuated and translated in both magnitude and duration respectively.

5.1.3 Average catchment slope and centroid

The GIS-based (DEM) results of the average catchment slope calculations of the quaternary catchments within the study area are listed in Table 5.3.

Table 5.3: Average slope of quaternary catchments

Quaternary catchment	Average slope (%)	Quaternary catchment	Average slope (%)
C51A	3.637	C52A	5.044
C51B	5.223	C52B	5.501
C51C	3.245	C52C	5.102
C51D	3.054	C52D	3.709
C51E	3.185	C52E	3.776
C51F	4.361	C52F	3.659
C51G	4.091	C52G	3.266
C51H	5.220	C52H	2.825
C51J	5.245	C52J	2.589
C51K	3.452	C52K	2.716
C51L	3.267	C52L	2.416
C51M	3.640		

The results of the average catchment slope calculations of the specific catchments used in the flood frequency analyses based on the grid method, empirical equation and GIS are listed in Tables 5.4 to 5.6, whilst the least-square scatter plots are shown in Figures 5.2 and 5.3.

The developed DEM was used as the baseline data for the evaluation of and/or comparisons with the two other methods (refer to Table 5.7).

Table 5.4: Average catchment slope: Grid method

Catchment description	Area (km²)	Number of grid points (N)	Average slope (%)
C5R001	921.6	250	2.072
C5R002	10 259.9	3 400	3.060
C5R003	936.7	450	4.123
C5R004	6 330.9	2 220	2.919
C5R005	116.4	50	3.713
C5H003	1 650	450	4.123
C5H012	2 366.3	1 030	3.610
C5H015	6 009	2 220	2.919
C5H016	33 277.2	7 200	2.461
C5H018	17 360.3	3 300	2.211
C5H022	38	40	3.713
C5H054	687.8	305	2.479

Table 5.5: Average catchment slope: Empirical equation

Catchment description	Area (km²)	Length of contours (m)	Average slope (%)
C5R001	921.6	1 126 973.4	2.446
C5R002	10 259.9	18 823 502.6	3.669
C5R003	936.7	2 166 950.9	4.627
C5R004	6 330.9	10 776 515.8	3.404
C5R005	116.4	319 988.3	5.499
C5H003	1 650	3 817 275	4.627
C5H012	2 366.3	4 753 023	4.017
C5H015	6 009	10 227 318	3.404
C5H016	33 277.2	44 534 606.5	2.677
C5H018	17 360.3	19 454 617.6	2.241
C5H022	38	104 477.2	5.499
C5H054	687.8	940 089.2	2.734

Table 5.6: Average catchment slope: GIS data

Catchment description	Area (km²)	Average slope (%)
C5R001	921.6	3.054
C5R002	10 259.9	4.369
C5R003	936.7	5.044
C5R004	6 330.9	4.186
C5R005	116.4	5.501
C5H003	1 650	5.044
C5H012	2 366.3	4.771
C5H015	6 009	4.186
C5H016	33 277.2	3.598
C5H018	17 360.3	3.211
C5H022	38	5.501
C5H054	687.8	3.659

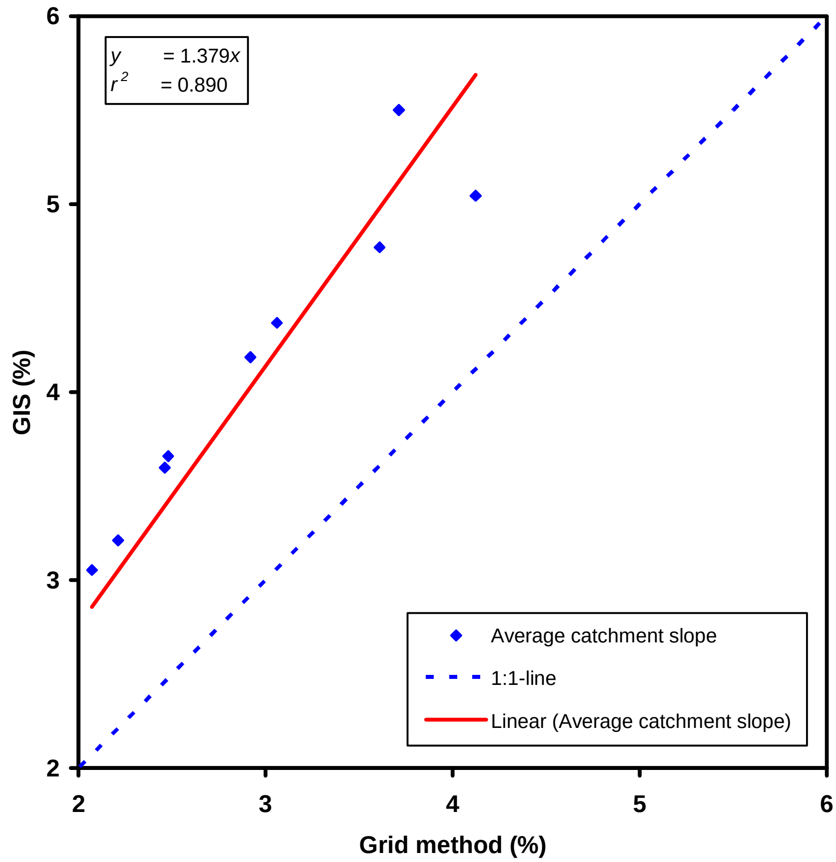

Figure 5.2: Average slope: GIS versus grid method

According to Alexander (1990), there must be at least 50 grid points within a catchment, whilst Van der Spuy and Rademeyer (2008) suggested that the minimum number of grid points in catchments smaller or larger than 10 km² must be 20 and 50 respectively. The number of grid points used varied from 40 to 7 200 with an overall average of 0.40 grid points per km².

The results indicated that either an increase or decrease in the number of grid points per km² does not necessarily guarantee higher accuracies when compared with the DEM (GIS) data. The grid method underestimated the average catchment slope in all the catchments under consideration compared to the DEM (GIS) data. The underestimation varied between 18.3% (0.48 grid points/km²) and 32.5% (0.34 grid points/km²). Thus, if the DEM (GIS) data are accepted as true and accurate, then the average slope calculation using the grid method must be increased with a value of between 18% and 32%. The inverse is also true. No definite relationship between the catchment area and these underestimations could be established. The coefficient of determination (r^2) of 0.890 is indicative of a high degree of association and confirms the usefulness of this method, especially for the development of slope frequency distribution classes used in the deterministic methods (ARM and RM). Although, the grid method is time-consuming and sensitive to biased user-input at different scale resolutions in terms of the grid density, extent of catchment areas and contour intervals used.

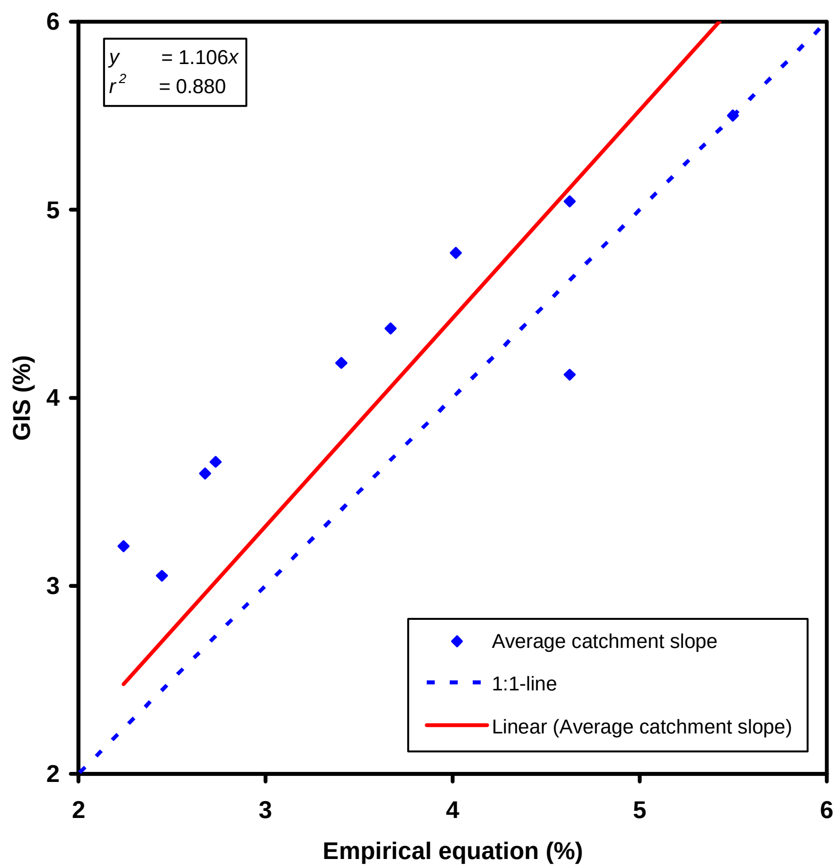

Figure 5.3: Average slope: GIS versus empirical equation

The results based on the empirical relationship (Equation 2.2, Chapter 2) compared well with the DEM (GIS) data (Figure 5.3). Since this equation is a function of the catchment area (*A*), contour interval (ΔH) and total length of all contour lines within the catchment (*M*), the influence of each variable was evaluated. The results showed that there is only a direct relationship between *A* and *M* for slopes steeper than 4%, since flatter slopes will result in a lower contour density and associated *M*-values. This trend was particularly evident for catchment areas exceeding 15 000 km². The empirical equation underestimated the average catchment slope in all the catchments under consideration. *M: A*-ratios of less than 1 500 resulted in an underestimation of between 20% and 30.2%, whilst *M: A*-ratios between 1 700 and 2 750 were associated with underestimations between 18.7% and 0%. Thus, the higher the *M:A*-ratios, the more accurate the empirical equation becomes. The coefficient of determination (r^2) of 0.880 is indicative of a high degree of association. This empirical equation, along with suitable tools in the ArcGIS™ environment, proved to be useful catchment parameter estimation tools.

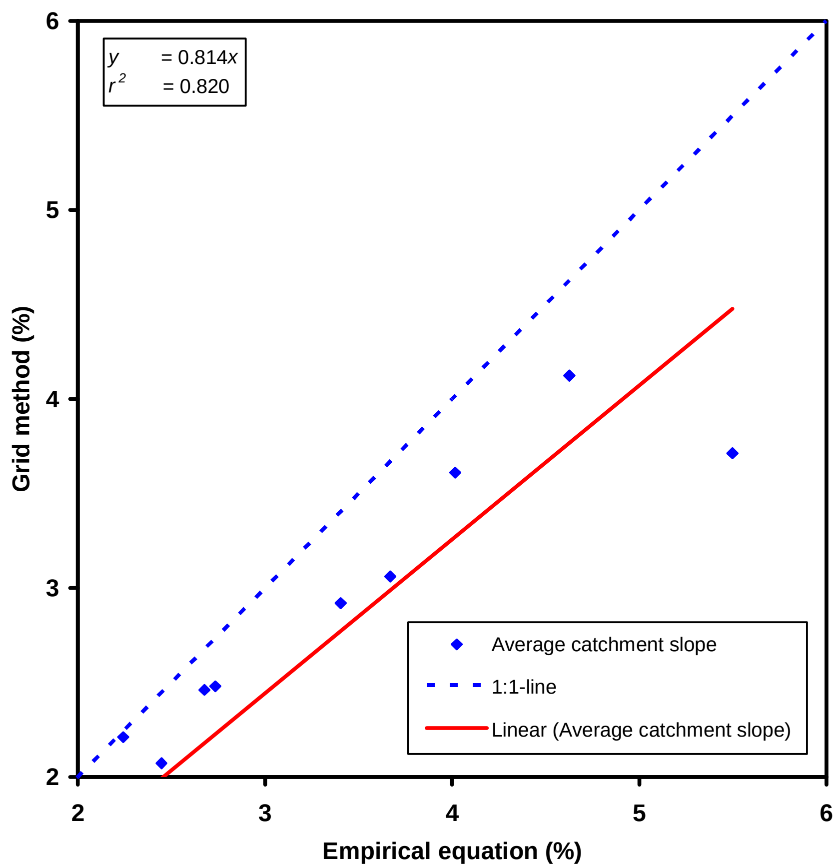

Figure 5.4: Average slope: Grid method versus empirical equation

Figure 5.4 provides a visual measure of performance between the grid method and empirical equation. The coefficient of determination (r^2) of 0.820 is indicative of a high degree of association. The visual comparison of results can be subjective. Therefore, the data pairs in each catchment under consideration were compared and evaluated using the array of conservation and regression statistics discussed in Chapter 2. Values of the *y*-intercept (*a*), slope (*b*), coefficients of efficiency (E_C) and determination (r^2), which provide quantitative amplification of the results discussed above, are reported in Table 5.7.

Table 5.7: Summary of GOF: GIS (DEM) baseline data

Conservation statistics	**Grid method**	**Empirical equation**	**GIS**
Observed mean (*x*)	3.12	3.74	4.34
Percentage-difference (%)	-28.11	-13.83	-
Observed standard deviation (S_x)	0.73	1.13	0.85
Percentage-difference (%)	-14.12	32.94	-
Regression statistics	**Grid method**	**Empirical equation**	**GIS**
Base constant/*y*-intercept (*a*)	0.93	1.74	-
Slope (*b*)	1.09	0.68	-
Coefficient of efficiency (E_C)	-1.42	0.22	-
Coefficient of determination (r^2)	0.89	0.88	-

The slope frequency distribution classes based on the developed DEM of the study area are listed in Table 5.8, whilst the slope frequency distribution classes of the specific catchments used in the flood frequency analyses based on the developed DEM are summarised in Table B.1, Addendum B.

Table 5.8: Slope frequency distribution

Catchment description	**Slope classification (%)**	**%-Distribution**
Study area (SDF basin 9)	0 - 3	62.8
	3 - 10	31.4
	10 - 30	4.8
	> 30	1

The results representing the centroid distance of each catchment, as discussed in Section 4.1.3, Chapter 4, are listed in Table 5.9.

Table 5.9: Centroid distances of catchments

Catchment description	Main watercourse length (L, km)	Centroid distance (L_C, km)	L_C: L-ratio	Average slope (%)
C5R001	86.44	53.18	0.62	3.054
C5R002	201.69	96.72	0.48	4.369
C5R003	53.80	31.11	0.58	5.044
C5R004	186.70	113.02	0.61	4.186
C5R005	16.20	7.90	0.49	5.501
C5H003	71.18	41.18	0.58	5.044
C5H012	86.96	47.62	0.55	4.771
C5H015	166.95	101.06	0.61	4.186
C5H016	430.72	237.14	0.55	3.598
C5H018	375.39	232.99	0.62	3.211
C5H022	7.91	3.86	0.49	5.501
C5H054	68.04	33.05	0.49	3.659

The results indicate that the centroid distance is influenced by the size and shape of the catchment area, but more importantly, influenced by the average catchment slope. The steeper the average catchment and main watercourse slope, the lower the L_C: L-ratio. The average L_C: L-ratio of 0.55 obtained from this evaluation confirms that the general assumption of using a L_C: L-ratio of between 0.5 and 0.6 in the various design flood estimation methods is sufficiently accurate.

5.1.4 Length and average slope of main watercourses

The main watercourse average slope results as determined in the DFET based on the Equal-area, 10-85 and Taylor-Schwarz methods are listed in Table 5.10, whilst the least-square scatter plots are shown in Figures 5.5 to 5.7. The longitudinal profile data are listed in Tables B.2 to B.13, Addendum B, and shown in Figures C.1 to C.12, Addendum C.

The degree of association between these methods is high, since the coefficient of determination varies between 0.995 and 0.998. In the past, preference was given to the 10-85 method, since the Equal-area method is largely a graphical procedure and the use of the Taylor-Schwarz method is not widely known in South Africa. The ease of use and numerical application of each method in the DFET is equal, thus the results as obtained with these method are the only selection criteria. The 10-85 method was used by default during this study, since it is part of the standard calculation procedures used in the SDF method.

Table 5.10: Average slope of main watercourses

Catchment description	Main watercourse length (L, km)	Average slope (%)		
		Equal-area	10-85	Taylor-Schwarz
C5R001	86.44	0.197	0.229	0.225
C5R002	201.69	0.113	0.133	0.108
C5R003	53.80	0.272	0.273	0.266
C5R004	186.70	0.102	0.131	0.113
C5R005	16.20	0.723	0.895	0.819
C5H003	71.18	0.195	0.232	0.195
C5H012	86.96	0.203	0.269	0.222
C5H015	166.95	0.099	0.139	0.103
C5H016	430.72	0.091	0.078	0.081
C5H018	375.39	0.073	0.079	0.075
C5H022	7.91	1.316	1.687	1.493
C5H054	68.04	0.252	0.261	0.283

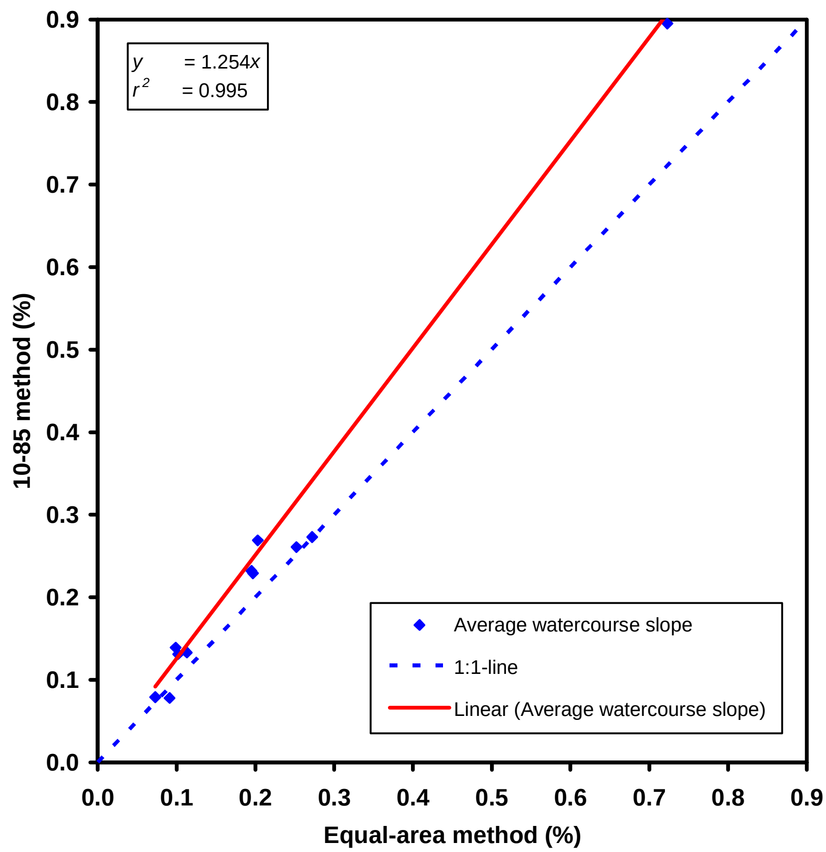

Figure 5.5: 10-85 method versus Equal-area method

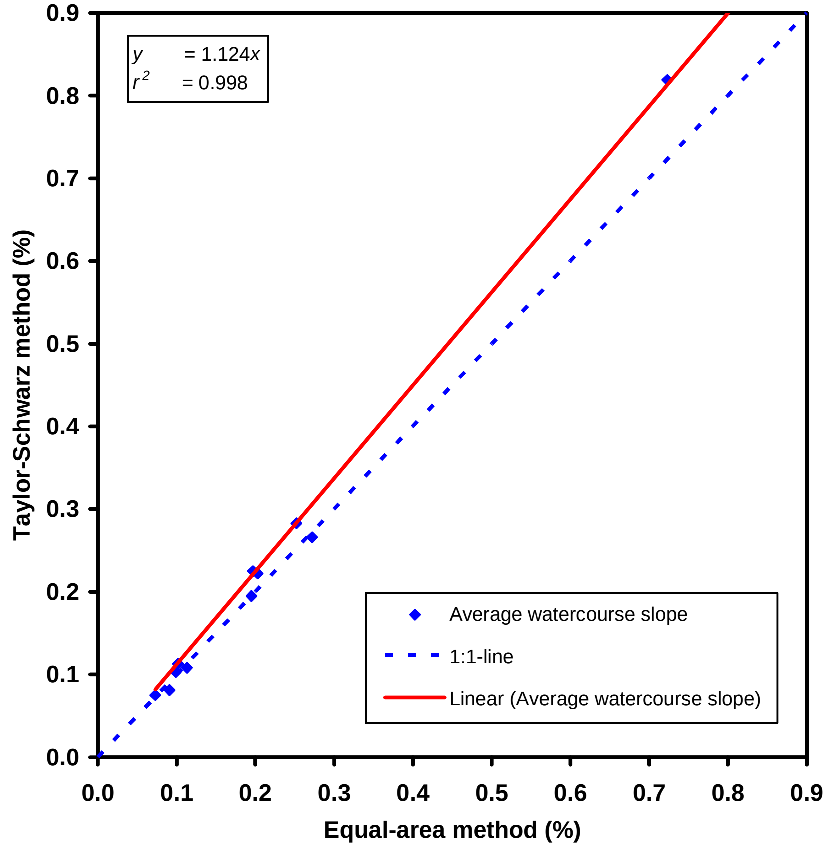

Figure 5.6: Taylor-Schwarz method versus Equal-area method

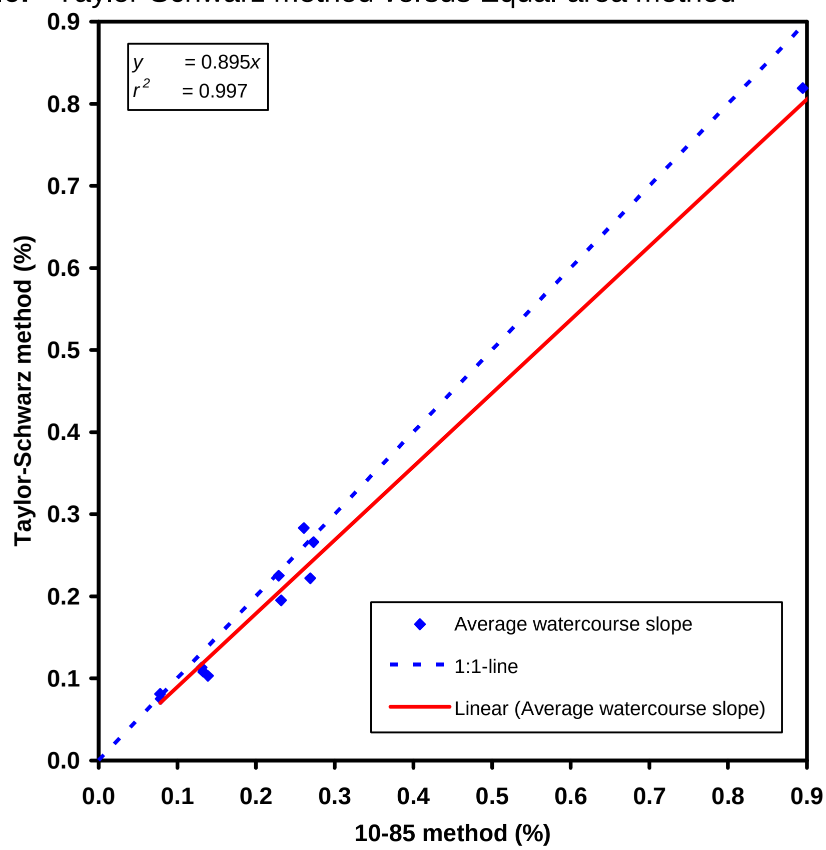

Figure 5.7: Taylor-Schwarz method versus 10-85 method

5.1.5 Soil classification

The percentage distribution of the different hydrological soil groups within the study area and the specific catchments used in the flood frequency analyses based on the binomial soil classification system are summarised in Tables 5.11 and 5.12.

Table 5.11: Hydrological soil groups of SDF basin 9

Soil form	Hydrological soil group	Area (km²)	%-Distribution
Clovelley	B	9 498.9	27.3
Hutton (Shorrocks)	A/B	8 072.4	23.2
Hutton (Mangano)	B/C	974.3	2.8
Sterkspruit	D	10 786.4	31
Vals River	C/D	5 462.8	15.7
	Total	**34 794.8**	**100**

Table 5.12: Hydrological soil groups of specific catchments

Catchment description	Hydrological soil groups	%-Distribution
C5R001	B	16.99
	C/D	28.75
	D	54.26
C5R002	A/B	2.70
	B	9.44
	C/D	2.82
	D	85.04
C5R003	C/D	100
C5R004	B	30.04
	C/D	69.96
C5R005	C/D	100
C5H003	C/D	100
C5H012	C/D	1.03
	D	98.97
C5H015	B	30.04
	C/D	69.96
C5H016	A/B	20.23
	B	28.55
	B/C	2.37
	C/D	16.41
	D	32.45
C5H018	A/B	10.52
	B	47.42
	B/C	0.58
	C/D	29.79
	D	11.69
C5H022	C/D	100
C5H054	B	74.19
	C/D	25.81

The results as contained in Tables 5.11 and 5.12 show that the infiltration and permeability rates are different in the two tertiary drainage regions, i.e. the RRC (C5R001, C5R002, C5H012 and C5H016) and MRC (C5R003, C5R004, C5R005, C5H003, C5H015, C5H018 and C5H054). The upper reaches of the RRC are dominated by semi-permeable (C/D) and impermeable (D) soil forms, whilst their dominance is less prevalent downstream of the confluence with the Modder River. Permeable (B) and semi-permeable (C/D) soil forms are the best presented in the MRC.

Thus, the hydrological response in each catchment will be different due to the difference in soil permeability which controls the infiltration rate and consequently the balance of precipitation that constitutes surface run-off and contributes to the flood peak. Apart from the permeability associated with each hydrological soil group, the volume, duration and intensity of precipitation should also be considered, since most of the effective precipitation and associated run-off are produced after the saturation of soil is reached.

5.1.6 Land use and vegetation

5.1.6.1 Reclassification and grouping of land use and vegetation

The percentage distribution of the lake, rural and urban components within the study area, as well as their association with the specific catchments used in the flood frequency analyses are listed in Table B.14, Addendum B.

Tables 5.13 and 5.14 represent the reclassification of land use and vegetation data of the study area according to the standard classification classes as used in the deterministic methods, whilst Tables B.15 and B.16, Addendum B, provide a summary of the standard classification classes applicable to the specific catchments used in the flood frequency analyses.

It is evident from all these data sets that the study area, as well as the individual catchments, can be classified as rural. Grasslands dominate the rural component, whilst residential areas dominate the urban component. The effect of the different land uses on the attenuation and translation of flood peaks will be discussed in Section 5.5.

Table 5.13: Urban component: Standard land-use classification classes

Standard classification	Original land-use description	%-Distribution
City centre	Commercial and mercantile Commercial, education, health and information technology	4.93
Heavy industry	Heavy industrial and transport areas	2.49
Light industry	Light industrial and transport areas	10.43
Residential (Flats)	Flats and hostels	0.57
Residential (Houses)	Residential houses Residential and formal townships Residential and informal squatter camps Residential and informal townships	51.50
Suburban	Formal suburban areas	30.08
	Total	**100**

Table 5.14: Rural component: Standard land-use classification classes

Standard classification	Original land-use description	%-Distribution
Cultivated land	Cultivated land (Commercial dry-land) Cultivated land (Commercial irrigation) Cultivated land (Subsistence dry-land) Cultivated land (Subsistence irrigation)	10.98
Grasslands	Improved natural grassland Smallholdings and grassland Unimproved natural grassland Wetlands	58.42
Light bush and farmlands	Degraded shrubland and low fynbos Shrubland and low fynbos Smallholdings, thickets and bushland	20.42
No vegetation	Bare rock and soil Mines and quarries Mines and quarries (Waste dumps)	0.83
Thick bush and plantations	Degraded thickets and bushland Forest, plantations and woodlands Thickets, bushland and high fynbos	9.35
	Total	**100**

5.1.6.2 Homogeneous veld-type regions

The following generalised veld-type regions were identified in the study area and were used in the deterministic (LRH and SUH) and empirical (MIPI) methods:

- Grassland of the interior plateau (Region 4).
- Karoo (Region 6).
- False Karoo (Region 7).

The details concerning these identified veld-type regions, both at a study area and specific catchment level, are listed in Table 5.15. Figure 5.8 is illustrative of these three regions within the study area.

Table 5.15: Percentage distribution of homogeneous veld-type regions

Catchment description	%-Distribution of homogeneous veld-type regions		
	Region 4 (Grassland)	**Region 6 (Karoo)**	**Region 7 (False Karoo)**
Study area	23.34	16.60	60.06
C5R001	60.27	-	39.73
C5R002	6.15	-	93.85
C5R003	100	-	-
C5R004	97.29	-	2.71
C5R005	100	-	-
C5H003	100	-	-
C5H012	3.21	-	96.79
C5H015	97.29	-	2.71
C5H016	24.40	12.80	62.80
C5H018	43.15	10.82	46.03
C5H022	100	-	-
C5H054	78	-	22

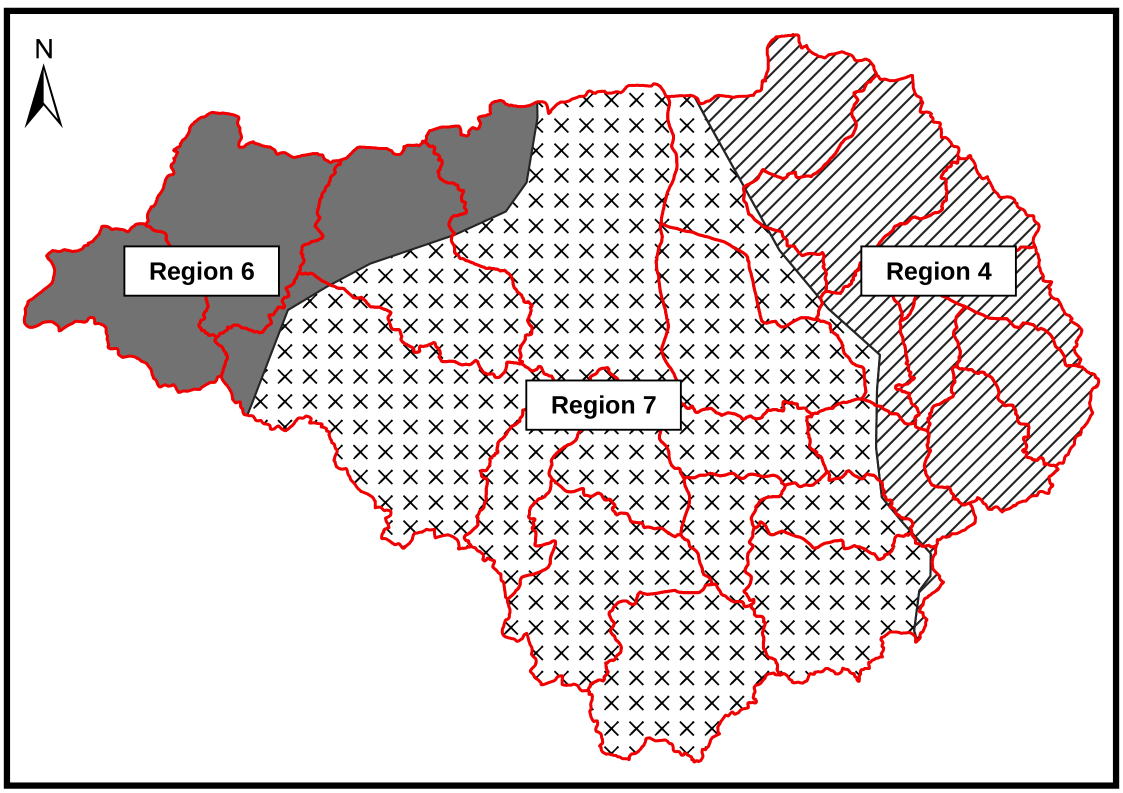

Figure 5.8: Homogeneous veld-type regions

5.1.6.3 Kovács flood regions

Three Kovács flood regions were identified in the study area and were used in the application of the empirical (RMF) method. The details concerning these identified flood regions, both at a study area and specific catchment level, are listed in Table 5.16. Figure 5.9 is illustrative of these three regions within the study area.

Table 5.16: Percentage distribution of Kovács flood regions

Catchment description	%-Distribution of Kovács flood regions		
	K3-Region	K4-Region	K5-Region
Study area	30.52	26.72	42.76
C5R001	-	-	100
C5R002	-	5.47	94.53
C5R003	-	-	100
C5R004	-	35.79	64.21
C5R005	-	-	100
C5H003	-	-	100
C5H012	-	-	100
C5H015	-	35.79	64.21
C5H016	27.35	27.93	44.72
C5H018	28.48	43.57	27.95
C5H022	-	-	100
C5H054	-	31.71	68.29

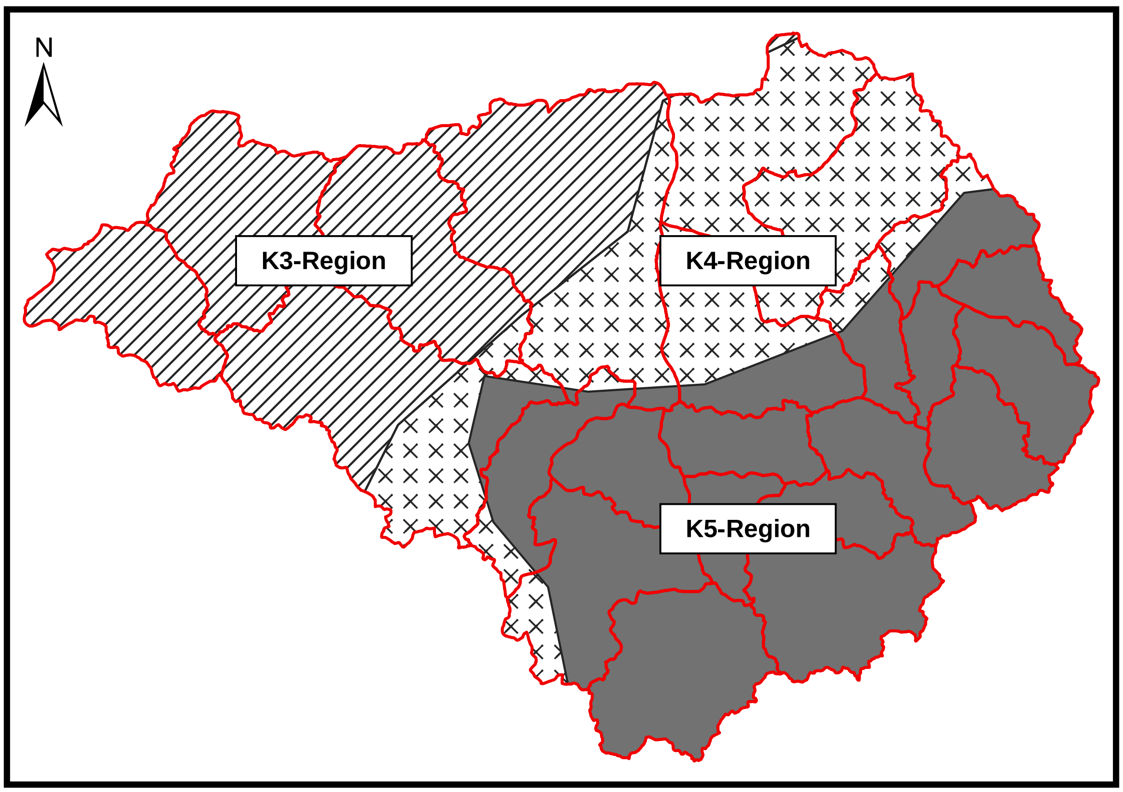

Figure 5.9: Kovács flood regions

5.2 METEOROLOGICAL DATA

5.2.1 Precipitation database

The SAWS and TR102 precipitation databases are not included in this report, due to the extent thereof, although both are included in the DFET enabling the user to have direct access to all the relevant information. The selection of the single precipitation stations used to evaluate, calibrate and verify the SDF method in each quaternary catchment under consideration is listed in Tables 5.17 and 5.18. Table 5.17 is only representative of the study area, whilst Table 5.18 shows the precipitation stations used in the rest of South Africa in this study. The SDF basin numbers are indicated in brackets in the latter table.

Table 5.17: Selected SDF precipitation stations used in SDF basin 9

Catchment description	Station number	MAP (mm)		Record length (*N*, years)
		Single SDF station	Thiessen polygon	
C5R001	0261750W	497	488	55
C5R002	0232018W	420	420	86
C5R003	0232123W	555	549	88
C5R004	0261523W	518	518	94
C5R005	0262734W	649	660	43
C5H003	0232123W	555	549	88
C5H008	0232018W	420	420	86
C5H012	0231395W	454	444	71
C5H015	0261523W	518	518	94
C5H016	0291899W	433	429	79
C5H018	0260163W	461	461	74
C5H022	0262734W	649	660	43
C5H054	0261523W	518	523	94

Table 5.18: Selected SDF precipitation stations used in South Africa

Catchment description	Station number	MAP (mm)		Record length (*N*, years)
		Single SDF station	Thiessen polygon	
A2H012 (1)	0476396W	697	692	92
A4H002 (2)	0588721W	635	637	81
A6H006 (2)	0589670W	625	630	82
B4H003 (4)	0516701W	712	702	50
B7H004 (5)	0594696W	1 230	1 086	64
C3H003 (8)	0434359W	527	525	77
C4H001 (7)	0294500W	553	568	76
C4H002 (7)	0294500W	553	541	76
C8H001 (6)	0369238W	691	680	92
C8H003 (6)	0369238W	691	647	92
D1H001(10)	0147777W	482	460	73
D1H004 (10)	0147777W	482	502	73

Table 5.18: Selected SDF precipitation stations used in South Africa (Continued)

Catchment description	Station number	MAP (mm)		Record length (*N*, years)
		Single SDF station	Thiessen polygon	
D1H005 (11)	0207391W	682	656	58
D2H001 (10)	0263859W	727	742	94
E2H003 (16)	0085309W	253	234	99
G1H008 (17)	0042227W	415	554	98
H3H001 (18)	0022113W	812	812	80
H7H004 (18)	0025414W	333	333	74
Q1H001 (21)	0146382W	378	343	81
Q7H003 (21)	0146382W	378	359	81
Q9H004 (21)	0078453W	561	631	89
Q9H008 (21)	0078453W	561	679	89
Q9H010 (21)	0146382W	378	398	81
Q9H012 (21)	0146382W	378	366	81
R1H001 (22)	0078700W	624	791	41
T3H004 (23)	0208840W	773	766	40
V2H002 (26)	0268441W	962	1 012	61
V6H002 (26)	0334825W	907	856	79
W5H005 (28)	0444203W	800	832	80
W5H006 (28)	0444540A	887	887	42
X2H010 (29)	0518460W	1 305	1 305	47

5.2.2 Averaging of precipitation depths

The results of the averaged design precipitation depth calculations applicable to the study area are listed in Tables 5.19 and 5.20. The station number, MAP and weighted area associated with each station are summarised in Table B.17, Addendum B.

Table 5.19: MAP of specific catchments within SDF basin 9

Catchment description	MAP (mm)		Number of precipitation stations (N_i)
	Arithmetic mean	Thiessen polygon	
Study area	439	424	185
C5R001	492	488	7
C5R002	421	420	61
C5R003	553	549	8
C5R004	530	518	47
C5R005	642	660	3
C5H003	553	549	8
C5H012	448	444	11
C5H015	530	518	47
C5H016	440	429	183
C5H018	479	461	93
C5H022	686	660	3
C5H054	542	523	13

Table 5.20: SAWS design precipitation depths of SDF basin 9

Arithmetic mean method							
MAP (mm)	439						
2-year Mean of annual daily maxima precipitation (*M*)	45						
Days of thunder per year (*R*)	57.1						
Duration (days)	**Return period (years)**						
	2	**5**	**10**	**20**	**50**	**100**	**200**
1	45	61.4	72.9	84.4	99.8	111.9	124.5
2	55.6	76.3	90.8	105.4	125.2	140.8	157.1
3	61.5	84.7	101.1	117.7	140.5	158.7	177.8
7	75.8	105.7	127.5	150	181.9	208	236.1
Thiessen polygon method							
MAP (mm)	424						
2-year Mean of annual daily maxima precipitation (*M*)	44.7						
Days of thunder per year (*R*)	56.7						
Duration (days)	**Return period (years)**						
	2	**5**	**10**	**20**	**50**	**100**	**200**
1	44.7	61.2	72.6	84.1	99.6	111.7	124.2
2	55.1	75.7	90.1	104.7	124.6	140.2	156.5
3	60.7	83.8	100.2	116.8	139.7	158	177.2
7	74.6	104.5	126.3	148.9	181	207.3	235.8

Figure 5.10 is illustrative of the Thiessen polygon weighted areas and location of the precipitation stations within the study area.

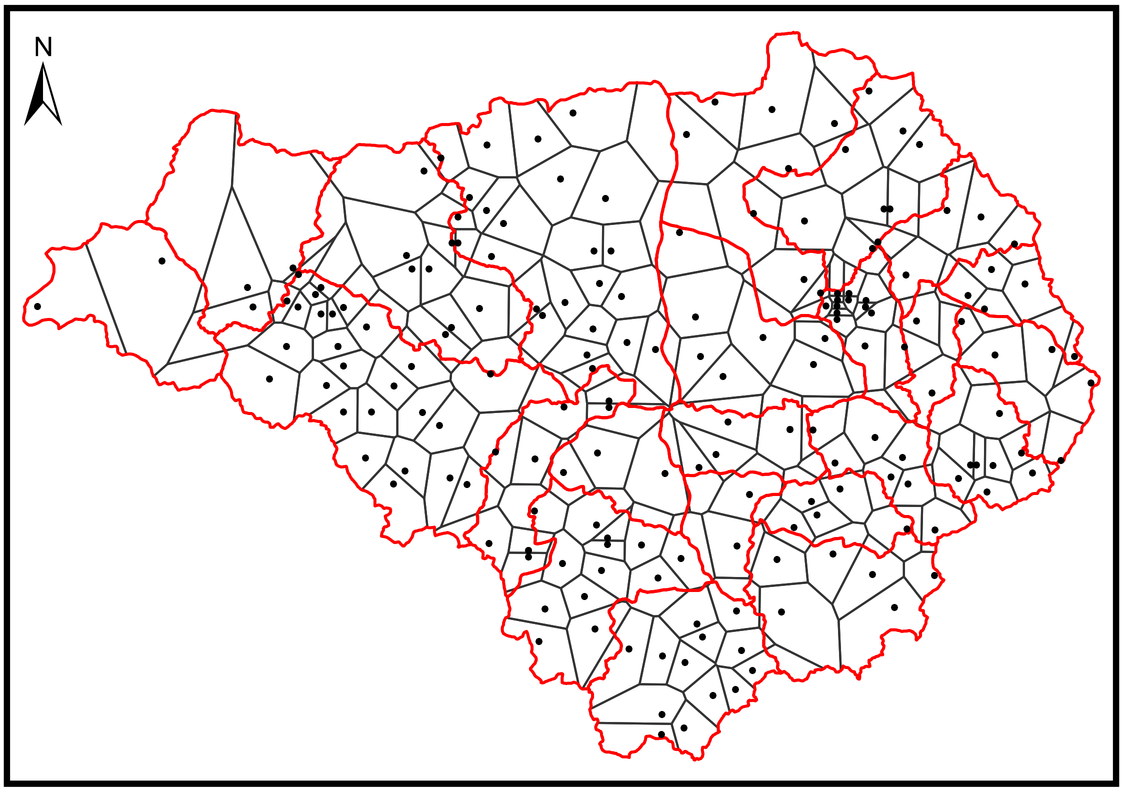

Figure 5.10: SDF basin 9: Thiessen polygons and precipitation stations

The number of precipitation stations used for averaging the precipitation varied from catchment to catchment with an overall average of one station per 100 km². The Arithmetic mean values exceeded the Thiessen polygon values in all the catchments, except in C5R005. However, this was also the only catchment where the polygons and isohyets were based on precipitation stations within and outside the catchment boundary. The percentage differences between the arithmetic mean and Thiessen polygon methods varied between -3% and 4%. Despite these percentage differences, the coefficient of determination (r^2) of 0.982 is indicative of a high degree of association between these two methods. This also confirmed the even areal distribution of the precipitation stations and the relative flat topography of the study area.

5.2.3 Critical storm duration precipitation

The critical storm duration precipitation depths based on the various DDF relationships as applicable to the specific catchments used in the flood frequency analyses are listed in Tables 5.21 to 5.23.

Table 5.21: Precipitation depths for $T_C \leq 6$ hours

Catchment description	**C5H022**						
Time of concentration	1.6 hours						
Return period (years)	**2**	**5**	**10**	**20**	**50**	**100**	**200**
Precipitation depth (mm) (Midgley and Pitman)	35.4	48.2	61	75.3	97.8	120.4	135.4
Precipitation depth (mm) (Hershfield)	28.7	48.4	63.3	78.3	98	112.9	127.8

The results contained in Table 5.21 indicate that the DDF relationship based on LEV1 distributions developed by Midgley and Pitman (1978) tends to slightly overestimate the design precipitation depths for the 100- and 200-year return periods compared to the DDF relationship based on the modified Hershfield equation. The degree of association between these two methods is, however, high, since the overall coefficient of determination equals 0.985.

Table 5.22: Precipitation depths for $6 < T_C \leq 24$ hours

Catchment description	**C5R001**						
Time of concentration	21.3 hours						
Return period (years)	**2**	**5**	**10**	**20**	**50**	**100**	**200**
Precipitation depth (mm) (Midgley and Pitman)	41.8	56.9	72.1	89	115.7	142.4	160.2
Precipitation depth (mm) (Hershfield/SAWS)	43.7	61	73.4	85.8	102.7	115.9	129.6
Catchment description	**C5R003**						
Time of concentration	13.9 hours						
Return period (years)	**2**	**5**	**10**	**20**	**50**	**100**	**200**
Precipitation depth (mm) (Midgley and Pitman)	43.6	59.4	75.2	92.8	120.6	148.5	167
Precipitation depth (mm) (Hershfield/SAWS)	42.3	64.2	80.5	96.8	118.8	135.7	152.9
Catchment description	**C5H003**						
Time of concentration	18.3 hours						
Return period (years)	**2**	**5**	**10**	**20**	**50**	**100**	**200**
Precipitation depth (mm) (Midgley and Pitman)	45.2	61.6	77.9	96.2	125.1	153.9	173.2
Precipitation depth (mm) (Hershfield/SAWS)	45.2	65	79.7	94.2	114.1	129.7	145.8
Catchment description	**C5H012**						
Time of concentration	20.2 hours						
Return period (years)	**2**	**5**	**10**	**20**	**50**	**100**	**200**
Precipitation depth (mm) (Midgley and Pitman)	38.5	52.4	66.4	81.9	106.5	131.1	147.5
Precipitation depth (mm) (Hershfield/SAWS)	41.2	58.3	70.5	82.7	99.1	111.8	124.8
Catchment description	**C5H054**						
Time of concentration	16.9 hours						
Return period (years)	**2**	**5**	**10**	**20**	**50**	**100**	**200**
Precipitation depth (mm) (Midgley and Pitman)	43.2	58.8	74.4	91.8	119.4	146.9	165.3
Precipitation depth (mm) (Hershfield/SAWS)	44.3	64.9	79.8	94.7	114.6	130	145.5

The results contained in Table 5.22 show that the DDF (LEV1, Midgley & Pitman) relationship tends to slightly overestimate the design precipitation depths for the 50-, 100- and 200-year return periods compared to the DDF relationship based on the linear interpolation between the modified Hershfield equation and the 1-day point precipitation depths from the SAWS database. The coefficient of determination (r^2) equals a constant value of ± 0.905 for each return period ranging from two to 200 years and is indicative of a high degree of association. This also confirms that a constant relationship exists between these two methods within the critical storm duration range under consideration.

The high degree of association between these methods does not necessarily guarantee acceptable accuracy, since both methods have shortcomings, as indicated in Section 2.3.4, Chapter 2.

Table 5.23: Precipitation depths for 24 < $T_C \leq$ 168 hours

Catchment description	**C5R002**						
Time of concentration	50.5 hours						
Return period (years)	**2**	**5**	**10**	**20**	**50**	**100**	**200**
Precipitation depth (mm) (Midgley and Pitman)	41.2	56.1	71.1	87.7	114	140.4	157.9
Precipitation depth (mm) (SAWS)	53.6	73.6	87.5	101.5	120.4	135.3	150.7
Catchment description	**C5R004**						
Time of concentration	47.9 hours						
Return period (years)	**2**	**5**	**10**	**20**	**50**	**100**	**200**
Precipitation depth (mm) (Midgley and Pitman)	48.6	66.1	83.7	103.4	134.4	165.4	186
Precipitation depth (mm) (SAWS)	61.1	82.3	97	111.9	132	147.8	164.2
Catchment description	**C5H015**						
Time of concentration	43 hours						
Return period (years)	**2**	**5**	**10**	**20**	**50**	**100**	**200**
Precipitation depth (mm) (Midgley and Pitman)	47.9	65.3	82.6	102	132.6	163.2	183.6
Precipitation depth (mm) (SAWS)	58.5	78.8	93	107.3	126.7	141.9	157.7
Catchment description	**C5H016**						
Time of concentration	111.1 hours						
Return period (years)	**2**	**5**	**10**	**20**	**50**	**100**	**200**
Precipitation depth (mm) (Midgley and Pitman)	46.1	62.8	79.5	98.1	127.6	157	176.6
Precipitation depth (mm) (SAWS)	66.6	92.4	110.9	129.7	156.1	177.4	200
Catchment description	**C5H018**						
Time of concentration	99.6 hours						
Return period (years)	**2**	**5**	**10**	**20**	**50**	**100**	**200**
Precipitation depth (mm) (Midgley and Pitman)	48.2	65.6	83	102.5	133.2	163.9	184.4
Precipitation depth (mm) (SAWS)	68.7	93.9	111.5	129.3	153.5	172.7	192.7

The results contained in Table 5.23 confirm that the DDF (LEV1, Midgley & Pitman) relationship tends to overestimate the design precipitation depths for the 50-, 100- and 200-year return periods up to a critical storm duration of 50 hours compared with the linear interpolated SAWS *n*-day point precipitation depths, whilst it underestimates all the design precipitation depths with a critical storm duration in excess or exceeding 100 hours.

The degree of association between these two methods is poor, since the coefficient of determination varies between 0.597 at a 2-year return period and decreases to a low value of 0.300 at a 200-year return period in some cases.

The critical storm duration precipitation depths based on the DDF relationships (RLMA&SI approach results as obtained from Parak and Pegram (2006) and results based on the modified Hershfield equation and/or SAWS daily precipitation data), as applicable to the randomly selected SDF basins, are listed in Tables 5.24 to 5.26.

Table 5.24: SDF precipitation depths for $T_C \leq 6$ hours

SDF basin	Catchment description	T_C (hours)	DDF relationship	Design precipitation depths (mm)				
				P_{10}	P_{20}	P_{50}	P_{100}	P_{200}
2	A6H006	4.4	RLMA&SI	72	83.8	100.3	113.5	127.5
			Hershfield	77.1	95.3	119.3	137.4	155.6
5	B7H004	3.7	RLMA&SI	94.6	112.4	148.8	160.8	185.3
			Hershfield	110.8	136.8	171.3	197.4	223.5
17	G1H008	4	RLMA&SI	41.2	46.2	52.6	57.4	62.1
			Hershfield	36.7	45.4	56.8	65.5	74.1
18	H7H004	2.3	RLMA&SI	49.3	59.6	74.7	87.5	101.6
			Hershfield	42.1	52	65.1	75	84.9
28	W5H006	5	RLMA&SI	82.4	98	120.8	140.1	161.4
			Hershfield	85.3	105.4	132	152.1	172.2
29	X2H010	3.3	RLMA&SI	82.3	97.8	120.5	139.8	161.1
			Hershfield	86.9	107.3	134.4	154.8	175.3

The results contained in Table 5.24 indicate that the modified Hershfield equation as used in the SDF method tends to slightly underestimate the design precipitation depths for the return periods ranging from 10 to 200 years in basins 17 and 18, whilst the precipitation depths are overestimated in the remaining basins.

The degree of association between these two methods is high, since the coefficient of determination varies between 0.984 at a 10-year return period and decreases to 0.923 at a 200-year return period.

Table 5.25: SDF precipitation depths for 6 < $T_C \leq$ 24 hours

SDF basin	Catchment description	T_C (hours)	DDF relationship	Design precipitation depths (mm)				
				P_{10}	P_{20}	P_{50}	P_{100}	P_{200}
1	A2H012	18	RLMA&SI	92.9	109.4	133.4	153.2	175
			Hershfield/SAWS	81.3	97.6	120.6	138.2	158.9
2	A4H002	18.1	RLMA&SI	94.3	109.7	131.2	148.6	166.9
			Hershfield/SAWS	92.6	109.8	133.3	151.8	171
4	B4H003	19.6	RLMA&SI	85.1	96.6	115.2	124.1	136.2
			Hershfield/SAWS	75.2	88.2	105.6	119.3	133.4
6	C8H003	19.2	RLMA&SI	83.5	95.4	111.6	124.4	137.7
			Hershfield/SAWS	79	92.4	110.3	124.2	138.4
9	C5H003	18.3	RLMA&SI	80.3	92.6	109.1	121.9	135.1
			Hershfield/SAWS	78.5	93	112.7	128	143.8
	C5H008	11.9	RLMA&SI	65.8	76.4	90.9	102.5	114.7
			Hershfield/SAWS	71	86.1	106.2	121.6	137.3
10	D1H001	19.9	RLMA&SI	66.9	76	87.8	96.5	105.3
			Hershfield/SAWS	68.5	79.7	94.7	106.2	117.8
18	H3H001	9.5	RLMA&SI	55.4	67.4	85.3	100.8	118.2
			Hershfield/SAWS	56.6	69.7	87.5	101.6	116.1
21	Q1H001	18	RLMA&SI	54.7	63.2	74.7	83.9	93.1
			Hershfield/SAWS	55	63.7	75.2	84.2	93.4
	Q9H004	6.3	RLMA&SI	60	70.2	84.5	95.9	108
			Hershfield/SAWS	67	82.7	103.5	119.2	134.9
	Q9H008	12.7	RLMA&SI	63.9	74.8	89.9	102.1	114.9
			Hershfield/SAWS	70.8	85.6	105.5	120.9	136.6
22	R1H001	6.2	RLMA&SI	62.2	72.8	87.5	99.3	111.9
			Hershfield/SAWS	75	92.7	115.9	133.6	151.2
23	T3H004	18.8	RLMA&SI	97.6	115.1	140.2	161.3	184.4
			Hershfield/SAWS	87.8	104.1	126.6	144.5	163.1
26	V2H002	18.9	RLMA&SI	98.7	115.1	138	156.7	176.7
			Hershfield/SAWS	86.5	102.5	124.7	142.3	160.7
28	W5H005	17.8	RLMA&SI	111.3	132.3	162.9	189	217.7
			Hershfield/SAWS	95	114.4	141.7	164.1	187.9

The results shown in Table 5.25 tend to follow in general a similar trend as the results in Table 5.24, although there are some differences. The DDF (Hershfield/SAWS) relationship tends to overestimate the design precipitation depths for the whole range of return periods under consideration compared to the DDF (RLMA&SI) relationship in basins 9, 10, 18, 21 and 22. The design precipitation depths are underestimated in the remaining basins, except for basins 2, 6 and 21 (Q1H001). The latter basins are characterised by almost a perfect fit.

The degree of association is acceptable, with r^2-values varying from 0.816 at a 10-year return period and decrease to 0.683 at a 200-year return period.

Table 5.26: SDF precipitation depths for 24 < T_C ≤ 168 hours

SDF basin	Catchment description	T_C (hours)	DDF relationship	Design precipitation depths (mm)				
				P_{10}	P_{20}	P_{50}	P_{100}	P_{200}
6	C8H001	122	RLMA&SI	131.8	152.5	179.3	201.3	224.5
			SAWS	126.6	141	159	172.1	184.7
7	C4H001	34	RLMA&SI	92.1	106.1	125.1	139.7	154.7
			SAWS	93.7	108.5	128.8	144.9	161.9
	C4H002	111	RLMA&SI	123.2	142.1	167.6	188.7	209.8
			SAWS	130.3	149.5	175.2	195.2	215.6
8	C3H003	78	RLMA&SI	110	127.1	149.8	167.7	184.9
			SAWS	113.6	129.6	150.2	165.5	180.7
9	C5H015	43	RLMA&SI	93.3	107.5	126.9	141.5	157
			SAWS	83.6	96.2	113.2	126.4	140.1
10	D2H001	106	RLMA&SI	117.7	136.7	162.2	183.4	205.6
			SAWS	111	127.2	149.2	166.2	183.6
11	D1H005	60	RLMA&SI	101.4	118.8	142.2	161.4	182.4
			SAWS	91.3	106	126.7	143.6	161.7
16	E2H003	59	RLMA&SI	54.9	63.1	74.3	82.6	91.5
			SAWS	71	82	96.5	107.3	118.3
21	Q7H003	59	RLMA&SI	106.8	125.1	149.9	170.5	191.8
			SAWS	70.8	81.8	96.5	107.8	119.2
	Q9H010	108	RLMA&SI	148	179.3	226.8	267.8	313.2
			SAWS	82.6	95.5	112.6	125.8	139.1
	Q9H012	85	RLMA&SI	130.9	153.9	184.5	210	236.3
			SAWS	77.9	90.1	106.3	118.8	131.4
26	V6H002	48	RLMA&SI	139.2	166.6	207.8	243.8	283.7
			SAWS	125.6	142.8	165.3	182.4	199.5

The results contained in Table 5.26 are characterised by a low degree of association, especially due to the RLMA&SI approach resulting in higher design precipitation depths for the 50- to 200-year return periods. This was especially the case for critical storm durations exceeding 50 hours, whilst the RLMA&SI design precipitation depths in basins 21 and 26 are questionable.

The RLMA&SI design precipitation depths, as indicated before, were obtained from the previous research conducted by Parak and Pegram (2006) and are generated by the software program, *Design Rainfall Estimation in South Africa* in their study. A number of locations (depending on the size of the catchment) along the main watercourse within the catchment were chosen for which design precipitation depth estimates based on the RLMA&SI approach were obtained. The average depth for each catchment was computed and thereafter the intensity, duration and frequency relationships were derived by fitting a simple power-law function of storm duration to the mean precipitation depths.

Thus, although Parak and Pegram (2006) averaged the precipitation depths following a different approach, the overall degree of association in Tables 5.24, 5.25 and 5.26 is acceptable. It also serves as confirmation that the new single precipitation stations (Tables 5.17 and 5.18) selected for the evaluation and calibration of the SDF method at a single or multiple quaternary catchment level is sufficiently representative of the average meteorological conditions at this level, or even at a smaller scale.

Since all the above-mentioned DDF relationships, except the RLMA&SI approach, are used as standard precipitation input data to the deterministic and empirical methods, the question arises whether it must remain as the standard procedure or whether the SAWS *n*-day point precipitation database in conjunction with the software program, *Design Rainfall Estimation in South Africa* should rather be used. If not, this could result in either under- or overestimations of the design flood, depending on the catchment area and critical storm duration under consideration.

5.2.4 Area reduction factors

The plotting results of the time of concentration against the catchment area in the various catchments under consideration were characterised by points clustered about a curve to which a power-law relationship could be fitted. The power-law fitted trendline with a coefficient of determination equal to unity represented the relationship shown in Equation 2.19. The results also showed a high degree of association between Equation 2.19 and the clustered points, with r^2 equal to 0.928. The power-law relationship associated with r^2 equal to 0.928 is shown in Equation 5.1 which provides a good indication of the time of concentration associated with any catchment area under consideration. Equation 5.1 can be substituted in Equation 2.19 and simplified to result in Equation 5.2:

$$T_C = 0.2284A^{0.5957} \qquad (5.1)$$

$$ARF = \left(-6944.3\ln A + 115731.9\right)^{0.4} \qquad (5.2)$$

Where:

ARF = Area reduction factor (%)

A = Catchment area (km²)

T_C = Time of concentration (hours)

A summary of the applicable results is shown in Table 5.27. Figures 5.11 and 5.12 illustrate the fitted power-law relationship and ARF diagram respectively.

Table 5.27: Comparison of ARF results: Equations 2.19 and 5.2

Catchment description	Area (km²)	T_C (hours)	ARF (%)	
			Equation 2.19	**Equation 5.2**
A2H012	2 551	18	80.6	82.2
A4H002	1 777	18.1	83.1	83.5
A6H006	168	4.4	91.1	91.5
B4H003	2 240	19.6	81.9	82.7
B7H004	136	3.7	91.6	92.2
C3H003	10 990	78	78.1	76.5
C4H001	5 590	34	78.4	79.2
C4H002	17 599	111	76.6	74.5
C5H003	1 650	18.3	83.6	83.8
C5H008	593	11.9	88.1	87.4
C5H012	2 366.3	20.2	81.7	82.5
C5H015	6 009	43	79.2	78.9
C5H016	33 277.2	111.1	71.5	71.6
C5H018	17 360.3	99.6	76.1	74.5
C5H022	38	1.6	95.1	96.1
C5H054	687.8	16.9	88.8	86.9
C5R001	921.5	21.3	88.2	85.9
C5R002	10 259.9	50.5	76.1	76.7
C5R003	936.7	13.9	86	85.8
C5R004	6 330.9	47.9	79.4	78.7
C5R005	116.4	3.5	92.2	92.7
C8H001	15 673	122	78.1	75
C8H003	806	19.2	88.5	86.3
D1H001	2397	19.9	81.5	82.4
D1H005	10 680	60	76.8	76.6
D2H001	13 421	106	78.4	75.6
E2H003	24 044	59	70.1	73.1
G1H008	395	4	85.4	88.8
H3H001	593	9.5	87	87.4
H7H004	28	2.3	98.3	97
Q1H001	9 091	18	70.7	77.2
Q7H003	18 534	59	72.4	74.2
Q9H004	404	6.3	87.5	88.7
Q9H008	748	12.7	87	86.6
Q9H010	29 328	108	72.4	72.2
Q9H012	23 067	85	72.9	73.3
R1H001	238	6.2	90.6	90.4
T3H004	1 029	18.8	86.9	85.5
V2H002	937	18.9	87.5	85.8
V6H002	12 862	48	74.1	75.8
W5H005	804	17.8	88.1	86.3
W5H006	180	5	91.3	91.3
X2H010	126	3.3	91.5	92.4

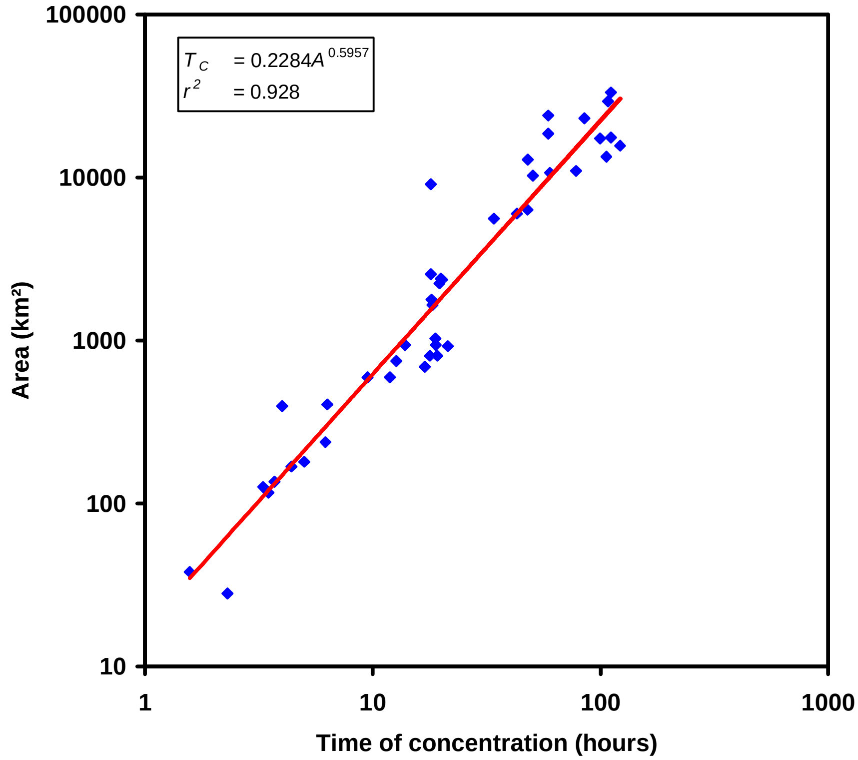

Figure 5.11: ARF: Area versus time of concentration power-law curve

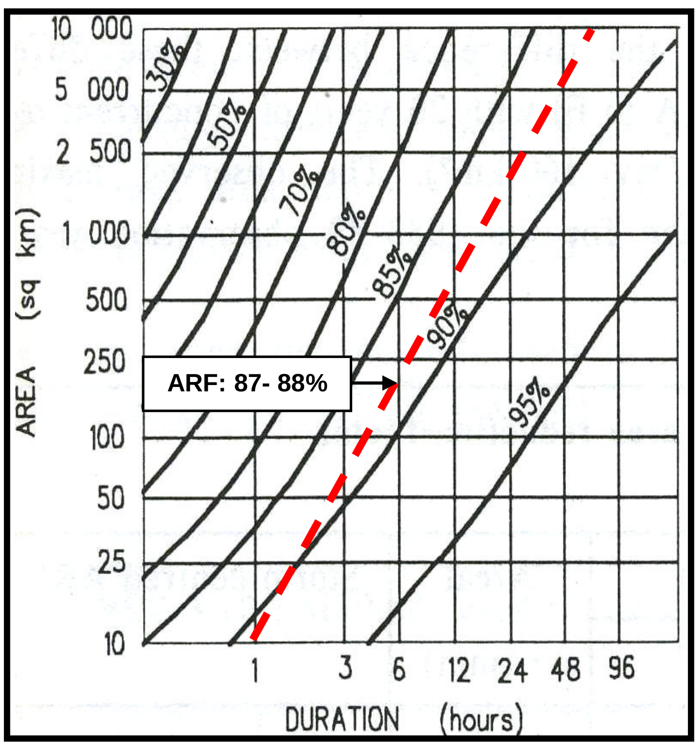

Figure 5.12: ARF diagram derived from fixed storm data
(NERC, 1975; as cited in Alexander, 1990: 3.31)

Figure 5.12 represents the ARF diagram published in the FSR (NERC, 1975) superimposed by Figure 5.11, the area-duration power-law curve. It is clearly evident that this power-law curve yielded a constant ARF of between 87% and 88% across the ARF diagram for durations exceeding 3 hours. This implies that for the catchments under consideration, the ARFs for point precipitation depths with durations equal to the time of concentration in a specific catchment appear to be fairly constant between 87% and 88%.

Similar results were obtained by Pegram (2003), although Equation 5.1 differed slightly with a coefficient of determination (r^2) close to unity (0.999).

5.2.5 Days of thunder per year

The 280 precipitation stations which were allocated to the Type 1 and Type 2 storm distribution regions with associated *R*- and *M*-values are listed in Tables B.18 and B.19, Addendum B. The isohyetal map representative of the distribution of *R*-values in South Africa and the SAWS precipitation station reference grid are respectively illustrated in Figures C.13 and C.14, Addendum C.

Figures 5.13 and 5.14 serve as a confirmation that there is no direct relationship between the *R*- and *M*-values of the precipitation stations under consideration as originally anticipated. The data points are randomly scattered about a curve to which a third order polynomial relationship could not even be fitted satisfactorily, especially in the case of the Type 2 storm distributions. The degree of association between the *R*- and *M*-values of the Type 1 storm distribution is higher compared to that of the Type 2 storm distribution, emphasising the more uniform areal and time distribution of precipitation and associated less thunder activities typical of the winter and/or coastal precipitation regions.

Thus, the number of days per year during which thunder was heard is not only influenced by the time distribution of storms, but the climate, type of precipitation, areal distribution of precipitation, location, altitude above mean sea level and topography must be taken into consideration.

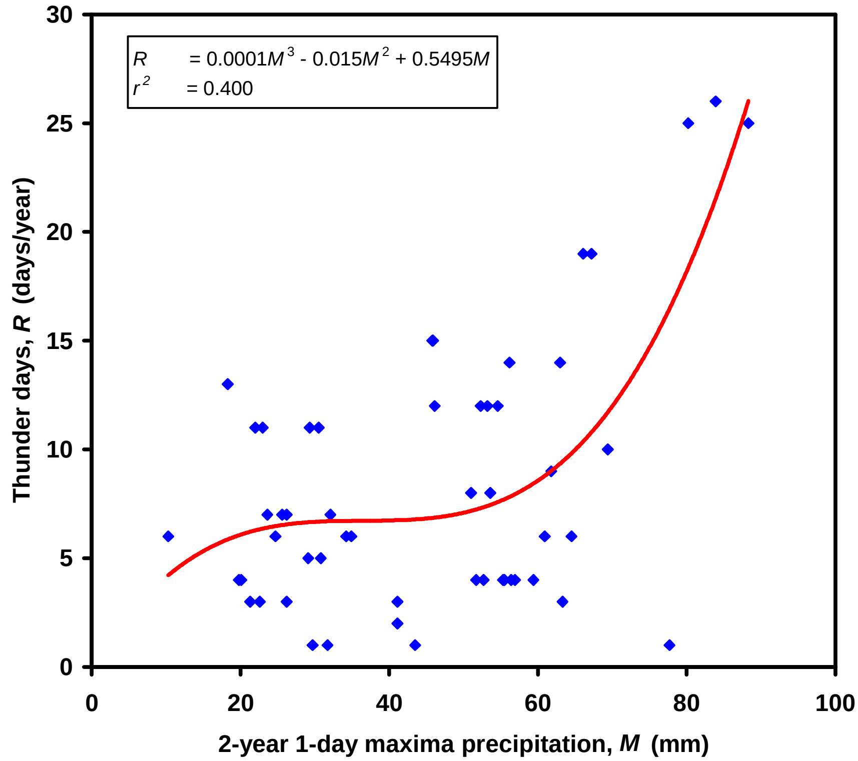

Figure 5.13: Type 1 storm distribution: *R*- versus *M*-values

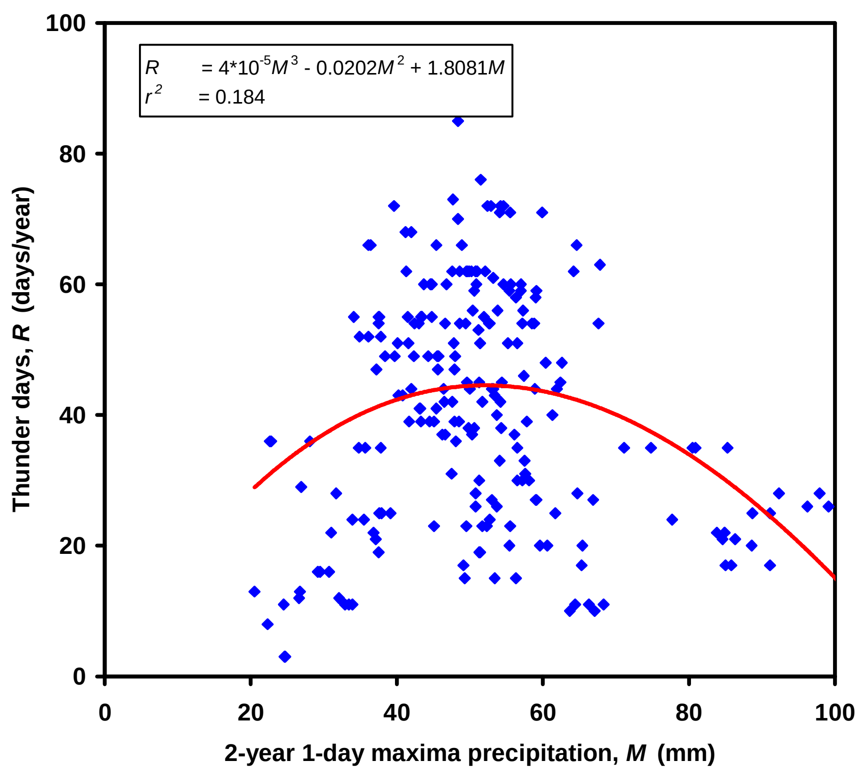

Figure 5.14: Type 2 storm distribution: *R*- versus *M*-values

5.3 HYDROLOGICAL DATA

5.3.1 Observed streamflow

5.3.1.1 Hydrological gauging stations

The particulars of each hydrological gauging station used during this study are listed in Tables 5.28 and 5.29. The SDF basin numbers are indicated in brackets in the latter table. The AMS of the 12 gauging stations used in the study area (SDF basin 9) are listed in Tables B.20 to B.31, Addendum B. The AMS of the gauging stations used to evaluate the SDF method in the rest of South Africa (SA) are listed in Tables B.32 to B.55, Addendum B.

Table 5.28: Hydrological gauging stations used in SDF basin 9

Station number	Station name	Catchment area (km²) (Tertiary/quaternary catchments)
C5R001	Tierpoort Dam	922 (C51D)
C5R002	Kalkfontein Dam	10 260 (C51A - H and J)
C5R003	Rustfontein Dam	937 (C52A)
C5R004	Krugersdrift Dam	6 331 (C52A - G)
C5R005	Groothoek Dam	116 (C52B)
C5H003	Modder River at Likatlong	1 650 (C52A - B)
C5H012 **	Riet River at Kromdraai	2 366 (C51A and C51B)
C5H015	Modder River at Stoomhoek	6 009 (C52A - G)
C5H016 **	Riet River at Biesiesbult	33 277 (C51 and C52 A - H and J - L)
C5H018	Modder River at Twee River	17 360 (C52 A - H, J - L)
C5H022 **	Kgabanyane River at Bedford	38 (C52B)
C5H054 **	Renosterspruit at Bishop's Glen	688 (C52F)

Table 5.29: Hydrological gauging stations used in the SA SDF basins

Station number	Station name	Catchment area (km²) (Tertiary/quaternary catchments)
A2H012 (1)	Krokodil River at Kalkheuwel	2 551 (A21A - E and H)
A4H002 (2)	Mokolo River at Zand River	1 777 (A42A - C)
A6H006 (2)*	Little Nyl River at Nylstroom	168 (A61A)
B4H003 (4)	Steelpoort River at Buffelskloof	2 240 (B41A - D)
B7H004 (5)	Klaserie River at Fleur de Lys	136 (B73A)
C3H003 (8)	Harts River at Taung	10 990 (C31B - F)
C4H001 (7)	Vet River at Paardevallei	5 590 (C41A - G)
C4H002 (7)	Vet River at Floorsdrift	17 599 (C41, C42D - H, J - L and C43A - C)
C5H008 (9)*	Riet River at Riviera	593 (C51B)
C8H001 (6)	Wilge River at Frankfort	15 673(C81, C82A - H, C83A - H and J)
C8H003 (6)*	Cornelius River at Warden	806 (C82A - B)
D1H001 (10)	Wonderboomspruit at Diepkloof	2 397 (D14B - E)
D1H004 (10)	Stormbergspruit at Molteno	348 (D14B)
D1H005 (11)	Orange River at Lesotho	10 680 (D11, D16, D17G - H and J - L)

Table 5.29: Hydrological gauging stations used in the SA SDF basins (Continued)

Station number	Station name	Catchment area (km²) (Tertiary/quaternary catchments)
D2H001 (11)	Caledon River at Jammerdrif	13 421 (D21, D22 and D23A - F)
E2H003 (16)	Doring River at Melkboom	24 044 (E21 - E24 and E40)
G1H008 (17)	Little Berg River at Nieuwkloof	395 (G10E)
H3H001 (18)*	Kingna River at Montagu	593 (H30A - B)
H7H004 (18)	Huis River at Barrydale	28 (H70C)
Q1H001 (21)	Great Fish River at Katkop	9 091 (Q11 - Q13A, B, Q14, Q21 and Q22)
Q7H003 (21)	Great Fish River at Leeuw Drift	18 534 (Q11- Q14, Q21, Q22, Q30, Q41 - Q44, Q50 - Q70A)
Q9H008 (21)*	Kat River at Heald Town Fingo	748 (Q94A - E)
Q9H010 (21)	Great Fish River at Blaauwdrift	29 328 (Q11 - Q14, Q21, Q22, Q30, Q41 - Q44, Q50 - Q80, Q91 - Q93 and Q94)
Q9H012 (21)	Great Fish River at Brandt Legte	23 067 (Q11 - Q14, Q21, Q22, Q30, Q41 - Q44, Q50 - Q80 and Q91A - B)
R1H001 (22)*	Tyume River at Goumahashe	238 (R10F- G)
T3H004 (23)*	Mzinthlava River at Slangfontein	1 029 (T32A - C)
V2H002 (26)*	Mooi River at Mooi River	937 (V20A - D)
V6H002 (26)*	Tugela River at Tugela Ferry	12 862 (V11 - V14, V60A - H and V70)
W5H005 (28)	Hlelo River at Ishlelo	804 (W52A - C)
W5H006 (28)*	Swartwater River at Zwartwater	180 (W51D)
X2H010 (29)*	Noordkaap River at Bellevue	126 (X23A)

The flow gauging station numbers marked with an *asterisk* (*) in column 1 of Tables 5.29 highlight that the observed streamflow of these stations are questionable and that the data and GEV/MM modelled flood peaks of Parak and Pegram (2006) will be used.

5.3.1.2 Data quality

Table B.56, Addendum B, provides a summary describing the main properties of each AMS used in the study area. The Square root-area method was only used in the study area to combine the observed streamflow data sets. In each case, if applicable, the particulars and record length of concern are indicated next to the *Additional record length* row.

The AMS of the river gauging stations were characterised by flood peaks that exceeded the hydraulic capacity on numerous events, resulting in a higher degree of uncertainty introduced, since no additional data or historical information quantifying these high outliers were available. These reduced record lengths are most likely to underestimate the higher frequency floods, since the magnitude of floods predicted by any probability distribution fitted to the observed data, is implicitly dependent on the statistical properties (mean, standard deviation and skewness) of the data set.

5.4 DESIGN FLOOD ESTIMATION TOOL

5.4.1 Development and application

The schematic layout and application guidelines for the DFET developed in Microsoft-Excel/VBA (2007) are included in Addendum D (DFET User manual, Figure D.3). The numerical results obtained with the DFET are included and discussed in Sections 5.5 and 5.6. All the graphical plot results are included in Addendum C.

5.5 FLOOD FREQUENCY ANALYSIS

5.5.1 Direct statistical analyses

A total of 36 catchments were evaluated, of which 12 are within the study area. Table 5.30 provides a summary describing the main statistical properties of each AMS used in the study area (SDF basin 9), whilst the statistical properties of each AMS used to evaluate the SDF method in the rest of South Africa are listed in Table B.57, Addendum B.

Table 5.30: Statistical properties of AMS used in SDF basin 9

Catchment description	Normal data				Log_{10}-transformed data			
	$\bar{x}$	***s***	***g***	c_v	$\bar{x}$	***s***	***g***	c_v
C5R001	75.448	144.612	4.128	1.917	1.506	0.559	0.096	0.372
C5R002	431.152	756.719	5.627	1.755	2.292	0.581	-0.470	0.253
C5R003	174.066	233.526	1.782	1.342	1.901	0.548	0.306	0.288
C5R004	398.321	421.916	2.571	1.059	2.351	0.543	-0.840	0.231
C5R005	60.548	69.292	1.962	1.144	1.557	0.452	0.129	0.291
C5H003	247.952	347.354	1.511	1.401	2	0.576	0.639	0.288
C5H012	68.596	61.187	1.408	0.892	1.543	0.689	-1.429	0.446
C5H015	425.945	385.695	1.249	0.906	2.389	0.563	-1.101	0.236
C5H016	129.556	103.404	0.979	0.798	1.955	0.403	-0.344	0.206
C5H018	162.654	269.287	5.226	1.656	1.883	0.586	-0.416	0.311
C5H022	15.167	15.814	1.563	1.043	0.906	0.565	-0.501	0.624
C5H054	32.640	59.765	4.077	1.831	1.220	0.461	0.312	0.378

The statistical properties listed in Tables 5.30 and B.57 are characterised by a high degree of variability and skewness typical of the flood peaks in South African rivers. In most of the catchments, due to the high variability, the dispersion about the mean (standard deviation) is relatively high. The skewness coefficients are indicative of the asymmetrical nature of the data, whilst the lower tail of the distribution curves was in general longer than the upper tail.

All the probability distributions based on MM estimation (except the Gamma distribution) and the GLO distribution based on LM/PWM estimation were evaluated during this study. The study area (SDF basin 9) results for return periods ranging from two to 200 years based on the most relevant distributions are listed in Table 5.31. The probability distribution results applicable to the hydrological gauging stations or catchments used to evaluate the SDF method in the rest of South Africa are listed in Table B.58, Addendum B. All the graphical plot results (data plotting positions and fitted probability distributions) are illustrated in Figures C.15 to C.50, Addendum C.

The problem associated with the AMS data sets characterised by short, insufficient record lengths was highlighted in Chapter 4 and the use of the mean values of the logarithms of two or more probability distributions to establish the most suitable probability distribution was suggested. This approach also takes cognisance of the strong evidence that in South Africa most of the high flood peaks are a result of rare, severe meteorological phenomena resulting in the AMS being a mixture of two or more statistical populations with different parameter values and associated flood peak frequency relationships. The mean values of the logarithms can be expressed by Equation 5.3 as follows:

$$Q_{Stats} = 10\exp\left[\frac{\log((Q_{EV1MM})(Q_{GEVMM})(Q_{LNMM})(Q_{LEV1MM})(Q_{LP3MM})(Q_{LMPWM}))}{N}\right] \tag{5.3}$$

Where:

Q_{Stats} = Peak flow based on the combined probability distributions (m^3/s)

Q_{EV1MM} = Peak flow based on the EV1/MM probability distribution (m^3/s)

Q_{GEVMM} = Peak flow based on the GEV/MM probability distribution (m^3/s)

Q_{LNMM} = Peak flow based on the LN/MM probability distribution (m^3/s)

Q_{LEV1MM} = Peak flow based on the LEV1/MM probability distribution (m^3/s)

Q_{LP3MM} = Peak flow based on the LP3/MM probability distribution (m^3/s)

Q_{LMPWM} = Peak flow based on the GLO probability distribution (m^3/s)

N = Number of probability distributions

The use of the mean values of the logarithms of the LP3-GEV/MM distributions dominated the direct statistical analyses in 42% of the catchments, followed by the LP3-GEV-LN/MM distributions in 28% of the catchments. The LP3/MM distribution was the only distribution which was used as a single most suitable distribution in 11% of the catchments. The remaining 19% of the catchments under consideration were characterised by a different combination of the above-mentioned distributions. The selection and use of probability distribution pair combinations in specific return period ranges was only based on the statistical properties, visual inspection of the plotted data and GOF statistics.

Thus, the LN/MM distribution was only used where the logarithms of the observed data have a near symmetrical distribution, in other words where the skewness coefficients were close to zero. In all other asymmetrical data sets, the LP3/MM distribution was used instead. The GEV/MM distributions were used at asymmetrical data sets characterised by either positive (EV2/MM) or negative (EV3/MM) skewness coefficients.

Apart from the problems associated with short record observed streamflow data and extrapolation beyond the record length, typical measurement errors at flow gauging stations, inconsistency, non-homogeneity and non-stationarity of data can violate the assumptions made when these probability distribution(s) are fitted to the data. Taking all these factors and results into consideration, it can be conclusively confirmed that the LN, LP3 and GEV distributions or a combination thereof are the most suitable probability distributions for flood frequency analyses in South Africa. This is thus in agreement with the statement made by Van der Spuy and Rademeyer (2008) (refer to Section 2.4.1.7, Chapter 2). However, when Equation 5.3 is used to establish the mean values of the logarithms of two or more probability distributions, it was impossible to give directives as to which probability distribution would be the best suited for a specific return period range. The use of GOF statistics, both regressive and descriptive, is suggested.

The further evaluation and GOF statistics of the fitted probability distributions are discussed and listed in Section 5.7.1.

Table 5.31: SDF basin 9: Probability distribution results

Station	Return period	Probability distributions (m^3/s)					Comments
		GEV/MM	LN/MM	LP3/MM	LM/PWM	Q_{Stats}	
C5R001	2	40	32	31	32	**31**	Return period range: 1.25 – 1 000 years LP3/MM distribution
	5	145	95	94	80	**94**	
	10	231	167	169	135	**169**	
	20	327	266	276	216	**276**	
	50	477	451	482	390	**482**	
	100	611	641	701	604	**701**	
	200	766	884	992	930	**992**	
C5R002	2	243	196	218	195	**218**	Return period range: 1.25 – 1 000 years LP3/MM distribution 10 – 1 000 years GEV/MM distribution
	5	765	604	616	470	**616**	
	10	1 201	1 089	1 004	762	**1 098**	
	20	1 704	1 770	1 460	1 177	**1 577**	
	50	2 506	3 059	2 160	2 024	**2 327**	
	100	3 242	4 405	2 758	3 015	**2 990**	
	200	4 115	6 150	3 410	4 468	**3 746**	
C5R003	2	126	80	75	66	**75**	Return period range: 10 – 1 000 years GEV/MM distribution 1.25 – 20 years LP3/MM distribution
	5	323	230	225	162	**225**	
	10	465	401	416	259	**440**	
	20	609	635	705	392	**655**	
	50	810	1 064	1 303	652	**810**	
	100	972	1 502	1 988	945	**972**	
	200	1 143	2 058	2 953	1 361	**1 143**	
C5R004	2	302	225	266	317	**290**	Return period range: 1.25 – 1 000 years LM/PWM distribution 1.25 – 20 years LP3/MM distribution
	5	637	643	654	637	**646**	
	10	893	1 114	961	910	**935**	
	20	1 168	1 755	1 266	1 241	**1 253**	
	50	1 571	2 925	1 654	1 807	**1 807**	
	100	1 913	4 112	1 933	2 366	**2 366**	
	200	2 293	5 617	2 195	3 075	**3 075**	
C5R005	2	46	36	35	34	**35**	Return period range: 1.25 – 1 000 years LP3/MM distribution 20 – 1 000 years GEV/MM distribution
	5	103	87	86	73	**86**	
	10	146	137	139	112	**139**	
	20	189	200	208	165	**198**	
	50	251	306	329	266	**287**	
	100	301	407	449	377	**368**	
	200	355	528	599	533	**461**	
C5H003	2	182	100	87	63	**87**	Return period range: 10 – 1 000 years GEV/MM distribution 1.25 – 10 years LP3/MM distribution
	5	481	305	287	164	**287**	
	10	689	546	583	268	**634**	
	20	897	884	1 095	411	**897**	
	50	1 179	1 521	2 337	697	**1 179**	
	100	1 400	2 182	3 993	1 023	**1 400**	
	200	1 629	3 038	6 659	1 492	**1 629**	

Table 5.31: SDF basin 9: Probability distribution results (Continued)

Station	Return period	Probability distributions (m^3/s)					Comments
		GEV/MM	LN/MM	LP3/MM	LM/PWM	Q_{Stats}	
C5H012	2	57	35	50	52	**57**	Return period range: 1.25 – 5 years GEV/MM distribution 5 – 1 000 years LP3/MM distribution
	5	110	133	130	98	**120**	
	10	147	267	180	133	**180**	
	20	183	474	219	173	**219**	
	50	231	907	256	234	**256**	
	100	269	1397	275	290	**275**	
	200	307	2075	288	356	**288**	
C5H015	2	359	245	309	331	**320**	Return period range: 1.25 – 1 000 years LM/PWM distribution 1.25 – 20 years LP3/MM distribution
	5	698	730	736	640	**686**	
	10	925	1 291	1 030	887	**956**	
	20	1 147	2 068	1 288	1 172	**1 229**	
	50	1 438	3 514	1 575	1 635	**1 635**	
	100	1 659	5 003	1 754	2 070	**2 070**	
	200	1 882	6 914	1 904	2 599	**2 599**	
C5H016	2	114	90	95	104	**104**	Return period range: 1.25 – 1 000 years GEV/MM distribution 1.25 – 10 years LP3/MM distribution
	5	206	197	199	186	**203**	
	10	266	296	284	249	**275**	
	20	322	414	376	321	**322**	
	50	392	605	508	433	**392**	
	100	444	780	615	536	**444**	
	200	494	983	728	659	**494**	
C5H018	2	96	76	84	105	**80**	Return period range: 1.25 – 1 000 years LN/MM distribution 1.25 – 1 000 years LP3/MM distribution
	5	284	238	242	243	**240**	
	10	440	431	401	377	**416**	
	20	619	703	593	556	**646**	
	50	903	1 221	895	896	**1 045**	
	100	1 163	1 763	1 161	1 269	**1 431**	
	200	1 469	2 469	1 457	1 786	**1 897**	
C5H022	2	12	8	9	10	**10**	Return period range: 1.25 – 1 000 years LP3/MM distribution 1.25 – 5 years GEV/MM distribution
	5	26	24	25	21	**25**	
	10	35	43	39	31	**39**	
	20	45	68	56	43	**56**	
	50	58	117	81	63	**81**	
	100	68	166	102	83	**102**	
	200	79	230	125	109	**125**	
C5H054	2	18	17	16	11	**16**	Return period range: 1.25 – 1 000 years LP3/MM distribution
	5	62	41	40	25	**40**	
	10	97	65	67	41	**67**	
	20	137	95	104	66	**104**	
	50	198	147	175	123	**175**	
	100	254	196	250	197	**250**	
	200	318	256	349	316	**349**	

5.5.2 Deterministic methods

The design flood estimation results based on the deterministic methods applied in the study area (SDF basin 9) are listed in Table 5.32, whilst the discussion, comparison and evaluation of these results are included in Section 5.7.2.

Table 5.32: SDF basin 9: Deterministic flood estimation results

Station	Return period	Design flood (m^3/s)					
		RM	ARM	SCS	SDF	SUH	LRH
C5R001	2	81	85	108	66	75	84
	5	121	130	190	198	122	136
	10	167	170	256	313	179	200
	20	231	222	325	448	253	284
	50	371	330	426	656	382	427
	100	551	448	509	850	532	595
	200	743	602	599	1 053	645	721
C5R002	2	328	426	455	351	217	227
	5	490	642	823	1 059	361	375
	10	675	831	1 111	1 692	520	541
	20	929	1 075	1 416	2 417	727	756
	50	1 490	1 573	1 850	3 590	1 103	1 146
	100	2 204	2 125	2 202	4 678	1 529	1 593
	200	2 970	2 834	2 576	5 929	1 852	1 927
C5R003	2	126	122	179	90	109	130
	5	188	203	316	291	178	213
	10	259	278	426	470	261	312
	20	357	373	545	677	370	443
	50	575	566	719	992	557	666
	100	851	778	864	1 271	778	931
	200	1 148	1 051	1 022	1 565	943	1 127
C5R004	2	245	308	311	236	232	223
	5	363	451	561	710	386	365
	10	497	576	759	1 134	562	535
	20	678	735	973	1 618	790	751
	50	1 075	1 057	1 285	2 402	1 205	1 134
	100	1 576	1 409	1 541	3 129	1 667	1 590
	200	2 108	1 891	1 819	3 966	2 014	1 933
C5R005	2	87	72	87	38	52	43
	5	130	133	154	133	85	70
	10	180	190	207	221	124	102
	20	248	262	265	320	176	145
	50	399	406	350	469	264	218
	100	591	563	421	594	370	304
	200	798	765	499	726	448	369
C5H003	2	169	169	239	125	146	172
	5	253	267	422	387	239	283
	10	349	356	568	616	352	415
	20	481	471	726	883	498	587
	50	773	705	959	1 294	750	884
	100	1 145	965	1 152	1 670	1 048	1 234
	200	1 544	1 300	1 362	2 063	1 269	1 497

Table 5.32: SDF basin 9: Deterministic flood estimation results (Continued)

Station	Return period	Design flood (m^3/s)					
		RM	ARM	SCS	SDF	SUH	LRH
C5H012	2	214	228	273	163	193	226
	5	320	356	487	497	322	375
	10	442	469	654	787	469	549
	20	609	615	831	1 126	664	774
	50	980	912	1 084	1 650	1 018	1 182
	100	1 453	1 239	1 291	2 135	1 411	1 640
	200	1 961	1 660	1 511	2 641	1 702	1 984
C5H015	2	255	311	330	239	207	233
	5	378	456	594	715	339	382
	10	517	582	804	1 139	497	560
	20	707	743	1 030	1 625	697	786
	50	1 120	1 080	1 360	2 407	1 054	1 187
	100	1 642	1 483	1 631	3 135	1 474	1 661
	200	2 196	1 996	1 925	3 960	1 792	2 019
C5H016	2	398	574	451	567	277	261
	5	594	873	893	1 745	457	431
	10	818	1 141	1 257	2 789	659	621
	20	1 124	1 486	1 655	4 017	923	878
	50	1 802	2 205	2 237	5 980	1 404	1 346
	100	2 663	3 009	2 721	7 788	1 958	1 874
	200	3 586	4 061	3 244	9 844	2 374	2 267
C5H018	2	262	374	290	344	277	223
	5	391	559	563	1 057	457	363
	10	537	722	785	1 688	659	527
	20	737	929	1 028	2 434	923	743
	50	1 177	1 356	1 382	3 626	1 404	1 124
	100	1 735	1 827	1 677	4 725	1 958	1 575
	200	2 331	2 435	1 995	5 976	2 374	1 913
C5H022	2	55	45	63	24	35	17
	5	83	83	111	83	57	28
	10	114	119	150	138	83	40
	20	157	164	192	200	117	57
	50	254	254	254	293	179	87
	100	376	353	305	372	248	121
	200	507	479	361	455	300	146
C5H054	2	92	95	115	59	80	83
	5	133	147	200	184	130	136
	10	177	190	266	295	191	199
	20	235	242	335	423	270	282
	50	352	338	434	620	408	424
	100	494	437	514	798	569	592
	200	637	561	599	985	689	718

5.5.3 Empirical methods

The design flood estimation results based on the empirical methods applied in the study area (SDF basin 9) are listed in Table 5.33, whilst the discussion, comparison and evaluation of these results are included in Section 5.7.3.

Table 5.33: SDF basin 9: Empirical flood estimation results

Station	Return period	Design flood (m^3/s)			RMF (m^3/s)	
		MIPI	CAPA	Q_T/RMF	Francou-Rodier	Kovács
C5R001	2	-	49	-	3 036	3 036
	5	-	112	-		
	10	271	173	-		
	20	337	251	-		
	50	468	381	1 345		
	100	593	485	1 659		
	200	-	589	1 997		
C5R002	2	-	253	-	6 935	7 444
	5	-	614	-		
	10	1 193	977	-		
	20	1 568	1 441	-		
	50	2 175	2 223	3 550		
	100	2 759	2 866	4 280		
	200	-	3 511	4 990		
C5R003	2	-	82	-	3 061	3 061
	5	-	180	-		
	10	366	274	-		
	20	422	392	-		
	50	589	588	1 358		
	100	744	744	1 674		
	200		897	2 015		
C5R004	2	-	206	-	6 928	7 045
	5	-	463	-		
	10	894	711	-		
	20	1 037	1 024	-		
	50	1 448	1 544	3 409		
	100	1 829	1 962	4 097		
	200	-	2 373	4 796		
C5R005	2	-	29	-	1 079	1 079
	5	-	60	-		
	10	156	89	-		
	20	180	125	-		
	50	251	184	413		
	100	317	230	529		
	200	-	274	658		
C5H003	2	-	116	-	4 062	4 062
	5	-	255	-		
	10	506	388	-		
	20	583	555	-		
	50	815	831	1 862		
	100	1 029	1 052	2 277		
	200	-	1 268	2 719		

Table 5.33: SDF basin 9: Empirical flood estimation results (Continued)

Station	Return period	Design flood (m^3/s)			RMF (m^3/s)	
		MIPI	CAPA	Q_T/RMF	Francou-Rodier	Kovács
C5H012	2	-	118	-	4 864	4 864
	5	-	280	-		
	10	585	441	-		
	20	792	646	-		
	50	1 096	991	2 291		
	100	1 392	1 272	2 782		
	200	-	1 553	3 302		
C5H015	2	-	207	-	6 745	6 860
	5	-	465	-		
	10	902	714	-		
	20	1 046	1 028	-		
	50	1 461	1 550	3 306		
	100	1 845	1 969	3 977		
	200	-	2 382	4 660		
C5H016	2	-	452	-	12 630	13 213
	5	-	1 087	-		
	10	2 078	1 723	-		
	20	2 651	2 535	-		
	50	3 683	3 902	6 980		
	100	4 668	5 022	8 240		
	200	-	6 144	9 418		
C5H018	2	-	283	-	8 854	9 330
	5	-	664	-		
	10	1 367	1 039	-		
	20	1 745	1 516	-		
	50	2 424	2 316	4 630		
	100	3 072	2 966	5 549		
	200	-	3 613	6 422		
C5H022	2	-	16	-	616	616
	5	-	32	-		
	10	90	48	-		
	20	104	67	-		
	50	146	99	254		
	100	184	123	319		
	200	-	147	390		
C5H054	2	-	49	-	2 255	2 308
	5	-	109	-		
	10	264	167	-		
	20	318	240	-		
	50	443	361	950		
	100	560	459	1 189		
	200	-	554	1 440		

5.6 EVALUATION AND CALIBRATION OF THE SDF METHOD

5.6.1 Input data requirements

The primary input data requirements in terms of precipitation and flows were extensively discussed in Sections 5.2 and 5.3 earlier in this chapter. The selected single precipitation and representative flow gauging stations used to evaluate, calibrate and verify the SDF method in each quaternary catchment under consideration are listed in Tables 5.17 and 5.18, Section 5.2.1, and Tables 5.28 and 5.29, Section 5.3.1.1. The AMS of these flow gauging stations are listed in Tables B.20 to B.55, Addendum B.

5.6.2 Evaluation and calibration of run-off coefficients

The original and calibrated C_2 (2-year return period) and C_{100} (100-year return period) run-off coefficients both applicable to the study area and the additional SDF basins evaluated in the rest of South Africa (SA) are listed in Tables 5.34 and 5.35 respectively. The SDF basin numbers are indicated in brackets in the latter table. The corresponding MAP, 2-year 1-day precipitation (*M*) and average number of days per year during which thunder was heard (*R*) are also shown. However, only the catchments for which both calibration and verification data were available are listed in Tables 5.34 and 5.35, whilst the calibrated C_2 and C_{100} run-off coefficients of the additional catchments used in the calibration exercise only, are listed in Table B.59, Addendum B.

The following notations will be used in Sections 5.6, 5.7 and Addendum B:

$SDF_{Original}$ Original SDF method as proposed by Alexander (2003);

$SDF_{Adjusted}$ Adjusted SDF method based on the adjustment factors proposed by Van Bladeren (2005);

$SDF_{Calibrated}$ Calibrated SDF method at a quaternary catchment level based on the methodology of this study;

$SDF_{Verified}$ Verified SDF method at a quaternary catchment level which is used to establish whether the calibrated version of the SDF method behaved in the probabilistic manner which it was designed for;

* Observed data and GEV/MM modelled flood peaks based on the research conducted by Parak and Pegram (2006); and

** Excluded from evaluation and calibration.

Table 5.34: SDF basin 9: Calibrated C_2 and C_{100} run-off coefficients

Catchment description	Method	Design information used in the SDF method				
		C_2	C_{100}	MAP (mm)	M (mm)	R (days)
C5R002	$SDF_{Original}$	15	60	376	43	47
	$SDF_{Adjusted}$	15	60	376	43	47
	$SDF_{Calibrated}$	9	54	420	42	54
C5R003	$SDF_{Original}$	15	60	376	43	47
	$SDF_{Adjusted}$	15	60	376	43	47
	$SDF_{Calibrated}$	9.5	47.5	555	48	54
C5R004	$SDF_{Original}$	15	60	376	43	47
	$SDF_{Adjusted}$	15	60	376	43	47
	$SDF_{Calibrated}$	18	59	518	44	62
C5R005	$SDF_{Original}$	15	60	376	43	47
	$SDF_{Adjusted}$	15	60	376	43	47
	$SDF_{Calibrated}$	11	33	649	48	66
C5H016 **	$SDF_{Original}$	15	60	376	43	47
	$SDF_{Adjusted}$	15	60	376	43	47
	$SDF_{Calibrated}$	3	20.5	461	48	60

Table 5.35: SA SDF basins: Calibrated C_2 and C_{100} run-off coefficients

Catchment description	Method	Design information used in the SDF method				
		C_2	C_{100}	MAP (mm)	M (mm)	R (days)
C8H001 (6)	$SDF_{Original}$	15	60	668	51	54
	$SDF_{Adjusted}$	15	60	668	51	54
	$SDF_{Calibrated}$	9	68	691	51	54
C4H002 (7)	$SDF_{Original}$	15	60	507	49	39
	$SDF_{Adjusted}$	15	60	507	49	39
	$SDF_{Calibrated}$	10	45	553	53	62
D1H001 (10)	$SDF_{Original}$	10	50	560	54	55
	$SDF_{Adjusted}$	10	50	560	54	55
	$SDF_{Calibrated}$	8	22.5	482	43	66
H3H001 (18)	$SDF_{Original}$	30	60	812	59	4
	$SDF_{Adjusted}$	30	60	812	59	4
	$SDF_{Calibrated}$	20	57	333	44	8
Q9H008 (21)*	$SDF_{Original}$	10	35	457	45	23
	$SDF_{Adjusted}$	10	35	457	45	23
	$SDF_{Calibrated}$	16	30	561	47	24
Q9H010 (21)	$SDF_{Original}$	10	35	457	45	23
	$SDF_{Adjusted}$	10	35	457	45	23
	$SDF_{Calibrated}$	6	50	378	32	54

The original and calibrated C_2 and C_{100} run-off coefficients of the study area (SDF basin 9) contained in Table 5.34 are characterised by large proportional differences between them. The proportional differences between the original run-off coefficients are characterised by a constant difference of 45%. In the case of the calibrated run-off coefficients, the proportional differences tend to decrease with an increase in the MAP, with a 45% difference for MAP less than 500 mm, a 38% to 41% difference for MAP ranging from 500 mm to 600 mm and a 22% difference for MAP exceeding 600 mm.

It is important to note that the original MAP (376 mm) in SDF basin 9 is also less than 500 mm and it confirms the trend identified. It also confirms that the antecedent soil moisture status in the quaternary catchment(s) under consideration introduces additional variability into the precipitation run-off process and that the hydrological response in each quaternary catchment will be different. This can be ascribed to the difference in soil permeability which controls the infiltration rate and consequently the balance of precipitation that constitutes surface run-off and contributes to the flood peak.

The large C_2 and C_{100} pair values listed in Table 5.35 indicate that a larger proportion of the representative precipitation contributes to the flood peak, whilst, as indicated above, the large proportional differences emphasised the important role of antecedent soil moisture status in the precipitation run-off process.

Tables 5.36 and 5.37 respectively provide a summary describing the results obtained during the numerical calibration of the SDF run-off coefficients both applicable to the study area and the additional SDF basins evaluated in the rest of South Africa (SA). The SDF basin numbers are indicated in brackets in the latter table. The original, adjusted and calibrated run-off coefficients (C_T) are shown and calculated by using Equation 2.49, Chapter 2. Again, as indicated before, these tables present only the catchments for which both calibration and verification data were available, whilst the run-off coefficients of the catchments used in the calibration exercise only, are listed in Table B.60, Addendum B.

Table 5.36: SDF basin 9: Calibrated run-off coefficients

Catchment description	Method	Run-off coefficients (C_T) for return period (T)						
		2	5	10	20	50	100	200
C5R002	$SDF_{Original}$ (C_{T1})	0.150	0.312	0.397	0.467	0.546	0.600	0.648
	$SDF_{Adjusted}$ (C_{T2})	0.155	0.383	0.719	1.338	1.130	1.422	1.878
	$SDF_{Calibrated}$ (C_{T3})	0.090	0.253	0.338	0.408	0.487	0.540	0.588
C5R003	$SDF_{Original}$ (C_{T1})	0.150	0.312	0.397	0.467	0.546	0.600	0.648
	$SDF_{Adjusted}$ (C_{T2})	0.125	0.287	0.446	0.870	0.753	0.902	1.137
	$SDF_{Calibrated}$ (C_{T3})	0.095	0.232	0.304	0.364	0.430	0.475	0.516
C5R004	$SDF_{Original}$ (C_{T1})	0.150	0.312	0.397	0.467	0.546	0.600	0.648
	$SDF_{Adjusted}$ (C_{T2})	0.148	0.361	0.653	1.226	1.042	1.299	1.696
	$SDF_{Calibrated}$ (C_{T3})	0.180	0.328	0.406	0.470	0.542	0.590	0.634
C5R005	$SDF_{Original}$ (C_{T1})	0.150	0.312	0.397	0.467	0.546	0.600	0.648
	$SDF_{Adjusted}$ (C_{T2})	0.103	0.224	0.294	0.597	0.529	0.607	0.733
	$SDF_{Calibrated}$ (C_{T3})	0.110	0.190	0.231	0.266	0.304	0.330	0.354
C5H016 **	$SDF_{Original}$ (C_{T1})	0.150	0.312	0.397	0.467	0.546	0.600	0.648
	$SDF_{Adjusted}$ (C_{T2})	0.172	0.441	0.911	1.656	1.382	1.780	2.400
	$SDF_{Calibrated}$ (C_{T3})	0.030	0.093	0.126	0.154	0.184	0.205	0.224

Table 5.37: SA SDF basins: Calibrated run-off coefficients

Catchment description	Method	Run-off coefficients (C_T) for return period (T)						
		2	5	10	20	50	100	200
C8H001 (6)	$SDF_{Original}$ (C_{T1})	0.150	0.312	0.397	0.467	0.546	0.600	0.648
	$SDF_{Adjusted}$ (C_{T2})	0.192	0.270	0.329	0.383	0.468	0.542	0.638
	$SDF_{Calibrated}$ (C_{T3})	0.090	0.303	0.415	0.507	0.611	0.680	0.743
C4H002 (7)	$SDF_{Original}$ (C_{T1})	0.150	0.312	0.397	0.467	0.546	0.600	0.648
	$SDF_{Adjusted}$ (C_{T2})	0.074	0.101	0.128	0.134	0.140	0.144	0.146
	$SDF_{Calibrated}$ (C_{T3})	0.100	0.227	0.293	0.347	0.409	0.450	0.488
D1H001 (10)	$SDF_{Original}$ (C_{T1})	0.100	0.244	0.320	0.382	0.452	0.500	0.543
	$SDF_{Adjusted}$ (C_{T2})	0.099	0.178	0.220	0.251	0.315	0.355	0.435
	$SDF_{Calibrated}$ (C_{T3})	0.080	0.132	0.160	0.183	0.208	0.225	0.241
H3H001 (18)	$SDF_{Original}$ (C_{T1})	0.300	0.408	0.465	0.511	0.564	0.600	0.632
	$SDF_{Adjusted}$ (C_{T2})	0.531	0.640	0.622	0.632	0.605	0.624	0.614
	$SDF_{Calibrated}$ (C_{T3})	0.200	0.334	0.404	0.462	0.527	0.570	0.610
Q9H008 (21)*	$SDF_{Original}$ (C_{T1})	0.100	0.190	0.237	0.276	0.320	0.350	0.377
	$SDF_{Adjusted}$ (C_{T2})	0.048	0.120	0.213	0.280	0.352	0.396	0.473
	$SDF_{Calibrated}$ (C_{T3})	0.160	0.211	0.237	0.259	0.284	0.300	0.315
Q9H010 (21)	$SDF_{Original}$ (C_{T1})	0.100	0.190	0.237	0.276	0.320	0.350	0.377
	$SDF_{Adjusted}$ (C_{T2})	0.163	0.343	0.498	0.678	0.912	1.061	1.356
	$SDF_{Calibrated}$ (C_{T3})	0.060	0.219	0.302	0.371	0.448	0.500	0.547

The original run-off coefficients of SDF basin 9 (study area) and the other basins evaluated ranged from 0.100 (2-year return period) to 0.648 (200-year return period), whilst the calibrated run-off coefficients ranged from 0.060 (2-year return period) to 0.743 (200-year return period). The adjusted run-off coefficients based on the adjustment factors proposed by Van Bladeren (2005) ranged from 0.025 (2-year return period) to 1.878 (200-year return period). According to Van Bladeren (2005), the latter run-off coefficient exceeding unity is justified, since it is used when the SDF method overestimates the more frequent events and underestimates the extreme events in a particular basin.

However, the question arises whether the adjustment factor can successfully describe a meaningful relationship between the regional descriptors (average catchment slope, catchment area, land-use distribution and MAP) and the C_T-coefficients as shown in Equation 5.4 (Van Bladeren, 2005: 32).

$$C_{T2} = \frac{C_{T1}}{F} \qquad (5.4)$$

Where:

C_{T1} = Original run-off coefficient (Alexander, 2003)

C_{T2} = Adjusted run-off coefficient (Van Bladeren, 2005)

F = Adjustment factor ($F = xA^y$)

A = Catchment area (km²)

x = Regional descriptor (multiplier)

y = Regional descriptor (exponent)

Based on the results listed in Tables 5.36 and 5.37, as well as Table B.60, Addendum B, it was interesting to note that the run-off coefficients adjusted by Equation 5.4 had a tendency to decrease in magnitude with increasing recurrence interval. This was especially the case in SDF basins 11 and 17. In SDF basin 9 (study area), the 20-year adjusted run-off coefficients exceeded the 50-year run-off coefficients. Similar results were also evident in SDF basin 18.

The adjusted run-off coefficients which exceeded unity and decreased in magnitude with increasing recurrence interval deviated from the norm. Run-off coefficients exceeding unity indicate that more than a 100% run-off can occur, but this is physically impossible.

An increase in the C_T-coefficients with return period is necessary to accommodate the known effects which also increase with return period, but are not accounted for in Equation 5.4. Thus, the likelihood that a catchment is to be more saturated at the start of a storm with a longer recurrence interval is ignored.

In conclusion, the effort at regionalisation made by Van Bladeren (2005) requires further refinement, since the relationships established between the parameters (multiplier and exponent) of the power-law function (Equation 5.4) fitted to the C_T-coefficients as a function of return period and regional descriptors are questionable. Nevertheless, these questionable results are in agreement with the conclusions of Parak and Pegram (2006) for conditions in South Africa and Pilgrim and Cordery (1993) for conditions in Australia. In both these studies, the calibrated run-off coefficients of the RM did not show much sensitivity to the above-mentioned regional descriptors. However, this does indicate that the C_T-coefficients are essentially functions of the return period and time of concentration as conjectured.

The coaxially plotted values of C_T with the regional SDF run-off coefficients from Alexander (2003) against the return period applicable to SDF basin 9 (study area) and the other basins evaluated during the calibration and verification exercises are shown in Figures 5.15 to 5.20.

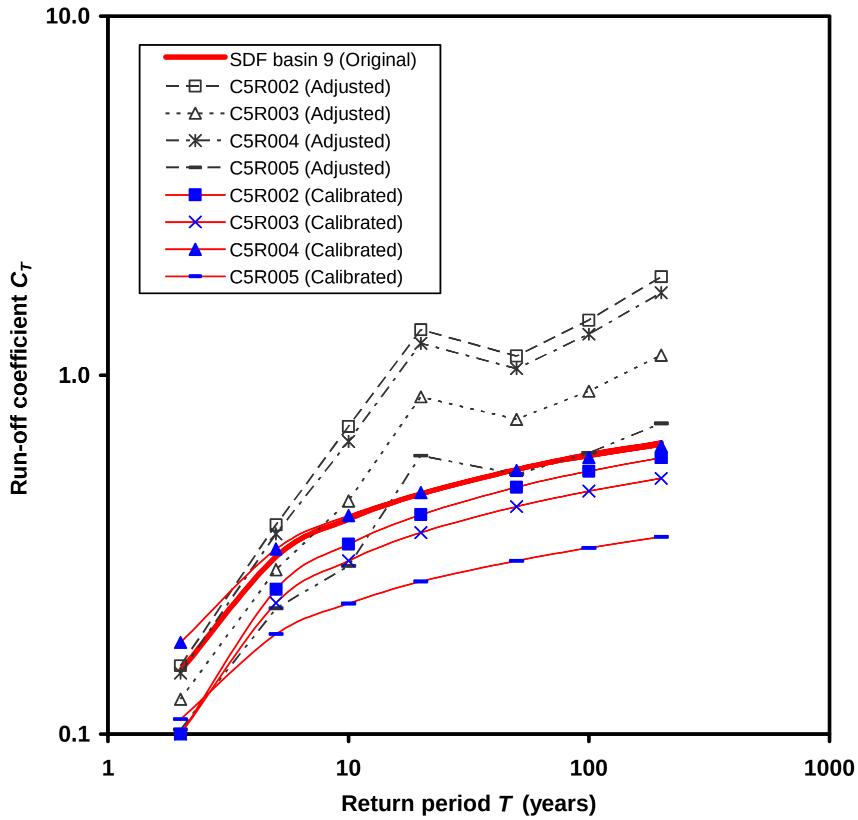

Figure 5.15: SDF basin 9: Comparison of run-off coefficients

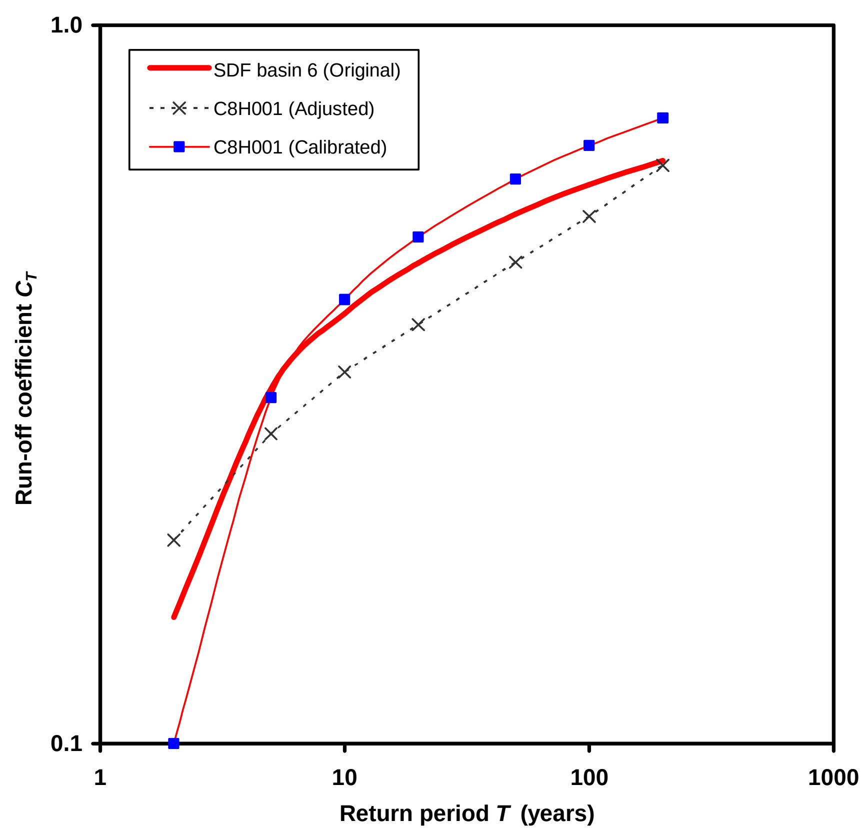

Figure 5.16: SDF basin 6: Comparison of run-off coefficients

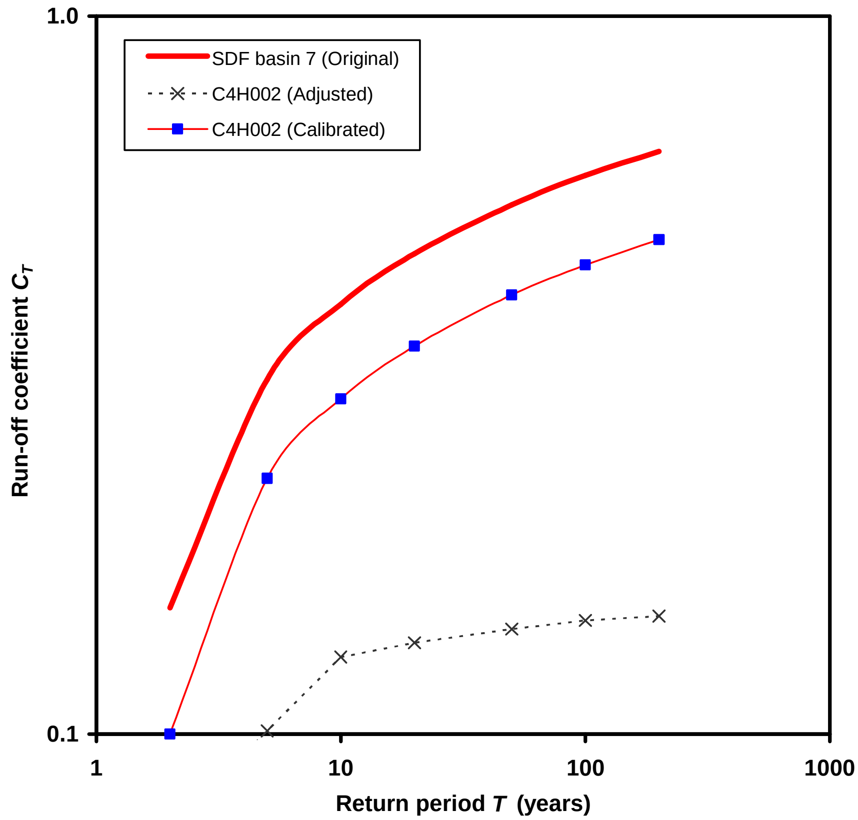

Figure 5.17: SDF basin 7: Comparison of run-off coefficients

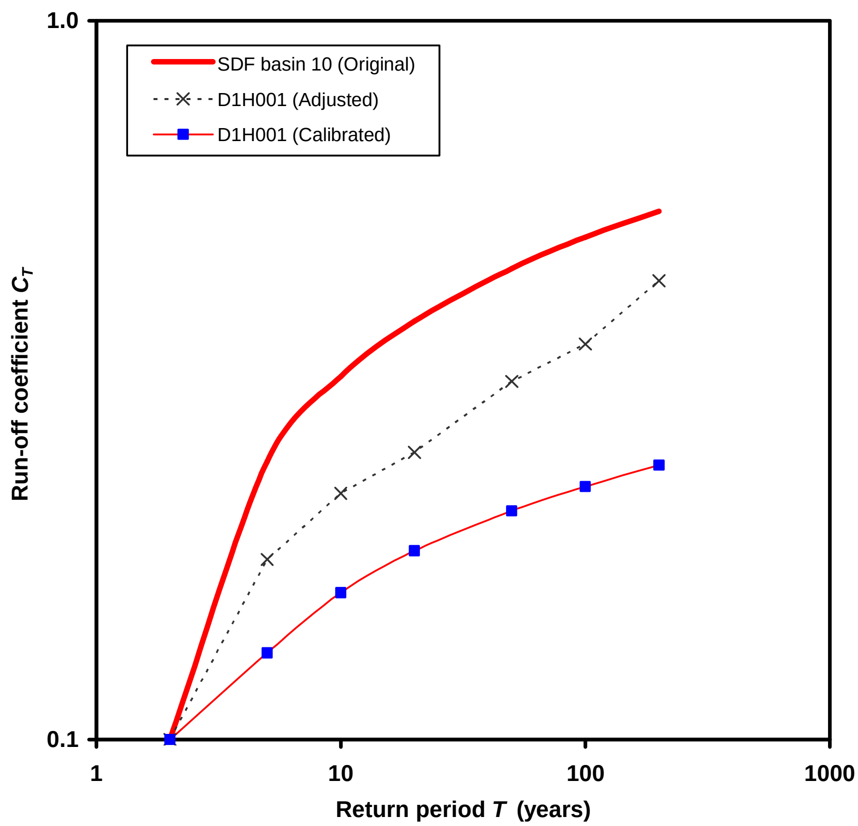

Figure 5.18: SDF basin 10: Comparison of run-off coefficients

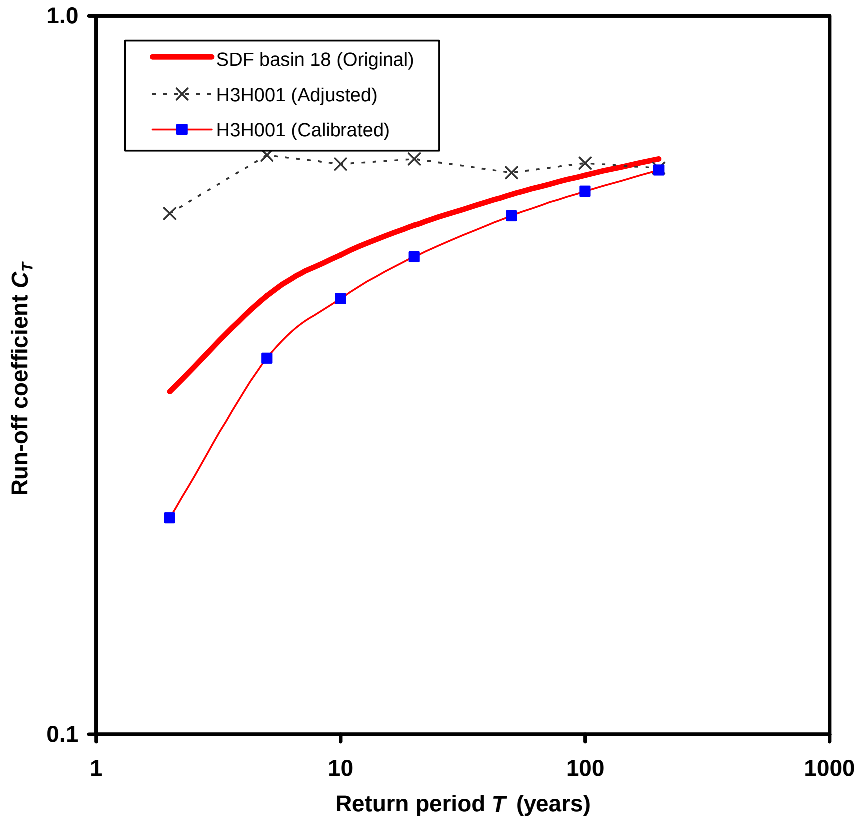

Figure 5.19: SDF basin 18: Comparison of run-off coefficients

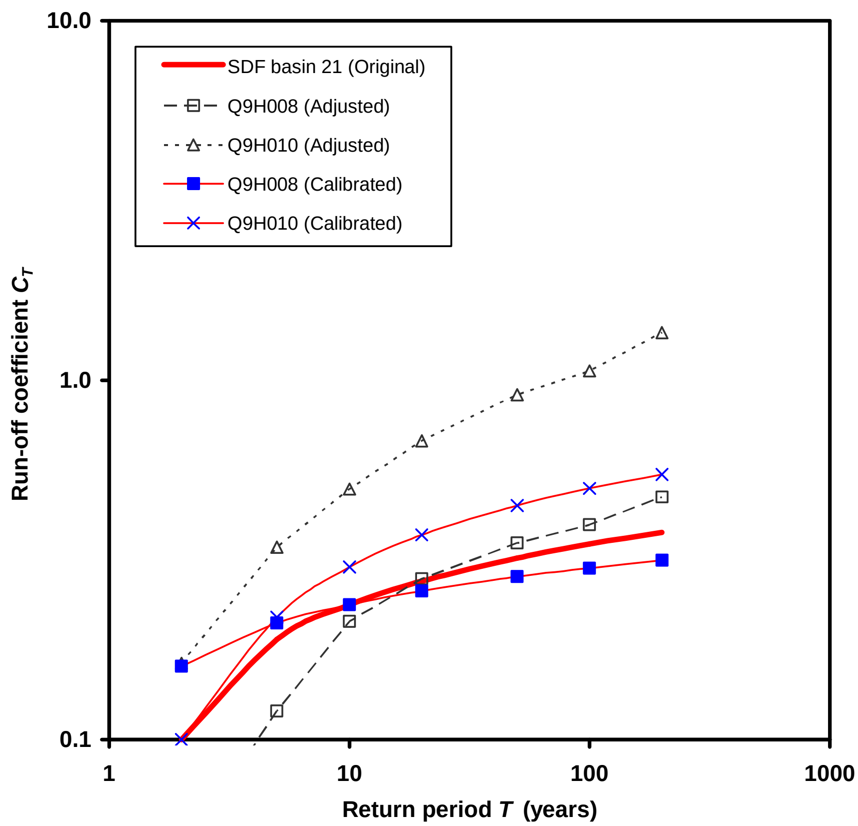

Figure 5.20: SDF basin 21: Comparison of run-off coefficients

It is evident from Figures 5.15 to 5.20 that the calibrated C_T - coefficients in the quaternary catchments obtained from this study are spread around those of Alexander (2003), but are generally lower in magnitude, except for SDF basins 6 and 21 (Q9H010). The curves representative of the calibrated run-off coefficients had similar growths as a function of the recurrence interval in most of the basins under consideration. The decreasing trend in the adjusted run-off coefficients with an increase in recurrence interval is clearly evident from Figures 5.15 and 5.19, with the adjusted 20-year run-off coefficients questionable in SDF basin 9, since they are larger than the 50- and 100-year coefficients.

5.6.3 Evaluation of calibrated flood peaks

The comparison between the design flood peak values based on the direct statistical analyses and the original, adjusted and calibrated versions of the SDF method is listed in Tables 5.38 and 5.39(a) – (e). The latter tables are representative of the additional SDF basins evaluated in the rest of South Africa. The average SDF/probability distribution-ratios representative of all the basins under consideration are also shown.

However, the direct statistical analysis results of C5H016 were excluded (marked with an *asterisk* **) when the average SDF/probability distribution-ratios were determined, since the AMS at this station are characterised by numerous flood events that exceeded the hydraulic capacity of the particular flow gauging station, resulting in the underestimation of flood peaks. In the following paragraphs, the calibration results obtained in the study area and the other SDF basins used in both the calibration and verification exercises are discussed in detail, whilst the results obtained in the SDF basins which were only used in the calibration exercise are discussed and summarised at the end of this section.

<u>SDF basin 9 (study area):</u>
According to Van Bladeren (2005), the SDF method tends to overestimate the more frequent design floods for return periods up to 20 years, whilst the extreme events are underestimated. Although, the results contained in Table 5.38 show that on average the SDF method overestimated all the statistical flood peaks. The overestimation varied between 18% and 45%.

Except for the 2-year return period, the adjusted SDF method overestimated all the flood peaks as well, with average overestimations up to 204%. The calibrated version of the SDF method proved to be the most accurate, with the 2-year return period being underestimated on average by 7%, whilst the maximum overestimation was limited to 12%.

Table 5.38: SDF basin 9: SDF flood estimation results

Catchment description	Method	Design flood (m^3/s) for return period (years)						
		2	**5**	**10**	**20**	**50**	**100**	**200**
C5R002	$Q_{Statistical}$	218	616	1 098	1 577	2 327	2 990	3 746
	$SDF_{Original}$ (Q_1)	351	1 059	1 692	2 417	3 590	4 678	5 929
	$SDF_{Adjusted}$ (Q_2)	362	1 298	3 065	6 926	7 438	11085	17183
	$SDF_{Calibrated}$ (Q_3)	204	773	1 221	1 703	2 404	3 010	3 712
C5R003	$Q_{Statistical}$	75	225	440	655	810	972	1 143
	$SDF_{Original}$ (Q_1)	90	291	470	677	992	1 271	1 565
	$SDF_{Adjusted}$ (Q_2)	75	267	528	1 261	1 368	1 912	2 744
	$SDF_{Calibrated}$ (Q_3)	64	237	389	559	812	1 024	1 253
C5R004	$Q_{Statistical}$	290	646	935	1 253	1 807	2 366	3 075
	$SDF_{Original}$ (Q_1)	236	710	1 134	1 618	2 402	3 129	3 966
	$SDF_{Adjusted}$ (Q_2)	233	821	1 866	4 251	4 585	6 766	10387
	$SDF_{Calibrated}$ (Q_3)	290	709	1 033	1 376	1 878	2 356	2 866
C5R005	$Q_{Statistical}$	35	86	139	198	287	368	461
	$SDF_{Original}$ (Q_1)	38	133	221	320	469	594	726
	$SDF_{Adjusted}$ (Q_2)	26	95	163	410	454	601	822
	$SDF_{Calibrated}$ (Q_3)	32	92	147	209	300	375	455
C5H016 **	$Q_{Statistical}$	104	203	275	322	392	444	495
	$SDF_{Original}$ (Q_1)	567	1 746	2 789	4 017	5 980	7 788	9 844
	$SDF_{Adjusted}$ (Q_2)	649	2 465	6 394	14225	15135	23080	36525
	$SDF_{Calibrated}$ (Q_3)	126	546	892	1 276	1 857	2 360	2 924
Average Q_{SDF}/Q_{Stats}	**$Q_1/Q_{Statistical}$**	**1.18**	**1.41**	**1.35**	**1.37**	**1.43**	**1.45**	**1.45**
	$Q_2/Q_{Statistical}$	**1.05**	**1.42**	**1.79**	**2.95**	**2.25**	**2.54**	**3.04**
	$Q_3/Q_{Statistical}$	**0.93**	**1.12**	**1.04**	**1.02**	**1.03**	**1.02**	**1.00**

<u>SDF basin 6:</u>

According to Van Bladeren (2005), the precipitation data associated with a time of concentration less than 24 hours are anomalous and requires some revision, whilst in the larger catchments the SDF method estimates all the events reasonably. In the smaller catchments it would seem to underestimate the flood magnitudes significantly.

The results contained in Table 5.39(a) confirm these findings applicable to large catchments, especially for return periods ranging from 50 to 200 years with the overestimation limited to 11%. The overall results of the adjusted SDF method are good, except for the 2-year return period which is overestimated by 96%. The calibrated version of the SDF method proved to be slightly less accurate than the adjusted method.

Table 5.39(a): SDF basin 6: SDF flood estimation results

Catchment description	Method	Design flood (m^3/s) for return period (years)						
		2	**5**	**10**	**20**	**50**	**100**	**200**
C8H001	$Q_{Statistical}$	227	713	1 099	1 656	2 424	3 280	4 325
	$SDF_{Original}$ (Q_1)	348	957	1 433	1 945	2 695	3 338	4 041
	$SDF_{Adjusted}$ (Q_2)	446	827	1 187	1 596	2 311	3 015	3 982
	$SDF_{Calibrated}$ (Q_3)	217	938	1 464	1 992	2 706	3 260	3 823
Average Q_{SDF}/Q_{Stats}	**$Q_1/Q_{Statistical}$**	**1.53**	**1.34**	**1.30**	**1.17**	**1.11**	**1.02**	**0.93**
	$Q_2/Q_{Statistical}$	**1.96**	**1.16**	**1.08**	**0.96**	**0.95**	**0.92**	**0.92**
	$Q_3/Q_{Statistical}$	**0.96**	**1.32**	**1.33**	**1.20**	**1.12**	**0.99**	**0.88**

<u>SDF basin 7:</u>

According to Van Bladeren (2005), the SDF method provides acceptable results and does not require any adjustment for all the return periods; however, adjustment factors based on Equation 5.4 are still suggested. Despite of this recommendation, the results contained in Table 5.39(b) indicate that the SDF method overestimated all the statistical flood peaks. On average, the overestimation varied between 38% and 61%.

The adjusted SDF method underestimated on average all the flood peaks, ranging from -30% to -69%. The calibrated version of the SDF method proved to be the most accurate, with good estimations of the extreme events, whilst the more frequent events being estimated reasonably.

Table 5.39(b): SDF basin 7: SDF flood estimation results

Catchment description	Method	Design flood (m^3/s) for return period (years)						
		2	5	10	20	50	100	200
C4H002	$Q_{Statistical}$	236	601	944	1 360	2 046	2 685	3 443
	$SDF_{Original}$ (Q_1)	336	965	1 512	2 111	3 031	3 843	4 761
	$SDF_{Adjusted}$ (Q_2)	165	313	486	607	779	919	1 072
	$SDF_{Calibrated}$ (Q_3)	249	755	1 146	1 560	2 152	2 637	3 157
Average Q_{SDF}/Q_{Stats}	**$Q_1/Q_{Statistical}$**	**1.42**	**1.61**	**1.60**	**1.55**	**1.48**	**1.43**	**1.38**
	$Q_2/Q_{Statistical}$	**0.70**	**0.52**	**0.51**	**0.45**	**0.38**	**0.34**	**0.31**
	$Q_3/Q_{Statistical}$	**1.06**	**1.26**	**1.21**	**1.15**	**1.05**	**0.98**	**0.92**

SDF basin 10:

According to Van Bladeren (2005), the SDF method tends to give a reasonable mix of results that are generally accepted in this basin, with the exception of small catchments where it overestimates the flood peaks significantly. However, the results contained in Table 5.39(c) indicate that the SDF method overestimated all the statistical flood peaks significantly in the large catchments as well. On average, the overestimation varied between 55% and 211%.

The adjusted SDF method also overestimated all the flood peaks for all the return periods, with the overall results being slightly better than those estimated by the original SDF method. The calibrated version of the SDF method proved to be the most accurate, with the estimations either almost correct (-2%) or slightly exceeding the statistical flood peaks with a maximum of 8%.

Table 5.39(c): SDF basin 10: SDF flood estimation results

Catchment description	Method	Design flood (m^3/s) for return period (years)						
		2	5	10	20	50	100	200
D1H001	$Q_{Statistical}$	89	190	286	388	535	654	783
	$SDF_{Original}$ (Q_1)	138	475	763	1 079	1 553	1 981	2 437
	$SDF_{Adjusted}$ (Q_2)	136	347	525	709	1 082	1 408	1 953
	$SDF_{Calibrated}$ (Q_3)	89	205	298	396	536	650	770
Average Q_{SDF}/Q_{Stats}	**$Q_1/Q_{Statistical}$**	**1.55**	**2.50**	**2.67**	**2.78**	**2.90**	**3.03**	**3.11**
	$Q_2/Q_{Statistical}$	**1.53**	**1.83**	**1.84**	**1.83**	**2.02**	**2.15**	**2.49**
	$Q_3/Q_{Statistical}$	**1.00**	**1.08**	**1.04**	**1.02**	**1.00**	**0.99**	**0.98**

SDF basin 18:

Van Bladeren (2005) identified two sub-basins within this basin based on the large variation in the MAP. The catchments evaluated during the calibration and verification exercise are both within the larger Breë River catchment, for which the results obtained were classified as reasonable. However, adjustment factors based on Equation 5.4 were still suggested. The results contained in Table 5.39(d) indicate that the SDF method overestimated all the statistical flood peaks, except those associated with the 100- and 200-year return periods, which were almost accurately estimated. Except for the 200-year return period, the adjusted SDF method overestimated all the flood peaks as well. The average overestimations showed a tendency to increase in magnitude with decreasing recurrence interval. The calibrated version of the SDF method proved to be the most accurate, with the estimations either slightly too low or too high, but limited to either an under- or overestimation of ± 14%.

Table 5.39(d): SDF basin 18: SDF flood estimation results

Catchment description	Method	Design flood (m^3/s) for return period (years)						
		2	5	10	20	50	100	200
H3H001*	$Q_{Statistical}$	95	210	304	436	661	881	1 156
	$SDF_{Original}$ (Q_1)	142	300	433	577	787	961	1 145
	$SDF_{Adjusted}$ (Q_2)	252	469	579	714	843	1 000	1 113
	$SDF_{Calibrated}$ (Q_3)	82	221	345	486	696	874	1 068
Average Q_{SDF}/Q_{Stats}	**$Q_1/Q_{Statistical}$**	**1.49**	**1.43**	**1.42**	**1.32**	**1.19**	**1.09**	**0.99**
	$Q_2/Q_{Statistical}$	**2.65**	**2.23**	**1.90**	**1.64**	**1.28**	**1.14**	**0.96**
	$Q_3/Q_{Statistical}$	**0.86**	**1.05**	**1.13**	**1.11**	**1.05**	**0.99**	**0.92**

SDF basin 21:

According to Van Bladeren (2005), the SDF estimates are acceptable for the more frequent design floods for return periods up to 20 years, whilst the extreme events are underestimated. However, the SDF/probability distribution-ratios in the larger catchments (A > 20 000 km²) varied between 0.5 and 0.8, whilst in the smaller catchments ratios of between 2 and 4 were witnessed. The results contained in Table 5.39(e) are in agreement with the findings of Van Bladeren (2005), although the SDF/probability distribution-ratios were lower in the smaller catchments, whilst in the larger catchments the ratios tend to be slightly higher to almost being equal to unity.

The use of adjustment factors did not improve the results, especially in the larger catchments where the adjusted SDF method overestimated all the flood peaks, with an average overestimation of between 103% and 294%. The calibrated version of the SDF method proved to be the most accurate, although the average overestimations showed a tendency to increase in magnitude with increasing recurrence interval in the smaller catchments, whilst the degree of association in the larger catchments was acceptable.

Table 5.39(e): SDF basin 21: SDF flood estimation results

Catchment description	Method	Design flood (m^3/s) for return period (years)						
		2	**5**	**10**	**20**	**50**	**100**	**200**
Q9H008*	$Q_{Statistical}$	105	215	305	362	486	604	723
	$SDF_{Original}$ (Q_1)	64	190	305	434	634	807	998
	$SDF_{Adjusted}$ (Q_2)	31	120	274	441	698	912	1 253
	$SDF_{Calibrated}$ (Q_3)	107	217	307	406	547	663	787
Average Q_{SDF}/Q_{Stats}	**$Q_1/Q_{Statistical}$**	**0.61**	**0.88**	**1.00**	**1.20**	**1.30**	**1.34**	**1.38**
	$Q_2/Q_{Statistical}$	**0.30**	**0.56**	**0.90**	**1.22**	**1.44**	**1.51**	**1.73**
	$Q_3/Q_{Statistical}$	**1.02**	**1.01**	**1.01**	**1.12**	**1.13**	**1.10**	**1.09**
Q9H010	$Q_{Statistical}$	231	856	1 366	1 962	2 887	3 694	4 596
	$SDF_{Original}$ (Q_1)	350	963	1 499	2 118	3 106	3 995	5 027
	$SDF_{Adjusted}$ (Q_2)	572	1 738	3 148	5 197	8 855	12100	18092
	$SDF_{Calibrated}$ (Q_3)	165	831	1 364	1 935	2 758	3435	4 158
Average Q_{SDF}/Q_{Stats}	**$Q_1/Q_{Statistical}$**	**1.52**	**1.13**	**1.10**	**1.08**	**1.08**	**1.08**	**1.09**
	$Q_2/Q_{Statistical}$	**2.48**	**2.03**	**2.30**	**2.65**	**3.07**	**3.28**	**3.94**
	$Q_3/Q_{Statistical}$	**0.71**	**0.97**	**1.00**	**0.99**	**0.96**	**0.93**	**0.90**

Additional SDF basins only used in the calibration exercise:

SDF basins 1, 2, 4, 5, 8, 11, 16, 17, 22, 23, 26, 28 and 29 were only evaluated and calibrated, since the available data (flow, area and time of concentration) were limited to those catchments investigated by Petras and Du Plessis (1987) and Parak and Pegram (2006). The comparison between the design flood peak values based on the direct statistical analyses and the original, adjusted and calibrated versions of the SDF method is listed in Tables B.61(a) – (m), Addendum B. The average SDF/probability distribution-ratios representative of all the basins under consideration are also shown. As indicated before, the flow gauging station numbers marked with an *asterisk* (*) in column 1 of Tables B.61(a) – (m) highlight that the GEV/MM modelled flood peaks of Parak and Pegram (2006) were used.

The overall results indicated that the use of the original SDF method in 62% of the SDF basins (2, 5, 16, 22, 23, 26, 28 and 29) evaluated were in agreement with the findings of Van Bladeren (2005). In other words, the SDF/probability distribution-ratios were of the same magnitude, irrespective whether the flows were over- or underestimated for the range of return periods under consideration. However, all the design flood peak values were overestimated, except in basin 26. On average, the SDF/probability distribution-ratios varied between 1.1 and 3.26.

The most reasonable results were demonstrated in SDF basins 16 and 26, with the more frequent events (2- and 5-year return periods) being underestimated. The best results were evident in SDF basin 16, with the overestimation limited to ± 12% for the return periods ranging from ten to 200 years.

The original SDF method results in basins 1, 4, 11 and 17 were in disagreement with the findings of Van Bladeren (2005), since the overestimations were almost double in magnitude. This confirms that the data sets used in these particular basins differ from the AMS used by Van Bladeren (2005), which possibly included higher peak flows or historical information. In SDF basin 11 this might be ascribed to the precipitation data originally used, since it was established that the precipitation data for a time of concentration less than 24 hours are anomalous and should be reviewed. Due to this, the recommended adjustment factors to be used in this basin will result in significant overestimations. The original SDF method results in basin 8 were also in disagreement with the findings of Van Bladeren (2005), since the overestimations were almost 50% better compared to the analysis done by Van Bladeren. The SDF/probability distribution-ratios ranged from 0.74 to 1.37.

The adjusted SDF method results were only better in 38% of the basins under consideration when compared to those estimated by the original SDF method. As in the case of the original SDF method, the most acceptable results were evident in SDF basin 16, whilst the flood peak values were significantly overestimated in basins 1, 11 and 17. On average, the adjusted SDF/probability distribution-ratios varied between 1.63 and 6.58, which is unacceptable.

The calibrated version of the SDF method proved to be the most accurate in all the basins under consideration, except for SDF basin 23. On average, the calibrated SDF/probability distribution-ratios varied between 0.85 and 1.15, whilst at some basins and individual return periods, less accurate results were evident.

In order to establish whether these calibrated run-off coefficients behaved in the probabilistic manner for which they were designed for, verification tests were conducted to convey confidence that the method works as anticipated. The verification of the calibrated run-off coefficients is discussed in the following section, Section 5.6.4, whilst the further evaluation and GOF statistics of the calibration results are discussed and listed in Section 5.7.4.

5.6.4 Verification of calibrated run-off coefficients and flood peaks

In Chapter 4 it was highlighted that the 16 catchments which were not used in the calibration exercise and for which AMS were available, were selected to verify the calibrated run-off coefficients in SDF basins 6, 7, 9 (study area), 10, 18 and 21. Verification was done, using the calibrated run-off coefficients previously calculated in Section 5.6.2 to estimate the SDF flood peaks in the same basin, but at another site. These verification catchments within the same basin were selected based on the fact that their physical and regional descriptors are similar, in other words, the catchments are situated within a smaller portion/number of quaternary catchments within the larger group of quaternary catchments used in the calibration exercise.

The flood peaks estimated for verification purposes with calibrated run-off coefficients will be referred to as $SDF_{Verified}$ (Q_3). The original and verified (similar to calibrated) C_2 and C_{100} run-off coefficients both applicable to the study area and the additional SDF basins evaluated in the rest of South Africa are listed in Tables B.62 and B.63, Addendum B, whilst Tables B.64 and B.65, Addendum B contain the verified (similar to calibrated) SDF run-off coefficients associated with return periods ranging from two to 200 years for all the basins under consideration. The comparison between the design flood peak values based on the direct statistical analyses and the original, adjusted and calibrated/verified versions of the SDF method is listed in Tables 5.40 and 5.41(a) – (e).

The flow gauging station numbers in brackets in column 1 of Tables 5.40 and 5.41(a) – (e) are the stations used for verification purposes. In the following paragraphs all the verification results obtained are discussed in detail and compared with the calibration results listed in Section 5.6.3.

SDF basin 9 (study area):

The verification results contained in Table 5.40 indicate that the original SDF method demonstrated the same trends of overestimating all the statistical flood peaks. Although, the magnitude of overestimation of the 2- and 5-year return period floods were slightly larger, whilst the flood peaks for the remaining return periods showed some improvement with the overestimation being limited to ± 30%. The adjusted SDF method results also improved slightly and were characterised by overestimations up to 163%. The verification results confirmed that the calibrated SDF method is the most accurate and similar trends were evident, although the flood peak associated with the 2-year return period being now correctly estimated. On average, the verified SDF/probability distribution-ratios varied between 1.01 and 1.18, which is acceptable.

Table 5.40: SDF basin 9: SDF flood estimation results (verification)

Catchment description	Method	Design flood (m^3/s) for return period (years)						
		2	**5**	**10**	**20**	**50**	**100**	**200**
C5R002 (C5R001)	$Q_{Statistical}$	31	94	169	276	482	701	992
	$SDF_{Original}$ (Q_1)	66	199	313	448	656	850	1 053
	$SDF_{Adjusted}$ (Q_2)	55	182	350	831	902	1 275	1 839
	$SDF_{Verified}$ (Q_3)	39	151	244	345	494	620	757
C5R002 (C5H008*)	$Q_{Statistical}$	45	175	325	432	585	712	851
	$SDF_{Original}$ (Q_1)	66	217	354	510	747	955	1 174
	$SDF_{Adjusted}$ (Q_2)	53	189	362	875	954	1 317	1 869
	$SDF_{Verified}$ (Q_3)	40	173	293	429	631	801	985
C5R002 (C5H012**)	$Q_{Statistical}$	57	120	180	219	256	275	288
	$SDF_{Original}$ (Q_1)	163	497	787	1 126	1 650	2 135	2 641
	$SDF_{Adjusted}$ (Q_2)	147	511	1 063	2 478	2 664	3 829	5 625
	$SDF_{Verified}$ (Q_3)	96	381	617	877	1 262	1 586	1 939
C5R003 (C5H003)	$Q_{Statistical}$	87	287	634	897	1 179	1 400	1 629
	$SDF_{Original}$ (Q_1)	125	387	616	883	1 294	1 670	2 063
	$SDF_{Adjusted}$ (Q_2)	109	381	775	1 822	1 966	2 797	4 074
	$SDF_{Verified}$ (Q_3)	89	313	501	709	1 016	1 274	1 554

Table 5.40: SDF basin 9: SDF flood estimation results (verification) (Continued)

Catchment description	Method	Design flood (m^3/s) for return period (years)						
		2	**5**	**10**	**20**	**50**	**100**	**200**
C5R004 (C5H015)	$Q_{Statistical}$	320	686	956	1 229	1 635	2 070	2 599
	$SDF_{Original}$ (Q_1)	239	715	1 139	1 625	2 407	3 135	3 960
	$SDF_{Adjusted}$ (Q_2)	234	823	1 855	4 229	4 553	6 711	10256
	$SDF_{Verified}$ (Q_3)	292	717	1 044	1 392	1 982	2 487	3 025
C5R004 (C5H054**)	$Q_{Statistical}$	16	40	67	104	175	250	349
	$SDF_{Original}$ (Q_1)	59	184	295	423	620	798	985
	$SDF_{Adjusted}$ (Q_2)	47	163	311	745	811	1 132	1 618
	$SDF_{Verified}$ (Q_3)	73	194	296	406	567	699	841
C5R005 (C5H022**)	$Q_{Statistical}$	10	25	39	56	81	102	125
	$SDF_{Original}$ (Q_1)	24	83	138	200	293	372	455
	$SDF_{Adjusted}$ (Q_2)	15	52	82	210	235	304	407
	$SDF_{Verified}$ (Q_3)	20	58	92	131	188	235	285
C5H016** (C5H018)	$Q_{Statistical}$	80	240	416	646	1 046	1 431	1 897
	$SDF_{Original}$ (Q_1)	344	1 058	1 688	2 434	3 626	4 725	5 976
	$SDF_{Adjusted}$ (Q_2)	371	1 382	3 399	7 667	8 216	12374	19341
	$SDF_{Verified}$ (Q_3)	76	329	536	765	1 110	1 407	1 739
Average Q_{SDF}/Q_{Stats}	**$Q_1/Q_{Statistical}$**	**1.44**	**1.44**	**1.28**	**1.28**	**1.30**	**1.32**	**1.31**
	$Q_2/Q_{Statistical}$	**1.23**	**1.39**	**1.59**	**2.63**	**1.99**	**2.23**	**2.62**
	$Q_3/Q_{Statistical}$	**1.02**	**1.18**	**1.06**	**1.04**	**1.04**	**1.03**	**1.01**

SDF basin 6:

The verification results contained in Table 5.41(a) applicable to both the original and adjusted SDF method confirm that similar trends as in the case of the calibration are present, although individual return period flood peaks are slightly less accurately estimated.

As in the case of calibration, the calibrated/verified version of the SDF method proved to be slightly less accurate than the adjusted method, with an average increase of 20% in the overestimations. However, the 200-year return period flood peak is correctly estimated.

Table 5.41(a): SDF basin 6: SDF flood estimation results (verification)

Catchment description	Method	Design flood (m^3/s) for return period (years)						
		2	**5**	**10**	**20**	**50**	**100**	**200**
C8H001 (C8H003*)	$Q_{Statistical}$	65	140	220	321	514	727	1 024
	$SDF_{Original}$ (Q_1)	74	208	313	429	594	735	888
	$SDF_{Adjusted}$ (Q_2)	73	121	172	279	505	761	1 174
	$SDF_{Verified}$ (Q_3)	44	206	338	483	695	872	1 062
Average Q_{SDF}/Q_{Stats}	**$Q_1/Q_{Statistical}$**	**1.14**	**1.49**	**1.42**	**1.34**	**1.16**	**1.01**	**0.87**
	$Q_2/Q_{Statistical}$	**1.12**	**0.86**	**0.78**	**0.87**	**0.98**	**1.05**	**1.15**
	$Q_3/Q_{Statistical}$	**0.68**	**1.47**	**1.54**	**1.50**	**1.35**	**1.20**	**1.04**

SDF basin 7:

The verification results contained in Table 5.41(b) show that both the original and verified versions of the SDF method demonstrated the opposite results, since the more frequent events (2- to 10-year return periods) are now being underestimated as opposed to the overestimations experienced during the calibration exercise. In essence, the verified SDF method follows this trend in all the return periods, but with some improvement. As in the case of calibration, the adjusted SDF method underestimated all the flood peaks, although the average underestimation increased to almost 70%. The original version of the SDF method proved to be the most accurate for return periods ranging from two to 20 years, whilst the verified version estimates the extreme events (50- to 200-year return periods) the best.

Table 5.41(b): SDF basin 7: SDF flood estimation results (verification)

Catchment description	Method	Design flood (m^3/s) for return period (years)						
		2	**5**	**10**	**20**	**50**	**100**	**200**
C4H002 (C4H001)	$Q_{Statistical}$	397	983	1 367	1 748	2 248	2 621	2 989
	$SDF_{Original}$ (Q_1)	292	849	1 315	1 828	2 576	3 365	4 187
	$SDF_{Adjusted}$ (Q_2)	143	276	423	525	662	805	943
	$SDF_{Verified}$ (Q_3)	210	642	983	1 350	1 979	2 509	3 077
Average Q_{SDF}/Q_{Stats}	**$Q_1/Q_{Statistical}$**	**0.74**	**0.86**	**0.96**	**1.05**	**1.15**	**1.28**	**1.40**
	$Q_2/Q_{Statistical}$	**0.36**	**0.28**	**0.31**	**0.30**	**0.29**	**0.31**	**0.32**
	$Q_3/Q_{Statistical}$	**0.53**	**0.65**	**0.72**	**0.77**	**0.88**	**0.96**	**1.03**

<u>SDF basin 10:</u>

The verification results contained in Table 5.41(c) confirm that the original SDF method demonstrated the same trends of overestimating all the statistical flood peaks. The magnitude of overestimation was limited to $\pm$ 138%, thus an improvement of almost 70%. The adjusted version of the SDF method demonstrated a slight improvement, but the results of the more frequent events (2- to 5-year return periods) are now being underestimated as opposed to the overestimations experienced during the calibration exercise. The verification results confirmed that the calibrated SDF method is the most accurate and similar trends were evident, although the estimated flood peaks were slightly underestimated. On average, the verified SDF/probability distribution-ratios varied between 0.82 and 1.01, which is still good.

Table 5.41(c): SDF basin 10: SDF flood estimation results (verification)

Catchment description	Method	Design flood (m^3/s) for return period (years)						
		2	**5**	**10**	**20**	**50**	**100**	**200**
D1H001 (D1H004)	$Q_{Statistical}$	34	73	114	164	241	309	386
	$SDF_{Original}$ (Q_1)	40	158	267	389	574	732	899
	$SDF_{Adjusted}$ (Q_2)	20	62	105	155	257	354	510
	$SDF_{Verified}$ (Q_3)	28	74	114	159	225	279	336
Average Q_{SDF}/Q_{Stats}	**$Q_1/Q_{Statistical}$**	**1.18**	**2.16**	**2.34**	**2.37**	**2.38**	**2.37**	**2.33**
	$Q_2/Q_{Statistical}$	**0.59**	**0.85**	**0.92**	**0.95**	**1.07**	**1.15**	**1.32**
	$Q_3/Q_{Statistical}$	**0.82**	**1.01**	**1.00**	**0.97**	**0.93**	**0.90**	**0.87**

<u>SDF basin 18:</u>

The verification results contained in Table 5.41(d) show that both the original and calibrated versions of the SDF method demonstrated the same trends as established during the calibration exercise. The adjusted SDF method overestimated all the flood peaks during the verification exercise as well, although the average overestimations showed a tendency to increase in magnitude with decreasing recurrence interval with overestimations up to 564%. The verification results confirmed that the calibrated SDF method is the most accurate with the verified SDF/probability distribution-ratios ranging from 0.93 to 1.19.

Table 5.41(d): SDF basin 18: SDF flood estimation results (verification)

Catchment description	Method	Design flood (m^3/s) for return period (years)						
		2	**5**	**10**	**20**	**50**	**100**	**200**
H3H001* (H7H004)	$Q_{Statistical}$	14	32	48	69	105	140	180
	$SDF_{Original}$ (Q_1)	20	47	70	95	131	160	191
	$SDF_{Adjusted}$ (Q_2)	93	148	139	169	209	248	285
	$SDF_{Verified}$ (Q_3)	13	36	57	80	114	142	172
Average Q_{SDF}/Q_{Stats}	**$Q_1/Q_{Statistical}$**	**1.43**	**1.47**	**1.46**	**1.38**	**1.25**	**1.14**	**1.06**
	$Q_2/Q_{Statistical}$	**6.64**	**4.63**	**2.90**	**2.45**	**1.99**	**1.77**	**1.58**
	$Q_3/Q_{Statistical}$	**0.93**	**1.13**	**1.19**	**1.16**	**1.09**	**1.01**	**0.96**

SDF basin 21:

The verification results contained in Table 5.41(e) indicate that both the original and calibrated versions of the SDF method demonstrated the same trends in the smaller catchments as established during the calibration exercise. However, the estimations were lower and more accurate with the SDF/probability distribution-ratios closer to unity. The adjusted version of the SDF method demonstrated a slight improvement, but the results of the more extreme events (20- to 200-year return periods) are now being underestimated as opposed to the overestimations experienced during the calibration exercise. The verification results in the smaller catchments confirmed that the calibrated SDF method is the most accurate with the verified SDF/probability distribution-ratios increasing from 0.83 to 1.10 with a decrease in recurrence interval.

In the larger catchments, the original SDF method overestimated all the flood peaks with the original SDF/probability distribution-ratios increasing from 0.97 to 2.27 with a decrease in recurrence interval. The adjusted SDF method displayed similar results as during the calibration with the degree of overestimation slightly higher. The calibrated SDF method exhibited the same tendency as in the smaller catchments, but the 5- to 20-year return period flood peaks were overestimated by 41% to 56%. However, the calibrated SDF method remains the preferred method based on the verification results obtained.

Table 5.41(e): SDF basin 21: SDF flood estimation results (verification)

Catchment description	Method	Design flood (m^3/s) for return period (years)						
		2	**5**	**10**	**20**	**50**	**100**	**200**
Q9H008* (Q9H004)	$Q_{Statistical}$	70	160	245	340	493	635	805
	$SDF_{Original}$ (Q_1)	46	147	240	345	501	632	771
	$SDF_{Adjusted}$ (Q_2)	16	71	173	278	431	553	736
	$SDF_{Verified}$ (Q_3)	77	169	249	335	460	560	666
Average Q_{SDF}/Q_{Stats}	**$Q_1/Q_{Statistical}$**	**0.66**	**0.92**	**0.98**	**1.01**	**1.02**	**1.00**	**0.96**
	$Q_2/Q_{Statistical}$	**0.23**	**0.44**	**0.71**	**0.82**	**0.87**	**0.87**	**0.91**
	$Q_3/Q_{Statistical}$	**1.10**	**1.06**	**1.02**	**0.99**	**0.93**	**0.88**	**0.83**
Q9H010 (Q1H001)	$Q_{Statistical}$	168	380	569	958	1 732	2 650	4 003
	$SDF_{Original}$ (Q_1)	310	844	1 315	1 861	2 740	3 538	4 471
	$SDF_{Adjusted}$ (Q_2)	332	1 059	2 060	3 367	5 626	7 628	11187
	$SDF_{Verified}$ (Q_3)	134	673	1 214	1 841	2 785	3 578	4 433
Q9H010 (Q7H003)	$Q_{Statistical}$	152	789	1 289	2 022	3 561	5 399	8 141
	$SDF_{Original}$ (Q_1)	365	1 006	1 562	2 227	3 288	4 250	5 373
	$SDF_{Adjusted}$ (Q_2)	505	1 575	2 925	4 849	8 242	11265	16770
	$SDF_{Verified}$ (Q_3)	163	824	1 351	1 917	2 732	3 410	4 225
Q9H010 (Q9H012)	$Q_{Statistical}$	132	514	869	1 342	2 209	3 104	4 265
	$SDF_{Original}$ (Q_1)	338	924	1 436	2 028	2 981	3 834	4 828
	$SDF_{Adjusted}$ (Q_2)	506	1 548	2 840	4 676	7 945	10831	16129
	$SDF_{Verified}$ (Q_3)	156	789	1 295	1 837	2 619	3 264	3 951
Average Q_{SDF}/Q_{Stats}	**$Q_1/Q_{Statistical}$**	**2.27**	**1.76**	**1.73**	**1.52**	**1.28**	**1.12**	**0.97**
	$Q_2/Q_{Statistical}$	**3.04**	**2.60**	**3.05**	**3.13**	**3.05**	**2.82**	**2.88**
	$Q_3/Q_{Statistical}$	**1.02**	**1.45**	**1.56**	**1.41**	**1.19**	**1.01**	**0.85**

The further evaluation and GOF statistics of the verification results are discussed and listed in Section 5.7.4.

5.7 ASSESSMENT OF RESULTS: COMPARISON

5.7.1 Direct statistical analyses

In Chapter 4 it was highlighted that regression (coefficient of determination) and descriptive (Chi-square) statistics would be used to evaluate the GOF of the fitted probability distributions. Firstly, the validity of Equation 2.46, Chapter 2, which can be used to determine the limiting critical value at confidence levels ranging from 90% to 99.5%, was evaluated. This was done by comparing the critical values obtained with Equation 2.46 with the critical values listed in Table 2.7, Chapter 2. The degrees of freedom and critical values listed in Table 2.7 were then plotted against one another to establish whether there exists any direct relationship which can be used to express the critical values in terms of the degrees of freedom.

The data points (as obtained from Table 2.7) are clustered around a curve to which a third order polynomial relationship could be fitted satisfactorily for confidence levels ranging from 90% to 99.5%. The results are also illustrative of a perfect fit, since the coefficient of determination (r^2) equals unity at all the different confidence levels. The degree of association between the data points (as obtained from Table 2.7) and Equation 2.46 was also good, since the coefficient of determination varied between 0.85 and 0.89. Based on these results, Equations 5.5a – 5.5e, as illustrated in Figure 5.21, can thus be used instead of Equation 2.46.

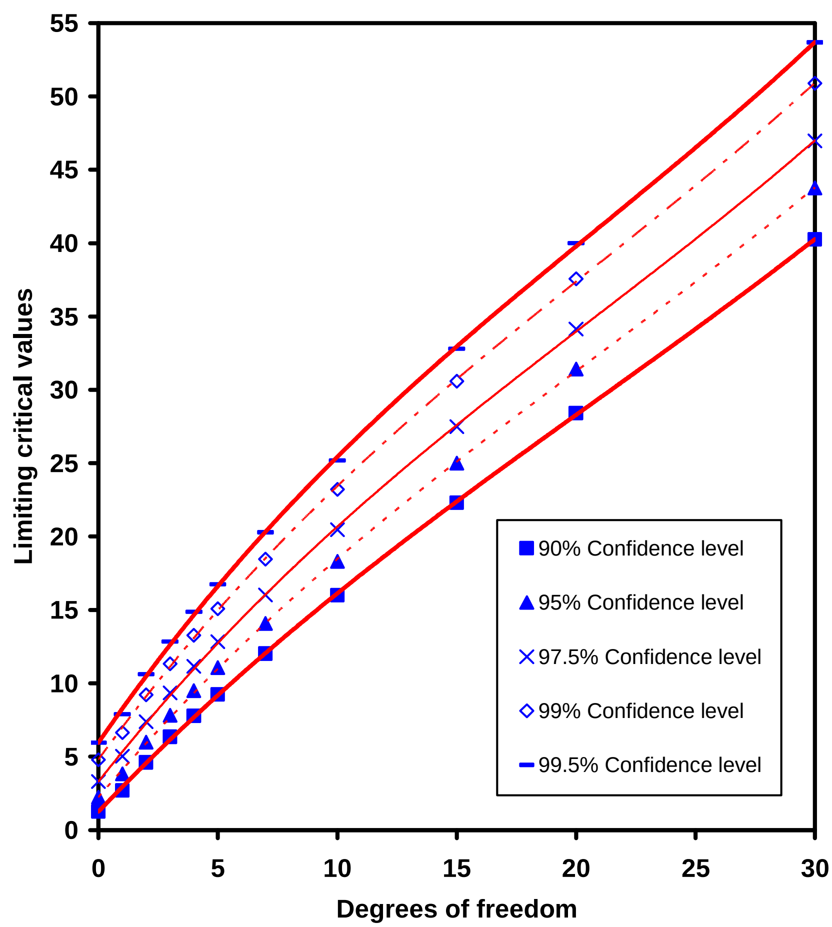

Figure 5.21: Limiting critical values and degrees of freedom

From Figure 5.21 it is evident that there exists a direct relationship between the limiting critical values and degrees of freedom used in the Chi-square statistic.

$$\chi^2_{v,90} = 0.0004v^3 - 0.0261v^2 + 1.7061v + 1.2541 \quad (5.5a)$$

$$\chi^2_{v,95} = 0.0005v^3 - 0.0332v^2 + 1.9028v + 2.2366 \quad (5.5b)$$

$$\chi^2_{v,97.5} = 0.0006v^3 - 0.0394v^2 + 2.0682v + 3.3003 \quad (5.5c)$$

$$\chi^2_{v,99} = 0.0007v^3 - 0.0450v^2 + 2.2424v + 4.7968 \quad (5.5d)$$

$$\chi^2_{v,99.5} = 0.0008v^3 - 0.0490v^2 + 2.3592v + 5.9569 \quad (5.5e)$$

Where:

$\chi^2_{v,1-\alpha}$ = Limiting critical value at a specific confidence level

v = Degrees of freedom

A confidence level of 95% and therefore Equation 5.5b was used during this study.

Table 5.42 provides a summary describing the GOF statistics of each fitted probability distribution used in the study area (SDF basin 9), whilst the GOF statistics of each fitted probability distribution used to evaluate the SDF method in the rest of South Africa (SA) are listed in Table B.66, Addendum B. The fitted probability distributions used in SDF basin 9 and SA are contained in Tables 5.31 (Section 5.5.1) and B.58 (Addendum B) respectively.

Table 5.42: SDF basin 9: GOF statistics of the fitted distributions

Catchment description	*T*-range (years)	r^2 *(2.40)*	χ^2 statistic *(2.42)*	χ^2 critical value *(5.5b)*	$C_{Contingency}$ *(2.47)*	C_{Max} *(2.48b)*	Confidence level (%)
C5R001	1 - 142	0.915	94.9	204.3	0.732	0.994	13.90
C5R002	1 - 160	0.978	114.2	294.2	0.741	0.995	6.73
C5R003	1 - 150	0.938	146.8	100.5	-	-	-
C5R004	1 - 100	0.991	29.9	101.6	0.576	0.992	99.94
C5R005	1 - 45	0.962	7.9	38.1	0.477	0.981	99.98
C5H003	1 - 71	0.864	319.9	84.3	-	-	-
C5H012	1 - 49	0.959	14.8	54	0.524	0.987	99.98
C5H015	1 - 54	0.982	35.6	45.5	0.720	0.985	30.38
C5H016	1 - 90	0.963	32.8	84.3	0.615	0.991	98.67
C5H018	1 - 85	0.852	191.2	72.4	-	-	-
C5H022	1 - 47	0.975	1.4	39.3	0.220	0.981	100
C5H054	1 - 65	0.904	24.6	54	0.622	0.987	95.47

The coefficients of determination (r^2) results are indicative of a high degree of association between the observed data and theoretical probability distributions, with 0.852 and 0.790 respectively as the poorest correlations in the study area (SDF basin 9) and additional catchments (SA SDF basins).

In all the study area catchments, except C5R003, C5H003 and C5H018, the Chi-square statistic was less than the limiting critical value and the confidence level larger than the significance level, in other words, the *null hypothesis* can be accepted. This was also the case in 60% of the catchments used to verify the SDF method in the rest of South Africa. However, acceptance of the *null hypothesis* at low confidence levels (< 50%), highlighted the likelihood of differences to be present, especially at C5R001, C5R002 and C5H015 in the study area. Similar detectable differences were present in 12% of the catchments used to evaluate the SDF method in the rest of South Africa.

The differences between Equations 2.47 and 2.48b are indicative of a moderate to good degree of association. Since Equation 2.47 is only a function of the Chi-square statistic (χ^2) and sample size *(N)*, it tends to give questionable results when the record length is either relatively long with a low associated Chi-square statistic or short with a high associated Chi-square statistic.

The overall results indicated that both the coefficient of determination and Chi-square statistic can be satisfactorily used to evaluate the GOF of fitted probability distributions. The Chi-square statistic tends to be more sensitive towards short record lengths, inconsistency, non-homogeneity and non-stationarity of data.

5.7.2 Deterministic methods

Figures C.51 to C.62, Addendum C, are illustrative of the probabilistic plot results as obtained by using the deterministic methods and also serve as a comparison with the empirical methods and direct statistical analyses. Tables 5.43(a) – (g) provide a summary describing the GOF statistics based on the least-square technique for each catchment used in the study area with return periods ranging from two to 200 years.

As indicated before, the direct statistical analysis results of C5H012, C5H016, C5H022 and C5H054 were excluded (marked with an *asterisk* **) from this comparison , since these AMS were characterised by numerous flood events that exceeded the hydraulic capacity of the particular gauging weirs, resulting in a higher degree of uncertainty and underestimation of flood peaks.

Table 5.43(a): 2-year Return period: Deterministic method results (m^3/s)

Catchment description	RM	ARM	SCS	$SDF_{Original}$	SUH	LRH	Q_{Stats}
C5R001	81	85	108	66	75	84	**31**
C5R002	328	426	455	351	217	227	**218**
C5R003	126	122	179	90	109	130	**75**
C5R004	245	308	311	236	232	223	**290**
C5R005	87	72	87	38	52	43	**35**
C5H003	169	169	239	125	146	172	**87**
C5H015	255	311	330	239	207	233	**320**
r^2-value	**0.73**	**0.73**	**0.65**	**0.69**	**0.86**	**0.80**	**-**
Average Q_D/Q_{Stats}	**1.70**	**1.77**	**2.18**	**1.29**	**1.35**	**1.46**	**-**

Table 5.43(b): 5-year Return period: Deterministic method results (m^3/s)

Catchment description	RM	ARM	SCS	$SDF_{Original}$	SUH	LRH	Q_{Stats}
C5R001	121	130	190	198	122	136	**94**
C5R002	490	642	823	1 059	361	375	**616**
C5R003	188	203	316	291	178	213	**225**
C5R004	363	451	561	710	386	365	**646**
C5R005	130	133	154	133	85	70	**86**
C5H003	253	267	422	387	239	283	**287**
C5H015	378	456	594	715	339	382	**686**
r^2-value	**0.87**	**0.85**	**0.82**	**0.83**	**0.95**	**0.91**	**-**
Average Q_D/Q_{Stats}	**0.92**	**1.02**	**1.39**	**1.45**	**0.80**	**0.85**	**-**

Table 5.43(c): 10-year Return period: Deterministic method results (m^3/s)

Catchment description	RM	ARM	SCS	$SDF_{Original}$	SUH	LRH	Q_{Stats}
C5R001	167	170	256	313	179	200	**169**
C5R002	675	831	1 111	1 692	520	541	**1 098**
C5R003	259	278	426	470	261	312	**440**
C5R004	497	576	759	1 134	562	535	**935**
C5R005	180	190	207	221	124	102	**139**
C5H003	349	356	568	616	352	415	**634**
C5H015	517	582	804	1 139	497	560	**956**
r^2-value	**0.96**	**0.92**	**0.95**	**0.91**	**0.96**	**0.95**	**-**
Average Q_D/Q_{Stats}	**0.73**	**0.79**	**1.08**	**1.35**	**0.67**	**0.70**	**-**

Table 5.43(d): 20-year Return period: Deterministic method results (m^3/s)

Catchment description	RM	ARM	SCS	$SDF_{Original}$	SUH	LRH	Q_{Stats}
C5R001	231	222	325	448	253	284	**276**
C5R002	929	1 075	1 416	2 417	727	756	**1 577**
C5R003	357	373	545	677	370	443	**655**
C5R004	678	735	973	1 618	790	751	**1 253**
C5R005	248	262	265	320	176	145	**198**
C5H003	481	471	726	883	498	587	**897**
C5H015	707	743	1 030	1 625	697	786	**1 229**
r^2-value	**0.97**	**0.94**	**0.98**	**0.93**	**0.93**	**0.93**	**-**
Average Q_D/Q_{Stats}	**0.70**	**0.73**	**0.95**	**1.34**	**0.65**	**0.69**	**-**

Table 5.43(e): 50-year Return period: Deterministic method results (m^3/s)

Catchment description	RM	ARM	SCS	$SDF_{Original}$	SUH	LRH	Q_{Stats}
C5R001	371	330	426	656	382	427	**482**
C5R002	1 490	1 573	1 850	3 590	1 103	1 146	**2 327**
C5R003	575	566	719	992	557	666	**810**
C5R004	1 075	1 057	1 285	2 402	1 205	1 134	**1 807**
C5R005	399	406	350	469	264	218	**287**
C5H003	773	705	959	1 294	750	884	**1 179**
C5H015	1 120	1 080	1 360	2 407	1 054	1 187	**1 635**
r^2-value	**0.98**	**0.96**	**0.98**	**0.97**	**0.91**	**0.88**	**-**
Average Q_D/Q_{Stats}	**0.78**	**0.76**	**0.88**	**1.38**	**0.69**	**0.72**	**-**

Table 5.43(f): 100-year Return period: Deterministic method results (m^3/s)

Catchment description	RM	ARM	SCS	$SDF_{Original}$	SUH	LRH	Q_{Stats}
C5R001	551	448	509	850	532	595	**701**
C5R002	2 204	2 125	2 202	4 678	1 529	1 593	**2 990**
C5R003	851	778	864	1 271	778	931	**972**
C5R004	1 576	1 409	1 541	3 129	1 667	1 590	**2 366**
C5R005	591	563	421	594	370	304	**368**
C5H003	1 145	965	1 152	1 670	1 048	1 234	**1 400**
C5H015	1 642	1 483	1 631	3 135	1 474	1 661	**2 070**
r^2-value	**0.97**	**0.95**	**0.97**	**0.98**	**0.91**	**0.86**	**-**
Average Q_D/Q_{Stats}	**0.90**	**0.81**	**0.82**	**1.39**	**0.75**	**0.79**	**-**

Table 5.43(g): 200-year Return period: Deterministic method results (m^3/s)

Catchment description	RM	ARM	SCS	$SDF_{Original}$	SUH	LRH	Q_{Stats}
C5R001	743	602	599	1 053	645	721	**992**
C5R002	2 970	2 834	2 576	5 929	1 852	1 927	**3 746**
C5R003	1 148	1 051	1 022	1 565	943	1 127	**1 143**
C5R004	2 108	1 891	1 819	3 966	2 014	1 933	**3 075**
C5R005	798	765	499	726	448	369	**461**
C5H003	1 544	1 300	1 362	2 063	1 269	1 497	**1 629**
C5H015	2 196	1 996	1 925	3 960	1 792	2 019	**2 599**
r^2-value	**0.95**	**0.93**	**0.95**	**0.97**	**0.90**	**0.83**	**-**
Average Q_D/Q_{Stats}	**0.97**	**0.87**	**0.78**	**1.38**	**0.72**	**0.76**	**-**

The results contained in Tables 5.43(a) – (g) are indicative of several trends associated with a specific return period, which will be highlighted in the following paragraph(s):

- 2-year Return period: All the deterministic flood peaks exceeded the statistical flood peaks, except in catchments C5R004 and C5H015. Although, both these catchments consist of the same quaternary catchments with similar hydrological responses. On average, the overestimation varied between 29% and 77%. The SUH method demonstrated the best results overall, with the coefficient of determination (r^2) equal to 0.86 with an associated average overestimation of 35%. The poorest results were demonstrated by the SCS method ($r^2 = 0.65$ and 118% overestimation).
- 5-year Return period: On average, only the SCS and SDF method exceeded the statistical flood peaks in all the catchments under consideration by 39% and 45% respectively. Again, the SUH method demonstrated the best results overall, with the coefficient of determination (r^2) equal to 0.95 with an associated average underestimation of 20%. The ARM also showed good results, with the coefficient of determination (r^2) equal to 0.85 with an average overestimation of 2%. The poorest results were demonstrated by the SDF method ($r^2 = 0.83$).

- 10-year Return period: Similar trends as identified at the 5-year return period range characterised the 10-year return period, however, on average, the over- and underestimation decreased and increased respectively. Again, the poorest results were demonstrated by the SDF method (r^2 = 0.91 and 35% overestimation). Figure 5.22 provides a visual measure of performance between the deterministic and statistical flood peaks.

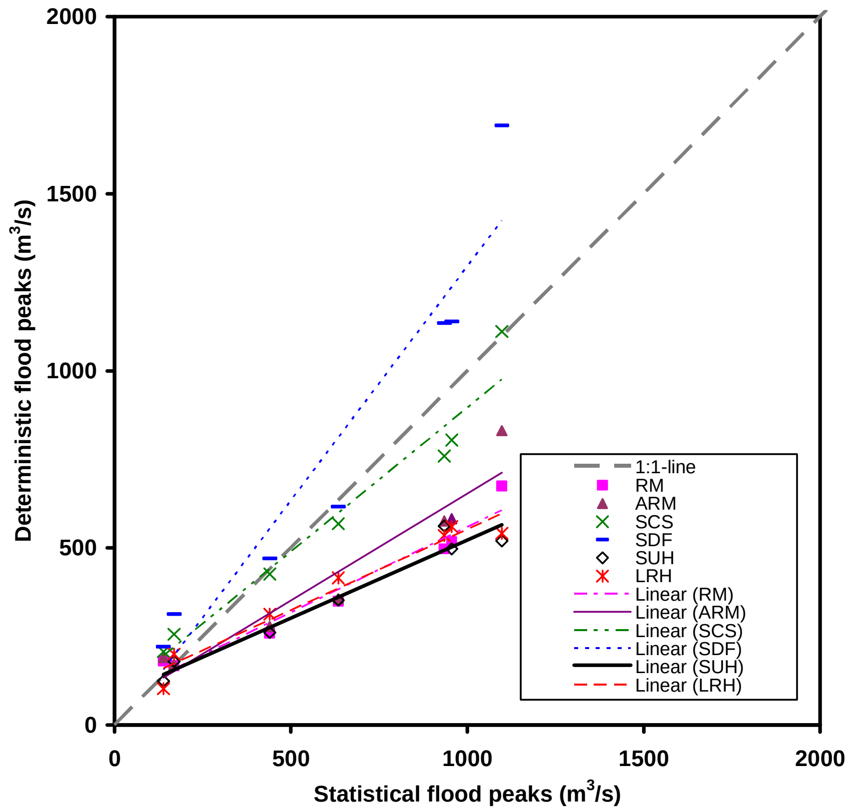

Figure 5.22: 1:10-year Deterministic versus statistical flood peaks

- 20-year Return period: On average, the poorest results were demonstrated by the SDF method, with the coefficient of determination (r^2) equal to 0.93 and an associated overestimation of 34%. However, on average, both the trends of over- and underestimation decreased compared to what was observed at the 10-year return period, whilst the degree of association improved.
- 50-year Return period: The results obtained were almost identical to the 20-year return period, except that the overestimation of flood peaks by the SDF method increased by another 4%, resulting in an overestimation of 38%.

- 100-year Return period: The results obtained were almost identical to the 50-year return period, except that both the under- and overestimation of flood peaks slightly improved. Figure 5.23 provides a visual measure of performance between the deterministic and statistical flood peaks.

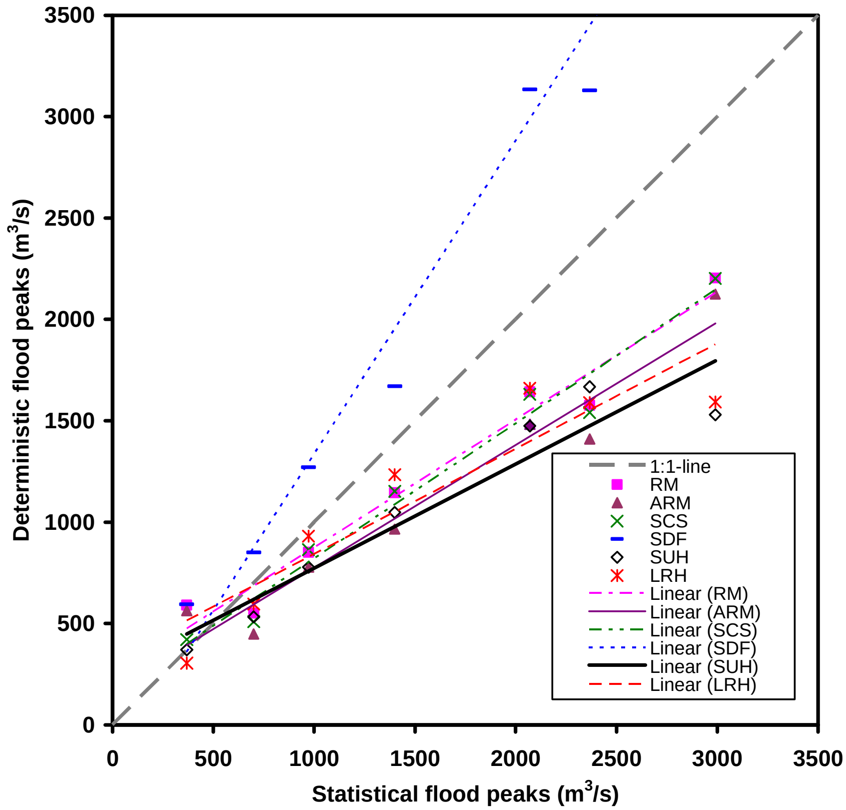

Figure 5.23: 1:100-year Deterministic versus statistical flood peaks

- 200-year Return period: The results obtained were almost identical to the 100-year return period, except that both the under- and overestimation of flood peaks slightly improved.

Apart from the trends identified and discussed in the paragraphs above, the overall results show that all the deterministic methods, except the SDF method, tend to underestimate the flood peaks when compared to the direct statistical analyses for return periods ranging from ten to 200 years. On average, the SDF method resulted in an overestimation of 37% for all the return periods under consideration. The degree of association between the individual deterministic methods, excluding the SDF method, was good, with r^2-values ranging from 0.76 to 0.99.

It is of utmost importance to realise that all the deterministic methods are based on average values derived from a large number of events at a regional level, consequently the acceptance or rejection of results based only on visual measures and GOF statistics can be subjective. Thus, the precipitation run-off relationship at a specific site will only be the same as that produced by direct statistical analysis if the site characteristics and hydrological and meteorological conditions are similar to the average conditions used in these methods. In addition, the field of application, limitations and assumptions associated with each method must also be taken into consideration before one can conclusively include or exclude a specific method.

5.7.3 Empirical methods

Figures C.51 to C.62, Addendum C, are illustrative of the probabilistic plot results as obtained by using the empirical methods and also serve as a comparison with the deterministic methods and direct statistical analyses. The GOF statistics of both the MIPI and CAPA methods were investigated in the same manner and to the same extent as discussed in Section 5.7.2. However, the MIPI method was only evaluated for return periods ranging from ten to 100 years.

The degree of association between these two methods was good for all the return periods under consideration, with r^2-values in the order of $\pm$ 0.98. Both these methods provided better results in comparison with the deterministic methods. Although, similar trends in the data were identified. On average, the degree of association between the MIPI method results and the direct statistical analyses increased from 0.93 to 0.98 for return periods ranging from ten to 100 years. On the other hand, the underestimation of flood peaks also increased to a maximum of 17%. The CAPA method proved to be slightly less accurate; with r^2-values ranging from 0.81 (2-year return period) to 0.98 (200-year return period) and a maximum underestimation of 23% at the higher order ($T > 20$ years) return periods.

Figures 5.24 and 5.25 provide a visual measure of performance between the empirical and statistical flood peaks for the 10- and 100-year return periods respectively.

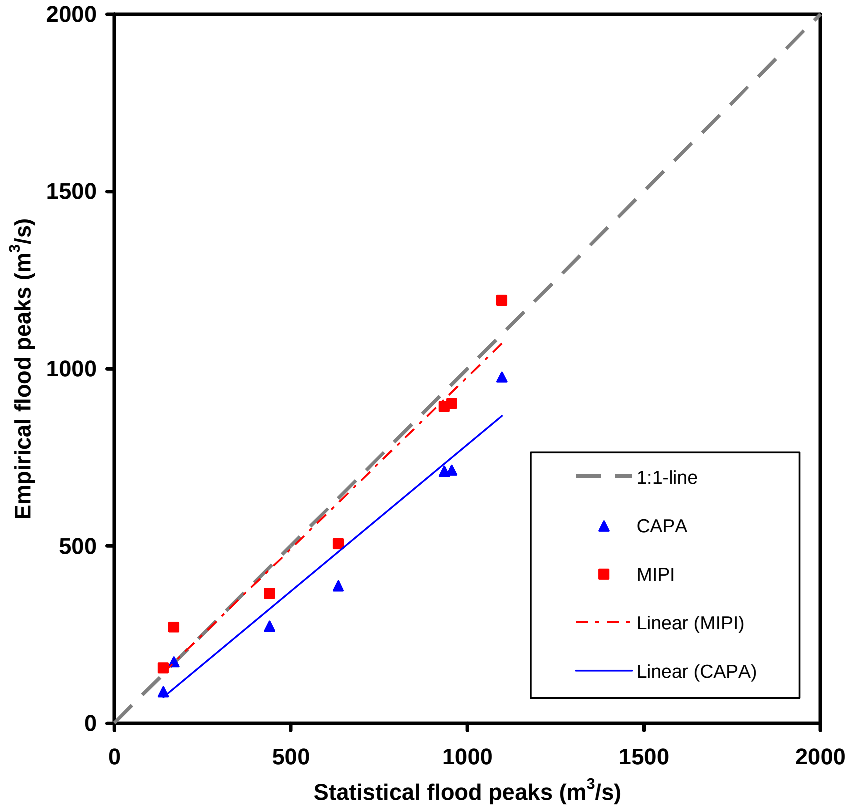

Figure 5.24: 1:10-year Empirical versus statistical flood peaks

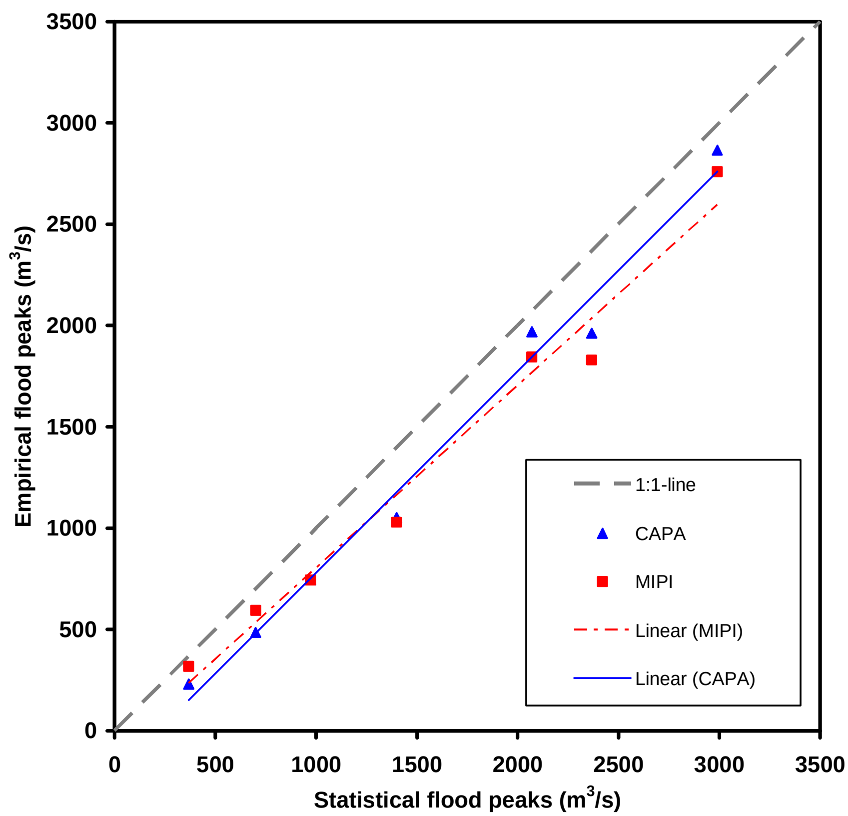

Figure 5.25: 1:100-year Empirical versus statistical flood peaks

5.7.4 SDF method for study area (SDF basin 9)

Figures C.63 to C.104, Addendum C, are illustrative of the probabilistic plot results as obtained by using the different versions of the SDF method during the calibration and verification exercises and also serve as a comparison with the direct statistical analyses. The GOF statistics of the original, adjusted, calibrated and verified versions of the SDF method applied in SDF basin 9 (study area) were investigated as discussed in Section 5.6.

Table 5.44(a): 2-year Return period: SDF method results (m^3/s)

Catchment description	$SDF_{Original}$	$SDF_{Adjusted}$	$SDF_{Calibrated}$	$SDF_{Verified}$	Q_{Stats}
C5R002	351	362	204	-	**218**
C5R003	90	75	64	-	**75**
C5R004	236	233	290	-	**290**
C5R005	38	26	32	-	**35**
***r*²-value**	**0.70**	**0.68**	**1**	**-**	**-**
Average Q_{SDF}/Q_{Stats}	**1.18**	**1.05**	**0.93**	**-**	**-**
C5R001	66	55	-	39	**31**
C5H003	125	109	-	89	**87**
C5H008*	66	53	-	40	**45**
C5H015	239	234	-	292	**320**
***r*²-value**	**0.97**	**0.98**	**-**	**1**	**-**
Average Q_{SDF}/Q_{Stats}	**1.44**	**1.23**	**-**	**1.02**	**-**

Table 5.44(b): 5-year Return period: SDF method results (m^3/s)

Catchment description	$SDF_{Original}$	$SDF_{Adjusted}$	$SDF_{Calibrated}$	$SDF_{Verified}$	Q_{Stats}
C5R002	1 059	1 298	773	-	**616**
C5R003	291	267	237	-	**225**
C5R004	710	821	709	-	**646**
C5R005	133	95	92	-	**86**
***r*²-value**	**0.85**	**0.84**	**0.98**	**-**	**-**
Average Q_{SDF}/Q_{Stats}	**1.41**	**1.42**	**1.12**	**-**	**-**
C5R001	199	182	-	151	**94**
C5H003	387	381	-	313	**287**
C5H008*	217	189	-	173	**175**
C5H015	715	823	-	717	**686**
***r*²-value**	**0.98**	**0.99**	**-**	**0.99**	**-**
Average Q_{SDF}/Q_{Stats}	**1.44**	**1.39**	**-**	**1.18**	**-**

Table 5.44(c): 10-year Return period: SDF method results (m^3/s)

Catchment description	$SDF_{Original}$	$SDF_{Adjusted}$	$SDF_{Calibrated}$	$SDF_{Verified}$	Q_{Stats}
C5R002	1 692	3 065	1 221	-	**1 098**
C5R003	470	528	389	-	**440**
C5R004	1 134	1 866	1 033	-	**935**
C5R005	221	163	147	-	**139**
r^2-value	**0.95**	**0.93**	**0.99**	**-**	**-**
Average Q_{SDF}/Q_{Stats}	**1.35**	**1.79**	**1.04**	**-**	**-**
C5R001	313	350	-	244	**169**
C5H003	616	775	-	501	**634**
C5H008*	354	362	-	293	**325**
C5H015	1 139	1 855	-	1 044	**956**
r^2-value	**0.94**	**0.90**	**-**	**0.92**	**-**
Average Q_{SDF}/Q_{Stats}	**1.28**	**1.59**	**-**	**1.06**	**-**

Table 5.44(d): 20-year Return period: SDF method results (m^3/s)

Catchment description	$SDF_{Original}$	$SDF_{Adjusted}$	$SDF_{Calibrated}$	$SDF_{Verified}$	Q_{Stats}
C5R002	2 417	6 926	1 703	-	**1 577**
C5R003	677	1 261	559	-	**655**
C5R004	1 618	4 251	1 376	-	**1 253**
C5R005	320	410	209	-	**198**
r^2-value	**0.96**	**0.94**	**0.99**	**-**	**-**
Average Q_{SDF}/Q_{Stats}	**1.37**	**2.95**	**1.02**	**-**	**-**
C5R001	448	831	-	345	**276**
C5H003	883	1 822	-	709	**897**
C5H008*	510	875	-	429	**432**
C5H015	1 625	4 229	-	1 392	**1 229**
r^2-value	**0.92**	**0.87**	**-**	**0.90**	**-**
Average Q_{SDF}/Q_{Stats}	**1.28**	**2.63**	**-**	**1.04**	**-**

Table 5.44(e): 50-year Return period: SDF method results (m^3/s)

Catchment description	$SDF_{Original}$	$SDF_{Adjusted}$	$SDF_{Calibrated}$	$SDF_{Verified}$	Q_{Stats}
C5R002	3 590	7 438	2 404	-	**2 327**
C5R003	992	1 368	812	-	**810**
C5R004	2 402	4 585	1 878	-	**1 807**
C5R005	469	454	300	-	**287**
r^2-value	**0.98**	**0.97**	**1**	**-**	**-**
Average Q_{SDF}/Q_{Stats}	**1.43**	**2.25**	**1.03**	**-**	**-**
C5R001	656	902	-	494	**482**
C5H003	1 294	1 966	-	1 016	**1 179**
C5H008*	747	954	-	631	**585**
C5H015	2 407	4 553	-	1 982	**1 635**
r^2-value	**0.94**	**0.90**	**-**	**0.93**	**-**
Average Q_{SDF}/Q_{Stats}	**1.30**	**1.99**	**-**	**1.04**	**-**

Table 5.44(f): 100-year Return period: SDF method results (m^3/s)

Catchment description	$SDF_{Original}$	$SDF_{Adjusted}$	$SDF_{Calibrated}$	$SDF_{Verified}$	Q_{Stats}
C5R002	4 678	11 085	3 010	-	**2 990**
C5R003	1 271	1 912	1 024	-	**972**
C5R004	3 129	6 766	2 356	-	**2 366**
C5R005	594	601	375	-	**368**
***r²*-value**	**0.98**	**0.97**	**1**	**-**	**-**
Average Q_{SDF}/Q_{Stats}	**1.45**	**2.54**	**1.02**	**-**	**-**
C5R001	850	1 275	-	620	**701**
C5H003	1 670	2 797	-	1 274	**1 400**
C5H008*	955	1 317	-	801	**712**
C5H015	3 135	6 711	-	2 487	**2 070**
***r²*-value**	**0.97**	**0.94**	**-**	**0.95**	**-**
Average Q_{SDF}/Q_{Stats}	**1.32**	**2.23**	**-**	**1.03**	**-**

Table 5.44(g): 200-year Return period: SDF method results (m^3/s)

Catchment description	$SDF_{Original}$	$SDF_{Adjusted}$	$SDF_{Calibrated}$	$SDF_{Verified}$	Q_{Stats}
C5R002	5 929	17 183	3 712	-	**3 746**
C5R003	1 565	2 744	1 253	-	**1 143**
C5R004	3 966	10 387	2 866	-	**3 075**
C5R005	726	822	455	-	**461**
***r²*-value**	**0.97**	**0.96**	**1**	**-**	**-**
Average Q_{SDF}/Q_{Stats}	**1.45**	**3.04**	**1**	**-**	**-**
C5R001	1 053	1 839	-	757	**992**
C5H003	2 063	4 074	-	1 554	**1 629**
C5H008*	1 174	1 869	-	985	**851**
C5H015	3 960	10 256	-	3 025	**2 599**
***r²*-value**	**0.98**	**0.97**	**-**	**0.96**	**-**
Average Q_{SDF}/Q_{Stats}	**1.31**	**2.62**	**-**	**1.01**	**-**

The results contained in Tables 5.44(a) – (g) indicate that both the original and adjusted SDF methods overestimated all the statistical flood peaks for the return periods ranging from two to 200 years during the calibration and verification exercises. The calibrated and verified versions of the SDF method proved to be the most accurate. On average, the calibrated and verified SDF/probability distribution-ratios varied between 0.93 and 1.18, with a high degree of association (r^2-values of between 0.9 and unity). The original and adjusted SDF methods also demonstrated a high degree of association, but it must be evaluated within the context of their poor SDF/probability distribution-ratios. Pair values of the coefficient of determination and these ratios must be evaluated in combination to get a true reflection of the accuracy.

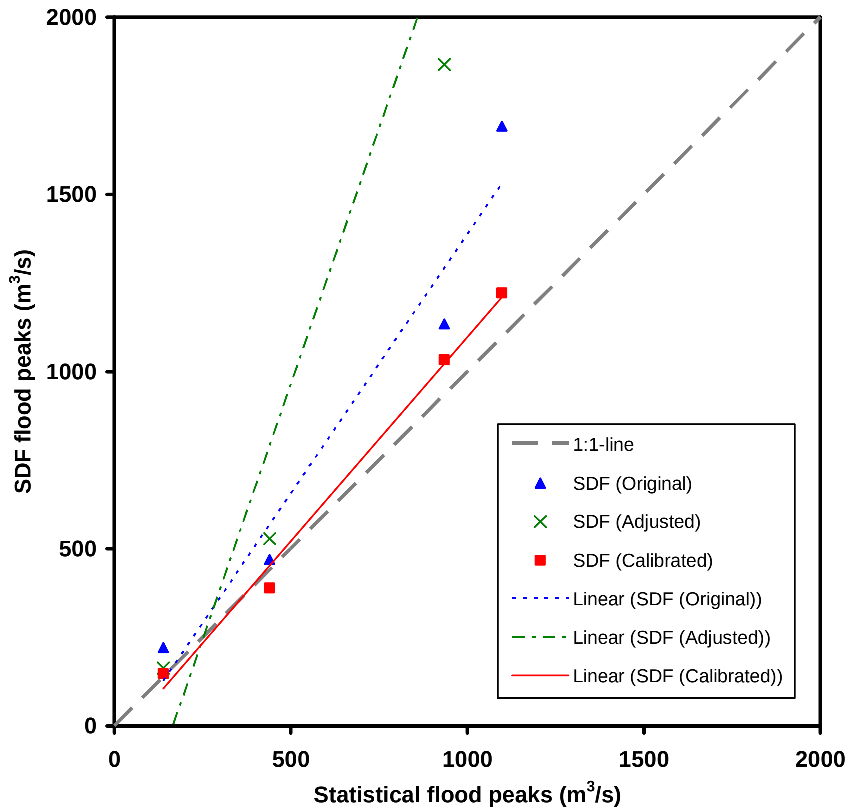

Figure 5.26: 1:10-year SDF versus statistical flood peaks (calibration)

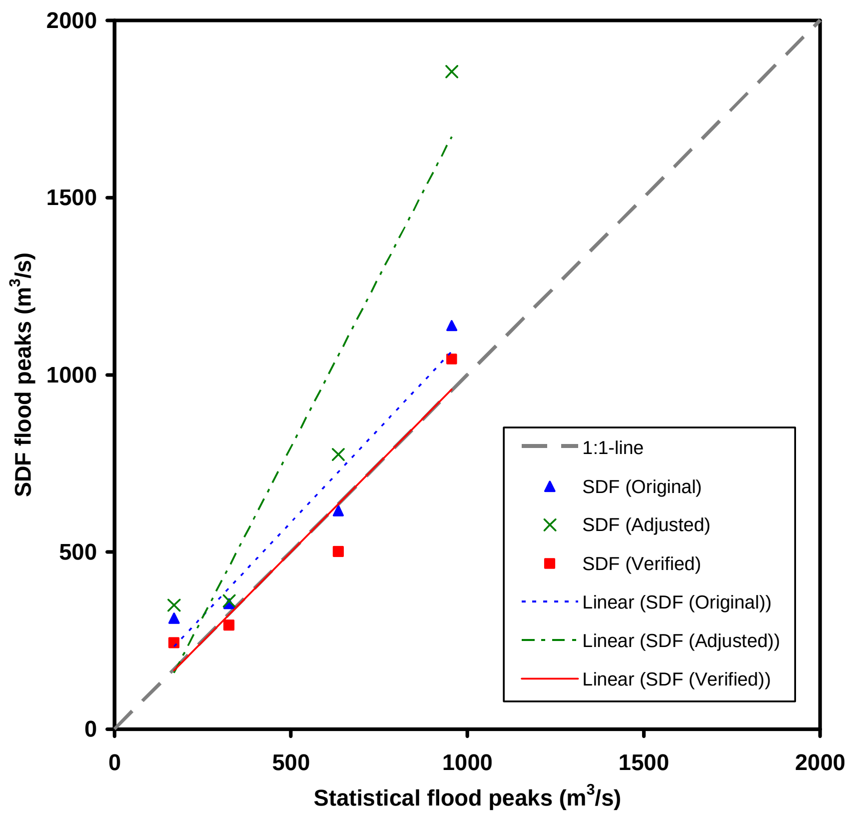

Figure 5.27: 1:10-year SDF versus statistical flood peaks (verification)

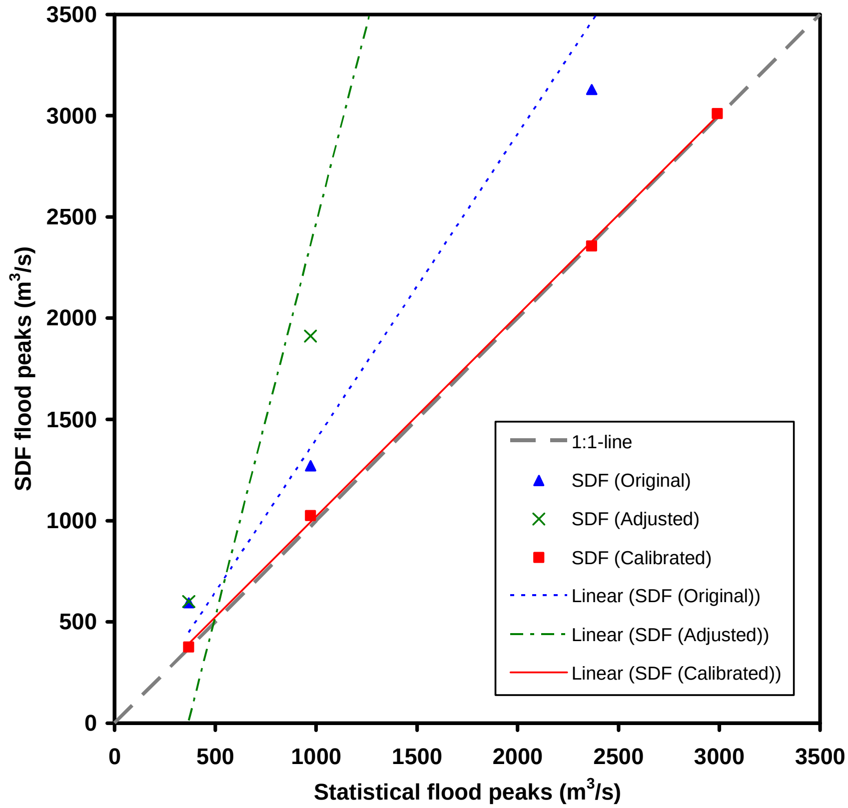

Figure 5.28: 1:100-year SDF versus statistical flood peaks (calibration)

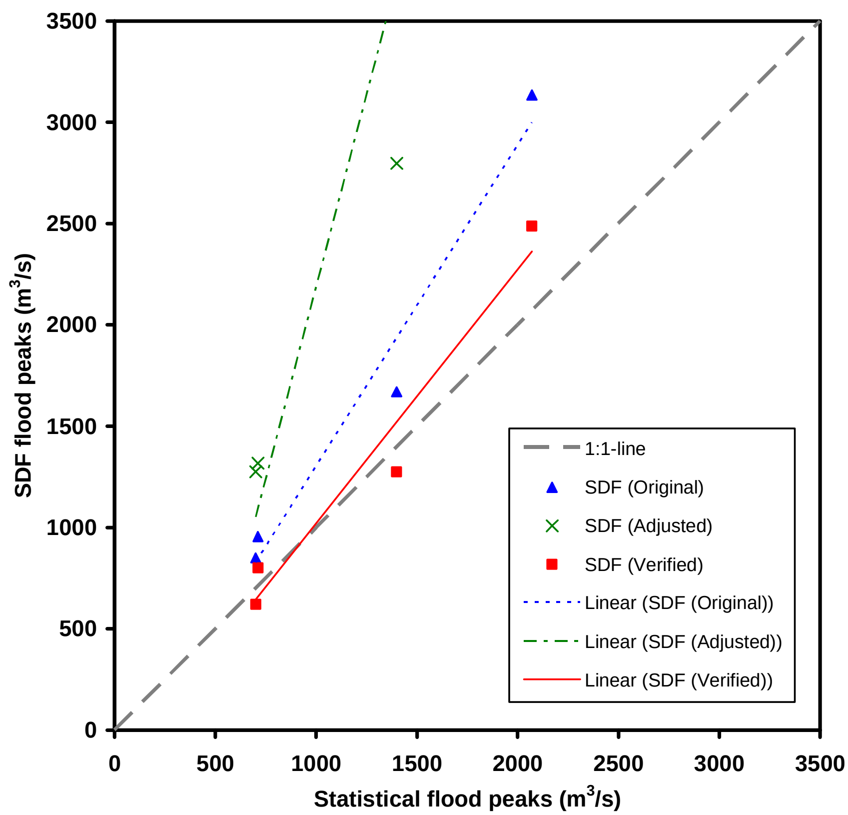

Figure 5.29: 1:100-year SDF versus statistical flood peaks (verification)

Figures 5.26 to 5.29 provide a visual measure of performance between the different versions of the SDF method and the statistical flood peaks for the 10- and 100-year return periods respectively. The original and adjusted SDF methods have a fairly large scatter above the 1:1 line and around their linear trendlines, which is indicative of their tendency to overestimate the flood peaks larger than $\pm$ 300 m^3/s and $\pm$ 500 m^3/s at the 10- and 100-year return periods respectively. Linear-space as opposed to log-space plots were used, since if the actual correlation is calculated in log-space it may disguise the fact that some flood peak ratios are occasionally different by up to a factor of 3.

All the other return period results of SDF basin 9 (study area), as well as all the other SDF basins investigated during this study, were evaluated in the same manner, but the graphical scatter plot results are not included. Similar trends were evident.

5.7.5 Summary of the flood frequency analyses in SDF basin 9

In this section the flood frequency analysis results of all the different design flood estimation methods used in the study area (SDF basin 9) are summarised. Tables 5.45(a) – (g) provide a summary of the GOF statistics for all the methods used for return periods ranging from two to 200 years. The notations SDF_1 (Original SDF), SDF_2 (Adjusted SDF) and SDF_3 (Calibrated SDF) were used in the above-mentioned tables. Figures 5.30 and 5.31 provide a visual measure of performance between the different design flood estimation methods and the statistical flood peaks for the 10- and 100-year return periods respectively.

Table 5.45(a): 2-year Return period: Flood frequency analyses (m^3/s)

Catchment	RM	ARM	SCS	SUH	LRH	CAPA	MIPI	SDF_1	SDF_2	SDF_3	Q_{Stats}
C5R001	81	85	108	75	84	49	-	66	55	39	**31**
C5R002	328	426	455	217	227	253	-	351	362	204	**218**
C5R003	126	122	179	109	130	82	-	90	75	64	**75**
C5R004	245	308	311	232	223	206	-	236	233	290	**290**
C5R005	87	72	87	52	43	29	-	38	26	32	**35**
C5H003	169	169	239	146	172	116	-	125	109	89	**87**
C5H015	255	311	330	207	233	207	-	239	234	292	**320**
***r*²-value**	**0.73**	**0.73**	**0.65**	**0.86**	**0.80**	**0.81**	**-**	**0.69**	**0.67**	**0.99**	**-**
Q_D/Q_{Stats}	**1.70**	**1.77**	**2.18**	**1.35**	**1.46**	**1.05**	**-**	**1.29**	**1.14**	**0.99**	**-**

Table 5.45(b): 5-year Return period: Flood frequency analyses (m^3/s)

Catchment	RM	ARM	SCS	SUH	LRH	CAPA	MIPI	SDF_1	SDF_2	SDF_3	Q_{Stats}
C5R001	121	130	190	122	136	112	-	198	182	151	**94**
C5R002	490	642	823	361	375	614	-	1 059	1 298	773	**616**
C5R003	188	203	316	178	213	180	-	291	267	237	**225**
C5R004	363	451	561	386	365	463	-	710	821	709	**646**
C5R005	130	133	154	85	70	60	-	133	95	92	**86**
C5H003	253	267	422	239	283	255	-	387	381	313	**287**
C5H015	378	456	594	339	382	465	-	715	823	717	**686**
r^2-value	**0.87**	**0.85**	**0.82**	**0.95**	**0.91**	**0.90**	**-**	**0.83**	**0.82**	**0.98**	**-**
Q_D/Q_{Stats}	**0.92**	**1.02**	**1.39**	**0.80**	**0.85**	**0.85**	**-**	**1.45**	**1.45**	**1.17**	**-**

Table 5.45(c): 10-year Return period: Flood frequency analyses (m^3/s)

Catchment	RM	ARM	SCS	SUH	LRH	CAPA	MIPI	SDF_1	SDF_2	SDF_3	Q_{Stats}
C5R001	167	170	256	179	200	173	271	313	350	244	**169**
C5R002	675	831	1 111	520	541	977	1 193	1 692	3 065	1 221	**1 098**
C5R003	259	278	426	261	312	274	366	470	528	389	**440**
C5R004	497	576	759	562	535	711	894	1 134	1 866	1 033	**935**
C5R005	180	190	207	124	102	89	156	221	163	147	**139**
C5H003	349	356	568	352	415	388	506	616	775	501	**634**
C5H015	517	582	804	497	560	714	902	1 139	1 855	1 044	**956**
r^2-value	**0.96**	**0.92**	**0.95**	**0.96**	**0.95**	**0.95**	**0.95**	**0.91**	**0.87**	**0.96**	**-**
Q_D/Q_{Stats}	**0.73**	**0.79**	**1.08**	**0.67**	**0.70**	**0.76**	**1.05**	**1.35**	**1.77**	**1.07**	**-**

Table 5.45(d): 20-year Return period: Flood frequency analyses (m^3/s)

Catchment	RM	ARM	SCS	SUH	LRH	CAPA	MIPI	SDF_1	SDF_2	SDF_3	Q_{Stats}
C5R001	231	222	325	253	284	251	337	448	831	345	**276**
C5R002	929	1 075	1 416	727	756	1 441	1 568	2 417	6 926	1 703	**1 577**
C5R003	357	373	545	370	443	392	422	677	1 261	559	**655**
C5R004	678	735	973	790	751	1 024	1 037	1 618	4 251	1 376	**1 253**
C5R005	248	262	265	176	145	125	180	320	410	209	**198**
C5H003	481	471	726	498	587	555	583	883	1 822	709	**897**
C5H015	707	743	1 030	697	786	1 028	1 046	1 625	4 229	1 392	**1 229**
r^2-value	**0.97**	**0.94**	**0.98**	**0.93**	**0.93**	**0.96**	**0.93**	**0.93**	**0.90**	**0.96**	**-**
Q_D/Q_{Stats}	**0.70**	**0.73**	**0.95**	**0.65**	**0.69**	**0.76**	**0.87**	**1.34**	**2.89**	**1.04**	**-**

Table 5.45(e): 50-year Return period: Flood frequency analyses (m^3/s)

Catchment	RM	ARM	SCS	SUH	LRH	CAPA	MIPI	SDF_1	SDF_2	SDF_3	Q_{Stats}
C5R001	371	330	426	382	427	381	468	656	902	494	**482**
C5R002	1 490	1 573	1 850	1 103	1 146	2 223	2 175	3 590	7 438	2 404	**2 327**
C5R003	575	566	719	557	666	588	589	992	1 368	812	**810**
C5R004	1 075	1 057	1 285	1 205	1 134	1 544	1 448	2 402	4 585	1 878	**1 807**
C5R005	399	406	350	264	218	184	251	469	454	300	**287**
C5H003	773	705	959	750	884	831	815	1 294	1 966	1 016	**1 179**
C5H015	1 120	1 080	1 360	1 054	1 187	1 550	1 461	2 407	4 553	1 982	**1 635**
r^2-value	**0.98**	**0.96**	**0.98**	**0.91**	**0.88**	**0.98**	**0.97**	**0.97**	**0.95**	**0.97**	**-**
Q_D/Q_{Stats}	**0.78**	**0.76**	**0.88**	**0.69**	**0.72**	**0.80**	**0.84**	**1.38**	**2.19**	**1.03**	**-**

Table 5.45(f): 100-year Return period: Flood frequency analyses (m^3/s)

Catchment	RM	ARM	SCS	SUH	LRH	CAPA	MIPI	SDF_1	SDF_2	SDF_3	Q_{Stats}
C5R001	551	448	509	532	595	485	593	850	1 275	620	**701**
C5R002	2 204	2 125	2 202	1 529	1 593	2 866	2 759	4 678	11085	3 010	**2 990**
C5R003	851	778	864	778	931	744	744	1 271	1 912	1 024	**972**
C5R004	1 576	1 409	1 541	1 667	1 590	1 962	1 829	3 129	6 766	2 356	**2 366**
C5R005	591	563	421	370	304	230	317	594	601	375	**368**
C5H003	1 145	965	1 152	1 048	1 234	1 052	1 029	1 670	2 797	1 274	**1 400**
C5H015	1 642	1 483	1 631	1 474	1 661	1 969	1 845	3 135	6 711	2 487	**2 070**
r^2-value	**0.97**	**0.95**	**0.97**	**0.91**	**0.86**	**0.99**	**0.98**	**0.98**	**0.96**	**0.97**	**-**
Q_D/Q_{Stats}	**0.90**	**0.81**	**0.82**	**0.75**	**0.79**	**0.80**	**0.83**	**1.39**	**2.46**	**1.01**	**-**

Table 5.45(g): 200-year Return period: Flood frequency analyses (m^3/s)

Catchment	RM	ARM	SCS	SUH	LRH	CAPA	MIPI	SDF_1	SDF_2	SDF_3	Q_{Stats}
C5R001	743	602	599	645	721	589	-	1 053	1 839	757	**992**
C5R002	2 970	2 834	2 576	1 852	1 927	3 511	-	5 929	17183	3 712	**3 746**
C5R003	1 148	1 051	1 022	943	1 127	897	-	1 565	2 744	1 253	**1 143**
C5R004	2 108	1 891	1 819	2 014	1 933	2 373	-	3 966	10387	2 866	**3 075**
C5R005	798	765	499	448	369	274	-	726	822	455	**461**
C5H003	1 544	1 300	1 362	1 269	1 497	1 268	-	2 063	4 074	1 554	**1 629**
C5H015	2 196	1 996	1 925	1 792	2 019	2 382	-	3 960	10256	3 025	**2 599**
r^2-value	**0.95**	**0.93**	**0.95**	**0.90**	**0.83**	**0.98**	**-**	**0.97**	**0.96**	**0.97**	**-**
Q_D/Q_{Stats}	**0.97**	**0.87**	**0.78**	**0.72**	**0.76**	**0.77**	**-**	**1.38**	**2.92**	**0.98**	**-**

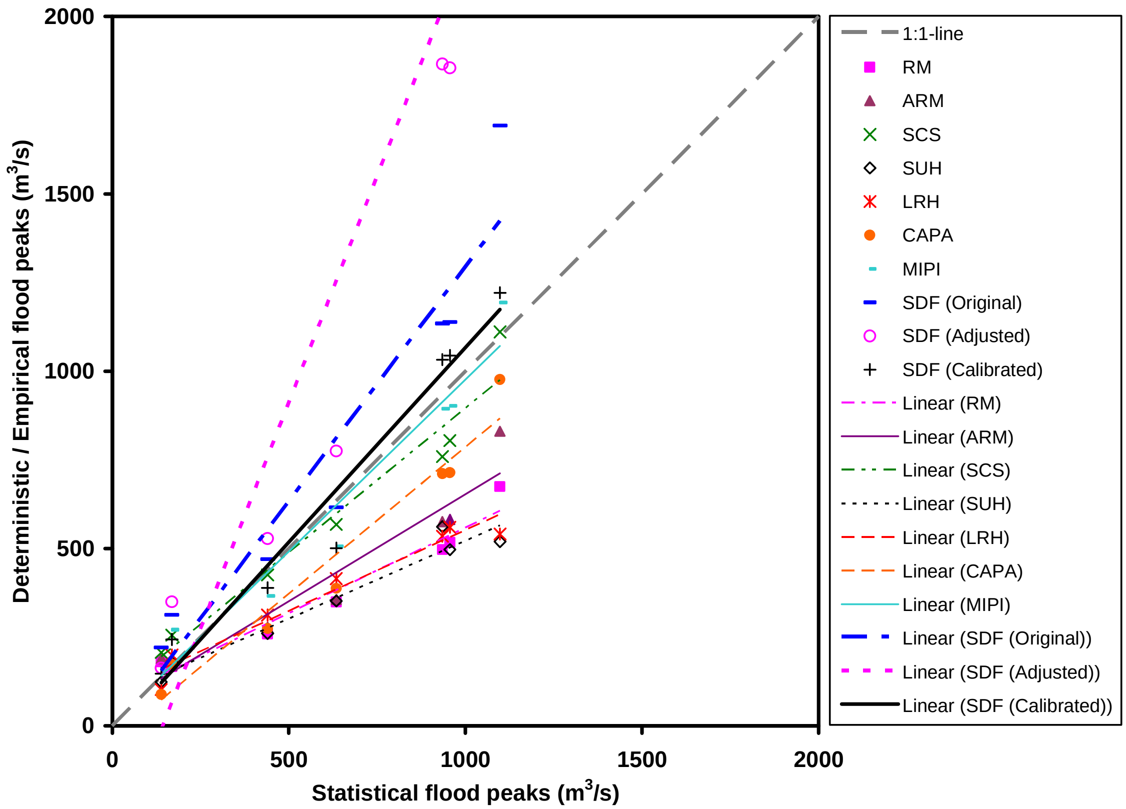

Figure 5.30: SDF basin 9: Comparison of 1:10-year flood peaks

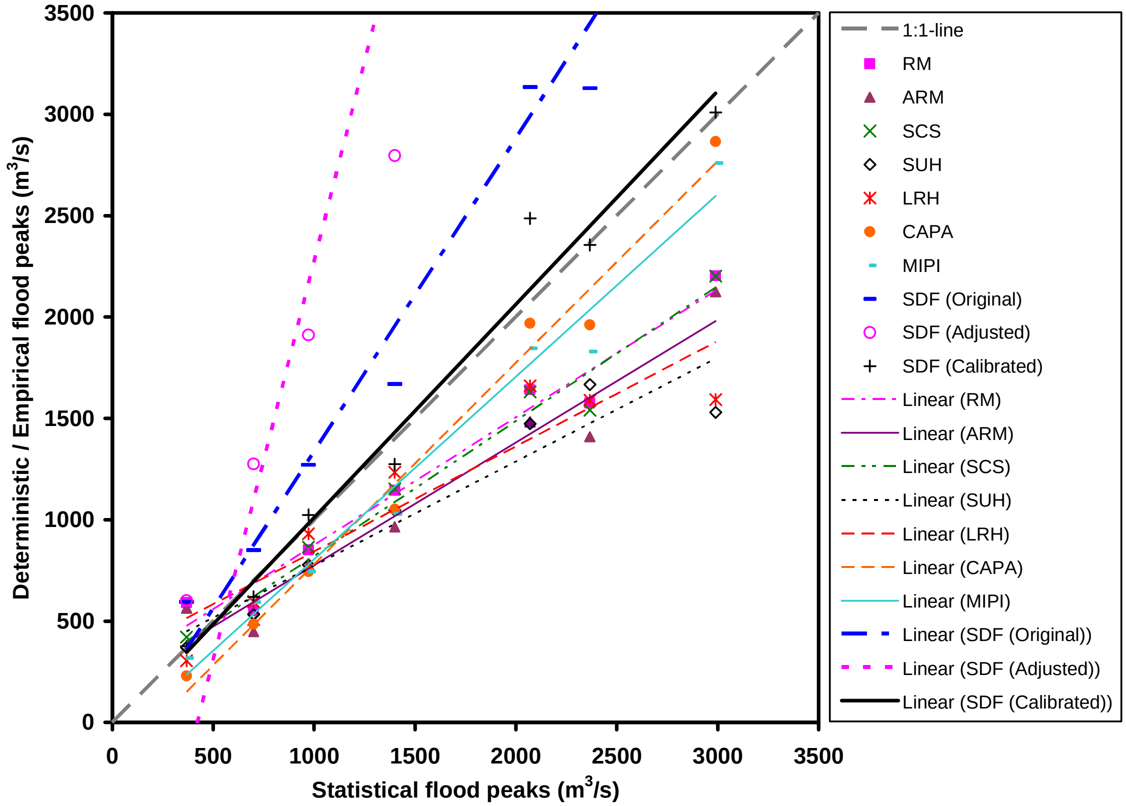

Figure 5.31: SDF basin 9: Comparison of 1:100-year flood peaks

The results contained in Tables 5.45 (a) – (g) prove that the calibrated version of the SDF method (SDF_3) is the most accurate method used in the study area (SDF basin 9) for all the return periods under consideration. On average, the calibrated SDF/probability distribution-ratios varied between 0.98 and 1.17, with a high degree of association. The r^2-values varied between 0.95 and 0.99.

In conclusion, the proposed quaternary catchment boundaries, single precipitation stations and calibrated C_2 and C_{100} run-off coefficients used during this study are recommended for future use in this basin. The probabilistic-based approach of the calibrated SDF method proved to have the essential qualities to overcome some of the deficiencies evident in the other techniques used for design flood estimation in this basin.

CHAPTER

6

CONCLUSIONS AND RECOMMENDATIONS

CHAPTER 6: CONCLUSIONS AND RECOMMENDATIONS

6.1 STUDY OBJECTIVES

The *primary aim* of this study was to evaluate, verify and calibrate SDF run-off coefficients at a quaternary catchment level in the C5 secondary drainage region by establishing the catchment parameters and SDF/probability distribution-ratios.

The *secondary aim* of this study was to develop a customised, user-friendly DFET in a MS-Excel and/or MS-VBA environment in order to assess the use and applicability of the various design flood estimation methods in comparison to the SDF method.

To achieve the research aims, the following specific objectives were identified:

- Evaluate, manipulate and prepare all hydrological and meteorological data from selected representative flow gauging and weather stations in the C5 secondary drainage region.
- Develop Geographical Information Systems (GIS) containing the relevant spatial information of the C5 secondary drainage region.
- Investigate the use of a GIS-based DEM as opposed to manual procedures and empirical equations to establish the average catchment slope and catchment centroid.
- Conduct direct statistical analyses of observed annual flood peak maxima at representative flow gauging stations in the quaternary catchments.
- Select daily precipitation stations representative of the meteorological conditions in each quaternary catchment of concern by making use of the design precipitation depths as proposed by Smithers and Schulze (2003).
- Numerically calibrate the run-off coefficients used in the SDF method to fit the results obtained by the direct statistical analyses in order to establish the quaternary SDF run-off coefficients for different return periods.
- Compare the quaternary and existing regional SDF run-off coefficients.
- Evaluate the validity of the run-off coefficient adjustment factors as proposed by Van Bladeren (2005).
- Apply the suite of deterministic, empirical and statistical methods available in the DFET in the selected quaternary catchments.

- Demonstrate the use of the DFET and compare the results obtained to establish whether the probabilistic-based approach of the SDF method does have the ability to overcome some of the deficiencies evident in the other techniques used for design flood estimation in the C5 secondary drainage region.
- Compile a user's manual for the DFET.

In the next section these objectives will be discussed individually.

6.2 DATA DEVELOPMENT AND EVALUATION

6.2.1 Catchment and GIS data

Catchment area and average catchment slope:

The DEM developed from the SRTM elevation data for Southern Africa at 90-metre resolution proved to provide accurate raster information which can be used to establish the various input parameters (area, length and slope) used in catchment parameter analyses.

The developed DEM was assumed to be the most accurate representation of the actual average catchment slope and was therefore used as the baseline data to evaluate the grid method and empirical equation in this regard. The grid method underestimated the average catchment slope in all the catchments under consideration, whilst the results confirmed that either an increase or decrease in the number of grid points per km² does not necessarily guarantee higher accuracies when compared with the DEM (GIS) data. The optimum number of grid points per km² is 0.5, which confirms the recommendation made by Alexander (1990) and Van der Spuy and Rademeyer (2008) that the minimum number of grid points in catchments smaller or larger than 10 km² must be 20 and 50 respectively.

The empirical equation underestimated the average catchment slope in all the catchments under consideration. The results confirmed that there is only a direct relationship between the area (*A*) and the total length of all contour lines within the catchment (*M*) for slopes steeper than 4% and catchment areas larger than 15 000 km². Thus, the higher the *M:A*-ratios, the more accurate the empirical equation becomes.

Both the grid method and empirical equation demonstrated equally high degrees of association with the DEM (GIS) data and can be used along with suitable tools in the ArcGIS™ environment to estimate the average catchment slope. The grid method is especially useful for the development of slope frequency distribution classes, but the method is sensitive to biased user-input at different scale resolutions in terms of the grid density, extent of catchment areas and contour intervals used. On the other hand, the empirical equation in conjunction with standard functions in ArcGIS™ is quicker to use and proved to be equally accurate.

Distance to catchment centroid (L_C):

The catchment centroid distances are influenced by the size and shape of the catchment area, but more importantly, influenced by the average catchment slope. The steeper the average catchment slope, the lower the L_C:L-ratio. The general assumption of using a L_C:L-ratio of between 0.5 and 0.6 proved to be sufficiently accurate to be used in the various design flood estimation methods.

Average main watercourse slope:

The main watercourse average slopes were determined by using the Equal-area, 10-85 and Taylor-Schwarz methods. The degree of association between these methods was high, since the coefficient of determination varied between 0.995 and 0.998. In the past, preference was given to the 10-85 method, since the Equal-area method is largely a graphical procedure and the use of the Taylor-Schwarz method is not widely known in South Africa. The ease of use and numerical application of each method in the DFET is equal, thus the results as obtained with these methods are the only selection criteria.

Soil classification, land use and vegetation:

The hydrological response in any catchment under consideration will be different due to the difference in soil permeability which controls the infiltration rate and consequently the balance of precipitation that constitutes surface run-off and contributes to the flood peak. Apart from the permeability associated with each hydrological soil group, the volume, duration and precipitation intensity should also be considered.

The reclassification and grouping of the land use and vegetation data contained in the National Landcover Database (CSIR, 2001) into standard classification classes as used in the deterministic methods proved to be useful. These classifications were used to determine weighted urban and rural run-off coefficients, which have a direct influence on the amount of run-off being estimated. The degree to which a specific land use can be classified as permeable or impermeable also had a direct influence on the precipitation run-off process, with specific reference to the attenuation and translation of flood peaks.

It was evident from all these data sets that the study area, as well as the individual catchments, can be classified as rural. Grasslands dominate the rural component, whilst residential areas dominate the urban component. Three homogeneous generalised veld-type regions were identified in the study area, namely Grassland of the interior plateau, Karoo and False Karoo, with the latter dominating the landscape (60%). Three Kovács flood regions, namely K3, K4 and K5 were also identified in the study area, with the latter region dominating the landscape (43%).

GIS applications in the ArcGIS™ environment for the purpose of catchment parameter analyses are recommended to be used as the standard procedure in any proposed hydrological assessments.

6.2.2 Meteorological data

Design precipitation:

The flood frequency analyses conducted in this study were only based on the SAWS precipitation database, since the TR102 precipitation database has ± 20 years less data available and is limited to 1 946 stations as opposed to the 3 946 SAWS precipitation stations. The SAWS precipitation database is also used in the software program, *Design Rainfall Estimation in South Africa* as developed by Smithers and Schulze (2003).

The arithmetic mean and/or Thiessen polygon methods were used to convert the point precipitation depths at precipitation stations to an average precipitation depth over the catchment area. The number of precipitation stations used varied from catchment to catchment with an overall average of one station per 100 km². The arithmetic mean values slightly exceeded the Thiessen polygon values in all the catchments, except for the catchments where the polygons were based on precipitation stations within and outside the catchment boundary. A high degree of association between these two methods was evident where the precipitation stations had an even areal distribution and associated relative flat catchment topography. Under any other conditions, the Thiessen polygon method would be the preferred method to use.

The critical storm duration precipitation depths used in this study, were based on the following approaches:

- DDF relationship based on LEV1 distributions (Midgley & Pitman).
- DDF relationship based on the 24-hour SAWS daily precipitation data.
- DDF relationship based on the modified Hershfield equation and/or SAWS daily precipitation data.
- DDF relationship based on the RLMA&SI approach.

The DDF (LEV1) relationship estimated the highest design precipitation depths in all the catchments under consideration for the 50- to 200-year return periods and critical storm durations up to 50 hours, whilst it underestimated all the design precipitation depths with critical storm duration in excess or exceeding 100 hours. The DDF (Hershfield/SAWS) relationship estimated the second highest design precipitation depths for the whole range of return periods under consideration, except in basins 2, 6 and 21 (Q1H001) where it was in agreement with the DDF (RLMA&SI) relationship. The lowest design precipitation depths were estimated by the DDF (RLMA&SI) relationship, except in cases where the critical storm duration exceeded 50 hours. However, it resulted in higher estimates compared to those of the DDF (Hershfield/SAWS) relationship and was in better agreement with the DDF (LEV1) relationship for the above-mentioned return periods.

The degree of association (r^2-values) between these methods was acceptable, although some trends were evident. On average, these methods demonstrated a high degree of association amongst each other, with r^2-values larger than 0.92 for critical storm durations less than 6 hours.

The critical storm duration range between 6 hours and 24 hours were characterised by a constant relationship (r^2-values equals 0.91) between the DDF (LEV1) and DDF (Hershfield/SAWS) relationships, whilst the degree of association between the DDF (Hershfield/SAWS) and DDF (RLMA&SI) relationships decreased with an increase in return period. The critical storm duration range between 24 hours and 168 hours was characterised by a low degree of association between all these methods. The results also showed a tendency of a decrease in association with an increase in return period.

Although, the reasonable to high degree of association between these methods does not necessarily guarantee acceptable accuracy, since all these methods have shortcomings as indicated in Section 2.3.4, Chapter 2. Since all the above-mentioned DDF relationships, except the RLMA&SI approach, are used as standard precipitation input data to the deterministic and empirical methods, the question arises whether it must remain as the standard procedure or whether the SAWS *n*-day point precipitation database in conjunction with the software program, *Design Rainfall Estimation in South Africa* should rather be used. If not, this could result in either under- or overestimations of the design flood, depending on the catchment area and critical storm duration under consideration.

<u>Area reduction factors:</u>

A high degree of association existed between the plotting results of the time of concentration (T_C) against the catchment area (A) and the ARF relationship shown in Equation 2.19, Chapter 2. The power-law trendline fitted to these clustered T_C:A points provided a good indication of the time of concentration associated with any catchment area under consideration and can be used to simplify the above-mentioned ARF relationship. Both these derived relationships (Equations 5.1 and 5.2) are shown in Equations 6.1 and 6.2 respectively:

$$T_C = 0.2284A^{0.5957} \tag{6.1}$$

$$ARF = \left(-6944.3\ln A + 115731.9\right)^{0.4} \tag{6.2}$$

A comparison between Equation 6.1 and the original ARF diagram published in the FSR (NERC, 1975) revealed that the ARF remains constant between 87% and 88% across the ARF diagram for durations exceeding 3 hours. This implied that for the catchments under consideration, the ARFs for point precipitation depths with durations equal to the time of concentration in a specific catchment appear to be fairly constant between 87% and 88%.

<u>Two-year mean annual daily maximum precipitation and thunder days per year</u>:

There was no direct relationship between the average number of days per year on which thunder was heard (*R)* and the 2-year mean of the annual daily maxima precipitation (*M)* values. The degree of association between the *R*- and *M*-values of the Type 1 storm distribution was higher compared to that of the Type 2 storm distribution, emphasising the more uniform areal and time distribution of precipitation and associated less thunder activities typical of the winter and/or coastal precipitation regions. Thus, the number of days per year during which thunder was heard is not only influenced by the time distribution of storms, but the climate, type of precipitation, areal distribution of precipitation, location, altitude above mean sea level and topography must be taken into consideration.

6.2.3 Hydrological data

The DWA website and related links used to obtain the monthly peak flows at flow gauging stations proved to be user-friendly, although the export format of the data required further manipulation.

The Square root-area method (Equation 2.20*,* Chapter 2) proved to be quite useful in combining or extending observed streamflow data sets at single sites up- or downstream from one another in cases where the observed streamflow data seemed unreliable due to short record lengths.

The AMS of the river gauging stations characterised by flood peaks that exceeded the hydraulic capacity on numerous events introduced a higher degree of uncertainty, since no additional data or historical information quantifying these high outliers were available. These reduced record lengths underestimated the higher frequency floods, since the magnitude of floods predicted by any probability distribution fitted to such an observed data set, is implicitly dependent on the statistical properties (mean, standard deviation and skewness) of the data set.

6.3 DESIGN FLOOD ESTIMATION TOOL

The developed DFET will provide designers with a software tool for the rapid investigation and evaluation of alternative design flood estimation methods either at a regional or site specific scale. The focus user group of application will comprise of engineering technicians, engineering technologist and engineers employed at civil engineering consultants, not necessarily specialists in the field of flood hydrology.

The developed DFET can process all the catchment (average catchment slope, catchment centroid, length and average slope of main watercourses, soil classification and land use/vegetation), meteorological (precipitation) and hydrological (observed flows, AMS and PDS) data used as input for the various design flood estimation methods. Both the data development and application phases of the DFET are characterised by a full graphical interface, enabling the printing/plotting of worksheets and graphs.

6.4 FLOOD FREQUENCY ANALYSIS

6.4.1 Direct statistical analyses

The flood peaks in South African rivers are characterised by a high degree of variability and skewness, whilst most flood peaks are a result of rare, severe meteorological phenomena resulting in the AMS being a mixture of two or more statistical populations with different parameter values and associated flood peak frequency relationships. The use of the mean values of the logarithms of two or more probability distributions to establish the most suitable probability distribution accommodating this phenomena, proved to be successful.

The selection of an appropriate distribution was always based on the assumption that the actual data points adhere to the Cunnane plotting position criteria. The direct statistical analyses of all the data sets evaluated were dominated by the use of the mean values of the logarithms of the LP3-GEV/MM and the LP3-GEV-LN/MM distributions. The LN/MM distribution was only used where the logarithms of the observed data have a near symmetrical distribution. In all other asymmetrical data sets, the LP3/MM distribution was used instead, whilst it was also the only distribution which was used as a single most suitable distribution in a catchment. The GEV/MM distributions were used at asymmetrical data sets characterised by either positive (EV2/MM) or negative (EV3/MM) skewness coefficients.

Apart from the problems associated with short record observed streamflow data and extrapolation beyond the record length, typical measurement errors at flow gauging stations, inconsistency, non-homogeneity and non-stationarity of data could violate the assumptions made when these probability distribution(s) were fitted to the data. Taking all these factors and results into consideration, it can be conclusively confirmed that the LN, LP3 and GEV distributions or a combination thereof are the most suitable probability distributions for flood frequency analyses in South Africa. However, when the mean values of the logarithms of two or more probability distributions were established, it was impossible to give directives to which probability distribution would be the best suited for a specific return period range.

The selection and use of probability distribution pair combinations in specific return period ranges can only be based on the statistical properties, visual inspection of the plotted data and GOF statistics.

6.4.2 Deterministic methods

Most of the deterministic methods overestimated the flood peaks for the 2- and 5-year return periods, whilst all the deterministic methods, except the SDF method, underestimated the flood peaks when compared to the direct statistical analyses for return periods ranging from 10 to 200 years. The degree of association between the individual deterministic methods and the direct statistical analyses, excluding the SDF method, was good.

The r^2-values ranged from 0.65 to 0.98. However, this reasonable to high degree of association must be evaluated within the context of the average deterministic/probability distribution-ratios, since some of these flood peak-ratios were occasionally different by up to a factor of 1.8. Therefore, pair values of the coefficient of determination and these ratios must be evaluated in combination to get a true reflection of the accuracy.

It is of utmost importance to realise that all the deterministic methods are based on average values derived from a large number of events at a regional level, consequently the acceptance or rejection of results only based on visual measures and GOF statistics alone can be subjective.

Thus, the precipitation run-off relationship at a specific site will only be the same as that produced by direct statistical analysis if the site characteristics and hydrological and meteorological conditions are similar to the average conditions used in these methods. In addition, the field of application, limitations and assumptions associated with each method must also be taken into consideration before one can conclusively include or exclude a specific method.

6.4.3 Empirical methods

The empirical methods proved to provide better results when compared with the results obtained by the various deterministic methods, but similar data trends were evident with an increase in accuracy associated with an increasing recurrence interval. The fact that empirical methods are more suitable to be used in larger catchments, contributed to these results, since most of the catchments evaluated can be classified as large with realistic delineated homogeneous hydrological response areas.

6.5 EVALUATION AND CALIBRATION OF THE SDF METHOD

6.5.1 Input data requirements

The criteria of *average meteorological conditions* and *record length* used to select the single precipitation stations in each quaternary catchment under consideration confirmed the initial hypothesis that the flood-producing characteristics within the current identified SDF basins are non-homogeneous. The newly identified single precipitation stations proved to be a better representation of the hydrological response at a smaller scale or quaternary catchment level.

6.5.2 Evaluation and calibration of run-off coefficients

The large C_2 and C_{100} run-off coefficient pair values indicated that a larger proportion of the representative precipitation contributes to the flood peak, whilst the large proportional differences emphasised the important role of antecedent soil moisture status in the precipitation run-off process. The proportional differences tend to decrease with an increase in the MAP.

It was evident from this study that the calibrated C_T-coefficients in the quaternary catchments obtained are spread around those of Alexander (2003) for SDF basin 9, but were generally lower in magnitude. The curves representative of the calibrated run-off coefficients had similar growths as a function of the recurrence interval in most of the basins under consideration.

The adjusted run-off coefficients based on the adjustment factors proposed by Van Bladeren (2005) had a tendency to decrease in magnitude with increasing recurrence interval and some of the adjusted run-off coefficients exceeded unity.

This deviation from the norm might be attributed to the fact that the flood peak data had a gentler growth curve, as a function of recurrence interval, than the design precipitation data used. An increase in C_T-coefficients with return period is necessary to accommodate the known effects which also increase with return period. The likelihood that a catchment is to be more saturated at the start of a storm with a longer recurrence interval was ignored by these adjustment factors.

The effort at regionalisation made by Van Bladeren (2005) requires further refinement, since the relationships established between the parameters (multiplier and exponent) of the power-law function (Equation 5.4, Chapter 5) fitted to the C_T-coefficients as a function of return period and regional descriptors are questionable. The fact that these questionable results were in agreement with similar studies conducted on the RM in South Africa and Australia confirmed that no relationship can be successfully established between the regional descriptors and the C_T-values in order to regress the run-off coefficients. However, this confirmed that the C_T-coefficients are essentially functions of the return period and time of concentration as conjectured.

6.5.3 Evaluation of calibrated flood peaks

The original SDF method overestimated the statistical flood peaks in all the SDF basins under consideration, except in SDF basins 18 and 26. On average, the original SDF/probability distribution-ratios varied between 1 and 3.3. The best results were evident in SDF basin 16, with the overestimation limited to $\pm$ 12% for the return periods ranging from 10 to 200 years.

The adjusted SDF method results were only better in 26% of all the basins under consideration when compared to those estimated by the original SDF method. As in the case of the original SDF method, the most acceptable results were evident in SDF basin 16, whilst the flood peak values were either significantly over- or underestimated in the remaining basins. On average, the adjusted SDF/probability distribution-ratios varied between 0.30 and 6.58, which is unacceptable.

The calibrated version of the SDF method proved to be the most accurate in all the basins under consideration, except in SDF basins 6 and 23, where it proved to be slightly less accurate than the adjusted SDF method. On average, the calibrated SDF/probability distribution-ratios varied between 0.85 and 1.15, whilst at some basins and individual return periods, less accurate results were evident.

6.5.4 Verification of calibrated run-off coefficients and flood peaks

The verification tests confirmed that the calibrated run-off coefficients behaved in the probabilistic manner as anticipated, since the verification results showed that the calibrated/verified SDF method is the most accurate and similar trends were evident in all the basins under consideration. However, individual return period flood peaks were either slightly more or less accurately estimated. On average, the verified SDF/probability distribution-ratios varied between 0.82 and 1.19, except in SDF basins 6 and 21 where the 5- to 20-year return period flood peaks were overestimated by 41% to 56%, which is still conservative.

The calibrated/verified SDF method remains the preferred method in the latter basins based on the higher degree of association and accuracy obtained. The original and adjusted versions of the SDF method also demonstrated similar trends as established during the calibration exercise, although some individual return period flood peaks were characterised by either a slightly improved or slightly worse estimation.

The degree or extent to which the original SDF method overestimated the magnitude and frequency of flood peaks varied form basin to basin. Apart from the previously discussed factors, this is also due to the influence of different climatic regions, types of weather and precipitation occurrence-frequencies on the depth, area, duration and movement of storm precipitation. The SDF/probability distribution-ratios were the highest in the Highveld and southern coastal (SDF basins 22, 23 and 26) regions with summer convective precipitation. Convective precipitation is characterised by a non-uniform areal and time distribution and more associated thunder activities. In these regions the flood peak-ratios were occasionally different by up to a factor of 3 or even more.

The southern coastal regions (SDF basins 16 - 18) with winter orographic/frontal precipitation demonstrated the best flood peak-ratios with flatter growth curves as a function of the recurrence interval and varied between 0.8 and 1.6.

6.6 ASSESSMENT OF RESULTS: GOF

There exists a direct relationship between the limiting critical values and degrees of freedom used in the Chi-square statistic. In 75% of the quaternary catchments within the study area and in 60% of the catchments used to evaluate the SDF method in the rest of South Africa could the *null hypothesis* be accepted. However, acceptance of the *null hypothesis* at low confidence levels (< 50%) highlighted the likelihood of differences to be present. The contingency coefficient used to measure the degree of association between the hypothesised probability distributions and observed data gave questionable results when the record length was either relatively long with a low associated Chi-square statistic or short with a high associated Chi-square statistic.

The overall results indicated that both the coefficient of determination and Chi-square statistic can be satisfactorily used to evaluate the GOF of theoretical probability distributions and design flood estimation methods (deterministic and empirical). However, the Chi-square statistic proved to be more sensitive towards short record lengths, inconsistency, non-homogeneity and non-stationarity of data.

6.7 FUTURE RESEARCH

Based on the findings, the following recommendations recognising possible future research on the SDF method are proposed:

- Review the current regional boundaries of the SDF basins by increasing the number of SDF basins based on the single or multiple quaternary catchment boundaries. The availability of hydrological (flow) and meteorological (precipitation) data, as well as the extent of the hydrological homogeneity within the identified catchments, will have an influence on the identification and delineation of the new basins.
- The data pool of hydrological and meteorological gauging sites should be increased and the data sets must be updated to ensure that periods of

observation are as long as possible. All available historical information of flood peaks should be included and made available from a central database.

- Conduct direct statistical analyses of the AMS for calibration purposes at a potential 326 reservoir gauging stations in the quaternary catchments. The number of reservoir gauging stations in the current SDF basins varies from three to 31 reservoirs per basin.
- Conduct direct statistical analyses of the AMS for verification purposes at all possible flow gauging stations in each quaternary catchment used during the calibration exercise.
- Investigate the use of the mean values of the logarithms of two or more probability distributions to accommodate the AMS consisting of a mixture of two or more statistical populations.
- Provide directives as to which probability distribution is the best suited for a specific return period range based on the statistical properties, visual inspection of the plotted data and GOF statistics.
- Select daily precipitation stations representative of the average meteorological conditions in each quaternary catchment of concern by making use of the precipitation database as proposed by Smithers and Schulze (2003).
- Numerically calibrate the run-off coefficients to be used in the revised SDF method to fit the results obtained by the direct statistical analyses for different return periods.
- Establish physical or regional descriptors on which to regress the calibrated run-off coefficients to enable the extension thereof to ungauged catchments. Descriptors such as the catchment area, slope, hydrological soil groups, land use and vegetation and MAP must be tested in combination with the calibrated run-off coefficients to examine if a relationship exists on which to regress the coefficients. In larger catchments, the effect of channel storage should also be taken into consideration.
- Improve the relationship which was established during this study between the time of concentration (T_C) and the catchment area (A) by investigating

as many catchments as possible. It is also recommended that not only the catchment area, but also the catchment shape, must be taken into consideration. This will enable future users to get a good indication of the time of concentration associated with any catchment area and shape without being required to go through the tedious exercise of determining the length and average slope of main watercourses.

- Use the SAWS *n*-hour/day point precipitation depths as estimated by the software program, *Design Rainfall Estimation in South Africa* for all the critical storm durations under consideration in the revised version of the SDF method. By doing this, the current DDF (Hershfield) relationship and the variable and questionable parameter (the number of days per year during which thunder was heard) can be excluded from the calculation procedures.
- Improve the ARF relationship established during this study by using the improved $T_C:A$ relationships.
- Update and improve the DFET by incorporating the revised version of the SDF method.
- Improve and extend the precipitation databases used in the developed DFET by incorporating the precipitation data beyond 2002.

CHAPTER

7

REFERENCES

CHAPTER 7: REFERENCES

Adamowski, K. 2000. Regional Analysis of Annual Maximum and Partial Duration Flood Data by Non-parametric and L-Moment methods. *Journal of Hydrology*, 229: 219 - 231.

Adamson, P.T. 1978. *The Statistics of Extreme Values and the Analyses of Floods in South Africa*. Technical Report TR186. Department of Water Affairs and Forestry. Pretoria, South Africa.

Adamson, P.T. 1981. *Southern African Storm Rainfall*. Technical Report TR102. Department of Environmental Affairs. Pretoria, South Africa.

Alexander, W.J.R. 1978. *Depth-Area-Duration-Frequency Properties of Storm Precipitation in South Africa*. Technical Report TR83. Department of Water Affairs and Forestry. Pretoria, South Africa.

Alexander, W.J.R. 1990. *Flood Hydrology for Southern Africa*. SANCOLD. Pretoria, South Africa.

Alexander, W.J.R. 2001. *Flood Risk Reduction Measures: Incorporating Flood Hydrology for Southern Africa*. Department of Civil and Biosystems Engineering, University of Pretoria. Pretoria, South Africa.

Alexander, W.J.R. 2002. *Statistical Analysis of Extreme Floods.* University of Pretoria. Pretoria, South Africa.

Alexander, W.J.R. 2002a. *The Standard Design Flood: Theory and Practice*. University of Pretoria. Pretoria, South Africa.

Alexander, W.J.R. 2002b. The Standard Design Flood. *Journal of the South African Institution of Civil Engineering*, 44(1) 2002: 26 - 30.

Alexander, W.J.R. 2003. *The Standard Design Flood: A New Design Philosophy*. University of Pretoria. Pretoria, South Africa.

Bauer, S.W. and Midgley, D.C. 1974. *A Simple Procedure for Synthesizing Direct Run-off Hydrographs*. Hydrological Research Unit. University of Witwatersrand. Johannesburg, South Africa.

Bouvard, M. 1988. *Rapporteur-General's Report on Design Flood and Operational Flood Control*. 16th Congress of the International Commission on Large Dams. San Francisco, United States of America.

Cameron, D.S., Beven, K.J., Tawn, J., Blazkova, S. and Naden, P. 1999. Flood Frequency Estimation by Continuous Simulation for a Gauged Upland Catchment. *Journal of Hydrology,* 219: 169 -187.

Chadwick, A.J. and Morfett, J.C. 2004. *Hydraulics in Civil and Environmental Engineering*. 4th Ed. E & FN Spon, Chapman and Hall. London, United Kingdom.

Chow, V.T., Maidment, D.R. and Mays, L.W. 1988. *Applied Hydrology*. McGraw-Hill. New York, United States of America.

Cordery, I. and Pilgrim, D.H. 2000. The State of the Art of Flood Prediction. In: Parker, D.J. (Ed.), *Floods: Volume II:* 185 - 197. Routledge, London, United Kingdom.

Council of Geosciences. 1995. *GIS Data: Simplified Lithology of South Africa*. Pretoria, South Africa.

CSIR (Council for Scientific and Industrial Research). 2001. *GIS Data: Classified Raster Data for National Coverage based on 31 Land Cover Types*. National Land Cover Database. Environmentek, CSIR. Pretoria, South Africa.

Cullis, J., Görgens, A.H.M. and Lyons, S. 2007. *Updated Guidelines and Design Flood Hydrology Techniques for Dam Safety*. Water Research Commission. WRC Report 1420/1/07. Cape Town, South Africa.

Cunnane, C. 1978. Unbiased Plotting Positions - A Review. *Journal of Hydrology,* 37: 205 - 222.

Cunnane, C. 1989. *Statistical Distributions for Flood Frequency Analysis*. WMO Report 718. World Meteorological Organisation. Geneva, Switzerland.

D’Agostino, R.B. and Stephens, M.A. 1986. *Goodness-of-Fit Techniques*. Marcel Dekker. New York, United States of America.

Davies, B. and Day, J. 1998. *Vanishing Waters*. 1st Ed. University of Cape Town Press. Cape Town, South Africa.

Dyson, L.L. and Van Heerden, J. 2001. The Heavy Rainfall and Floods over the Northeastern Interior of South Africa during February 2000. *South African Journal of Science,* 1997: 80 - 86.

DWAF (Department of Water Affairs and Forestry). 1995. *GIS Data: Primary Drainage Regions of South Africa.* Pretoria, South Africa.

DWAF (Department of Water Affairs and Forestry). 1999. *Catchment Management Strategy for the Modder and Riet Rivers. Phase 1: Situation and Draft Management Strategy.* Pretoria, South Africa.

DWAF (Department of Water Affairs and Forestry). 2004. *Internal Strategic Perspective: Upper Orange Water Management Area*. Directorate National Water Resources Planning. Report PWMA 13/000/00/0304. Pretoria, South Africa.

ESRI (Environmental Systems Research Institute). 2006. *ArcGIS Desktop Help: Map Projections and Coordinate Systems.*

Görgens, A.H.M. 1997. *Design Flood Analysis*. Proceedings of Lecture Course: Design of Small Dams. University of Stellenbosch, South Africa. 4.1 – 22.

Görgens, A.H.M. 2002. *Design Flood Hydrology: Design and Rehabilitation of Dams*. G. Basson (Ed.). University of Stellenbosch, South Africa. 460 - 524.

Gupta, R.D. and Kundu, D. 2007. Generalised Exponential Distribution: Existing Methods and Recent Developments. *Journal of the Statistical Planning and Inference,* 137 (11): 3 537 - 3 547.

Hershfield, D.M. 1962. *Extreme Rainfall Relationships*. Proceedings of the American Society of Civil Engineers. HY6 (11): 73 - 92.

Hirsch, R.M., Helsel, D.R., Cohn, T.A. and Gilroy, E.J. 1993. Statistical Treatment of Hydrological Data. *Handbook of Hydrology*. McGraw-Hill, New York, United States of America.

Hogg, W.D. 1992. *Inhomogeneities in Time Series of Extreme Rainfall*. 5th International Meeting on Statistical Climatology. The Steering Committee for International Meetings on Statistical Climatology, Toronto, Canada. 481 - 484.

Hosking, J.R.M. and Wallis, J.R. 1997. *Regional Frequency Analysis: An Approach Based on L-Moments.* Cambridge University Press. Cambridge, United Kingdom.

HRU (Hydrological Research Unit). 1972. *Design Flood Determination in South Africa*. HRU Report 1/72. University of the Witwatersrand. Johannesburg, South Africa.

IH (Institute of Hydrology). 1999. *Flood Estimation Handbook*. Institute of Hydrology. Wallingford, United Kingdom.

Kachroo, R.K., Mkhandi, S.H. and Parida, B.P. 2000. Flood Frequency Analysis of Southern Africa: Delineation of Homogeneous Regions. *Hydrological Sciences Journal,* 45 (3): 437 - 447.

Kirpich, Z.P. 1940. Time of Concentration of Small Agricultural Watersheds. *Civil Engineering,* 10 (6): 362.

Kite, G.W. 1988. *Frequency and Risk Analysis in Hydrology*. Revised Ed. Water Resources Publications. Littleton, Colorado, United States of America.

Kjeldsen, T.R. and Jones, D.A. 2004. Sampling Variance of Flood Quantiles from the Generalised Logistic Distribution estimated using the Method of L-Moments. *Hydrology and Earth System Sciences,* 8: 183 - 190.

Kovács, Z.P. 1988. *Regional Maximum Flood Peaks in Southern Africa*. Technical Report TR137. Department of Water Affairs. Pretoria, South Africa.

Madsen, H., Pearson, C.P. and Rosbjerg, D. 1997. Comparison of Annual Maximum Series and Partial Duration Series Methods for Modelling Extreme Hydrologic Events. *Water Resources Research,* 33: 759 - 769.

McPherson, D.R. 1983. *Comparison of Mean Annual Flood Peaks calculated by Various Methods*. South African National Hydrology Symposium, Technical Report TR119. Department of Environmental Affairs. Pretoria, South Africa.

Midgley, D.C. and Pitman, W.V. 1971. *Amendments to Design Flood Manual HRU 4/69*. HRU Report 1/71. University of Witwatersrand. Johannesburg, South Africa.

Midgley, D.C. and Pitman, W.V. 1978. *A Depth-Duration-Frequency Diagram for Point Rainfall in Southern Africa*. HRU Report 2/78. University of Witwatersrand. Johannesburg, South Africa.

Midgley, D.C., Pitman, W.V. and Middleton, B.J. 1994. *Surface Water Resources of South Africa.* Volume 2, Drainage Region C, Vaal: Appendices. Water Research Commission. WRC Report 298/2.1/94. Pretoria, South Africa.

Milton, J.S. and Arnold, J.C. 1986. *Probability and Statistics in the Engineering and Computer Sciences*. International Ed. McGraw-Hill. Singapore.

NASA (National Aeronautics and Space Administration). 2002. *Shuttle Radar Topography Mission (SRTM) elevation data for Southern Africa at 90-metre resolution.*

NERC (Natural Environment Research Council). 1975. *Flood Studies Report*. Natural Environment Research Council. London, United Kingdom.

Parak, M. 2007. *Flood Estimation for Roads, Bridges and Dams*. Unpublished MSc Eng. Dissertation, Civil Engineering Programme, University of KwaZulu-Natal. Durban, South Africa.

Parak, M. and Pegram, G.G.S. 2006. Rational Formula from Runhydrograph. *Water SA,* 32 (2): 163 - 180.

Pegram, G.G.S. 2003. Rainfall, Rational Formula and Regional Maximum Flood: Some Scaling Links. Keynote Paper. *Australian Journal of Water Resources,* 7 (1): 29 - 39.

Pegram, G.G.S. and Adamson, P.T. 1988. Revised Risk Analysis for Extreme Storms and Floods in Natal/Kwazulu. *The Civil Engineer in South Africa:* 331 - 336.

Pegram, G.G.S and Parak, M. 2004. A Review of the Regional Maximum Flood and Rational Formula using Geomorphological Information and Observed Floods. *Water SA,* 30 (3): 377 - 392.

Petras, V. and Du Plessis, P.H. 1987. *Catalogue of Hydrological Catchment Parameters.* Department of Water Affairs, Flood Studies. Technical Note 6. Pretoria, South Africa.

Pilgrim, D.H. and Cordery, I. 1993. Flood Run-off. *Handbook of Hydrology*. McGraw-Hill. New York, United States of America.

Pilon, P.J., Condie, R. and Harvey, K.D. 1985. *Flood Frequency Analysis with Zero Flows, Low Outliers and Historical Information*. Inland Waters Directorate: Environment Canada. Ottawa, Canada.

Pullen, R.A. 1969. *Synthetic Unitgraphs for South Africa*. Hydrological Research Unit Report 3/69. University of the Witwatersrand. Johannesburg, South Africa.

Rademeyer, P.F. 2008. *Personal correspondence or communication*.

Roberts, D.F. 1963. *Annual Flood Peak Probabilities*. Department of Water Affairs, Professional Paper No. 20. Pretoria, South Africa.

Roberts, P.J.T. 1987. The Role of Objective Functions in Digital Simulation Modelling. *In*: Thornton, J.A. (Ed.) *Proceedings and Symposium on Modelling of Aquatic Systems*. Ecosystem Programme, FRD-CSIR, Pretoria. Occasional Report, 24: 159 - 171.

Rooseboom, A., Basson, M.S., Loots, C.H. and Wiggett, J.H. 1993. *Manual for Road Drainage.* 4th Ed. Department of Transport. Pretoria, South Africa.

SANRAL (South African National Roads Agency Limited). 2006. *Drainage Manual*. 5th Ed. South African National Roads Agency Limited. Pretoria, South Africa.

SAWB (South African Weather Bureau). 1956. *Climate of South Africa. Part 3: Maximum 24-hour Rainfall*. South African Weather Bureau Publication WB21. Pretoria, South Africa.

SAWB (South African Weather Bureau). 1992. *Climate Tables of South Africa.* South African Weather Bureau Publication WB42. Pretoria, South Africa.

Seaman, M.T., Roos, J.C. and Watson, M. 2001. *The State of the Modder River, First Quarter 2001: A Bio-monitoring Report*. Report to Bloem Water by the Centre for Environmental Management. University of the Free State. Bloemfontein, South Africa.

Schulze, R.E. 1980. *Potential Flood-Producing Rainfall for Medium and Long Duration in Southern Africa*. Report to Water Research Commission. Pretoria, South Africa.

Schulze, R.E. 1984. *Depth-duration-frequency Studies in Natal based on Digitised Data*. South African National Hydrology Symposium, Technical Report TR119. Department of Environment Affairs. Pretoria, South Africa.

Schulze, R.E. 1989. Non-stationary Catchment Responses and other Problems in Determining Flood Series: A Case for a Simulation Modelling Approach. *In:* Kienzle, S.W. and Maaren, H. (Eds.). Proceedings of 4th South African National Hydrological Symposium. *SANCIAHS:* 135 - 157. Pretoria, South Africa.

Schulze, R.E. 1995. *Hydrology and Agrohydrology: A Text to Accompany the ACRU 3.00 Agrohydrological Modelling System.* Water Research Commission. WRC Report TT 69/95. Pretoria, South Africa.

Schulze, R.E., Schmidt, E.J. and Smithers, J.C. 1992. *SCS-SA User Manual: PC-Based SCS Design Flood Estimates for Small Catchments in Southern Africa*. Agricultural Catchments Research Unit Report 40. Department of Agricultural Engineering, University of Natal. Pietermaritzburg, South Africa.

Sinske, B.H. 1982. Bepaling van Uiterste Neerslag vir Intermediêre Reënvalduurtes in Suidelike Afrika. *Water SA,* 8 (3): 149 - 154.

Smithers, J.C. and Schulze, R.E. 2000a. *Development and Evaluation of Techniques for Estimating Short Duration Design Rainfall in South Africa*. Water Research Commission. WRC Report 681/1/00. Pretoria, South Africa.

Smithers, J.C. and Schulze, R.E. 2000b. *Long Duration Design Rainfall Estimates for South Africa. Water Research Commission*. WRC Report 811/1/00. Pretoria, South Africa.

Smithers, J.C. and Schulze, R.E. 2003. *Design Rainfall and Flood Estimation in South Africa*. Water Research Commission. WRC Report 1060/01/03. Pretoria, South Africa.

Smithers, J.C. and Schulze, R.E. 2004. The Estimation of Design Rainfalls for South Africa using a Regional Scale Invariant Approach. *Water SA,* 30 (4): 435 - 44.

Stedinger, J.R., Vogel, R.M. and Foufoula-Georgiou, E. 1993. Frequency Analysis of Extreme Events. *Handbook of Hydrology*. McGraw-Hill. New York, United States of America.

Van Bladeren, D. 2005. *Verification of the Proposed Standard Design Flood (SDF).* SRK Consulting Engineers and Scientists. SRK Report 344512/1. Pretoria, South Africa.

Van der Spuy, D. and Rademeyer, P.F. 2008. *Flood Frequency Estimation Methods*. Proceedings of Course: Flood Hydrology. University of Stellenbosch, South Africa.

Viessman, W., Lewis, G.L. and Knapp, J.W. 1989. *Introduction to Hydrology*. 3rd Ed. Harper and Row Publishers Incorporated. New York, United States of America.

Weddepohl, J.P. 1988. *Design Rainfall Distributions for Southern Africa*. Unpublished MSc. Dissertation, Department of Agricultural Engineering, University of Natal. Pietermaritzburg, South Africa.

Willmott, C.J. 1982. Some Comments on the Evaluation of Model-Performance. *Bulletin of American Meteorological Society,* 63: 1 309 - 1 313.

Wilson, E.M. 1990. *Engineering Hydrology.* 4th Ed. The Macmillan Press Ltd. London, United Kingdom.

WRC (Water Research Commission). 1995. *GIS Data: Soil Coverage based on the 1989 Revised Broad Homogeneous Natural Regions Map.* Pretoria, South Africa.

Yevjevich, V. 1982. *Probability and Statistics in Hydrology*. 1st Ed. Water Resources Publications. Littleton, Colorado, United States of America.

LIST OF ADDENDA

ADDENDUM A:

SPATIAL GIS DATA OF THE C5 DRAINAGE REGION

ADDENDUM B:

TABULATED RESULTS

ADDENDUM C:

GRAPHICAL PLOT RESULTS

Page

ADDENDUM D:

USER MANUAL: DESIGN FLOOD ESTIMATION TOOL

Page

Page

LIST OF TABLES

LIST OF FIGURES

Page

ADDENDUM

A

SPATIAL GIS DATA

DRAINAGE REGIONS OF THE STUDY AREA

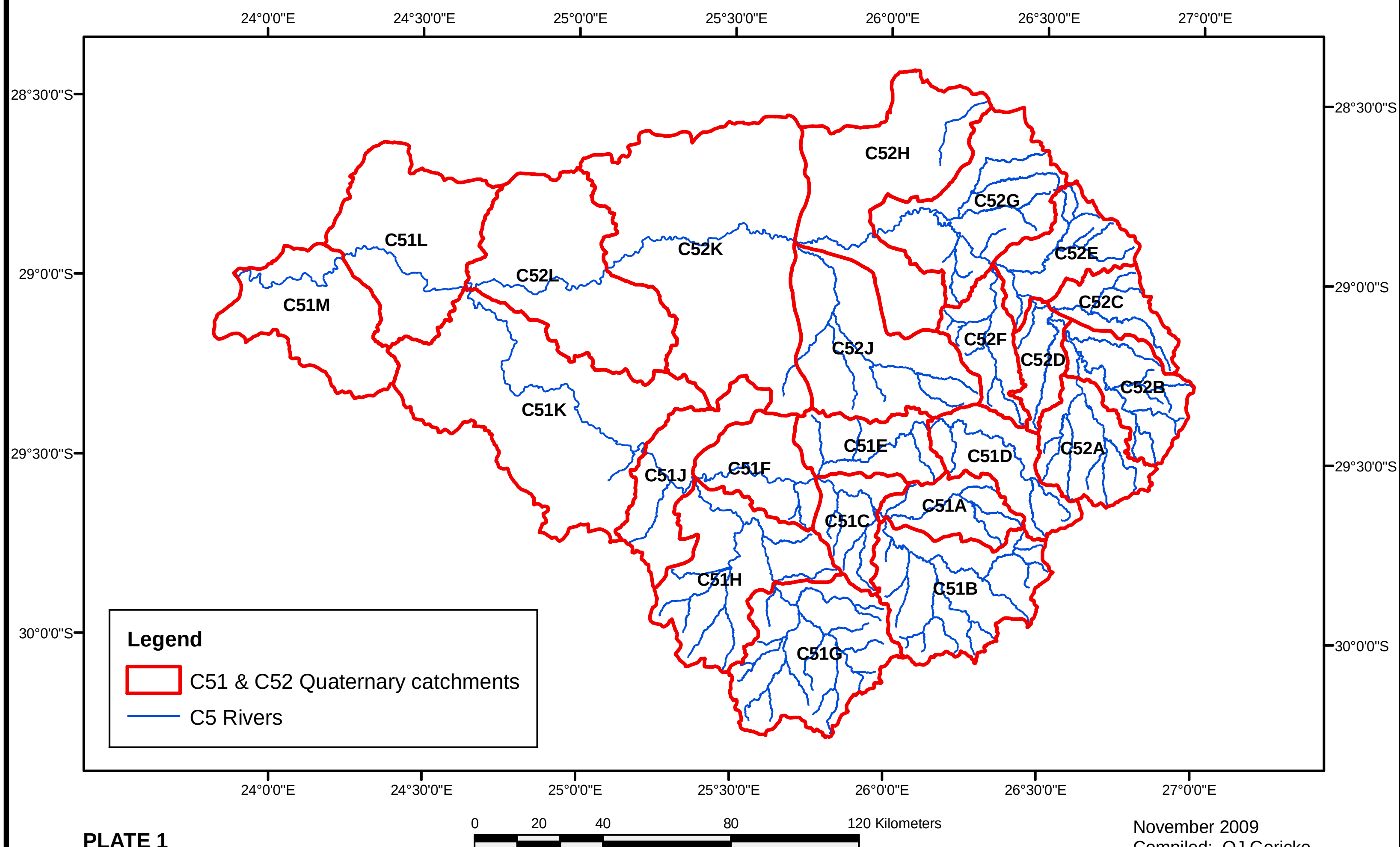

PLATE 1

Albers-Equal Area Projection

November 2009
Compiled: OJ Gericke
Source: DWAF (1995)

ADDENDUM A: SPATIAL GIS DATA

TOPOGRAPHY (DEM) OF THE STUDY AREA

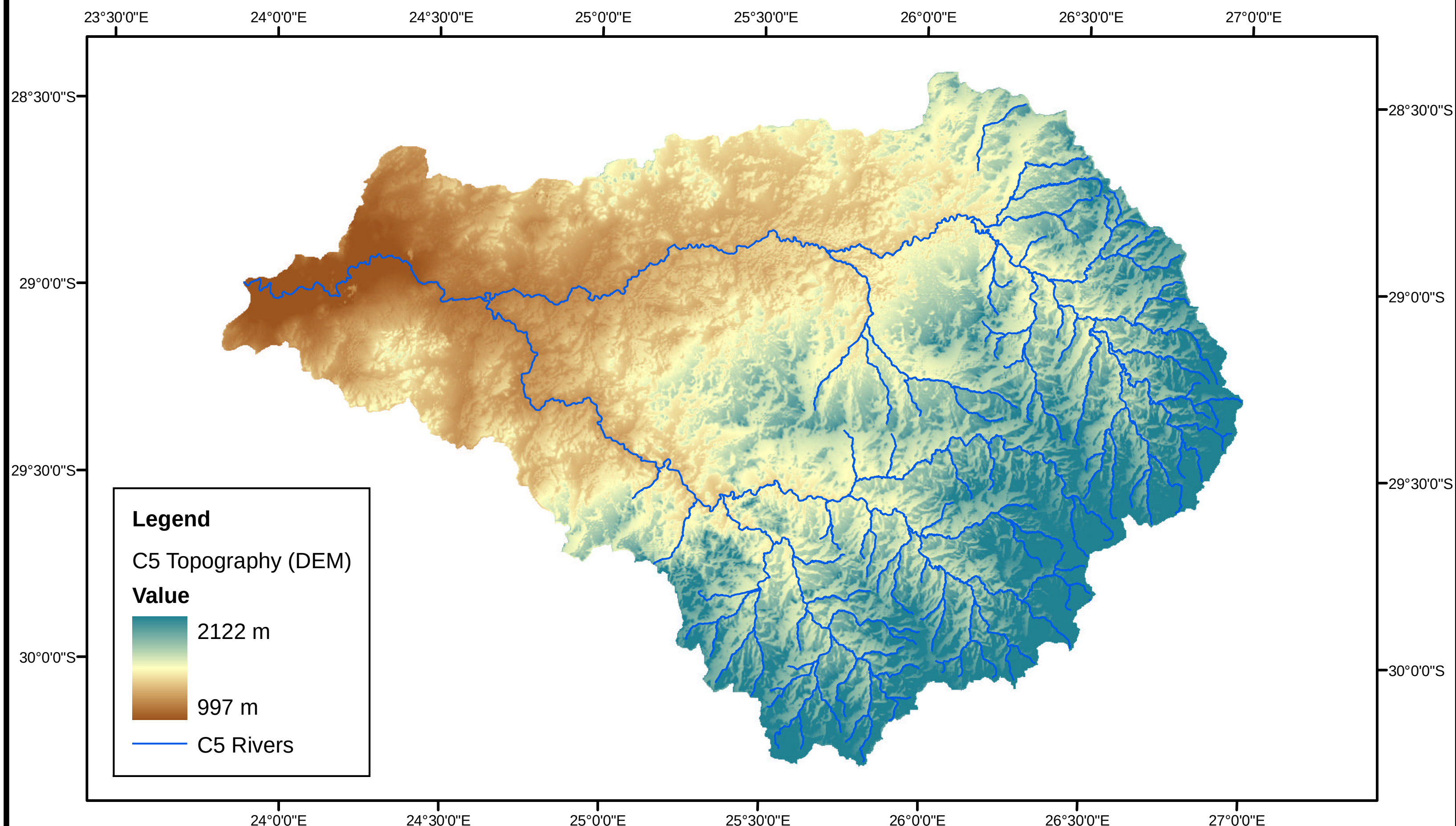

PLATE 2

0 20 40 80 120 Kilometers

Albers-Equal Area Projection

November 2009
Compiled: OJ Gericke
Source: NASA (2002)

GEOLOGICAL DATA OF THE STUDY AREA

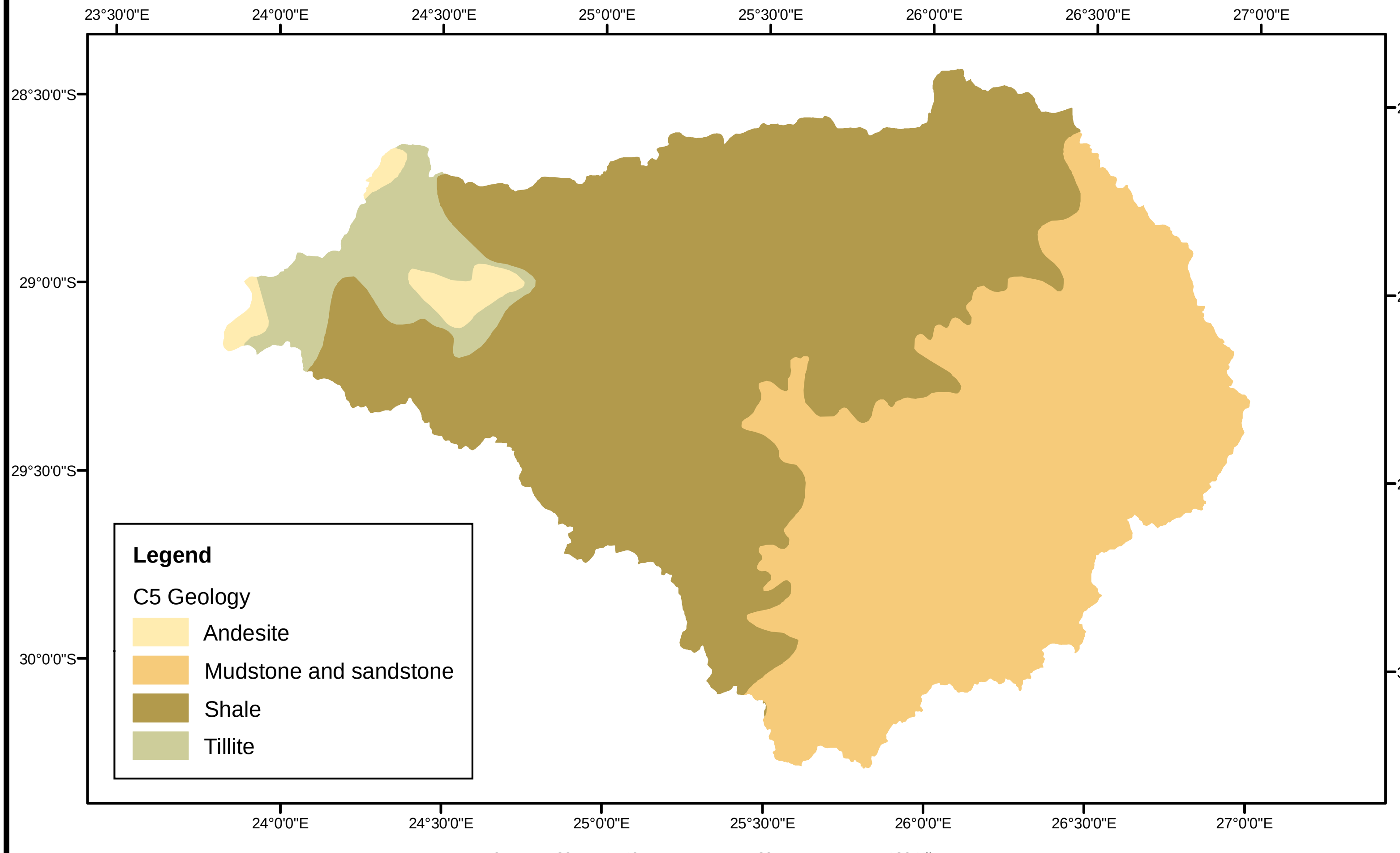

Albers-Equal Area Projection

PLATE 3

November 2009
Compiled: OJ Gericke
Source: Council of Geosciences (1995)

SOIL CLASSIFICATION OF THE STUDY AREA

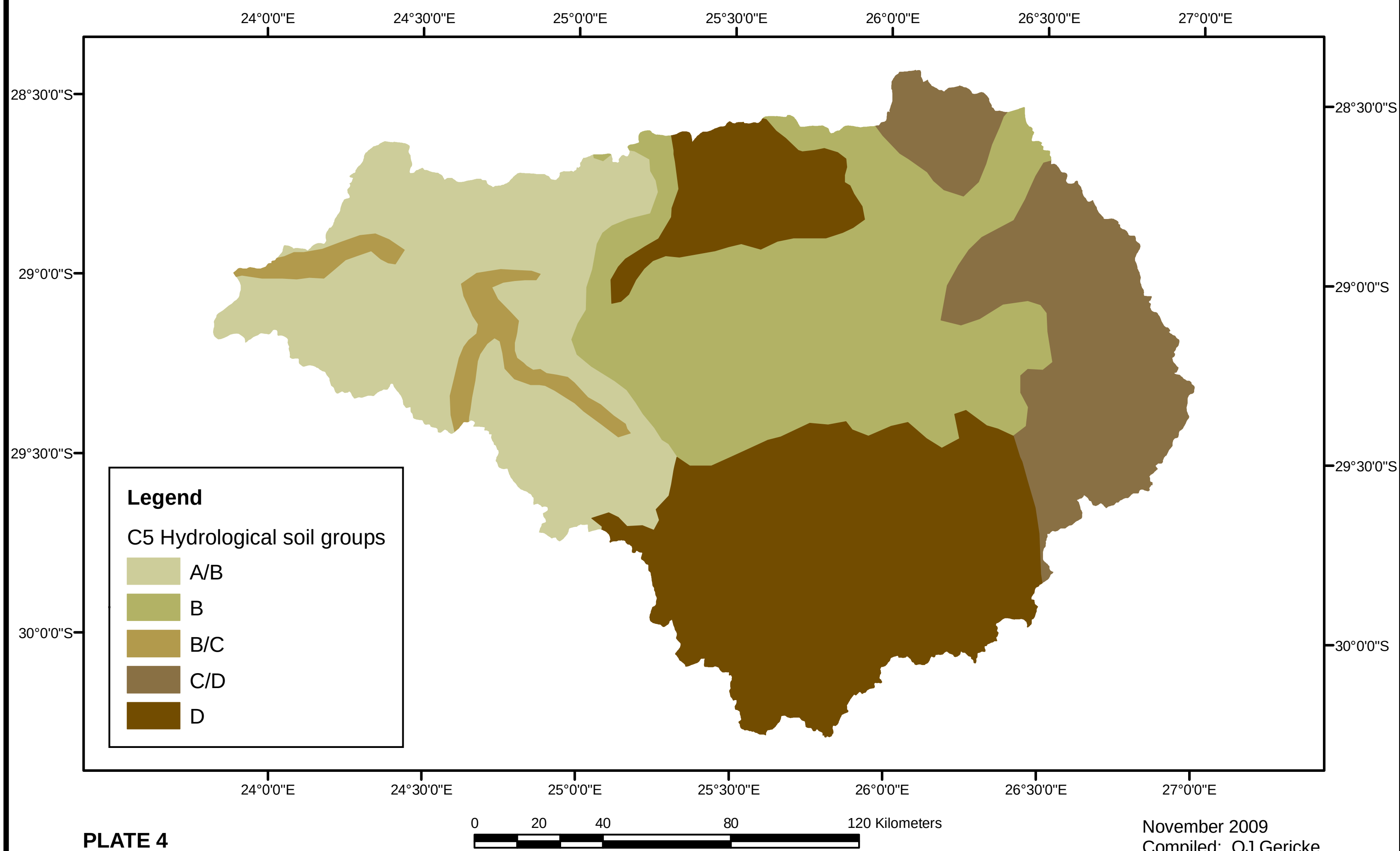

PLATE 4

November 2009
Compiled: OJ Gericke
Source: WRC (1995)

LAND-USE AND VEGETATION OF THE STUDY AREA

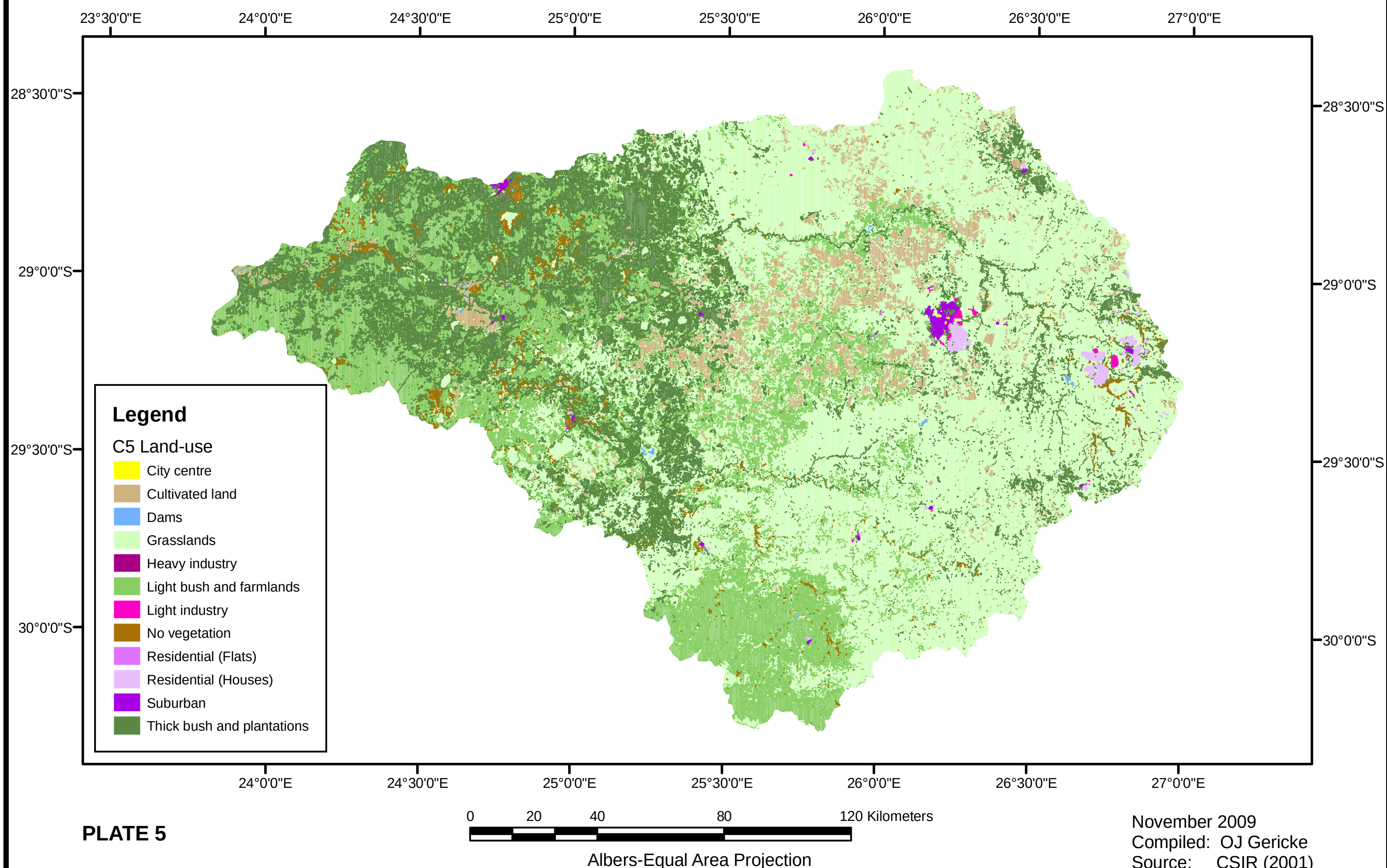

PLATE 5

November 2009
Compiled: OJ Gericke
Source: CSIR (2001)

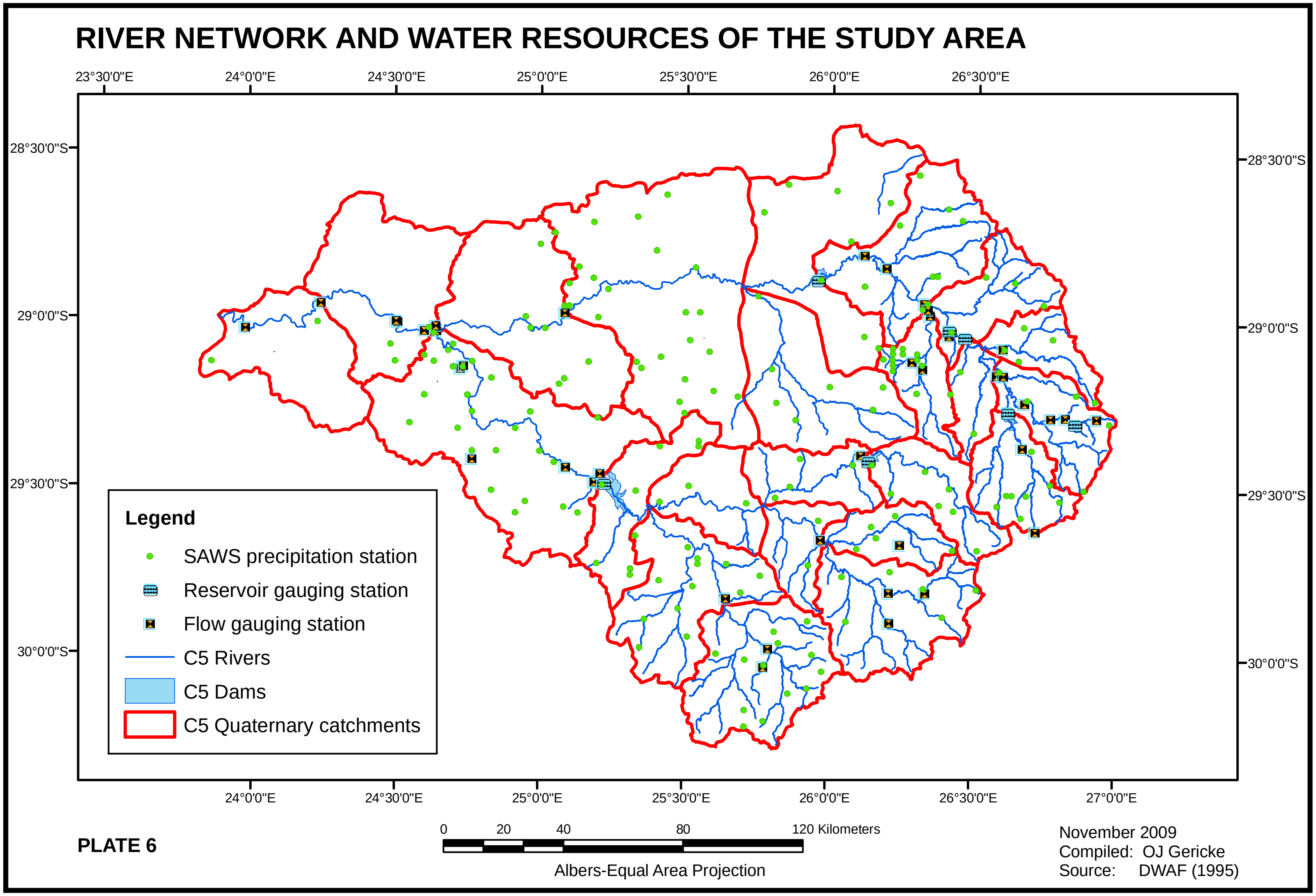
RIVER NETWORK AND WATER RESOURCES OF THE STUDY AREA
23°30'0"E
24°0'0"E
24°30'0"E
25°0'0"E
25°30'0"E
26°0'0"E
26°30'0"E
27°0'0"E
28°30'0"S
29°0'0"S
29°30'0"S
30°0'0"S
Legend
SAWS precipitation station
Reservoir gauging station
Flow gauging station
C5 Rivers
C5 Dams
C5 Quaternary catchments
0 20 40 80 120 Kilometers
Albers-Equal Area Projection
PLATE 6
November 2009
Compiled: OJ Gericke
Source: DWAF (1995)

ADDENDUM

B

TABULATED RESULTS

EVALUATION OF THE SDF METHOD USING A CUSTOMISED DESIGN FLOOD ESTIMATION TOOL

ADDENDUM B: TABULATED RESULTS

Table B.1: Slope frequency distribution of quaternary catchments

Catchment description	Slope classification (%)	%-Distribution
C5R001	0 - 3	62
	3 - 10	34.8
	10 - 30	2.9
	> 30	0.3
C5R002	0 - 3	59.2
	3 - 10	32.3
	10 - 30	6.6
	> 30	1.90
C5R003	0 - 3	51.7
	3 - 10	35.7
	10 - 30	10.9
	> 30	1.7
C5R004, C5H015	0 - 3	57.6
	3 - 10	34.3
	10 - 30	6.7
	> 30	1.4
C5R005	0 - 3	47.3
	3 - 10	31
	10 - 30	12.6
	> 30	9.1
C5H003	0 - 3	51.7
	3 - 10	35.7
	10 - 30	10.9
	> 30	1.7
C5H012	0 - 3	56
	3 - 10	34.2
	10 - 30	7.5
	> 30	2.3
C5H022	0 - 3	47.3
	3 - 10	31
	10 - 30	12.6
	> 30	9.1
C5H054	0 - 3	59.7
	3 - 10	34.3
	10 - 30	5.1
	> 30	0.9

Table B.2: C5R001: Longitudinal profile data

Progressive distance (m)	Reduced height (m)	Progressive distance (m)	Reduced height (m)
0	1 372.820	74 975	1 540
19 272	1 400	78 648	1 560
32 138	1 420	81 959	1 580
43 927	1 440	83 841	1 600
51 121	1 460	84 700	1 620
54 905	1 480	85 633	1 640
64 682	1 500	86 207	1 660
70 212	1 520	86 441	1 679.30

Table B.3: C5R002: Longitudinal profile data

Progressive distance (m)	Reduced height (m)	Progressive distance (m)	Reduced height (m)
0	1 210.06	169 068	1 420
29	1 220	174 063	1 440
49 443	1 240	180 018	1 460
67 583	1 260	183 418	1 480
87 244	1 280	186 673	1 500
100 320	1 300	190 435	1 520
113 275	1 320	193 212	1 540
127 910	1 340	196 027	1 560
146 595	1 360	198 448	1 580
155 045	1 380	200 949	1 600
162 026	1 400	201 689	1 613

Table B.4: C5R003: Longitudinal profile data

Progressive distance (m)	Reduced height (m)	Progressive distance (m)	Reduced height (m)
0	1 356.27	40 061	1 460
183	1 360	46 025	1 480
11 828	1 380	49 768	1 500
15 047	1 400	52 857	1 520
21 967	1 420	53 775	1 530
32 703	1 440	40 061	1 460

Table B.5: C5R004: Longitudinal profile data

Progressive distance (m)	Reduced height (m)	Progressive distance (m)	Reduced height (m)
0	1 229.85	147 968	1 400
40 950	1 260	154 887	1 420
72 056	1 280	165 623	1 440
90 711	1 300	172 982	1 460
106 691	1 320	178 945	1 480
126 587	1 340	182 688	1 500
133 104	1 360	185 778	1 520
144 749	1 380	186 696	1 530

Table B.6: C5R005: Longitudinal profile data

Progressive distance (m)	Reduced height (m)	Progressive distance (m)	Reduced height (m)
0	1 484.69	14 402	1 620
3 930	1 500	15 118	1 640
6 643	1 520	15 538	1 660
9 509	1 540	15 931	1 680
11 613	1 560	16 112	1 700
12 941	1 580	16 200	1 706.10
13 782	1 600		

Table B.7: C5H003: Longitudinal profile data

Progressive distance (m)	Reduced height (m)	Progressive distance (m)	Reduced height (m)
0	1 340	50 103	1 440
11 000	1 350	57 461	1 460
17 400	1 356.27	63 425	1 480
17 583	1 360	67 168	1 500
29 228	1 380	70 257	1 520
32 447	1 400	71 175	1 530
39 367	1 420		

Table B.8: C5H012: Longitudinal profile data

Progressive distance (m)	Reduced height (m)	Progressive distance (m)	Reduced height (m)
0	1 325	68 693	1 480
13 185	1 340	71 948	1 500
31 870	1 360	75 710	1 520
40 320	1 380	78 487	1 540
47 301	1 400	81 302	1 560
54 343	1 420	83 723	1 580
59 338	1 440	86 224	1 600
65 293	1 460	86 964	1 613

Table B.9: C5H015: Longitudinal profile data

Progressive distance (m)	Reduced height (m)	Progressive distance (m)	Reduced height (m)
0	1 253	128 218	1 400
21 200	1 260	135 137	1 420
52 306	1 280	145 874	1 440
70 961	1 300	153 232	1 460
86 941	1 320	159 195	1 480
106 838	1 340	162 939	1 500
113 354	1 360	166 028	1 520
124 999	1 380	166 946	1 530

Table B.10: C5H016: Longitudinal profile data

Progressive distance (m)	Reduced height (m)	Progressive distance (m)	Reduced height (m)
0	1 025	334 734	1 300
24 922	1 040	350 713	1 320
34 187	1 060	370 610	1 340
42 255	1 080	377 126	1 360
50 208	1 100	388 771	1 380
82 416	1 120	391 990	1 400
106 466	1 140	398 910	1 420
127 128	1 160	409 646	1 440
171 321	1 180	417 004	1 460
199 321	1 200	422 968	1 480
237 455	1 220	426 711	1 500
243 975	1 240	429 800	1 520
284 972	1 260	430 718	1 530
316 078	1 280		

Table B.11: C5H018: Longitudinal profile data

Progressive distance (m)	Reduced height (m)	Progressive distance (m)	Reduced height (m)
0	1 110	315 276	1 340
27 083	1 120	321 793	1 360
51 133	1 140	333 438	1 380
71 795	1 160	336 657	1 400
115 988	1 180	343 576	1 420
143 987	1 200	354 312	1 440
182 121	1 220	361 671	1 460
188 641	1 240	367 634	1 480
229 639	1 260	371 377	1 500
260 745	1 280	374 466	1 520
279 400	1 300	375 385	1 530
295 380	1 320		

Table B.12: C5H022: Longitudinal profile data

Progressive distance (m)	Reduced height (m)	Progressive distance (m)	Reduced height (m)
0	1 531.48	6 830	1 640
1 221	1 540	7 250	1 660
3 325	1 560	7 643	1 680
4 653	1 580	7 824	1 700
5 495	1 600	7 912	1 706.10
6 114	1 620		

Table B.13: C5H054: Longitudinal profile data

Progressive distance (m)	Reduced height (m)	Progressive distance (m)	Reduced height (m)
0	1 278.67	50 299	1 400
790	1 280	55 597	1 420
7 299	1 300	59 474	1 440
17 220	1 320	63 298	1 460
27 404	1 340	66 126	1 480
36 300	1 360	67 600	1 500
44 031	1 380	68 039	1 517.40

Table B.14: %-Distribution of lake, rural and urban components

Catchment description	%-Distribution of land-use components		
	Lakes	Rural	Urban
Study area	0.21	99.07	0.72
C5R001	0.56	99.44	-
C5R002	0.35	99.56	0.09
C5R003	1.12	98.54	0.34
C5R004	0.34	96.62	3.04
C5R005	0.45	99.47	0.08
C5H003	1.12	98.54	0.34
C5H012	0.29	99.64	0.07
C5H015	0.34	96.62	3.04
C5H016	0.21	99.04	0.75
C5H018	0.16	98.52	1.32
C5H022	0.45	99.47	0.08
C5H054	0.09	86.05	13.86

Table B.15: Rural component: Standard classification classes

Catchment description	Standard classification classes	%-Distribution
C5R001	Cultivated land	11.41
	Grasslands	86
	Light bush and farmlands	0.04
	No vegetation	0.03
	Thick bush and plantations	2.52
C5R002	Cultivated land	4.45
	Grasslands	76.17
	Light bush and farmlands	16.09
	No vegetation	0.37
	Thick bush and plantations	2.92
C5R003	Cultivated land	8.08
	Grasslands	86.96
	No vegetation	0.32
	Thick bush and plantations	4.64

Table B.15: Rural component: Standard classification classes (Continued)

Catchment description	Standard classification classes	%-Distribution
C5R004	Cultivated land	14.29
	Grasslands	80.18
	Light bush and farmlands	0.73
	No vegetation	0.46
	Thick bush and plantations	4.34
C5R005	Cultivated land	10.81
	Grasslands	81.85
	No vegetation	0.29
	Thick bush and plantations	7.05
C5H003	Cultivated land	8.08
	Grasslands	86.96
	No vegetation	0.32
	Thick bush and plantations	4.64
	Cultivated land	8.08
C5H012	Cultivated land	6.77
	Grasslands	90.76
	Light bush and farmlands	1.36
	No vegetation	0.21
	Thick bush and plantations	0.90
C5H015	Cultivated land	14.29
	Grasslands	80.18
	Light bush and farmlands	0.73
	No vegetation	0.46
	Thick bush and plantations	4.34
C5H016	Cultivated land	11.33
	Grasslands	61.07
	Light bush and farmlands	17.82
	No vegetation	0.81
	Thick bush and plantations	8.97
C5H018	Cultivated land	17.22
	Grasslands	62.07
	Light bush and farmlands	10.66
	No vegetation	0.71
	Thick bush and plantations	9.34
C5H022	Cultivated land	10.81
	Grasslands	81.85
	Light bush and farmlands	0.29
	No vegetation	7.05
C5H054	Cultivated land	13.44
	Grasslands	81.13
	No vegetation	0.05
	Thick bush and plantations	5.38

Table B.16: Urban component: Standard classification classes

Catchment description	Standard classification classes	%-Distribution
C5R002	City centre	2.78
	Light industry	2.26
	Residential (Houses)	46.68
	Suburban	48.28
C5R003	City centre	1.85
	Light industry	2.90
	Residential (Houses)	74.34
	Suburban	20.91
C5R004	City centre	4.62
	Heavy industry	0.03
	Light industry	11.53
	Residential (Flats)	0.15
	Residential (Houses)	59.12
	Suburban	24.55
C5R005	Residential (Houses)	100
C5H003	City centre	1.85
	Light industry	2.90
	Residential (Houses)	74.34
	Suburban	20.91
C5H012	City centre	1.64
	Light industry	2
	Residential (Houses)	37.90
	Suburban	58.46
C5H015	City centre	4.62
	Heavy industry	0.03
	Light industry	11.53
	Residential (Flats)	0.15
	Residential (Houses)	59.12
	Suburban	24.55
C5H016	City centre	4.95
	Heavy industry	2.48
	Light industry	10.43
	Residential (Flats)	0.57
	Residential (Houses)	51.48
	Suburban	30.09
C5H018	City centre	4.79
	Heavy industry	2.45
	Light industry	11.02
	Residential (Flats)	0.62
	Residential (Houses)	52.23
	Suburban	28.89
C5H022	Residential (Houses)	100
C5H054	City centre	7.60
	Light industry	13.05
	Residential (Flats)	0.25
	Residential (Houses)	36.56
	Suburban	42.54

Table B.17: Thiessen polygon weighted areas within SDF basin 9

Precipitation station number	MAP (mm)	Weighted area (km²)
0201361W	414	140.7
0201370W	435	227.9
0201373W	453	143.4
0201482W	414	108.8
0201492W	453	129
0201637W	340	123.9
0201756W	361	81.7
0201843W	382	147.6
0228571W	332	171.5
0228725W	314	223.6
0228783W	334	133.9
0229124W	370	178.2
0229215W	366	176.6
0229344W	401	190.8
0229555W	420	75.8
0229556W	422	109.7
0229571W	368	172.7
0229579W	398	210.1
0229629W	405	209
0229654W	374	178.6
0229723W	368	158.5
0229737W	414	138.4
0229862W	384	115.3
0230011W	426	194.9
0230027W	466	220.9
0230048W	376	124.1
0230073W	419	48.2
0230074W	395	52.7
0230210W	395	286.1
0230254W	359	178.2
0230349W	409	194.9
0230363W	275	342.9
0230466W	389	233.2
0230542W	384	181
0230566W	368	147
0230598W	410	79.1
0230764W	427	244.4
0230774W	431	186.8
0230810W	408	118.8
0230816W	489	265.2
0231076W	386	180
0231114W	431	422.3
0231161W	406	128.2
0231247W	463	120.9
0231279W	479	80.2
0231361W	459	139.4
0231375W	403	241.1
0231395W	454	146.2

Table B.17: Thiessen polygon weighted areas within SDF basin 9 (Continued)

Precipitation station number	MAP (mm)	Weighted area (km²)
0231588W	443	237.7
0231663W	496	112.4
0231713W	479	362.4
0231754W	516	111.8
0231761W	564	191
0232011W	530	129.1
0232018W	420	97.7
0232123W	555	127
0232181W	555	96.2
0232211W	555	40.1
0232275W	585	102.4
0232301W	488	74
0232512W	599	98.5
0256638W	293	389.5
0257391W	332	1 583
0257845W	364	381.8
0257878W	358	332.9
0258079W	305	483.8
0258157W	385	67.9
0258164W	322	161.6
0258182W	359	858.9
0258213W	404	57.7
0258218W	359	49.1
0258306W	348	27.5
0258335W	375	156.6
0258339W	374	49.2
0258380W	275	147.3
0258399W	325	33.2
0258434W	363	90
0258458W	376	115.6
0258467W	349	101.8
0258474W	313	128.2
0258581W	342	197.7
0258624W	338	129.9
0258740W	350	115.4
0258812W	349	129.6
0258827W	360	179.4
0258894W	450	145
0259002W	363	127.3
0259086W	359	189.3
0259102W	371	155.2
0259131W	392	109.1
0259278W	414	211.3
0259348W	369	378.2
0259390W	408	239.6
0259578W	426	154.3
0259609W	399	141.3

Table B.17: Thiessen polygon weighted areas within SDF basin 9 (Continued)

Precipitation station number	MAP (mm)	Weighted area (km²)
0259727W	411	144.6
0259743W	309	272.9
0259855W	463	118.7
0259881W	433	105.5
0259887W	457	98.5
0260004W	449	98.4
0260030W	374	238.3
0260082W	448	126.3
0260083W	424	172.5
0260126W	454	199.8
0260163W	461	127.8
0260314W	440	218.4
0260519W	471	367.2
0260555W	516	181.2
0260660W	459	140.8
0260678W	478	213.1
0260715W	373	253.3
0260882W	495	336
0261146A	479	250.9
0261183W	484	276
0261256W	325	248
0261266W	519	176.9
0261275W	570	50
0261307W	537	51.4
0261312W	538	103.5
0261365W	558	43.7
0261366W	563	7
0261367W	552	7
0261368W	545	10.9
0261369W	613	39.7
0261425W	553	45.5
0261426W	553	15
0261516W	537	56
0261517W	514	16.2
0261523W	518	191.9
0261548W	518	73
0261597W	426	256.7
0261722W	534	221.9
0261733W	486	171.5
0261750W	497	149.3
0261789W	551	142.8
0261890W	523	342.6
0262129W	516	143.5
0262155W	473	132.7
0262247W	566	113.6
0262271W	435	140.5
0262314W	526	250.4

Table B.17: Thiessen polygon weighted areas within SDF basin 9 (Continued)

Precipitation station number	MAP (mm)	Weighted area (km²)
0262353W	530	296.5
0262453W	548	183.9
0262479W	554	125.6
0262613W	590	242.2
0262690W	548	115.3
0262734W	649	70.4
0262828W	686	147.2
0290810W	380	357.5
0290887W	392	487.5
0291075W	441	146
0291148W	397	70
0291174W	375	109.5
0291178W	396	66.1
0291231W	333	107.9
0291313W	431	242.4
0291323W	404	100.3
0291360W	403	196.8
0291415W	394	209.2
0291582W	449	225.2
0291708W	390	292.1
0291758W	418	337.4
0291899W	433	201.7
0292051W	398	379.6
0292089W	430	162.8
0292446W	438	509
0292461W	432	576.3
0292606W	455	155.5
0292833W	453	435.5
0293007W	453	446.7
0293106W	471	301.5
0293204W	478	293.7
0293339W	406	224.3
0293403W	463	240.2
0293514W	486	300.9
0293568W	464	140.6
0293597W	529	90.1
0293622W	500	153.7
0293652W	500	141.7
0293700W	476	189.6
0293792W	536	228.1
0294052W	428	284.5
0294233W	471	213.6

Table B.18: Type 1 storm distribution (winter/all year precipitation)

Station number	*M* (mm)	*R* (days/year)	Station number	*M* (mm)	*R* (days/year)
0003020W	29.1	5	0037541A	66.1	19
0004891W	26.2	3	0037541W	67.2	19
0007699A	34.2	6	0038152A	64.5	6
0007699W	34.9	6	0038152W	60.9	6
0010456W	41.1	3	0041347A	31.7	1
001225W	32.1	7	0041347W	29.7	1
0017582A	53.6	8	0059572A	80.2	25
0017582W	51	8	005972W	88.3	25
0020779W	77.7	1	0060620A	21.3	3
0020866W	41.1	2	0060620W	22.6	3
0021778W	63.3	3	0061298W	24.7	6
0021823W	56.9	4	0062379A	55.5	4
0021825W	59.4	4	0062379W	55.3	4
0021860A	51.7	4	0080569W	83.9	26
0022113A	52.7	4	0084558W	43.5	1
0022113W	56.4	4	0106850W	20.1	4
0023710A	30.8	5	0106880W	19.8	4
0028771W	61.8	9	0110385W	18.3	13
0029058W	69.4	10	0134478A	25.6	7
0034705W	53.2	12	0134478W	26.2	7
0034706W	54.6	12	0157874A	23	11
0034762W	52.3	12	0157874W	22	11
0034767A	46.1	12	0160807A	30.5	11
0035179A	56.2	14	0160807W	29.3	11
0035179W	63	14	0214636W	23.6	7
0035334A	45.9	15	0274034W	10.3	6
0035334W	45.8	15			

Table B.19: Type 2 storm distribution (summer precipitation)

Station number	*M* (mm)	*R* (days/year)	Station number	*M* (mm)	*R* (days/year)
0054805W	37.5	19	0190868W	24.7	3
0069483W	30.7	16	0207560W	39.6	72
0074296A	29.2	16	0224430A	36.8	22
0074296W	29.5	16	0224430W	31	22
0076133W	55.5	23	0228420W	37.5	54
0076134A	49.5	23	0229555W	42.3	49
0076884W	45.1	23	0229556A	45.5	49
0079683A	50.8	26	0229556W	45.7	49
0079712W	53.7	26	0233044W	37.5	55
0079811A	57.5	33	0233049W	51.9	55
0079811W	54.1	33	0236521W	36.1	66
0088293A	32.1	12	0237606W	64.6	66
0088293W	26.6	12	0239138W	53.2	61
0092141W	37.1	21	0239482A	54.6	60
0096045A	37.9	25	0239482W	55.6	60
0096045B	39.1	25	0239577W	50.9	60
0096045W	37.6	25	0239605P	57	60
0113025W	26.7	13	0240269W	71.1	35
0123654A	43.1	41	0240682W	85.3	35
0123654W	43.2	41	0240808AW	80.9	35
0123716W	45.4	41	0240862W	74.8	35
0127485A	48.1	36	0240883A	84.9	22
0129068A	88.6	20	0241042A	84.9	22
0129068W	65.4	20	0241042W	83.8	22
0143258W	34.9	52	0247242W	20.5	13
0145029A	37.8	52	0253363A	35.7	35
0145059W	36.1	52	0253363W	34.8	35
0148352A	42	68	0256453W	39.7	49
0148352W	41.2	68	0256483W	38.4	49
0165898A	33.4	11	0258213A	45.6	47
0165898W	32.9	11	0258458W	37.2	47
0166238A	33.9	11	0261307A	50.2	62
0166238W	24.5	11	0261365W	49.5	62
0170009A	35.5	24	0261366W	50.8	62
0170009W	33.9	24	0261367W	48.6	62
0175311W	46.8	60	0261368W	49.9	62
0175342W	43.7	60	0261369W	64.2	62
0175371A	44.6	60	0261425W	51	62
0175371W	44.8	60	0261426W	47.6	62
0180439W	62.4	45	0261517W	50.8	62
0180721A	49.6	45	0277177W	22.3	8
0180721W	51.3	45	0284361W	34.1	55
0180722A	54.4	45	0290463W	43.3	55
0182379A	108.7	11	0290464A	41.5	55
0182794A	99.1	26	0290468A	43.4	55
0182794W	96.2	26	0290468W	37.6	55
0190868A	24.6	3	0293568W	41.3	62

Table B.19: Type 2 storm distribution (summer precipitation) (Continued)

Station number	*M* (mm)	*R* (days/year)	Station number	*M* (mm)	*R* (days/year)
0293597A	49.7	62	0436887W	52.9	72
0293597W	52.1	62	0437100W	54.6	72
0300439A	57.3	56	0437104W	52.4	72
0300567A	53.8	56	0438550W	41.6	51
0300690W	50.4	56	0438729W	50	44
0303833W	107	26	0438731A	53	44
0305167W	91.1	17	0442811A	53.4	43
0317447A	22.8	36	0442811W	40.2	43
0317447AW	28.1	36	0444540A	58.9	44
0317447W	22.6	36	0461208W	31.7	28
0317474W	26.9	29	0474680W	52.7	24
0322071W	45.1	39	0475455A	59	27
0323075W	41.7	39	0475455W	66.9	27
0323102A	47.9	39	0475456A	59.1	27
0323102W	48.5	39	0475456W	53	27
0323160W	43.3	39	0475528W	40.8	43
0323221W	44.5	39	0476072W	61.3	40
0328636W	44.3	49	0476111W	40.1	51
0328726W	48	49	0476396W	47.7	73
0331554W	48.4	85	0480184A	52.7	54
0336283W	65.3	17	0480184W	42.4	54
0339357W	85.8	17	0483193W	67.6	54
0339415W	85	17	0508261W	53.7	40
0339720W	97.9	28	0511400W	59.9	71
0360597A	44.8	55	0511523A	54.1	71
0360597W	43.4	55	0511523W	55.5	71
0363470W	48.9	66	0511855A	58.8	54
0364322W	48.4	70	0511855B	52.6	54
0365400A	43	54	0511855W	58.5	54
0365400W	46.6	54	0511858W	57.2	54
0365430W	48.6	54	0512488W	50.8	28
0369030W	49.4	54	0512545A	52.3	23
0370655A	67.8	63	0512545W	51.7	23
0393778W	46.2	37	0513284W	55.2	51
0399894A	46.6	37	0513314A	56.5	51
0400203W	50.3	37	0513382W	52.8	87
0403886A	45.4	66	0513465A	57.8	39
0403886W	36.4	66	0517072W	47.9	47
0406682A	60.4	48	0519077W	57.6	31
0406682W	62.6	48	0546204W	51.3	30
0410878W	80.5	35	0546630A	56.5	30
0411294S	37.8	35	0547359W	47.5	31
0432237A	47.8	51	0548165W	57.4	46
0432237W	51.4	51	0552610A	59.1	59
0434888W	51.5	76	0552610W	55.4	59
0436887A	54.2	72	0552654A	57	59

Table B.19: Type 2 storm distribution (summer precipitation) (Continued)

Station number	*M* (mm)	*R* (days/year)	Station number	*M* (mm)	*R* (days/year)
0552654W	50.6	59	0633881W	53.4	15
0553351W	55.4	20	0634011W	49.3	15
0554752W	54.3	38	0636486W	77.7	24
0554786W	49.8	38	0637801W	61.7	25
0554816A	50.6	38	0675125W	61.9	44
0555837A	59	58	0677802A	46.4	44
0555837W	56.3	58	0677802W	42	44
0556088W	66.3	11	0679290A	91.1	25
0556460A	68.3	11	0679290W	88.7	25
0556460W	64.4	11	0680059W	67.1	10
0589476A	46.5	42	0681180W	63.7	10
0589476W	47.6	42	0719370A	53.2	44
0589594A	54.2	42	0722099A	57.2	30
0589594W	51.7	42	0722099W	58.1	30
0591538W	49.1	17	0723485A	86.3	21
0593581W	56.1	37	0723485W	84.6	21
0594493W	56.5	35	0766324W	64.7	28
0596179A	60.6	20	0766863A	92.3	28
0596179W	59.6	20	0809706A	51.4	19
0632044W	51.2	53	0809706W	51.3	19
0633881A	56.3	15			

Table B.20: C5R001: Annual maximum peak flow

Hydrological year	AMS (m^3/s)	Hydrological year	AMS (m^3/s)
1923/1924	25	1966/1967	19
1924/1925	851	1967/1968	13
1925/1926	3.5	1968/1969	34
1926/1927	95	1969/1970	26
1927/1928	23	1970/1971	35
1928/1929	72	1971/1972	92
1929/1930	17	1972/1973	5
1930/1931	33	1973/1974	60
1931/1932	66	1974/1975	9.9
1932/1933	14	1975/1976	177
1933/1934	91	1976/1977	96
1934/1935	16	1977/1978	57
1935/1936	7.8	1978/1979	5.8
1936/1937	26	1979/1980	7.6
1937/1938	2.2	1980/1981	108
1938/1939	17	1981/1982	19
1939/1940	56	1982/1983	13
1940/1941	30	1983/1984	27
1941/1942	28	1984/1985	47
1942/1943	62	1985/1986	36
1943/1944	86	1986/1987	91
1944/1945	25	1987/1988	7 100
1945/1946	60	1988/1989	-1
1946/1947	6.6	1989/1990	-1
1947/1948	751	1990/1991	48
1948/1949	2.1	1991/1992	74
1949/1950	70	1992/1993	3.1
1950/1951	19	1993/1994	71
1951/1952	4.9	1994/1995	3.3
1952/1953	14	1995/1996	136
1953/1954	17	1996/1997	7.3
1954/1955	393	1997/1998	19
1955/1956	166	1998/1999	2.7
1956/1957	45	1999/2000	97
1957/1958	18	2000/2001	60
1958/1959	24	2001/2002	143
1959/1960	91	2002/2003	36
1960/1961	30	2003/2004	33
1961/1962	18	2004/2005	11
1962/1963	67	2005/2006	153
1963/1964	50	2006/2007	25
1964/1965	6.9	2007/2008	139
1965/1966	647		

Table B.21: C5R002: Annual maximum peak flow

Hydrological year	AMS (m^3/s)	Hydrological year	AMS (m^3/s)
1912/1913	165.9	1960/1961	138
1913/1914	141.6	1961/1962	422
1914/1915	515.2	1962/1963	402
1915/1916	255.2	1963/1964	72
1916/1917	394.9	1964/1965	117
1917/1918	83.4	1965/1966	695
1918/1919	296.9	1966/1967	335
1919/1920	1 750.2	1967/1968	76
1920/1921	130	1968/1969	735
1921/1922	310.5	1969/1970	169
1922/1923	1 579.5	1970/1971	172
1923/1924	502.6	1971/1972	1 590
1924/1925	1 426.2	1972/1973	12
1925/1926	251.3	1973/1974	6 400
1926/1927	335.7	1974/1975	142
1927/1928	213.4	1975/1976	1 040
1928/1929	269.7	1976/1977	130
1929/1930	1 060.4	1977/1978	185
1930/1931	284.3	1978/1979	183
1931/1932	571.4	1979/1980	63
1932/1933	330.8	1980/1981	123
1933/1934	772.3	1981/1982	5.1
1934/1935	447.3	1982/1983	14
1935/1936	41.7	1983/1984	288
1936/1937	918.8	1984/1985	73
1937/1938	5.8	1985/1986	205
1938/1939	186	1986/1987	71
1939/1940	195	1987/1988	15 250
1940/1941	496	1988/1989	425
1941/1942	175	1989/1990	50
1942/1943	1 444	1990/1991	1 436
1943/1944	161	1991/1992	345
1944/1945	25	1992/1993	198
1945/1946	204	1993/1994	889
1946/1947	58	1994/1995	22
1947/1948	2 005	1995/1996	95
1948/1949	99	1996/1997	61
1949/1950	1 272	1997/1998	40
1950/1951	61	1998/1999	3.4
1951/1952	182	1999/2000	81
1952/1953	85	2000/2001	117
1953/1954	321	2001/2002	326
1954/1955	807	2002/2003	84
1955/1956	266	2003/2004	144
1956/1957	167	2004/2005	27
1957/1958	436	2005/2006	332
1958/1959	70	2006/2007	397
1959/1960	84	2007/2008	176

Table B.22: C5R003: Annual maximum peak flow

Hydrological year	AMS (m^3/s)	Hydrological year	AMS (m^3/s)
1918/1919	21.9	1963/1964	66
1919/1920	685.6	1964/1965	26
1920/1921	54.2	1965/1966	204
1921/1922	128.1	1966/1967	104
1922/1923	667.6	1967/1968	101
1923/1924	97.9	1968/1969	100
1924/1925	739.1	1969/1970	34
1925/1926	36.9	1970/1971	19
1926/1927	366.2	1971/1972	160
1927/1928	65.6	1972/1973	19
1928/1929	612.6	1973/1974	204
1929/1930	54.2	1974/1975	12
1930/1931	137.1	1975/1976	167
1931/1932	88.2	1976/1977	68
1932/1933	33.2	1977/1978	35
1933/1934	627.6	1978/1979	8.9
1934/1935	183.8	1979/1980	16
1935/1936	23.4	1980/1981	130
1936/1937	627.6	1981/1982	27
1937/1938	44.5	1982/1983	12
1938/1939	11.3	1983/1984	12
1939/1940	54.2	1984/1985	9.7
1940/1941	723.3	1985/1986	96
1941/1942	33.2	1986/1987	92
1942/1943	646.5	1987/1988	2 597
1943/1944	137.1	1988/1989	204
1944/1945	334.5	1989/1990	66
1945/1946	128.1	1990/1991	29
1946/1947	20.3	1991/1992	154
1947/1948	914.7	1992/1993	17
1948/1949	49	1993/1994	501
1949/1950	780.6	1994/1995	12
1950/1951	36.2	1995/1996	457
1951/1952	296.9	1996/1997	83
1952/1953	54.2	1997/1998	118
1953/1954	55	1998/1999	32
1954/1955	200	1999/2000	90
1955/1956	583	2000/2001	111
1956/1957	49	2001/2002	876
1957/1958	30	2002/2003	66
1958/1959	53	2003/2004	44
1959/1960	22	2004/2005	10
1960/1961	40	2005/2006	200
1961/1962	23	2006/2007	47
1962/1963	51	2007/2008	31

Table B.23: C5R004: Annual maximum peak flow

Hydrological year	AMS (m^3/s)	Hydrological year	AMS (m^3/s)
1948/1949	137.5	1978/1979	41
1949/1950	773.9	1979/1980	12
1950/1951	240.2	1980/1981	350
1951/1952	339.8	1981/1982	260
1952/1953	1 090.1	1982/1983	5.1
1953/1954	187.8	1983/1984	22
1954/1955	570.7	1984/1985	36
1955/1956	1 642.3	1985/1986	426
1956/1957	86.2	1986/1987	398
1957/1958	56.5	1987/1988	2 456
1958/1959	362.3	1988/1989	217
1959/1960	374.6	1989/1990	77
1960/1961	154	1990/1991	230
1961/1962	60.6	1991/1992	741
1962/1963	636.4	1992/1993	72
1963/1964	985.4	1993/1994	466
1964/1965	482.4	1994/1995	53
1965/1966	1 087	1995/1996	616
1966/1967	555.3	1996/1997	121
1967/1968	537.9	1997/1998	281
1968/1969	366.4	1998/1999	135
1969/1970	162.2	1999/2000	210
1970/1971	453.7	2000/2001	208
1971/1972	792	2001/2002	315
1972/1973	20	2002/2003	377
1973/1974	625	2003/2004	128
1974/1975	336	2004/2005	35
1975/1976	687	2005/2006	836
1976/1977	318	2006/2007	456
1977/1978	158	2007/2008	40

Table B.24: C5R005: Annual maximum peak flow

Hydrological year	AMS (m^3/s)	Hydrological year	AMS (m^3/s)
1981/1982	51	1995/1996	78
1982/1983	6.1	1996/1997	24
1983/1984	4.9	1997/1998	192
1984/1985	11	1998/1999	34
1985/1986	31	1999/2000	56
1986/1987	49	2000/2001	22
1987/1988	264	2001/2002	47
1988/1989	35	2002/2003	34
1989/1990	85	2003/2004	20
1990/1991	23	2004/2005	13
1991/1992	32	2005/2006	239
1992/1993	15	2006/2007	137
1993/1994	93	2007/2008	27
1994/1995	8.8		

Table B.25: C5H003: Annual maximum peak flow

Hydrological year	AMS (m^3/s)	Hydrological year	AMS (m^3/s)
1918/1919	29	1963/1964	-1
1919/1920	910	1964/1965	-1
1920/1921	72	1965/1966	-1
1921/1922	170	1966/1967	-1
1922/1923	886	1967/1968	-1
1923/1924	130	1968/1969	-1
1924/1925	981	1969/1970	-1
1925/1926	49	1970/1971	-1
1926/1927	486	1971/1972	-1
1927/1928	87	1972/1973	-1
1928/1929	813	1973/1974	-1
1929/1930	72	1974/1975	-1
1930/1931	182	1975/1976	-1
1931/1932	117	1976/1977	-1
1932/1933	44	1977/1978	-1
1933/1934	833	1978/1979	-1
1934/1935	244	1979/1980	-1
1935/1936	31	1980/1981	-1
1936/1937	833	1981/1982	-1
1937/1938	59	1982/1983	-1
1938/1939	15	1983/1984	-1
1939/1940	72	1984/1985	-1
1940/1941	960	1985/1986	-1
1941/1942	44	1986/1987	-1
1942/1943	858	1987/1988	-1
1943/1944	182	1988/1989	-1
1944/1945	444	1989/1990	-1
1945/1946	170	1990/1991	60.4
1946/1947	27	1991/1992	61.2
1947/1948	1 214	1992/1993	20.2
1948/1949	65	1993/1994	61.2
1949/1950	1 036	1994/1995	21.1
1950/1951	48	1995/1996	48.2
1951/1952	394	1996/1997	13.3
1952/1953	72	1997/1998	48.2
1953/1954	73	1998/1999	32.5
1954/1955	-1	1999/2000	38.4
1955/1956	-1	2000/2001	48.2
1956/1957	-1	2001/2002	47.4
1957/1958	-1	2002/2003	48.2
1958/1959	-1	2003/2004	25.6
1959/1960	-1	2004/2005	33
1960/1961	-1	2005/2006	27.1
1961/1962	-1	2006/2007	22.6
1962/1963	-1	2007/2008	30.9

Table B.26: C5H012: Annual maximum peak flow

Hydrological year	AMS (m^3/s)	Hydrological year	AMS (m^3/s)
1931/1932	85.7	1970/1971	52.4
1932/1933	131.4	1971/1972	52.4
1933/1934	131.4	1972/1973	52.4
1934/1935	131.4	1973/1974	2.4
1935/1936	131.4	1974/1975	52.4
1936/1937	28.8	1975/1976	4.4
1937/1938	131.4	1976/1977	120.9
1938/1939	66.5	1977/1978	34.6
1939/1940	131.4	1978/1979	75.4
1940/1941	69.2	1979/1980	7.6
1941/1942	131.4	1980/1981	102.5
1942/1943	35.1	1981/1982	266.2
1943/1944	131.4	1982/1983	3.6
1944/1945	131.4	1983/1984	32.9
1945/1946	0.4	1984/1985	140.6
1946/1947	131.4	1985/1986	98.6
1947/1948	131.4	1986/1987	63.3
1948/1949	131.4	1987/1988	52.4
1949/1950	103.2	1988/1989	52.4
1950/1951	131.4	1989/1990	52.4
1951/1952	88.5	1990/1991	1
1952/1953	131.4	1991/1992	52.4
1953/1954	131.3	1992/1993	52.4
1954/1955	131.4	1993/1994	-1
1955/1956	131.4	1994/1995	52.4
1956/1957	140.8	1995/1996	-1
1957/1958	79.1	1996/1997	-1
1958/1959	237	1997/1998	15.2
1959/1960	52.3	1998/1999	-1
1960/1961	52.4	1999/2000	18.7
1961/1962	46	2000/2001	52.4
1962/1963	52.4	2001/2002	52.4
1963/1964	52.4	2002/2003	52.4
1964/1965	52.4	2003/2004	37.4
1965/1966	44.2	2004/2005	27.2
1966/1967	52.4	2005/2006	0.6
1967/1968	52.4	2006/2007	52.4
1968/1969	52.4	2007/2008	47
1969/1970	52.4		

Table B.27: C5H015: Annual maximum peak flow

Hydrological year	AMS (m^3/s)	Hydrological year	AMS (m^3/s)
1948/1949	134.2	1965/1966	1 059
1949/1950	753.7	1966/1967	541.3
1950/1951	234.2	1967/1968	523.8
1951/1952	331.2	1968/1969	356.9
1952/1953	1 062.2	1969/1970	158.5
1953/1954	182.5	1970/1971	441.6
1954/1955	555.7	1971/1972	1 039.4
1955/1956	1 600.2	1972/1973	-1
1956/1957	83.8	1973/1974	24.3
1957/1958	54.9	1974/1975	157.6
1958/1959	353.3	1975/1976	888.4
1959/1960	365.3	1976/1977	272.3
1960/1961	150.2	1977/1978	157.6
1961/1962	59.3	1978/1979	9.2
1962/1963	619.8	1979/1980	7.7
1963/1964	960.1	1980/1981	305.7
1964/1965	470.2	1981/1982	141.9

Table B.28: C5H016: Annual maximum peak flow

Hydrological year	AMS (m^3/s)	Hydrological year	AMS (m^3/s)
1952/1953	301.7	1979/1980	16.9
1953/1954	132.2	1980/1981	74.7
1954/1955	301.7	1981/1982	24.9
1955/1956	301.7	1982/1983	20.4
1956/1957	66	1983/1984	26.8
1957/1958	95.5	1984/1985	33.6
1958/1959	217.2	1985/1986	104.2
1959/1960	190.1	1986/1987	104.2
1960/1961	55.9	1987/1988	98.1
1961/1962	19.1	1988/1989	363.6
1962/1963	301.7	1989/1990	297.5
1963/1964	301.7	1990/1991	102.3
1964/1965	224.7	1991/1992	118.3
1965/1966	239.1	1992/1993	127.2
1966/1967	104.2	1993/1994	148.5
1967/1968	104.2	1994/1995	104.9
1968/1969	104.2	1995/1996	121.4
1969/1970	21.3	1996/1997	31.4
1970/1971	37.2	1997/1998	26
1971/1972	104.2	1998/1999	134.4
1972/1973	34.3	1999/2000	148.8
1973/1974	104.2	2000/2001	89.3
1974/1975	83.5	2001/2002	30.5
1975/1976	104.2	2002/2003	396.5
1976/1977	86.1	2003/2004	325.4
1977/1978	48.8	2004/2005	210.3
1978/1979	17.8	2005/2006	14.1

Table B.29: C5H018: Annual maximum peak flow

Hydrological year	AMS (m^3/s)	Hydrological year	AMS (m^3/s)
1959/1960	152.7	1984/1985	12.4
1960/1961	59.2	1985/1986	69.3
1961/1962	22.9	1986/1987	59
1962/1963	261.9	1987/1988	1 826.9
1963/1964	330.5	1988/1989	118.4
1964/1965	171.8	1989/1990	6.1
1965/1966	395.6	1990/1991	110.6
1966/1967	210.8	1991/1992	285
1967/1968	254	1992/1993	13.1
1968/1969	127.1	1993/1994	124.9
1969/1970	32	1994/1995	5.3
1970/1971	52.3	1995/1996	178.4
1971/1972	219.8	1996/1997	20.4
1972/1973	303.1	1997/1998	157.5
1973/1974	319.1	1998/1999	10.5
1974/1975	131.6	1999/2000	17.8
1975/1976	379	2000/2001	30.1
1976/1977	101.5	2001/2002	197.5
1977/1978	54.6	2002/2003	77.1
1978/1979	62.9	2003/2004	8.7
1979/1980	57	2004/2005	3.5
1980/1981	109.3	2005/2006	287.1
1981/1982	61.7	2006/2007	244.2
1982/1983	62.5	2007/2008	10.5
1983/1984	-1		

Table B.30: C5H022: Annual maximum peak flow

Hydrological year	AMS (m^3/s)	Hydrological year	AMS (m^3/s)
1980/1981	7.2	1994/1995	3.4
1981/1982	19.4	1995/1996	21.4
1982/1983	1.9	1996/1997	1.2
1983/1984	3.6	1997/1998	35.9
1984/1985	7	1998/1999	24.1
1985/1986	7.5	1999/2000	10.6
1986/1987	15.7	2000/2001	5.5
1987/1988	63.7	2001/2002	18.2
1988/1989	13.8	2002/2003	10.3
1989/1990	21.1	2003/2004	0.6
1990/1991	1.7	2004/2005	0.5
1991/1992	9.6	2005/2006	46
1992/1993	4.1	2006/2007	43.9
1993/1994	25	2007/2008	1.9

Table B.31: C5H054: Annual maximum peak flow

Hydrological year	AMS (m^3/s)	Hydrological year	AMS (m^3/s)
1922/1923	81.4	1965/1966	11.2
1923/1924	81.4	1966/1967	11.2
1924/1925	81.4	1967/1968	11.2
1925/1926	81.4	1968/1969	11.2
1926/1927	39.1	1969/1970	11.2
1927/1928	11.9	1970/1971	11.2
1928/1929	92	1971/1972	11.2
1929/1930	19.1	1972/1973	9.3
1930/1931	37.5	1973/1974	11.2
1931/1932	313.8	1974/1975	11.2
1932/1933	56	1975/1976	11.2
1933/1934	314.2	1976/1977	11.2
1934/1935	50.6	1977/1978	9
1935/1936	62.7	1978/1979	2.3
1936/1937	44.6	1979/1980	4.7
1937/1938	19.5	1980/1981	11.2
1938/1939	61.4	1981/1982	8.4
1939/1940	71.9	1982/1983	1.5
1940/1941	314.2	1983/1984	6.3
1941/1942	22.6	1984/1985	2.1
1942/1943	-1	1985/1986	11.2
1943/1944	-1	1986/1987	11.2
1944/1945	-1	1987/1988	11.2
1945/1946	-1	1988/1989	11.2
1946/1947	-1	1989/1990	0.5
1947/1948	11.2	1990/1991	11.2
1948/1949	11.2	1991/1992	11.2
1949/1950	11.2	1992/1993	5
1950/1951	11.2	1993/1994	11.2
1951/1952	11.2	1994/1995	-1
1952/1953	11.2	1995/1996	23.8
1953/1954	11.2	1996/1997	23.8
1954/1955	11.2	1997/1998	23.8
1955/1956	11.2	1998/1999	12.8
1956/1957	11.2	1999/2000	23.8
1957/1958	11.1	2000/2001	23.8
1958/1959	11.2	2001/2002	23.8
1959/1960	11.2	2002/2003	23.8
1960/1961	11.2	2003/2004	23.8
1961/1962	8.3	2004/2005	19.6
1962/1963	11.2	2005/2006	23.8
1963/1964	11.2	2006/2007	23.8
1964/1965	11.2	2007/2008	23.8

Table B.32: A2H012 (1): Annual maximum peak flow

Hydrological year	AMS (m^3/s)	Hydrological year	AMS (m^3/s)
1922/1923	91.8	1966/1967	369.1
1923/1924	81.5	1967/1968	27
1924/1925	-1	1968/1969	22.4
1925/1926	-1	1969/1970	149.3
1926/1927	33.8	1970/1971	176.2
1927/1928	87.3	1971/1972	313.2
1928/1929	108.9	1972/1973	84.6
1929/1930	-1	1973/1974	75
1930/1931	-1	1974/1975	289.1
1931/1932	-1	1975/1976	316.5
1932/1933	-1	1976/1977	660.7
1933/1934	-1	1977/1978	453
1934/1935	96.3	1978/1979	36.2
1935/1936	-1	1979/1980	202
1936/1937	-1	1980/1981	163.4
1937/1938	-1	1981/1982	70
1938/1939	-1	1982/1983	57
1939/1940	-1	1983/1984	89.8
1940/1941	-1	1984/1985	276.3
1941/1942	62.7	1985/1986	399.4
1942/1943	90.3	1986/1987	247.9
1943/1944	-1	1987/1988	273.7
1944/1945	-1	1988/1989	213.1
1945/1946	-1	1989/1990	97
1946/1947	108.9	1990/1991	99.8
1947/1948	50.7	1991/1992	49.7
1948/1949	63.8	1992/1993	55
1949/1950	-1	1993/1994	155.1
1950/1951	96	1994/1995	312.4
1951/1952	46.7	1995/1996	495.6
1952/1953	39	1996/1997	353.2
1953/1954	50.5	1997/1998	124.1
1954/1955	-1	1998/1999	166.5
1955/1956	-1	1999/2000	839.7
1956/1957	-1	2000/2001	160.1
1957/1958	102.5	2001/2002	125.7
1958/1959	86.9	2002/2003	116.6
1959/1960	70.5	2003/2004	98.9
1960/1961	73	2004/2005	252.4
1961/1962	37.2	2005/2006	312.8
1962/1963	120.8	2006/2007	117.8
1963/1964	131.9	2007/2008	164.4
1964/1965	63	2008/2009	171.3
1965/1966	72.7		

Table B.33: A6H006 (2): Annual maximum peak flow

Hydrological year	AMS (m^3/s)	Hydrological year	AMS (m^3/s)
1948/1949	36.9	1978/1979	4.1
1949/1950	2.4	1979/1980	9.4
1950/1951	30.1	1980/1981	0.8
1951/1952	53.3	1981/1982	1.1
1952/1953	26.8	1982/1983	2
1953/1954	53.3	1983/1984	1.6
1954/1955	24.6	1984/1985	-1
1955/1956	6.5	1985/1986	1.2
1956/1957	1.2	1986/1987	3.7
1957/1958	10.3	1987/1988	1.7
1958/1959	24.2	1988/1989	0.4
1959/1960	17	1989/1990	38.8
1960/1961	17	1990/1991	1.4
1961/1962	2.4	1991/1992	5.1
1962/1963	53.3	1992/1993	1.4
1963/1964	3.4	1993/1994	1.1
1964/1965	1	1994/1995	27.7
1965/1966	-1	1995/1996	24.5
1966/1967	-1	1996/1997	1.7
1967/1968	-1	1997/1998	3.3
1968/1969	4.8	1998/1999	22.3
1969/1970	28.5	1999/2000	26.9
1970/1971	14.6	2000/2001	26.3
1971/1972	8.3	2001/2002	1
1972/1973	26.6	2002/2003	7.2
1973/1974	45.2	2003/2004	4.3
1974/1975	73	2004/2005	44.4
1975/1976	8.8	2005/2006	4.6
1976/1977	60.3	2006/2007	15.2
1977/1978	2.4	2007/2008	8.9

Table B.34: B4H003 (4): Annual maximum peak flow

Hydrological year	AMS (m^3/s)	Hydrological year	AMS (m^3/s)
1956/1957	41.8	1982/1983	122.7
1957/1958	100	1983/1984	24.4
1958/1959	195.5	1984/1985	68.1
1959/1960	81.5	1985/1986	92.4
1960/1961	43.1	1986/1987	90.1
1961/1962	74.4	1987/1988	51
1962/1963	142	1988/1989	25.6
1963/1964	100	1989/1990	145.4
1964/1965	33.9	1990/1991	65.1
1965/1966	114	1991/1992	35.1
1966/1967	63.2	1992/1993	146.3
1967/1968	101.3	1993/1994	68
1968/1969	113	1994/1995	237.3
1969/1970	46.2	1995/1996	113.1
1970/1971	202.3	1996/1997	33.4
1971/1972	41.2	1997/1998	54.8
1972/1973	96.4	1998/1999	131.9
1973/1974	102.8	1999/2000	279.7
1974/1975	58.5	2000/2001	108.3
1975/1976	73.2	2001/2002	90.1
1976/1977	29.8	2002/2003	62
1977/1978	35.6	2003/2004	37.2
1978/1979	68.8	2004/2005	77.6
1979/1980	84.9	2005/2006	51.1
1980/1981	52.7	2006/2007	239.7
1981/1982	45.5	2007/2008	83.6

Table B.35: B7H004 (5): Annual maximum peak flow

Hydrological year	AMS (m^3/s)	Hydrological year	AMS (m^3/s)
1949/1950	5.2	1979/1980	50.4
1950/1951	11.4	1980/1981	9.5
1951/1952	73.3	1981/1982	3.5
1952/1953	27.8	1982/1983	31.4
1953/1954	99.1	1983/1984	55
1954/1955	223.9	1984/1985	10
1955/1956	16.3	1985/1986	27.2
1956/1957	154.9	1986/1987	273.3
1957/1958	111.8	1987/1988	21.3
1958/1959	129.1	1988/1989	145.9
1959/1960	0.6	1989/1990	14.5
1960/1961	14.9	1990/1991	1.7
1961/1962	16.2	1991/1992	241.6
1962/1963	14.1	1992/1993	70.4
1963/1964	28.5	1993/1994	141.1
1964/1965	28.3	1994/1995	73.8
1965/1966	55.5	1995/1996	17.2
1966/1967	9.1	1996/1997	24.5
1967/1968	125.5	1997/1998	141.6
1968/1969	4.4	1998/1999	0.6
1969/1970	94.1	1999/2000	-1
1970/1971	352.1	2000/2001	-1
1971/1972	6.3	2001/2002	8.8
1972/1973	91.7	2002/2003	45.1
1973/1974	21.5	2003/2004	18.1
1974/1975	336	2004/2005	87.4
1975/1976	127.3	2005/2006	3.3
1976/1977	69.1	2006/2007	16.8
1977/1978	13.3	2007/2008	76.2
1978/1979	5.9		

Table B.36: C3H003 (8): Annual maximum peak flow

Hydrological year	AMS (m^3/s)	Hydrological year	AMS (m^3/s)
1922/1923	103.4	1965/1966	298.6
1923/1924	91.6	1966/1967	160.5
1924/1925	-1	1967/1968	113.1
1925/1926	136.6	1968/1969	140.5
1926/1927	160.9	1969/1970	67
1927/1928	230.3	1970/1971	140.2
1928/1929	39.6	1971/1972	38.3
1929/1930	230.3	1972/1973	204.7
1930/1931	110.4	1973/1974	152.6
1931/1932	171.6	1974/1975	298.6
1932/1933	130.7	1975/1976	55.5
1933/1934	122.3	1976/1977	77.8
1934/1935	116.7	1977/1978	29.7
1935/1936	233.1	1978/1979	65.5
1936/1937	198.7	1979/1980	129.3
1937/1938	49.6	1980/1981	38.1
1938/1939	97.7	1981/1982	21.9
1939/1940	69.9	1982/1983	83.7
1940/1941	-1	1983/1984	103.5
1941/1942	79	1984/1985	132.7
1942/1943	298.6	1985/1986	165.5
1943/1944	21.5	1986/1987	298.6
1944/1945	88.1	1987/1988	181.8
1945/1946	190	1988/1989	46.4
1946/1947	180.4	1989/1990	298.6
1947/1948	149.3	1990/1991	0.2
1948/1949	69.9	1991/1992	40.4
1949/1950	230.8	1992/1993	185.3
1950/1951	102.5	1993/1994	185.3
1951/1952	69.9	1994/1995	133.5
1952/1953	-1	1995/1996	112.5
1953/1954	298.6	1996/1997	47.9
1954/1955	271.6	1997/1998	16.3
1955/1956	90.6	1998/1999	118.4
1956/1957	12.3	1999/2000	30.3
1957/1958	57.2	2000/2001	47.3
1958/1959	298.6	2001/2002	56.3
1959/1960	196.5	2002/2003	134.5
1960/1961	41.9	2003/2004	32.7
1961/1962	207.9	2004/2005	134.5
1962/1963	72.2	2005/2006	69.1
1963/1964	298.6	2006/2007	29.6
1964/1965	221.5		

Table B.37: C4H001 (7): Annual maximum peak flow

Hydrological year	AMS (m^3/s)	Hydrological year	AMS (m^3/s)
1932/1933	131.7	1944/1945	955.8
1933/1934	107.6	1945/1946	317.1
1934/1935	243.6	1946/1947	-1
1935/1936	388	1947/1948	24.4
1936/1937	115.3	1948/1949	68
1937/1938	321.4	1949/1950	1 565.8
1938/1939	68	1950/1951	603.6
1939/1940	1 565.8	1951/1952	1 130.3
1940/1941	603.6	1952/1953	1 275.8
1941/1942	1 130.3	1953/1954	235.1
1942/1943	1 275.8	1954/1955	955.8
1943/1944	235.1	1955/1956	317.1

Table B.38: C4H002 (7): Annual maximum peak flow

Hydrological year	AMS (m^3/s)	Hydrological year	AMS (m^3/s)
1949/1950	38.6	1960/1961	36.8
1950/1951	198.2	1961/1962	113.8
1951/1952	736.6	1962/1963	195.3
1952/1953	474.8	1963/1964	142.1
1953/1954	735.3	1964/1965	221
1954/1955	748.8	1965/1966	1 822.6
1955/1956	655.6	1966/1967	38.7
1956/1957	1 110.6	1967/1968	149.8
1957/1958	80.8	1968/1969	49
1958/1959	38.2	1969/1970	145.7
1959/1960	98.6	1970/1971	543.1

Table B.39: C8H001 (6): Annual maximum peak flow

Hydrological year	AMS (m^3/s)	Hydrological year	AMS (m^3/s)
1912/1913	176	1960/1961	-1
1913/1914	-1	1961/1962	128.3
1914/1915	-1	1962/1963	88.7
1915/1916	147.8	1963/1964	1 186.9
1916/1917	-1	1964/1965	188.5
1917/1918	-1	1965/1966	727.2
1918/1919	168.4	1966/1967	153.9
1919/1920	173.2	1967/1968	62
1920/1921	-1	1968/1969	78.7
1921/1922	-1	1969/1970	143.6
1922/1923	-1	1970/1971	312.7
1923/1924	-1	1971/1972	120.9
1924/1925	-1	1972/1973	673.3
1925/1926	-1	1973/1974	1 829.7
1926/1927	-1	1974/1975	1 188.2
1927/1928	-1	1975/1976	784.4
1928/1929	-1	1976/1977	732.5
1929/1930	-1	1977/1978	75.7
1930/1931	-1	1978/1979	87.6
1931/1932	-1	1979/1980	151.3
1932/1933	-1	1980/1981	68
1933/1934	-1	1981/1982	140.1
1934/1935	-1	1982/1983	342.1
1935/1936	-1	1983/1984	118.4
1936/1937	-1	1984/1985	75.7
1937/1938	-1	1985/1986	1 405.3
1938/1939	-1	1986/1987	2 472.8
1939/1940	-1	1987/1988	1 263
1940/1941	-1	1988/1989	183.9
1941/1942	-1	1989/1990	160.1
1942/1943	-1	1990/1991	37.9
1943/1944	-1	1991/1992	89.2
1944/1945	-1	1992/1993	581.6
1945/1946	-1	1993/1994	71.1
1946/1947	-1	1994/1995	2 472.8
1947/1948	-1	1995/1996	1 396
1948/1949	-1	1996/1997	471.2
1949/1950	-1	1997/1998	256.5
1950/1951	-1	1998/1999	1 003.2
1951/1952	74.3	1999/2000	319.3
1952/1953	-1	2000/2001	359.6
1953/1954	-1	2001/2002	144.3
1954/1955	-1	2002/2003	57.5
1955/1956	-1	2003/2004	396.8
1956/1957	-1	2004/2005	364.7
1957/1958	-1	2005/2006	82.5
1958/1959	-1	2006/2007	166.9
1959/1960	-1		

Table B.40: C8H003 (6): Annual maximum peak flow

Hydrological year	AMS (m^3/s)	Hydrological year	AMS (m^3/s)
1953/1954	42.4	1981/1982	-1
1954/1955	69.1	1982/1983	2.8
1955/1956	32.3	1983/1984	92.3
1956/1957	153.9	1984/1985	10.5
1957/1958	153.9	1985/1986	16.4
1958/1959	83.8	1986/1987	69.3
1959/1960	116.5	1987/1988	156.4
1960/1961	111.8	1988/1989	42.7
1961/1962	14.4	1989/1990	55.7
1962/1963	36.9	1990/1991	8.7
1963/1964	111.8	1991/1992	16.2
1964/1965	29	1992/1993	13.1
1965/1966	31.9	1993/1994	33.5
1966/1967	146.2	1994/1995	0.6
1967/1968	90.9	1995/1996	167.8
1968/1969	25.8	1996/1997	103.9
1969/1970	71	1997/1998	20.7
1970/1971	7.4	1998/1999	64.6
1971/1972	25.2	1999/2000	51.7
1972/1973	118.3	2000/2001	34.8
1973/1974	38.1	2001/2002	13.2
1974/1975	171.5	2002/2003	3.9
1975/1976	98.4	2003/2004	0.8
1976/1977	57.2	2004/2005	21
1977/1978	71.2	2005/2006	67.1
1978/1979	30.8	2006/2007	4.1
1979/1980	8.1	2007/2008	89.6
1980/1981	32.3		

Table B.41: D1H001 (10): Annual maximum peak flow

Hydrological year	AMS (m^3/s)	Hydrological year	AMS (m^3/s)
1912/1913	282.6	1960/1961	35.9
1913/1914	78.9	1961/1962	150.8
1914/1915	160.4	1962/1963	319
1915/1916	96.7	1963/1964	79.5
1916/1917	160.4	1964/1965	47.4
1917/1918	133.9	1965/1966	10.5
1918/1919	19.3	1966/1967	321.5
1919/1920	160.4	1967/1968	4.3
1920/1921	136.2	1968/1969	74.5
1921/1922	92.7	1969/1970	41.5
1922/1923	113.7	1970/1971	59.1
1923/1924	160.4	1971/1972	226.7
1924/1925	160.4	1972/1973	18.4
1925/1926	165.5	1973/1974	347.1
1926/1927	165.5	1974/1975	18
1927/1928	55.5	1975/1976	347.1
1928/1929	160.4	1976/1977	222.3
1929/1930	160.4	1977/1978	44.9
1930/1931	150.5	1978/1979	13.9
1931/1932	160.4	1979/1980	27.9
1932/1933	160.4	1980/1981	145.1
1933/1934	160.4	1981/1982	7.6
1934/1935	160.4	1982/1983	38
1935/1936	28.8	1983/1984	5.2
1936/1937	55.5	1984/1985	41.3
1937/1938	105.9	1985/1986	116.9
1938/1939	160.4	1986/1987	16.5
1939/1940	118.2	1987/1988	347.1
1940/1941	160.4	1988/1989	70.3
1941/1942	160.4	1989/1990	18.1
1942/1943	160.4	1990/1991	82.3
1943/1944	112.4	1991/1992	109.1
1944/1945	36.9	1992/1993	3.8
1945/1946	160.4	1993/1994	135.8
1946/1947	140	1994/1995	0.2
1947/1948	147	1995/1996	25.4
1948/1949	23.8	1996/1997	77.2
1949/1950	160.4	1997/1998	0.9
1950/1951	77.4	1998/1999	35
1951/1952	60.3	1999/2000	28.7
1952/1953	109.4	2000/2001	2.3
1953/1954	160.4	2001/2002	60
1954/1955	148.1	2002/2003	20.4
1955/1956	32.7	2003/2004	309.8
1956/1957	53.9	2004/2005	119.2
1957/1958	62.4	2005/2006	183.3
1958/1959	34.1	2006/2007	4.2
1959/1960	25.5	2007/2008	11.6

Table B.42: D1H004 (10): Annual maximum peak flow

Hydrological year	AMS (m^3/s)	Hydrological year	AMS (m^3/s)
1924/1925	115.7	1953/1954	67.3
1925/1926	15.3	1954/1955	26.1
1926/1927	26.1	1955/1956	5.5
1927/1928	23.6	1956/1957	34.2
1928/1929	160	1957/1958	90.4
1929/1930	17.2	1958/1959	51
1930/1931	127.5	1959/1960	0.7
1931/1932	43.7	1960/1961	6.5
1932/1933	69.4	1961/1962	21.4
1933/1934	63.3	1962/1963	91.9
1934/1935	27.3	1963/1964	21.4
1935/1936	24.8	1964/1965	-1
1936/1937	11.1	1965/1966	21.4
1937/1938	43.7	1966/1967	91.9
1938/1939	107.3	1967/1968	-1
1939/1940	19.2	1968/1969	67.3
1940/1941	51	1969/1970	21.4
1941/1942	146.9	1970/1971	7.7
1942/1943	47.3	1971/1972	5.5
1943/1944	61.3	1972/1973	-1
1944/1945	4.1	1973/1974	10.4
1945/1946	17.2	1974/1975	-1
1946/1947	21.4	1975/1976	160
1947/1948	8.4	1976/1977	99.8
1948/1949	26.1	1977/1978	-1
1949/1950	75.6	1978/1979	3.1
1950/1951	28.6	1979/1980	9.2
1951/1952	42	1980/1981	2.9
1952/1953	6		

Table B.43: D1H005 (11): Annual maximum peak flow

Hydrological year	AMS (m^3/s)	Hydrological year	AMS (m^3/s)
1931/1932	206.1	1966/1967	-1
1932/1933	829.9	1967/1968	66.4
1933/1934	695.5	1968/1969	63.1
1934/1935	269.3	1969/1970	56.8
1935/1936	1 128.3	1970/1971	105.2
1936/1937	464.4	1971/1972	-1
1937/1938	572.1	1972/1973	105.2
1938/1939	386.8	1973/1974	-1
1939/1940	671.3	1974/1975	105.2
1940/1941	674.9	1975/1976	742.5
1941/1942	538.1	1976/1977	670.6
1942/1943	1 132.7	1977/1978	1 514
1943/1944	988.3	1978/1979	411.6
1944/1945	467.4	1979/1980	409.6
1945/1946	220.8	1980/1981	-1
1946/1947	105.2	1981/1982	-1
1947/1948	-1	1982/1983	-1
1948/1949	-1	1983/1984	-1
1949/1950	-1	1984/1985	-1
1950/1951	-1	1985/1986	356
1951/1952	-1	1986/1987	925.1
1952/1953	-1	1987/1988	1 722.9
1953/1954	-1	1988/1989	423.8
1954/1955	5	1989/1990	817
1955/1956	11.9	1990/1991	531.6
1956/1957	39.5	1991/1992	479.1
1957/1958	40.8	1992/1993	1 262.1
1958/1959	36.7	1993/1994	207.6
1959/1960	36.7	1994/1995	1 197.3
1960/1961	39.5	1995/1996	626.2
1961/1962	38.3	1996/1997	749
1962/1963	38.1	1997/1998	614
1963/1964	38.9	1998/1999	224.2
1964/1965	-1	1999/2000	406
1965/1966	-1	2000/2001	-1

Table B.44: E2H003 (16): Annual maximum peak flow

Hydrological year	AMS (m^3/s)	Hydrological year	AMS (m^3/s)
1924/1925	4 569	1966/1967	1 610
1925/1926	-1	1967/1968	236
1926/1927	435	1968/1969	67
1927/1928	104	1969/1970	171
1928/1929	691	1970/1971	207
1929/1930	390	1971/1972	63
1930/1931	294	1972/1973	189
1931/1932	189	1973/1974	662
1932/1933	623	1974/1975	89
1933/1934	394	1975/1976	363
1934/1935	742	1976/1977	632
1935/1936	410	1977/1978	97
1936/1937	294	1978/1979	198
1937/1938	162	1979/1980	159
1938/1939	343	1980/1981	654
1939/1940	136	1981/1982	82
1940/1941	1 570	1982/1983	232
1941/1942	1 884	1983/1984	733
1942/1943	649	1984/1985	298
1943/1944	474	1985/1986	297
1944/1945	36	1986/1987	260
1945/1946	1 011	1987/1988	128
1946/1947	294	1988/1989	303
1947/1948	437	1989/1990	485
1948/1949	279	1990/1991	530
1949/1950	496	1991/1992	489
1950/1951	446	1992/1993	578
1951/1952	505	1993/1994	263
1952/1953	277	1994/1995	119
1953/1954	1 347	1995/1996	529
1954/1955	1 316	1996/1997	1 400
1955/1956	648	1997/1998	337
1956/1957	2 304	1998/1999	500
1957/1958	272	1999/2000	148
1958/1959	827	2000/2001	709
1959/1960	87	2001/2002	655
1960/1961	544	2002/2003	159
1961/1962	1 060	2003/2004	50
1962/1963	1 742	2004/2005	245
1963/1964	334	2005/2006	424
1964/1965	52	2006/2007	1 100
1965/1966	185	2007/2008	1 435

Table B.45: G1H008 (17): Annual maximum peak flow

Hydrological year	AMS (m^3/s)	Hydrological year	AMS (m^3/s)
1953/1954	169.2	1981/1982	27.5
1954/1955	220.2	1982/1983	209.3
1955/1956	61.6	1983/1984	267
1956/1957	132.7	1984/1985	247.5
1957/1958	169.2	1985/1986	149.1
1958/1959	111.3	1986/1987	90.2
1959/1960	140.9	1987/1988	37.6
1960/1961	21.8	1988/1989	87.6
1961/1962	267	1989/1990	112.3
1962/1963	267	1990/1991	267
1963/1964	98.3	1991/1992	196.3
1964/1965	40	1992/1993	121.4
1965/1966	62	1993/1994	213.2
1966/1967	267	1994/1995	54.1
1967/1968	84.9	1995/1996	134.6
1968/1969	33.9	1996/1997	142.7
1969/1970	65.4	1997/1998	69.5
1970/1971	49.2	1998/1999	46.7
1971/1972	51.6	1999/2000	68.1
1972/1973	144.6	2000/2001	201.9
1973/1974	88	2001/2002	107.5
1974/1975	-1	2002/2003	42.9
1975/1976	123.7	2003/2004	-1
1976/1977	195.7	2004/2005	78.4
1977/1978	33.2	2005/2006	70.6
1978/1979	-1	2006/2007	243.4
1979/1980	32.1	2007/2008	133.2
1980/1981	103.4		

Table B.46: H3H001 (18): Annual maximum peak flow

Hydrological year	AMS (m^3/s)	Hydrological year	AMS (m^3/s)
1924/1925	10.2	1936/1937	48.9
1925/1926	22.3	1937/1938	146.7
1926/1927	48.9	1938/1939	146.7
1927/1928	114.2	1939/1940	4.2
1928/1929	146.7	1940/1941	62.3
1929/1930	37.2	1941/1942	17.9
1930/1931	146.7	1942/1943	255.9
1931/1932	48.9	1943/1944	-1
1932/1933	-1	1944/1945	15.4
1933/1934	146.7	1945/1946	102.9
1934/1935	17.9	1946/1947	102.9
1935/1936	94.9		

Table B.47: H7H004 (18): Annual maximum peak flow

Hydrological year	AMS (m^3/s)	Hydrological year	AMS (m^3/s)
1950/1951	6.6	1979/1980	2.5
1951/1952	7	1980/1981	108.5
1952/1953	17.6	1981/1982	17.7
1953/1954	59.8	1982/1983	37.4
1954/1955	6	1983/1984	5.5
1955/1956	2.3	1984/1985	15.5
1956/1957	21.7	1985/1986	32
1957/1958	57.2	1986/1987	15.5
1958/1959	25.1	1987/1988	6.6
1959/1960	5.7	1988/1989	17.3
1960/1961	9.7	1989/1990	25.6
1961/1962	-1	1990/1991	3.6
1962/1963	-1	1991/1992	16.1
1963/1964	-1	1992/1993	27.5
1964/1965	-1	1993/1994	4.6
1965/1966	8.1	1994/1995	6.5
1966/1967	36	1995/1996	9.2
1967/1968	3.3	1996/1997	57
1968/1969	9.7	1997/1998	22.2
1969/1970	4	1998/1999	24.4
1970/1971	9.2	1999/2000	16.5
1971/1972	3.4	2000/2001	30.6
1972/1973	2.8	2001/2002	8.7
1973/1974	7.1	2002/2003	53.9
1974/1975	6.7	2003/2004	7.6
1975/1976	1.9	2004/2005	56.9
1976/1977	36.6	2005/2006	69.7
1977/1978	10.7	2006/2007	6.9
1978/1979	3.9	2007/2008	73.9

Table B.48: Q1H001 (21): Annual maximum peak flow

Hydrological year	AMS (m^3/s)	Hydrological year	AMS (m^3/s)
1917/1918	29.5	1955/1956	125.6
1918/1919	50.5	1956/1957	355.3
1919/1920	343.8	1957/1958	166.7
1920/1921	512	1958/1959	78.5
1921/1922	203.6	1959/1960	100.9
1922/1923	233.2	1960/1961	307.3
1923/1924	203.6	1961/1962	6.2
1924/1925	512	1962/1963	181.4
1925/1926	16.1	1963/1964	113
1926/1927	122.1	1964/1965	78.5
1927/1928	167.5	1965/1966	58.4
1928/1929	512	1966/1967	375.2
1929/1930	253.8	1967/1968	262.5
1930/1931	437.3	1968/1969	181.4
1931/1932	1 515.6	1969/1970	93.1
1932/1933	335.8	1970/1971	145.2
1933/1934	597.6	1971/1972	78.1
1934/1935	245.3	1972/1973	187.1
1935/1936	36.9	1973/1974	234.8
1936/1937	204.3	1974/1975	88.1
1937/1938	549.7	1975/1976	182.9
1938/1939	672.5	1976/1977	105.2
1939/1940	119.4	1977/1978	22.8
1940/1941	204.3	1978/1979	27.6
1941/1942	196.7	1979/1980	56.2
1942/1943	152.5	1980/1981	88.1
1943/1944	610	1981/1982	90
1944/1945	245.3	1982/1983	115.2
1945/1946	145.7	1983/1984	26.5
1946/1947	610	1984/1985	584.1
1947/1948	426.8	1985/1986	324.9
1948/1949	29.4	1986/1987	40.8
1949/1950	1 533.8	1987/1988	108.8
1950/1951	271.1	1988/1989	232.7
1951/1952	220.3	1989/1990	172.9
1952/1953	280.1	1990/1991	42.3
1953/1954	236.8	1991/1992	46.8
1954/1955	166.7	1992/1993	34

Table B.49: Q9H008 (21): Annual maximum peak flow

Hydrological year	AMS (m^3/s)	Hydrological year	AMS (m^3/s)
1920/1921	59	1945/1946	144.8
1921/1922	283.3	1946/1947	415.4
1922/1923	17.2	1947/1948	34.9
1923/1924	-1	1948/1949	114.3
1924/1925	4.3	1949/1950	144.8
1925/1926	37.4	1950/1951	87.8
1926/1927	209.8	1951/1952	79
1927/1928	114.3	1952/1953	310.2
1928/1929	98.2	1953/1954	34.9
1929/1930	87.8	1954/1955	-1
1930/1931	310.2	1955/1956	261.8
1931/1932	144.8	1956/1957	34.9
1932/1933	330	1957/1958	144.8
1933/1934	218.7	1958/1959	48.4
1934/1935	32.6	1959/1960	26.8
1935/1936	114.3	1960/1961	120.1
1936/1937	218.7	1961/1962	23.5
1937/1938	87.8	1962/1963	197.6
1938/1939	-1	1963/1964	19.3
1939/1940	36.5	1964/1965	109.6
1940/1941	48.4	1965/1966	45.8
1941/1942	31.9	1966/1967	65.6
1942/1943	120.1	1967/1968	181.9
1943/1944	15.4	1968/1969	240.8
1944/1945	23.5	1969/1970	240.8

Table B.50: Q9H010 (21): Annual maximum peak flow

Hydrological year	AMS (m^3/s)	Hydrological year	AMS (m^3/s)
1929/1930	28.8	1943/1944	5 457.9
1930/1931	266.9	1944/1945	56
1931/1932	6 156.7	1945/1946	474.6
1932/1933	345	1946/1947	105.6
1933/1934	831.3	1947/1948	2 135.7
1934/1935	440.6	1948/1949	24.3
1935/1936	46.1	1949/1950	1 478.4
1936/1937	130.6	1950/1951	556
1937/1938	1 783.3	1951/1952	145.4
1938/1939	659.7	1952/1953	193.9
1939/1940	868.9	1953/1954	4 603.4
1940/1941	113.7	1954/1955	21.5
1941/1942	1 448	1955/1956	9.7
1942/1943	122.1		

Table B.51: Q9H012 (21): Annual maximum peak flow

Hydrological year	AMS (m^3/s)	Hydrological year	AMS (m^3/s)
1957/1958	31.6	1983/1984	59.8
1958/1959	95.4	1984/1985	254.1
1959/1960	236.1	1985/1986	31
1960/1961	152.6	1986/1987	255.7
1961/1962	286.6	1987/1988	111.5
1962/1963	58.1	1988/1989	1 389.2
1963/1964	168.8	1989/1990	19.8
1964/1965	190	1990/1991	116.9
1965/1966	286.6	1991/1992	118.3
1966/1967	148.7	1992/1993	81.9
1967/1968	80.1	1993/1994	1 088.5
1968/1969	286.6	1994/1995	34.4
1969/1970	2 082.6	1995/1996	289.3
1970/1971	80.1	1996/1997	87.6
1971/1972	168.8	1997/1998	32.1
1972/1973	2 083.5	1998/1999	62.1
1973/1974	58.1	1999/2000	1 009
1974/1975	1 328.2	2000/2001	189
1975/1976	369.7	2001/2002	37.3
1976/1977	32.3	2002/2003	112.6
1977/1978	489.5	2003/2004	94.4
1978/1979	13.7	2004/2005	695.6
1979/1980	32.1	2005/2006	107.4
1980/1981	46.2	2006/2007	114.4
1981/1982	1 967	2007/2008	149.7
1982/1983	84.6		

Table B.52: V2H002 (26): Annual maximum peak flow

Hydrological year	AMS (m^3/s)	Hydrological year	AMS (m^3/s)
1949/1950	27.6	1979/1980	35
1950/1951	61.5	1980/1981	172.6
1951/1952	108.1	1981/1982	87.3
1952/1953	168.3	1982/1983	41.6
1953/1954	50.9	1983/1984	45.4
1954/1955	164.6	1984/1985	215
1955/1956	111.1	1985/1986	70.7
1956/1957	367.9	1986/1987	1 381
1957/1958	50.9	1987/1988	294.8
1958/1959	242.2	1988/1989	143.3
1959/1960	53.4	1989/1990	96.2
1960/1961	52.1	1990/1991	278.3
1961/1962	88.4	1991/1992	36.9
1962/1963	48.7	1992/1993	53.6
1963/1964	57	1993/1994	145.4
1964/1965	85.5	1994/1995	24.6
1965/1966	145.1	1995/1996	345.6
1966/1967	233.7	1996/1997	51.7
1967/1968	38.5	1997/1998	49.7
1968/1969	51.4	1998/1999	38.7
1969/1970	56.7	1999/2000	40.1
1970/1971	46.7	2000/2001	35.6
1971/1972	66.4	2001/2002	43.5
1972/1973	47.9	2002/2003	27.2
1973/1974	192.8	2003/2004	32.4
1974/1975	333.5	2004/2005	46.5
1975/1976	358	2005/2006	39.8
1976/1977	83.4	2006/2007	57.7
1977/1978	99	2007/2008	37.3
1978/1979	122.6		

Table B.53: V6H002 (26): Annual maximum peak flow

Hydrological year	AMS (m^3/s)	Hydrological year	AMS (m^3/s)
1926/1927	582.9	1967/1968	348
1927/1928	640.5	1968/1969	-1
1928/1929	1 035.5	1969/1970	765.6
1929/1930	1 837.7	1970/1971	892
1930/1931	853.6	1971/1972	1 548.9
1931/1932	882.9	1972/1973	652.3
1932/1933	376.6	1973/1974	949.7
1933/1934	973.3	1974/1975	1 828.2
1934/1935	1 467.5	1975/1976	1 710.2
1935/1936	1 035.5	1976/1977	997.9
1936/1937	1 252.3	1977/1978	-1
1937/1938	549.7	1978/1979	891.8
1938/1939	1 482.9	1979/1980	449.3
1939/1940	946.2	1980/1981	864.6
1940/1941	1 237.5	1981/1982	628.4
1941/1942	1 514.4	1982/1983	340.8
1942/1943	2 296.8	1983/1984	497.8
1943/1944	2 437.6	1984/1985	704.9
1944/1945	918.2	1985/1986	534.2
1945/1946	753.6	1986/1987	2 134
1946/1947	857.7	1987/1988	-1
1947/1948	1 082.8	1988/1989	1 424.7
1948/1949	623.2	1989/1990	673.2
1949/1950	1 190.8	1990/1991	566.2
1950/1951	890	1991/1992	427.4
1951/1952	961.8	1992/1993	410.7
1952/1953	961.8	1993/1994	934.7
1953/1954	1 352.7	1994/1995	368.2
1954/1955	2 186.9	1995/1996	1 174
1955/1956	1 036.3	1996/1997	900.6
1956/1957	1 563.2	1997/1998	612.5
1957/1958	1 579.2	1998/1999	345
1958/1959	1 172.8	1999/2000	1 097.4
1959/1960	871.8	2000/2001	525.8
1960/1961	898	2001/2002	548.2
1961/1962	1 018.5	2002/2003	-1
1962/1963	1 244.9	2003/2004	766.1
1963/1964	1 516.5	2004/2005	691.3
1964/1965	1 101.7	2005/2006	772.8
1965/1966	1 172.8	2006/2007	459.4
1966/1967	1 318.4	2007/2008	-1

Table B.54: W5H005 (28): Annual maximum peak flow

Hydrological year	AMS (m^3/s)	Hydrological year	AMS (m^3/s)
1949/1950	4.2	1979/1980	93
1950/1951	41.9	1980/1981	35.5
1951/1952	538.3	1981/1982	38.2
1952/1953	33.4	1982/1983	19.2
1953/1954	89	1983/1984	215.4
1954/1955	220.3	1984/1985	22.4
1955/1956	67.7	1985/1986	58.9
1956/1957	50.6	1986/1987	54.3
1957/1958	64.8	1987/1988	51.7
1958/1959	76.2	1988/1989	55.6
1959/1960	24.3	1989/1990	19.9
1960/1961	57.7	1990/1991	30.2
1961/1962	67.9	1991/1992	12.7
1962/1963	48.9	1992/1993	38.2
1963/1964	72	1993/1994	26.5
1964/1965	43.6	1994/1995	16.6
1965/1966	47.6	1995/1996	108.4
1966/1967	37.1	1996/1997	27.6
1967/1968	29	1997/1998	38.1
1968/1969	24.3	1998/1999	9.1
1969/1970	147.4	1999/2000	82.1
1970/1971	29.6	2000/2001	14.2
1971/1972	67.9	2001/2002	31.1
1972/1973	129.2	2002/2003	13.3
1973/1974	53.1	2003/2004	16.2
1974/1975	88.8	2004/2005	9.8
1975/1976	231.1	2005/2006	67.6
1976/1977	32.9	2006/2007	100.9
1977/1978	32.1	2007/2008	15.4
1978/1979	12.9	2008/2009	19.7

Table B.55: X2H010 (29): Annual maximum peak flow

Hydrological year	AMS (m^3/s)	Hydrological year	AMS (m^3/s)
1947/1948	58.9	1978/1979	0.7
1948/1949	47.2	1979/1980	2
1949/1950	51.2	1980/1981	9.1
1950/1951	52.9	1981/1982	2.2
1951/1952	64.2	1982/1983	4
1952/1953	48.8	1983/1984	77.2
1953/1954	28	1984/1985	14.3
1954/1955	79.1	1985/1986	30.8
1955/1956	103.5	1986/1987	10.9
1956/1957	47.2	1987/1988	36
1957/1958	55.4	1988/1989	15.5
1958/1959	62.4	1989/1990	16.6
1959/1960	103.5	1990/1991	9.2
1960/1961	112.1	1991/1992	10.9
1961/1962	47.2	1992/1993	3.3
1962/1963	73.4	1993/1994	1.2
1963/1964	64.2	1994/1995	6.1
1964/1965	52.1	1995/1996	89.6
1965/1966	39.4	1996/1997	74.2
1966/1967	89.6	1997/1998	15.9
1967/1968	28.2	1998/1999	25
1968/1969	21.4	1999/2000	30.6
1969/1970	29.4	2000/2001	5.6
1970/1971	12.2	2001/2002	6
1971/1972	18.4	2002/2003	28.1
1972/1973	20.5	2003/2004	8
1973/1974	1.6	2004/2005	7.6
1974/1975	2	2005/2006	18.6
1975/1976	71.6	2006/2007	5.6
1976/1977	1.7	2007/2008	2.1
1977/1978	3.7	2008/2009	5.4

Table B.56: SDF basin 9: Properties of AMS

Station description	C5R001: Tierpoort Dam		
Parameter description	**Type of recorded data (years)**		
	Continuous	**Historical**	**Combined**
Record length (*N*)	85	-	-
Additional record length	-	-	-
Equivalent record length	-	-	85
Outliers > $threshold_{Max}$	1	-	1
Peaks between thresholds	82	-	82
Outliers < $threshold_{Min}$	-	-	-
Missing data	2	-	2
Data not used in analysis	**3**	**-**	**3**
Station description	C5R002: Kalkfontein Dam		
Parameter description	**Type of recorded data (years)**		
	Continuous	**Historical**	**Combined**
Record length (*N*)	70	-	-
Additional record length	26	C5H001/45 Riet River at Ebani (1912 - 1938)	
Equivalent record length	-	-	96
Outliers > $threshold_{Max}$	1	-	1
Peaks between thresholds	95	-	95
Outliers < $threshold_{Min}$	-	-	-
Missing data	-	-	-
Data not used in analysis	**1**	**-**	**1**
Station description	C5R003: Rustfontein Dam		
Parameter description	**Type of recorded data (years)**		
	Continuous	**Historical**	**Combined**
Record length (*N*)	54	-	-
Additional record length	36	C5H003/17 Modder River at Likatlong (1918 - 1954)	
Equivalent record length	-	-	90
Outliers > $threshold_{Max}$	1	-	1
Peaks between thresholds	89	-	89
Outliers < $threshold_{Min}$	-	-	-
Missing data	-	-	-
Data not used in analysis	**1**	**-**	**1**
Station description	C5R004: Krugersdrift Dam		
Parameter description	**Type of recorded data (years)**		
	Continuous	**Historical**	**Combined**
Record length (*N*)	37	-	-
Additional record length	23	C5H015 Modder River at Stoomhoek (1948 -1971)	
Equivalent record length	-	-	60
Outliers > $threshold_{Max}$	-	-	-
Peaks between thresholds	60	-	60
Outliers < $threshold_{Min}$	-	-	-
Missing data	-	-	-
Data not used in analysis	**-**	**-**	**-**

Table B.56: SDF basin 9: Properties of AMS (Continued)

Station description	C5R005: Groothoek Dam		
Parameter description	**Type of recorded data (years)**		
	Continuous	**Historical**	**Combined**
Record length (*N*)	27	-	-
Additional record length	-	-	-
Equivalent record length	-	-	27
Outliers > $threshold_{Max}$	-	-	-
Peaks between thresholds	27	-	27
Outliers < $threshold_{Min}$	-	-	-
Missing data	-	-	-
Data not used in analysis	**-**	**-**	**-**
Station description	C5H003: Modder River at Likatlong		
Parameter description	**Type of recorded data (years)**		
	Continuous	**Historical**	**Combined**
Record length (*N*)	90	-	-
Additional record length	-	-	-
Equivalent record length	-	-	90
Outliers > $threshold_{Max}$	-	-	-
Peaks between thresholds	54	-	54
Outliers < $threshold_{Min}$	-	-	-
Missing data	36	-	36
Data not used in analysis	**36**	**-**	**36**
Station description	C5H012: Riet River at Kromdraai		
Parameter description	**Type of recorded data (years)**		
	Continuous	**Historical**	**Combined**
Record length (*N*)	34	-	-
Additional record length	43	C5H008 Riet River at Kromdraai (1931- 1959, 1961, 1965 & 1976- 86)	
Equivalent record length	-	-	77
Outliers > $threshold_{Max}$	-	-	-
Peaks between thresholds	39	-	39
Outliers < $threshold_{Min}$	-	-	-
Missing data	38	-	38
Data not used in analysis	**38**	**-**	**38**
Station description	C5H015: Modder River at Stoomhoek		
Parameter description	**Type of recorded data (years)**		
	Continuous	**Historical**	**Combined**
Record length (*N*)	34	-	-
Additional record length	-	-	-
Equivalent record length	-	-	34
Outliers > $threshold_{Max}$	-	-	-
Peaks between thresholds	33	-	33
Outliers < $threshold_{Min}$	-	-	-
Missing data	1	-	1
Data not used in analysis	**1**	**-**	**1**

Table B.56: SDF basin 9: Properties of AMS (Continued)

Station description	C5H016: Riet River at Biesiesbult		
Parameter description	**Type of recorded data (years)**		
	Continuous	**Historical**	**Combined**
Record length (*N*)	35	-	-
Additional record length	19	C5H014 Riet River at Klipdrift and C5H048 Riet River at Zoutpansdrift (1987 - 2006)	
Equivalent record length	-	-	54
Outliers > $threshold_{Max}$	-	-	-
Peaks between thresholds	54	-	54
Outliers < $threshold_{Min}$	-	-	-
Missing data	-	-	-
Data not used in analysis	**-**	**-**	**-**
Station description	C5H018: Modder River at Twee River		
Parameter description	**Type of recorded data (years)**		
	Continuous	**Historical**	**Combined**
Record length (*N*)	40		
Additional record length	9	C5H035 Modder River at Tweeriviere (1999 - 2008)	
Equivalent record length	-	-	49
Outliers > $threshold_{Max}$	-	-	-
Peaks between thresholds	48	-	48
Outliers < $threshold_{Min}$	-	-	-
Missing data	1	-	1
Data not used in analysis	**1**	**-**	**1**
Station description	C5H022: Kgabanyane River at Bedford		
Parameter description	**Type of recorded data (years)**		
	Continuous	**Historical**	**Combined**
Record length (*N*)	28	-	-
Additional record length	-	-	-
Equivalent record length	-	-	28
Outliers > $threshold_{Max}$	-	-	-
Peaks between thresholds	28	-	28
Outliers < $threshold_{Min}$	-	-	-
Missing data	-	-	-
Data not used in analysis	**-**	**-**	**-**
Station description	C5H054: Renoster Spruit at Bishop's Glen		
Parameter description	**Type of recorded data (years)**		
	Continuous	**Historical**	**Combined**
Record length (*N*)	13		
Additional record length	73	C5H006 Renoster Spruit at Glen and C5H007 Renoster Spruit at Shannon (1922 - 1927) & (1927 - 1995)	
Equivalent record length	-	-	86
Outliers > $threshold_{Max}$	-	-	-
Peaks between thresholds	80	-	80
Outliers < $threshold_{Min}$	-	-	-
Missing data	6	-	6
Data not used in analysis	**6**	**-**	**6**

Table B.57: SA SDF basins: Statistical properties of AMS

Catchment description	Normal data				Log$_{10}$-transformed data			
	$\bar{x}$	s	g	c_v	$\bar{x}$	s	g	c_v
A2H012 (1)	165.665	151.485	2.234	0.914	2.081	0.343	0.251	0.165
A6H006 (2)*	16.570	18.251	1.270	1.101	0.879	0.612	-0.147	0.696
B4H003 (4)	89.915	57.242	1.546	0.637	1.879	0.256	0.163	0.136
B7H004 (5)	68.020	82.685	1.873	1.216	1.475	0.646	-0.547	0.438
C3H003 (8)	128.758	84.030	0.632	0.653	1.976	0.442	-2.801	0.224
C4H001 (7)	592.823	516.276	0.683	0.871	2.553	0.505	-0.541	0.198
C4H002 (7)	380.644	446.651	1.900	1.173	2.297	0.528	0.125	0.230
C8H001 (6)	469.691	593.750	2.021	1.264	2.396	0.482	0.505	0.201
C8H003 (6)*	58.170	49.061	0.842	0.843	1.533	0.558	-1.198	0.364
D1H001 (10)	105.997	86.366	1.020	0.815	1.793	0.586	-1.656	0.327
D1H004 (10)	45.154	42.786	1.245	0.948	1.423	0.514	-0.665	0.361
D1H005 (11)	461.899	422.709	1.002	0.915	2.372	0.620	-0.781	0.261
E2H003 (16)	543.139	616.015	3.977	1.134	2.555	0.403	-0.142	0.158
G1H008 (17)	124.107	76.086	0.587	0.613	2.002	0.300	-0.322	0.150
H3H001 (18)*	82.770	65.696	0.854	0.794	1.734	0.469	-0.737	0.271
H7H004 (18)	21.148	22.526	1.828	1.065	1.107	0.446	0.161	0.403
Q1H001 (21)	246.359	269.822	3.024	1.095	2.188	0.452	-0.457	0.207
Q9H008 (21)*	122.807	101.126	1	0.823	1.914	0.435	-0.561	0.227
Q9H010 (21)	511.918	613.475	1.464	1.198	2.330	0.665	-0.297	0.285
Q9H012 (21)	341.165	533.574	2.347	1.564	2.168	0.543	0.516	0.251
V2H002 (26)*	128.500	190.177	5.193	1.480	1.917	0.364	0.981	0.190
V6H002 (26)*	1001.480	475.494	0.984	0.475	2.953	0.207	-0.132	0.070
W5H005 (28)	63.427	79.275	4.153	1.250	1.623	0.381	0.211	0.235
X2H010 (29)*	33.276	30.712	0.872	0.923	1.248	0.576	-0.584	0.461

Table B.58: SA SDF basins: Probability distributions

Station	Return period	Probability distributions (m^3/s)					Comments
		GEV/MM	LN/MM	LP3/MM	LM/PWM	Q_{Stats}	
A2H012 (SDF 1)	2	132	121	117	109	**117**	Return period range:
	5	256	234	232	201	**243**	
	10	348	332	338	284	**343**	1.25 – 1 000 years
	20	445	442	466	389	**466**	LP3/MM distribution
	50	585	610	677	578	**677**	
	100	701	757	875	774	**875**	5 – 10 years
	200	828	922	1 110	1 032	**1 110**	GEV/MM distribution
A6H006* (SDF 2)	2	13	8	8	9	**7**	Return period range:
	5	29	25	25	19	**25**	1.25 – 1 000 years
	10	40	46	45	28	**45**	LP3/MM distribution
	20	51	77	72	39	**74**	1.25 – 1 000 years
	50	65	136	122	58	**102**	LN/MM distribution
	100	75	200	172	77	**137**	50 – 1 000 years
	200	86	284	234	100	**179**	GEV/MM distribution
B4H003 (SDF 4)	2	79	76	74	76	**74**	Return period range:
	5	128	124	124	120	**124**	
	10	162	161	163	156	**163**	1.25 – 1 000 years
	20	197	200	205	197	**205**	
	50	244	254	267	264	**267**	LP3/MM distribution
	100	281	298	320	328	**320**	
	200	319	345	378	406	**378**	
B7H004 (SDF 5)	2	51	30	34	28	**42**	Return period range:
	5	120	104	107	66	**113**	1.25 – 1 000 years
	10	170	201	180	101	**190**	LP3/MM distribution
	20	222	345	268	146	**304**	10 – 1 000 years
	50	294	633	403	228	**505**	LN/MM distribution
	100	353	950	518	314	**702**	1.25 – 5 years
	200	415	1 376	643	431	**941**	GEV/MM distribution
C3H003 (SDF 8)	2	120	95	139	115	**120**	Return period range:
	5	195	223	186	185	**209**	
	10	241	349	195	233	**349**	5 – 1 000 years
	20	282	505	202	283	**505**	LN/MM distribution
	50	330	766	209	356	**766**	
	100	363	1 011	212	418	**1 011**	1.25 – 5 years
	200	394	1 303	215	486	**1 303**	GEV/MM distribution
C4H001 (SDF 7)	2	533	357	397	321	**397**	Return period range:
	5	998	951	968	610	**983**	
	10	1 282	1 585	1 458	827	**1 367**	1.25 – 1 000 years
	20	1 536	2 418	1 990	1 068	**1 748**	LP3/MM distribution
	50	1 842	3 890	2 744	1 440	**2 248**	
	100	2 055	7 136	3 343	1 775	**2 621**	5 – 1 000 years
	200	2 254	10 142	3 962	2 167	**2 989**	GEV/MM distribution

Table B.58: SA SDF basins: Probability distributions (Continued)

Station	Return period	Probability distributions (m^3/s)					Comments
		GEV/MM	LN/MM	LP3/MM	LM/PWM	Q_{Stats}	
C4H002 (SDF 7)	2	287	198	193	173	**236**	Return period range:
	5	660	552	547	395	**601**	
	10	931	942	956	604	**944**	1.25 – 1 000 years
	20	1 211	1 465	1 528	875	**1 360**	LP3/MM distribution
	50	1 603	2 408	2 611	1 375	**2 046**	
	100	1 922	3 354	3 749	1 908	**2 685**	1.25 – 1 000 years
	200	2 263	4 543	5 240	2 628	**3 443**	GEV/MM distribution
C8H001 (SDF 6)	2	343	249	227	173	**227**	Return period range:
	5	834	632	609	402	**713**	10 – 1 000 years
	10	1 195	1 030	1 079	634	**1 099**	LN/MM distribution
	20	1 570	1 541	1 781	951	**1 656**	1.25 – 5 years
	50	2 102	2 424	3 233	1 576	**2 424**	LP3/MM distribution
	100	2 539	3 280	4 905	2 281	**3 280**	1.25 – 2 years
	200	3 008	4 325	7 284	3 283	**4 325**	GEV/MM distribution
C8H003* (SDF 6)	2	52	34	44	40	**48**	Return period range:
	5	96	101	101	75	**101**	10 – 1 000 years
	10	123	177	138	100	**177**	LN/MM distribution
	20	149	282	169	129	**282**	1.25 – 20 years
	50	180	477	201	173	**477**	LP3/MM distribution
	100	203	678	220	212	**678**	5 – 10 years
	200	225	934	235	258	**934**	GEV/MM distribution
D1H001 (SDF 10)	2	93	62	89	95	**89**	Return period range:
	5	170	193	186	166	**190**	
	10	220	350	233	217	**286**	1.25 – 1 000 years
	20	267	571	264	271	**388**	LP3/MM distribution
	50	327	992	288	351	**535**	
	100	371	1 432	299	420	**654**	5 – 1 000 years
	200	414	2 005	305	497	**783**	LN/MM distribution
D1H004 (SDF 10)	2	38	27	30	26	**34**	Return period range:
	5	75	72	73	52	**73**	1.25 – 1 000 years
	10	101	121	108	73	**114**	LP3/MM distribution
	20	125	185	145	99	**164**	5 – 1 000 years
	50	157	300	194	142	**241**	LN/MM distribution
	100	182	414	231	183	**309**	1.25 – 5 years
	200	207	557	268	235	**386**	GEV/MM distribution
D1H005 (SDF 11)	2	398	236	283	410	**398**	Return period range:
	5	774	784	801	790	**787**	
	10	1 018	1 470	1 252	1 078	**1 129**	1.25 – 1 000 years
	20	1 247	2 469	1 729	1 398	**1 469**	GEV/MM distribution
	50	1 539	4 426	2 373	1 894	**1 911**	
	100	1 753	6 532	2 855	2 342	**2 237**	5 – 1 000 years
	200	1 963	9 328	3 326	2 867	**2 555**	LP3/MM distribution

Table B.58: SA SDF basins: Probability distributions (Continued)

Station	Return period	Probability distributions (m^3/s)					Comments
		GEV/MM	LN/MM	LP3/MM	LM/PWM	Q_{Stats}	
E2H003 (SDF 16)	2	393	359	367	394	**367**	Return period range:
	5	844	785	789	765	**789**	
	10	1 209	1 180	1 163	1 106	**1 163**	1.25 – 1 000 years
	20	1 619	1 653	1 591	1 540	**1 591**	
	50	2 254	2 416	2 250	2 327	**2 250**	LP3/MM distribution
	100	2 820	3 112	2 824	3 150	**2 824**	
	200	3 475	3 923	3 467	4 245	**3 467**	
G1H008 (SDF 17)	2	116	101	104	109	**110**	Return period range:
	5	185	180	181	172	**183**	10 – 1 000 years
	10	226	243	237	216	**240**	LN/MM distribution
	20	262	313	293	262	**313**	1.25 – 10 years
	50	305	415	367	329	**415**	LP3/MM distribution
	100	334	501	424	386	**501**	1.25 – 5 years
	200	361	595	483	450	**595**	GEV/MM distribution
H3H001* (SDF 18)	2	74	54	62	62	**74**	Return period range:
	5	133	135	137	109	**134**	
	10	170	216	193	142	**216**	5 – 1 000 years
	20	204	320	249	176	**320**	LN/MM distribution
	50	247	499	320	226	**499**	
	100	277	669	370	269	**669**	1.25 – 5 years
	200	306	876	419	317	**876**	GEV/MM distribution
H7H004 (SDF 18)	2	17	13	12	10	**14**	Return period range:
	5	35	30	30	21	**32**	1.25 – 1 000 years
	10	49	48	49	32	**48**	LN/MM distribution
	20	63	69	73	45	**69**	1.25 – 10 years
	50	83	105	115	69	**105**	GEV/MM distribution
	100	98	140	157	94	**140**	1.25 – 10 years
	200	115	180	211	127	**180**	LP3/MM distribution
Q1H001 (SDF 21)	2	183	154	167	130 **	**168**	Return period range:
	5	391	370	375	326 **	**380**	2 – 1 000 years
	10	553	585	550	600 **	**569**	LN/MM distribution
	20	731	853	738	1 077 **	**958**	20 – 1 000 years **
	50	998	1 306	1 004	2 297 **	**1 732**	LEV1/MM distribution
	100	1 229	1 734	1 217	4 050 **	**2 650**	1.25 – 10 years
	200	1 490	2 248	1 439	7 130 **	**4 003**	GEV/MM distribution
Q9H008* (SDF 21)	2	108	82	90	98	**98**	Return period range:
	5	198	191	194	180	**194**	1.25 – 1 000 years
	10	256	296	275	243	**275**	GEV/MM distribution
	20	311	427	358	314	**362**	5 – 1 000 years
	50	380	643	470	427	**486**	LN/MM distribution
	100	432	845	556	530	**604**	1.25 – 50 years
	200	482	1 085	641	653	**723**	LP3/MM distribution

Table B.58: SA SDF basins: Probability distributions (Continued)

Station	Return period	Probability distributions (m^3/s)					Comments
		GEV/MM	LN/MM	LP3/MM	LM/PWM	Q_{Stats}	
Q9H010 (SDF 21)	2	397	214	231	230	**231**	Return period range:
	5	927	777	790	555	**856**	
	10	1 294	1 523	1 442	856	**1 366**	1.25 – 1 000 years
	20	1 659	2 658	2 320	1 243	**1 962**	LP3/MM distribution
	50	2 151	4 971	3 874	1 948	**2 887**	
	100	2 535	7 547	5 383	2 692	**3 694**	5 – 1 000 years
	200	2 930	11 060	7 208	3 688	**4 596**	GEV/MM distribution
Q9H012 (SDF 21)	2	222	147	132	117	**132**	Return period range:
	5	653	423	405	302	**514**	
	10	977	733	773	508	**869**	1.25 – 1 000 years
	20	1 321	1 155	1 363	811	**1 342**	LP3/MM distribution
	50	1 820	1 926	2 682	1 454	**2 209**	
	100	2 238	2 709	4 306	2 233	**3 104**	5 – 1 000 years
	200	2 696	3 701	6 746	3 412	**4 265**	GEV/MM distribution
V2H002* (SDF 26)	2	81	83	72	58	**72**	Return period range:
	5	214	167	156	117	**183**	
	10	325	242	254	181	**287**	1.25 – 1 000 years
	20	451	327	396	273	**423**	LP3/MM distribution
	50	652	461	689	464	**670**	
	100	835	579	1 026	691	**926**	5 – 1 000 years
	200	1 051	714	1 510	1 028	**1 260**	GEV/MM distribution
V6H002* (SDF 26)	2	930	898	907	918	**898**	Return period range:
	5	1 354	1 342	1 345	1 306	**1 342**	
	10	1 628	1 655	1 644	1 584	**1 655**	1.25 – 1 000 years
	20	1 885	1 969	1 933	1 881	**1 969**	
	50	2 210	2 393	2 313	2 321	**2 393**	LN/MM distribution
	100	2 448	2 726	2 601	2 702	**2 726**	
	200	2 681	3 070	2 893	3 134	**3 070**	
W5H005 (SDF 28)	2	44	42	41	36 **	**41**	Return period range:
	5	102	88	87	79 **	**83**	
	10	149	129	132	132 **	**132**	5 – 1 000 years **
	20	201	178	187	217 **	**217**	LEV1/MM distribution
	50	283	255	281	411 **	**411**	
	100	357	324	371	663 **	**663**	1.25 – 5 years
	200	442	403	480	1 068 **	**1 068**	LP3/MM distribution
X2H010* (SDF 29)	2	29	18	20	23	**24**	Return period range:
	5	57	54	55	45	**55**	5 – 1 000 years
	10	74	97	87	63	**97**	LN/MM distribution
	20	90	157	123	82	**157**	1.25 – 2 years
	50	110	270	175	112	**270**	LP3/MM distribution
	100	125	387	218	139	**387**	2 – 5 years
	200	138	539	262	172	**539**	GEV/MM distribution

Table B.59: SA SDF basins: Calibrated C_2 and C_{100} run-off coefficients

Catchment description	Method	Design information used in the SDF method				
		C_2	C_{100}	MAP (mm)	*M* (mm)	*R* (days)
A2H012 (1)	$SDF_{Original}$	10	40	549	56	30
	$SDF_{Adjusted}$	10	40	549	56	30
	$SDF_{Calibrated}$	7	19.5	697	48	73
A6H006 (2)*	$SDF_{Original}$	5	30	452	62	44
	$SDF_{Adjusted}$	5	30	452	62	44
	$SDF_{Calibrated}$	5	10.5	625	53	42
B4H003 (4)	$SDF_{Original}$	10	50	627	58	20
	$SDF_{Adjusted}$	10	50	627	58	20
	$SDF_{Calibrated}$	6.2	10.3	712	48	48
B7H004 (5)	$SDF_{Original}$	15	70	625	78	10
	$SDF_{Adjusted}$	15	70	625	78	10
	$SDF_{Calibrated}$	7	38	1 230	102	33
C3H003 (8)	$SDF_{Original}$	5	20	377	47	39
	$SDF_{Adjusted}$	5	20	377	47	39
	$SDF_{Calibrated}$	6.2	20	527	51	73
D1H005 (11)	$SDF_{Original}$	40	80	429	39	66
	$SDF_{Adjusted}$	40	80	429	39	66
	$SDF_{Calibrated}$	18	41	682	41	76
E2H003 (16)	$SDF_{Original}$	10	40	212	28	11
	$SDF_{Adjusted}$	10	40	212	28	11
	$SDF_{Calibrated}$	7.5	33	253	32	7
G1H008 (17)	$SDF_{Original}$	40	80	498	45	1
	$SDF_{Adjusted}$	40	80	498	45	1
	$SDF_{Calibrated}$	20	53	253	32	7
R1H001 (22)*	$SDF_{Original}$	15	60	821	84	26
	$SDF_{Adjusted}$	15	60	821	84	26
	$SDF_{Calibrated}$	9	49	624	55	24
T3H004 (23)*	$SDF_{Original}$	10	80	890	60	45
	$SDF_{Adjusted}$	10	80	890	60	45
	$SDF_{Calibrated}$	5	95	773	54	63
V2H002 (26)*	$SDF_{Original}$	15	50	760	61	17
	$SDF_{Adjusted}$	15	50	760	61	17
	$SDF_{Calibrated}$	41	67	962	53	80
V6H002 (26)*	$SDF_{Original}$	15	50	760	61	17
	$SDF_{Adjusted}$	15	50	760	61	17
	$SDF_{Calibrated}$	32	55.4	907	65	70
W5H005 (28)	$SDF_{Original}$	15	60	740	75	54
	$SDF_{Adjusted}$	15	60	740	75	54
	$SDF_{Calibrated}$	7	40	800	59	44
W5H006 (28)*	$SDF_{Original}$	15	60	740	75	54
	$SDF_{Adjusted}$	15	60	740	75	54
	$SDF_{Calibrated}$	10	48	887	59	44
X2H010 (29)*	$SDF_{Original}$	15	50	737	66	11
	$SDF_{Adjusted}$	15	50	737	66	11
	$SDF_{Calibrated}$	6	25.5	1 305	71	38

Table B.60: SA SDF basins: Calibrated run-off coefficients

Catchment description	Method	Run-off coefficients (C_T) for return period (T)						
		2	5	10	20	50	100	200
A2H012 (1)	$SDF_{Original}$ (C_{T1})	0.100	0.208	0.265	0.311	0.364	0.400	0.432
	$SDF_{Adjusted}$ (C_{T2})	0.160	0.170	0.239	0.277	0.336	0.330	0.468
	$SDF_{Calibrated}$ (C_{T3})	0.070	0.115	0.139	0.158	0.180	0.195	0.208
A6H006 (2)*	$SDF_{Original}$ (C_{T1})	0.050	0.140	0.187	0.226	0.270	0.300	0.327
	$SDF_{Adjusted}$ (C_{T2})	0.028	0.051	0.057	0.064	0.075	0.084	0.126
	$SDF_{Calibrated}$ (C_{T3})	0.050	0.070	0.080	0.089	0.099	0.105	0.111
B4H003 (4)	$SDF_{Original}$ (C_{T1})	0.100	0.244	0.20	0.382	0.452	0.500	0.543
	$SDF_{Adjusted}$ (C_{T2})	0.060	0.086	0.106	0.119	0.136	0.149	0.164
	$SDF_{Calibrated}$ (C_{T3})	0.062	0.077	0.085	0.091	0.098	0.103	0.107
B7H004 (5)	$SDF_{Original}$ (C_{T1})	0.150	0.348	0.452	0.537	0.634	0.700	0.759
	$SDF_{Adjusted}$ (C_{T2})	0.167	0.339	0.389	0.473	0.614	0.757	0.918
	$SDF_{Calibrated}$ (C_{T3})	0.070	0.182	0.241	0.289	0.344	0.380	0.413
C3H003 (8)	$SDF_{Original}$ (C_{T1})	0.050	0.104	0.132	0.156	0.182	0.200	0.216
	$SDF_{Adjusted}$ (C_{T2})	0.025	0.034	0.043	0.045	0.047	0.048	0.049
	$SDF_{Calibrated}$ (C_{T3})	0.062	0.112	0.138	0.160	0.184	0.200	0.215
D1H005 (11)	$SDF_{Original}$ (C_{T1})	0.400	0.544	0.620	0.682	0.752	0.800	0.843
	$SDF_{Adjusted}$ (C_{T2})	1.379	1.110	1.051	1.049	1.059	1.081	1.109
	$SDF_{Calibrated}$ (C_{T3})	0.180	0.263	0.307	0.343	0.383	0.410	0.435
E2H003 (16)	$SDF_{Original}$ (C_{T1})	0.100	0.208	0.265	0.311	0.364	0.400	0.432
	$SDF_{Adjusted}$ (C_{T2})	0.154	0.226	0.265	0.291	0.334	0.367	0.400
	$SDF_{Calibrated}$ (C_{T3})	0.075	0.167	0.215	0.255	0.300	0.330	0.357
G1H008 (17)	$SDF_{Original}$ (C_{T1})	0.400	0.544	0.620	0.682	0.752	0.800	0.843
	$SDF_{Adjusted}$ (C_{T2})	1.487	1.778	1.558	1.451	1.377	1.358	1.291
	$SDF_{Calibrated}$ (C_{T3})	0.200	0.319	0.382	0.433	0.491	0.530	0.565
R1H001 (22)*	$SDF_{Original}$ (C_{T1})	0.150	0.312	0.397	0.467	0.546	0.600	0.648
	$SDF_{Adjusted}$ (C_{T2})	0.125	0.152	0.174	0.187	0.201	0.209	0.220
	$SDF_{Calibrated}$ (C_{T3})	0.090	0.235	0.310	0.373	0.443	0.490	0.533
T3H004 (23)*	$SDF_{Original}$ (C_{T1})	0.100	0.352	0.485	0.593	0.716	0.800	0.875
	$SDF_{Adjusted}$ (C_{T2})	0.159	0.282	0.326	0.364	0.407	0.440	0.465
	$SDF_{Calibrated}$ (C_{T3})	0.050	0.376	0.546	0.686	0.845	0.950	1.047
V2H002 (26)*	$SDF_{Original}$ (C_{T1})	0.150	0.276	0.342	0.396	0.458	0.500	0.538
	$SDF_{Adjusted}$ (C_{T2})	0.294	0.285	0.320	0.350	0.379	0.391	0.405
	$SDF_{Calibrated}$ (C_{T3})	0.410	0.504	0.553	0.594	0.640	0.670	0.698
V6H002 (26)*	$SDF_{Original}$ (C_{T1})	0.150	0.276	0.342	0.396	0.458	0.500	0.538
	$SDF_{Adjusted}$ (C_{T2})	0.294	0.285	0.320	0.350	0.379	0.391	0.405
	$SDF_{Calibrated}$ (C_{T3})	0.320	0.405	0.449	0.485	0.527	0.554	0.579
W5H005 (28)	$SDF_{Original}$ (C_{T1})	0.150	0.312	0.397	0.467	0.546	0.600	0.648
	$SDF_{Adjusted}$ (C_{T2})	0.121	0.104	0.137	0.157	0.191	0.225	0.266
	$SDF_{Calibrated}$ (C_{T3})	0.070	0.189	0.252	0.303	0.361	0.400	0.435
W5H006 (28)*	$SDF_{Original}$ (C_{T1})	0.150	0.312	0.397	0.467	0.546	0.600	0.648
	$SDF_{Adjusted}$ (C_{T2})	0.121	0.104	0.137	0.157	0.191	0.225	0.266
	$SDF_{Calibrated}$ (C_{T3})	0.100	0.237	0.309	0.369	0.435	0.480	0.521
X2H010 (29)*	$SDF_{Original}$ (C_{T1})	0.150	0.276	0.342	0.396	0.458	0.500	0.538
	$SDF_{Adjusted}$ (C_{T2})	0.156	0.117	0.127	0.188	0.146	0.129	0.108
	$SDF_{Calibrated}$ (C_{T3})	0.060	0.131	0.167	0.198	0.232	0.255	0.276

Table B.61(a): SDF basin 1: SDF flood estimation results

Catchment description	Method	Design flood (m^3/s) for return period (years)						
		2	**5**	**10**	**20**	**50**	**100**	**200**
A2H012	$Q_{Statistical}$	117	243	343	466	677	875	1 110
	$SDF_{Original}$ (Q_1)	156	485	775	1 104	1 624	2 092	2 610
	$SDF_{Adjusted}$ (Q_2)	249	397	699	983	1 497	1 727	2 829
	$SDF_{Calibrated}$ (Q_3)	99	239	358	491	690	861	1 051
Average Q_{SDF}/Q_{Stats}	$Q_1/Q_{Statistical}$	**1.33**	**2.00**	**2.26**	**2.37**	**2.40**	**2.39**	**2.35**
	$Q_2/Q_{Statistical}$	**2.13**	**1.63**	**2.04**	**2.11**	**2.21**	**1.97**	**2.55**
	$Q_3/Q_{Statistical}$	**0.85**	**0.98**	**1.04**	**1.05**	**1.02**	**0.98**	**0.95**

Table B.61(b): SDF basin 2: SDF flood estimation results

Catchment description	Method	Design flood (m^3/s) for return period (years)						
		2	**5**	**10**	**20**	**50**	**100**	**200**
A6H006*	$Q_{Statistical}$	16	38	59	79	110	137	168
	$SDF_{Original}$ (Q_1)	19	89	156	233	348	446	550
	$SDF_{Adjusted}$ (Q_2)	11	33	48	66	96	125	212
	$SDF_{Calibrated}$ (Q_3)	17	40	60	82	114	139	167
Average Q_{SDF}/Q_{Stats}	$Q_1/Q_{Statistical}$	**1.19**	**2.34**	**2.64**	**2.95**	**3.16**	**3.26**	**3.27**
	$Q_2/Q_{Statistical}$	**0.69**	**0.87**	**0.81**	**0.84**	**0.87**	**0.91**	**1.26**
	$Q_3/Q_{Statistical}$	**1.06**	**1.05**	**1.02**	**1.04**	**1.04**	**1.01**	**0.99**

Table B.61(c): SDF basin 4: SDF flood estimation results

Catchment description	Method	Design flood (m^3/s) for return period (years)						
		2	**5**	**10**	**20**	**50**	**100**	**200**
B4H003	$Q_{Statistical}$	74	124	163	205	267	320	378
	$SDF_{Original}$ (Q_1)	136	455	713	992	1 420	1 784	2 180
	$SDF_{Adjusted}$ (Q_2)	82	160	236	310	426	533	657
	$SDF_{Calibrated}$ (Q_3)	72	125	166	209	271	321	374
Average Q_{SDF}/Q_{Stats}	$Q_1/Q_{Statistical}$	**1.84**	**3.67**	**4.37**	**4.84**	**5.32**	**5.58**	**5.77**
	$Q_2/Q_{Statistical}$	**1.11**	**1.29**	**1.45**	**1.51**	**1.60**	**1.67**	**1.74**
	$Q_3/Q_{Statistical}$	**0.97**	**1.01**	**1.02**	**1.02**	**1.01**	**1.00**	**0.99**

Table B.61(d): SDF basin 5: SDF flood estimation results

Catchment description	Method	Design flood (m^3/s) for return period (years)						
		2	**5**	**10**	**20**	**50**	**100**	**200**
B7H004	$Q_{Statistical}$	42	113	190	304	505	702	941
	$SDF_{Original}$ (Q_1)	46	181	307	451	666	847	1 040
	$SDF_{Adjusted}$ (Q_2)	51	176	265	397	645	916	1 256
	$SDF_{Calibrated}$ (Q_3)	33	144	249	370	551	701	864
Average Q_{SDF}/Q_{Stats}	$Q_1/Q_{Statistical}$	**1.10**	**1.60**	**1.62**	**1.48**	**1.32**	**1.21**	**1.11**
	$Q_2/Q_{Statistical}$	**1.21**	**1.56**	**1.39**	**1.31**	**1.28**	**1.30**	**1.33**
	$Q_3/Q_{Statistical}$	**0.79**	**1.27**	**1.31**	**1.22**	**1.09**	**1.00**	**0.92**

Table B.61(e): SDF basin 8: SDF flood estimation results

Catchment description	Method	Design flood (m^3/s) for return period (years)						
		2	**5**	**10**	**20**	**50**	**100**	**200**
C3H003	$Q_{Statistical}$	120	209	349	505	766	1 011	1 303
	$SDF_{Original}$ (Q_1)	89	287	467	687	1 045	1 382	1 774
	$SDF_{Adjusted}$ (Q_2)	44	93	150	197	269	331	400
	$SDF_{Calibrated}$ (Q_3)	120	294	425	561	748	897	1 052
Average Q_{SDF}/Q_{Stats}	$Q_1/Q_{Statistical}$	**0.74**	**1.37**	**1.34**	**1.36**	**1.36**	**1.37**	**1.36**
	$Q_2/Q_{Statistical}$	**0.37**	**0.44**	**0.43**	**0.39**	**0.35**	**0.33**	**0.31**
	$Q_3/Q_{Statistical}$	**1.00**	**1.41**	**1.22**	**1.11**	**0.98**	**0.89**	**0.81**

Table B.61(f): SDF basin 11: SDF flood estimation results

Catchment description	Method	Design flood (m^3/s) for return period (years)						
		2	**5**	**10**	**20**	**50**	**100**	**200**
D1H005	$Q_{Statistical}$	398	787	1 129	1 469	1 911	2 237	2 555
	$SDF_{Original}$ (Q_1)	760	1 427	1 966	2 551	3 428	4 210	5 060
	$SDF_{Adjusted}$ (Q_2)	2 620	2 912	3 332	3 924	4 829	5 689	6 658
	$SDF_{Calibrated}$ (Q_3)	394	771	1 064	1 380	1 843	2 236	2 670
Average Q_{SDF}/Q_{Stats}	$Q_1/Q_{Statistical}$	**1.91**	**1.81**	**1.74**	**1.74**	**1.79**	**1.88**	**1.98**
	$Q_2/Q_{Statistical}$	**6.58**	**3.70**	**2.95**	**2.67**	**2.53**	**2.54**	**2.61**
	$Q_3/Q_{Statistical}$	**0.99**	**0.98**	**0.94**	**0.94**	**0.96**	**1.00**	**1.05**

Table B.61(g): SDF basin 16: SDF flood estimation results

Catchment description	Method	Design flood (m^3/s) for return period (years)						
		2	**5**	**10**	**20**	**50**	**100**	**200**
E2H003	$Q_{Statistical}$	367	789	1 163	1 591	2 250	2 824	3 467
	$SDF_{Original}$ (Q_1)	285	816	1 268	1 761	2 520	3 197	3 932
	$SDF_{Adjusted}$ (Q_2)	439	887	1 268	1 646	2 312	2 933	3 640
	$SDF_{Calibrated}$ (Q_3)	255	793	1 215	1 663	2 299	2 812	3 357
Average Q_{SDF}/Q_{Stats}	$Q_1/Q_{Statistical}$	**0.78**	**1.03**	**1.09**	**1.11**	**1.12**	**1.13**	**1.13**
	$Q_2/Q_{Statistical}$	**1.20**	**1.12**	**1.09**	**1.03**	**1.03**	**1.04**	**1.05**
	$Q_3/Q_{Statistical}$	**0.69**	**1.01**	**1.04**	**1.05**	**1.02**	**1.00**	**0.97**

Table B.61(h): SDF basin 17: SDF flood estimation results

Catchment description	Method	Design flood (m^3/s) for return period (years)						
		2	**5**	**10**	**20**	**50**	**100**	**200**
G1H008	$Q_{Statistical}$	120	190	288	400	603	813	1 092
	$SDF_{Original}$ (Q_1)	135	310	461	627	866	1 061	1 266
	$SDF_{Adjusted}$ (Q_2)	502	1 010	1 160	1 334	1 585	1 802	1 938
	$SDF_{Calibrated}$ (Q_3)	78	210	328	460	653	811	980
Average Q_{SDF}/Q_{Stats}	**$Q_1/Q_{Statistical}$**	**1.13**	**1.63**	**1.60**	**1.57**	**1.44**	**1.31**	**1.16**
	$Q_2/Q_{Statistical}$	**4.18**	**5.32**	**4.03**	**3.34**	**2.63**	**2.22**	**1.77**
	$Q_3/Q_{Statistical}$	**0.65**	**1.11**	**1.14**	**1.15**	**1.08**	**1.00**	**0.90**

Table B.61(i): SDF basin 22: SDF flood estimation results

Catchment description	Method	Design flood (m^3/s) for return period (years)						
		2	**5**	**10**	**20**	**50**	**100**	**200**
R1H001*	$Q_{Statistical}$	28	105	178	269	442	632	895
	$SDF_{Original}$ (Q_1)	68	238	395	574	843	1 069	1 311
	$SDF_{Adjusted}$ (Q_2)	56	116	173	230	310	373	445
	$SDF_{Calibrated}$ (Q_3)	30	131	227	336	500	636	784
Average Q_{SDF}/Q_{Stats}	**$Q_1/Q_{Statistical}$**	**2.43**	**2.27**	**2.22**	**2.13**	**1.91**	**1.69**	**1.46**
	$Q_2/Q_{Statistical}$	**2.00**	**1.10**	**0.97**	**0.86**	**0.70**	**0.59**	**0.50**
	$Q_3/Q_{Statistical}$	**1.07**	**1.25**	**1.28**	**1.25**	**1.13**	**1.01**	**0.88**

Table B.61(j): SDF basin 23: SDF flood estimation results

Catchment description	Method	Design flood (m^3/s) for return period (years)						
		2	**5**	**10**	**20**	**50**	**100**	**200**
T3H004*	$Q_{Statistical}$	35	145	297	534	1 083	1 801	2 963
	$SDF_{Original}$ (Q_1)	72	356	597	867	1 284	1 642	2 038
	$SDF_{Adjusted}$ (Q_2)	114	285	401	532	730	902	1 084
	$SDF_{Calibrated}$ (Q_3)	33	356	631	942	1 409	1 808	2 249
Average Q_{SDF}/Q_{Stats}	**$Q_1/Q_{Statistical}$**	**2.06**	**2.46**	**2.01**	**1.62**	**1.19**	**0.91**	**0.69**
	$Q_2/Q_{Statistical}$	**3.26**	**1.97**	**1.35**	**1.00**	**0.67**	**0.50**	**0.37**
	$Q_3/Q_{Statistical}$	**0.94**	**2.46**	**2.12**	**1.76**	**1.30**	**1.00**	**0.76**

Table B.61(k): SDF basin 26: SDF flood estimation results

Catchment description	Method	Design flood (m^3/s) for return period (years)						
		2	5	10	20	50	100	200
V2H002*	$Q_{Statistical}$	225	425	548	716	954	1 149	1 357
	$SDF_{Original}$ (Q_1)	96	254	389	539	774	983	1 214
	$SDF_{Adjusted}$ (Q_2)	189	262	363	477	640	768	913
	$SDF_{Calibrated}$ (Q_3)	244	429	576	734	961	1 148	1 351
V6H002*	$Q_{Statistical}$	1 450	2 400	3 096	3 791	4 790	5 620	6 523
	$SDF_{Original}$ (Q_1)	628	1 598	2 415	3 321	4 720	5 980	7 407
	$SDF_{Adjusted}$ (Q_2)	1 232	1 648	2 257	2 939	3 901	4 672	5 569
	$SDF_{Calibrated}$ (Q_3)	1 436	2 404	3 108	3 821	4 798	5 613	6 642
Average Q_{SDF}/Q_{Stats}	**$Q_1/Q_{Statistical}$**	**0.43**	**0.63**	**0.74**	**0.81**	**0.90**	**0.96**	**1.02**
	$Q_2/Q_{Statistical}$	**0.84**	**0.65**	**0.70**	**0.72**	**0.74**	**0.75**	**0.76**
	$Q_3/Q_{Statistical}$	**1.04**	**1.01**	**1.03**	**1.02**	**1.00**	**1.00**	**1.01**

Table B.61(l): SDF basin 28: SDF flood estimation results

Catchment description	Method	Design flood (m^3/s) for return period (years)						
		2	5	10	20	50	100	200
W5H005	$Q_{Statistical}$	41	83	132	217	411	663	1 068
	$SDF_{Original}$ (Q_1)	110	334	530	750	1 090	1 391	1 726
	$SDF_{Adjusted}$ (Q_2)	89	112	183	252	381	521	707
	$SDF_{Calibrated}$ (Q_3)	40	160	265	384	566	726	905
Average Q_{SDF}/Q_{Stats}	**$Q_1/Q_{Statistical}$**	**2.68**	**4.02**	**4.02**	**3.46**	**2.65**	**2.10**	**1.62**
	$Q_2/Q_{Statistical}$	**2.17**	**1.35**	**1.39**	**1.16**	**0.93**	**0.79**	**0.66**
	$Q_3/Q_{Statistical}$	**0.98**	**1.93**	**2.01**	**1.77**	**1.38**	**1.10**	**0.85**
W5H006*	$Q_{Statistical}$	45	85	192	292	474	662	970
	$SDF_{Original}$ (Q_1)	65	229	381	553	810	1 025	1 254
	$SDF_{Adjusted}$ (Q_2)	53	77	131	186	283	384	514
	$SDF_{Calibrated}$ (Q_3)	35	141	241	355	525	666	819
Average Q_{SDF}/Q_{Stats}	**$Q_1/Q_{Statistical}$**	**1.44**	**2.69**	**1.98**	**1.89**	**1.71**	**1.55**	**1.29**
	$Q_2/Q_{Statistical}$	**1.18**	**0.91**	**0.68**	**0.64**	**0.60**	**0.58**	**0.53**
	$Q_3/Q_{Statistical}$	**0.78**	**1.66**	**1.26**	**1.22**	**1.11**	**1.01**	**0.84**

Table B.61(m): SDF basin 29: SDF flood estimation results

Catchment description	Method	Design flood (m^3/s) for return period (years)						
		2	5	10	20	50	100	200
X2H010*	$Q_{Statistical}$	24	55	97	157	270	387	539
	$SDF_{Original}$ (Q_1)	43	132	214	306	443	558	679
	$SDF_{Adjusted}$ (Q_2)	44	56	80	145	141	144	136
	$SDF_{Calibrated}$ (Q_3)	23	84	141	206	303	383	469
Average Q_{SDF}/Q_{Stats}	**$Q_1/Q_{Statistical}$**	**1.79**	**2.40**	**2.21**	**1.95**	**1.64**	**1.44**	**1.26**
	$Q_2/Q_{Statistical}$	**1.83**	**1.02**	**0.82**	**0.92**	**0.52**	**0.37**	**0.25**
	$Q_3/Q_{Statistical}$	**0.96**	**1.53**	**1.45**	**1.31**	**1.12**	**0.99**	**0.87**

Table B.62: SDF basin 9: Verified C_2 and C_{100} run-off coefficients

Catchment description	Method	Design information used in the SDF method				
		C_2	C_{100}	MAP (mm)	*M* (mm)	*R* (days)
C5R001 (C5R001, C5H008* & C5H012**)	$SDF_{Original}$	15	60	376	43	47
	$SDF_{Adjusted}$	15	60	376	43	47
	$SDF_{Verified}$	9	54	420	42	54
C5R003 (C5H003)	$SDF_{Original}$	15	60	376	43	47
	$SDF_{Adjusted}$	15	60	376	43	47
	$SDF_{Verified}$	9.5	47.5	555	48	54
C5R004 (C5H015 & C5H054**)	$SDF_{Original}$	15	60	376	43	47
	$SDF_{Adjusted}$	15	60	376	43	47
	$SDF_{Verified}$	18	59	518	44	62
C5R005 (C5H022**)	$SDF_{Original}$	15	60	376	43	47
	$SDF_{Adjusted}$	15	60	376	43	47
	$SDF_{Verified}$	11	33	649	48	66
C5H016** (C5H018)	$SDF_{Original}$	15	60	376	43	47
	$SDF_{Adjusted}$	15	60	376	43	47
	$SDF_{Verified}$	3	20.5	461	48	60

Table B.63: SA SDF basins: Verified C_2 and C_{100} run-off coefficients

Catchment description	Method	Design information used in the SDF method				
		C_2	C_{100}	MAP (mm)	*M* (mm)	*R* (days)
SDF basin 6 C8H001 (C8H003)	$SDF_{Original}$	15	60	668	51	54
	$SDF_{Adjusted}$	15	60	668	51	54
	$SDF_{Verified}$	9	68	691	51	54
SDF basin 7 C4H002 (C4H001)	$SDF_{Original}$	15	60	507	49	39
	$SDF_{Adjusted}$	15	60	507	49	39
	$SDF_{Verified}$	10	45	553	53	62
SDF basin 10 D1H001 (D1H004)	$SDF_{Original}$	10	50	560	54	55
	$SDF_{Adjusted}$	10	50	560	54	55
	$SDF_{Verified}$	8	22.5	482	43	66
SDF basin 18 H3H001 (H7H004)	$SDF_{Original}$	30	60	812	59	4
	$SDF_{Adjusted}$	30	60	812	59	4
	$SDF_{Verified}$	20	57	333	44	8
SDF basin 21 Q9H008* (Q9H004)	$SDF_{Original}$	10	35	457	45	23
	$SDF_{Adjusted}$	10	35	457	45	23
	$SDF_{Verified}$	16	30	561	47	24
Q9H010 (Q1H001, Q7H003 & Q9H012)	$SDF_{Original}$	10	35	457	45	23
	$SDF_{Adjusted}$	10	35	457	45	23
	$SDF_{Verified}$	6	50	378	32	54

Table B.64: SDF basin 9: Verified run-off coefficients

Catchment description	Method	Run-off coefficients (C_T) for return period (T) 2	5	10	20	50	100	200
C5R002 (C5R001)	$SDF_{Original}$ (C_{T1})	0.150	0.312	0.397	0.467	0.546	0.600	0.648
	$SDF_{Adjusted}$ (C_{T2})	0.124	0.287	0.444	0.866	0.751	0.900	1.133
	$SDF_{Verified}$ (C_{T3})	0.090	0.253	0.338	0.408	0.487	0.540	0.588
C5R002 (C5H008*)	$SDF_{Original}$ (C_{T1})	0.150	0.312	0.397	0.467	0.546	0.600	0.648
	$SDF_{Adjusted}$ (C_{T2})	0.120	0.272	0.407	0.801	0.696	0.828	1.032
	$SDF_{Verified}$ (C_{T3})	0.090	0.253	0.338	0.408	0.487	0.540	0.588
C5R002 (C5H012**)	$SDF_{Original}$ (C_{T1})	0.150	0.312	0.397	0.467	0.546	0.600	0.648
	$SDF_{Adjusted}$ (C_{T2})	0.135	0.321	0.537	1.029	0.882	1.075	1.379
	$SDF_{Verified}$ (C_{T3})	0.090	0.253	0.338	0.408	0.487	0.540	0.588
C5R003 (C5H003)	$SDF_{Original}$ (C_{T1})	0.150	0.312	0.397	0.467	0.546	0.600	0.648
	$SDF_{Adjusted}$ (C_{T2})	0.131	0.307	0.499	0.963	0.830	1.005	1.281
	$SDF_{Verified}$ (C_{T3})	0.095	0.232	0.304	0.364	0.430	0.475	0.516
C5R004 (C5H015)	$SDF_{Original}$ (C_{T1})	0.150	0.312	0.397	0.467	0.546	0.600	0.648
	$SDF_{Adjusted}$ (C_{T2})	0.147	0.359	0.647	1.216	1.032	1.285	1.679
	$SDF_{Verified}$ (C_{T3})	0.180	0.328	0.406	0.470	0.542	0.590	0.634
C5R004 (C5H054**)	$SDF_{Original}$ (C_{T1})	0.150	0.312	0.397	0.467	0.546	0.600	0.648
	$SDF_{Adjusted}$ (C_{T2})	0.121	0.277	0.419	0.822	0.715	0.851	1.064
	$SDF_{Verified}$ (C_{T3})	0.180	0.328	0.406	0.470	0.542	0.590	0.634
C5R005 (C5H022**)	$SDF_{Original}$ (C_{T1})	0.150	0.312	0.397	0.467	0.546	0.600	0.648
	$SDF_{Adjusted}$ (C_{T2})	0.093	0.196	0.235	0.489	0.437	0.491	0.580
	$SDF_{Verified}$ (C_{T3})	0.110	0.190	0.231	0.266	0.304	0.330	0.354
C5H016** (C5H018)	$SDF_{Original}$ (C_{T1})	0.150	0.312	0.397	0.467	0.546	0.600	0.648
	$SDF_{Adjusted}$ (C_{T2})	0.162	0.407	0.799	1.473	1.238	1.571	2.097
	$SDF_{Verified}$ (C_{T3})	0.030	0.093	0.126	0.154	0.184	0.205	0.224

Table B.65: SA SDF basins: Verified run-off coefficients

Catchment description	Method	Run-off coefficients (C_T) for return period (T)						
		2	**5**	**10**	**20**	**50**	**100**	**200**
SDF basin 6 C8H001 (C8H003*)	$SDF_{Original}$ (C_{T1})	0.150	0.312	0.397	0.467	0.546	0.600	0.648
	$SDF_{Adjusted}$ (C_{T2})	0.150	0.181	0.218	0.304	0.464	0.621	0.857
	$SDF_{Verified}$ (C_{T3})	0.090	0.303	0.415	0.507	0.611	0.680	0.743
SDF basin 7 C4H002 (C4H001)	$SDF_{Original}$ (C_{T1})	0.150	0.312	0.397	0.467	0.546	0.600	0.648
	$SDF_{Adjusted}$ (C_{T2})	0.074	0.101	0.128	0.134	0.140	0.144	0.146
	$SDF_{Verified}$ (C_{T3})	0.100	0.227	0.293	0.347	0.409	0.450	0.488
SDF basin 10 D1H001 (D1H004)	$SDF_{Original}$ (C_{T1})	0.100	0.244	0.320	0.382	0.452	0.500	0.543
	$SDF_{Adjusted}$ (C_{T2})	0.049	0.096	0.126	0.152	0.202	0.242	0.308
	$SDF_{Verified}$ (C_{T3})	0.080	0.132	0.160	0.183	0.208	0.225	0.241
SDF basin 18 H3H001 (H7H004)	$SDF_{Original}$ (C_{T1})	0.300	0.408	0.465	0.511	0.564	0.600	0.632
	$SDF_{Adjusted}$ (C_{T2})	1.370	1.291	0.925	0.911	0.898	0.929	0.942
	$SDF_{Verified}$ (C_{T3})	0.200	0.334	0.404	0.462	0.527	0.570	0.610
SDF basin 21 Q9H008* (Q9H004)	$SDF_{Original}$ (C_{T1})	0.100	0.190	0.237	0.276	0.320	0.350	0.377
	$SDF_{Adjusted}$ (C_{T2})	0.035	0.091	0.171	0.223	0.275	0.307	0.360
	$SDF_{Verified}$ (C_{T3})	0.160	0.211	0.237	0.259	0.284	0.300	0.315
SDF basin 21 Q9H010 (Q1H001)	$SDF_{Original}$ (C_{T1})	0.100	0.190	0.237	0.276	0.320	0.350	0.377
	$SDF_{Adjusted}$ (C_{T2})	0.107	0.238	0.372	0.499	0.657	0.754	0.943
	$SDF_{Verified}$ (C_{T3})	0.060	0.219	0.302	0.371	0.448	0.500	0.547
SDF basin 21 Q9H010 (Q7H003)	$SDF_{Original}$ (C_{T1})	0.100	0.190	0.237	0.276	0.320	0.350	0.377
	$SDF_{Adjusted}$ (C_{T2})	0.138	0.297	0.444	0.601	0.802	0.928	1.178
	$SDF_{Verified}$ (C_{T3})	0.060	0.219	0.302	0.371	0.448	0.500	0.547
SDF basin 21 Q9H010 (Q9H012)	$SDF_{Original}$ (C_{T1})	0.100	0.190	0.237	0.276	0.320	0.350	0.377
	$SDF_{Adjusted}$ (C_{T2})	0.150	0.318	0.468	0.636	0.853	0.989	1.261
	$SDF_{Verified}$ (C_{T3})	0.060	0.219	0.302	0.371	0.448	0.500	0.547

Table B.66: SA SDF basins: GOF statistics of the fitted distributions

Catchment description	*T*-range (years)	r^2 *(2.40)*	χ^2 statistic *(2.42)*	χ^2 critical value *(5.5b)*	$C_{Contingency}$ *(2.47)*	C_{Max} *(2.48b)*	Confidence level (%)
A2H012 (1)	1 - 68	0.993	13.9	127	0.415	0.993	100
A6H006 (2)*	1 - 57	0.891	18.9	89.7	0.503	0.991	100
B4H003 (4)	1 - 53	0.985	11.4	79.3	0.424	0.990	100
B7H004 (5)	1 - 58	0.946	32.5	92.5	0.603	0.991	99.50
C3H003 (8)	1 - 11	0.968	38.3	163.9	0.581	0.993	99.98
C4H001 (7)	1 - 14	0.956	67.9	32.2	-	-	-
C4H002 (7)	1 - 37	0.979	64.1	31	-	-	-
C8H001 (6)	1 - 65	0.959	154.1	76.9	-	-	-
C8H003 (6)*	1 - 89	0.670	171.5	84.3	-	-	-
D1H001 (10)	1 - 97	0.921	126.7	108	-	-	-
D1H004 (10)	1 - 97	0.910	50.5	81.7	0.698	0.991	53.38
D1H005 (11)	1 - 54	0.981	135.7	81.7	-	-	-
E2H003 (16)	1 - 84	0.907	280.5	210.7	-	-	-
G1H008 (17)	1 - 53	0.899	31.9	79.3	0.617	0.990	98.35
H3H001 (18)*	1 - 22	0.882	20.5	31	0.747	0.976	15.05
H7H004 (18)	1 - 55	0.974	12.3	84.3	0.430	0.991	100
Q1H001 (21)	1 - 77	0.947	95.8	169.1	0.747	0.993	5.33
Q9H008 (21)*	1 - 48	0.971	20.5	100	0.551	0.989	99.96
Q9H010 (21)	1 - 28	0.975	128.7	34.5	-	-	-
Q9H012 (21)	1 - 52	0.930	213.6	76.9	-	-	-
V2H002 (26)*	1 - 60	0.835	116.1	98.5	-	-	-
V6H002 (26)*	1 - 78	0.991	34.9	174.6	0.558	0.993	99.98
W5H005 (28)	1 - 61	0.975	10.6	101.6	0.388	0.992	100
X2H010 (29)*	1 - 63	0.789	64.5	108.3	0.715	0.992	34.31

ADDENDUM

C

GRAPHICAL PLOT RESULTS

EVALUATION OF THE SDF METHOD USING A CUSTOMISED DESIGN FLOOD ESTIMATION TOOL

ADDENDUM C: GRAPHICAL PLOT RESULTS

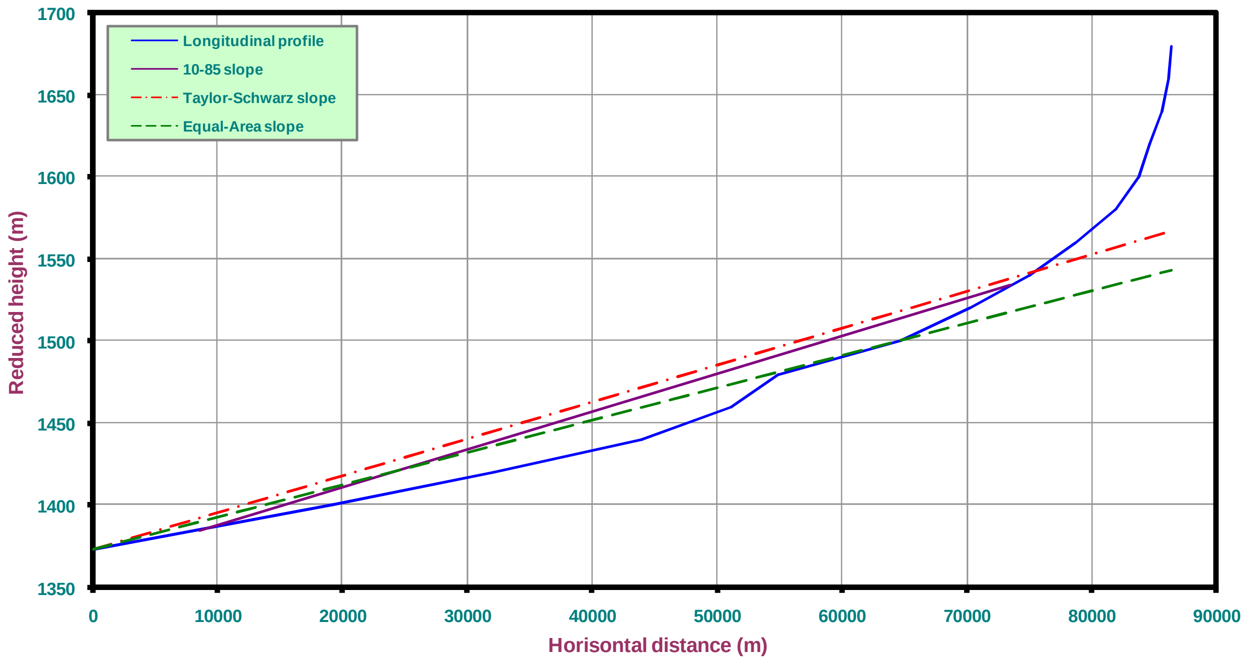

Figure C.1: C5R001: Longitudinal profile

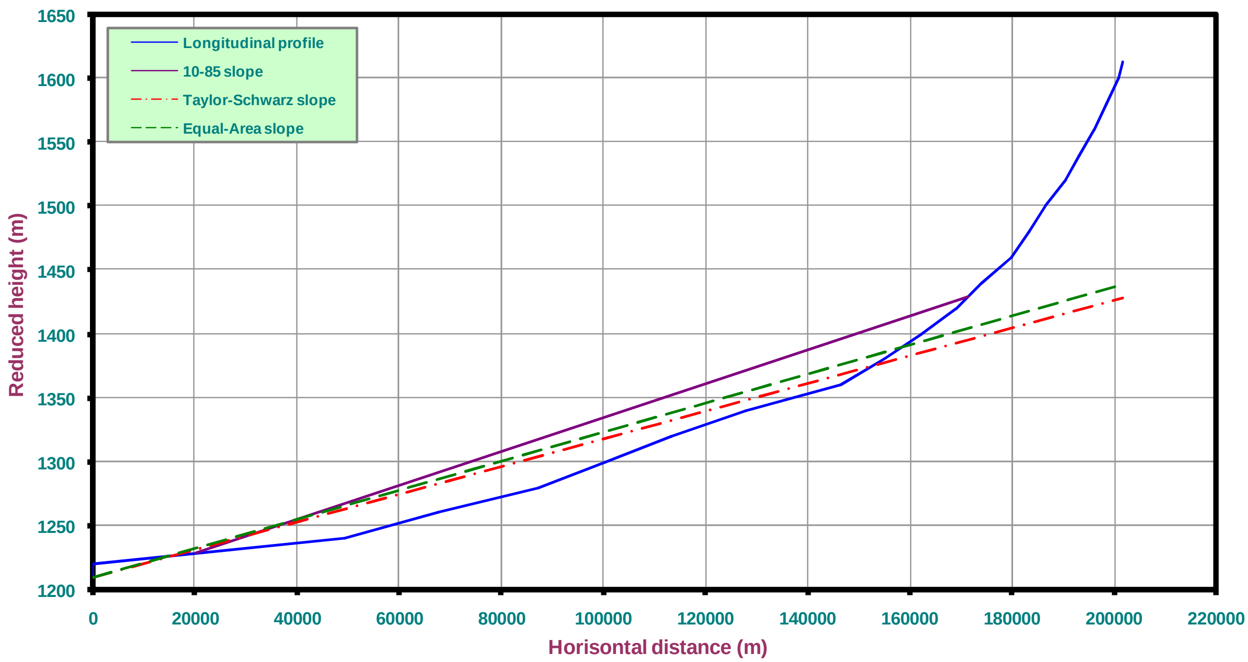

Figure C.2: C5R002: Longitudinal profile

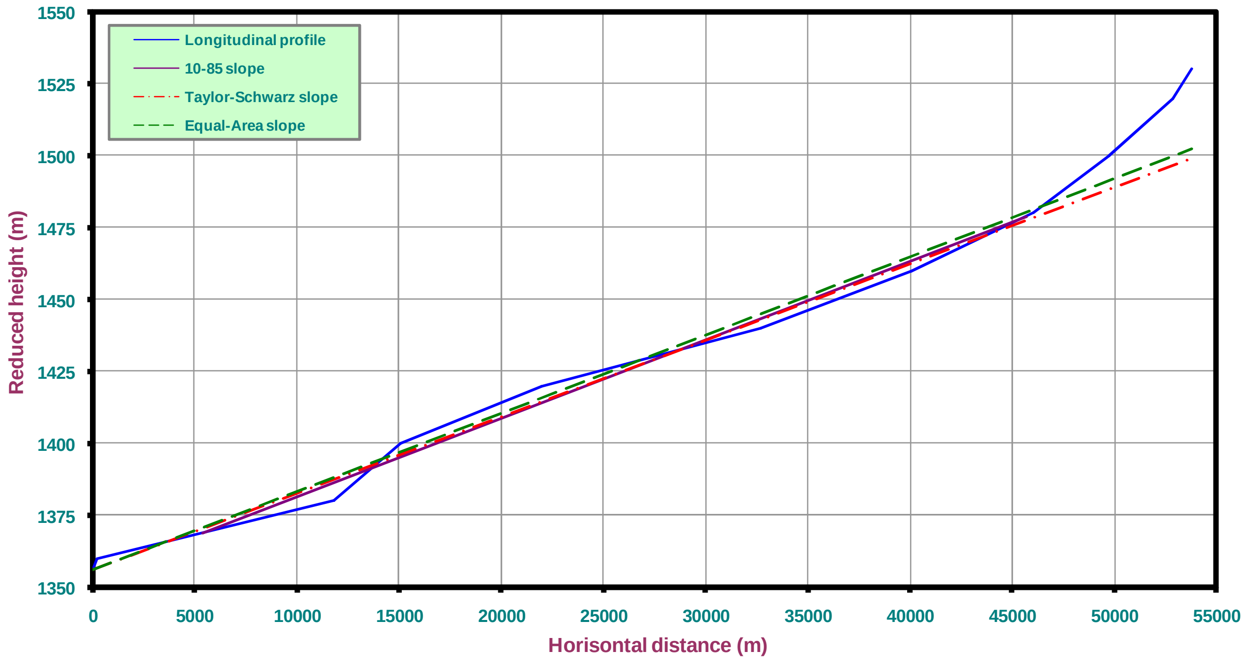

Figure C.3: C5R003: Longitudinal profile

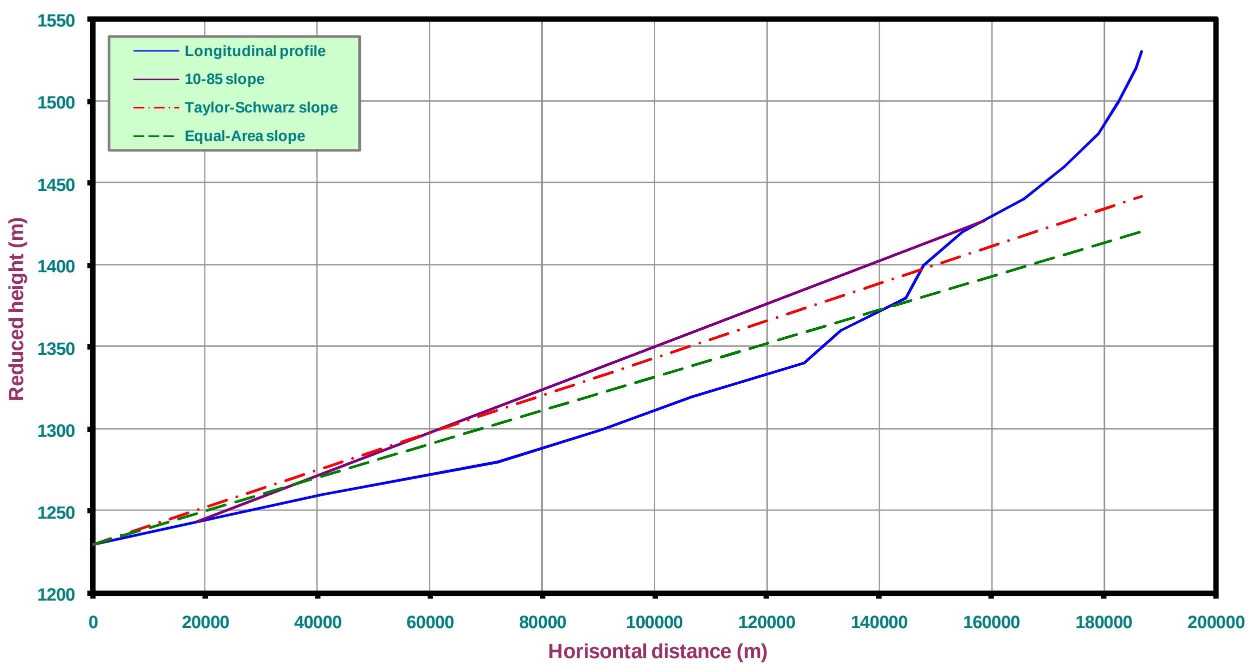

Figure C.4: C5R004: Longitudinal profile

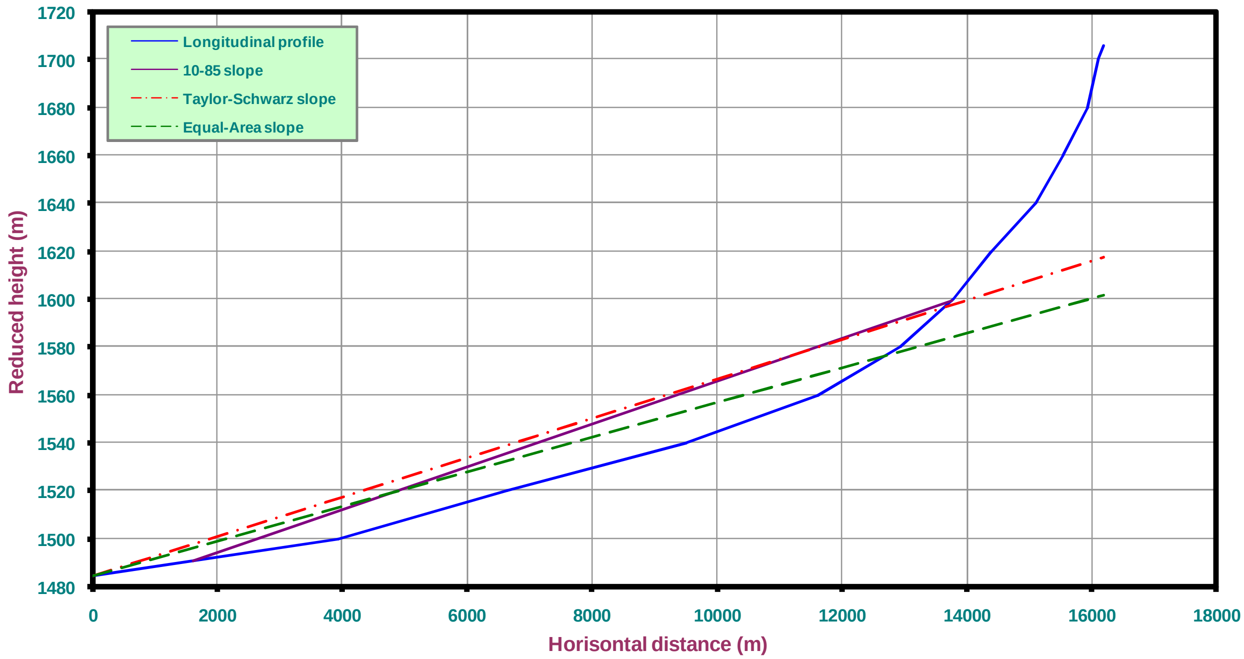

Figure C.5: C5R005: Longitudinal profile

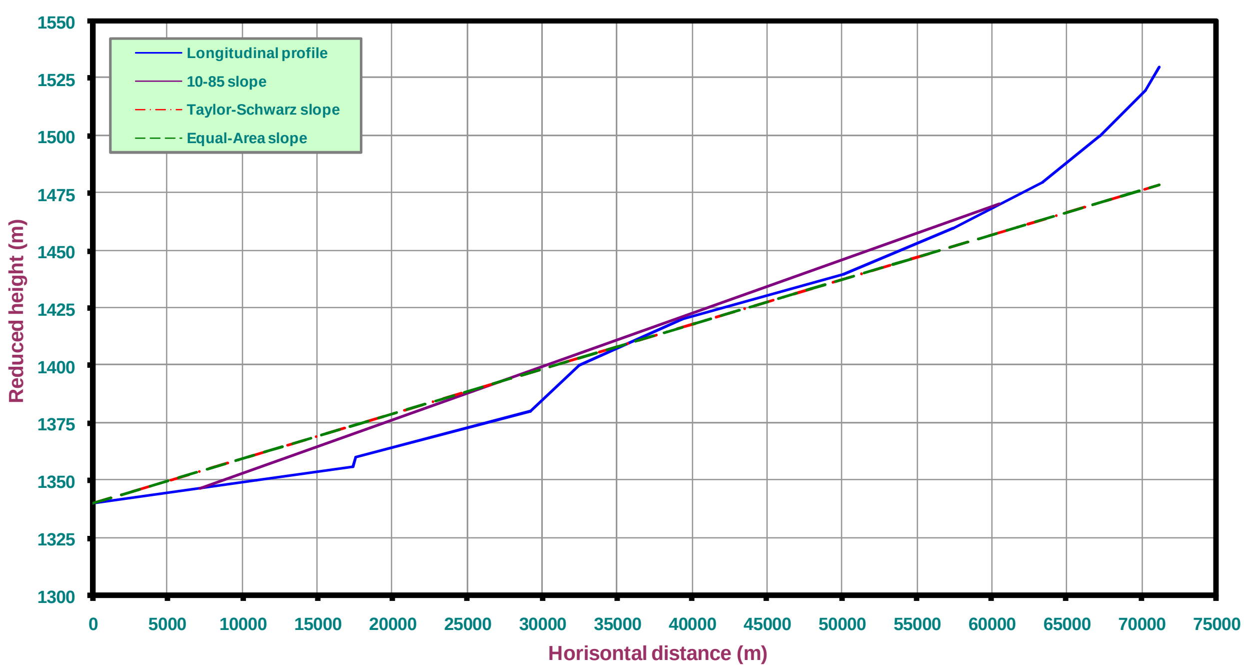

Figure C.6: C5H003: Longitudinal profile

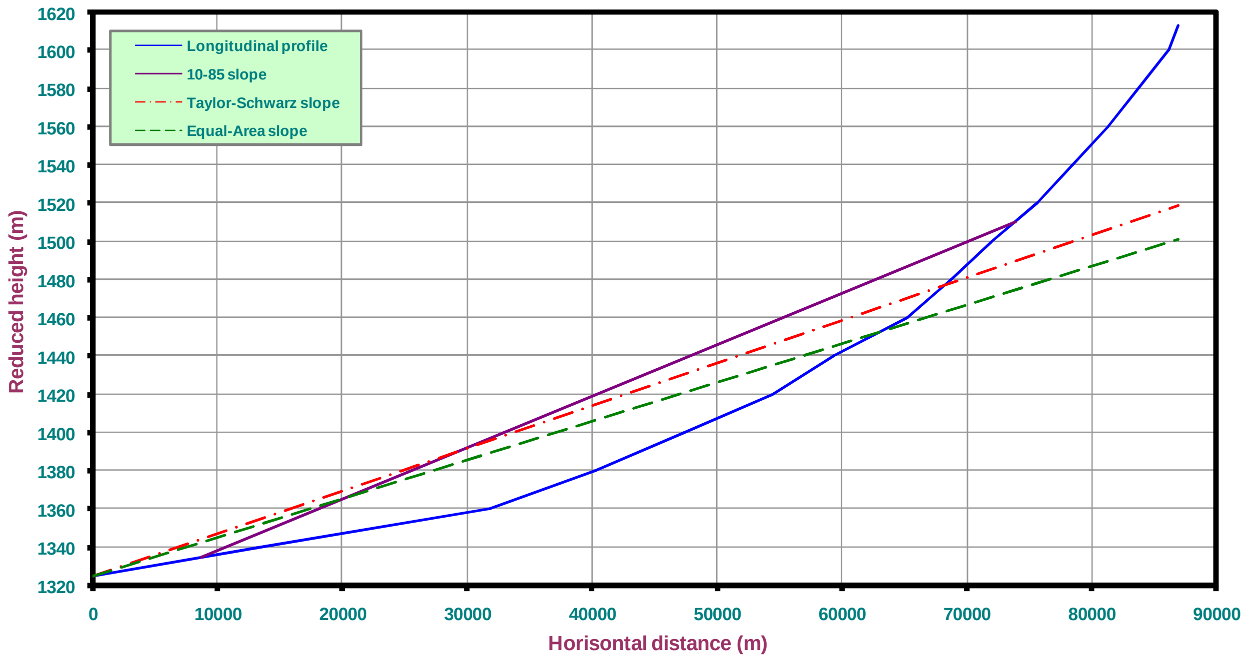

Figure C.7: C5H012: Longitudinal profile

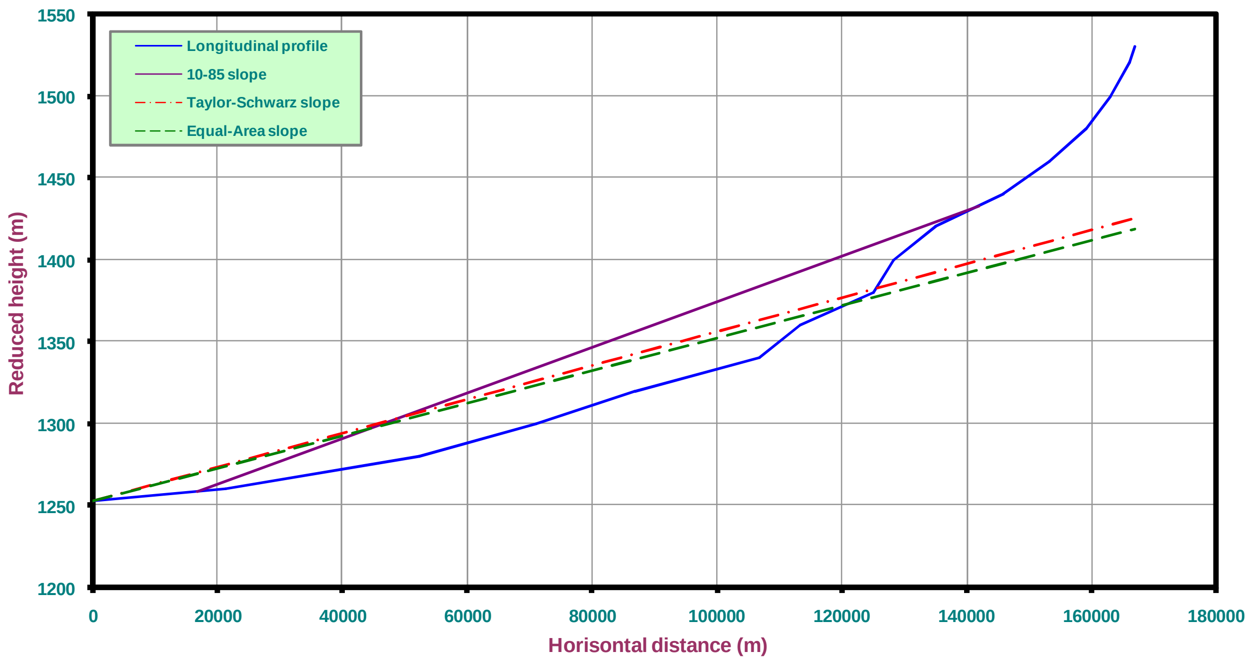

Figure C.8: C5H015: Longitudinal profile

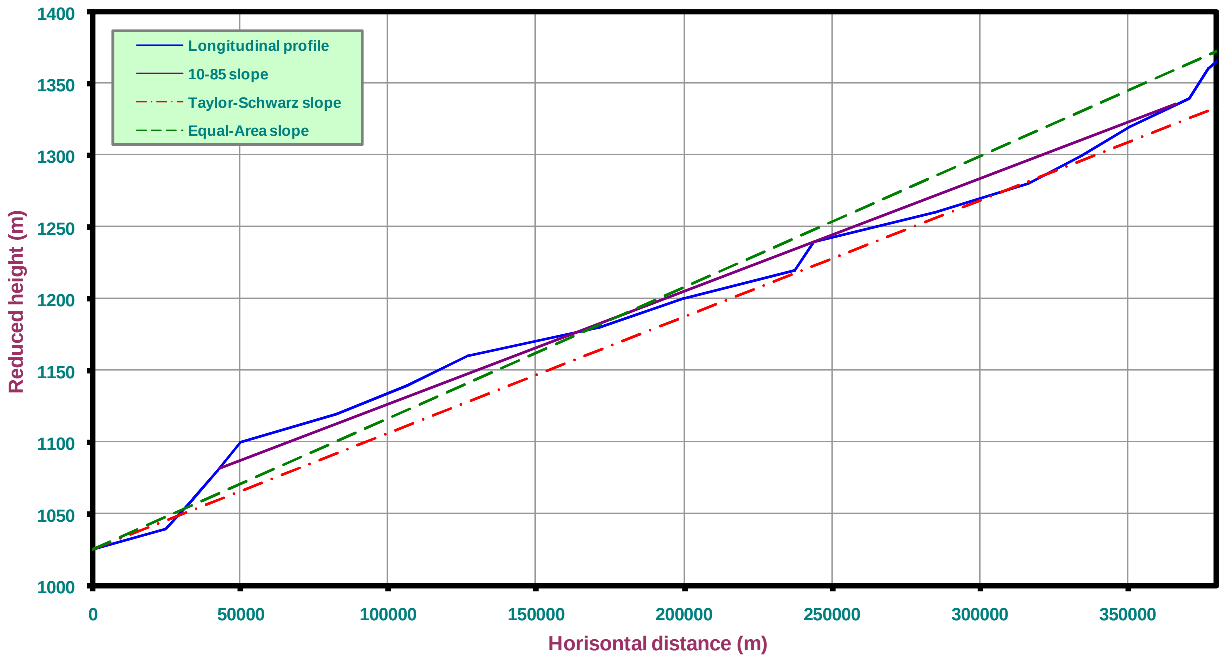

Figure C.9: C5H016: Longitudinal profile

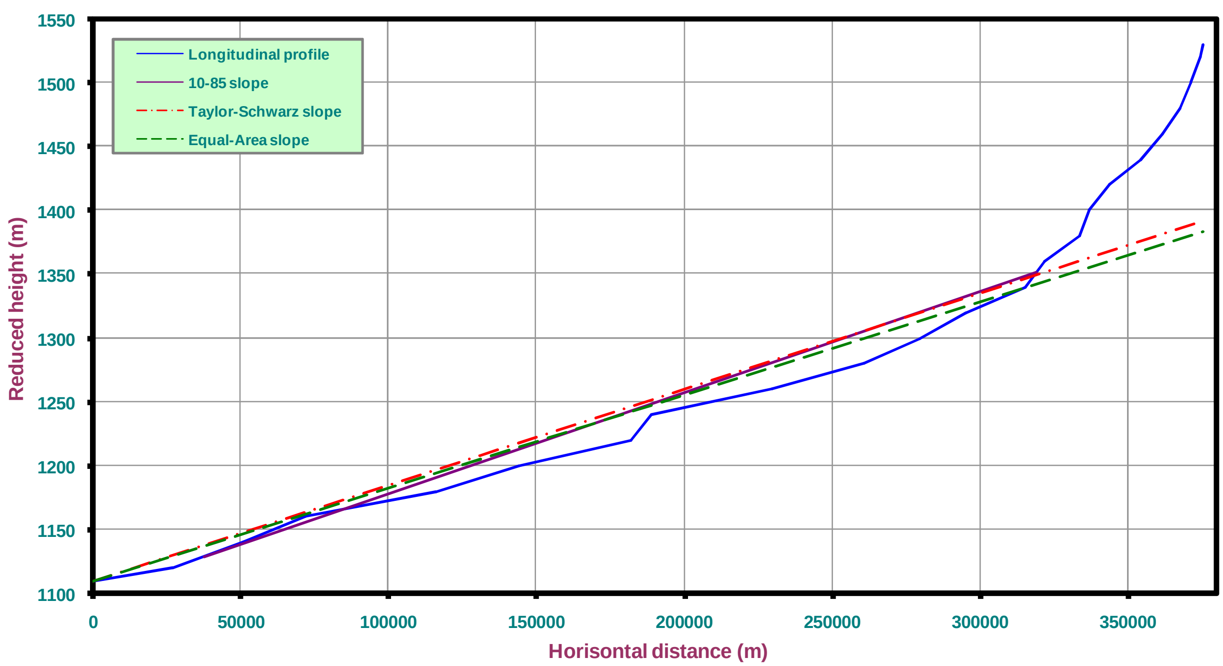

Figure C.10: C5H018: Longitudinal profile

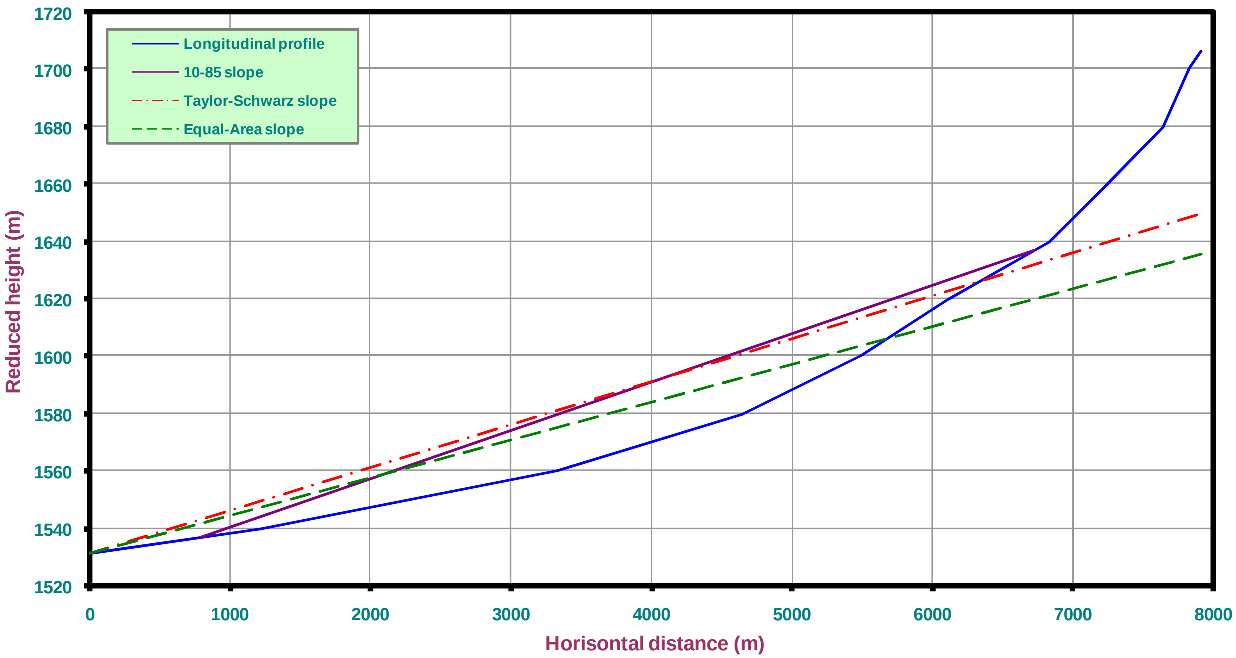

Figure C.11: C5H022: Longitudinal profile

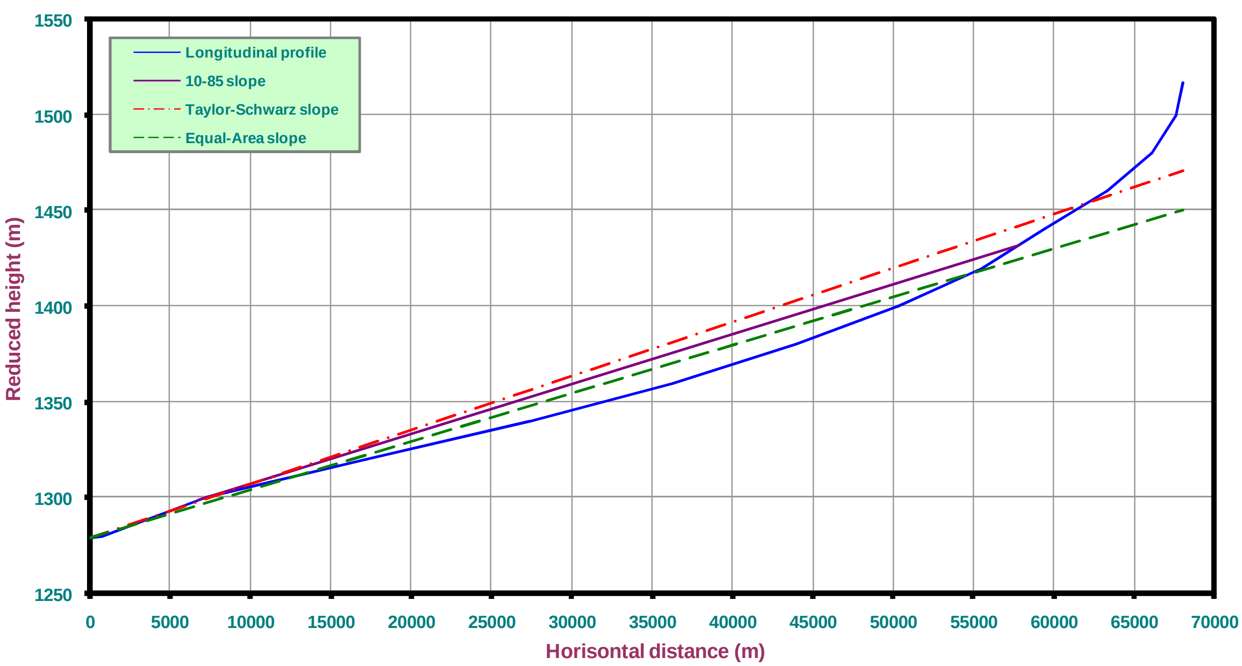

Figure C.12: C5H054: Longitudinal profile

Figure C.13: Average number of thunder days per year (SANRAL, 2006: 3.23)

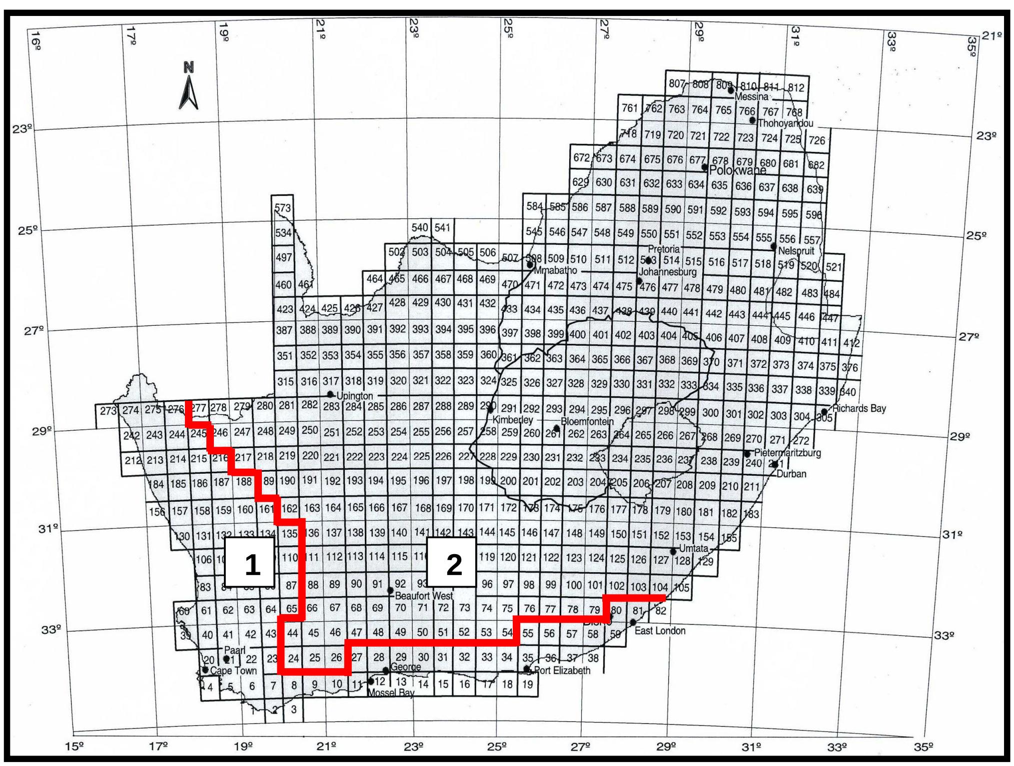

Figure C.14: SAWS precipitation station reference grid (Type 1/2) (SANRAL, 2006: 3.24; Rooseboom *et al.*, 1993: 2.47)

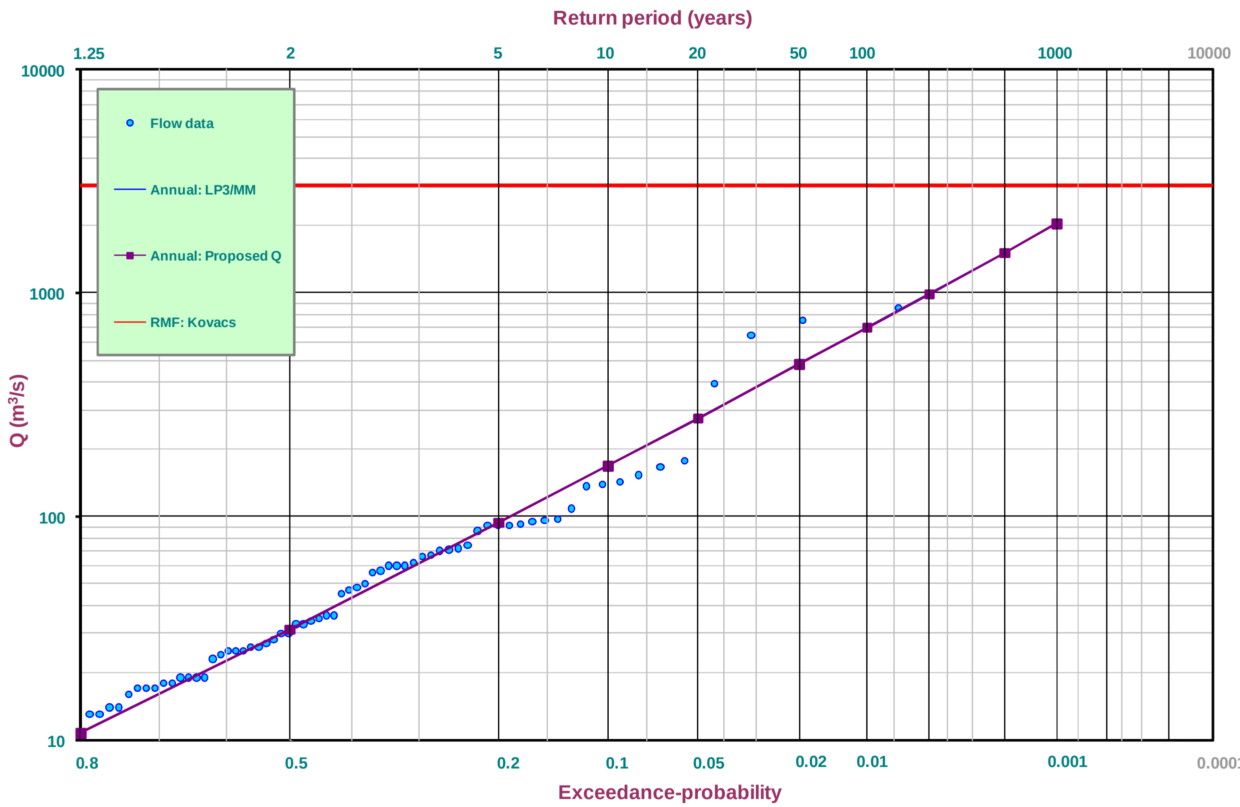

Figure C.15: C5R001: Probability distribution plot

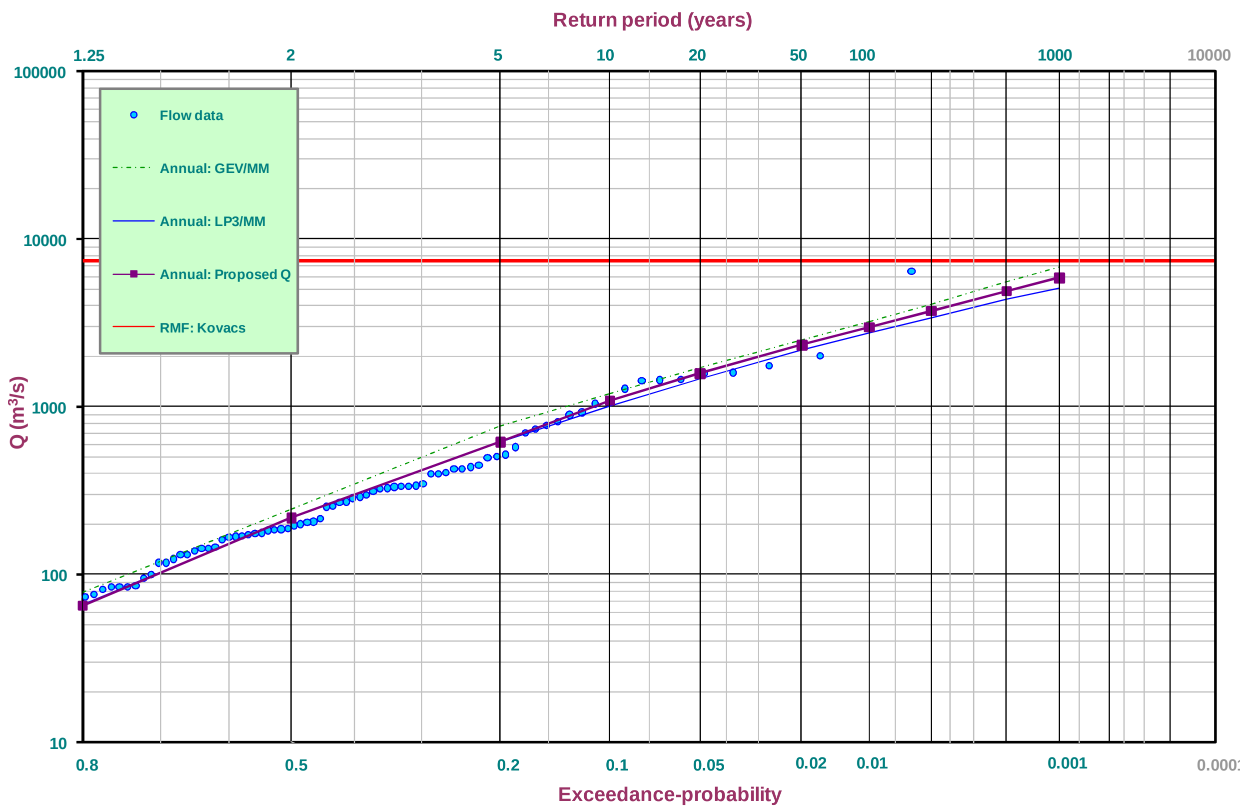

Figure C.16: C5R002: Probability distribution plot

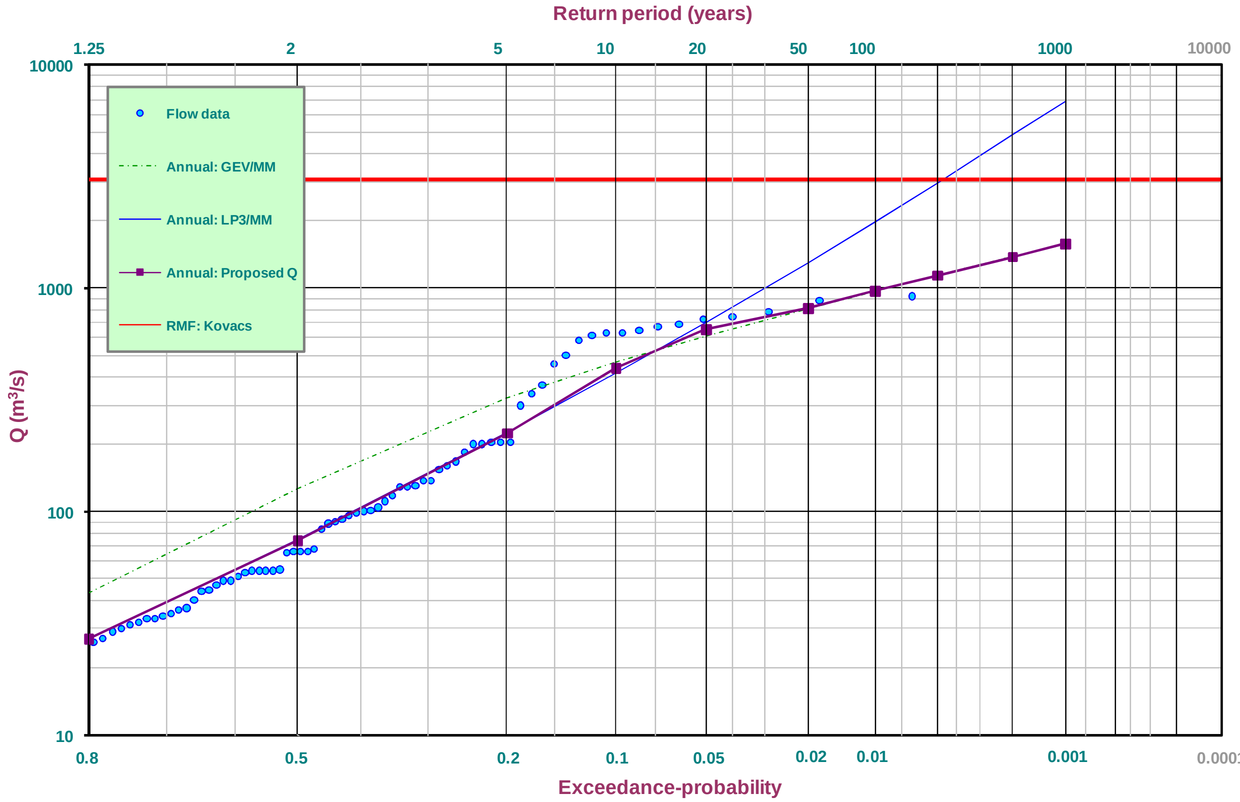

Figure C.17: C5R003: Probability distribution plot

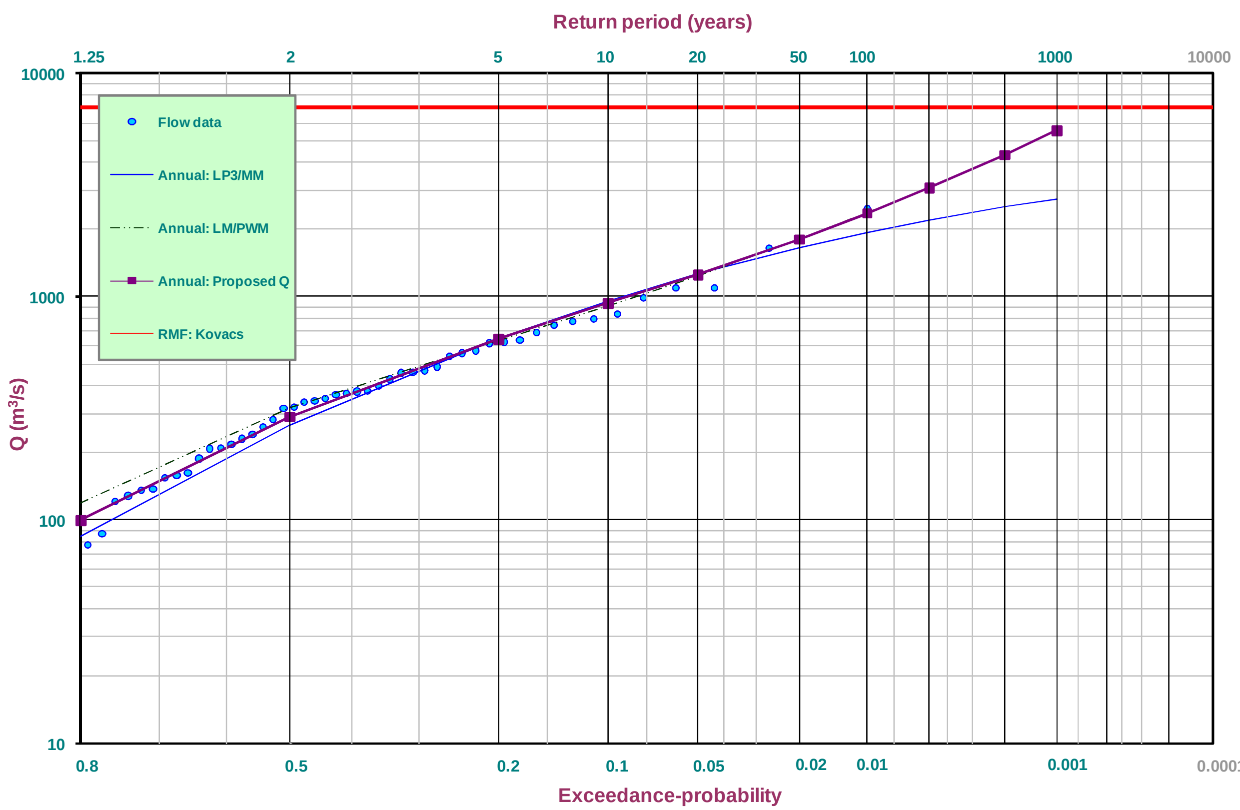

Figure C.18: C5R004: Probability distribution plot

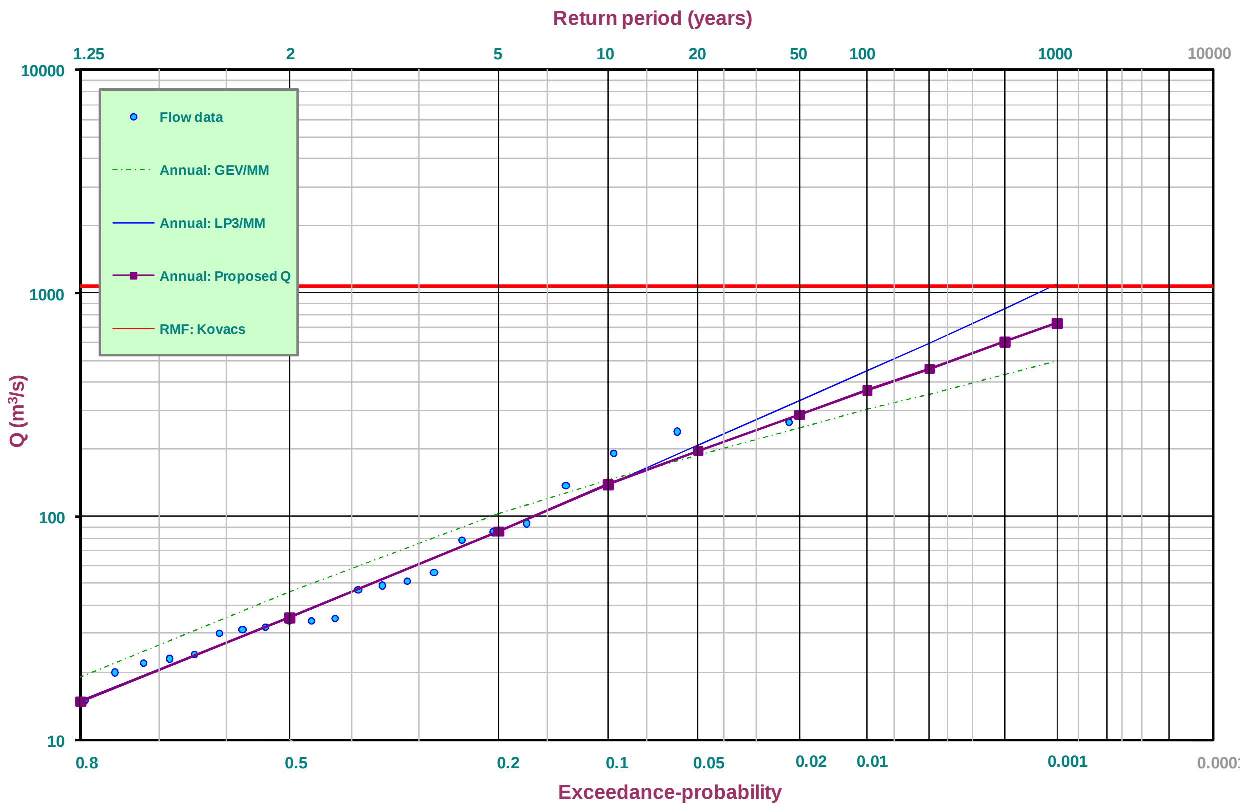

Figure C.19: C5R005: Probability distribution plot

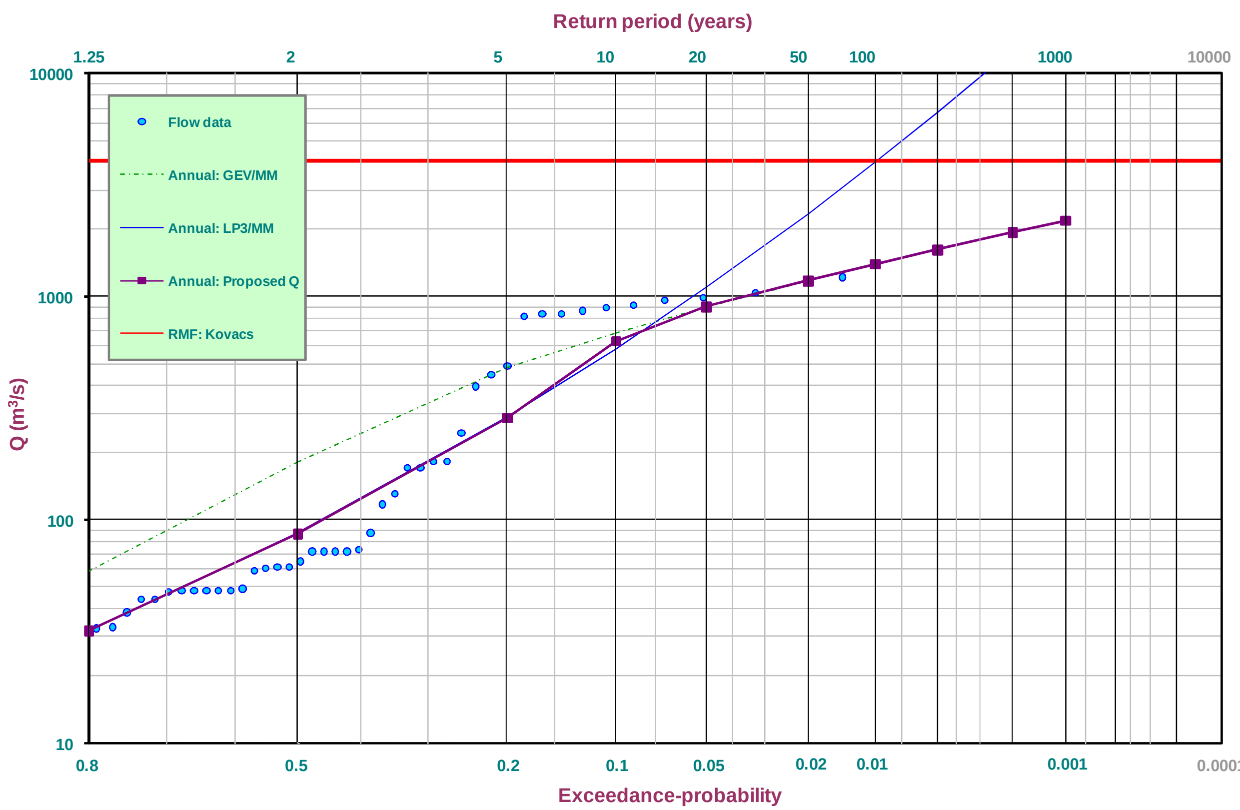

Figure C.20: C5H003: Probability distribution plot

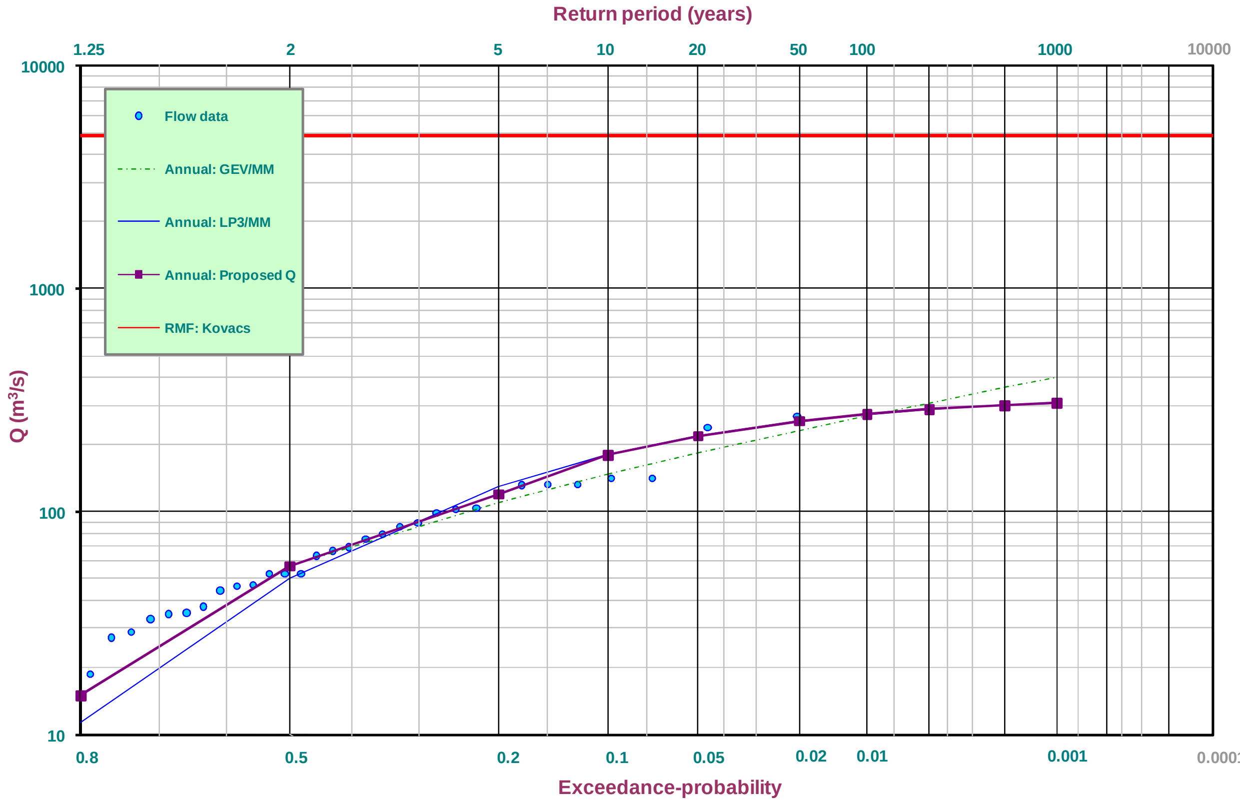

Figure C.21: C5H012: Probability distribution plot

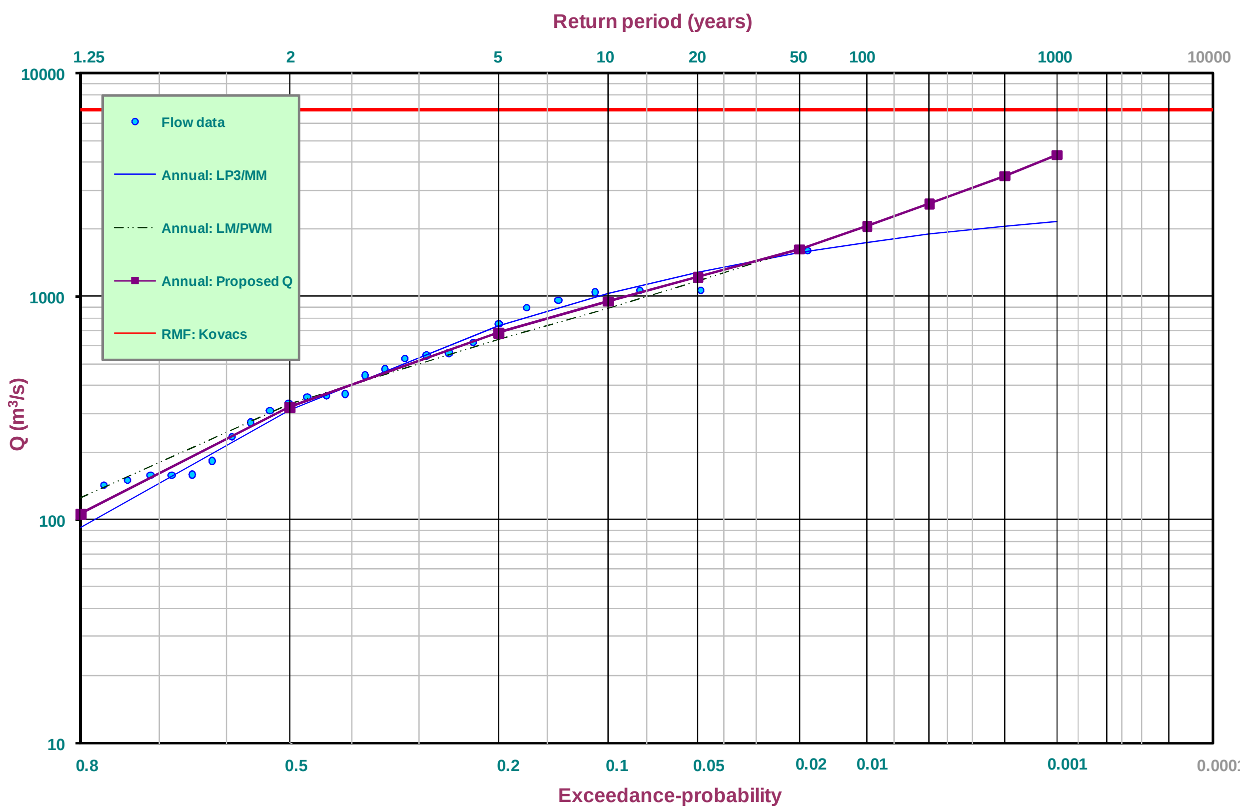

Figure C.22: C5H015: Probability distribution plot

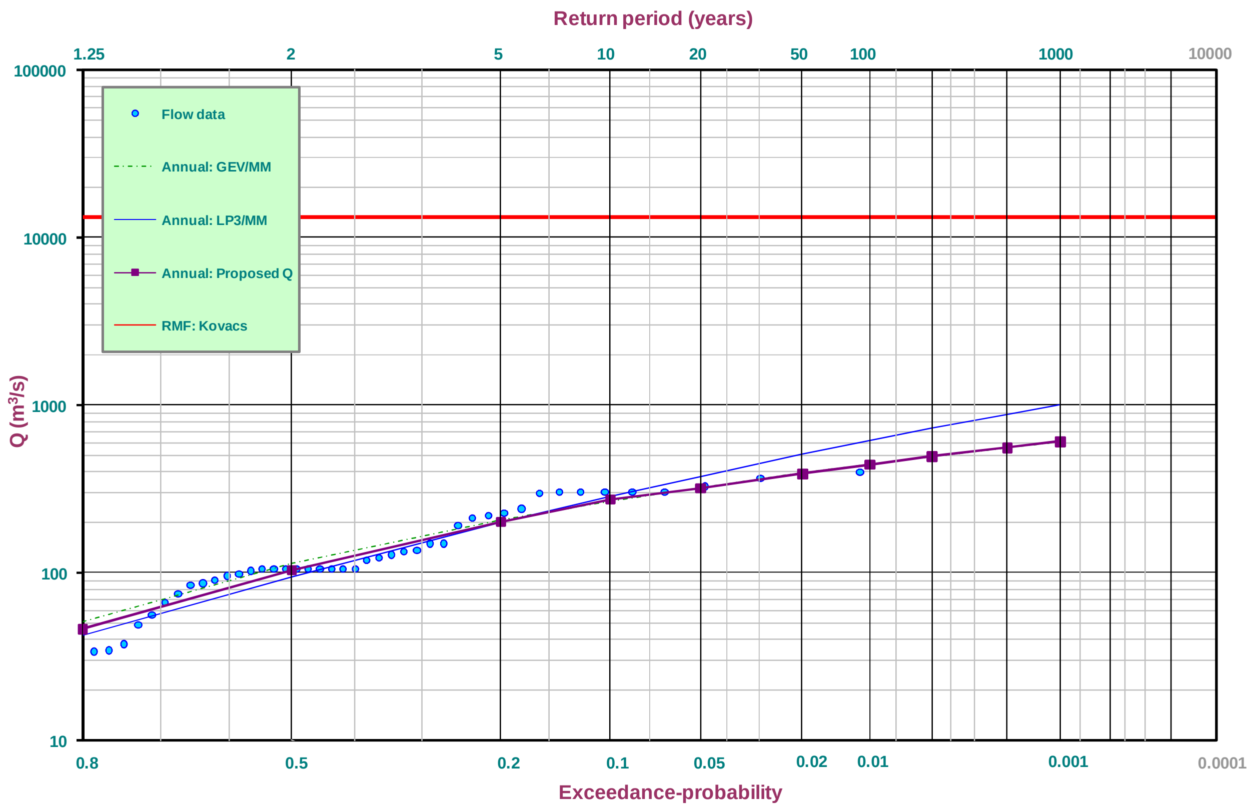

Figure C.23: C5H016: Probability distribution plot

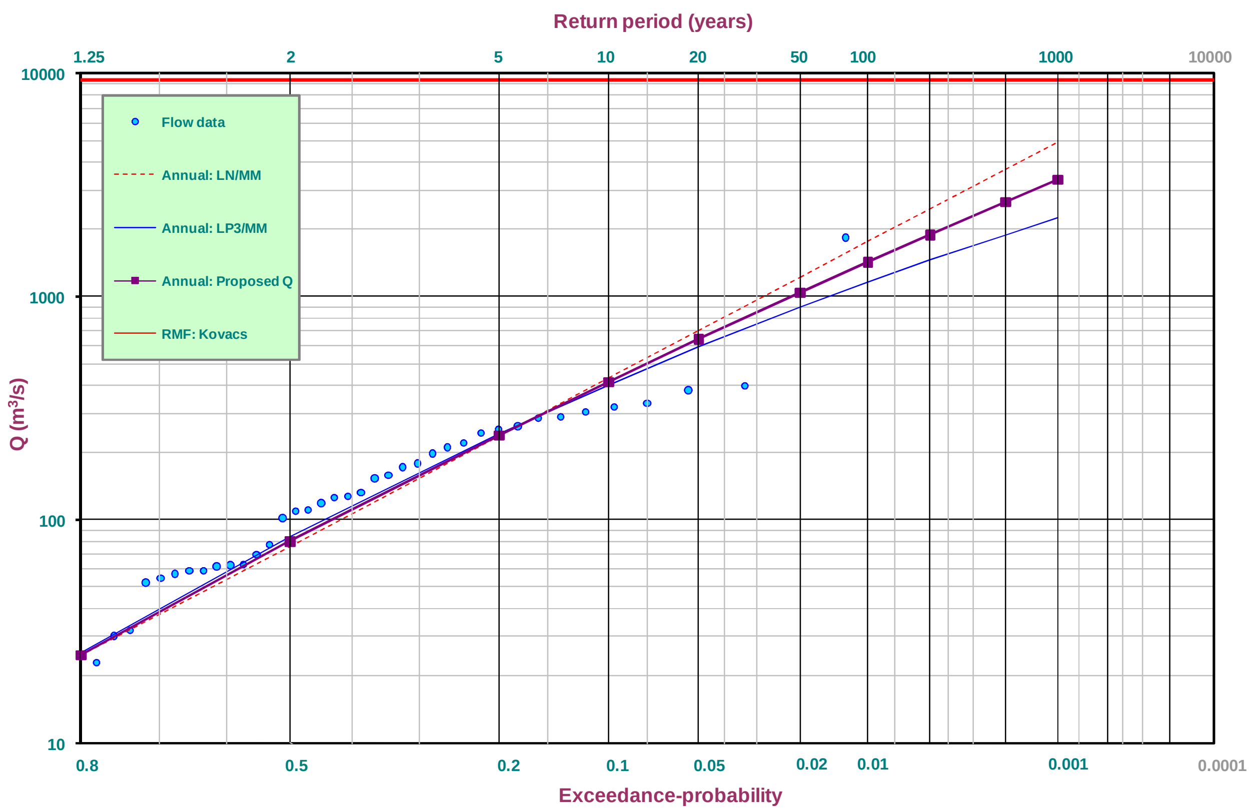

Figure C.24: C5H018: Probability distribution plot

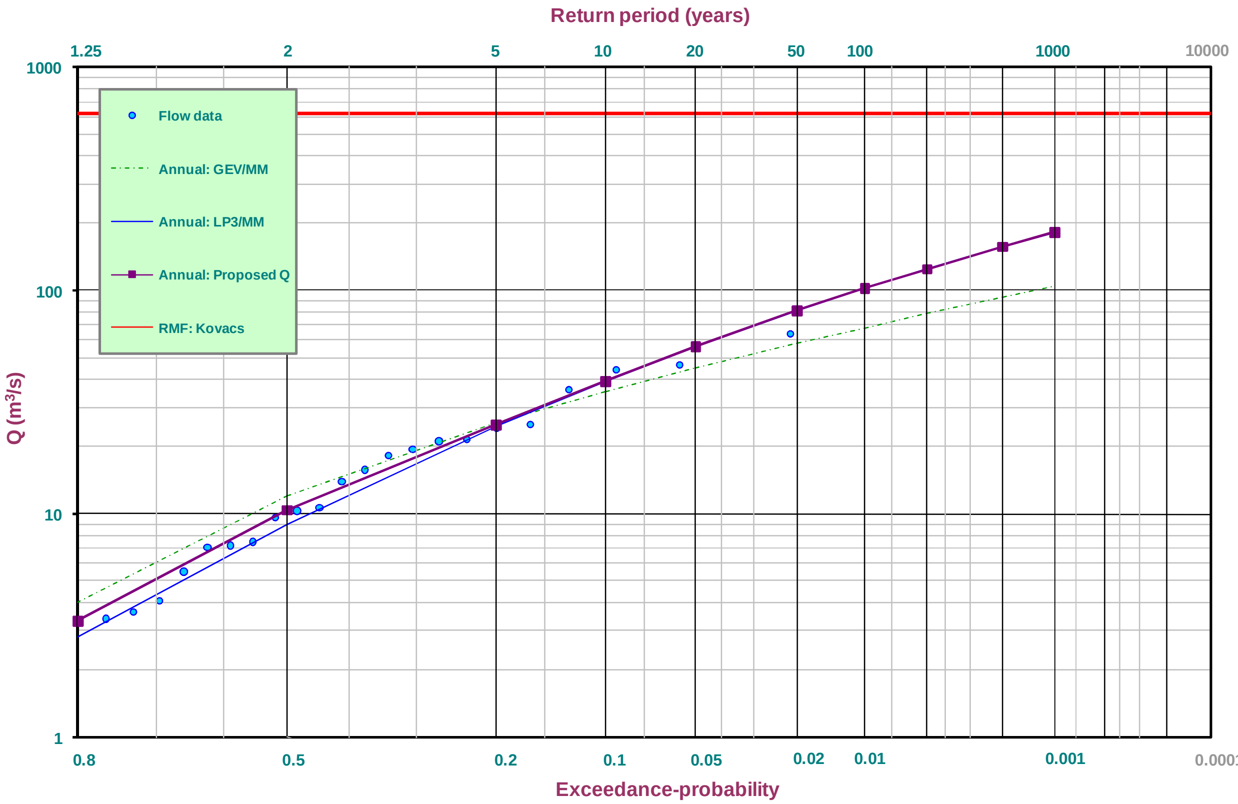

Figure C.25: C5H022: Probability distribution plot

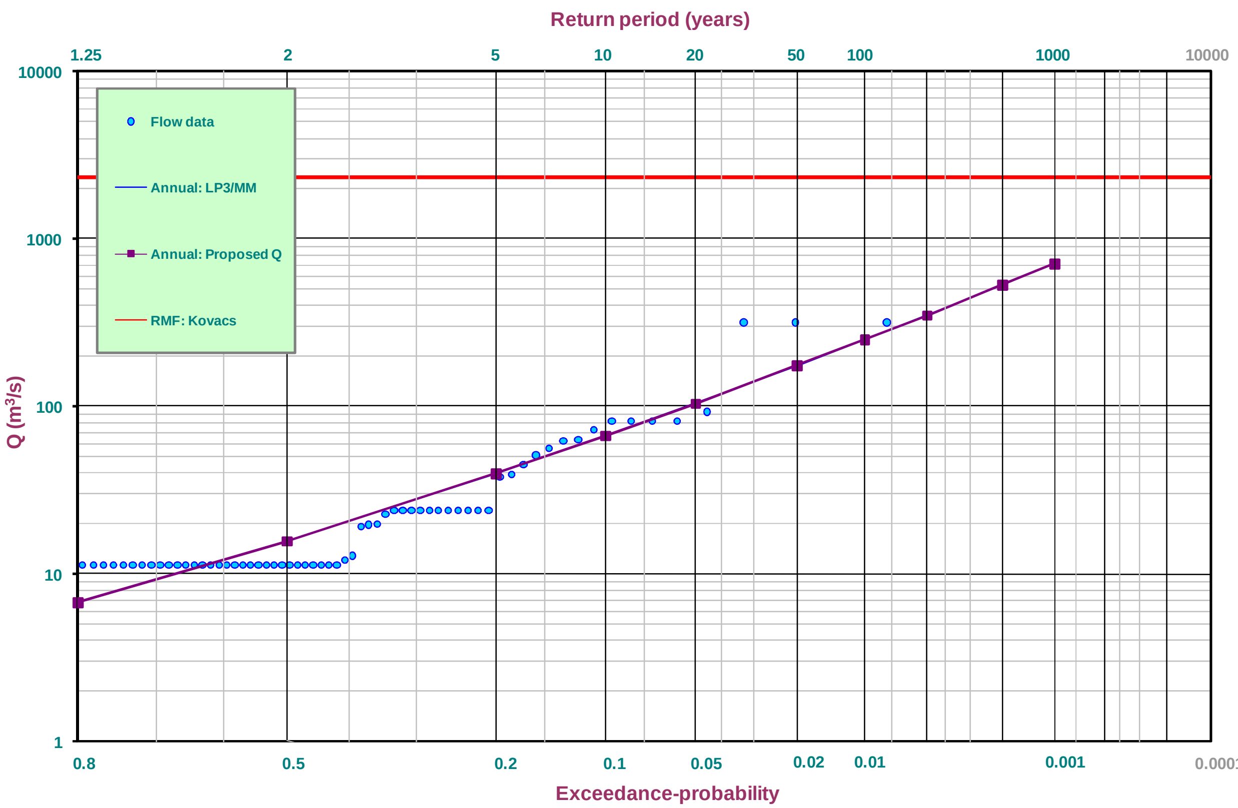

Figure C.26: C5H054: Probability distribution plot

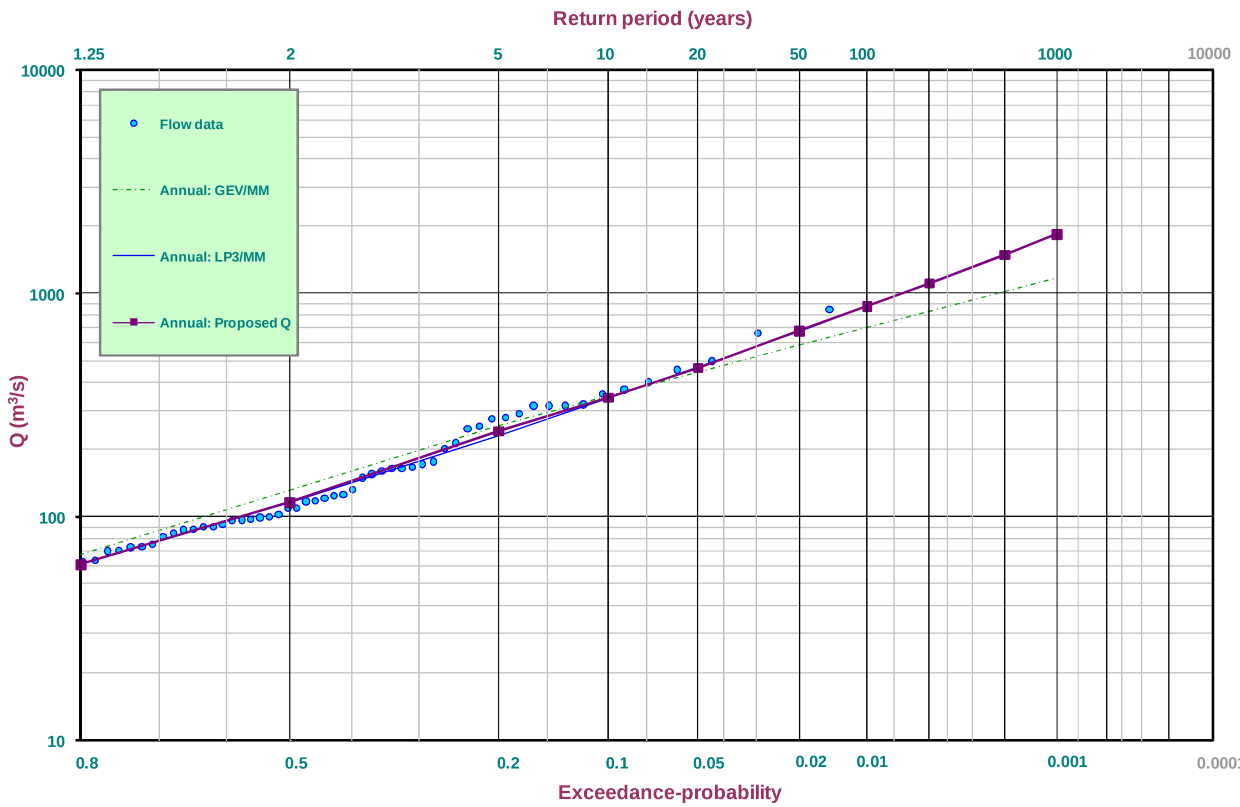

Figure C.27: A2H012 (1): Probability distribution plot

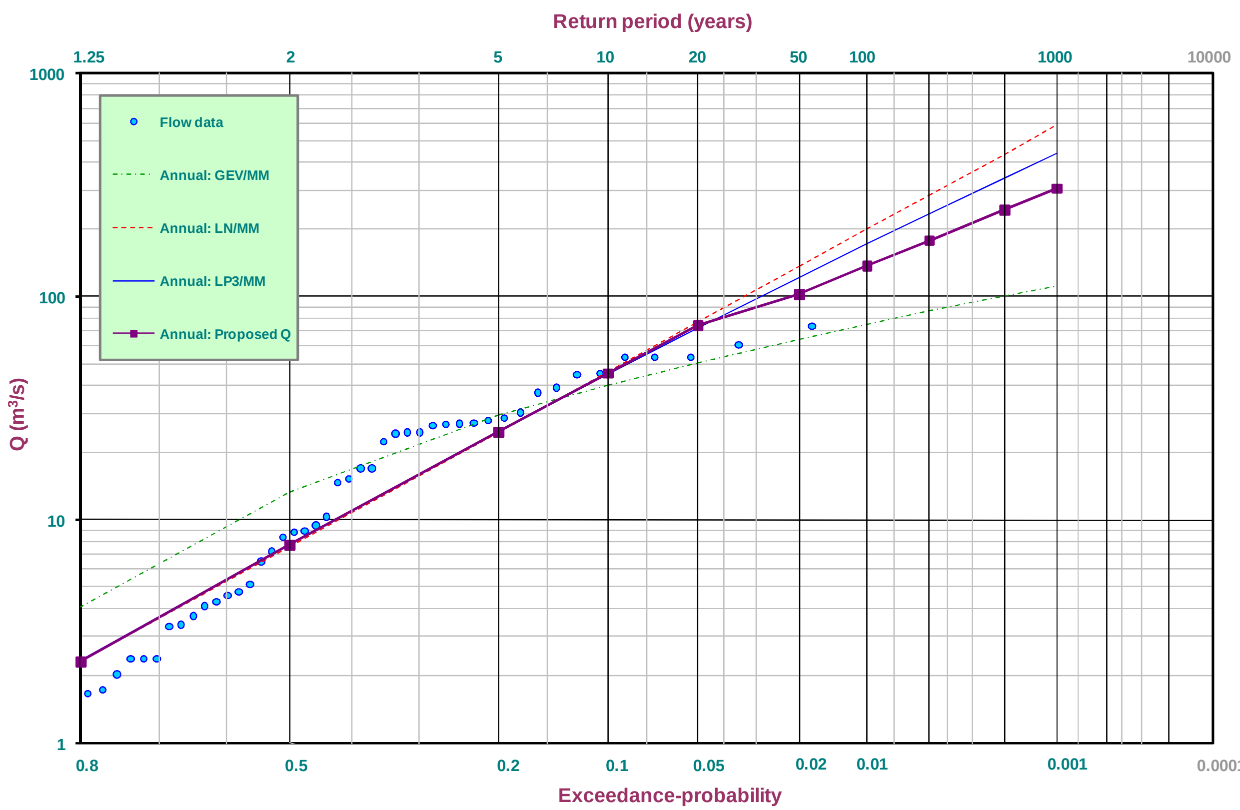

Figure C.28: A6H006 (2): Probability distribution plot

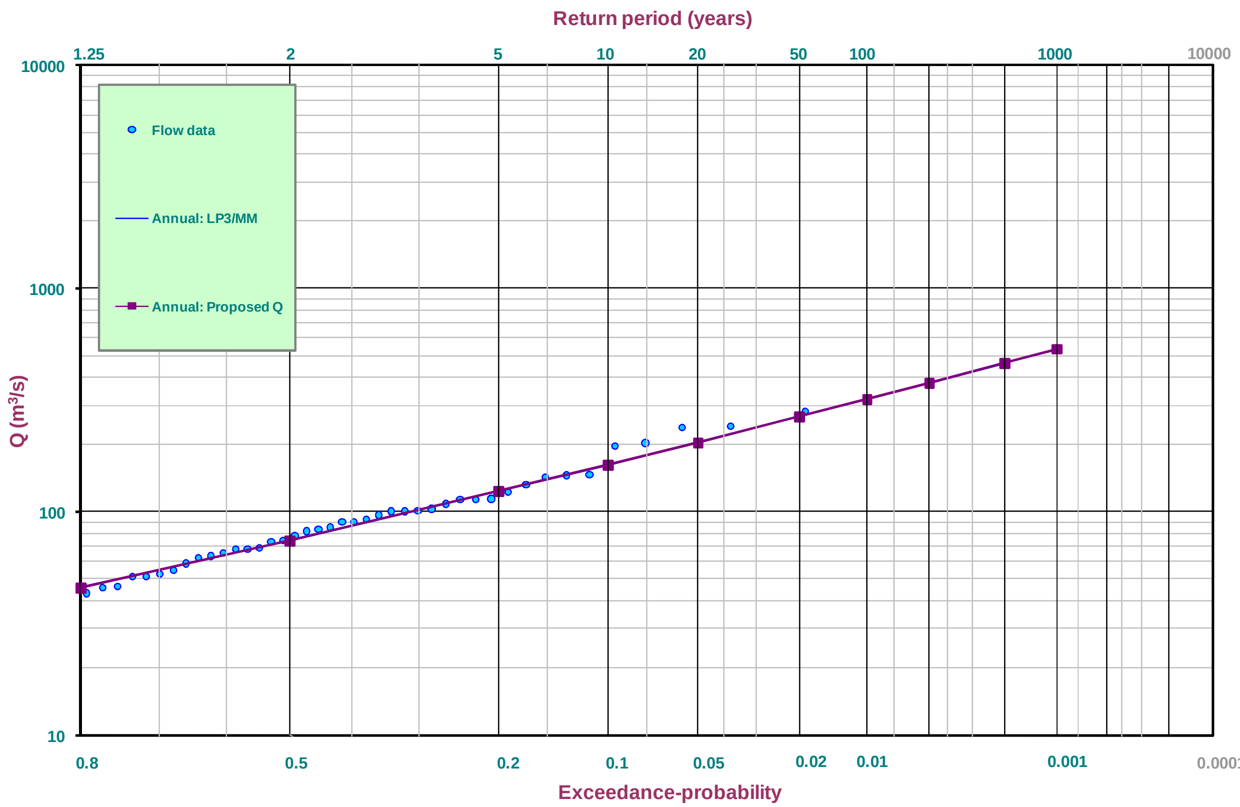

Figure C.29: B4H003 (4): Probability distribution plot

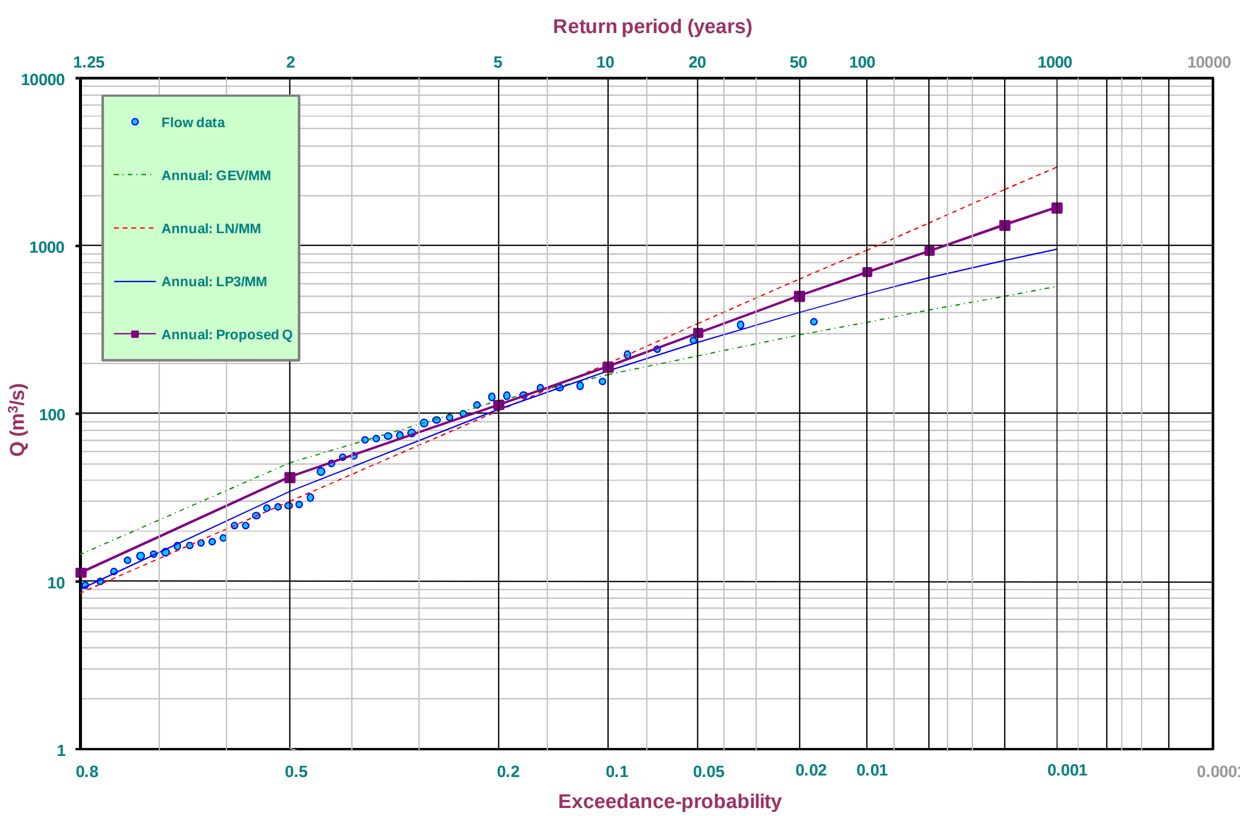

Figure C.30: B7H004 (5): Probability distribution plot

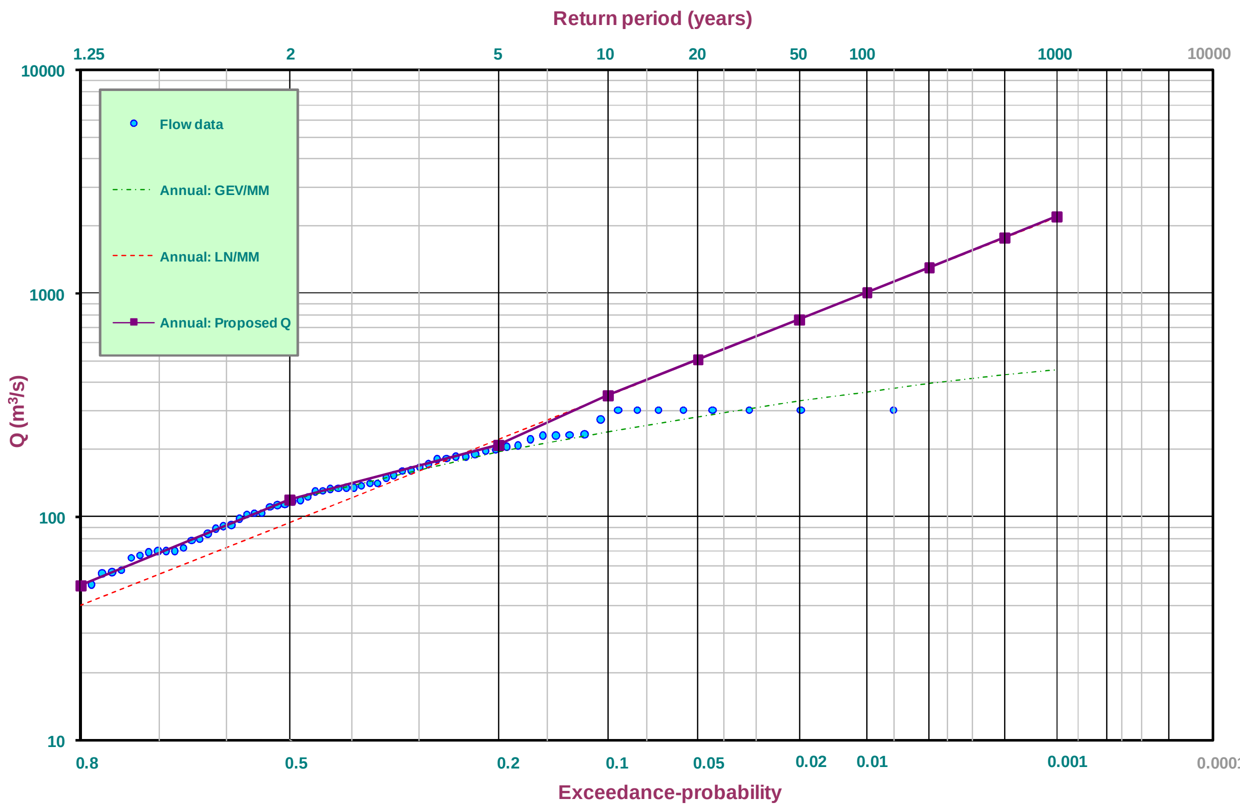

Figure C.31: C3H003 (8): Probability distribution plot

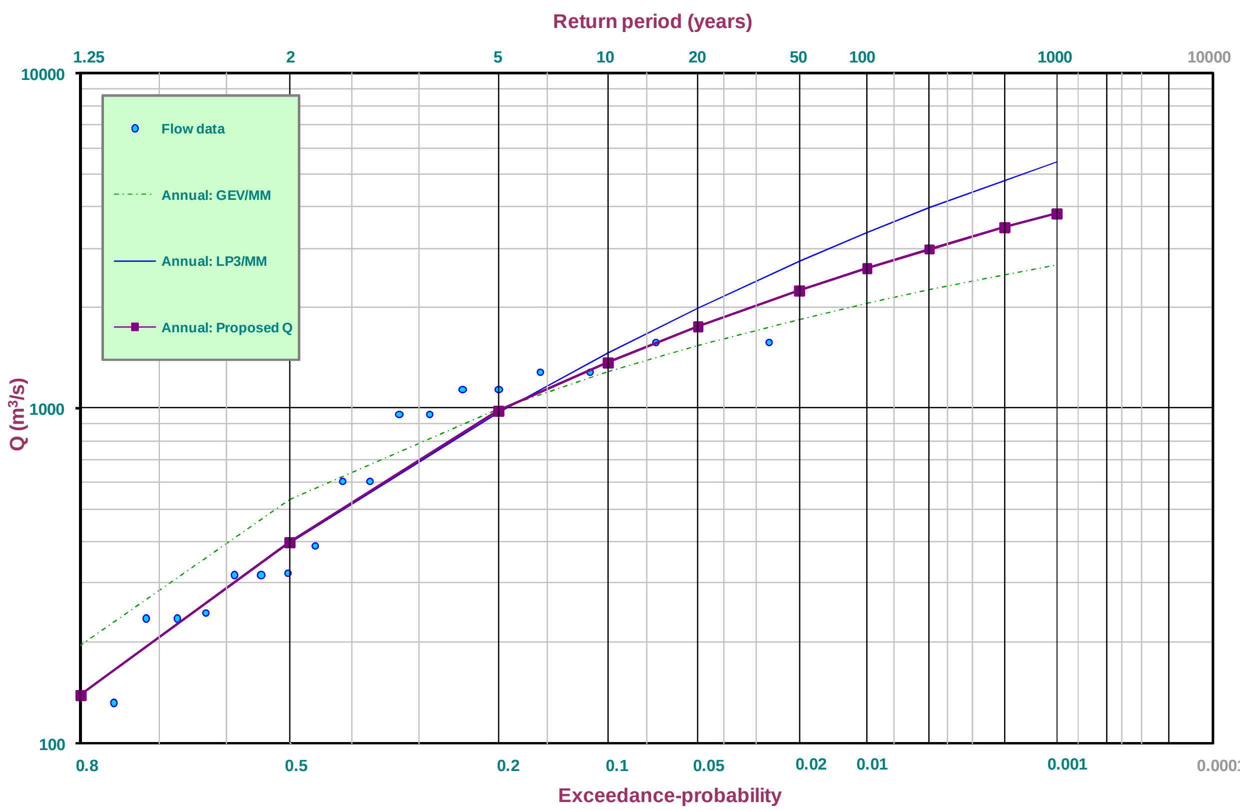

Figure C.32: C4H001 (7): Probability distribution plot

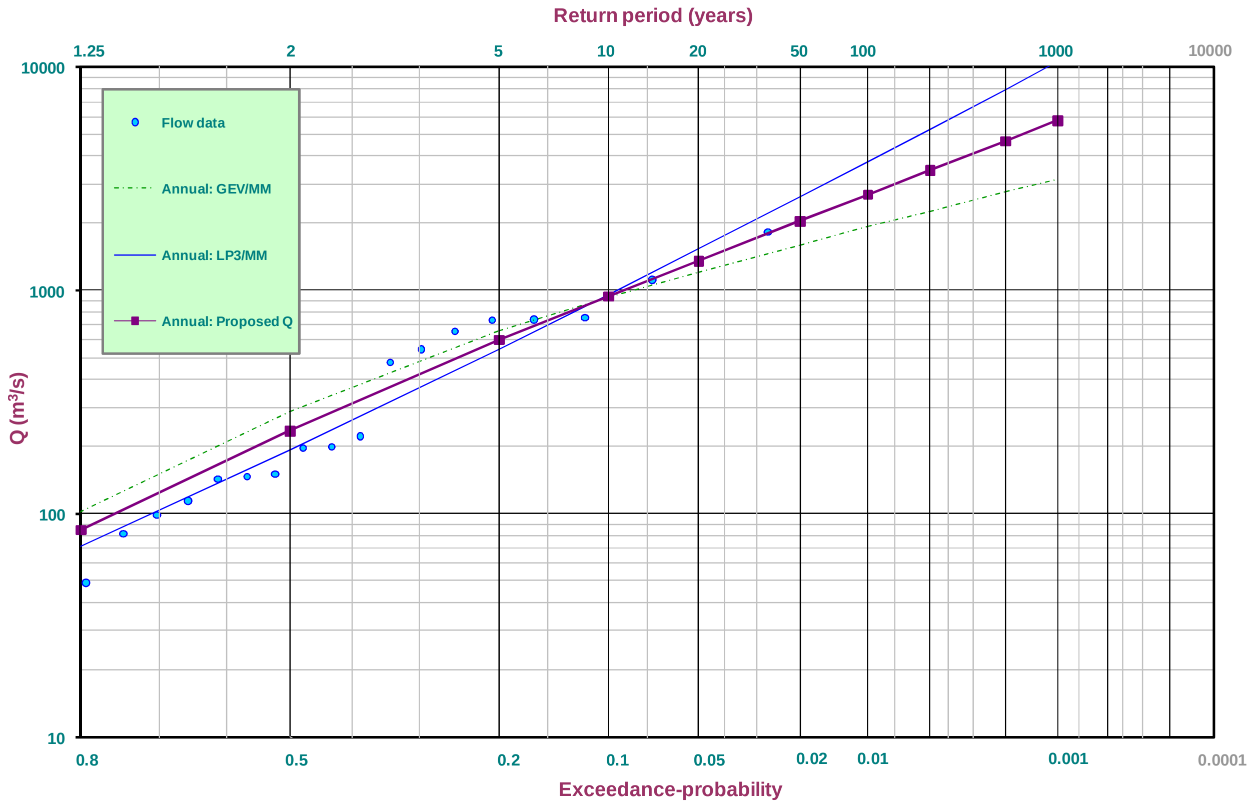

Figure C.33: C4H002 (7): Probability distribution plot

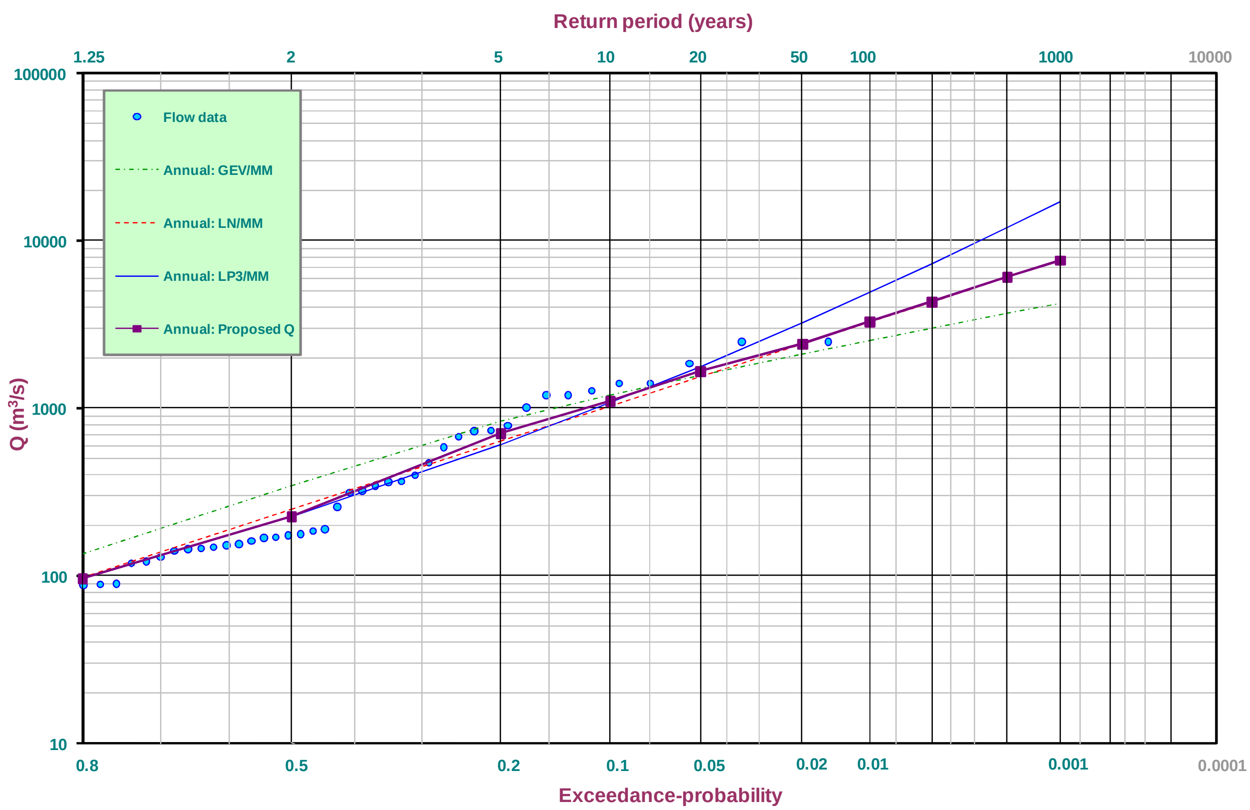

Figure C.34: C8H001 (6): Probability distribution plot

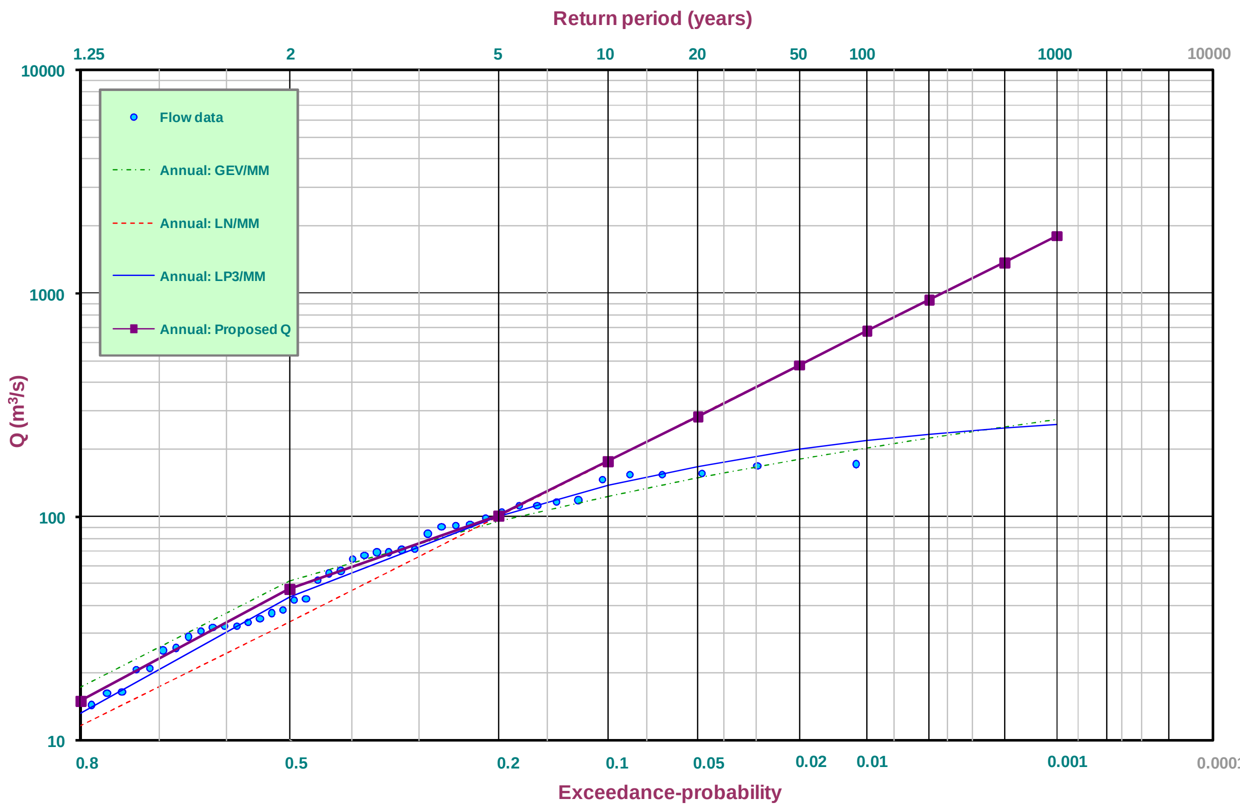

Figure C.35: C8H003 (6): Probability distribution plot

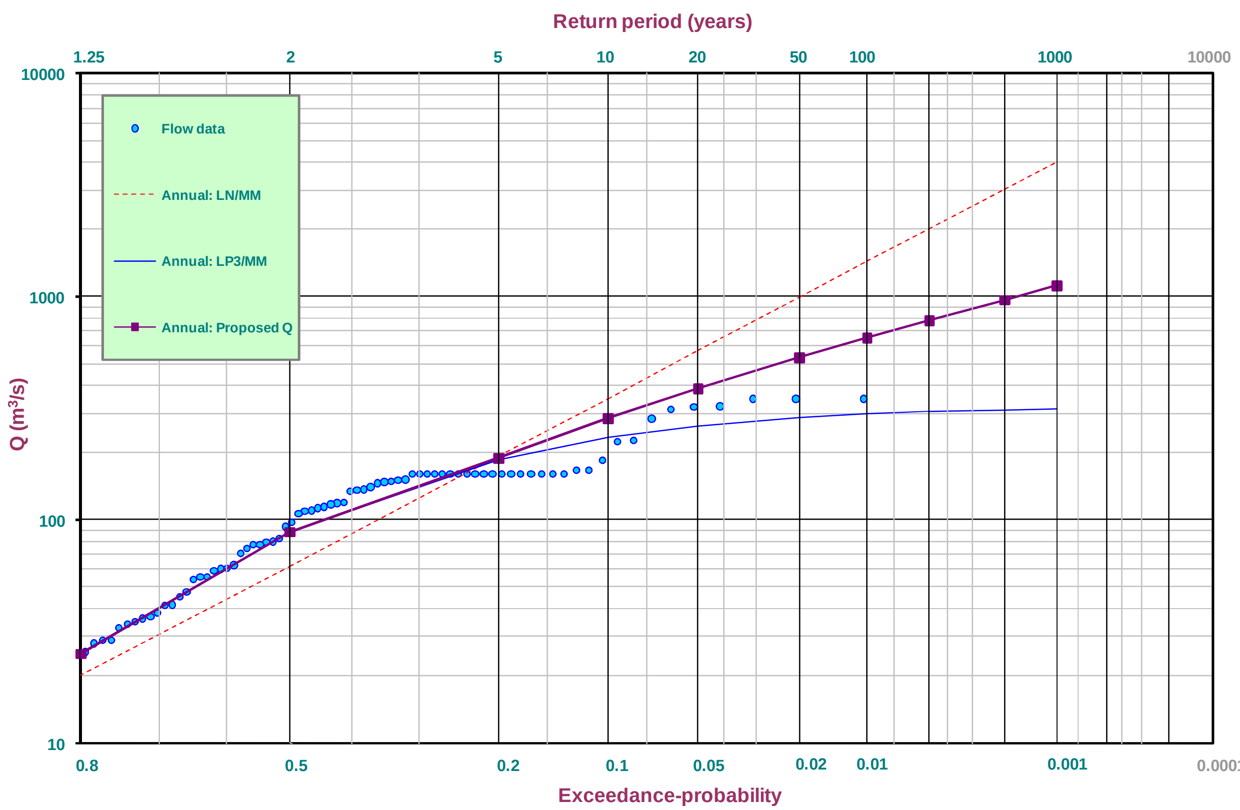

Figure C.36: D1H001 (10): Probability distribution plot

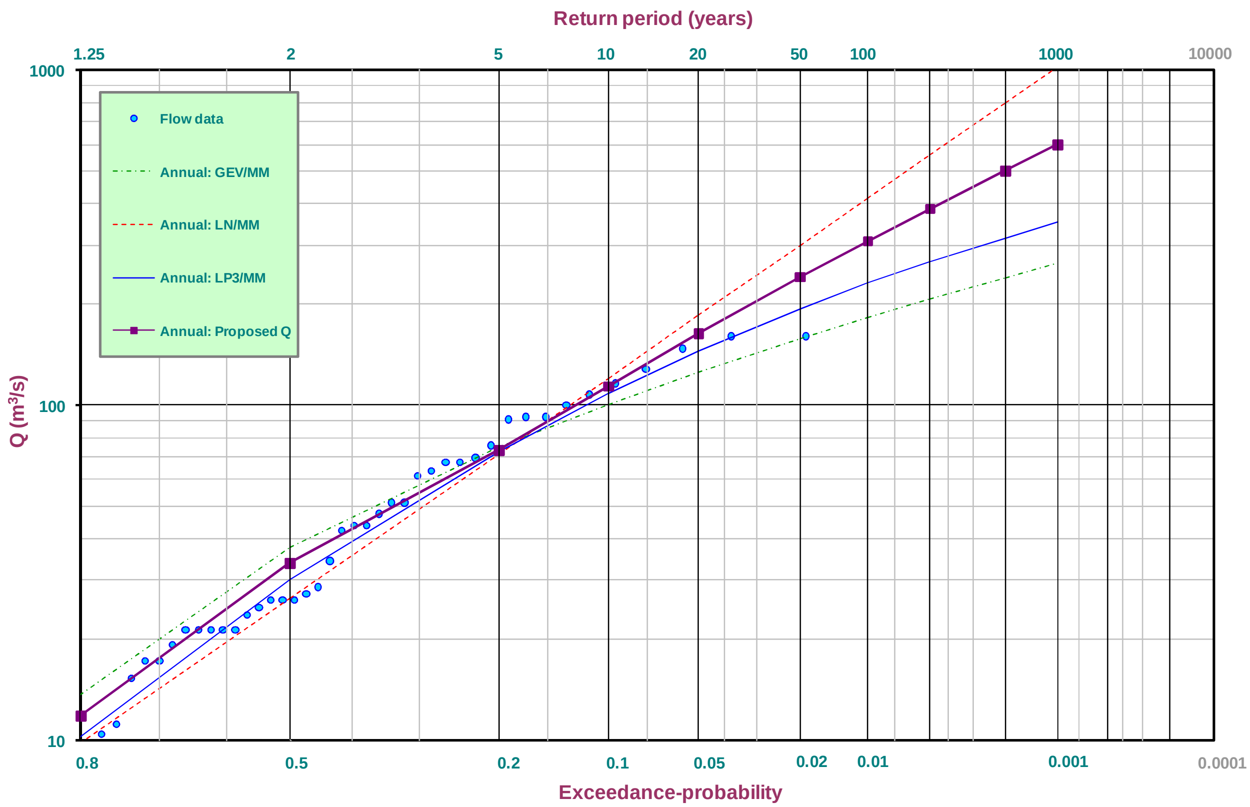

Figure C.37: D1H004 (10): Probability distribution plot

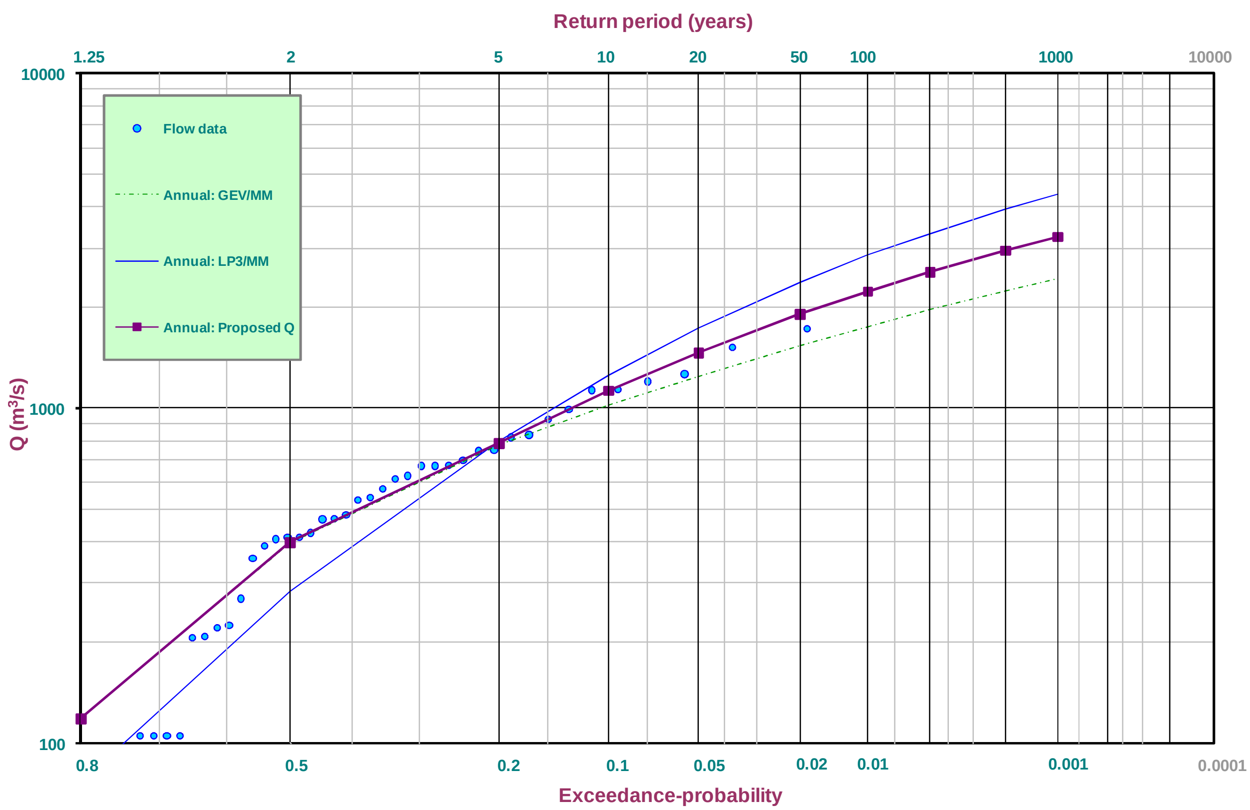

Figure C.38: D1H005 (11): Probability distribution plot

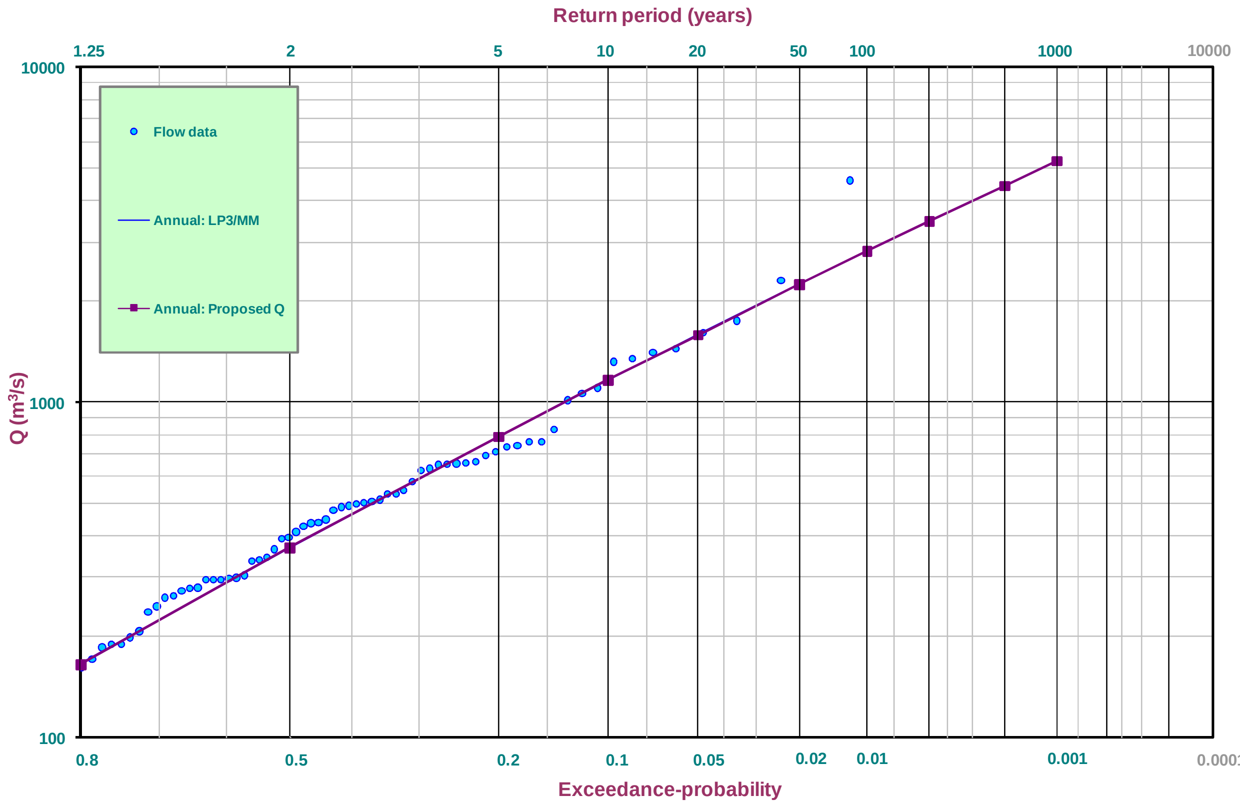

Figure C.39: E2H003 (16): Probability distribution plot

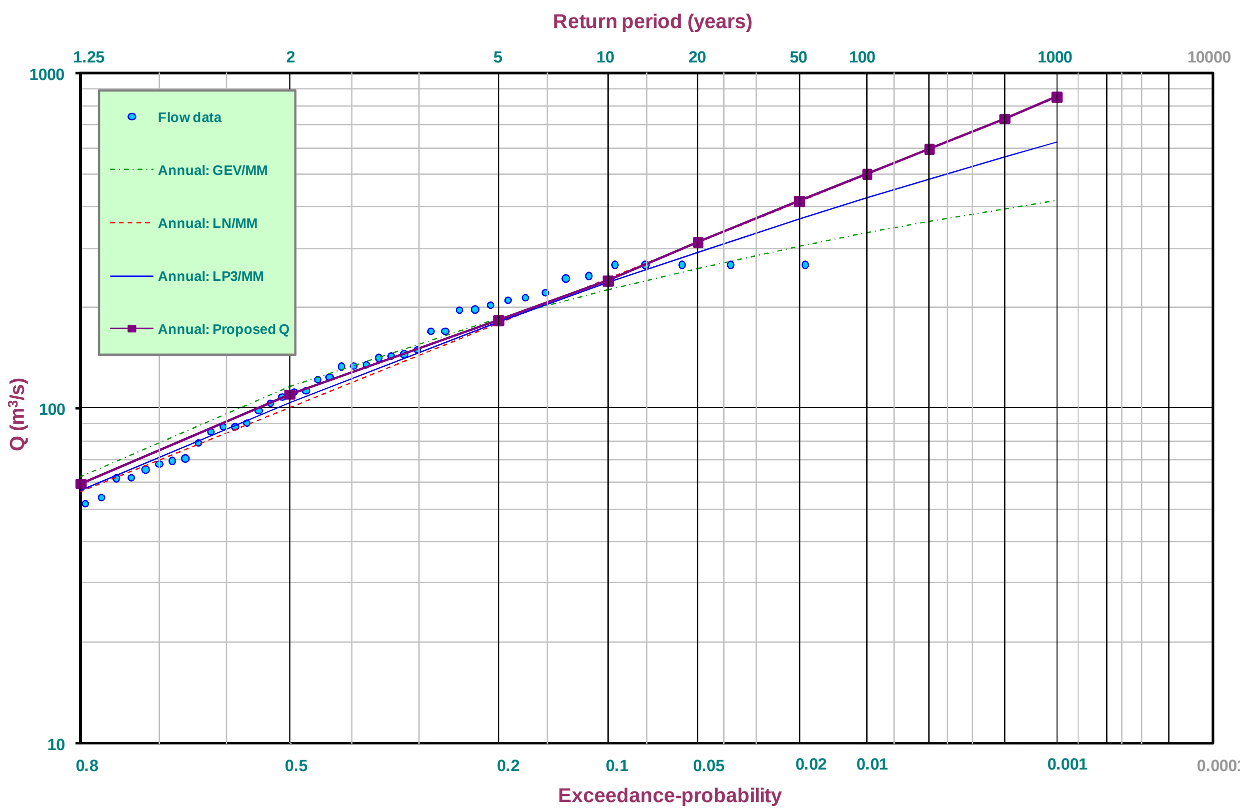

Figure C.40: G1H008 (17): Probability distribution plot

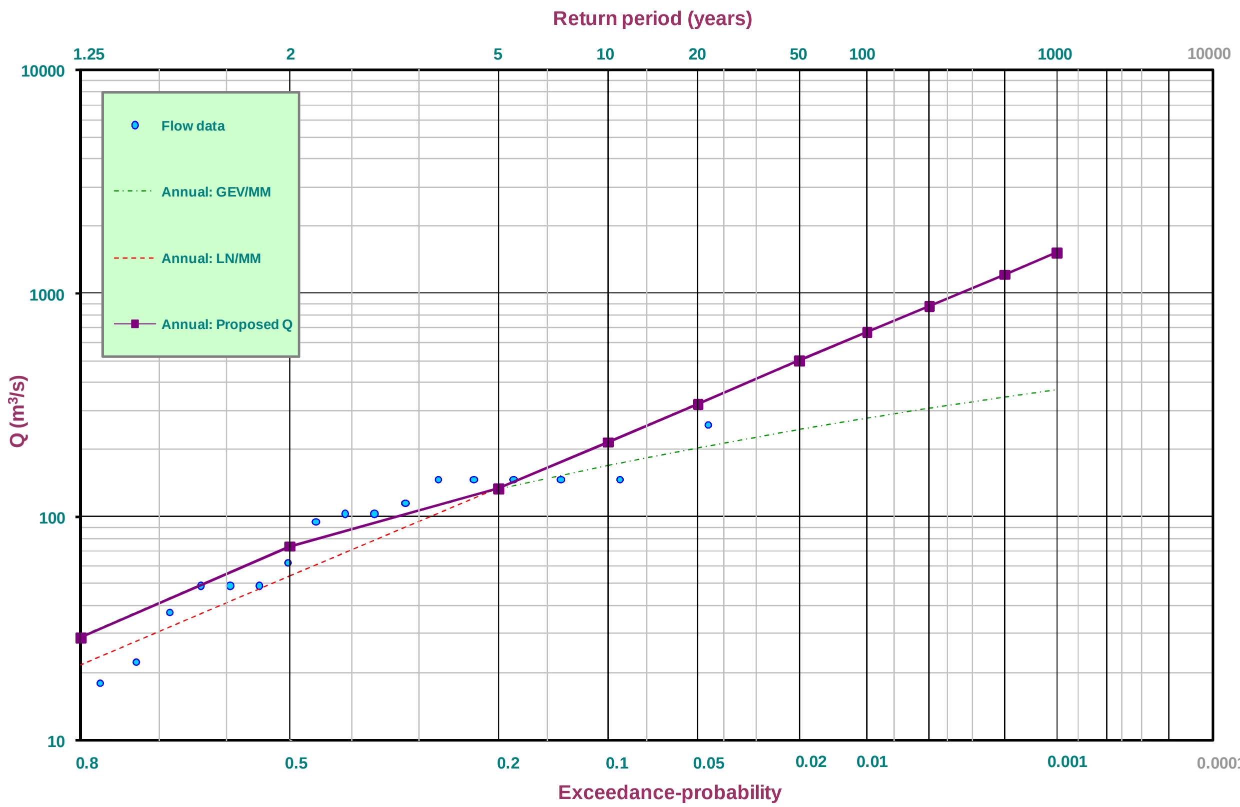

Figure C.41: H3H001 (18): Probability distribution plot

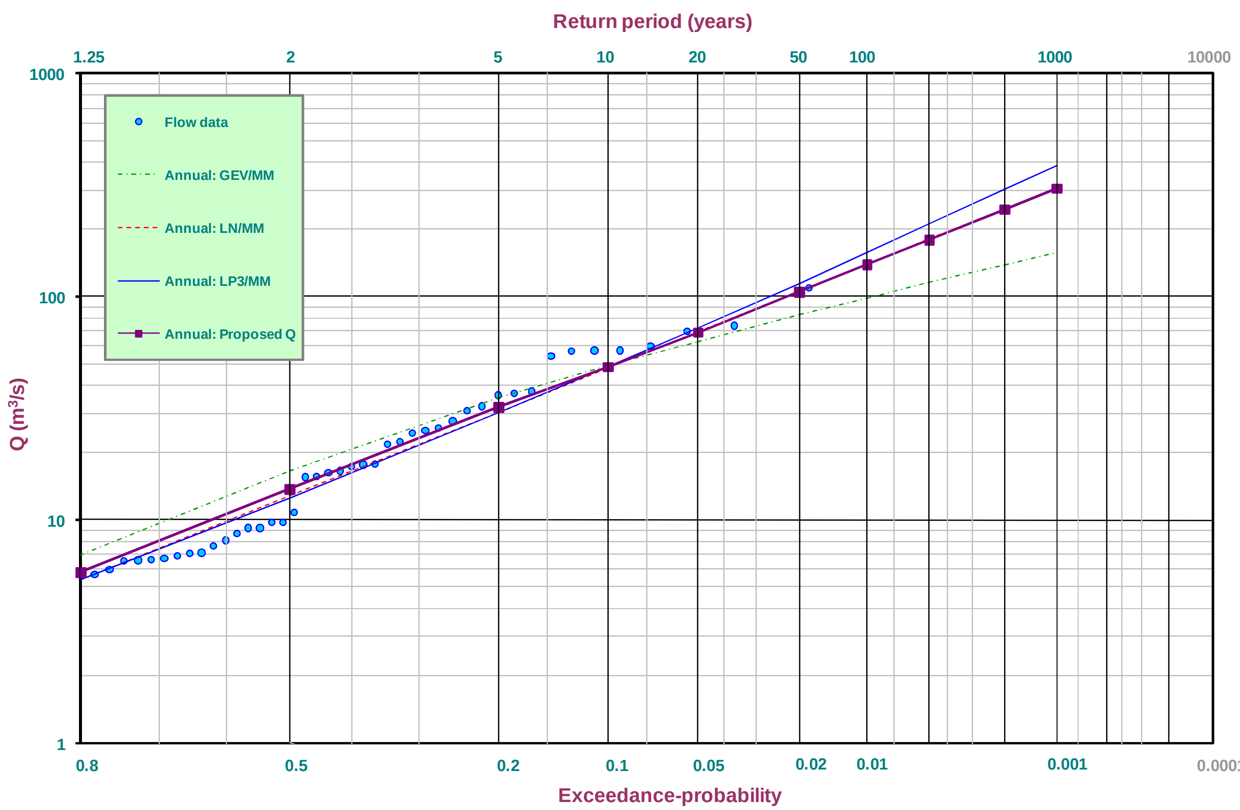

Figure C.42: H7H004 (18): Probability distribution plot

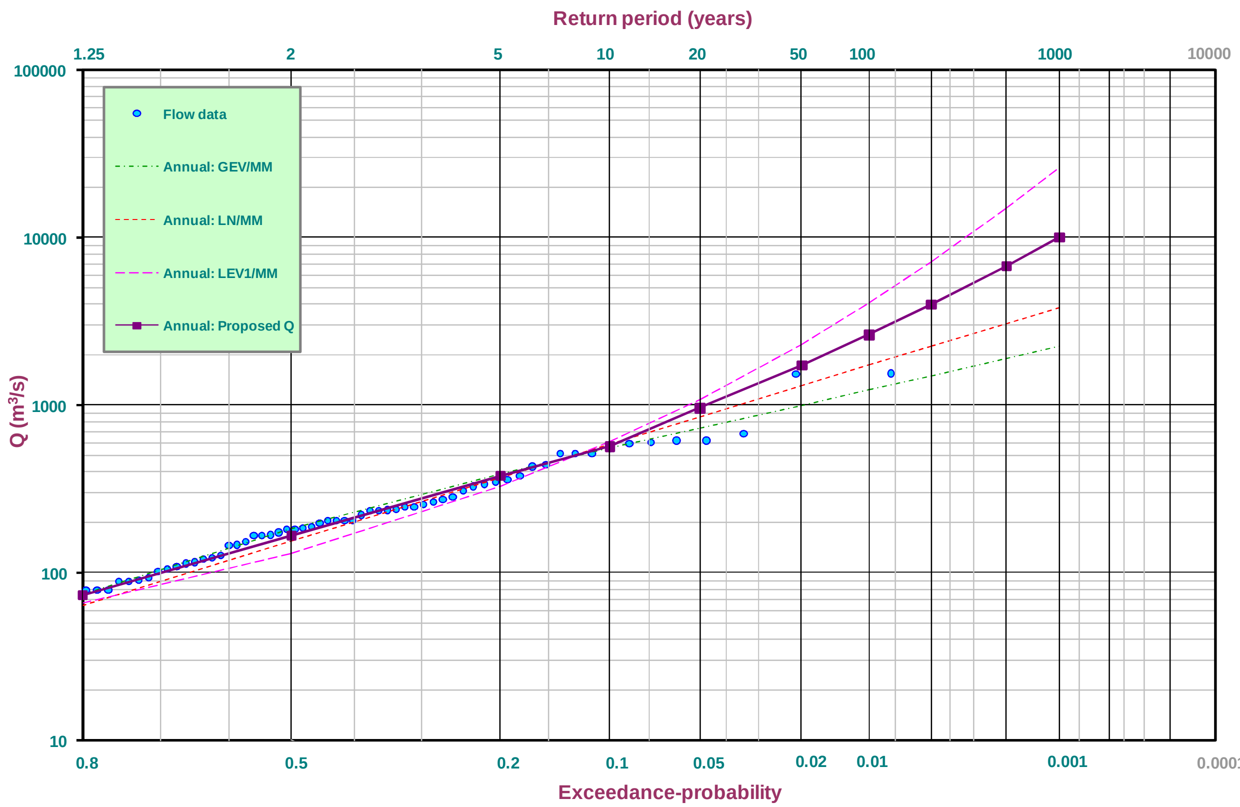

Figure C.43: Q1H001 (21): Probability distribution plot

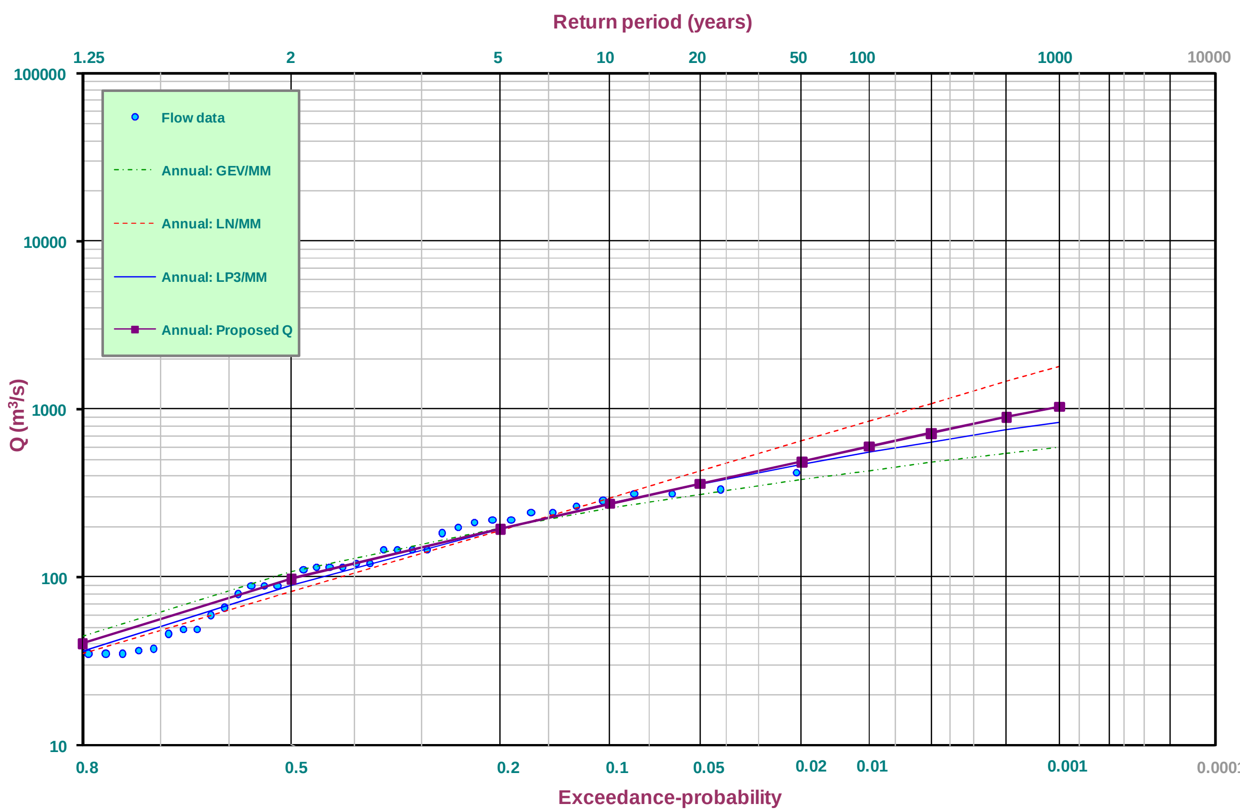

Figure C.44: Q9H008 (21): Probability distribution plot

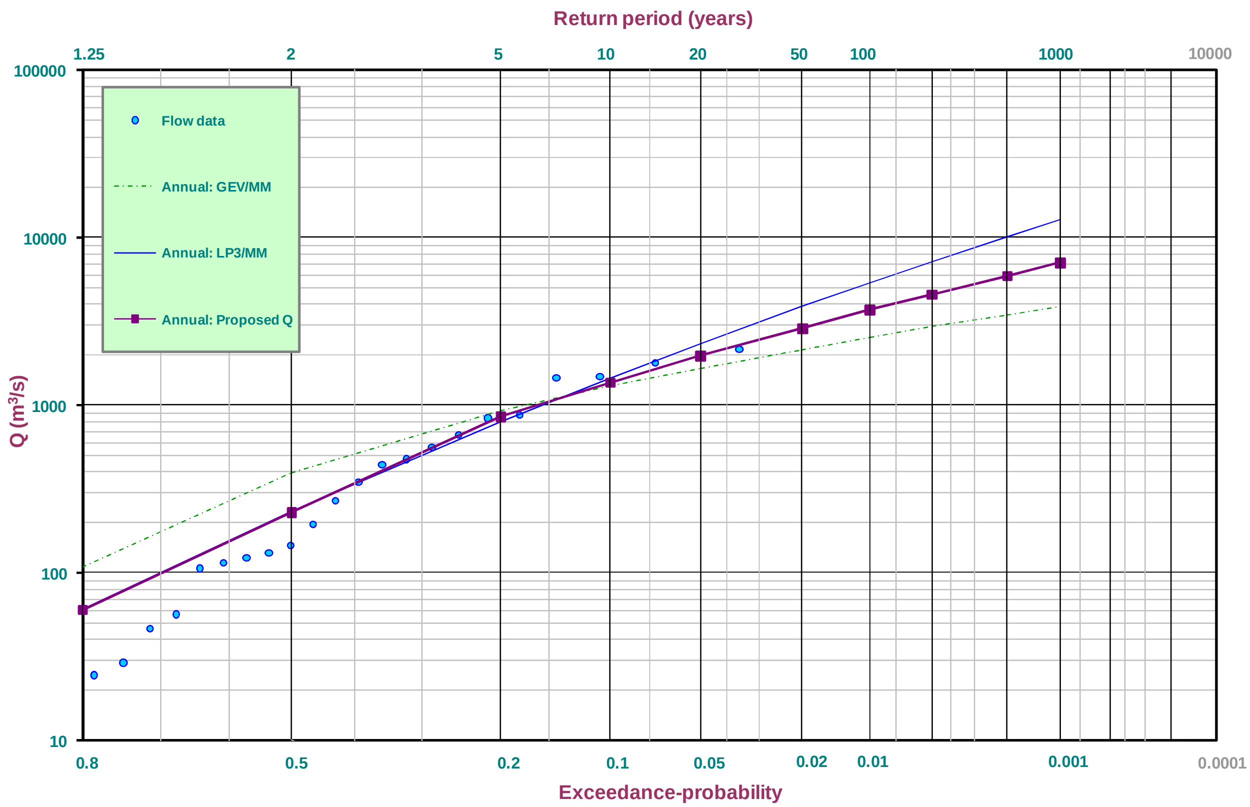

Figure C.45: Q9H010 (21): Probability distribution plot

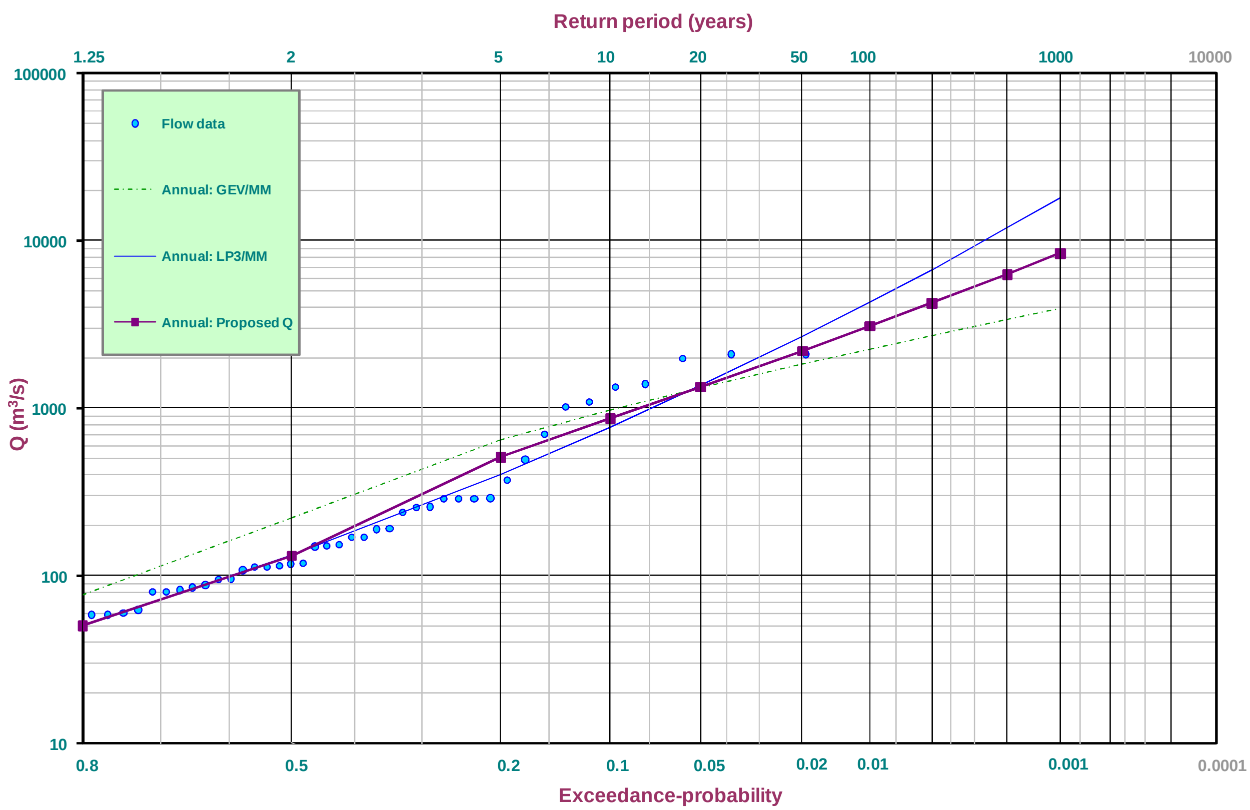

Figure C.46: Q9H012 (21): Probability distribution plot

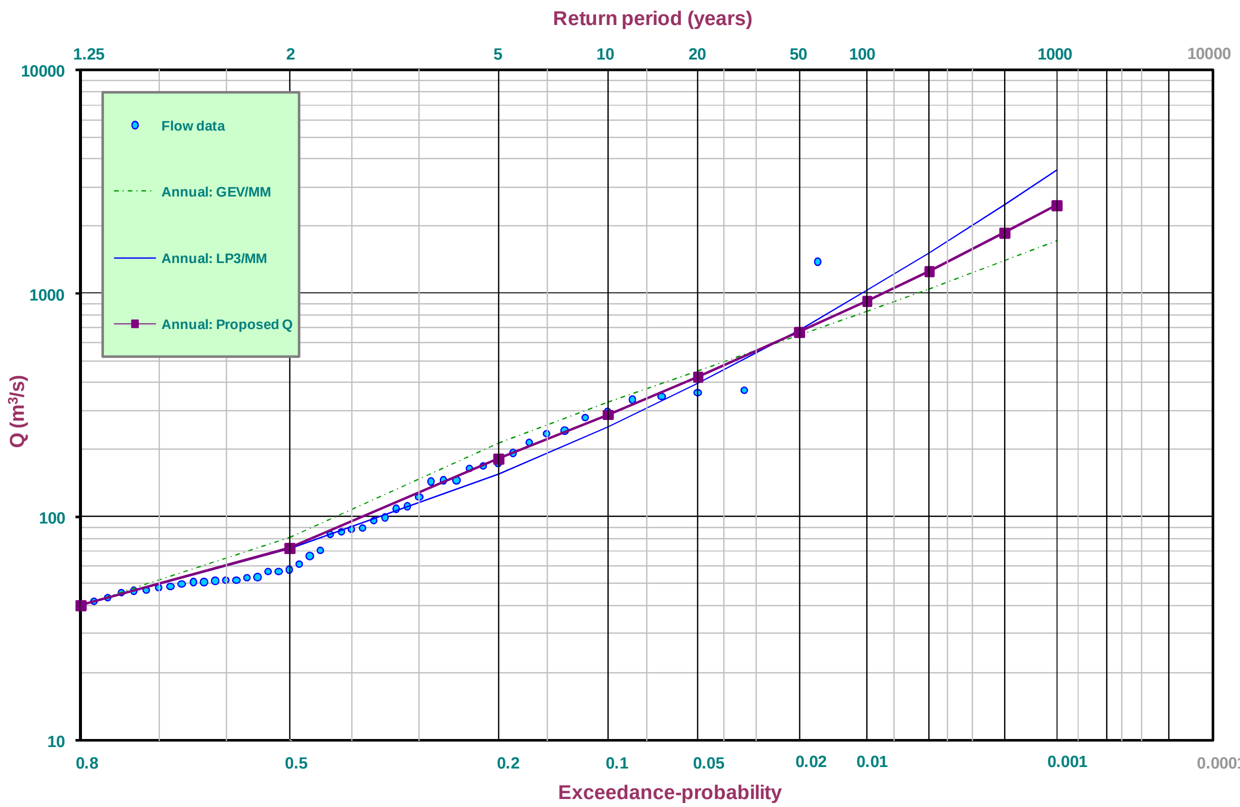

Figure C.47: V2H002 (26): Probability distribution plot

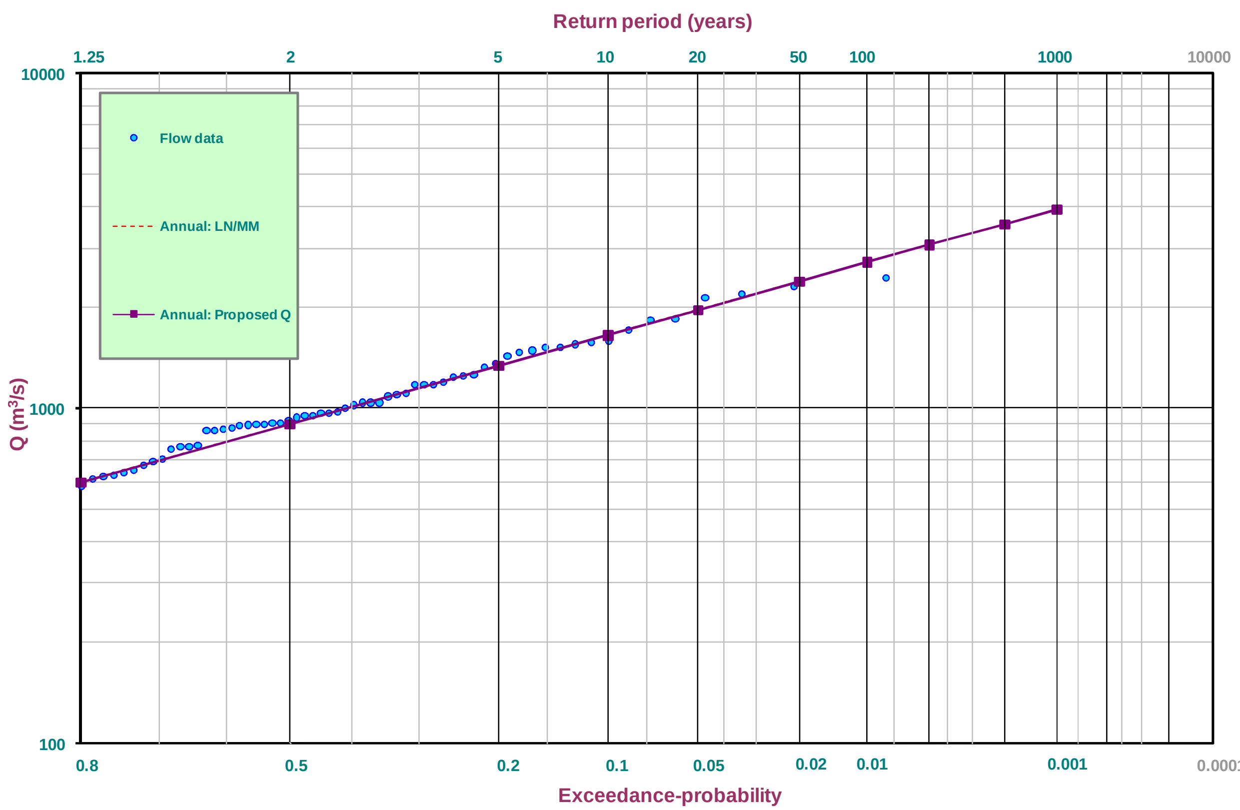

Figure C.48: V6H002 (26): Probability distribution plot

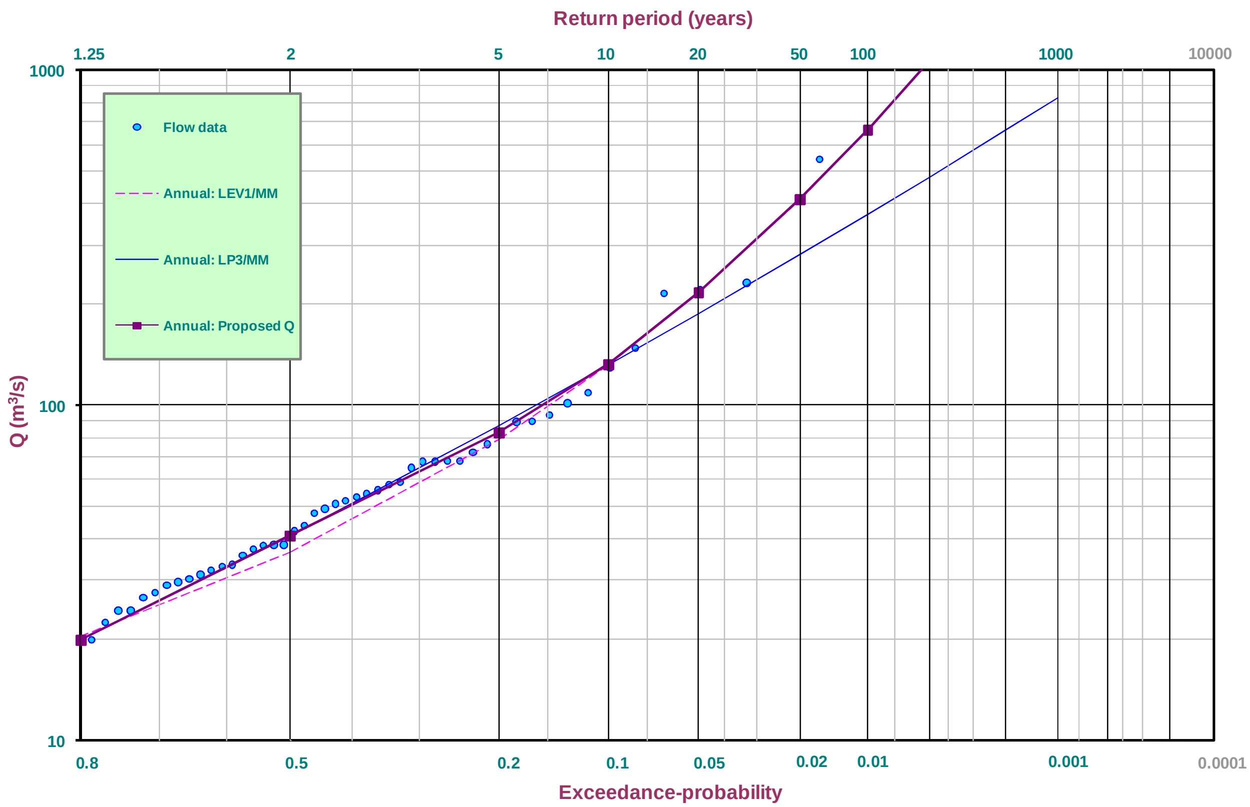

Figure C.49: W5H005 (28): Probability distribution plot

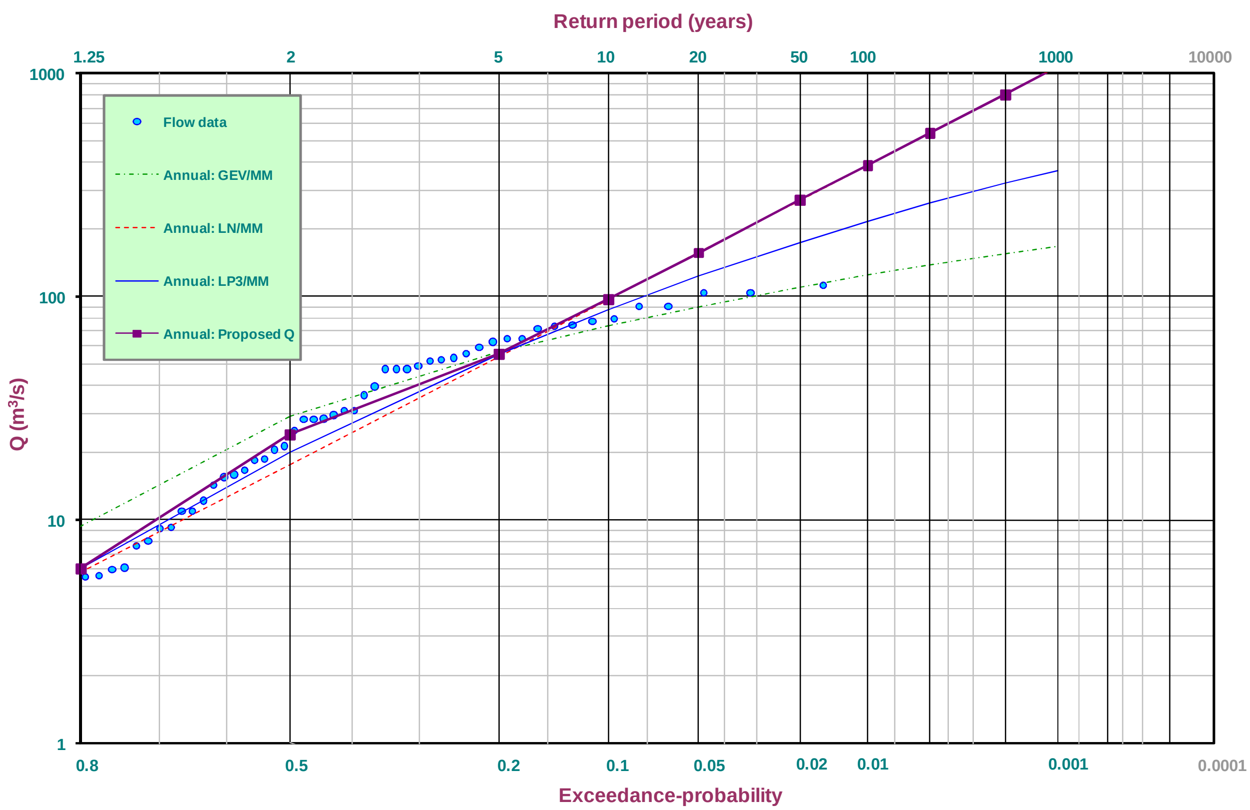

Figure C.50: X2H010 (29): Probability distribution plot

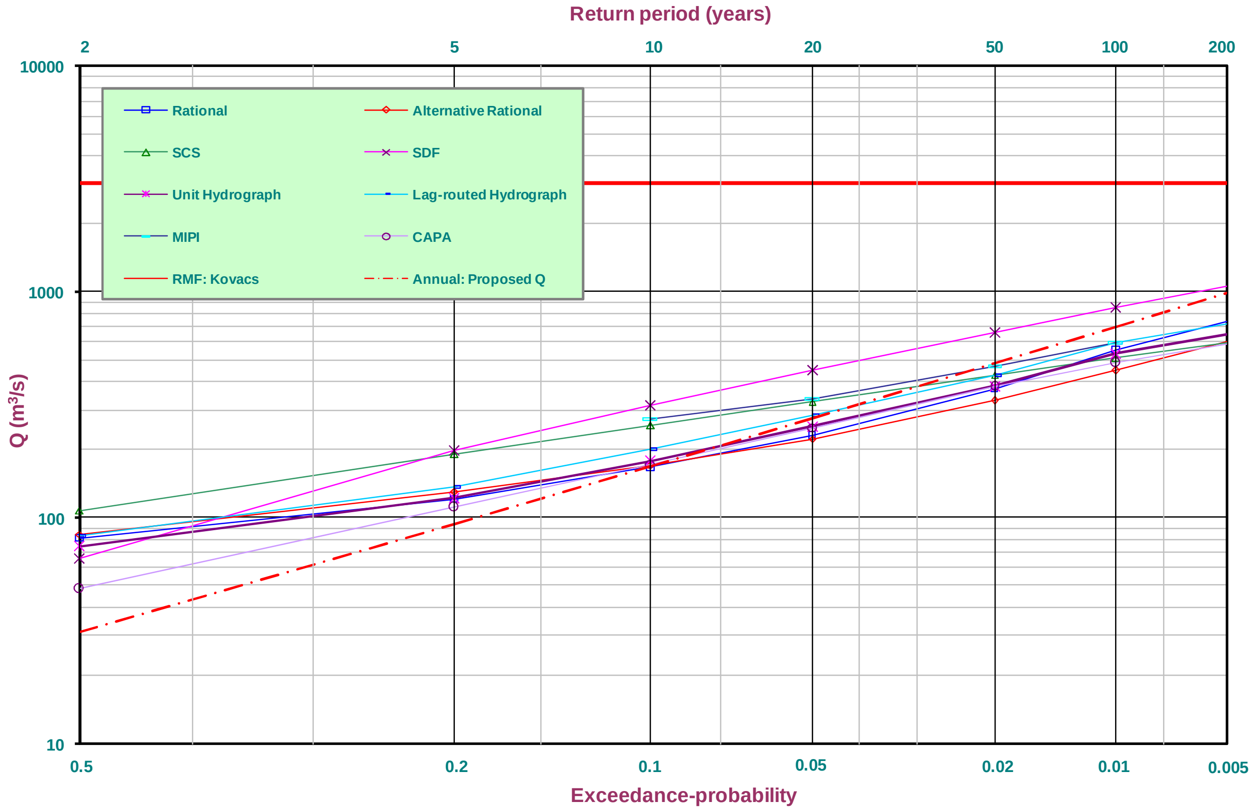

Figure C.51: C5R001: Probabilistic plot of flood estimation methods

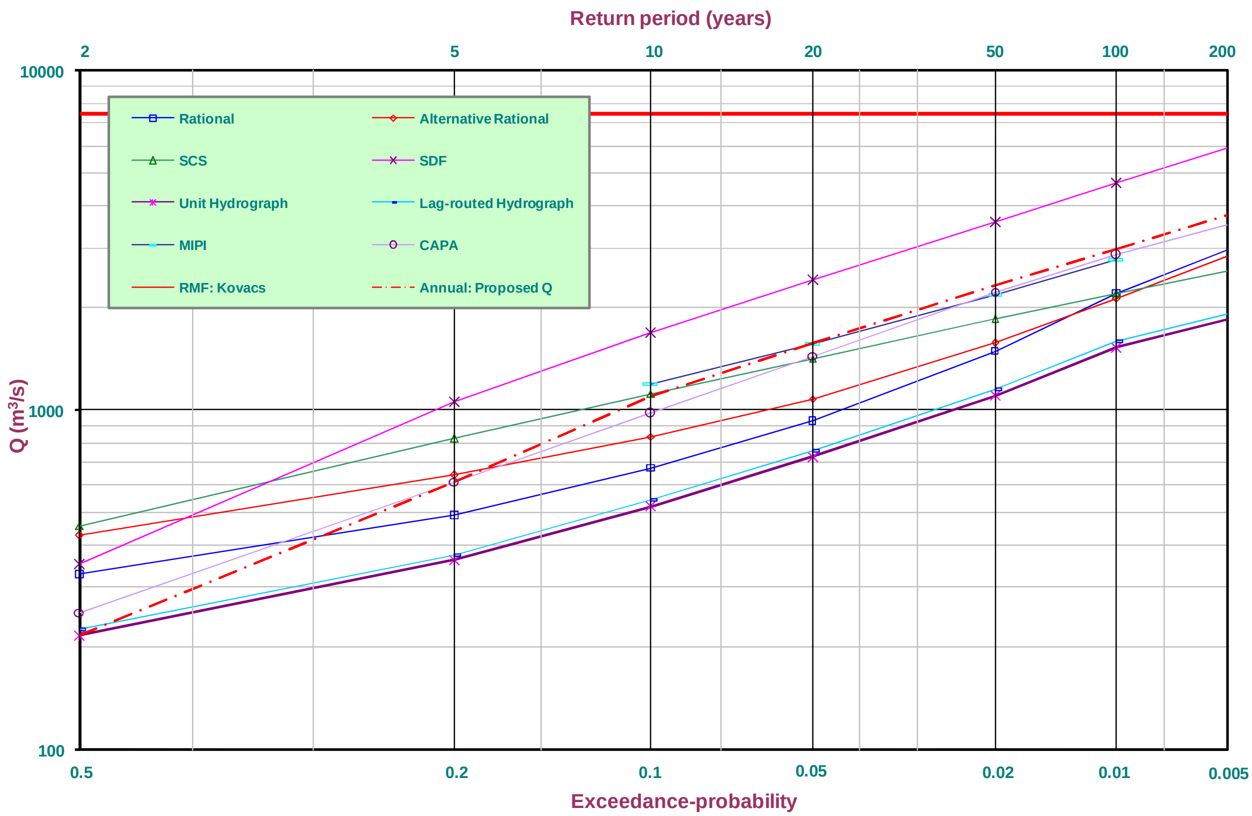

Figure C.52: C5R002: Probabilistic plot of flood estimation methods

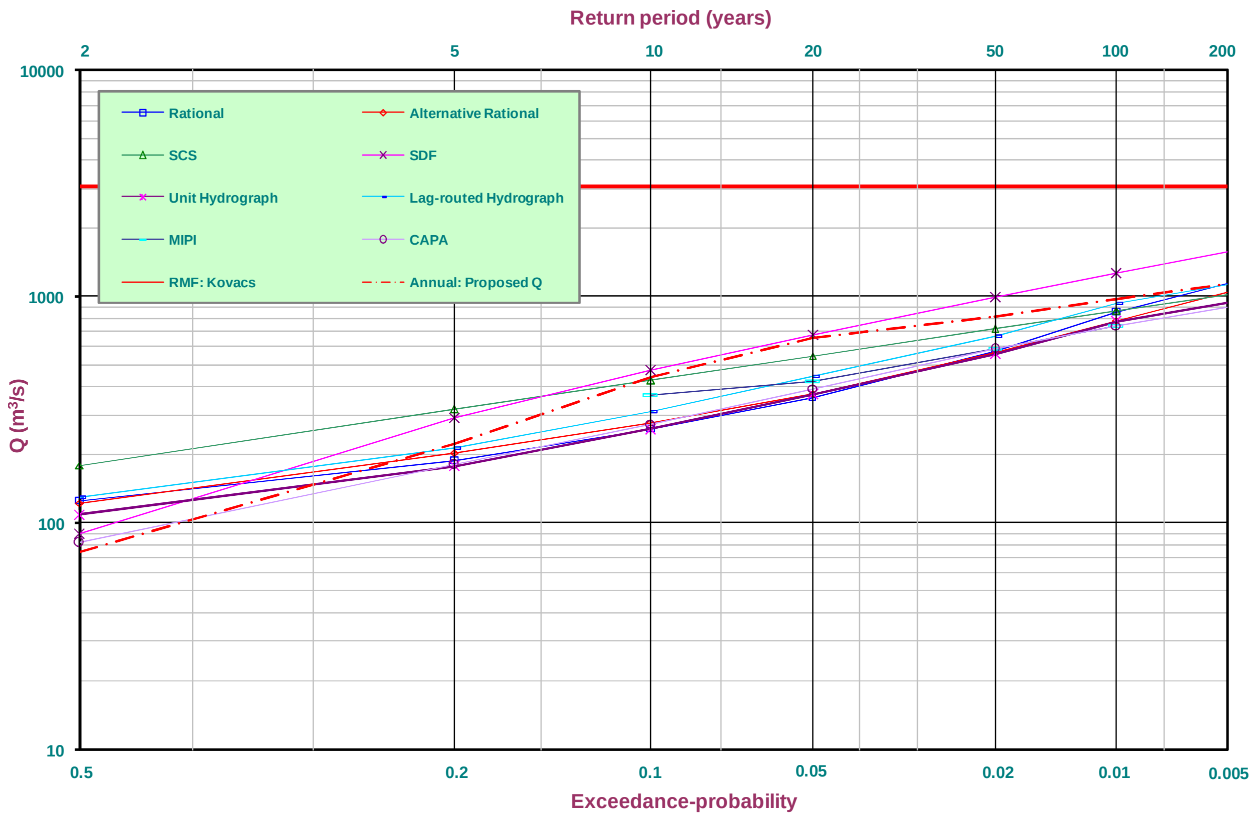

Figure C.53: C5R003: Probabilistic plot of flood estimation methods

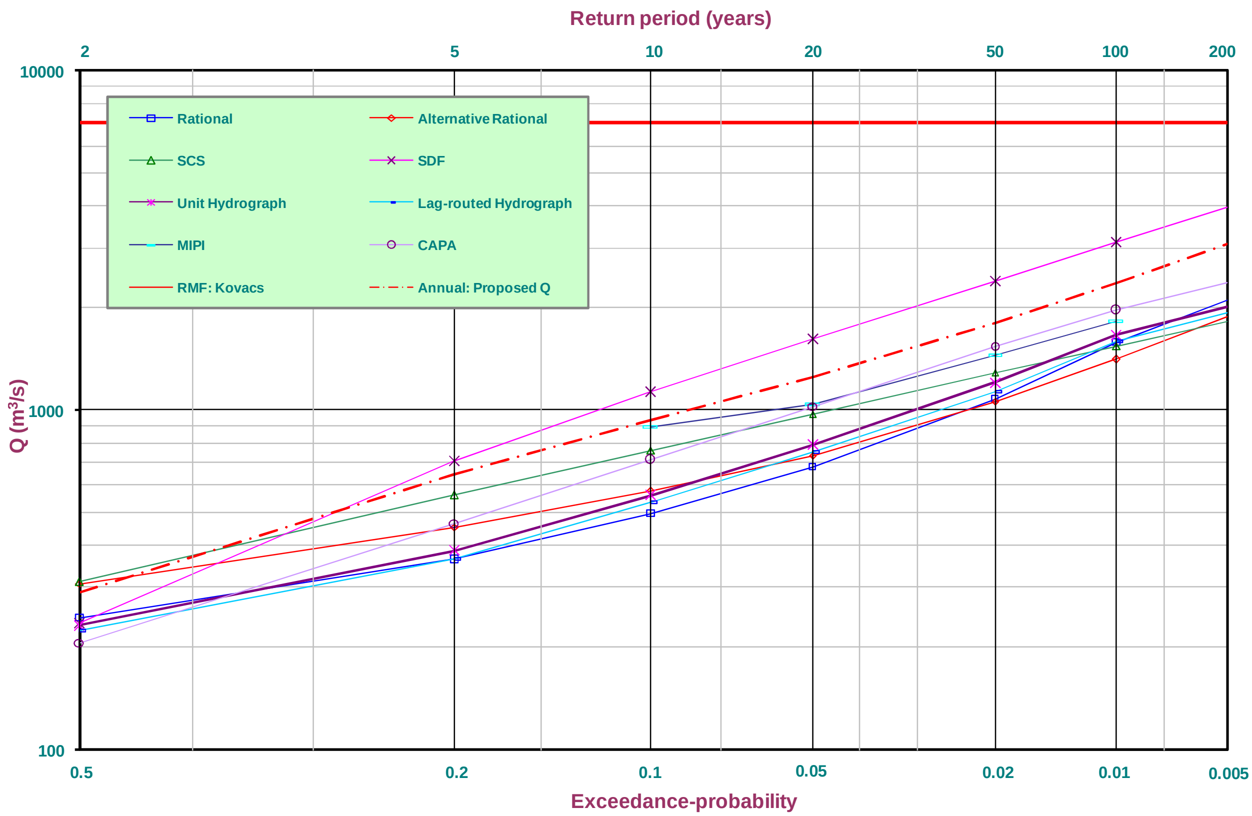

Figure C.54: C5R004: Probabilistic plot of flood estimation methods

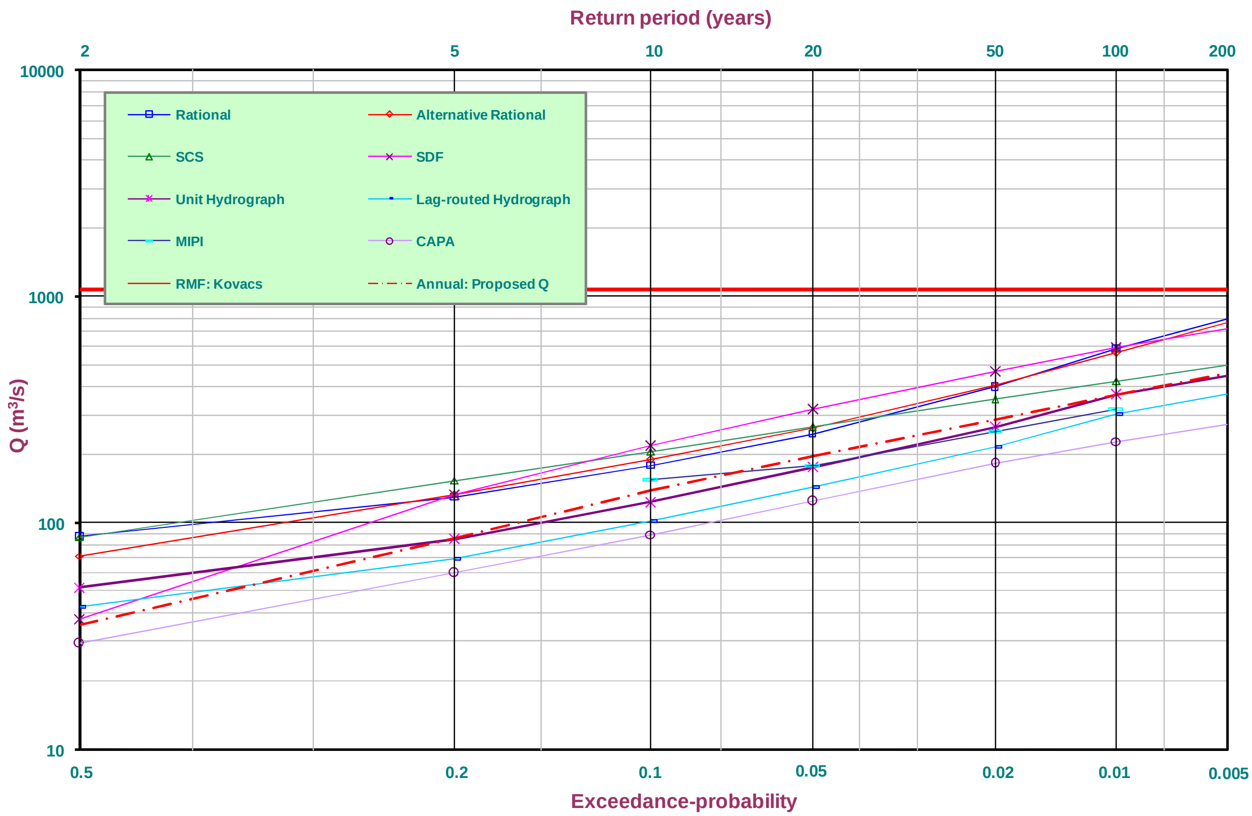

Figure C.55: C5R005: Probabilistic plot of flood estimation methods

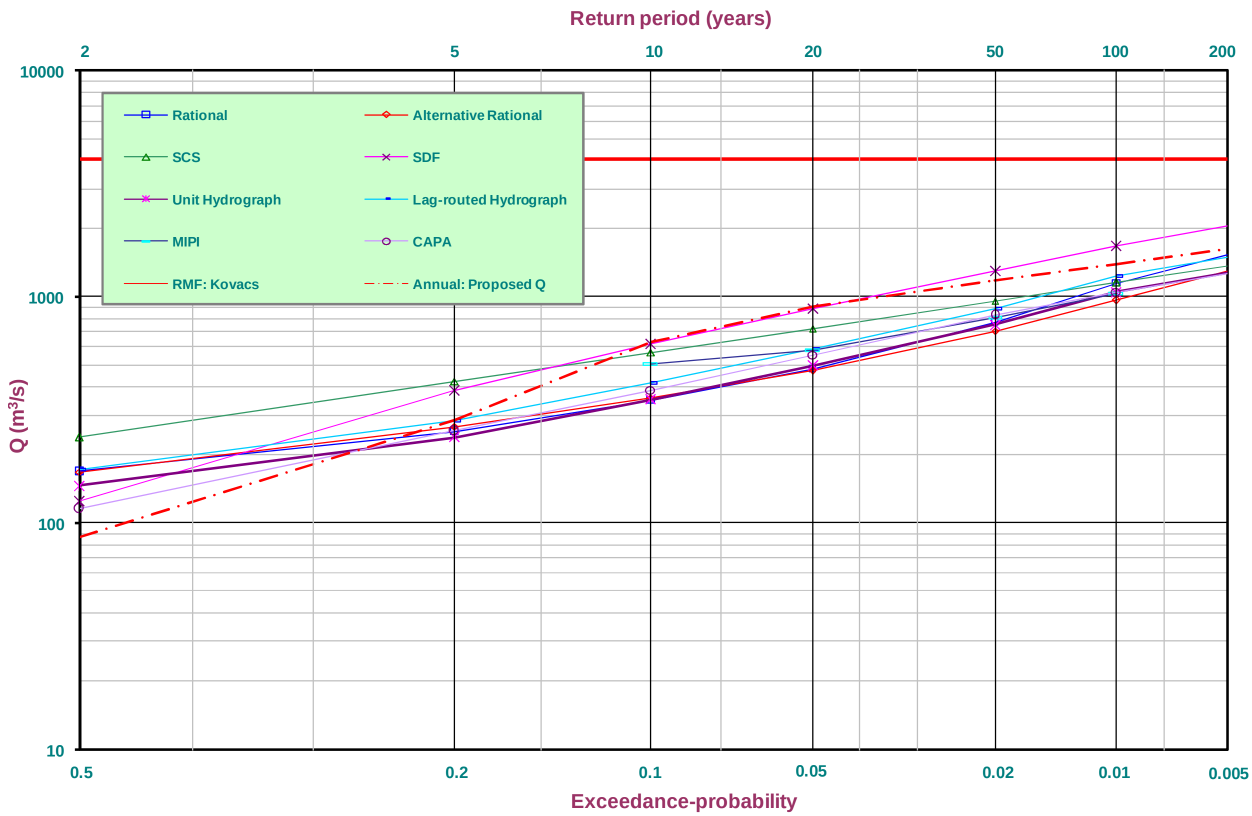

Figure C.56: C5H003: Probabilistic plot of flood estimation methods

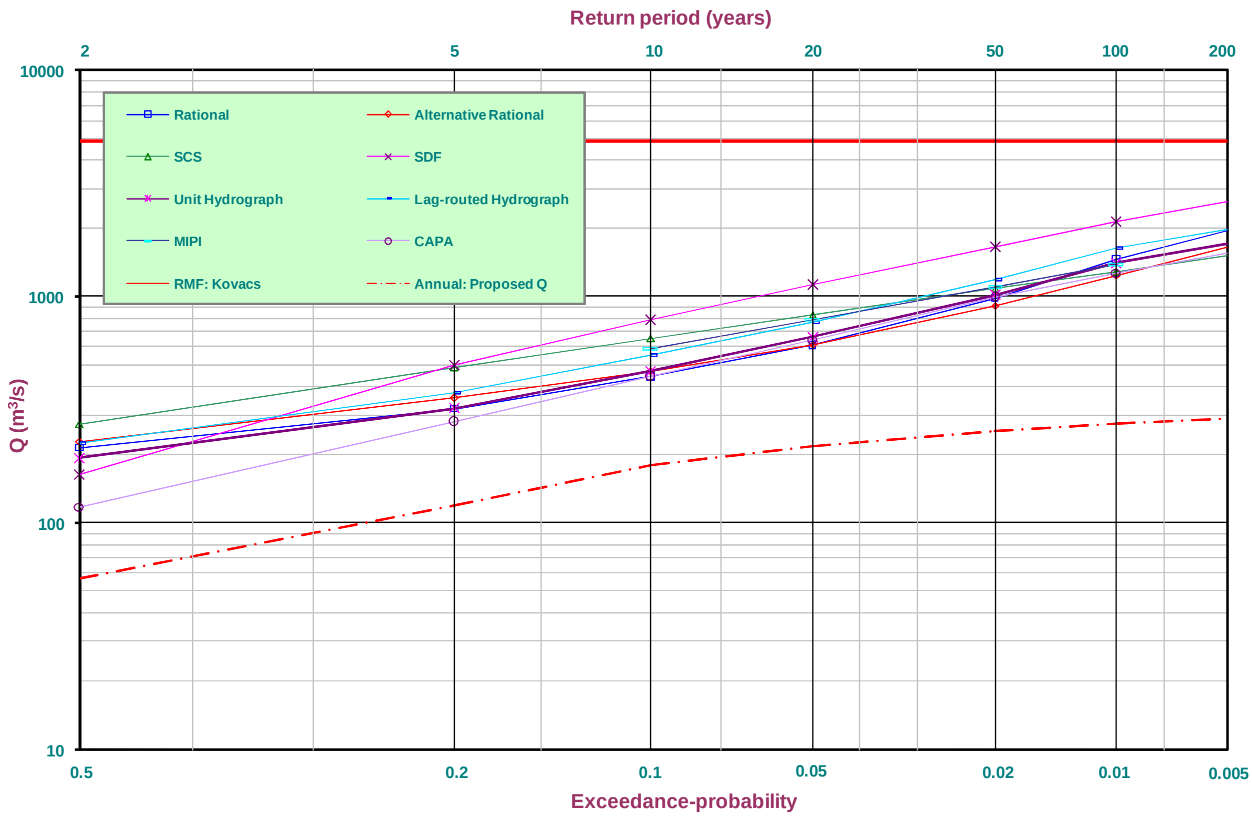

Figure C.57: C5H012: Probabilistic plot of flood estimation methods

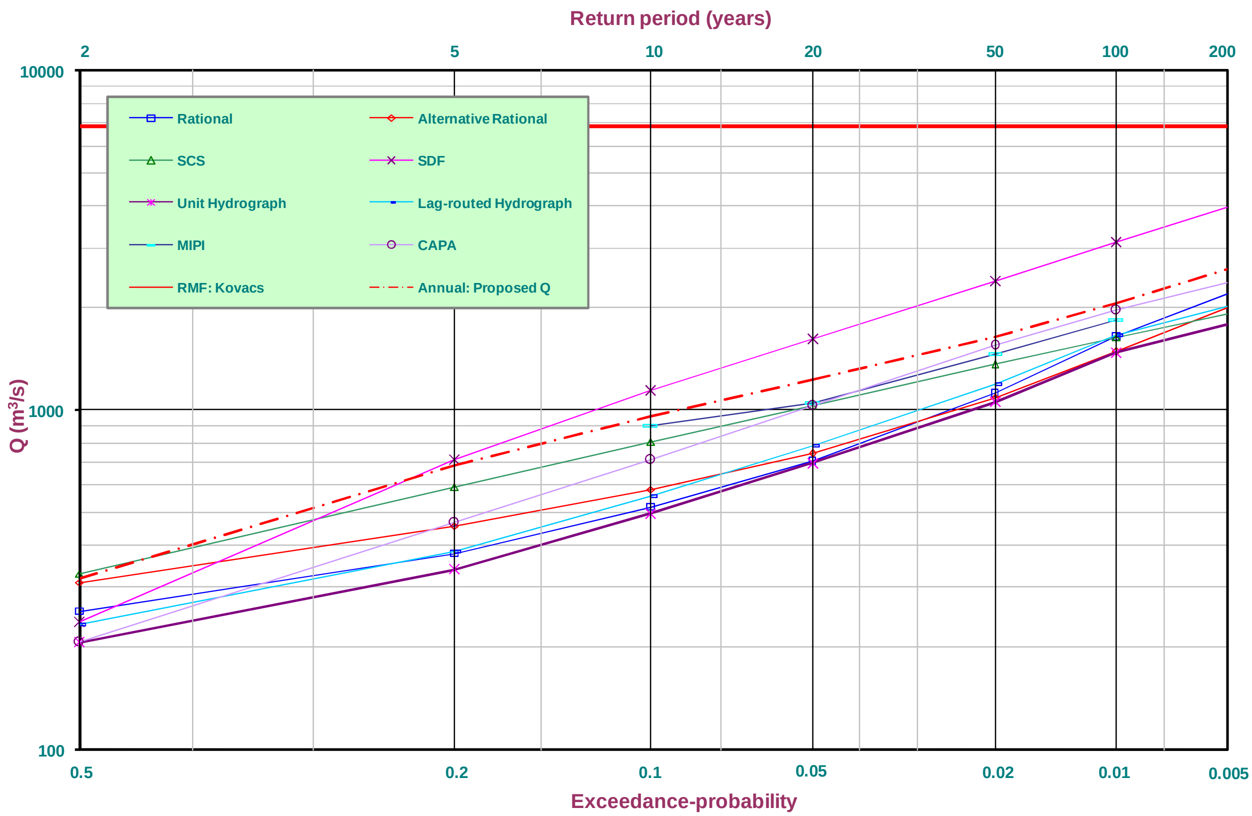

Figure C.58: C5H015: Probabilistic plot of flood estimation methods

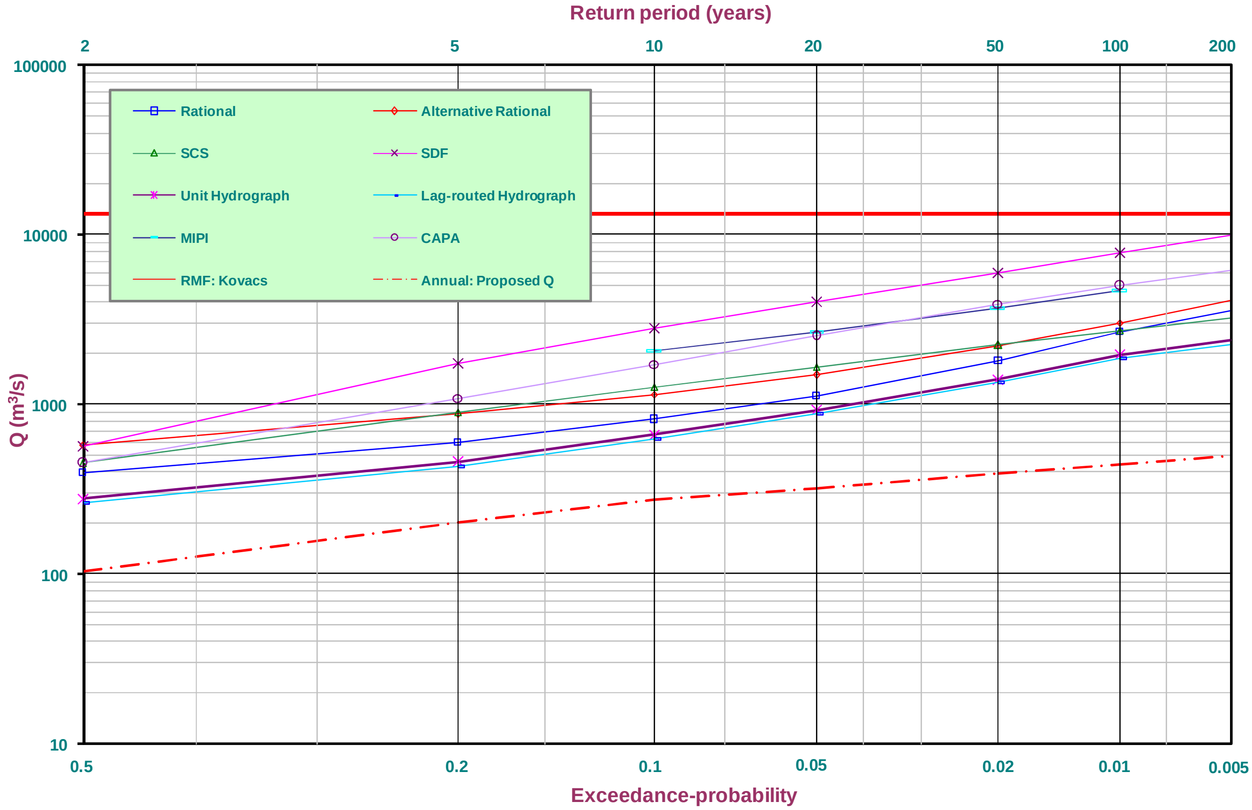

Figure C.59: C5H016: Probabilistic plot of flood estimation methods

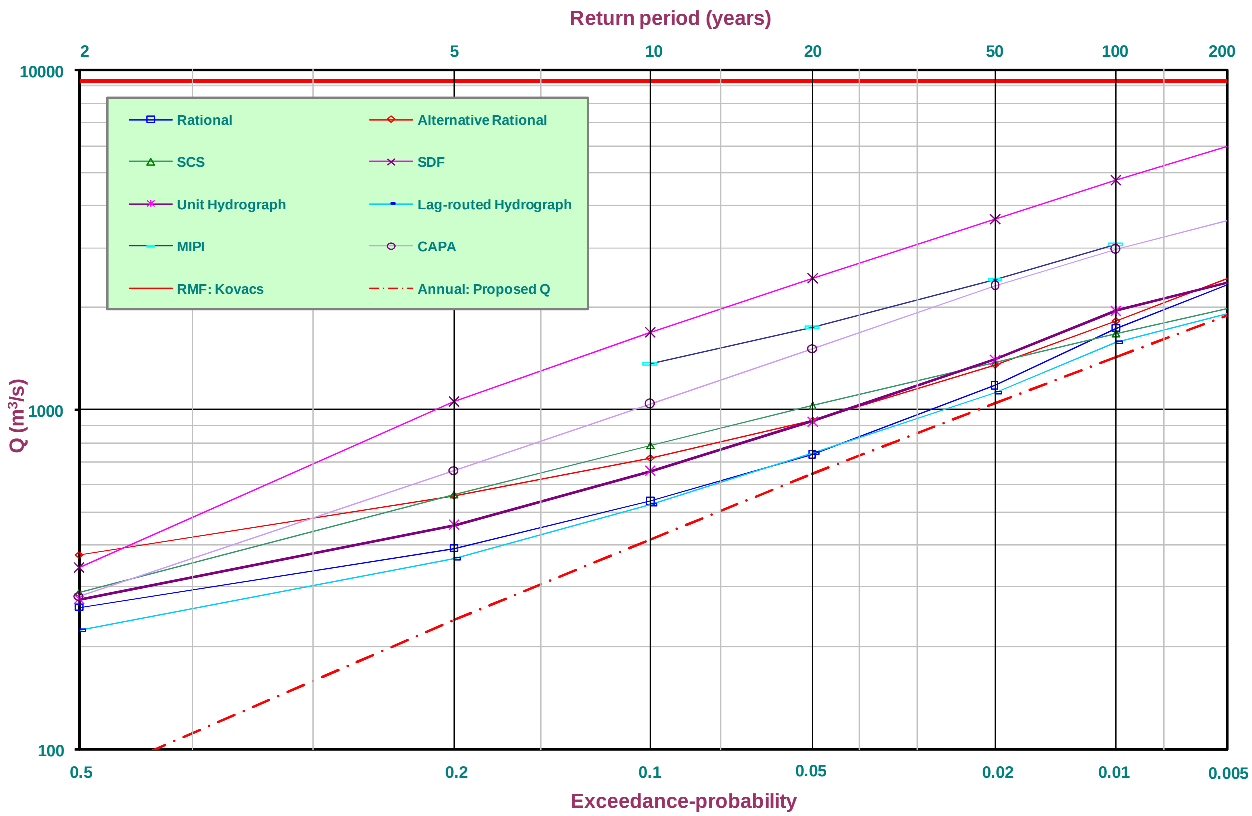

Figure C.60: C5H018: Probabilistic plot of flood estimation methods

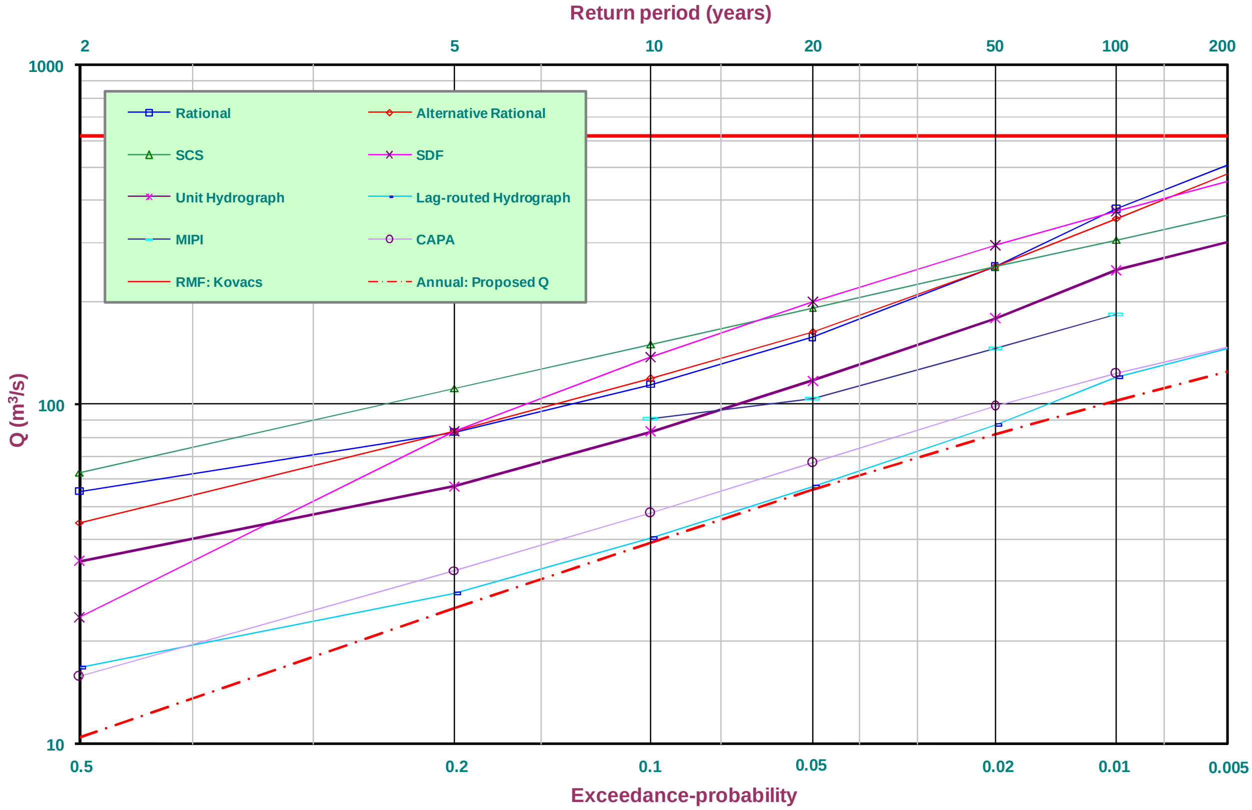

Figure C.61: C5H022: Probabilistic plot of flood estimation methods

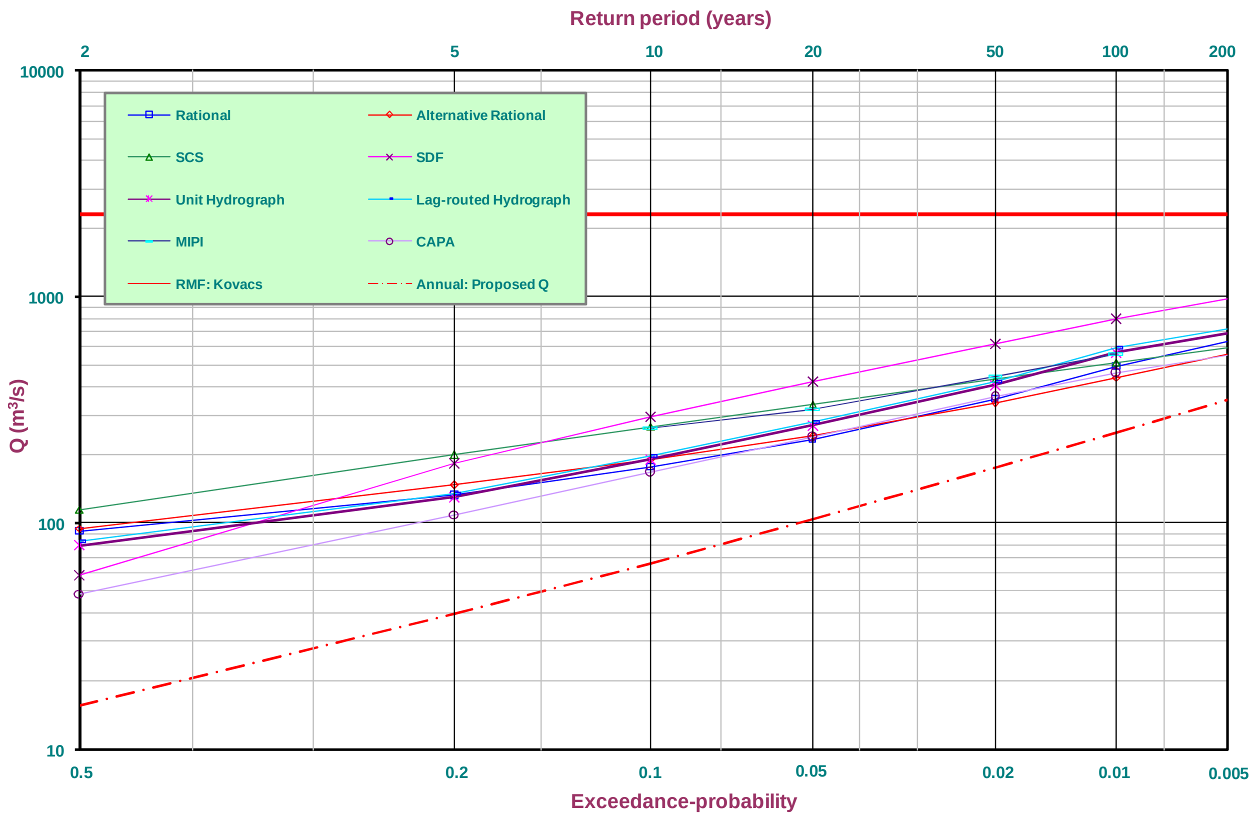

Figure C.62: C5H054: Probabilistic plot of flood estimation methods

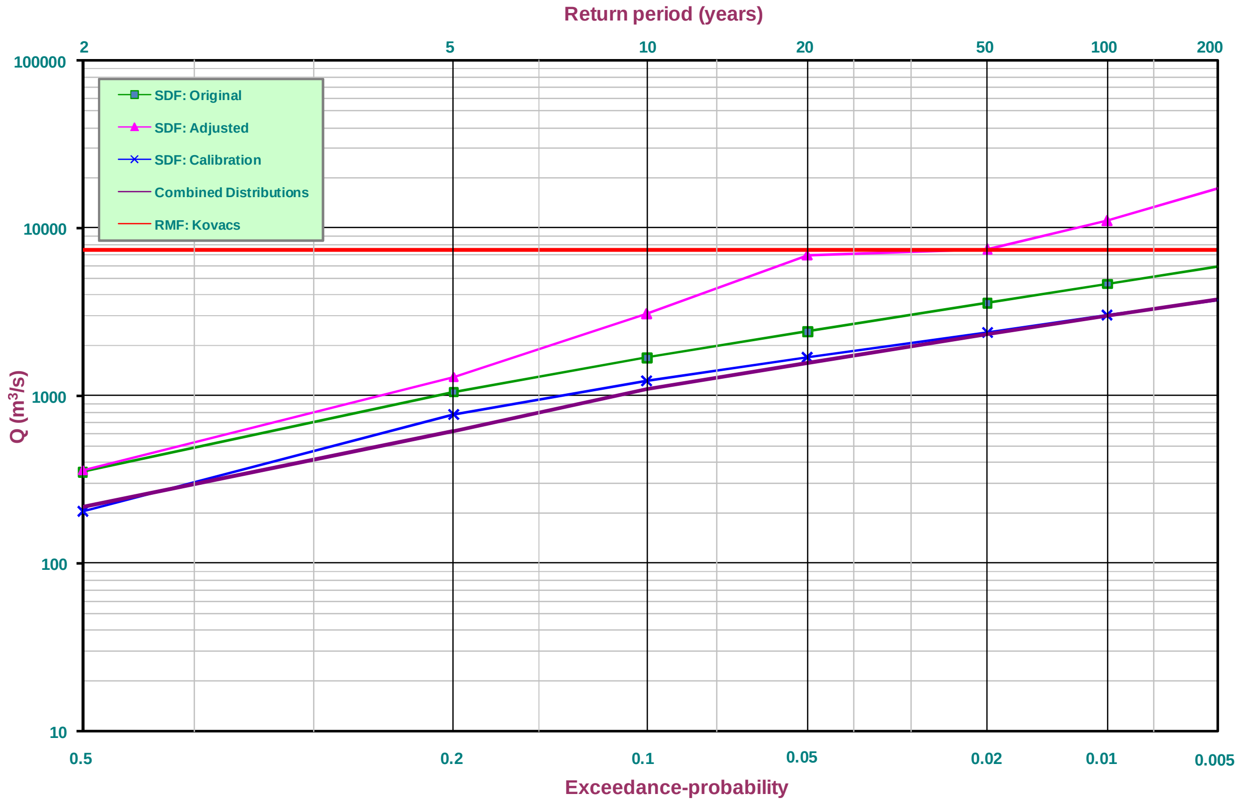

Figure C.63: C5R002: Probabilistic plot (calibrated SDF method)

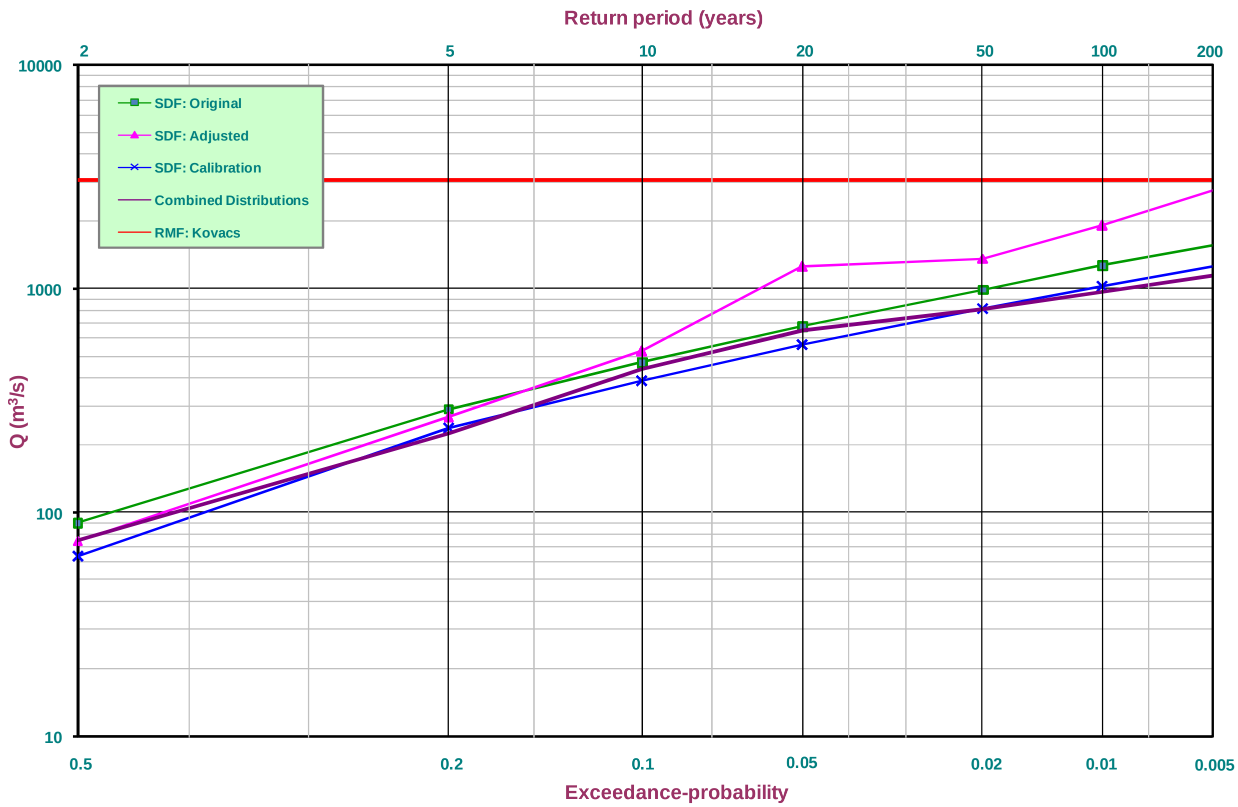

Figure C.64: C5R003: Probabilistic plot (calibrated SDF method)

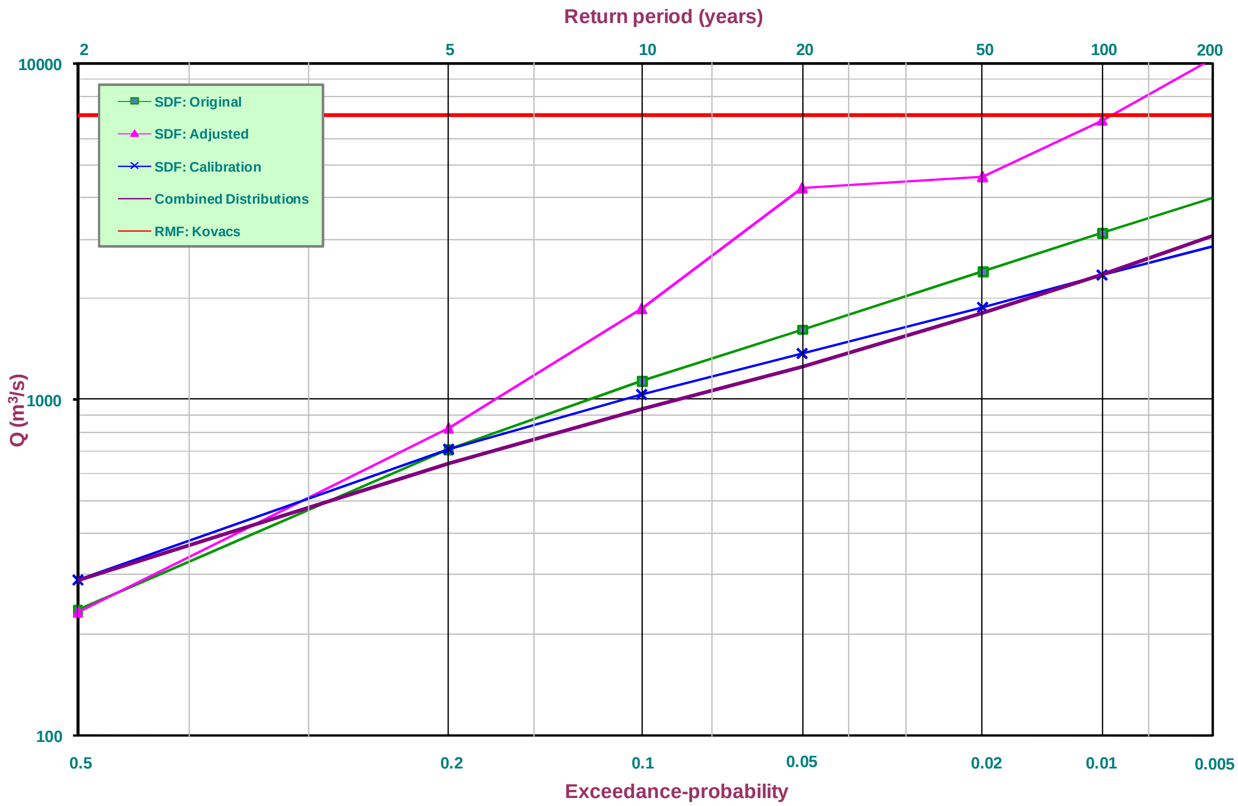

Figure C.65: C5R004: Probabilistic plot (calibrated SDF method)

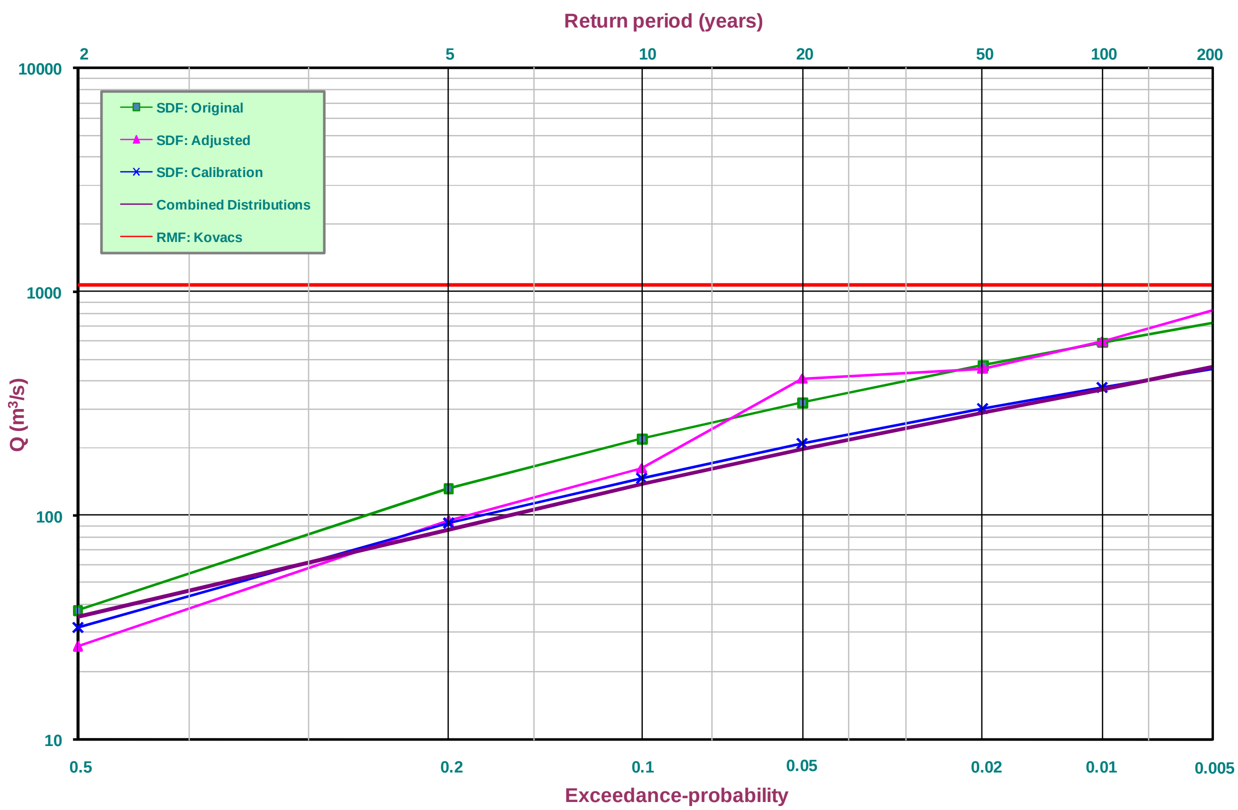

Figure C.66: C5R005: Probabilistic plot (calibrated SDF method)

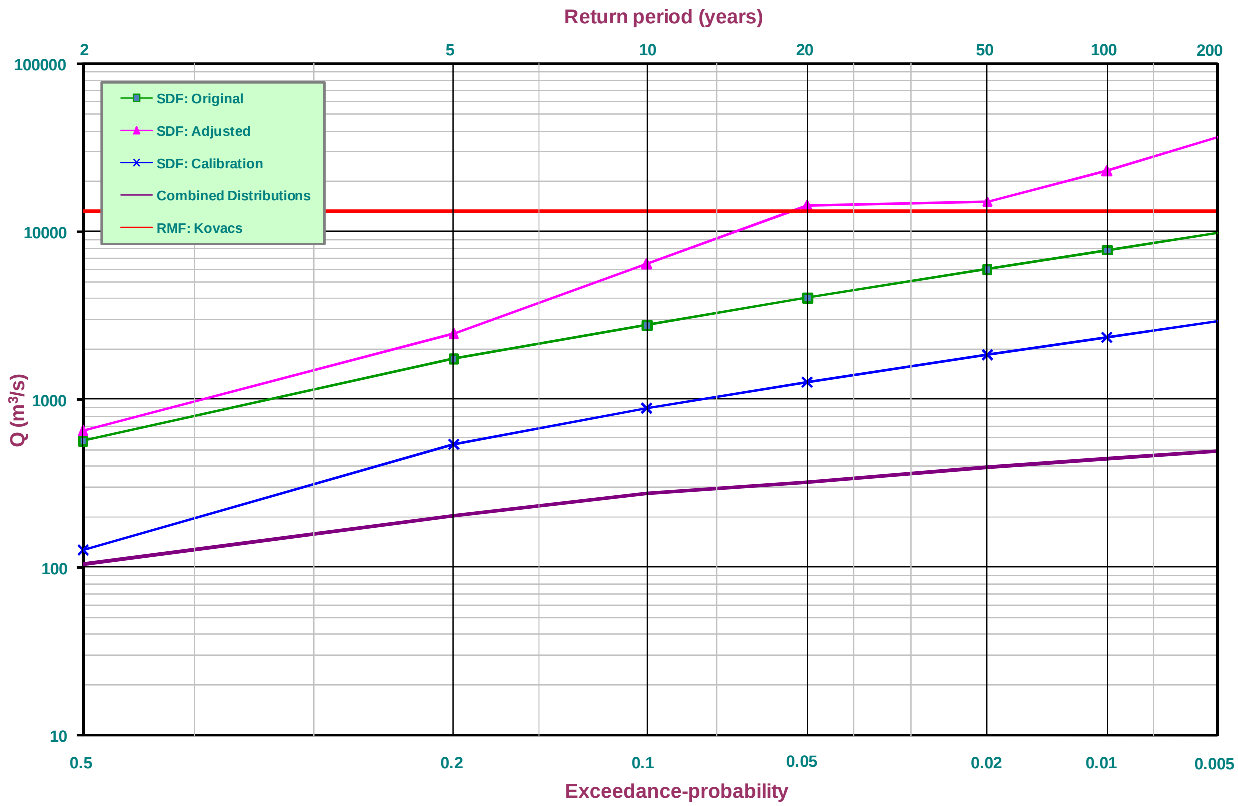

Figure C.67: C5H016: Probabilistic plot (calibrated SDF method)

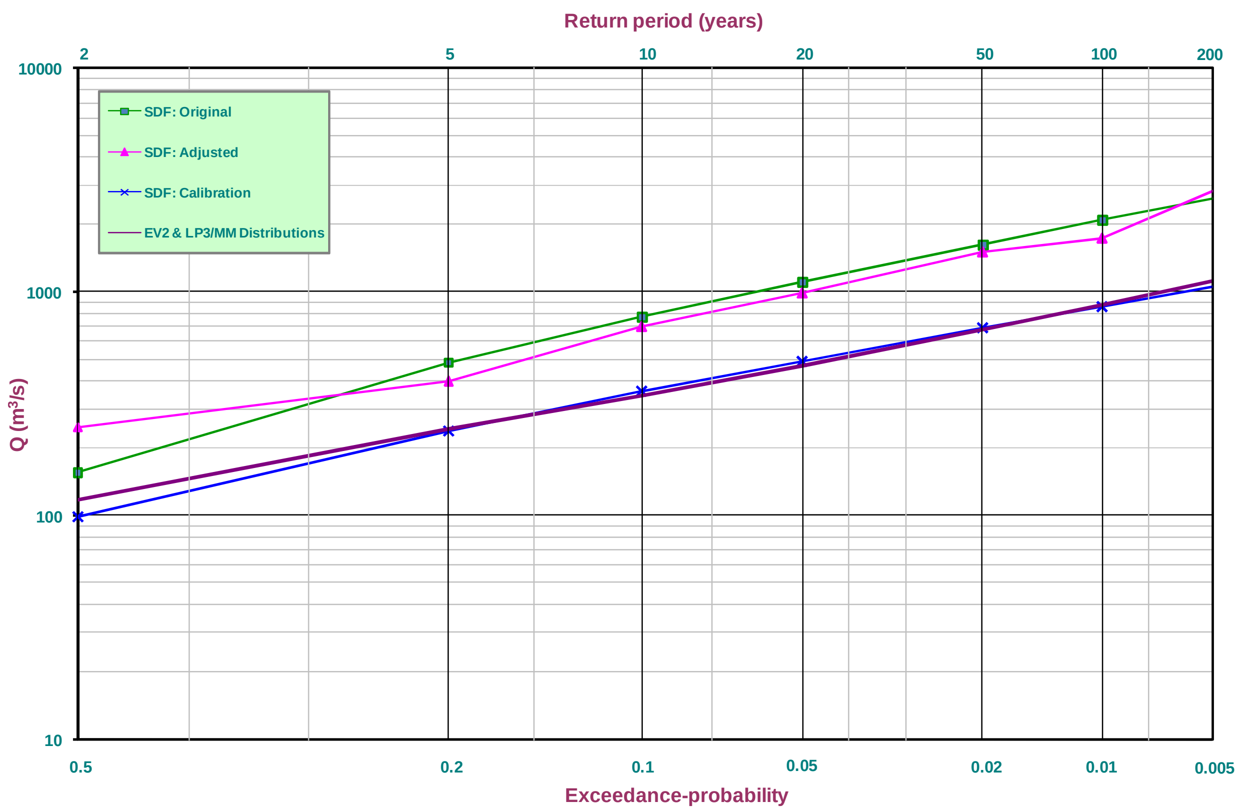

Figure C.68: A2H012 (1): Probabilistic plot (calibrated SDF method)

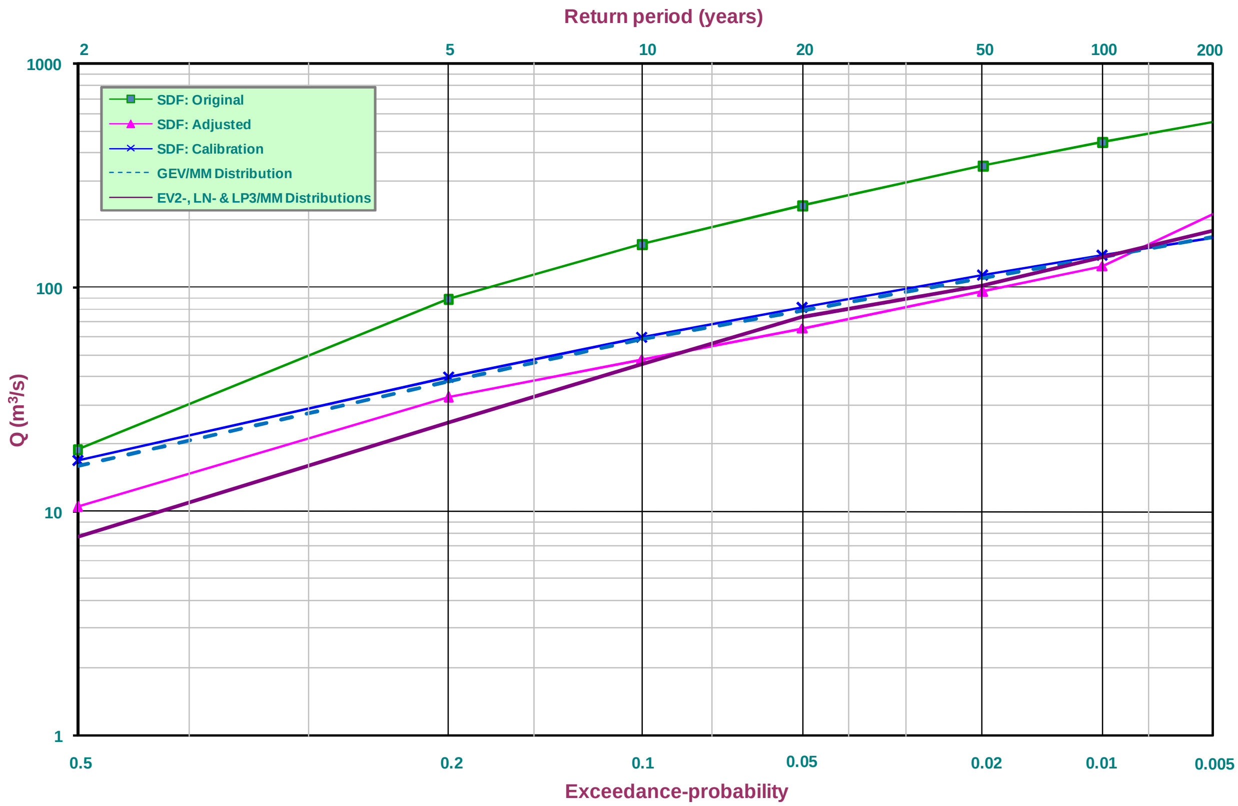

Figure C.69: A6H006 (2): Probabilistic plot (calibrated SDF method)

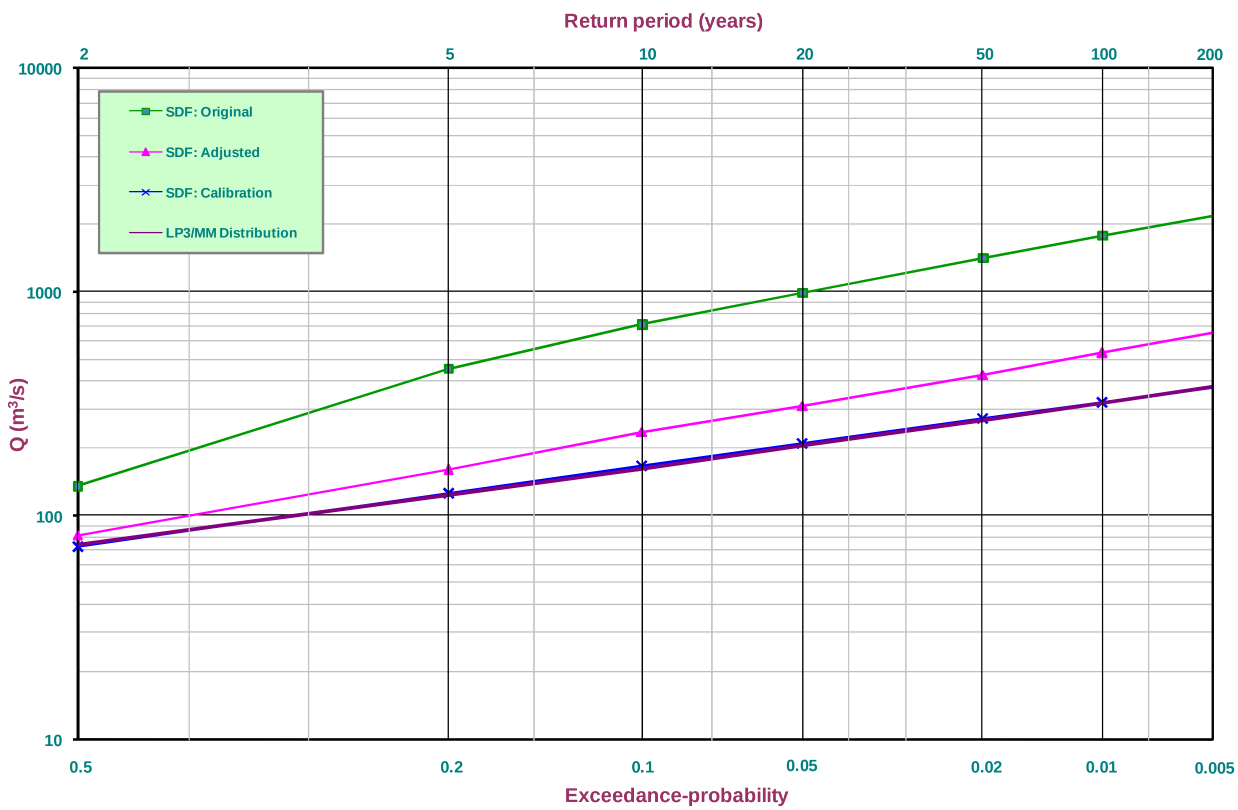

Figure C.70: B4H003 (4): Probabilistic plot (calibrated SDF method)

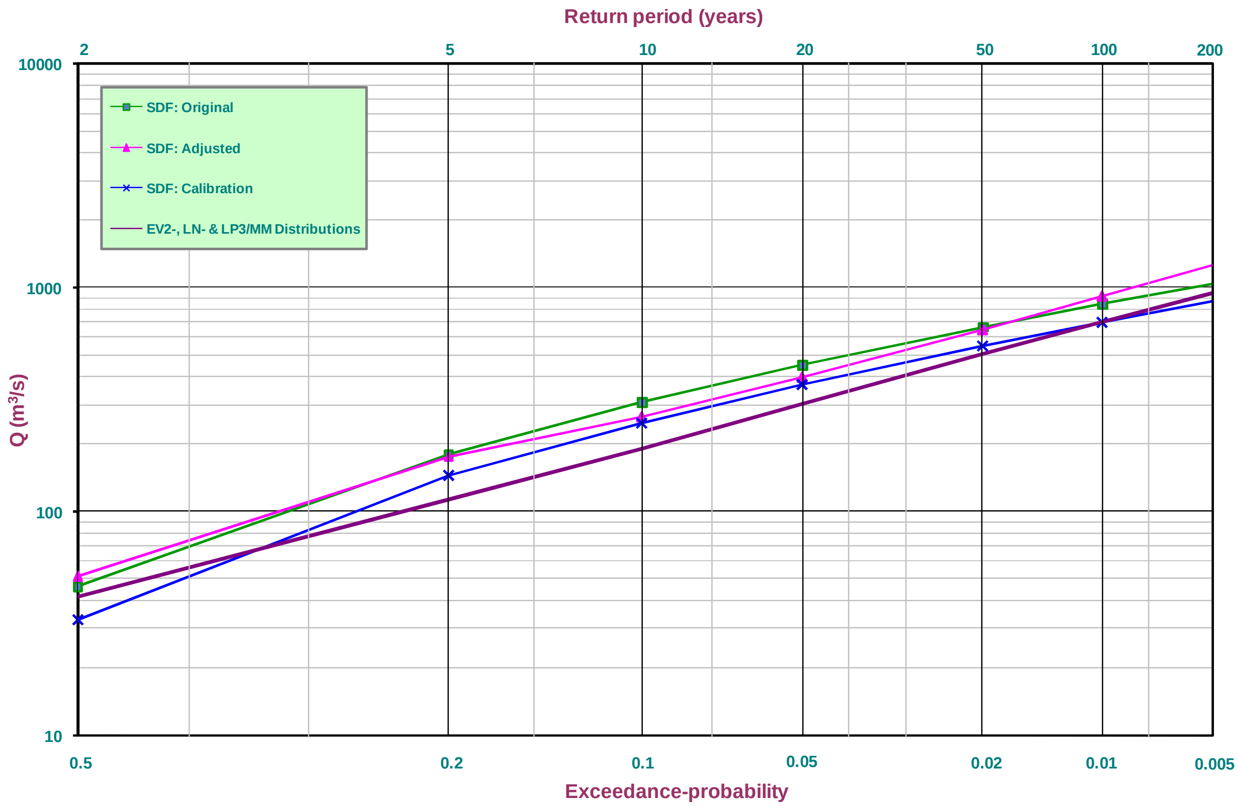

Figure C.71: B7H004 (5): Probabilistic plot (calibrated SDF method)

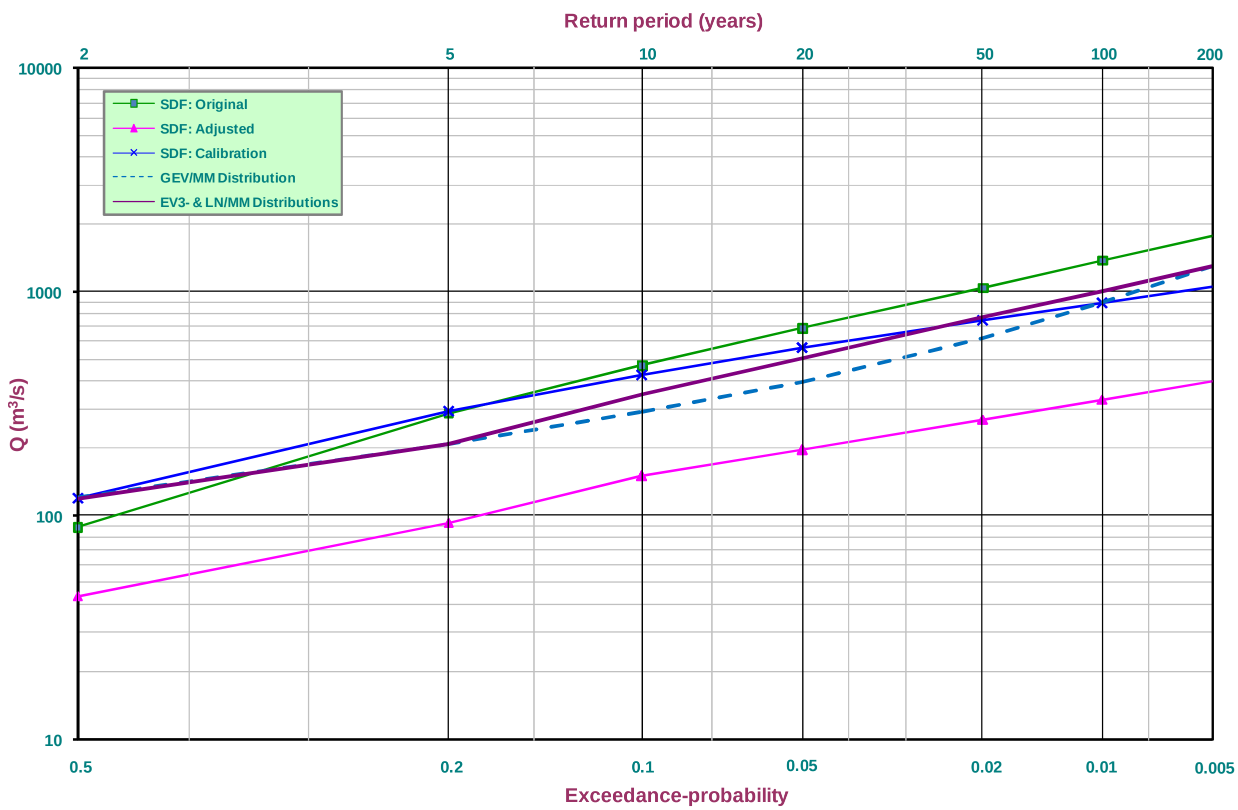

Figure C.72: C3H003 (8): Probabilistic plot (calibrated SDF method)

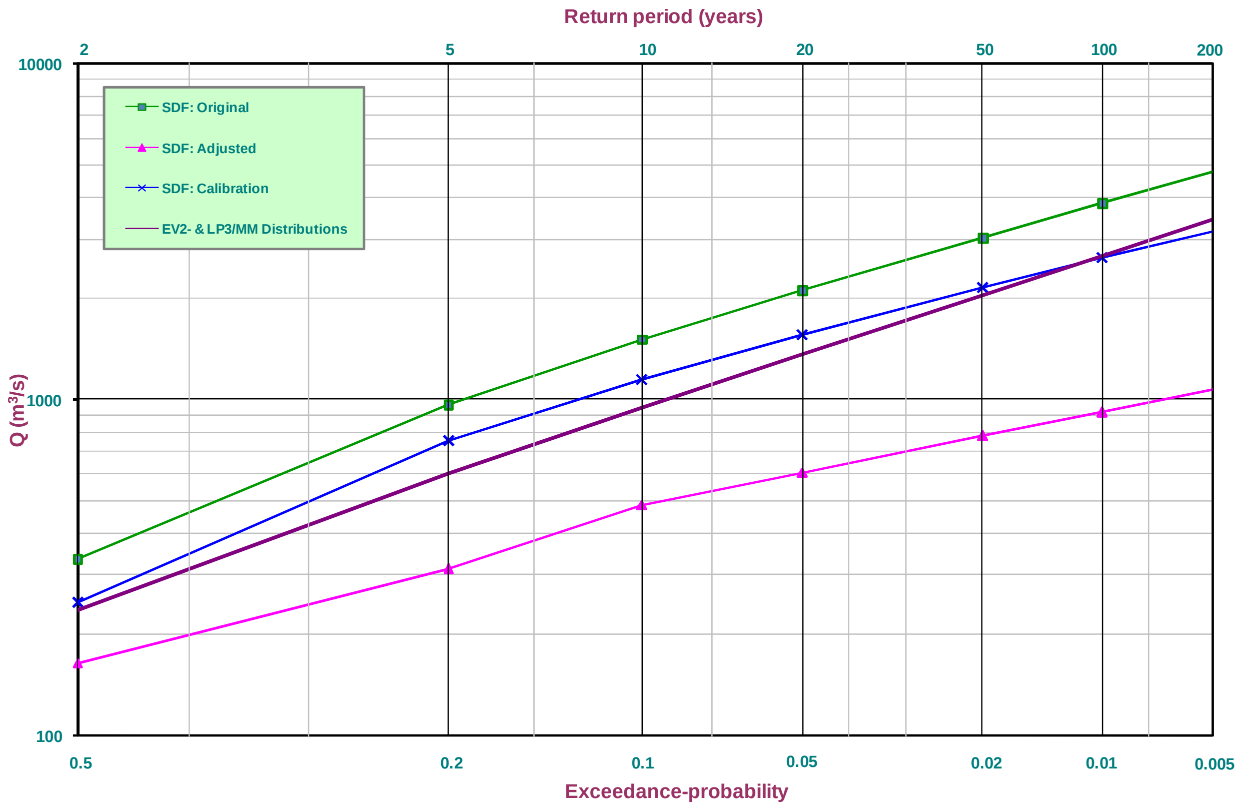

Figure C.73: C4H002 (7): Probabilistic plot (calibrated SDF method)

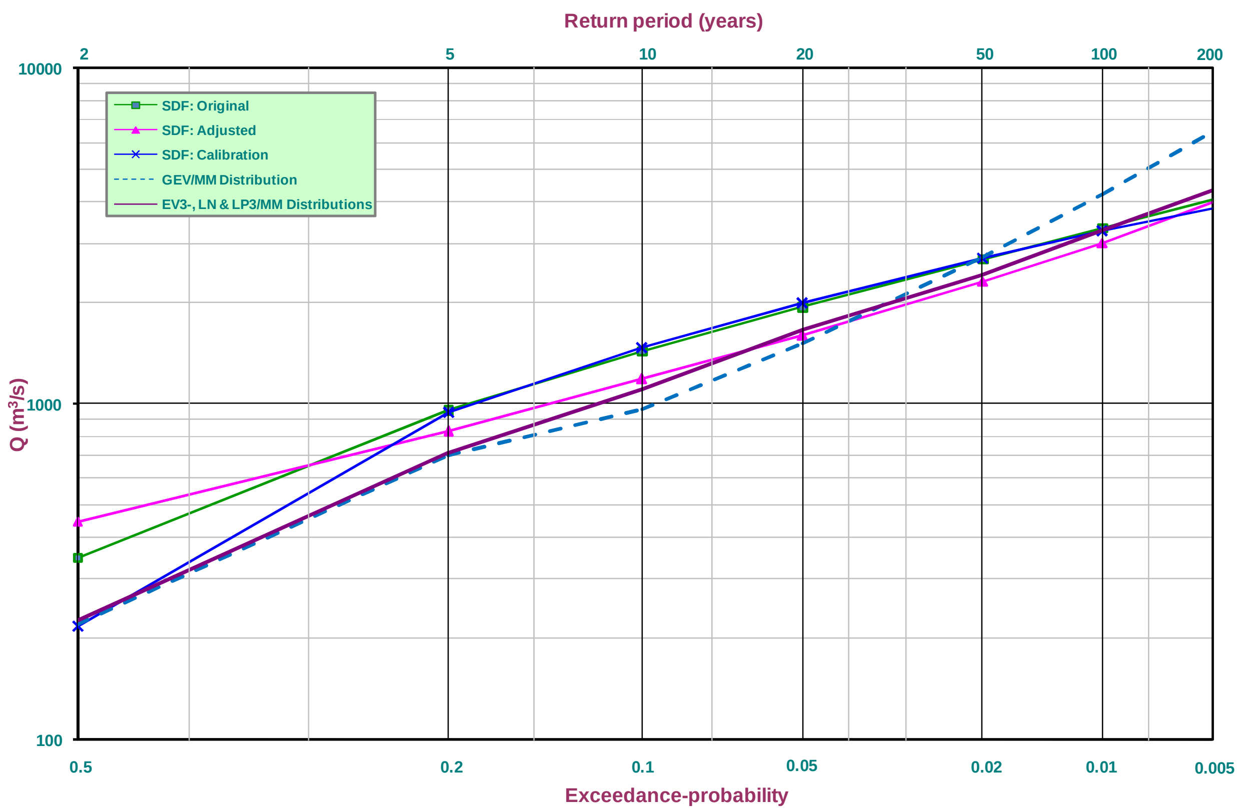

Figure C.74: C8H001 (6): Probabilistic plot (calibrated SDF method)

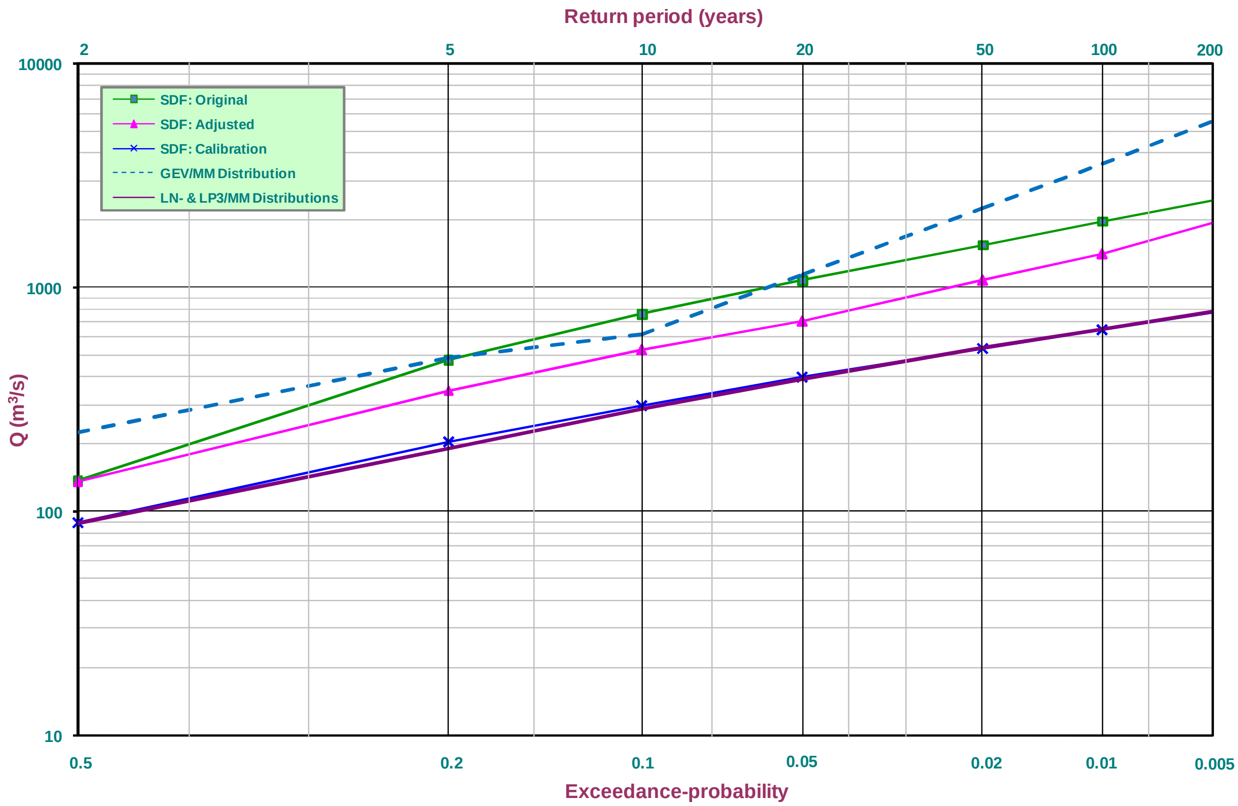

Figure C.75: D1H001 (10): Probabilistic plot (calibrated SDF method)

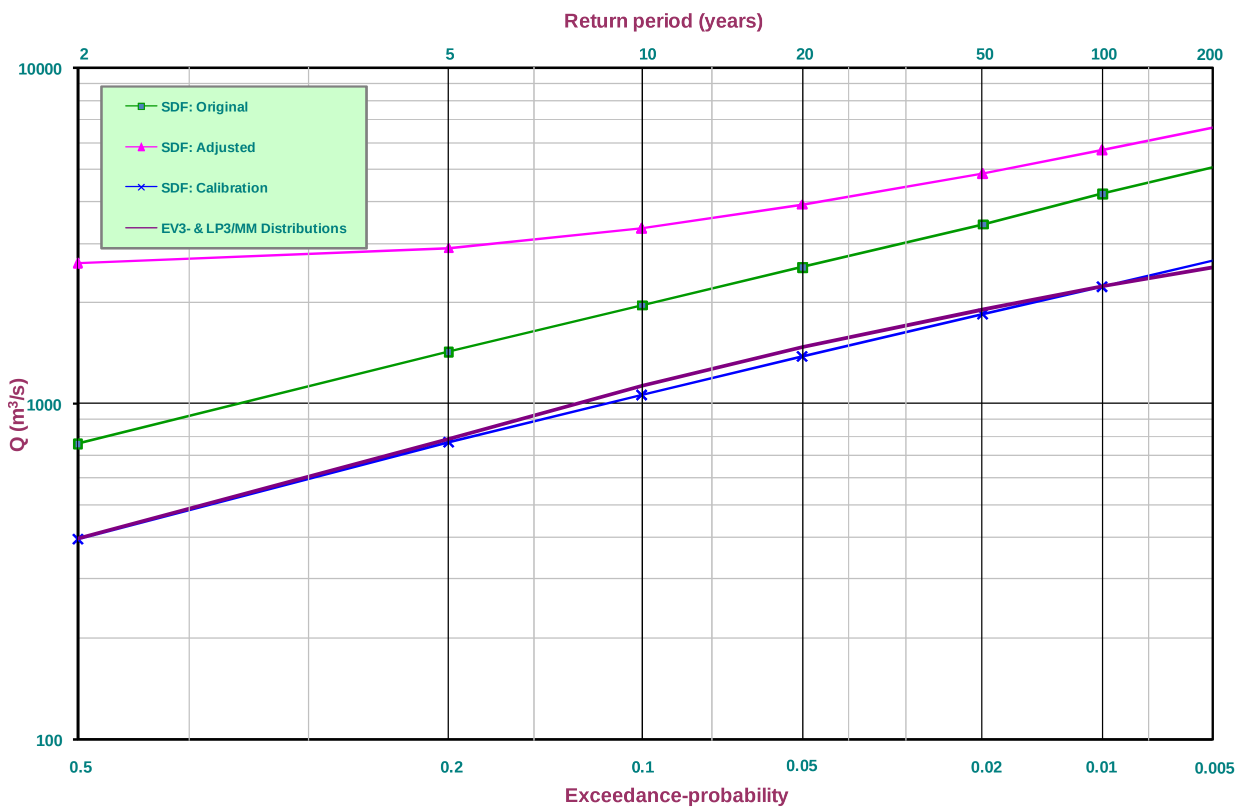

Figure C.76: D1H005 (11): Probabilistic plot (calibrated SDF method)

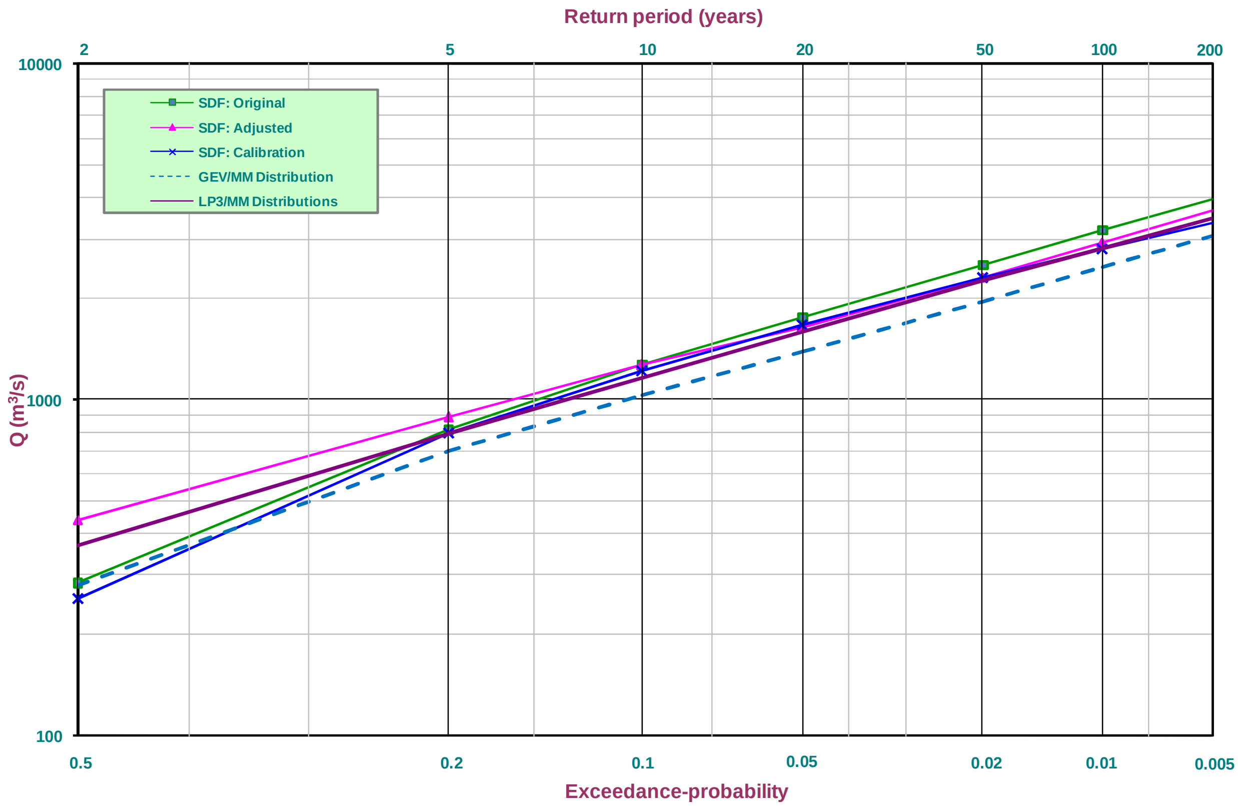

Figure C.77: E2H003 (16): Probabilistic plot (calibrated SDF method)

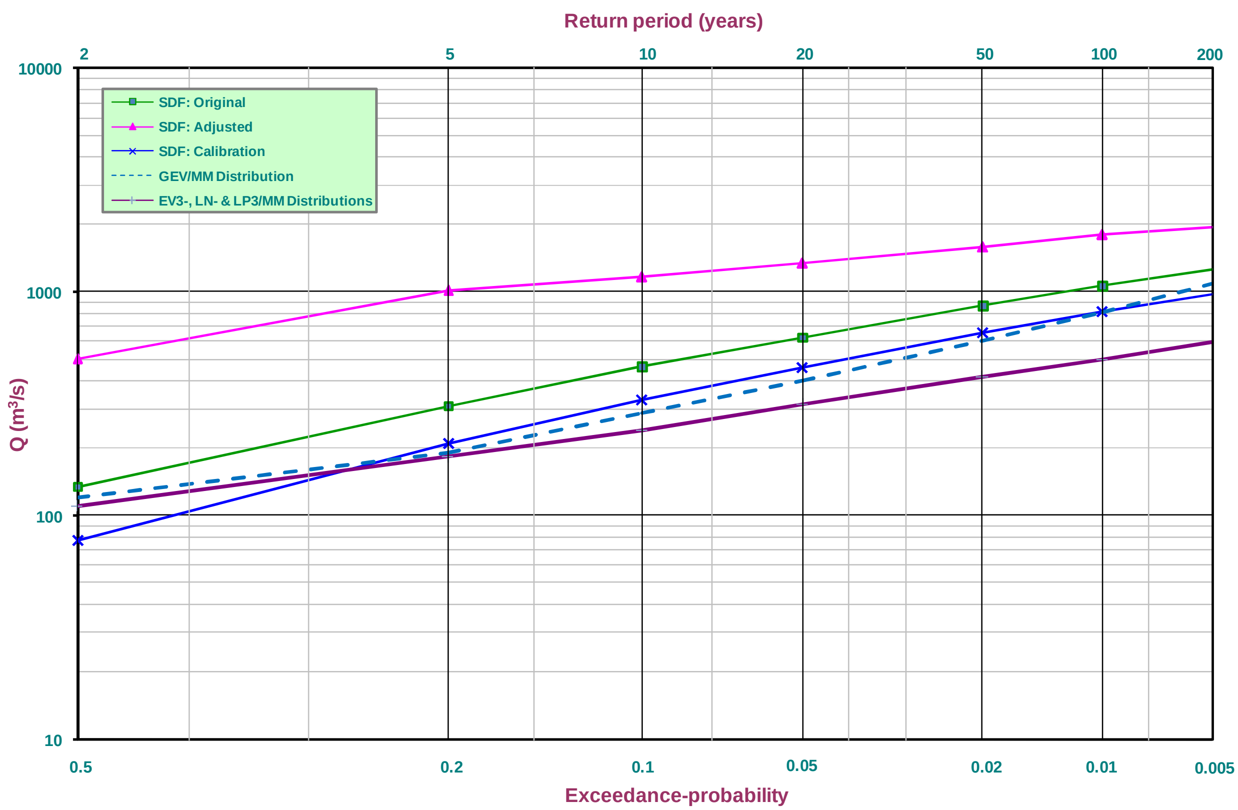

Figure C.78: G1H008 (17): Probabilistic plot (calibrated SDF method)

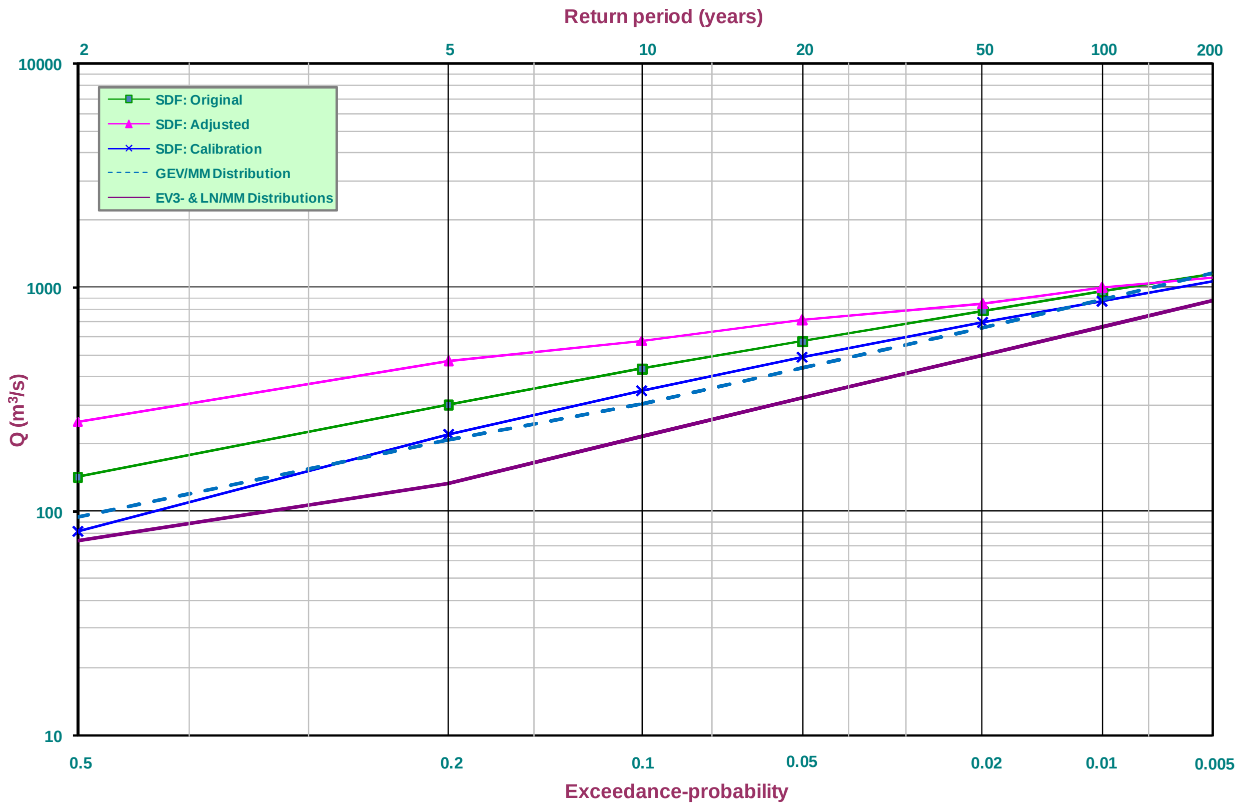

Figure C.79: H3H001 (18): Probabilistic plot (calibrated SDF method)

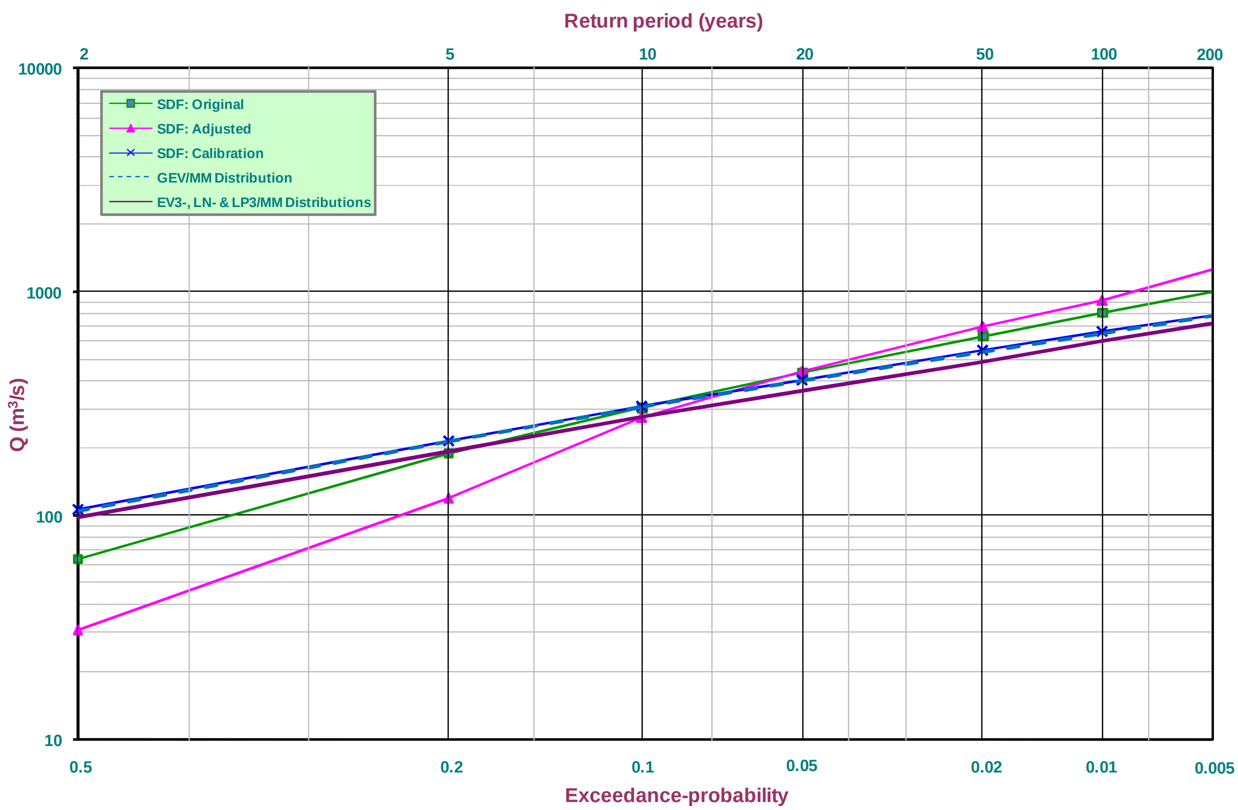

Figure C.80: Q9H008 (21): Probabilistic plot (calibrated SDF method)

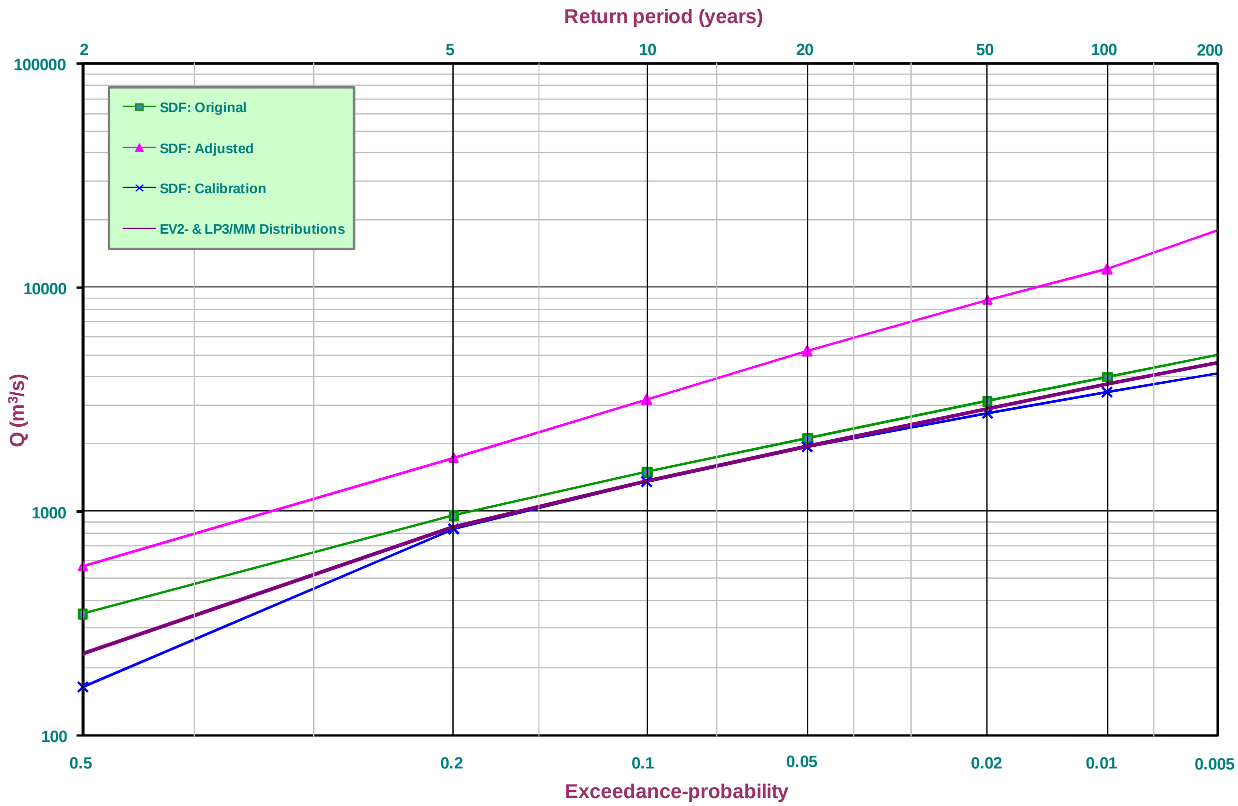

Figure C.81: Q9H010 (21): Probabilistic plot (calibrated SDF method)

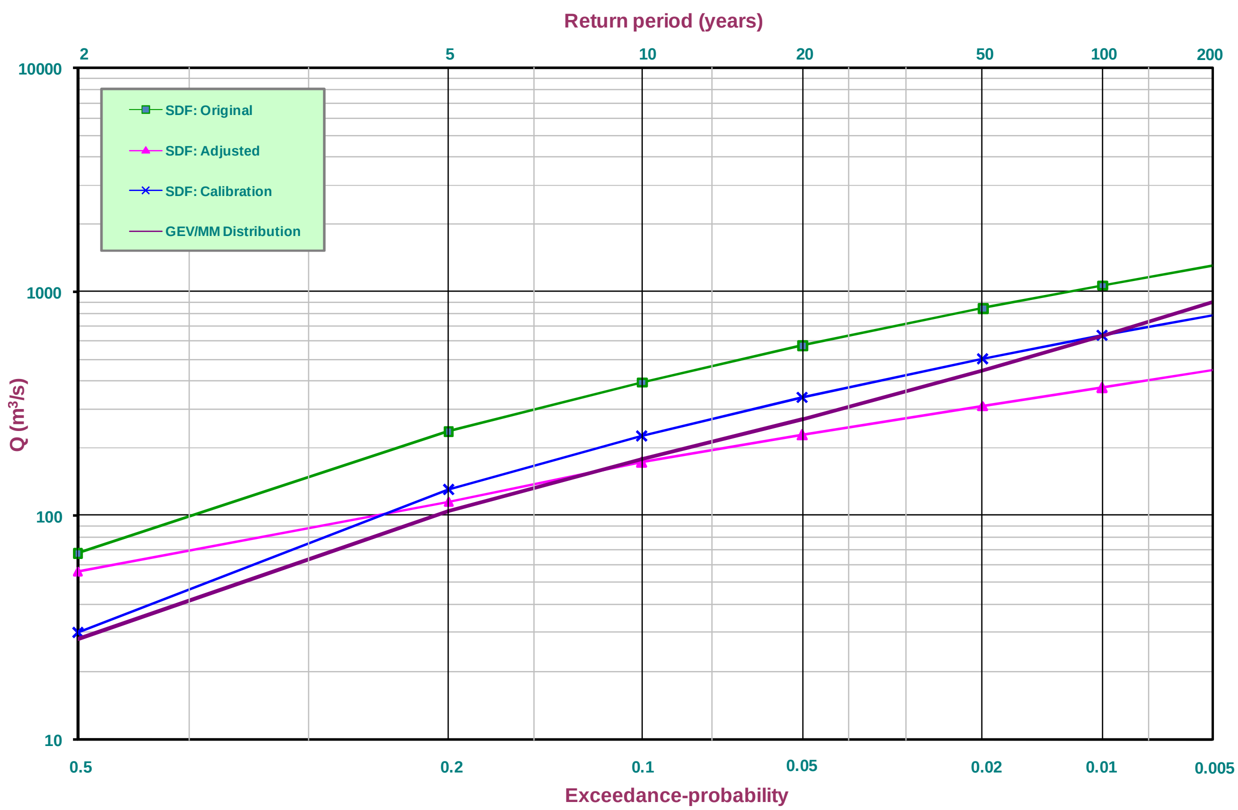

Figure C.82: R1H001 (22): Probabilistic plot (calibrated SDF method)

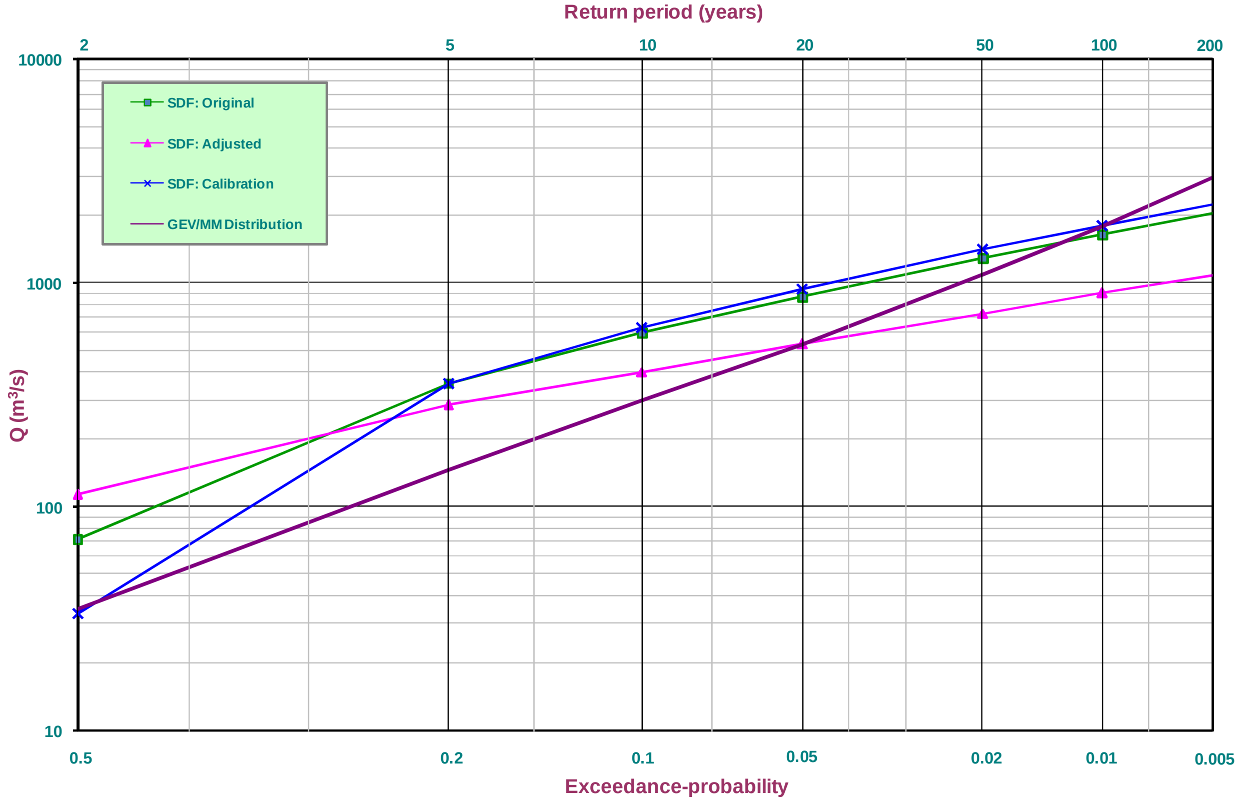

Figure C.83: T3H004 (23): Probabilistic plot (calibrated SDF method)

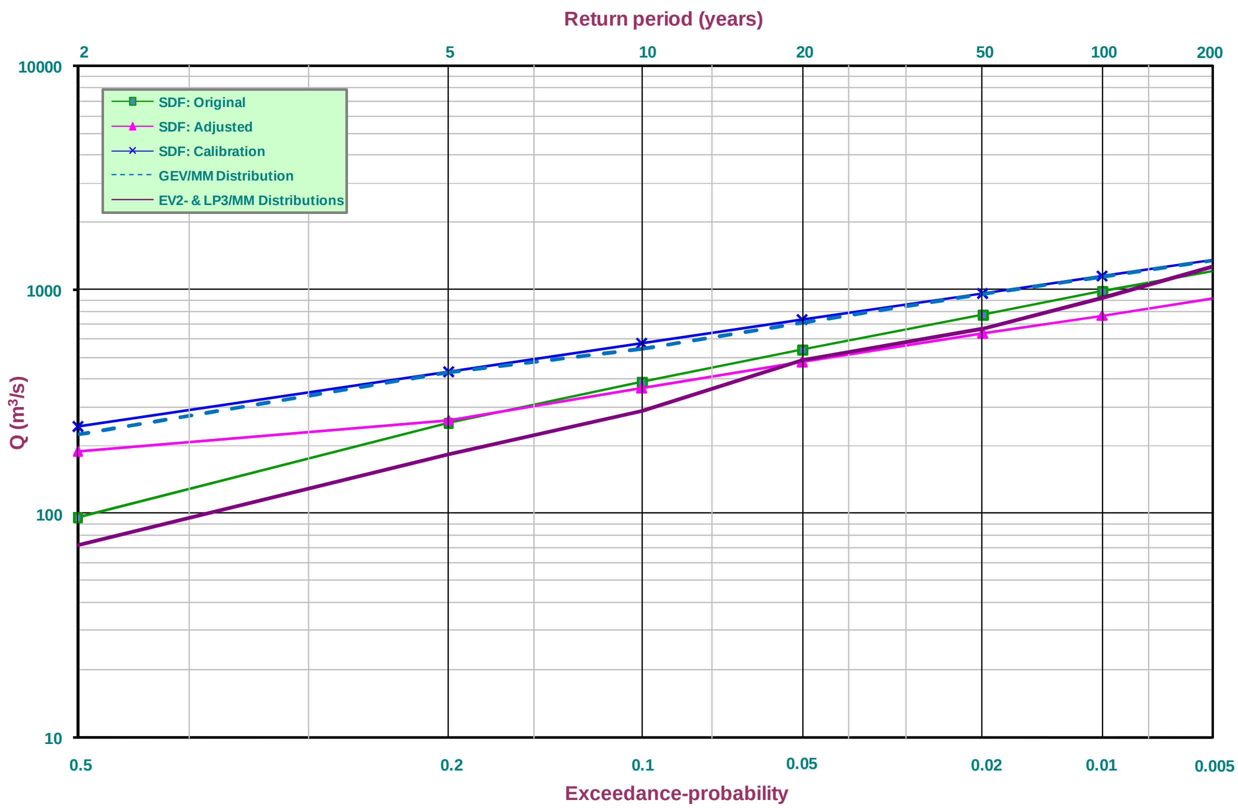

Figure C.84: V2H002 (26): Probabilistic plot (calibrated SDF method)

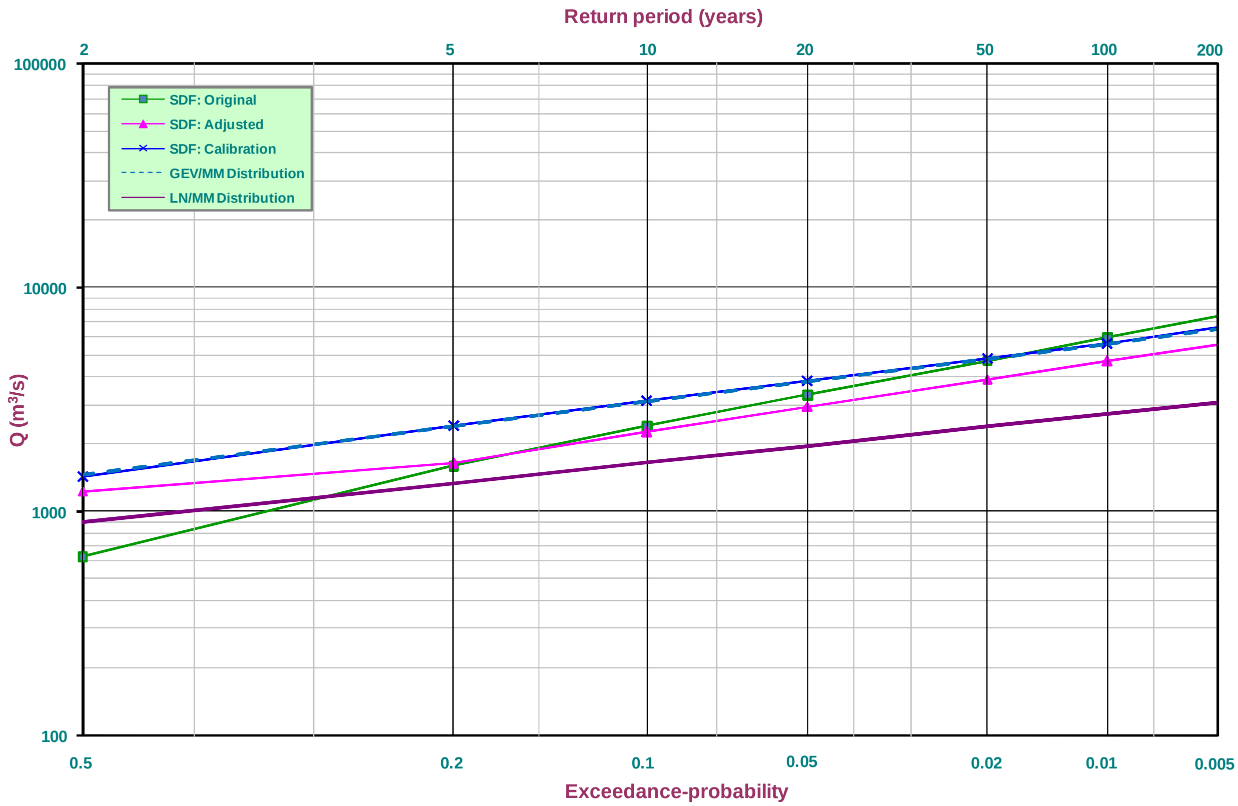

Figure C.85: V6H002 (26): Probabilistic plot (calibrated SDF method)

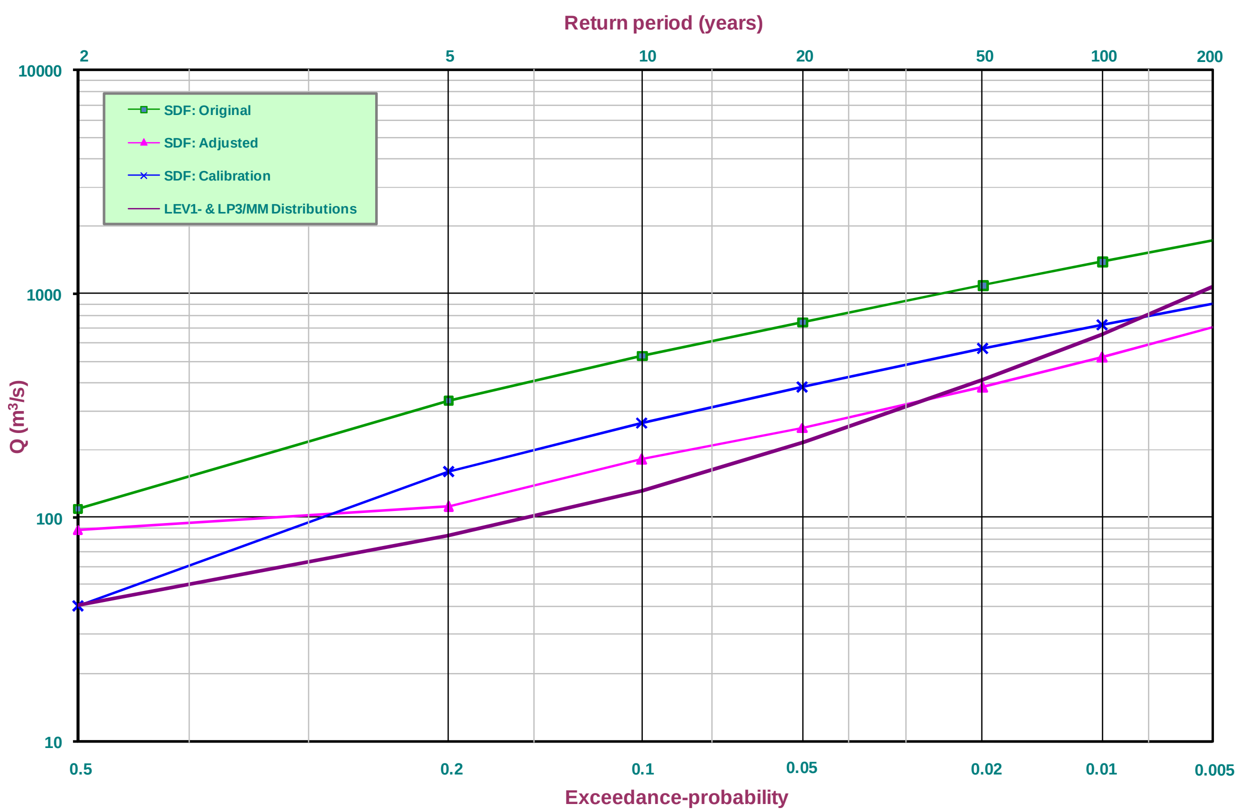

Figure C.86: W5H005 (28): Probabilistic plot (calibrated SDF method)

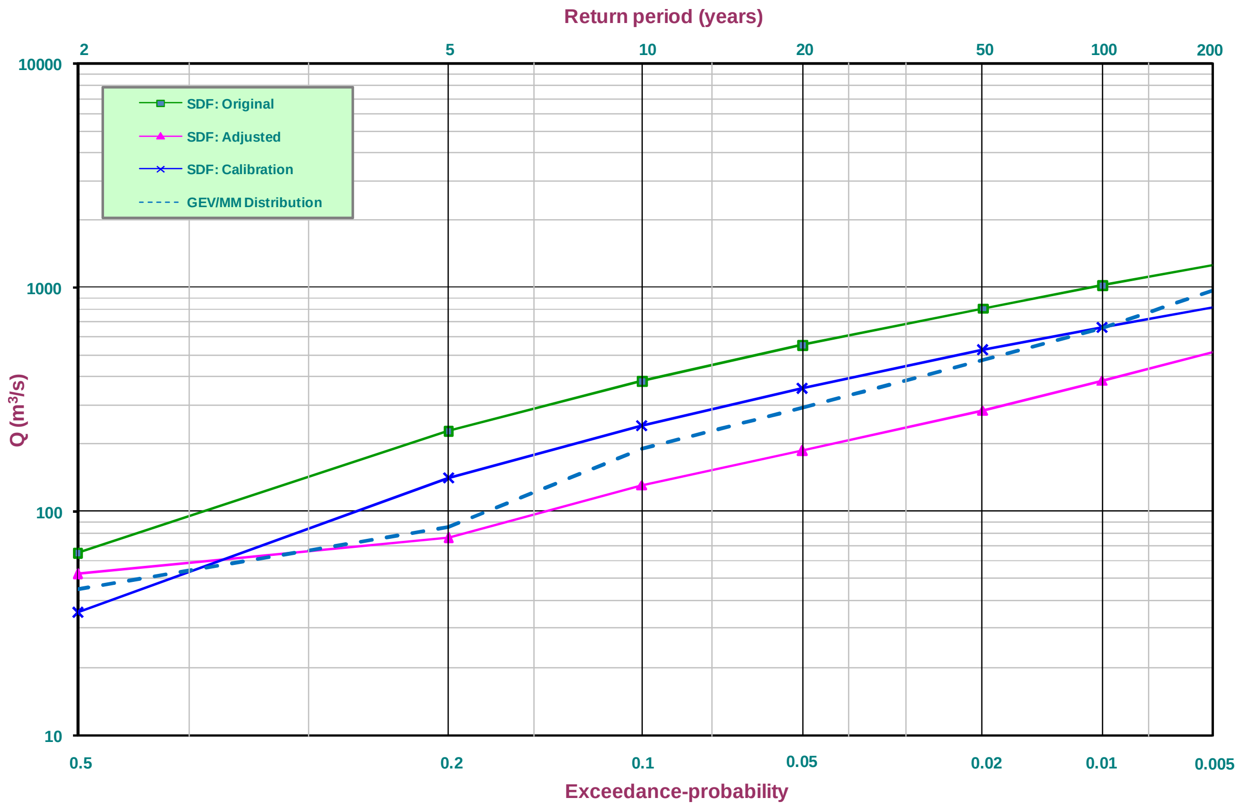

Figure C.87: W5H006 (28): Probabilistic plot (calibrated SDF method)

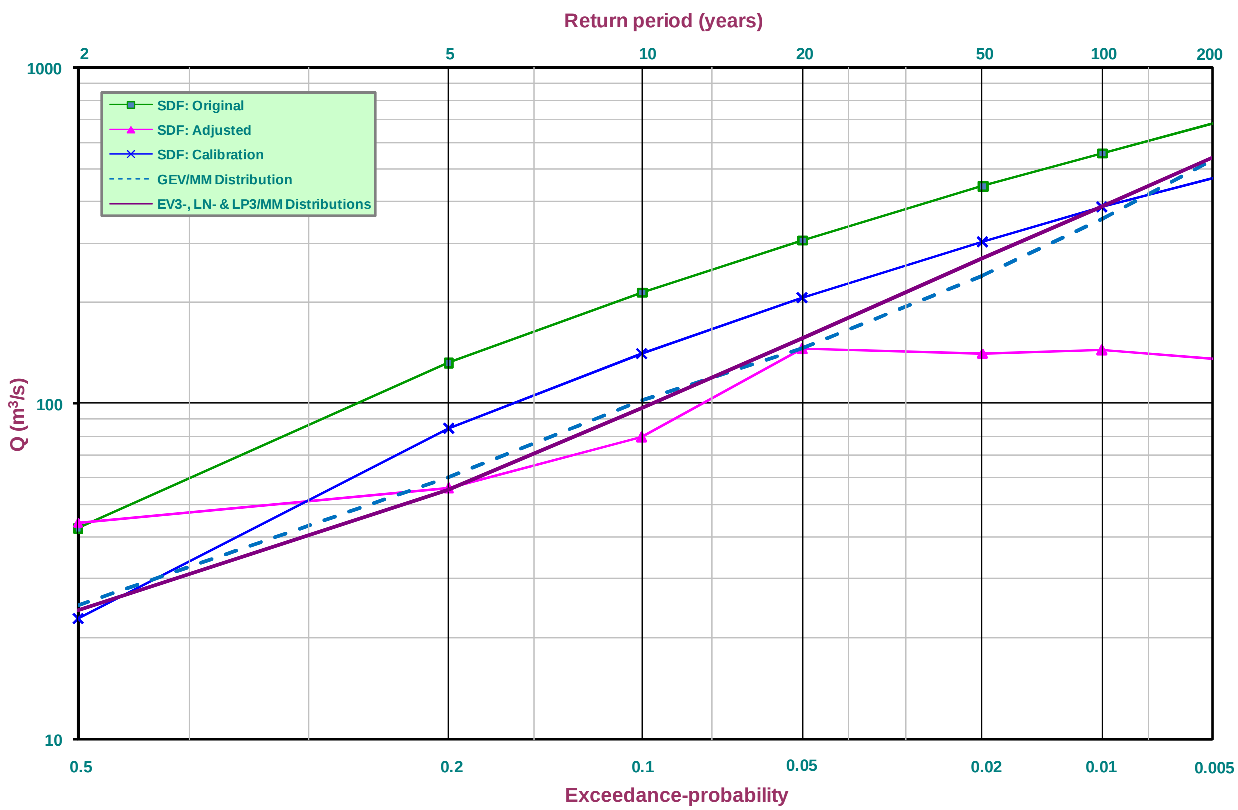

Figure C.88: X2H010 (29): Probabilistic plot (calibrated SDF method)

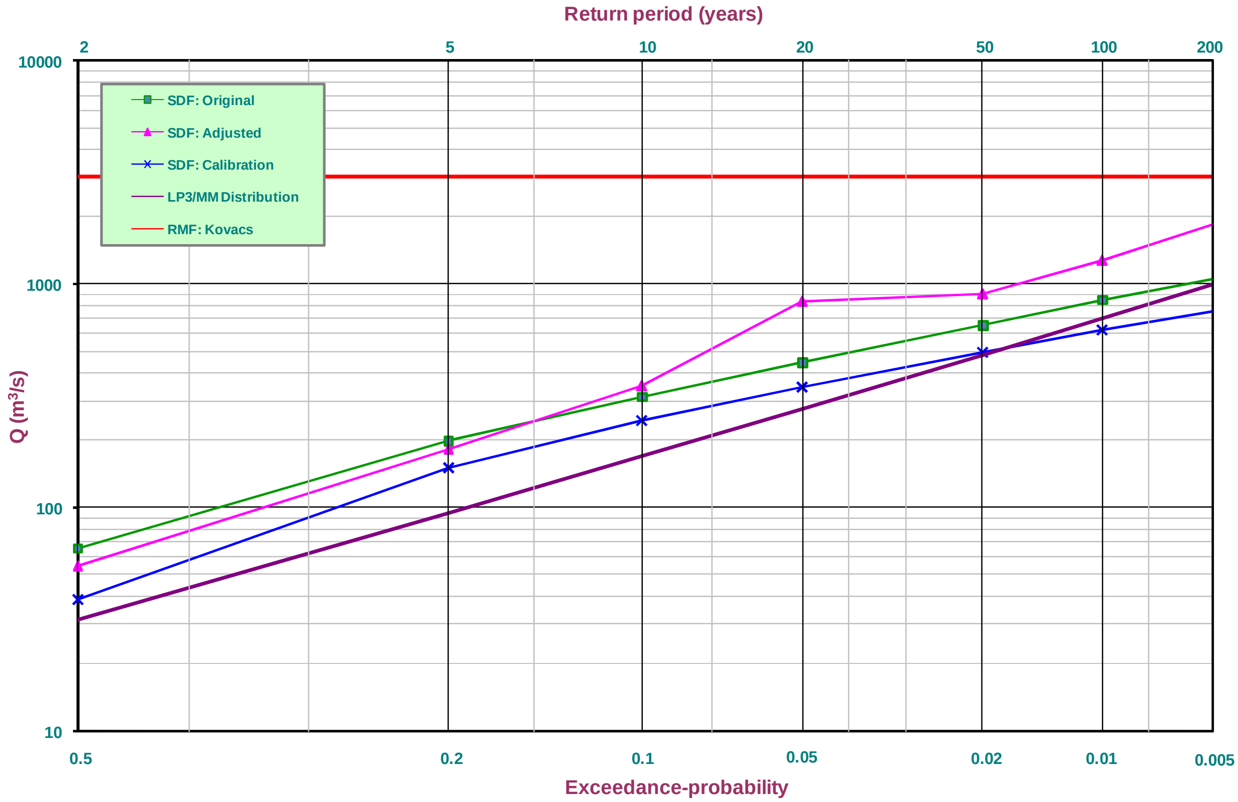

Figure C.89: C5R001: Probabilistic plot (verified SDF method)

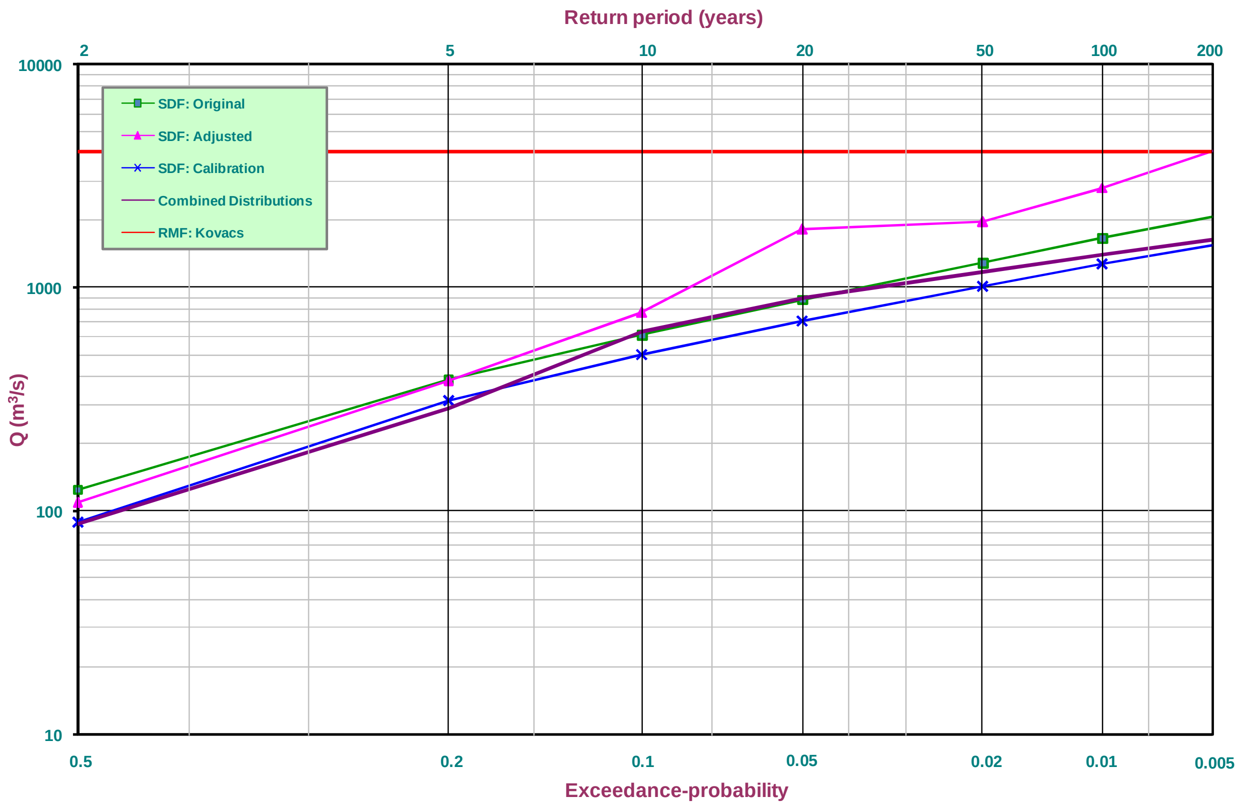

Figure C.90: C5H003: Probabilistic plot (verified SDF method)

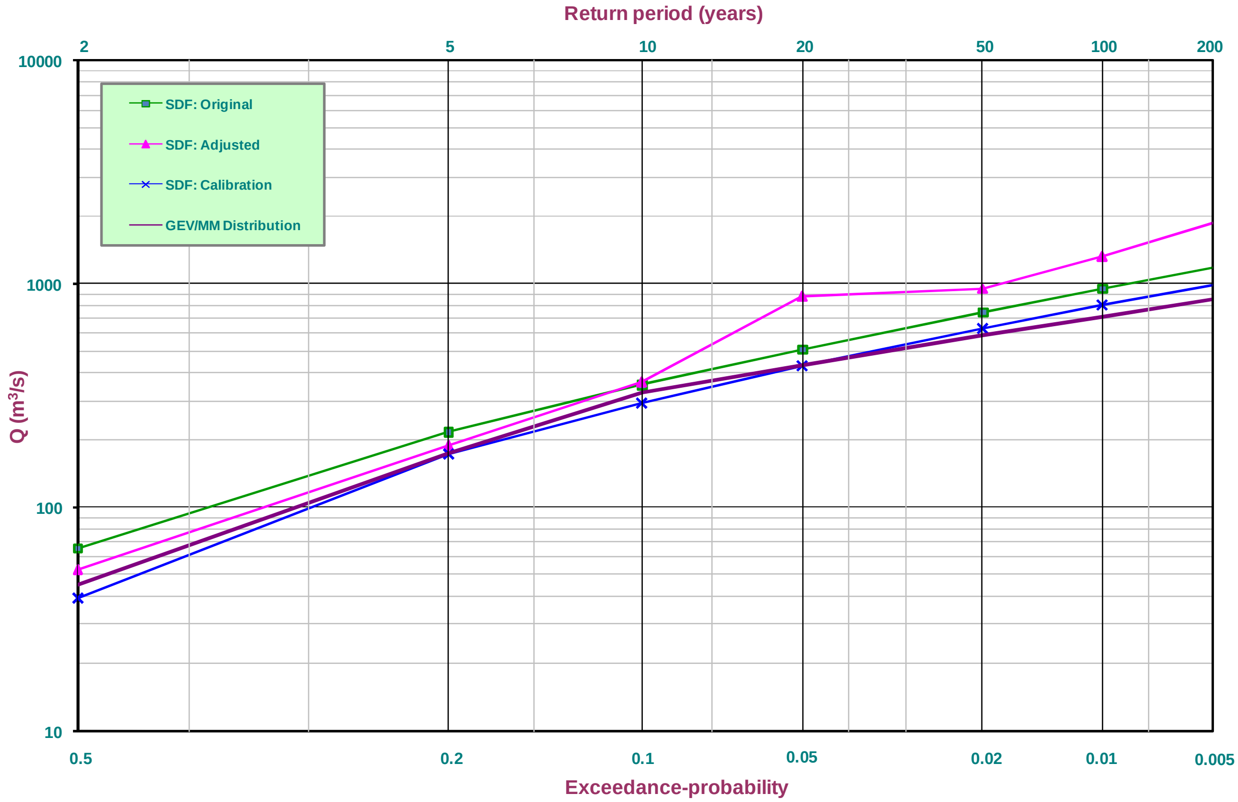

Figure C.91: C5H008: Probabilistic plot (verified SDF method)

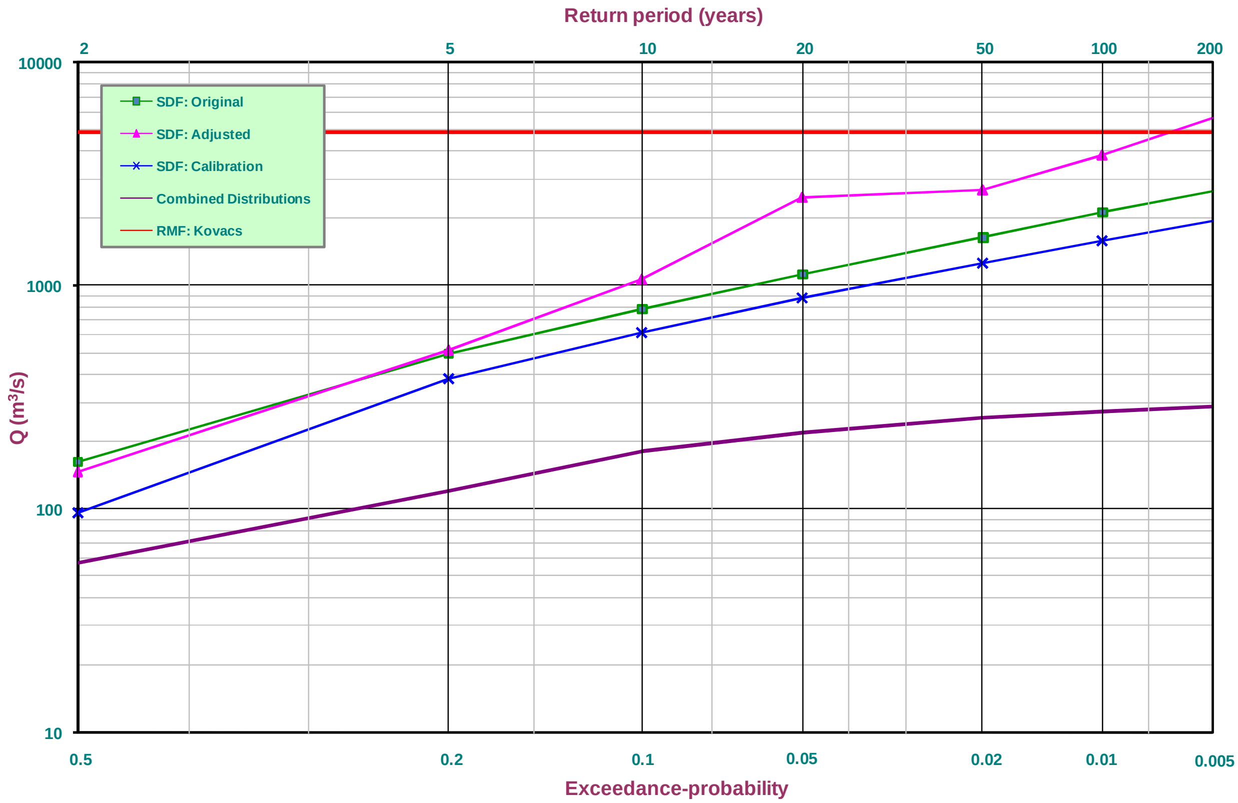

Figure C.92: C5H012: Probabilistic plot (verified SDF method)

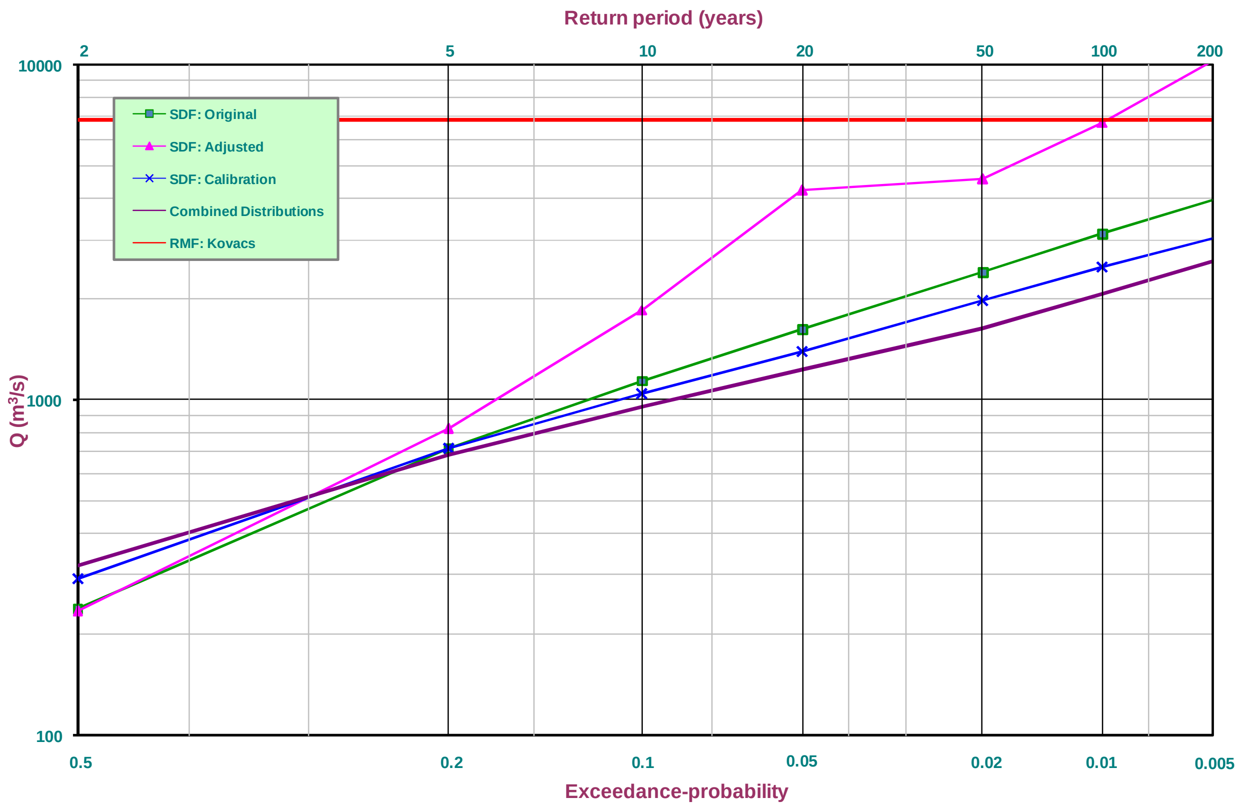

Figure C.93: C5H015: Probabilistic plot (verified SDF method)

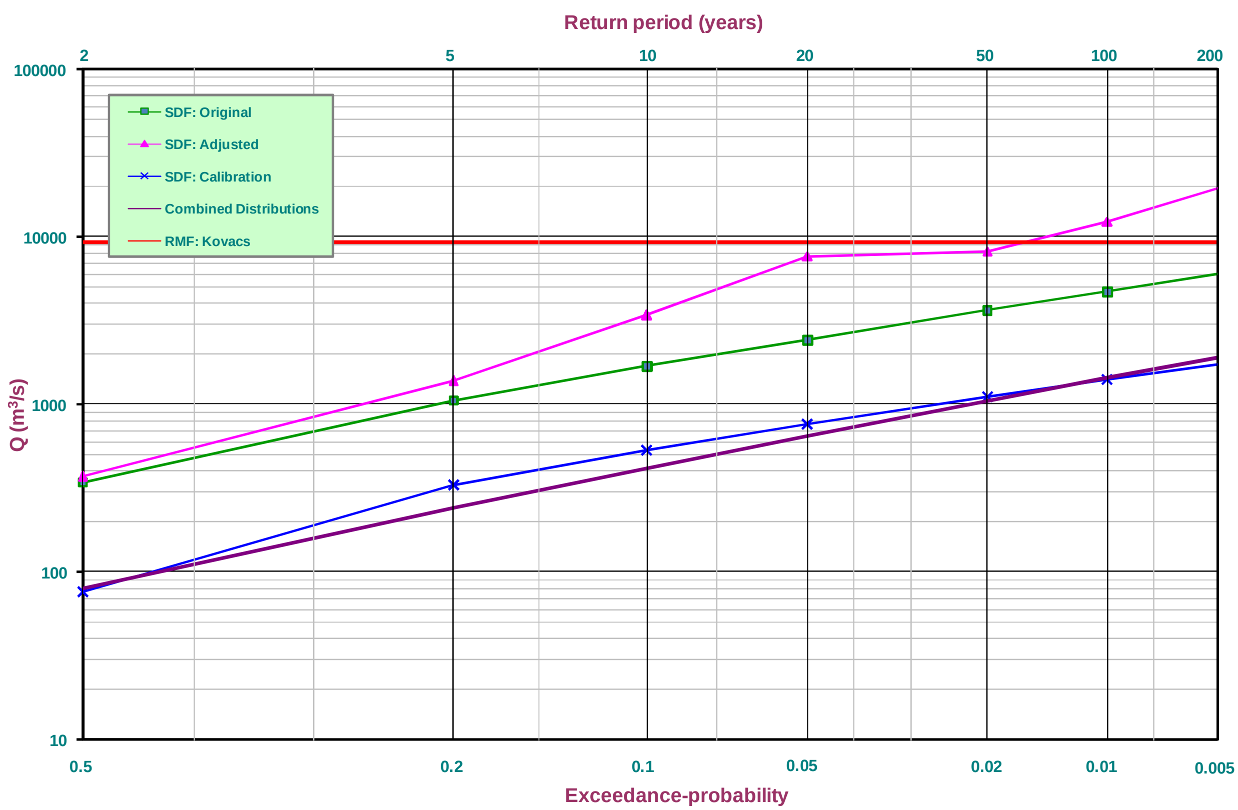

Figure C.94: C5H018: Probabilistic plot (verified SDF method)

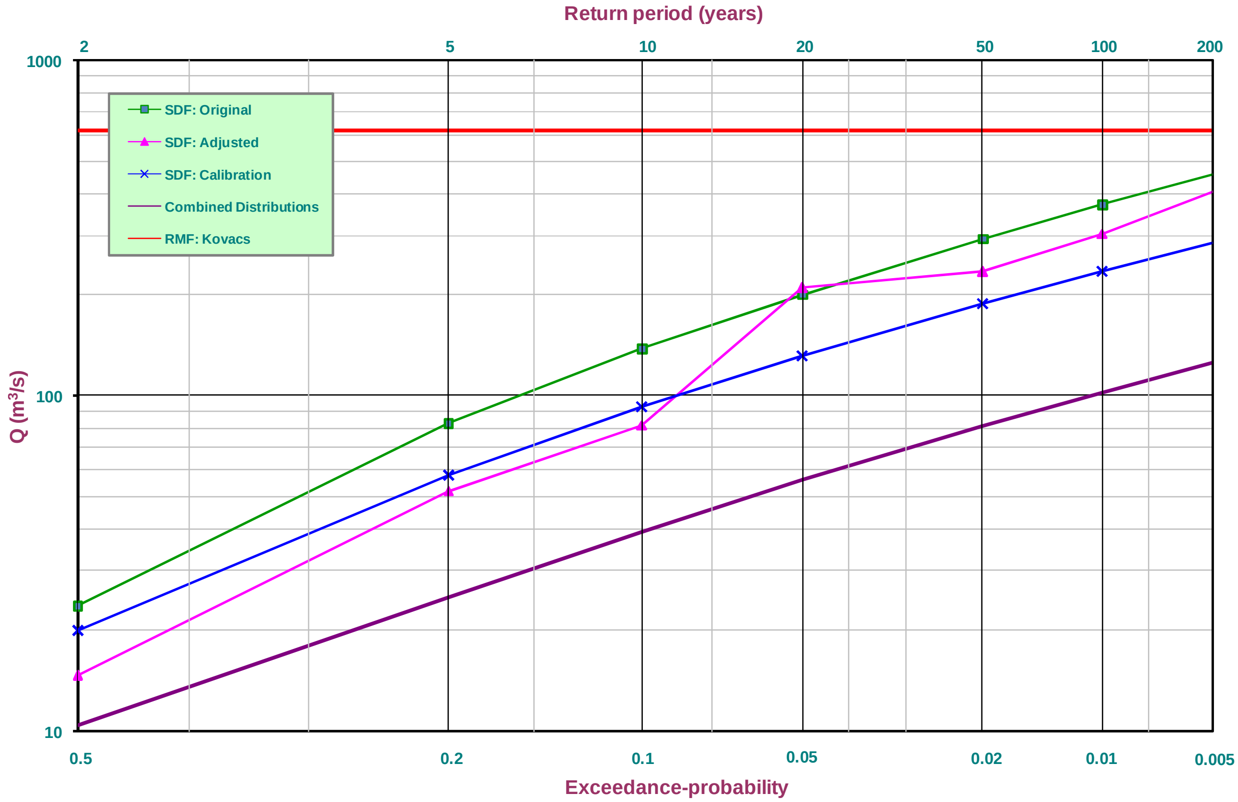

Figure C.95: C5H022: Probabilistic plot (verified SDF method)

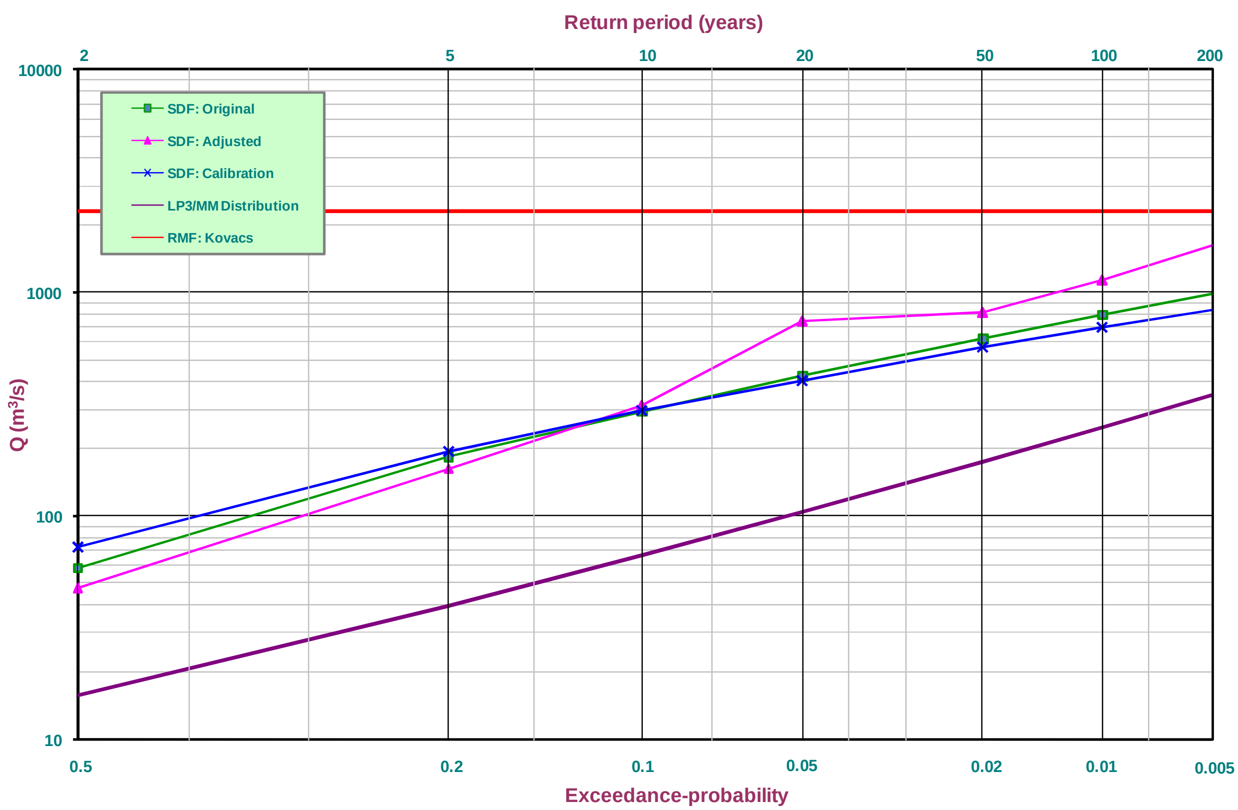

Figure C.96: C5H054: Probabilistic plot (verified SDF method)

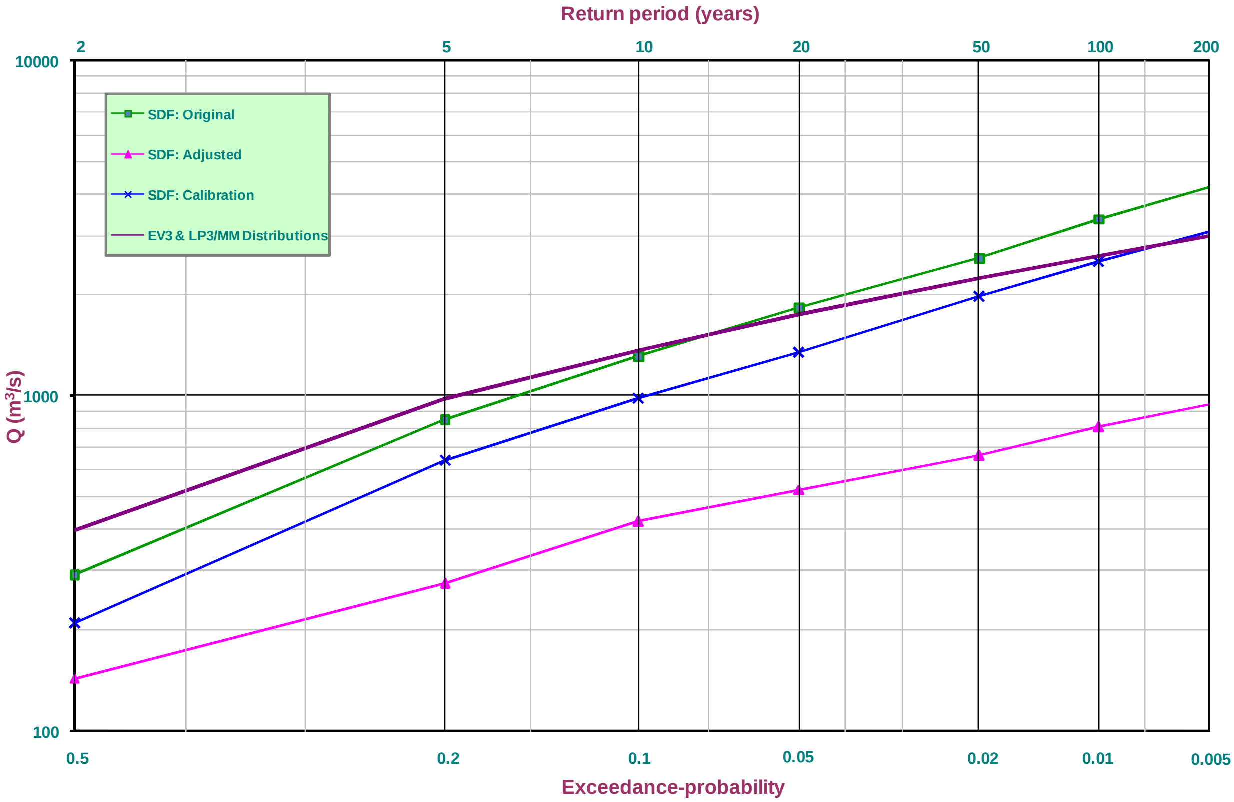

Figure C.97: C4H001 (7): Probabilistic plot (verified SDF method)

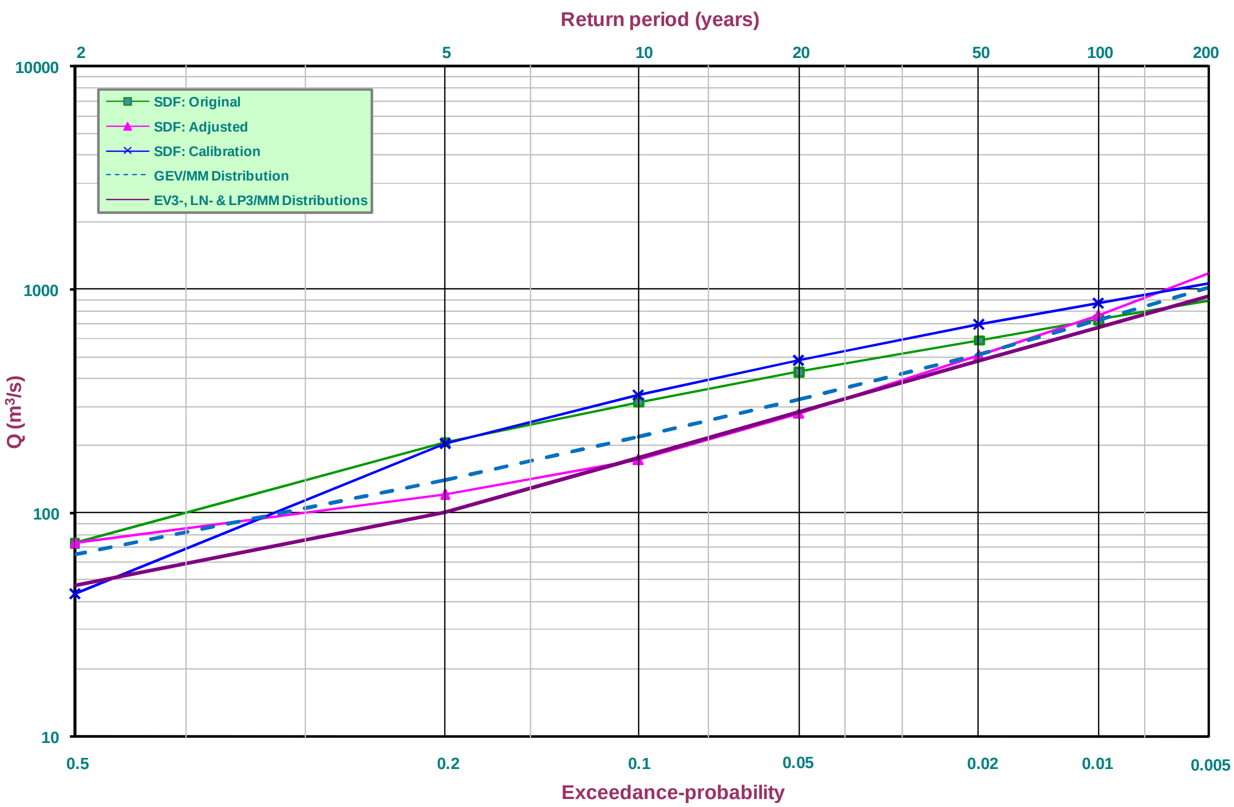

Figure C.98: C8H003 (6): Probabilistic plot (verified SDF method)

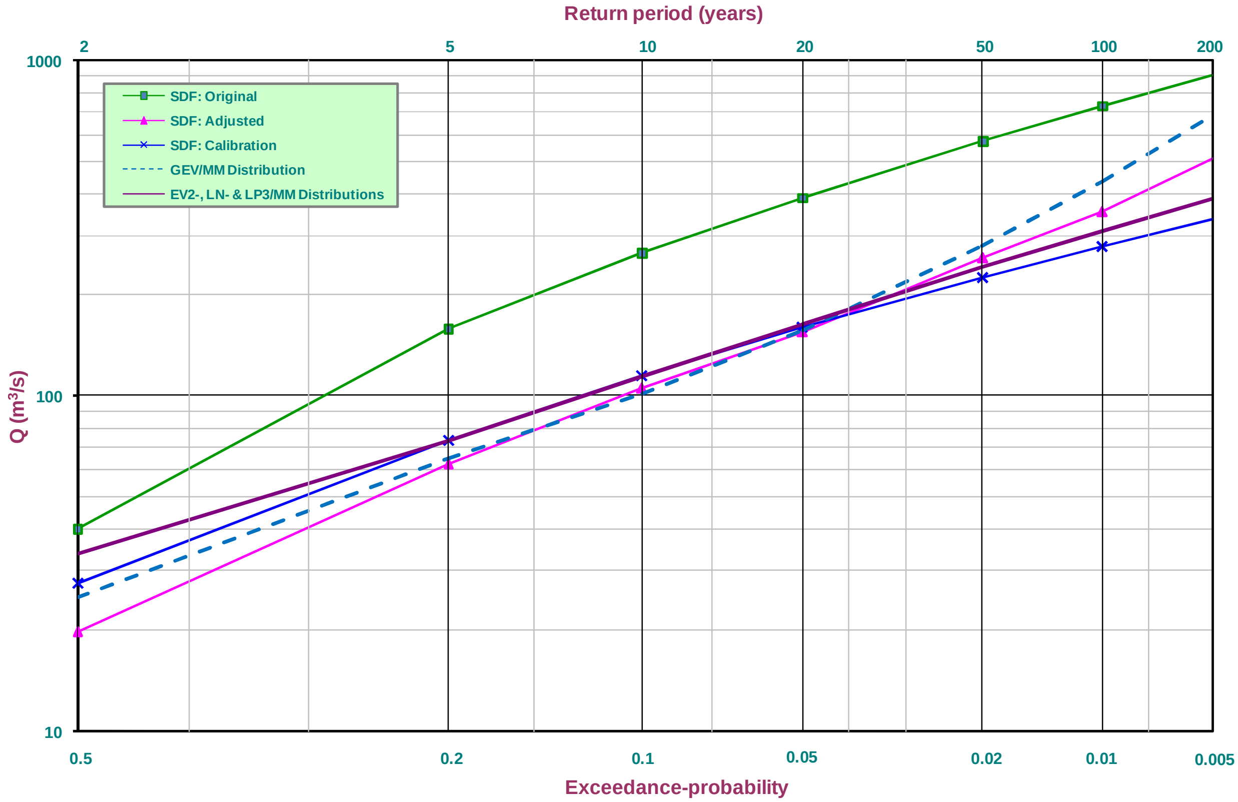

Figure C.99: D1H004 (10): Probabilistic plot (verified SDF method)

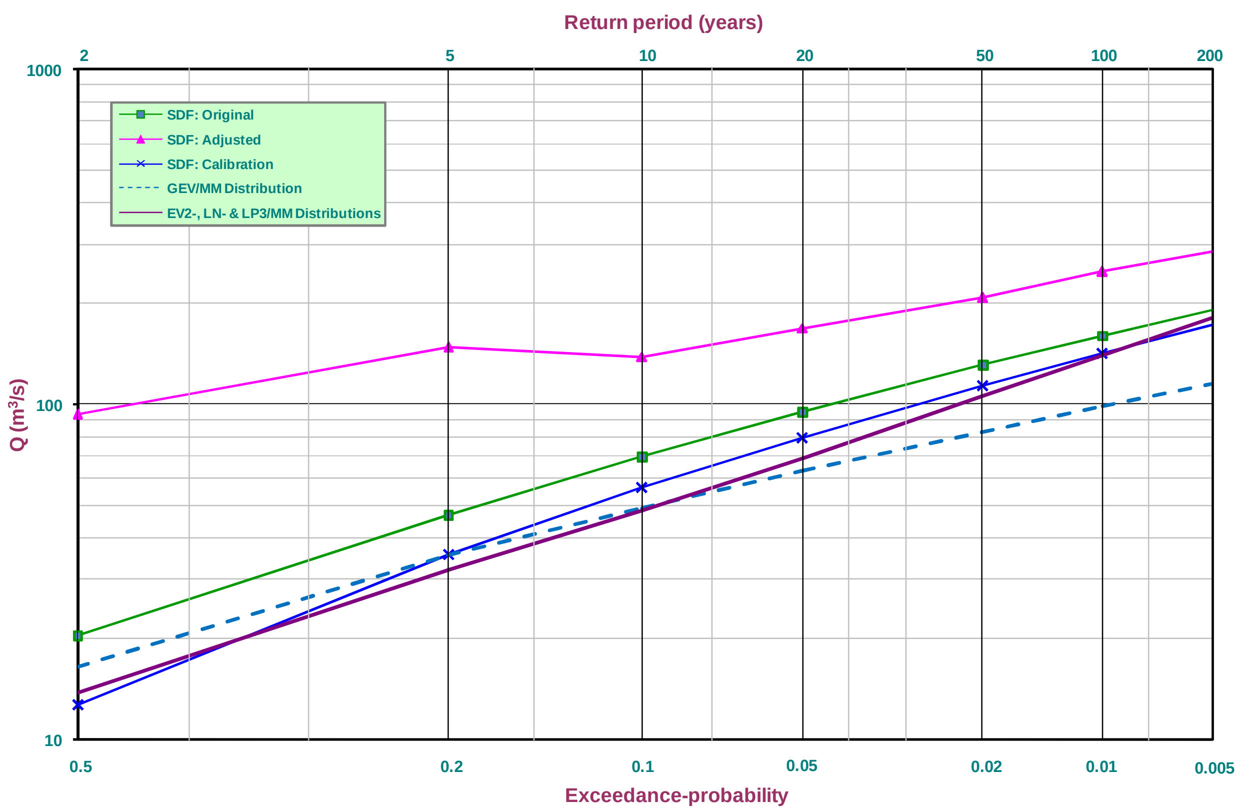

Figure C.100: H7H004 (18): Probabilistic plot (verified SDF method)

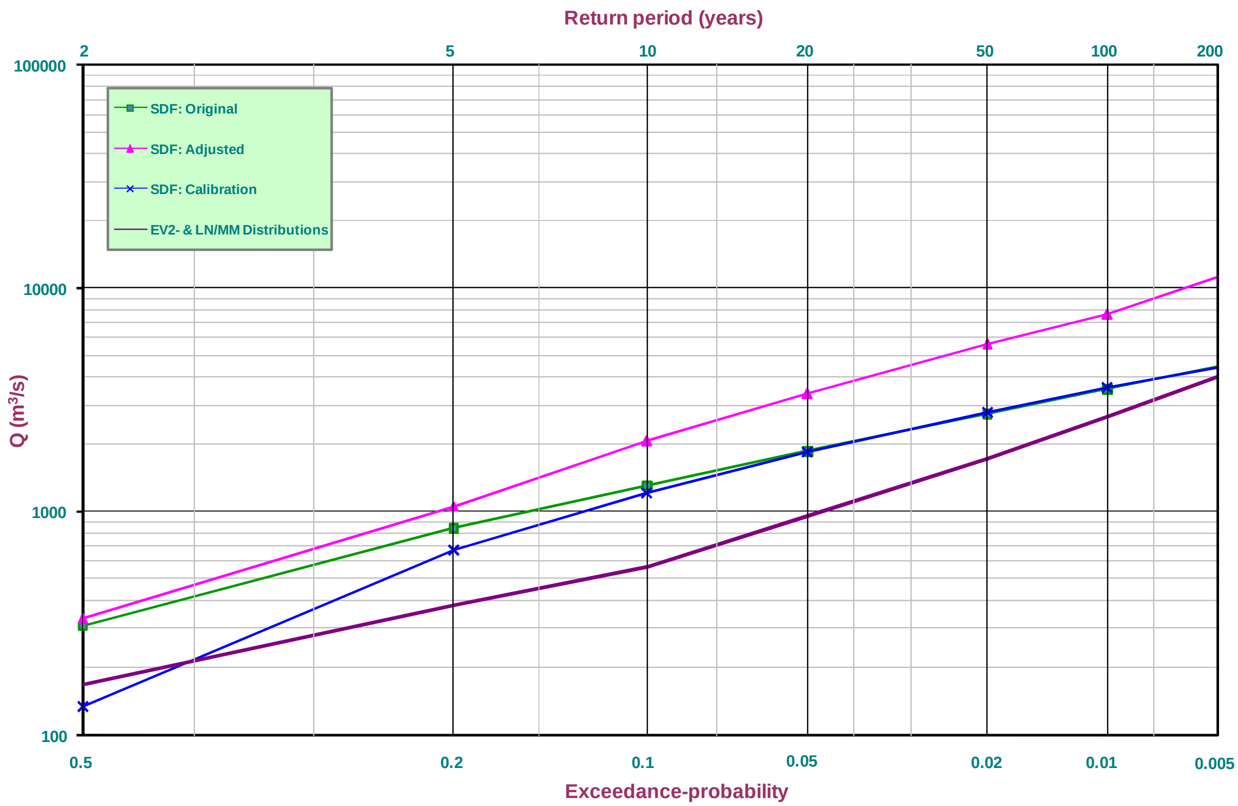

Figure C.101: Q1H001 (21): Probabilistic plot (verified SDF method)

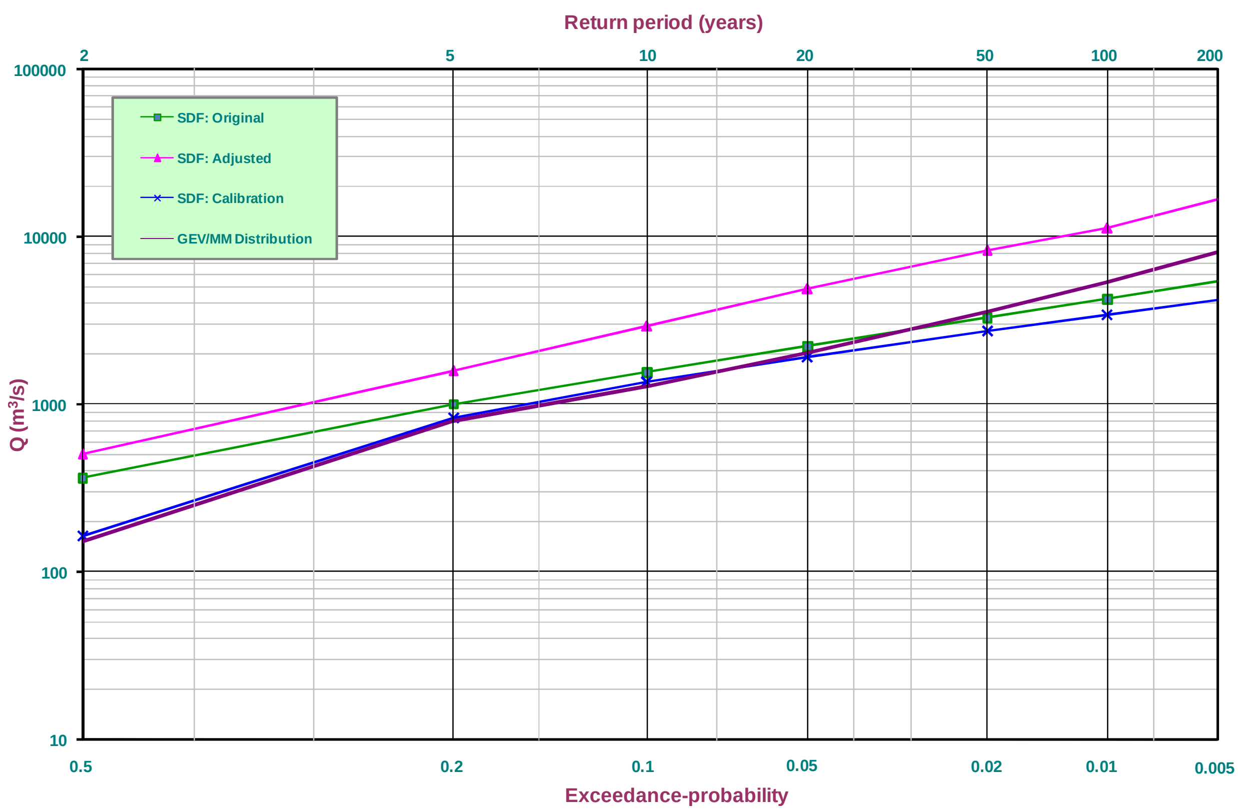

Figure C.102: Q7H003 (21): Probabilistic plot (verified SDF method)

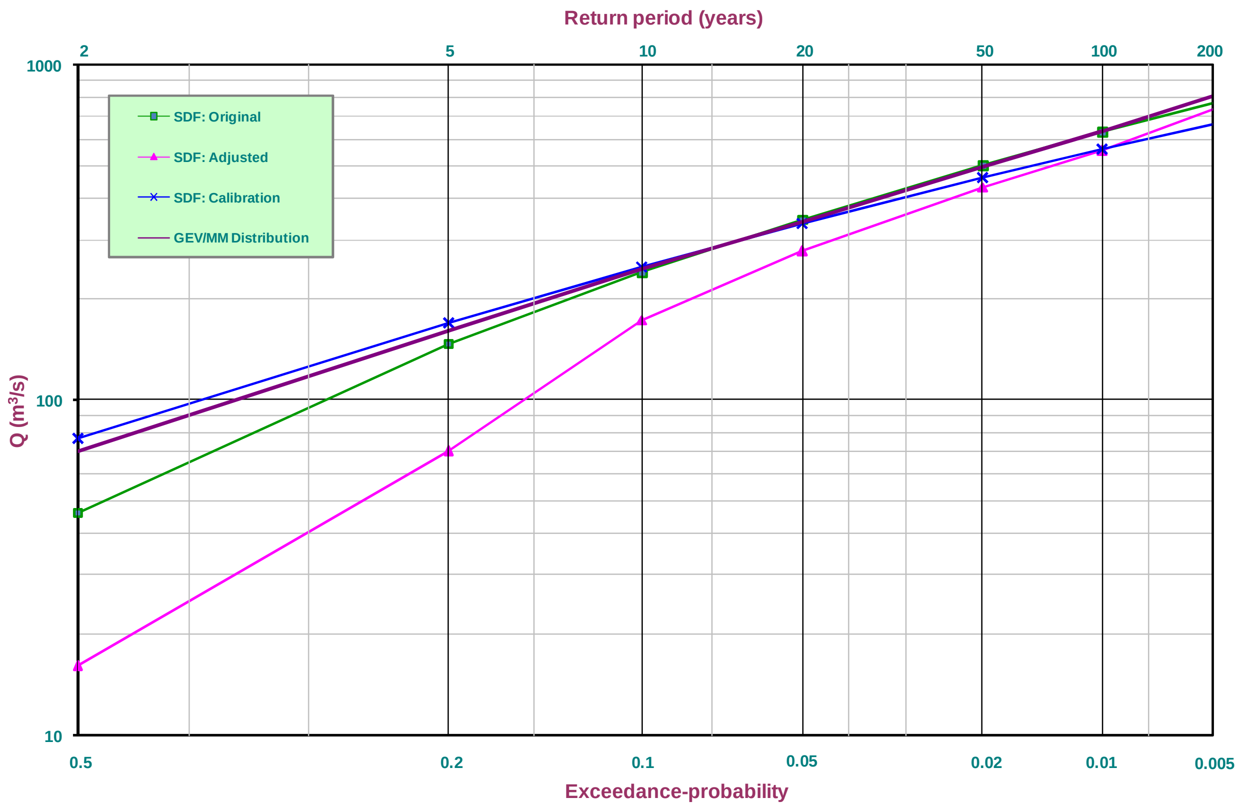

Figure C.103: Q9H004 (21): Probabilistic plot (verified SDF method)

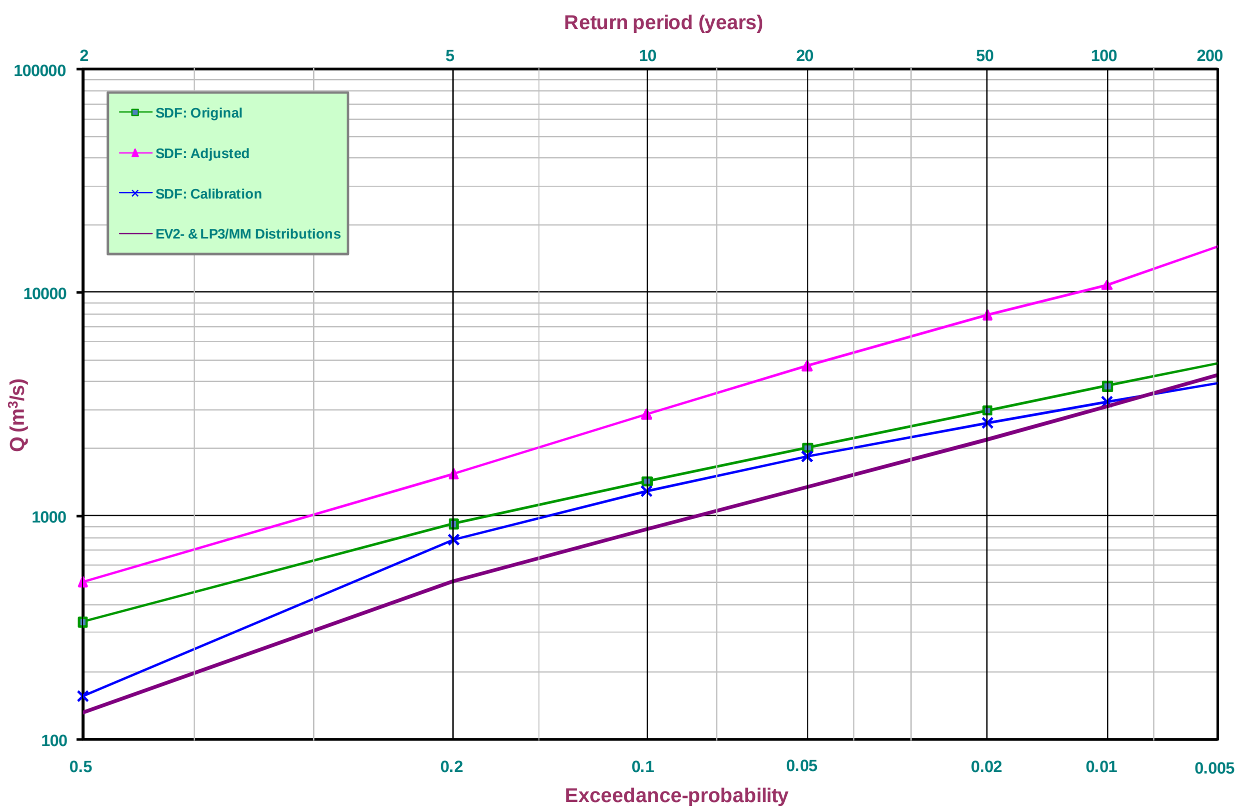

Figure C.104: Q9H012 (21): Probabilistic plot (verified SDF method)

ADDENDUM

D

USER MANUAL:

DESIGN FLOOD ESTIMATION TOOL

EVALUATION OF THE SDF METHOD USING A CUSTOMISED DESIGN FLOOD ESTIMATION TOOL

ADDENDUM D:
USER MANUAL: DESIGN FLOOD ESTIMATION TOOL

1. OPERATIONAL INSTRUCTIONS

A computer program with a graphical user interface, known as the Design Flood Estimation Tool (DFET) Version 1.1, has been developed in a Microsoft Office Excel (MS-Excel) and/or Visual Basic for Applications (MS-VBA) environment in order to assess the use and applicability of the various design flood estimation methods used in South Africa. This software implements the procedures detailed in Chapters 2 and 4 of the *Master of Science in Engineering (Civil)* thesis submitted at the Stellenbosch University. The objective of the first section in this user manual is to assist users with the installation and running of the software. The second section presents the application guidelines and instructions.

<u>Disclaimer</u>:

Although every effort has been made as to the accuracy and applicability contained in this software and supporting databases, the Stellenbosch University and the developer cannot accept any legal responsibility or liability for any errors or omissions or for any other reason whatsoever.

1.1 MINIMUM SYSTEM REQUIREMENTS

The minimum system requirements on a computer running the Windows operating system are:

- 512 Mb of RAM;
- 150 Mb Hard Disk capacity;
- Windows 2000/2000XP or more recent Windows operating system; and
- Microsoft Office 2007.

<u>Note</u>: The DFET is not compatible with Microsoft Office 2003 products.

The unprotected, light-green shaded cells in each worksheet are used as the primary input data cells and must be data free before commencing with a new example. Thus, any information entered in previous application files/examples must be deleted.

1.2 INSTALLATION OF SOFTWARE

The software may be installed from the CD which accompanies this report. The following files are contained on the CD:

- DFET_Excel2007.xlsm (MS-Excel Macro-enabled worksheet, 9.5 Mb).
- DesignPrecipitation_Excel2007.xlsx (MS-Excel worksheet, 7.4 Mb).
- DFET_UserManual.pdf (Adobe Acrobat 7.0 document, 23.3 Mb).

It is suggested that these files be saved in the *C:\Design_Flood*\directory, as the instructions in this manual will assume that the files are at that location. However, any user-defined directory can be used and the relevant path will need to be substituted in these instructions.

1.3 RUNNING OF SOFTWARE

Once these files are saved in the applicable directory, the DFET can be executed by running MS-Excel 2007 from Start\Programs\Microsoft Office\Microsoft Office Excel 2007 or by double-clicking the MS-Excel 2007 icon on the desktop.

Make use of the following steps:

- In MS-Excel 2007 click on the button and select open and browse to the relevant directory and DFET_Excel2007.xlsm file.
- Once the file is opened, a *Security Warning* (Macros have been disabled) will be displayed.
- Click on the *Options* button, after which the window displayed in Figure D.1 will appear.
- Select the option button next to *Enable this content*.
- Click OK.
- Save the DFET_Excel2007.xlsm file by making use of *Save As* and rename the file as desired. This must be done in order to retain the original template file in the *C:\Design_Flood*\directory.

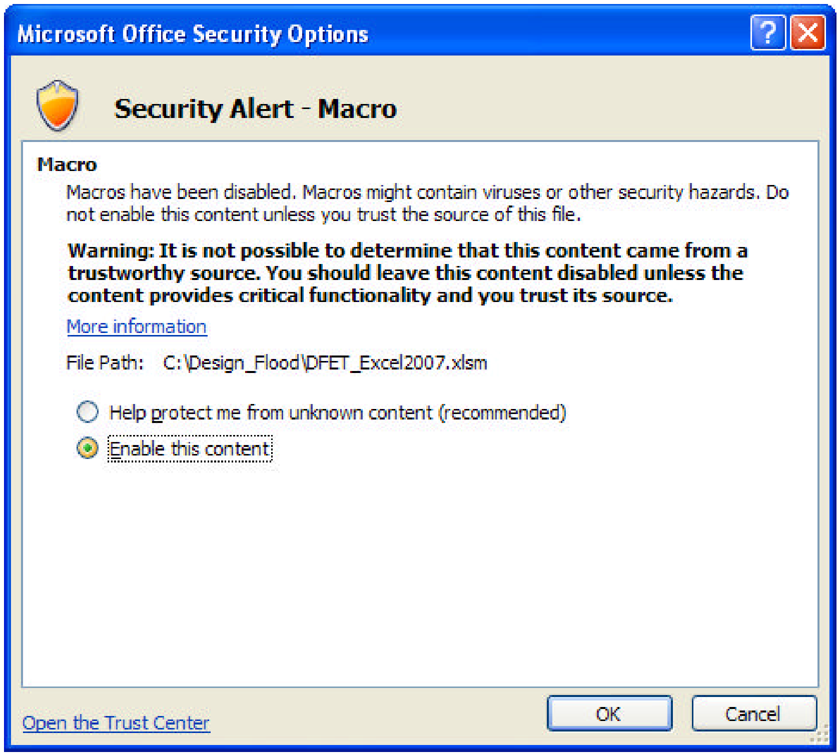

Figure D.1: Microsoft Office Security Options

2. APPLICATION GUIDELINES AND INSTRUCTIONS

2.1 HOME PAGE

The HOME page gives the user the ability to examine and view the contents of the relevant databases and design tables, design flood estimation methods, GIS-based maps and graphical plots contained in the various worksheets. It also serves as the primary worksheet with *click buttons* which activate macros to direct or redirect the user to any required worksheet. Figure D.2 is illustrative of the HOME page as contained in the DFET, whilst the schematic layout of the DFET is shown in Figure D.3.

2.1.1 Database and design tables

This group of 15 *click buttons* will either enable the user to view, examine, edit and update the applicable worksheets or only view the content thereof. The Catchment data, Precipitation, S-curve lag, Raw flow data, Annual and Partial series and Statistical plot worksheets are available for editing and updating, whilst the remaining eight worksheets are for viewing purposes only.

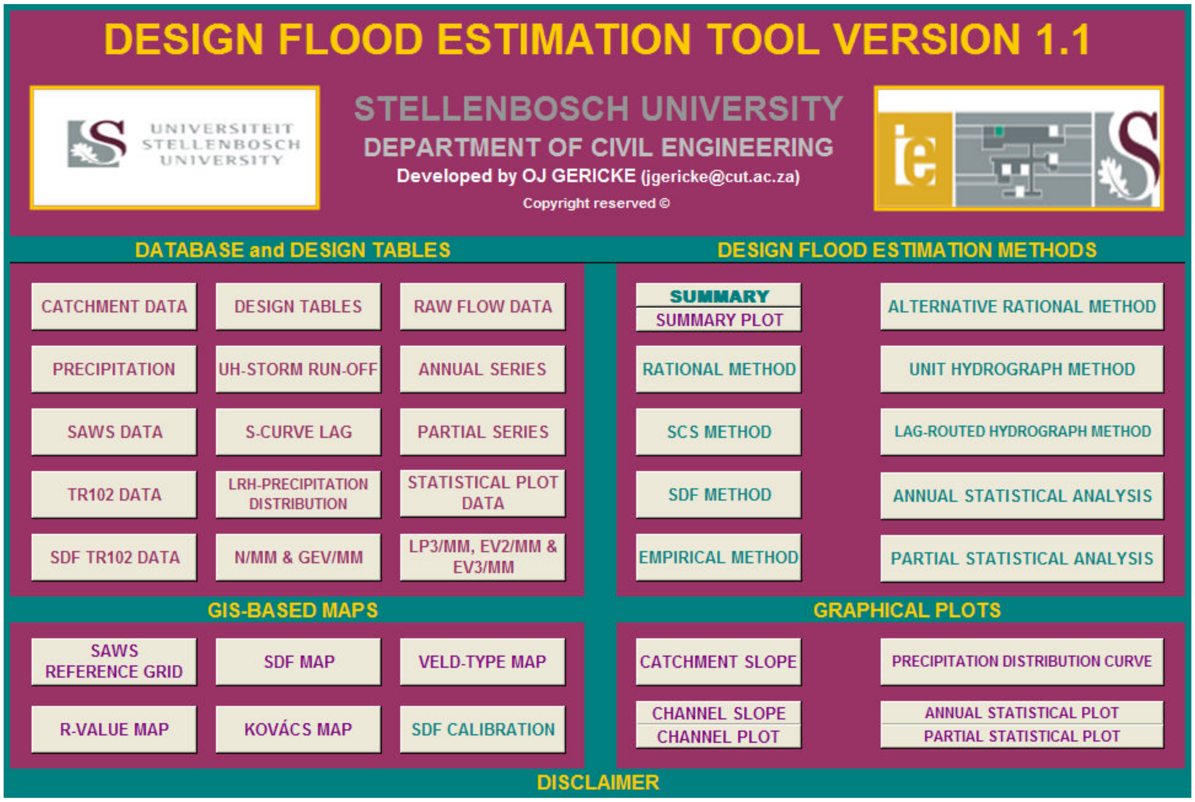

Figure D.2: DFET HOME page

2.1.2 Design flood estimation methods

Nine *click buttons* in this group give the user access to the deterministic, empirical and statistical methods used in South Africa to estimate the design flood. The editing and updating of all these worksheets are allowed, although the user input is restricted to the light-green shaded, unprotected cells. The **SUMMARY** and **SUMMARY PLOT** buttons enable the user to view and examine the flood estimation results summarised in both a tabular and graphical format.

2.1.3 Graphical plots

This group of six *click buttons* will enable the user to view, examine, edit and update the graphical plot results as obtained from the catchment data entries and design flood estimation methods listed in Section 2.1.2. It also allows the user to view the precipitation distribution curves of the Lag-routed hydrograph (LRH) method.

2.1.4 GIS-based maps

This group of six *click buttons* will enable the user to view all the standard GIS-based maps, inclusive of the SAWS reference grid, R-value, SDF, Kovács and Veld-type maps.

The SDF CALIBRATION button will enable the user to have a glimpse at the procedures followed to evaluate, calibrate en verify the original SDF method.

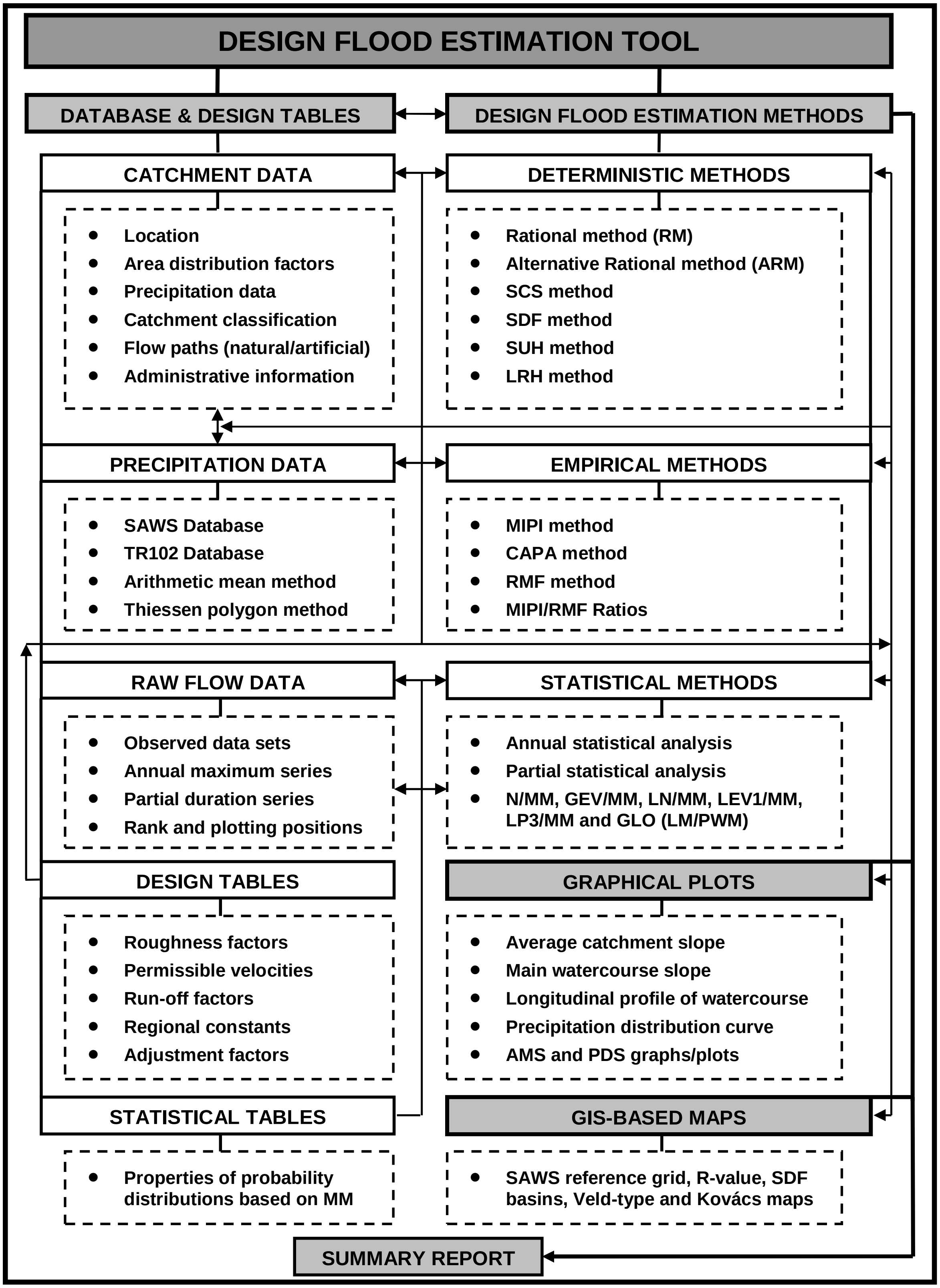

Figure D.3: Schematic layout of the DFET

2.2 CATCHMENT DATA

The layout of the Catchment data worksheet is displayed in Figure D.4.

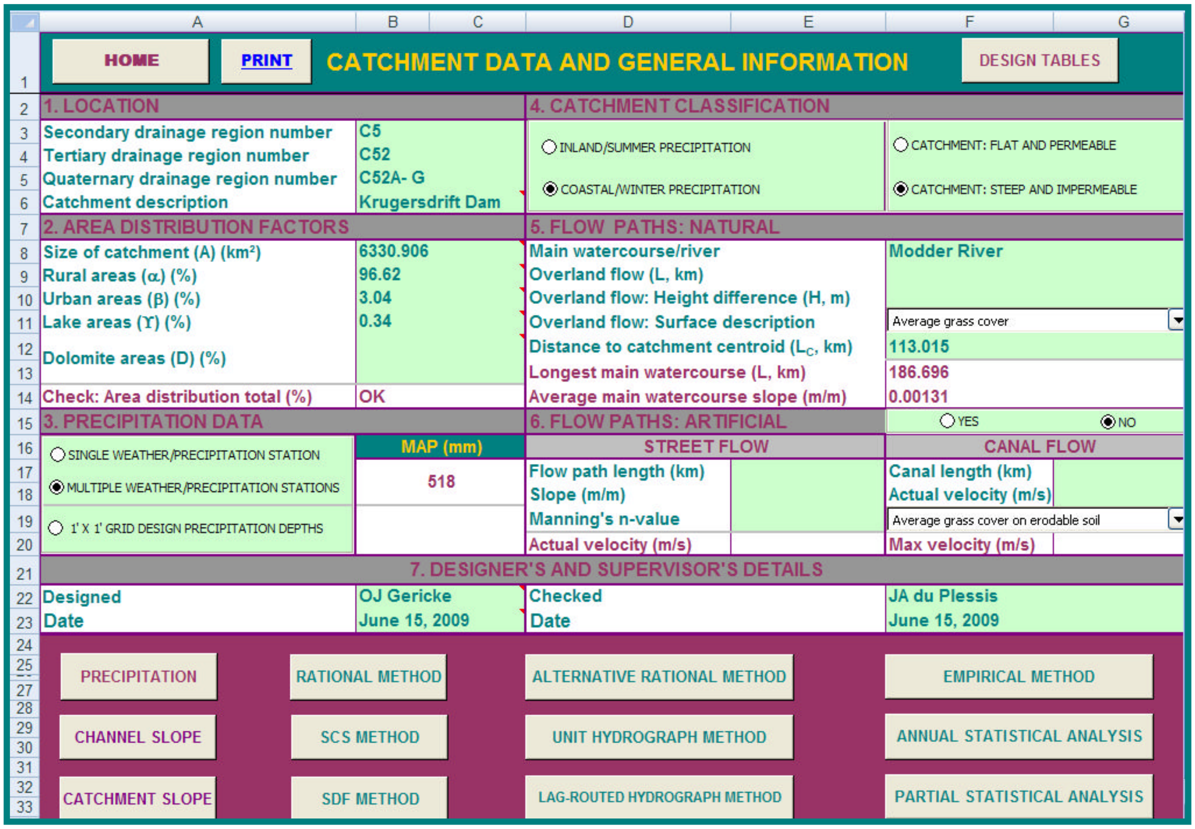

Figure D.4: Catchment data worksheet

2.2.1 Prerequisite input data and linked worksheets

The Weather data and Channel slope worksheets must be completed to provide the MAP, length and average slope of the main watercourse listed under catchment data; however, it is not a prerequisite.

The Catchment data worksheet is linked to several other worksheets (as indicated in Figure D.4), since it serves as input data for these worksheets.

2.2.2 Input data ranges and comments

Input data range identifier:

Single cell or cell range entries (light-green shaded and unprotected), option buttons and group boxes (drop-down lists with multiple options). Click and hold the mouse cursor in position to read any comment box (cells with red flags).

Location:

Cell B3: Enter the secondary drainage region number consisting of a descriptive letter and numerical value, e.g. C5.

Cell B4: Enter the tertiary drainage region number consisting of a descriptive letter and numerical values, e.g. C52.

Cell B5: Enter the quaternary drainage region number consisting of descriptive letters and numerical values, e.g. C52A.

Cell B6: Compulsory.
Enter the catchment description/name, e.g. Krugersdrift Dam.

Area distribution factors:

Cell B8: Compulsory.
Enter the catchment area (km^2).

Cell B9: Compulsory, if applicable.
Indicate the %-rural areas in catchment.

Cell B10: Compulsory, if applicable.
Indicate the %-urban areas in catchment.

Cell B11: Compulsory, if applicable.
Indicate the %-lake areas in catchment.

Cell B12: Compulsory, if applicable.
Indicate the %-dolomite areas in catchment.

Precipitation data:

Select the appropriate option button contained in the precipitation group box by indicating either whether a single or multiple weather/precipitation stations will be used. The MAP (mm) in *cell B17* will only be listed if the Weather data worksheet is completed. The MAP estimation can be based on either the TR102 or SAWS precipitation database.

Alternatively, the 1' x 1'-Grid design precipitation depths can also be selected. These precipitation depths are based on the output generated by the software program, *Design Rainfall Estimation in South Africa* as developed by Smithers and Schulze (2003). The MAP (mm) will then be listed in *cell B19*, but is also reliant on the prerequisite completion of the Weather data worksheet.

Catchment classification:

Two group boxes, precipitation regions and catchment description must be completed. In precipitation regions, select the appropriate option by indicating either whether the region can be classified as an “inland/summer precipitation” or a “coastal/winter precipitation” region. In catchment description, select the appropriate option by indicating either whether the catchment can be classified as “flat and permeable” or “steep and impermeable”. The selections made here will have an influence on the return period adjustment factors (F_T) used in both the Rational method (RM) and alternative Rational method (ARM).

Flow paths: Natural:

Cell F8: Compulsory.
Enter the main watercourse/river name, e.g. Modder River.

Cell F9: Compulsory, if applicable.
Enter the distance of overland flow (km).

Cell F10: Compulsory, if *cell F9* was completed.
Enter the height difference (m) along the overland flow path.

Cell F11: Select the appropriate overland flow surface description from the group box (drop-down list, 14 options available).

Cell F12: Compulsory, if the SUH, LRH and empirical methods are to be used.
Enter the distance to the catchment centroid (km), normally between 0.5 - 0.6 times the longest watercourse length.

Flow paths*:* Artificial:

Select the appropriate option button contained in the artificial flow path group box by indicating either “Yes” or “No”. If “Yes” is selected, then complete *cell ranges E17:E19 and G17:G18*, otherwise these cells can be left blank. The artificial flow path can consist of either street or canal flow or a combination thereof and the applicable cell ranges must be completed accordingly. The following applies:

Cell E17: Enter the length of the street flow path (km), if applicable.

Cell E18: Enter the slope of the street flow path (m/m), if *cell E17* was completed.

Cell E19: Enter a Manning’s *n*-value, if *cell range E17:E18* were completed.

Cell G17: Enter the canal flow path length (km), if applicable.

Cell G18: Enter the design/actual velocity if different from the maximum velocity indicated in *cell G20.* Manning's or Chézy's equation for open-channel flow can be used.

Cell G19: Select the appropriate canal lining material description from the group box (drop-down list, 16 options available) to establish the maximum allowable velocity in *cell G20*.

Designer's and supervisor's details:

Cell B22: Enter the details of the person responsible for the design.

Cell B23: Enter the design date (month, day, year), e.g. June 15, 2009.

Cell F22: Enter the details of the person responsible for the supervision.

Cell F23: Enter the approval date.

2.2.3 Calculation procedure

Area distribution factors:

Cell B14: Calculate the sum of *cell range B9:B11*. If # 100%, a "%-Error" message will appear. Revisit the input data used.

Precipitation data:

Cell B17: Input data from linked worksheet, Weather data.

Cell B19: Input data from linked worksheet, Weather data.

Flow paths: Natural:

Cell F13: Input data from linked worksheet, Channel slope.

Cell F14: Input data from linked worksheet, Channel slope.

Flow paths: Artificial:

Cell E20: The actual velocity is based on Manning's equation for street flow and a cross-slope of 2%.

$$v = \frac{1}{n}\left(\frac{0.1225}{3.57}\right)^{\frac{2}{3}} S^{\frac{1}{2}} \qquad (D.1)$$

Where:

n = Manning's *n*-value

S = Longitudinal slope (m/m)

v = Actual velocity (m/s)

Cell G20: Maximum allowable velocity based on the canal lining material selected from the drop-down list in *cell G19*.

2.3 PRECIPITATION DATA

Two precipitation databases, which are based on the SAWS and TR102 data, are available in the DFET. The SAWS database consist of design precipitation depths at 3 946 precipitation stations with data up to the year 2002 for durations ranging from one to 7 days and for return periods two to 200 years. This database is also used in the software program, *Design Rainfall Estimation in South Africa* as developed by Smithers and Schulze (2003). The TR102 database consists of design precipitation depths at 1 946 precipitation stations with data up to the year 1981 for durations of 1, 2, 3 and 7 days and for return periods ranging from two to 200 years.

2.3.1 Prerequisite input data and linked worksheets

The Catchment data worksheet is prerequisite input data for this worksheet. The Weather data worksheet is linked to the Catchment data worksheet and also serves as the primary input data for all the deterministic and empirical methods.

2.3.2 Input data ranges and comments

The following three options are available:

- 1' x 1'-Grid design precipitation depths based on the output generated by the software program, *Design Rainfall Estimation in South Africa*.
- SAWS precipitation depths based on either the arithmetic mean or Thiessen polygon methods.
- TR102 precipitation depths based on either the arithmetic mean or Thiessen polygon methods.

Only one option can be selected at a time.

Input data range identifier:

Single cell or cell range entries (light-green shaded and unprotected), option buttons and check boxes. The weather station numbers are used as the primary identifier in both the SAWS and TR102 precipitation databases. Click and hold the mouse cursor in position to read any comment box (cells with red flags).

1' x 1'-Grid design precipitation depths:

The following guidelines and/or instructions are based on the assumption that the output file generated by the software program, *Design Rainfall Estimation in South Africa* is ready for use in the DFET. In other words, the user-defined ASCII output file, which echoes the user selections and lists the design precipitation depths, is converted to a MS-Excel file, of which the averages of the grid-based precipitation estimates associated with durations in excess of the time of concentration, were calculated.

Cell D41: Compulsory, if applicable. By entering a MAP-value, all other calculated MAP-values are overwritten. This cell must be left blank if any of the other methods (SAWS/TR102) are used.

Cell A43: Click and hold the mouse cursor in position. The following comment box with instructions will appear on screen:

> **SEVEN (7) DESIGN PRECIPITATION DEPTHS ASSOCIATED WITH EACH RETURN PERIOD AND TWO (2) GROUPED USER-DEFINED STORM DURATIONS OF BETWEEN 0.083 hour (5 minutes) & 168 hours (7 days) CAN BE SELECTED BY ACTIVATING THE CHECK BOXES "10 min, 6 hr, 5 day, etc." IN CELL RANGE A44: B51.**
>
> **STORM DURATIONS WITHIN THE SAME ROW (e.g. 10 min, 6 hr & 2 day) CANNOT BE SELECTED SIMULTANEOUSLY.**
>
> **THE SELECTED STORM DURATIONS MUST FOLLOW ONE ANOTHER/BE GROUPED WITHIN A CONTINUOUS TIME PERIOD AND THE TIME OF CONCENTRATION MUST BE WITHIN THE SELECTED TIME PERIOD.**
>
> **IN ALL CASES, USE COPY & PASTE VALUES FOR MULTIPLE ENTRIES.**

Cell range

C44:I51: Compulsory, if applicable.

The seven design precipitation depths associated with each return period and selected storm durations (activated check boxes) must be copied into the relevant cells.

Figure D.5 displays the layout of the data screen representative of the 1' x 1'-Grid design precipitation depths.

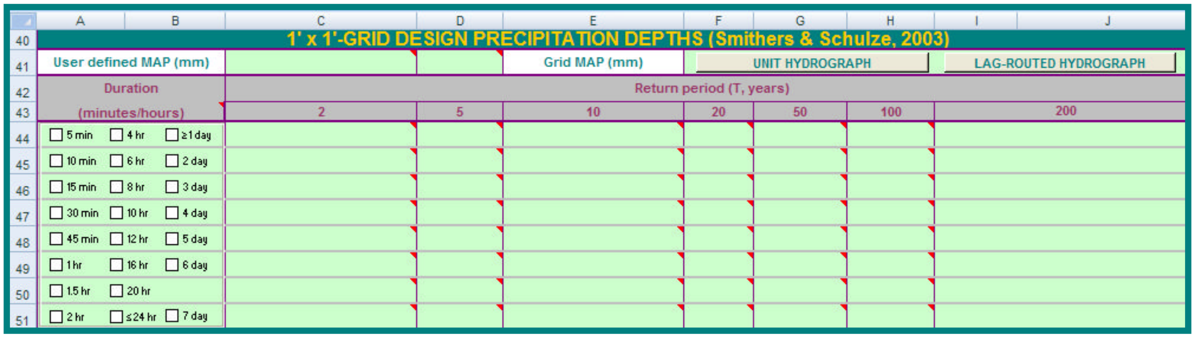

Figure D.5: 1' x 1'-Grid design precipitation depths

SAWS/TR102 precipitation depths:

The procedure to follow will depend on whether or not a user-defined MAP value is specified or whether or not the user want to use a selection of precipitation stations in the catchment under consideration. The user-defined MAP value must be entered in *cell C41* if the first option is applicable. This MAP value will overwrites any other calculated MAP value. The following procedure is relevant to the second option in cases where the user still has to identify the precipitation stations within/nearby the catchment boundary:

- Click on the **SAWS REFERENCE GRID** button to view the SAWS precipitation station reference grid map in order to establish in which grid the catchment under consideration is situated. The grid reference, e.g. 262, contains all the weather stations with numbering starting with 0262??? This 7-digit number will either be followed by an A, B, P, S or W, depending on which institution/company is responsible for the station. Click on the **PRECIPITATION** button to return to the Weather data worksheet. The SAWS precipitation station reference grid map is illustrated in Figure D.6.
- Click on either the **SAWS DATA** or **TR102 DATA** buttons to view the weather stations numbered in an ascending order and their associated design precipitation depths. The station numbers can be individually copied to the Weather data worksheet (refer to instructions below, *cell A56*) or a customised data file/sheet can be populated for later use. Click on the **PRECIPITATION** button to return to the Weather data worksheet.

Alternatively, if the GIS-based data of the precipitation stations are available, the relevant database file (.dbf) can be accessed in MS-Excel, highlighted and copied to the Weather data worksheet (refer to instructions below, *cell A56*).

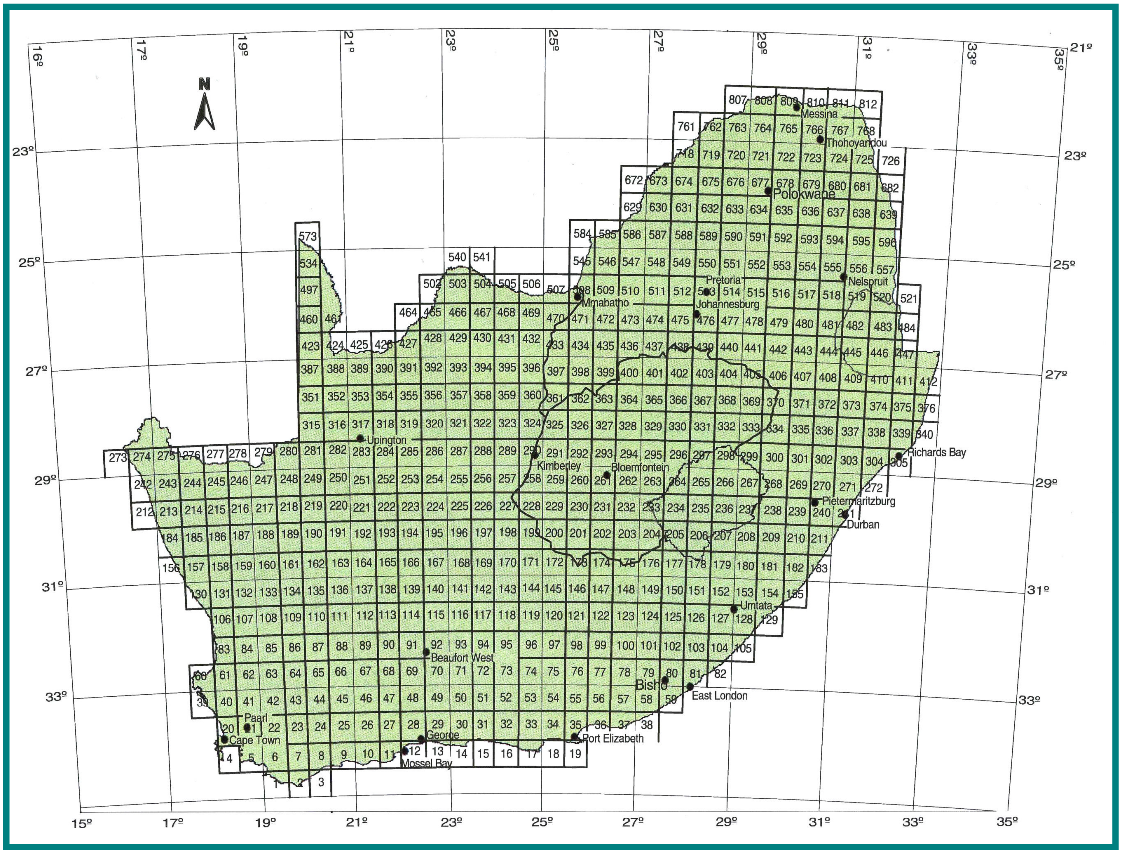

Figure D.6: SAWS reference grid map (SANRAL, 2006: 3.24)

Cell A56: Click and hold the mouse cursor in position. The following comment box with instructions will appear on screen:

> CLICK ON THE SAWS DATA/TR102 DATA BUTTON TO ACCESS THE APPLICABLE DATABASE.
>
> THE WEATHER SERVICE STATION NUMBERS OF UP TO 200 PRECIPITATION STATIONS WITHIN/NEARBY THE CATCHMENT BOUNDARY CAN BE ENTERED IN CELL RANGE A58: A157 & G58: G157, IF APPLICABLE.
>
> THE WEATHER SERVICE STATION NUMBER MUST BE A 7-DIGIT NUMBER FOLLOWED EITHER BY AN A, B, P, S OR W.
>
> THE CHECK BOXES “Outside catchment”, CELL RANGE C58: C157 & G58: G157 MUST BE SELECTED IN CASES WHERE THE THIESSEN POLYGON METHOD IS BASED ON STATIONS OUTSIDE THE CATCHMENT BOUNDARY. THESE SELECTIONS WILL ALSO HAVE AN INFLUENCE ON THE ARITHMETIC MEAN METHOD, SINCE THIS METHOD CONSIDERS ONLY THE STATIONS WITHIN THE CATCHMENT BOUNDARY.
>
> ENTER THE THIESSEN POLYGON AREAS IN CELL RANGE D58: D157 & I58: I157, IF THE THIESSEN POLYGON METHOD IS TO BE CONSIDERED.
>
> IN ALL CASES, USE COPY & PASTE VALUES FOR MULTIPLE ENTRIES.

Figure D.7 is illustrative of the data entries based on the instructions listed in the above-mentioned comment box. On completion of the above-mentioned instructions, the user can view the results applicable to both the SAWS and TR102 database. The weighted MAP, design precipitation depths associated with different return periods and number of thunder days per year are contained in *cell range A6:I39* and illustrated in Figure D.8.

WEATHER SERVICE STATIONS (SAWS/TR102)							
Number	**Station number**	**Area (km²)**	**Station name**	**Number**	**Station number**	**Area (km²)**	**Station name**
1	0232123W ☐ Outside catchment	118.728	ROODEPOORT	101	☐ Outside catchment		
2	0232181W ☐ Outside catchment	100.857	ROODEPOORT	102	☐ Outside catchment		
3	0232211W ☐ Outside catchment	40.136	NIEUWEJAARSFONTEIN	103	☐ Outside catchment		
4	0232275W ☐ Outside catchment	86.589	DEWETSDORP (Police)	104	☐ Outside catchment		
5	0232301W ☐ Outside catchment	74.032	KILDARE	105	☐ Outside catchment		
6	0232512W ☐ Outside catchment	98.538	THORLEY	106	☐ Outside catchment		
7	0261307W ☐ Outside catchment	20.406	BLOEMFONTEIN	107	☐ Outside catchment		
8	0261365W ☐ Outside catchment	60.038	BLOEMFONTEIN (BAYSWATER)	108	☐ Outside catchment		
9	0261366W ☐ Outside catchment	7.003	BLOEMFONTEIN (ARBORETUM)	109	☐ Outside catchment		
10	0261367W ☐ Outside catchment	6.978	BLOEMFONTEIN (ST. MICHAEL'S)	110	☐ Outside catchment		
11	0261368W ☐ Outside catchment	10.861	BLOEMFONTEIN (KING'S PARK)	111	☐ Outside catchment		
12	0261369W ☐ Outside catchment	39.344	BLOEMFONTEIN (HAMILTON)	112	☐ Outside catchment		
13	0261425W ☐ Outside catchment	45.539	BLOEMFONTEIN (WAVERLEY)	113	☐ Outside catchment		
14	0261426W ☐ Outside catchment	14.995	BLOEMFONTEIN (ESTIORE)	114	☐ Outside catchment		
15	0261516W ☐ Outside catchment	55.974	BLOEMFONTEIN (ESTIORE)	115	☐ Outside catchment		
16	0261517W ☐ Outside catchment	16.205	BLOEMSPRUIT	116	☐ Outside catchment		
17	0261523W ☐ Outside catchment	160.343	GROOTVLEI	117	☐ Outside catchment		
18	0261548W ☐ Outside catchment	73.016	SHANNON VALLEY	118	☐ Outside catchment		
19	0261722W ☐ Outside catchment	221.912	MAZELSPOORT DAM	119	☐ Outside catchment		
20	0261733W ☐ Outside catchment	171.472	TUSSENVIER	120	☐ Outside catchment		

Figure D.7: SAWS precipitation station data entries

HOME	CATCHMENT DATA	PRINT 1	PRECIPITATION DATA	PRINT 2	SAWS DATA	TR102 DATA

Secondary drainage region number	C5	Main watercourse/river	Modder River
Tertiary drainage region number	C52	Designed	OJ Gericke
Quaternary drainage region number	C52A- G	Checked	JA du Plessis
Catchment description	Krugersdrift Dam	Date	June 15, 2009

SAWS REFERENCE GRID

SAWS PRECIPITATION DATABASE

ARITHMETIC MEAN METHOD

Weighted MAP (mm)	530.2	Weighted number of thunder days/year (R)	61.8

Duration (days)	Return period (T, years) 2	5	10	20	50	100	200
1	48.7	65.8	77.9	90.0	106.5	119.5	133.1
2	61.6	82.9	97.8	112.7	133.0	148.9	165.4
3	68.6	92.0	108.0	123.9	145.2	161.7	178.5
7	86.2	116.0	136.3	156.2	182.7	203.1	223.8

THIESSEN POLYGON METHOD

Weighted MAP (mm)	518.5	Weighted number of thunder days/year (R)	62.3

Duration (days)	Return period (T, years) 2	5	10	20	50	100	200
1	48.5	65.5	77.5	89.6	106.0	119.0	132.5
2	61.2	82.3	97.1	112.0	132.1	147.9	164.4
3	68.0	91.2	107.2	122.9	144.0	160.4	177.1
7	85.9	115.7	135.9	155.8	182.2	202.5	223.2

TR102 PRECIPITATION DATABASE

ARITHMETIC MEAN METHOD

Weighted MAP (mm)	522.5	Weighted number of thunder days/year (R)	61.7

Duration (days)	Return period (T, years) 2	5	10	20	50	100	200
1	49.0	67.7	77.8	97.3	119.8	138.6	159.6
2	61.1	84.9	102.7	121.8	149.7	172.8	198.0
3	67.9	94.5	114.7	136.3	167.7	193.0	222.6
7	85.2	121.4	148.6	175.2	218.9	253.3	287.4

THIESSEN POLYGON METHOD

Weighted MAP (mm)	511.2	Weighted number of thunder days/year (R)	62.1

Duration (days)	Return period (T, years) 2	5	10	20	50	100	200
1	48.7	67.2	77.2	96.3	118.4	136.8	157.5
2	60.6	84.1	101.7	120.3	147.6	170.3	195.0
3	67.3	93.7	113.6	135.0	165.9	190.9	219.8
7	84.3	120.2	147.2	173.6	217.0	251.2	284.9

Figure D.8: Design precipitation depth results

Based on the results viewed and evaluated in the previous step, the appropriate option buttons contained in the design precipitation results group box (*cell range F53:J54*) must be selected by indicating either whether the SAWS or TR102 precipitation database will be used and whether the results based on the Thiessen polygon or Arithmetic mean method must be included. The design precipitation results group box is displayed in Figure D.9.

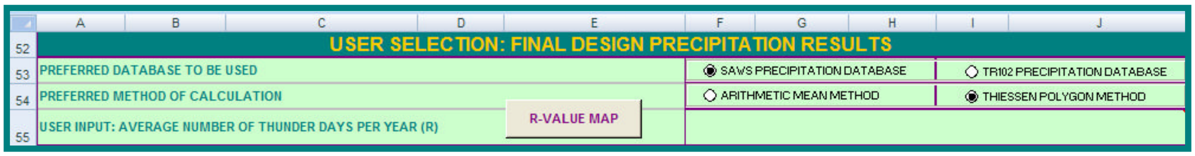

Figure D.9: Design precipitation results group box

In cases where the calculated weighted number of thunder days per year is deemed as questionable, the user can enter a user-defined *R*-value in *cell F55* with the use of the *R*-value map (Figure D.10). This value entered overwrites the calculated values.

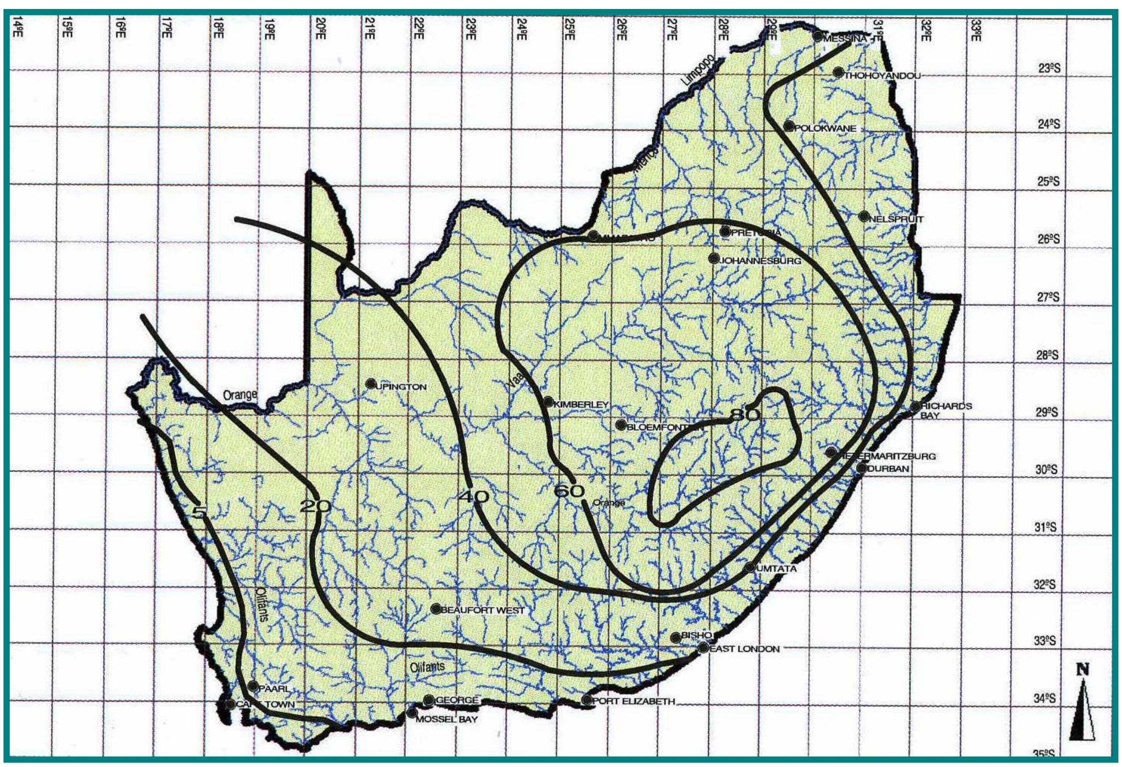

Figure D.10: Average number of thunder days per year (SANRAL, 2006: 3.23)

2.3.3 Calculation procedure

Arithmetic mean method:

$$\overline{X} = \sum \frac{X_i}{N_i} \quad (D.2)$$

Thiessen polygon method:

$$\overline{X} = \frac{\sum X_i A_i}{\sum A_i} \quad (D.3)$$

Where:

A = Area (km²)

N_i = Number of precipitation stations within area

$\overline{X}$ = Weighted MAP (mm), weighted point precipitation depth (mm) or weighted thunder days/year

X_i = MAP (mm), point precipitation depth (mm) or thunder days/year

2.4 AVERAGE CATCHMENT SLOPE

2.4.1 Prerequisite input data and linked worksheets

The Catchment data worksheet is prerequisite input data for this worksheet. The Catchment slope worksheet is linked to all the worksheets containing the deterministic and empirical methods.

2.4.2 Input data ranges and comments

Input data range identifier:

Single cell and cell range entries (light-green shaded and unprotected) and option buttons. Click and hold the mouse cursor in position to read any comment box (cells with red flags).

The layout of the Catchment slope worksheet is displayed in Figure D.11.

	A	B	C	D	E	F	G	H	I
1	HOME	PRINT	AVERAGE CATCHMENT SLOPE					CATCHMENT DATA	
2	Secondary drainage region number	C5			Main watercourse/river			Modder River	
3	Tertiary drainage region number	C52			Designed			OJ Gericke	
4	Quaternary drainage region number	C52A- G			Checked			JA du Plessis	
5	Catchment description	Krugersdrift Dam			Date			June 15, 2009	
6	USER INPUT/GRID METHOD/EMPIRICAL EQUATION								
7	Contour interval (ΔH, m)	20			Map scale (1:X)			50000	
8	Sum of contour lines in catchment (m)	10776515.778			Average slope (User input, m/m)			0.04186	
9	Number of grid points (N)	2220			Average slope (Alexander, m/m)			0.02919	
10	Sum of horisontal distances (m)	1520901.832			Average slope (Schulze, m/m)			0.03404	
11	PREFERRED METHOD OF CALCULATION	◉ AVERAGE SLOPE: USER INPUT			○ AVERAGE SLOPE: ALEXANDER			○ AVERAGE SLOPE: SCHULZE	
12	FREQUENCY DISTRIBUTION OF GRID POINTS (%)								
13	0-3% Slope	40.6%			10- 30% Slope			17.4%	
14	3-10% Slope	28.4%			> 30% Slope			13.6%	
15	HORISONTAL DISTANCES BETWEEN CONSECUTIVE CONTOURS (L_i)				Unit of measurement		◉ METRES	○ MILLIMETRES	
16	L_i (1)	L_i (2)	L_i (3)	L_i (4)	L_i (5)	L_i (6)	L_i (7)	L_i (8)	L_i (9)
17	455.528	1097.569	716.775	1354.745	495.303	1167.265	103.195	884.918	577.794
18	710.563	832.916	817.544	716.269	1170.613	683.076	214.482	1123.665	398.061
19	759.956	92.130	329.824	314.050	1133.771	362.170	272.185	976.753	818.630
20	432.349	888.657	152.769	283.368	1348.716	176.315	463.034	1186.414	1275.530
21	1021.848	365.607	121.937	2251.562	606.373	409.959	856.379	1558.020	608.861
22	610.638	336.021	1245.117	1466.786	1398.645	737.146	1083.361	1458.320	727.940
23	463.924	519.589	233.786	3376.404	625.470	809.243	338.645	1104.519	1467.619
24	104.574	1226.638	53.150	2723.262	703.148	417.843	989.719	1032.078	271.831
25	86.993	614.254	130.000	2153.730	142.459	727.931	809.438	1881.625	36.218
26	145.849	1956.578	614.358	2100.528	94.406	401.781	979.958	420.372	116.965
27	100.954	976.222	43.782	997.445	74.077	803.645	745.462	295.632	533.646
28	446.831	376.919	49.673	1521.217	53.425	365.614	369.326	296.763	1530.591
29	407.331	189.464	37.686	831.712	51.563	440.465	874.094	722.744	1733.500
30	562.389	581.986	120.263	1075.250	392.777	647.265	920.023	1877.907	1543.243
31	759.993	446.303	513.049	3646.257	144.929	705.857	1077.676	1649.992	823.526

Figure D.11: Layout of the Catchment slope worksheet

Grid method/Empirical equation/User input:

Cell B7: Compulsory, applicable to both the grid method and empirical equation.

Enter the contour interval in metres as obtained from GIS, orthophotos or topographical maps, e.g. 20 m.

Cell B8: Compulsory, if the empirical equation is to be used.

Use ArcGIS^{TM} (Hawth's Analysis Tools) to sum the contour line lengths in the catchment (polygons).

Cell H7: Compulsory, if the grid method is to be used.

Enter the map scale (1*:* X) as obtained from GIS, orthophotos or topographical maps, e.g. 50 000.

Cell H8: Enter the average slope (m/m) as obtained from a digital elevation model (DEM) in ArcGIS^{TM}.

Cell B11: Based on the values entered and results viewed in the previous steps, the appropriate option button contained in the average slope group box (*cell range B11:I11*) must be selected by indicating either whether the average slope results based on the DEM (user input), grid method (Alexander) or empirical equation (Schulze) must be used.

Cell A15: Comment: "A total of 7 506 horisontal distances between consecutive contours can be entered in *cell range A17:I850*, if applicable. In all cases, use *Copy & Paste values* for multiple entries."

Cell E15: Comment: "Indicate the unit in which the actual distances between consecutive contours on a map were measured, either in metres or millimetres."

Cell G15: Unit of measurement group box: Select the appropriate option button by indicating either whether the unit of measurement was in "metres" or "millimetres".

Cell range A17:I850: Refer to the comment made in *cell A15*.

2.4.3 Calculation procedure

Grid method (Alexander):

$$S = \frac{\Delta H}{\sum_{i=1}^{N} \frac{L_i}{N}} \qquad (D.4)$$

Empirical equation (Schulze):

$$S = \frac{M\Delta H * 10^{-2}}{A} \qquad (D.5)$$

Where:

A = Catchment area (km²)

ΔH = Contour interval (m)

L_i = Horisontal distance between consecutive contours (m)

M = Total length of all contour lines within the catchment (m)

N = Number of grid points

S = Average catchment slope (m/m)

Frequency distribution of grid points:

The results contained in *cells B13, B14, H13 and H14* are representative of the frequency distribution of the grid points based on the four standard slope classification classes used in the RM and ARM, e.g. 0 - 3%, 3 - 10%, 10 - 30% and > 30%.

2.5 AVERAGE MAIN WATERCOURSE SLOPE

2.5.1 Prerequisite input data and linked worksheets

The Catchment data worksheet is prerequisite input data for this worksheet. The Channel slope worksheet is linked to the Channel plot chart, the Catchment data worksheet and all the worksheets containing the deterministic and empirical methods.

2.5.2 Input data ranges and comments

Input data range identifier:

Single cell and cell range entries (light-green shaded and unprotected) and option buttons. Click and hold the mouse cursor in position to read any comment box (cells with red flags).

Longitudinal profile:

Cell B20: Click and hold the mouse cursor in position. The following comment box with instructions will appear on screen:

A TOTAL OF 150 HORISONTAL DISTANCES AND REDUCED HEIGHTS REPRESENTATIVE OF THE LONGITUDINAL PROFILE CAN BE ENTERED IN CELL RANGE B22: C171.

IN ALL CASES, USE COPY & PASTE VALUES FOR MULTIPLE ENTRIES.

CLICK ON THE CHANNEL PLOT BUTTON TO ACCESS THE CHANNEL PROFILE CHART.

THE X (HORISONTAL DISTANCE) AND Y (REDUCED HEIGHT) SCALES OF THE CHANNEL PROFILE CHART MUST BE EDITED ACCORDING TO THE INPUT DATA USED IN CELL RANGE B22: C171.

RIGHT-CLICK ON THE RELEVANT SCALE BAR (X- OR Y-AXIS) AND SELECT FORMAT AXIS FOLLOWED BY AXIS OPTIONS.

SET THE MAXIMUM AND MINIMUM VALUES, AS WELL AS THE MAJOR AND MINOR UNITS IF REQUIRED.

CLICK ON THE CHANNEL SLOPE BUTTON TO RETURN TO THE CHANNEL SLOPE WORKSHEET.

Average slope results:

Cell C19: Based on the values entered and results viewed in the previous steps, the appropriate option button contained in the average slope group box (*cell range C19:J19*) must be selected by indicating either whether the 10-85, Taylor-Schwarz or Equal-area methods must be used.

2.5.3 Calculation procedure

10-85 method:

$$S_{Avg} = \frac{(H_{0.85L} - H_{0.10L})}{(750L)} \qquad (D.6)$$

Taylor-Schwarz method:

$$S_{Avg} = \left(\frac{L}{\sum_{i=1}^{N} \frac{L_i}{\sqrt{S_i}}} \right)^2 \qquad (D.7)$$

Equal-area method:

$$S_{Avg} = \frac{(H_T - H_B)}{L} \qquad (D.8)$$

Where:

$$A_i = \left(\frac{(H_i + H_{i+1})}{2} - H_B \right) L_i$$

$$H_T = \frac{\left(\sum_{i=1}^{N} A_i * 2 \right)}{L} + H_B$$

H_B = Height at catchment outlet (m)

H_i = Specific contour interval height (m)

$H_{0.85L}$ = Height of main watercourse at length 0.85*L*

$H_{0.10L}$ = Height of main watercourse at length 0.10*L*

L = Length of main watercourse (m)

L_i = Distance between two consecutive contours (m)

S_{Avg} = Average main watercourse slope (m/m)

S_i = Slope between two consecutive contours (m/m)

The layout of the Channel slope worksheet is displayed in Figure D.12, whilst a typical longitudinal profile plot is shown in Figure D.13.

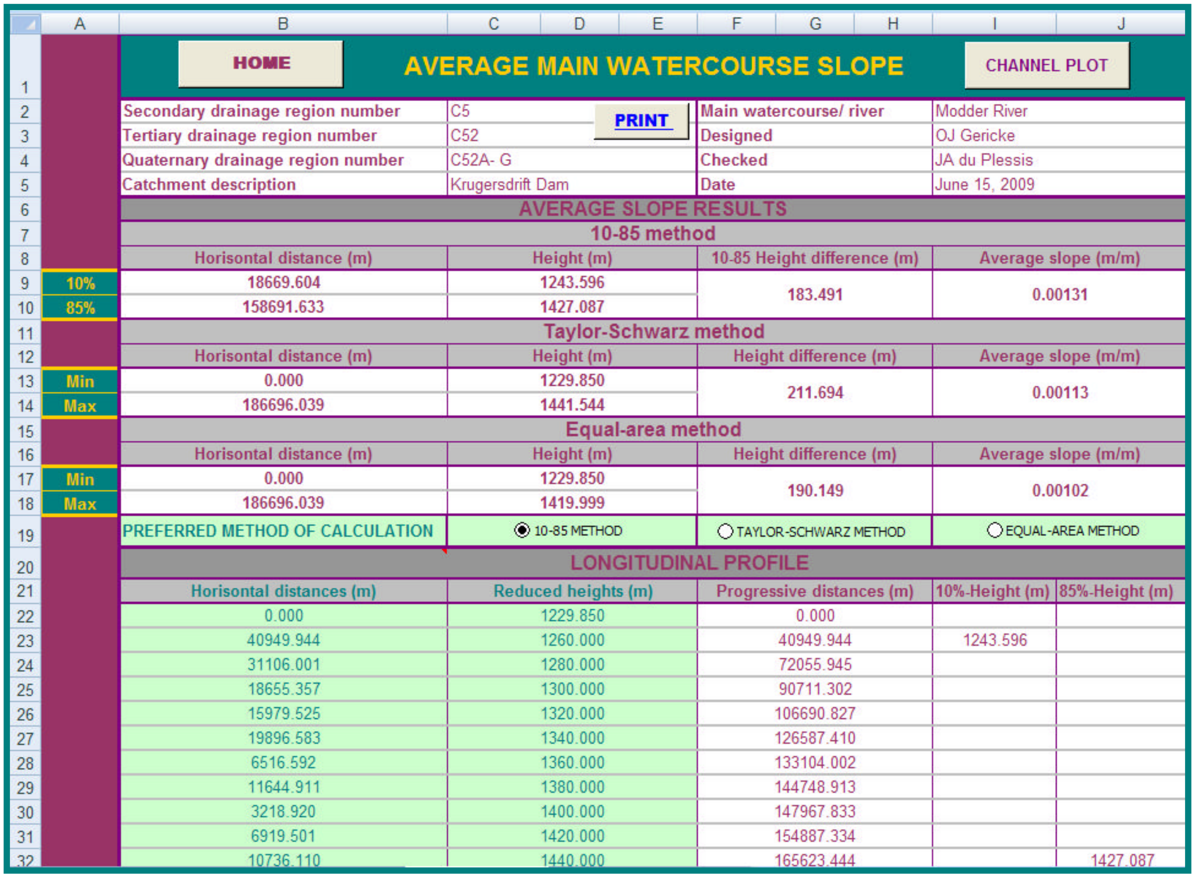

HOME | AVERAGE MAIN WATERCOURSE SLOPE | CHANNEL PLOT | PRINT

Secondary drainage region number	C5	Main watercourse/ river	Modder River
Tertiary drainage region number	C52	Designed	OJ Gericke
Quaternary drainage region number	C52A- G	Checked	JA du Plessis
Catchment description	Krugersdrift Dam	Date	June 15, 2009

AVERAGE SLOPE RESULTS

10-85 method

	Horisontal distance (m)	Height (m)	10-85 Height difference (m)	Average slope (m/m)
10%	18669.604	1243.596	183.491	0.00131
85%	158691.633	1427.087		

Taylor-Schwarz method

	Horisontal distance (m)	Height (m)	Height difference (m)	Average slope (m/m)
Min	0.000	1229.850	211.694	0.00113
Max	186696.039	1441.544		

Equal-area method

	Horisontal distance (m)	Height (m)	Height difference (m)	Average slope (m/m)
Min	0.000	1229.850	190.149	0.00102
Max	186696.039	1419.999		

PREFERRED METHOD OF CALCULATION: ◉ 10-85 METHOD ○ TAYLOR-SCHWARZ METHOD ○ EQUAL-AREA METHOD

LONGITUDINAL PROFILE

Horisontal distances (m)	Reduced heights (m)	Progressive distances (m)	10%-Height (m)	85%-Height (m)
0.000	1229.850	0.000		
40949.944	1260.000	40949.944	1243.596	
31106.001	1280.000	72055.945		
18655.357	1300.000	90711.302		
15979.525	1320.000	106690.827		
19896.583	1340.000	126587.410		
6516.592	1360.000	133104.002		
11644.911	1380.000	144748.913		
3218.920	1400.000	147967.833		
6919.501	1420.000	154887.334		
10736.110	1440.000	165623.444		1427.087

Figure D.12: Layout of the Channel slope worksheet

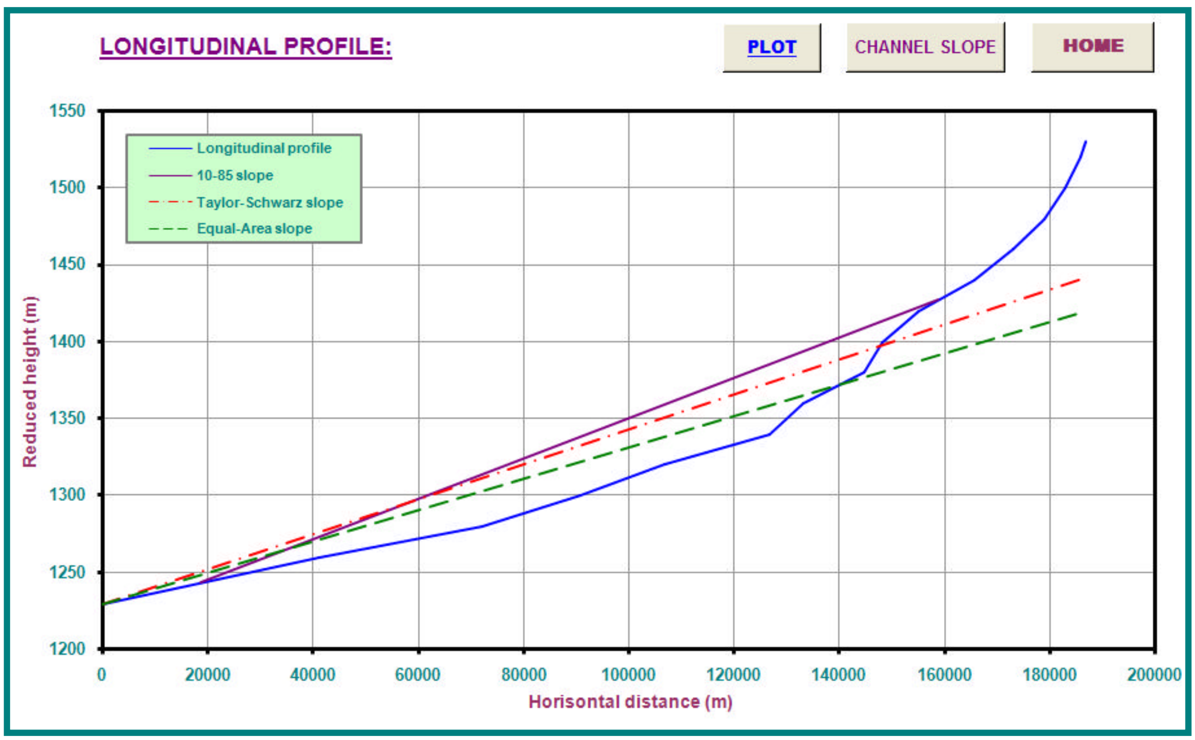

Figure D.13: Typical longitudinal profile plot

2.6 RATIONAL METHOD (RM)

2.6.1 Prerequisite input data and linked worksheets

The Catchment data and Weather data worksheets are prerequisite input data for this worksheet. The Rational method worksheet is also linked to the Catchment slope, Channel slope and Design tables worksheets. The Design tables worksheet contains all the input data and design parameters used in both the deterministic and empirical methods. This worksheet can be accessed by clicking on the DESIGN TABLES button.

2.6.2 Input data ranges and comments

Input data range identifier:

Single cell and cell range entries (light-green shaded and unprotected) and option buttons. Click and hold the mouse cursor in position to read any comment box (cells with red flags).

Physical characteristics:

Rural run-off coefficients (C_1):

The average catchment slope, hydrological soil group/permeability and land use/vegetation classes are used to describe the physical characteristics of the rural component of the RM. The following applies:

Cell range

B19:B22: Average catchment slope: Enter the %-distribution of the area associated with the slope class description in *cell range A19:A22*, if applicable. Alternatively, use the results contained in *cells B13, B14, H13 and H14* of the Catchment slope worksheet, which are representative of the frequency distribution of the grid points used in the grid method.

Note: The sum of *cell range B19:B22* must be equal to 100% (*cell B23*).

Cell range

B25:B31: Hydrological soil group/permeability: Enter the %-distribution of the area associated with the soil class description in *cell range A25:A31*, if applicable.

Note: The sum of *cell range B25:B31* must be equal to 100% (*cell B32*).

Cell range

B34:B39: Land use/vegetation: Enter the %-distribution of the area associated with the land use/vegetation description in *cell range A34:A39*, if applicable.

Note: The sum of *cell range B34:B39* must be equal to 100% (*cell B40*).

Urban run-off coefficients (C_2):

Lawns, residential areas, industry and business are used to describe the physical characteristics of the urban component of the RM. The following applies:

Cell range

G19:G22: Lawns: Enter the %-distribution of the area associated with the lawn description in *cell range E19:E22*, if applicable.

Cell range

G25:G26: Residential areas: Enter the %-distribution of the area associated with the residential area description in *cell range E25:E26*, if applicable.

Cell range

G29:G31: Industry: Enter the %-distribution of the area associated with the industry description in *cell range E29:E31*, if applicable.

Cell range

G34:G37: Business: Enter the %-distribution of the area associated with the business description in *cell range E34:E37*, if applicable.

Note: The sum of *cell ranges G19:G22;* G25*:G26; G29:G31 and G34:G37* must be equal to 100% (*cell G41*).

Figure D.14 displays the layout of the input data screen representative of the rural and urban run-off coefficients used in the RM.

	A	B	C	D	E	F	G	H	I
17	RURAL RUN-OFF COEFFICIENTS (C_1)				URBAN RUN-OFF COEFFICIENTS (C_2)				
18	Average catchment slope	%	Factor	C_s	Lawns		%	Factor	C_2
19	Vleis and pans (0-3%)	57.6	0.010	0.006	Sandy, flat (<2%)			0.100	
20	Flat areas (3-10%)	34.3	0.060	0.021	Sandy, steep (>7%)			0.200	
21	Hilly (10-30%) CATCHMENT SLOPE	6.7	0.120	0.008	Heavy soil, flat (<2%)			0.170	
22	Steep areas (>30%)	1.4	0.220	0.003	Heavy soil, steep (>7%)			0.350	
23	Total	100	Total	0.037	Total		0	Total	0.000
24	Hydrological soil group/permeability	%	Factor	C_p	Residential areas		%	Factor	C_2
25	Very permeable (A)		0.030		Houses		59.12	0.500	0.296
26	Very permeable (A/B)	23.15	0.040	0.009	Flats		0.14	0.700	0.001
27	Permeable (B)	27.31	0.060	0.016	Total		59.26	Total	0.297
28	Permeable (B/C)	2.82	0.080	0.002	Industry		%	Factor	C_2
29	Semi-permeable (C)		0.120		Light industry		11.53	0.800	0.092
30	Semi-permeable (C/D)	15.69	0.160	0.025	Average industry			0.850	
31	Impermeable (D)	31.03	0.210	0.065	Heavy industry		0.03	0.900	0.000
32	Total	100	Total	0.118	Total		11.56	Total	0.093
33	Land use/vegetation	%	Factor	C_v	Business		%	Factor	C_2
34	Thick bush and plantations	4.34	0.030	0.001	City centre		4.63	0.950	0.044
35	Light bush and farm lands	0.73	0.070	0.001	Suburban		24.55	0.700	0.172
36	Grasslands	80.18	0.170	0.136	Streets			0.950	
37	Cultivated land, contoured		0.070	0.000	Maximum flood			1.000	
38	Cultivated land	14.29	0.170	0.024					
39	No vegetation	0.46	0.260	0.001					
40	Total	100	Total	0.164	Total		29.18	Total	0.216
41	Total	100	Total C_1	0.319	Total		100	Total C_2	0.605

Figure D.14: Rural and urban run-off coefficients

Time of concentration:

Cell range

D43:E43: Select the appropriate option button contained in the time of concentration group box by indicating either “Yes” or “No”. If “Yes” is selected, the time of concentration in a defined main watercourse will be adjusted by a correction factor (τ). By selecting “No”, the use of a correction factor is excluded.

The correction factor, which is a function of the catchment area, was proposed by Kovács (unpublished report; as cited in Van der Spuy & Rademeyer, 2008: 2.8). Refer to Section 2.6.3 for more details.

Design notes:

Cell range

A47:A50: The user can enter any comments/design notes/recommendations in this cell range.

Precipitation:

Cell B64: Only applicable if the 1' x 1'-Grid design precipitation method was selected.

<u>Comment:</u> "Enter a user-defined ARF or an ARF equal to the default ARF in *cell range B63:H63*. To exclude the use of an ARF, enter a value of 100 (recommended)."

2.6.3 Calculation procedure

Time of concentration (T_C):

$$T_{C1} = 0.604\left(\frac{rL_1}{\sqrt{\frac{H}{1000L_1}}}\right)^{0.467} \qquad (D.9)$$

$$T_{C2} = \left(\frac{0.87L_2^{\,2}}{1000S_{Avg}}\right)^{0.385} \qquad (D.10)$$

$$T_{C3} = \left(\frac{L_3}{3.6\bar{v}}\right) \qquad (D.11)$$

$$T_C = T_{C1} + T_{C2} + T_{C3} \qquad (D.12)$$

Where:

H = Height of most remote point above the catchment outlet (m)

L_1 = Hydraulic length of catchment (km)

L_2 = Length of longest watercourse (km)

L_3 = Length of artificial flow path (km)

r = Roughness coefficient

S_{Avg} = Average slope (m/m) as determined in Section 2.5

$\bar{v}$ = Average/design velocity (m/s)

Equation D.10 tends to result in too high values in some cases and too low in others. The correction factors proposed by Kovács to overcome this problem are listed in Table D.1.

Table D.1: Correction factors (τ) for T_C

Area (A, km²)	Correction factor (τ)
< 1	2
1 - 100	2-0.5logA
100 - 5 000	1
5000 - 100 000	2.42-0.385logA
> 100 000	0.5

Adjusted/weighted run-off coefficients:

$$C_1 = C_s + C_p + C_v \quad (D.13)$$

$$C_{1D} = C_1(1 - D_{\%}) + C_1 D_{\%}\left(\sum\left(D_{factor} C_{S\%}\right)\right) \quad (D.14)$$

$$C_{1T} = F_T C_{1D} \quad (D.15)$$

$$C_T = \alpha C_{1T} + \beta C_2 + \gamma C_3 \quad (D.16)$$

Where:

α = Rural area distribution factor

β = Urban area distribution factor

C_1 = Rural run-off coefficient between zero and one

C_{1D} = Rural run-off coefficient incorporating the effect of dolomite areas

C_{1T} = Rural run-off coefficient incorporating the effect of initial saturation

C_2 = Urban run-off coefficient between zero and one

C_3 = Lake run-off coefficient

C_p = Run-off coefficient according to average soil permeability

C_s = Run-off coefficient according to average catchment slope

C_T = Weighted run-off coefficient for T-year return period

C_v = Run-off coefficient according to average land use/vegetation

F_T = Adjustment factor

γ = Lake area distribution factor

Precipitation:

Point precipitation ($P_{T\ Alexander}$):

$$P = (P_{iTw,\ s})\ (T_C)\ (M_F)\ (F) \quad (D.17)$$

Winter/coastal region (P_{iTw}):

$$P_{iTw} = \frac{122.8}{(1 + 4.779 T_C)^{0.7372}} \quad (D.17a)$$

Summer/inland region (P_{iTs}):

$$P_{iTs} = \frac{217.8}{(1+4.164T_C)^{0.8832}} \quad (D.17b)$$

MAP factor (M_F):

$$M_F = \frac{(18.79+0.17MAP)}{100} \quad (D.17c)$$

<u>Point precipitation</u> ($P_{T\ Smithers\ \&\ Schulze}$):

These point precipitation values are based on the input data (1' x 1'-Grid design precipitation) from the linked worksheet, Weather data.

<u>General:</u>

$$P_{iT} = \frac{P_T}{T_C} \quad (D.18)$$

$$ARF = (90000 - 12800\ln A + 9830\ln(60T_C))^{0.4} \quad (D.19)$$

$$I_T = P_{iT}\left(\frac{ARF}{100}\right) \quad (D.20)$$

<u>Peak flow:</u>

$$Q_T = \frac{C_T I_T A}{3.6} \quad (D.21)$$

Where:

A = Catchment area (km²)

ARF = Area reduction factor (%)

F = Frequency factor

I_T = Average precipitation intensity (mm/h)

MAP = Mean annual precipitation (mm)

M_F = MAP factor

P_T = Point precipitation (mm)

$P_{iTw,\ s}$ = Point precipitation intensity (mm/h)

Q_T = Peak flow for T-year return period (m^3/s)

T_C = Time of concentration (hours)

Figure D.15 displays the layout of the input data screen associated with the time of concentration and the design notes, whilst the calculation results of the time of concentration, adjusted/weighted run-off coefficients, precipitation and peak flow are also shown.

	A	B	C	D	E	F	G	H	I
42	TIME OF CONCENTRATION (T_C)					TIME OF CONCENTRATION (T_C)			
43	Correction factor (τ) for defined main watercourse		0.956	YES	NO				
44	Overland flow (T_{C1})		Defined main watercourse (T_{C2})			Artificial flow (T_{C3})		Total T_C	
45	0.000	hours	47.894		hours	0.000	hours	47.9	hours
46	DESIGN NOTES								
47									
48									
49									
50									
51	ADJUSTED/WEIGHTED RUN-OFF COEFFICIENTS								
52	**Return period (T, years)**	2	5	10	20	50	100	200	
53	Rural run-off coefficient (C_1)	0.319	0.319	0.319	0.319	0.319	0.319	0.319	
54	Dolomitic rural run-off coefficient (C_{1D})	0.319	0.319	0.319	0.319	0.319	0.319	0.319	
55	Adjustment factor (F_T)	0.500	0.550	0.600	0.670	0.830	1.000	1.200	
56	Adjusted rural run-off coefficient (C_{1T})	0.160	0.176	0.192	0.214	0.265	0.319	0.383	
57	**Weighted run-off coefficient (C_T)**	**0.173**	**0.188**	**0.203**	**0.225**	**0.274**	**0.327**	**0.389**	
58	PRECIPITATION								
59	**Return period (T, years)**	2	5	10	20	50	100	200	
60	Point precipitation ($P_{T\ Alexander}$, mm)	48.578	66.149	83.719	103.357	134.365	165.372	186.043	
61	Point precipitation ($P_{T\ Smithers\ \&\ Schulze}$, mm)								
62	Point precipitation intensity (P_{iT}, mm/h)	1.014	1.381	1.748	2.158	2.805	3.453	3.884	
63	Area reduction factor (ARF, %)	79.435	79.435	79.435	79.435	79.435	79.435	79.435	
64	**Area reduction factor ($ARF_{Smithers\ \&\ Schulze}$)**								
65	Average precipitation intensity (I_T, mm/h)	0.806	1.097	1.389	1.714	2.229	2.743	3.086	
66	**Peak flow (Q_T, m^3/s)**	**245**	**363**	**497**	**678**	**1075**	**1576**	**2108**	

Figure D.15: Input data and calculation results

2.7 ALTERNATIVE RATIONAL METHOD (ARM)

2.7.1 Prerequisite input data and linked worksheets

The Catchment data, Weather data and Rational method worksheets are prerequisite input data for this worksheet. The alternative Rational method worksheet is also linked to the Catchment slope, Channel slope and Design tables worksheets.

2.7.2 Input data ranges and comments

Input data range identifier:

Single cell and cell range entries (light-green shaded and unprotected) and option buttons.

Time of concentration:

Cell range

D53:E53: Select the appropriate option button contained in the time of concentration group box by indicating either “Yes” or “No”. If “Yes” is selected, the time of concentration in a defined main watercourse will be adjusted by a correction factor (τ). By selecting “No”, the use of a correction factor is excluded.

Design notes:

Cell range

A57:A60: The user can enter any comments/design notes/recommendations in this cell range.

2.7.3 Calculation procedure

Time of concentration (T_C):

Refer to Section 2.6.3, calculation procedures associated with the RM.

Adjusted/weighted run-off coefficients:

Refer to Section 2.6.3, calculation procedures associated with the RM.

Precipitation:

Point precipitation ($P_{T\ Hershfield,\ Tc \leq 6\text{-}h}$):

$$P_T = 1.13(0.41 + 0.64 \ln T)(-0.11 + 0.27 \ln(60T_C))(0.79M^{0.69}R^{0.20}) \quad (D.22)$$

Where:

- M = 2-year Mean of the annual daily maxima precipitation (mm)
- P_T = Point precipitation (mm)
- R = Average number of days per year on which thunder was heard
- T = Return period (years)
- T_C = Time of concentration (hours)

Point precipitation ($P_{T\ SAWS,\ 6\text{-}h < Tc \leq 168\text{-}h}$):

If the time of concentration (T_C) is longer than 6 hours and less than 24 hours, then linear interpolation between Equation D.22 and the 1-day point precipitation depth from either the TR102 or the SAWS database is used. If the time of concentration exceeds 24 hours, then linear interpolation between the *n*-day point precipitation depth values is used.

Point precipitation ($P_{T\ Smithers\ \&\ Schulze}$):

These point precipitation values are based on the input data (1' x 1'-Grid design precipitation) from the linked worksheet, Weather data.

General:

Refer to Section 2.6.3, calculation procedures associated with the RM.

Peak flow:

Refer to Section 2.6.3, calculation procedures associated with the RM.

The SAWS/TR102 *n*-day precipitation data and the physical catchment characteristics of the particular catchment are shown in Figure D.16.

	A	B	C	D	E	F	G	H	I
1	HOME	DESIGN TABLES	ALTERNATIVE RATIONAL METHOD				CATCHMENT DATA	PRECIPITATION	
2	Secondary drainage region number	C5		PRINT	Main watercourse/river			Modder River	
3	Tertiary drainage region number	C52			Designed			OJ Gericke	
4	Quaternary drainage region number	C52A- G			Checked			JA du Plessis	
5	Catchment description	Krugersdrift Dam			Date			June 15, 2009	
6	SAWS/TR102 N-DAY PRECIPITATION DATA								
7	Weather service station number	Multiple stations			Number of thunder days/year (R)			62	
8	Weather service station name	Multiple station numbers			2-year 1-day precipitation (M, mm)			48	
9	Precipitation region	Inland/summer			MAP (mm)			518	
10	Duration (days)	Return period (T, years)							
11		2	5	10	20	50	100	200	
12	1	48	66	78	90	106	119	133	
13	2	61	82	97	112	132	148	164	
14	3	68	91	107	123	144	160	177	
15	7	86	116	136	156	182	203	223	
16	PHYSICAL CHARACTERISTICS								
17	NATURAL FLOW				AREA DISTRIBUTION FACTORS				
18					Rural areas (α)			96.62	%
19	Size of catchment (A)	6330.906		km²	Urban areas (β)			3.04	%
20	Overland flow (L)			km	Lakes (Ƴ)			0.34	%
21	Overland flow: Height difference (H)			m	Dolomite area (D)			0	%
22	Overland flow: Average slope (S)			m/m	ARTIFICIAL FLOW				
23	Overland flow: r-Value				Street flow			Canal flow	
24	Longest main watercourse (L)	186.696		km	Flow path length (km)			Canal length (km)	
25	Average channel slope (S_{avg}) CHANNEL SLOPE	0.00131		m/m	Slope (m/m)			Actual velocity (m/s)	
26					Actual velocity (m/s)			Max velocity (m/s)	

Figure D.16: SAWS/TR102 *n*-day precipitation data

Figure D.17 displays the calculated design precipitation and associated peak flows.

	A	B	C	D	E	F	G	H	I
68	PRECIPITATION								
69	**Return period (T, years)**	**2**	**5**	**10**	**20**	**50**	**100**	**200**	
70	Point precipitation ($P_{T\ Hershfield,\ Tc \leq 6\text{-}h}$, mm)	37.478	63.225	82.702	102.179	127.926	147.403	166.880	
71	Point precipitation ($P_{T\ SAWS,\ 6\text{-}h < Tc \leq 168\text{-}h}$, mm)	61.117	82.271	97.040	111.912	132.030	147.802	164.222	
72	Point precipitation ($P_{T\ Smithers\ \&\ Schulze}$, mm)								
73	Point precipitation intensity (P_{iT}, mm/h)	1.276	1.718	2.026	2.337	2.757	3.086	3.484	
74	Area reduction factor (ARF, %)	79.435	79.435	79.435	79.435	79.435	79.435	79.435	
75	Area reduction factor ($ARF_{Smithers\ \&\ Schulze}$)								
76	Average precipitation intensity (I_T, mm/h)	1.014	1.365	1.609	1.856	2.190	2.451	2.768	
77	**Peak flow (Q_T, m^3/s)**	**308**	**451**	**576**	**735**	**1057**	**1409**	**1891**	

Figure D.17: Design precipitation and associated peak flows

2.8 SOIL CONSERVATION SERVICES (SCS) METHOD

2.8.1 Prerequisite input data and linked worksheets

The Catchment data, Weather data and Rational method worksheets are prerequisite input data for this worksheet. The SCS method worksheet is also linked to the Catchment slope and Channel slope worksheets.

2.8.2 Input data ranges and comments

Input data range identifier:

Single cell and cell range entries (light-green shaded and unprotected) and option buttons. Click and hold the mouse cursor in position to read any comment box (cells with red flags).

SAWS/TR102 24 hour precipitation data:

Cell range

B13:L13: Only applicable if the 1’ x 1’-Grid design precipitation method was selected.

Comment: “Enter the 24 hour 2-year grid precipitation depth (Smithers & Schulze, 2003) as obtained from the Precipitation worksheet.” The same applies to the 5-, 10-, 20-, 50-, 100- and 200-year return periods.

Run-off volume:

Initial weighted CN: Land use and hydrological soil groups:

Cell range

D26:J71: Select the appropriate option button contained in the CN-hydrological soil group box next to the identified/appropriate land-use description by indicating either “A, A/B, B, B/C, C, C/D or D”.

Cell K23: Comment: “Enter the area (%) associated with the selected hydrological soil groups (*cell range D26:J71*), if applicable.”

Cell range

P26:V71: Select the appropriate option button contained in the CN-hydrological soil group box next to the identified/appropriate land-use description by indicating either “A, A/B, B, B/C, C, C/D or D”.

Cell W23: Comment: “Enter the area (%) associated with the selected hydrological soil groups (*cell range P26:V71*), if applicable.”

Figure D.18 is illustrative of an extract from the *option button-based table* used in the DFET to establish the initial weighted Curve Numbers for the selected land use and hydrological soil groups.

	A	B–C	D	E	F	G	H	I	J	K	L
22	INITIAL WEIGHTED CURVE NUMBER (CN): LAND USE AND HYDROLOGICAL SOIL GROUPS										
23–24	Description	Run-off potential	Hydrological soil group							Area (%)	Weighted CN-value
25	Generalised CN-numbers		A	A/B	B	B/C	C	C/D	D	100	75.146
26	Agriculture		○	○	○	●	○	○	○	14.1	10.434
27	Open space		○	○	○	○	○	●	○	78.2	59.432
28	Forest		○	○	●	○	○	○	○	4.2	2.31
29	Disturbed land		○	○	○	○	○	●	○	0.4	0.356
30	Residential		○	○	●	○	○	○	○	1.8	1.368
31	Paved		○	○	○	○	○	●	○	0.9	0.882
32	Commercial: Industrial		○	○	○	○	○	●	○	0.4	0.364
33	Garden crops		A	A/B	B	B/C	C	C/D	D	0	0
34	Straight row	High	●	○	○	○	○	○	○		0
35	Straight row	Low	●	○	○	○	○	○	○		0
36	Small grain		A	A/B	B	B/C	C	C/D	D	0	0
37	Straight row	High	●	○	○	○	○	○	○		0
38	Straight row	Low	●	○	○	○	○	○	○		0
39	Straight row & conservation tillage	High	●	○	○	○	○	○	○		0
40	Straight row & conservation tillage	Low	●	○	○	○	○	○	○		0
41	Planted on contour	High	●	○	○	○	○	○	○		0
42	Planted on contour	Low	●	○	○	○	○	○	○		0
43	Planted on contour & conservation tillage	High	●	○	○	○	○	○	○		0
44	Planted on contour & conservation tillage	Low	●	○	○	○	○	○	○		0
45	Planted on contour: Winter	Low	●	○	○	○	○	○	○		0
46	Conservation structures	High	●	○	○	○	○	○	○		0
47	Conservation structures	Low	●	○	○	○	○	○	○		0

Figure D.18: Initial weighted CN-values

Catchment response time:

Cell Q18: Based on the values entered and results viewed in the previous steps, the appropriate option button contained in the lag time group box (*cell range Q18:X18*) must be selected by indicating either whether the T_C / T_L lag, SCS-lag or Schmidt-Schulze lag methods must be used to calculate the lag time.

2.8.3 Calculation procedure

Run-off volume:

$$CN = \frac{25400}{(S + 254)} \qquad (D.23)$$

$$S = \frac{25400}{CN} - 254 \qquad (D.24)$$

$$I_A = cS \qquad (D.25)$$

$$Q_v = \frac{(P - I_A)^2}{P - I_A + S} \qquad (D.26)$$

Where:

c = Seasonal-soil moisture status coefficient

CN = Curve Number

I_A = Initial losses/abstractions, normally 0.1S (mm)

P = 24-hour point precipitation depth for T-year return period (mm)

Q_v = Stormflow depth (mm)

S = Potential maximum soil water retention (mm)

Note:

The total area distribution of CN (*cell range B17:L17*) must be equal to 100%. The following comment(s) will appear on screen if this cell range is accessed by clicking and holding the mouse cursor in position: "If the %-area distribution of CN (*cell range B17:L17*) equals "%-Error", check the sum-total of *cells K72* + *W72* (%-area), since it must be equal to 100%."

Warning:

The initial CN is not adjusted for any variations in the soil moisture status of the catchment.

Catchment response time:

$$T_{L1} = 0.6T_C \quad (D.27)$$

$$T_{L2} = \frac{L^{0.8}(S+25.4)^{0.7}}{7069 S_{Avg}^{0.5}} \quad (D.28)$$

$$T_{L3} = \frac{A^{0.35} MAP^{1.1}}{41.67 S_{Avg}^{0.3} \overline{I_{30}}^{0.87}} \quad (D.29)$$

Where:

A = Catchment area (km²)

$\overline{I_{30}}$ = 2-year return period 30-minute precipitation intensity (mm/h)

L = Hydraulic length of catchment (m)

MAP = Mean annual precipitation (mm)

S = Potential maximum soil water retention (mm)

S_{Avg} = Average catchment slope (%)

T_{L1} = Lag time based on the T_C / T_L relationship (hours)

T_{L2} = Lag time based on the SCS-lag equation (hours)

T_{L3} = Lag time based on the Schmidt-Schulze lag equation (hours)

T_C = Time of concentration (hours)

Peak flow:

$$Q_T = \frac{0.2083 A Q_v}{\frac{T_C}{2} + T_L} \quad (D.30)$$

Where:

A = Catchment area (km²)

Q_T = Peak flow for T-year return period (m^3/s)

Q_v = Stormflow depth (mm)

T_C = Time of concentration (hours)

T_L = Lag time based on either Equations D.27, D.28 or D.29 (hours)

The layout of the SCS method worksheet, with specific reference to the calculation procedural part, is shown in Figures D.19 and D.20.

	A	B	C–D	E–F	G–H	I–J	K	L
2	GENERAL INFORMATION							
3	Secondary drainage region number	C5	PRINT	Main watercourse/river			Modder River	
4	Tertiary drainage region number	C52		Designed			OJ Gericke	
5	Quaternary drainage region number	C52A- G		Checked			JA du Plessis	
6	Catchment description	Krugersdrift Dam		Date			June 15, 2009	
7	SAWS/TR102 24 hour PRECIPITATION DATA							
8	Weather service station number	Multiple station numbers		Thunder days/year (R)			62	
9	Weather service station name	Multiple stations		2-year 1-day precipitation			48	
10	Precipitation region	Inland/summer		MAP (mm)			518	
11	Return period (T, years)	2	5	10	20	50	100	200
12	SAWS/TR102 precipitation depth (mm)	48	66	78	90	106	119	133
13	1' x 1'-24 hour Grid precipitation depth (mm)							
14	RUN-OFF VOLUME							
15	Return period (T, years)	2	5	10	20	50	100	200
16	Weighted catchment Curve Number (CN)	75.146	75.146	75.146	75.146	75.146	75.146	75.146
17	Total area distribution of CN (%)	100.000	100.000	100.000	100.000	100.000	100.000	100.000
18	Potential maximum soil water retention (S, mm)	84.009	84.009	84.009	84.009	84.009	84.009	84.009
19	Initial losses/abstractions (I_a, mm)	8.401	8.401	8.401	8.401	8.401	8.401	8.401
20	Stormflow depth (Q_v, mm)	12.936	23.121	31.197	39.880	52.477	62.855	74.040
21	WARNING: The initial Curve Number (CN) is not adjusted for any variations in the soil moisture status of the catchment							

Figure D.19: General information, precipitation and run-off volume

	M	N	O–P	Q–V	W	X
2	PHYSICAL CHARACTERISTICS					
3	NATURAL FLOW			ARTIFICIAL FLOW		
4	Size of catchment (A)	6330.906	km²	Street flow		
5	Overland flow (L)	0.000	km	Flow path length	0.000	km
6	Overland flow: Average slope (S)		m/m	Slope		m/m
7	Overland flow: r-Value CHANNEL SLOPE			Actual velocity		m/s
8	Longest main watercourse (L)	186.696	km	Canal flow		
9	Average channel slope (S_{avg}) CATCHMENT SLOPE	0.00131	m/m	Canal length	0.000	km
10	Average catchment slope (S)	0.04186	m/m	Actual velocity		m/s
11	TIME OF CONCENTRATION (T_C)					
12	Overland flow (T_{C1}, hours)	0.000		Defined main watercourse (T_{C2}, hours)		47.894
13	Artificial flow (T_{C3}, hours)	0.000		Total time of concentration (T_C ,hours)		47.9
14	CATCHMENT RESPONSE TIME					
15	T_C-T_L relationship (T_{L1})			28.737		hours
16	SCS-lag time (T_{L2})			30.478		hours
17	Schmidt-Schulze lag time (T_{L3})			21.748		hours
18	PREFERRED METHOD FOR LAG TIME (T_L)-CALCULATION			◉ TC/TL LAG	○ SCS-LAG	○ SCHMIDT-SCHULZE LAG

Figure D.20: Physical characteristics, lag time and peak flow

2.9 STANDARD DESIGN FLOOD (SDF) METHOD

2.9.1 Prerequisite input data and linked worksheets

The Catchment data and Weather data worksheets are prerequisite input data for this worksheet. The SDF method worksheet is also linked to the Catchment slope, Channel slope, Design tables and SDF TR102 worksheets, as well as the SDF regional map. The latter worksheet and map can be accessed by clicking on the SDF TR102 DATA and SDF MAP buttons.

2.9.2 Input data ranges and comments

Input data range identifier:

Single cell and cell range entries (light-green shaded and unprotected) and option buttons. Click and hold the mouse cursor in position to read any comment box (cells with red flags).

TR102 *n*-day precipitation data:

Cell B7: Comment: "Enter the SDF basin number, between 1 and 29. Click on the SDF Map button to view the SDF regional map for Southern Africa."

Cell range D24:E24: Select the appropriate option button contained in the time of concentration group box by indicating either "Yes" or "No". If "Yes" is selected, the time of concentration in a defined main watercourse will be adjusted by a correction factor (τ). By selecting "No", the use of a correction factor is excluded.

Cell A38: Click and hold the mouse cursor in position. The following comment box with instructions will appear on screen:

> **CLICK ON THE TABLE 8 BUTTON TO VIEW THE "DESIGN TABLES WORKSHEET".**
>
> **THE (a) & (b) CONSTANTS ARE LISTED IN TABLE 8: SDF ADJUSTMENT FACTORS (F) (Van Bladeren, 2005).**
>
> **ENTER THE (a) CONSTANTS OF THE SDF ADJUSTMENT FACTORS (F) APPLICABLE TO THE SELECTED SDF BASIN IN CELL RANGE B38: H38 (2- 200 years).**
>
> **IF NO (a) & (b) CONSTANTS ARE DEFINED, ENTER THE SDF ADJUSTMENT FACTORS (F) IN CELL RANGE B38: H38.**
>
> **LEAVE CELL RANGE B38: H38 BLANK, IF NO ADJUSTMENTS ARE REQUIRED.**

Cell A39: Click and hold the mouse cursor in position. The following comment box with instructions will appear on screen:

> **CLICK ON THE TABLE 8 BUTTON TO VIEW THE "DESIGN TABLES WORKSHEET".**
>
> **THE (a) & (b) CONSTANTS ARE LISTED IN TABLE 8: SDF ADJUSTMENT FACTORS (F) (Van Bladeren, 2005).**
>
> **ENTER THE (b) CONSTANTS OF THE SDF ADJUSTMENT FACTORS (F) APPLICABLE TO THE SELECTED SDF BASIN IN CELL RANGE B39: H39 (2- 200 years).**
>
> **IF NO (a) & (b) CONSTANTS ARE DEFINED, ENTER A VALUE OF ONE (1) IN CELL RANGE B39: H39.**
>
> **LEAVE CELL RANGE B38: H38 BLANK, IF NO ADJUSTMENTS ARE REQUIRED.**

Design notes:

Cell range

A44:A51: The user can enter any comments/design notes/recommendations in this cell range.

2.9.3 Calculation procedure

Time of concentration (T_C):

Refer to Section 2.7.3, calculation procedures associated with the ARM.

Adjusted/weighted run-off coefficients:

Refer to Section 2.7.3, calculation procedures associated with the ARM.

Precipitation:

Refer to Section 2.7.3, calculation procedures associated with the ARM.

Run-off coefficients:

$$C_T = \frac{C_2}{100} + \left(\frac{Y_T}{2.33}\right)\left(\frac{C_{100}}{100} - \frac{C_2}{100}\right) \quad (D.31)$$

Peak flow:

$$Q_T = 0.278 C_T I_T A \quad (D.32)$$

$$Q_{SDF} = \frac{Q_T}{F} \quad (D.33)$$

Where:

A = Catchment area (km²)

C_2 = Calibrated run-off coefficient for the 2-year return period

C_{100} = Calibrated run-off coefficient for the 100-year return period

C_T = Run-off coefficient

F = Adjustment factor (Van Bladeren, 2005)

I_T = Average precipitation intensity (mm/h)

Q_{SDF} = Adjusted peak flow for *T*-year return period (m^3/s)

Q_T = Original peak flow for *T*-year return period (m^3/s)

Y_T = Return period factor

The layout of the SDF method worksheet is shown in Figure D.21, whilst the location of the SDF basins is shown in Figure D.22.

	A	B	C	D	E	F	G	H	I
1	HOME / DESIGN TABLES	STANDARD DESIGN FLOOD METHOD					CATCHMENT DATA	SDF TR102 DATA	
2	Secondary drainage region number	C5		PRINT	Main watercourse/river			Modder River	
3	Tertiary drainage region number	C52			Designed			OJ Gericke	
4	Quaternary drainage region number	C52A- G			Checked			JA du Plessis	
5	Catchment description	Krugersdrift Dam			Date			June 15, 2009	
6	TR102 N-DAY PRECIPITATION DATA								
7	SDF Basin number / SDF MAP	9			MAP (mm)			376	
8	Weather service station number	0258458W			Number of thunder days/year (R)			47	
9	Weather service station name	Jacobsdal (Police)			2-year 1-day precipitation (M, mm)			43	
10	Duration (days)	Return period (T, years)							
11		2	5	10	20	50	100	200	
12	1	43	61	75	91	114	135	155	
13	2	54	78	98	119	151	179	210	
14	3	59	87	109	134	171	203	238	
15	7	70	104	131	160	203	240	280	
16	PHYSICAL CHARACTERISTICS								
17	NATURAL FLOW				ARTIFICIAL FLOW				
18	Size of catchment (A)	6330.906		km²	Street flow			Canal flow	
19	Overland flow (L)			km	Flow path length (km)			Canal length (km)	
20	Overland flow: Average slope (S)			m/m	Slope (m/m)			Actual velocity (m/s)	
21	Longest main watercourse (L) / CHANNEL SLOPE	186.696		km	Actual velocity (m/s)			Max velocity (m/s)	
22	Average channel slope (S_{avg})	0.00131		m/m					
23	TIME OF CONCENTRATION (T_C)					TIME OF CONCENTRATION (T_C)			
24	Correction factor (τ) for defined main watercourse	0.956		○ YES ◉ NO					
25	Overland flow (T_{C1})		Defined main watercourse (T_{C2})			Artificial flow (T_{C3})		Total T_C	
26	0.000	hours	47.894		hours	0.000	hours	47.9	hours
27	PRECIPITATION								
28	Return period (T, years)	2	5	10	20	50	100	200	
29	Point precipitation ($P_{T\ Hershfield,\ Tc \leq 6\text{-}h}$, mm)	32.623	55.034	71.988	88.942	111.353	128.307	145.261	
30	Point precipitation ($P_{T\ SAWS,\ 6\text{-}h < Tc \leq 168\text{-}h}$, mm)	53.951	77.925	97.899	118.877	150.837	178.806	209.757	
31	Point precipitation intensity (P_{iT}, mm/h)	1.126	1.627	2.044	2.482	3.149	3.733	4.380	
32	Area reduction factor (ARF, %)	79.435	79.435	79.435	79.435	79.435	79.435	79.435	
33	Average precipitation intensity (I_T, mm/h)	0.895	1.292	1.624	1.972	2.502	2.966	3.479	
34	RUN-OFF COEFFICIENTS								
35	Return period (T, years)	2	5	10	20	50	100	200	
36	Calibration factors	C_2	15		%	C_{100}	60		%
37	Run-off coefficient (C_T)	0.150	0.312	0.397	0.467	0.546	0.600	0.648	
38	Constant (a) / TABLE 8	2.230	2.470	3.500	1.840	2.320	2.440	2.400	
39	Constant (b)	-0.090	-0.120	-0.200	-0.180	-0.170	-0.190	-0.210	
40	SDF Adjustment factor (F)	1.014	0.864	0.608	0.381	0.524	0.462	0.382	
41	Original Peak flow (Q_T, m³/s)	236	710	1134	1618	2402	3129	3966	
42	Adjusted Peak flow (Q_{SDF}, m³/s)	233	821	1866	4251	4585	6766	10387	
43	DESIGN NOTES								
44									
45									
46									
47									
48									
49									
50									
51									

Figure D.21: SDF method worksheet

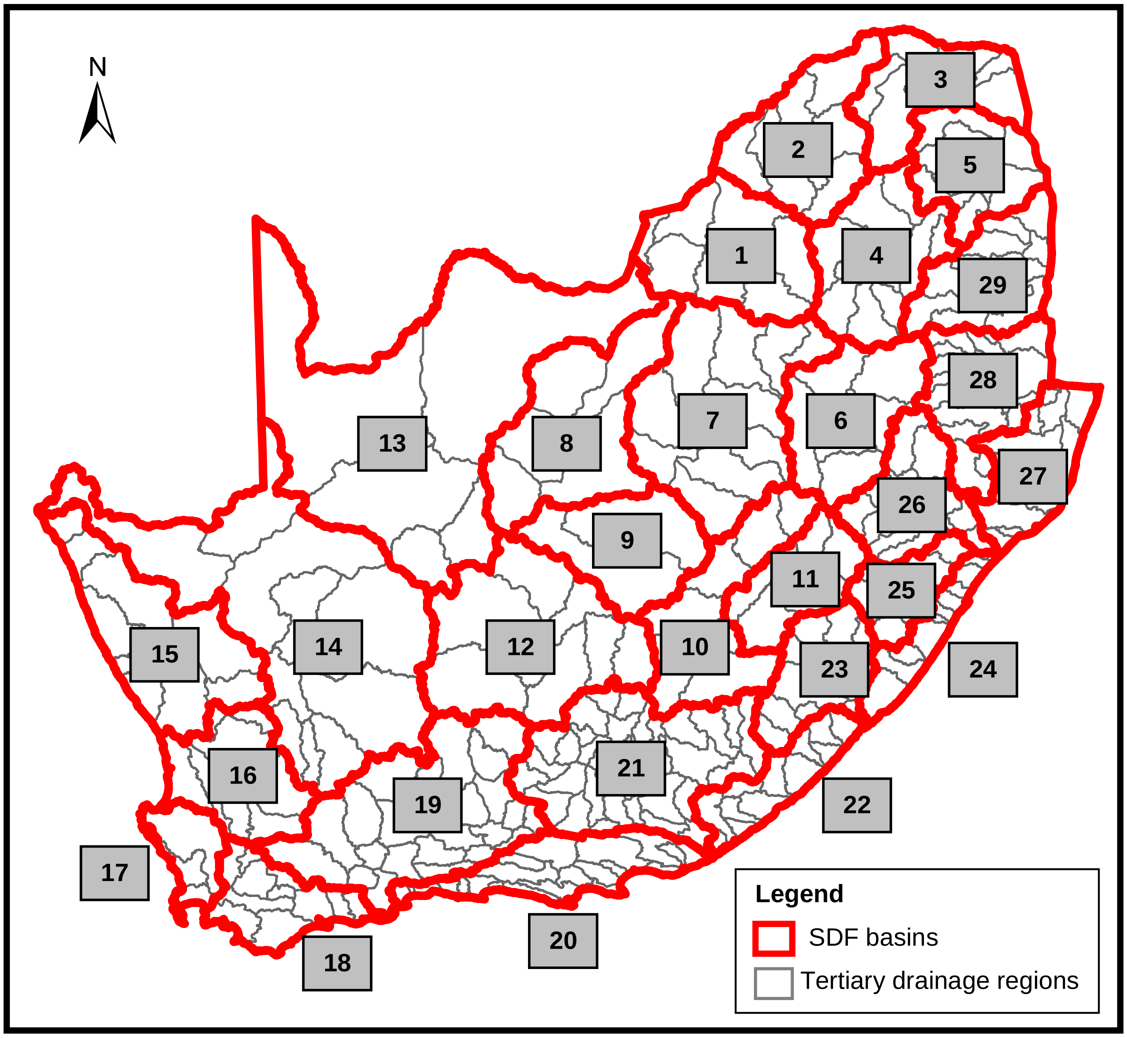

Figure D.22: SDF basins: Regional map (Alexander, 2003: 14)

2.10 SYNTHETIC UNIT HYDROGRAPH (SUH) METHOD

2.10.1 Prerequisite input data and linked worksheets

The Catchment data and Weather data worksheets are prerequisite input data for this worksheet. The Unit hydrograph method worksheet is also linked to the Catchment slope, Channel slope, Unit hydrograph storm run-off, Q/Q_P Data and S-curve lag worksheets.

2.10.2 Input data ranges and comments

Input data range identifier:

Single cell and cell range entries (light-green shaded and unprotected) and spinner buttons which enables the user to increase or decrease the veld-type number associated with a specific veld-type region. Click and hold the mouse cursor in position to read any comment box (cells with red flags).

Physical characteristics:

Cell range

B9:B11: Enter the area distribution (%) associated with the veld-type region number in *cell range D9:D11*. Use the spinner button to increase or decrease the veld region number in the latter cell range. Click on the **VELD-TYPE MAP** button to view the "*General Veld-type Region*" map to enable the selection of the appropriate region.

<u>*Note:*</u> The sum of *cell range B9:B11* must be equal to 100%.

Precipitation data:

Cells

D15 & H15: Select the appropriate return period (years) from the group box (drop-down list, 7 options available) to be used in the precipitation and design flood estimation. Repeat this process until all the return periods were evaluated.

Cell A17: Click and hold the mouse cursor in position. The following comment box with instructions will appear on screen:

1' x 1'-GRID DESIGN PRECIPITATION (Smithers & Schulze, 2003):
5 GROUPED USER-DEFINED STORM DURATIONS OF BETWEEN 0.250 hour (15 minutes) & 168 hour (7 days) CAN BE USED IN CELL RANGE C17: G17, BUT THESE DURATIONS MUST CORRESPOND WITH THE DURATIONS SELECTED IN THE PRECIPITATION WORKSHEET.

SAWS/TR102 PRECIPITATION DATABASE:
5 GROUPED USER-DEFINED STORM DURATIONS RELATED TO THE TIME OF CONCENTRATION (T_C) AND LAG TIME (T_L), e.g. 0.25, 0.5, 1, 1.5 and 2 T_C or T_L CAN BE USED IN CELL RANGE C17: G17.

THE DECIMAL ACCURACY OF THE STORM DURATIONS IS TO THE NEAREST 0.125 hour, HOWEVER, THE DECIMAL ACCURACY OF THE SELECTED DURATIONS MUST ALSO CORRESPOND WITH THE INCREMENTAL TIME INTERVAL (e.g. 0.25, 0.5 or 1 hour) SELECTED IN CELL E55.

Cell range

C17:G17: Comment: "Storm duration range (0.25 - 168 hours): Use the same incremental time interval (0.25, 0.5 or 1 hour) as selected in *cell E55*."

Cell range

C22:G22: Only applicable if the 1' x 1'-Grid design precipitation method was selected.

Comment: "Enter a user-defined ARF or an ARF equal to the default ARF in *cell range C21:G21*. To exclude the use of an ARF, enter a value of 100 (recommended)."

An extract of the SUH method precipitation data layout screen for data entering and calculations is shown in Figure D.23.

	A	B	C	D	E	F	G
14	PRECIPITATION DATA						
15	Return period (T, years)		100			years	
17	Storm duration (T_{SD}, hours)		12.00	24.00	38.00	48.00	72.00
18	Point precipitation ($P_{T\ Alexander}$, mm)	PRECIPITATION	138.858	151.884	160.777	165.416	173.693
19	Point precipitation ($P_{T\ Smithers\ \&\ Schulze}$, mm)						
20	Point precipitation intensity (P_{iT}, mm/h)		11.571	6.329	4.231	3.446	2.412
21	Area reduction factor (ARF, %)		71.105	75.449	78.134	79.448	81.653
22	Area reduction factor ($ARF_{Smithers\ \&\ Schulze}$, %)						
23	Average point precipitation (P_{AvgiT}, mm)		98.700	114.600	125.600	131.400	141.800
24	Flood run-off factor (f_{iT}, % & Area ≤1 000 km^2)	UH-STORM RUN-OFF					
25	Flood run-off factor (f_{iT}, % & Area >1 000 km^2)		30.204	33.057	35.014	36.038	37.874
46	Effective point precipitation (P_{eiT}, mm)		29.811	37.883	43.978	47.354	53.706

Figure D.23: SUH precipitation data layout screen

S-curve lagging:

Cell E55: Comment: "An incremental time interval (t) of 0.25, 0.5 or 1 hour can be used to represent the storm duration (T_{SD})."

Click on the S-CURVE LAG button to access the S-curve lag worksheet. The following applies:

Unit hydrograph S-curve lag: 1 hour:

Only to be used if *cell E55* (Unit hydrograph method worksheet) equals 1 hour. Time intervals ranging from zero to 168 hours (7 days) can be evaluated.

Cell FS11: Click and hold the mouse cursor in position. The following comment box with the S-curve lagging instructions will appear on screen:

THE BEGINNING OF ANY S-CURVE LAG IN COLUMNS FT to FX IS WHERE THE TIME-VALUE (t, hours) IN COLUMN A12: A179 EQUALS THE NUMERICAL VALUE, e.g. 12.0 IN THE FT, FU, FV, FW & FX COLUMN HEADINGS.

SET THE BEGINNING OF THE S-CURVE LAG (BASED ON A SPECIFIC STORM DURATION) IN COLUMNS FT, FU, FV, FW & FX EQUAL TO CELL FS11 BY ENTERING THE FOLLOWING FORMULA, =FS11.

USE COPY & PASTE FORMULAS TO COPY THIS FORMULA UP UNTIL THE END OF EACH COLUMN IN CELL RANGE FT12: FX179.

Unit hydrograph S-curve lag: 0.5 hour:

Only to be used if *cell E55* (Unit hydrograph method worksheet) equals 0.5 hour. Time intervals ranging from zero to 84 hours (3½ days) can be evaluated.

Cell FS186: Click and hold the mouse cursor in position. The following comment box with the S-curve lagging instructions will appear on screen:

THE BEGINNING OF ANY S-CURVE LAG IN COLUMNS FT to FX IS WHERE THE TIME-VALUE (t, hours) IN COLUMN A187: A354 EQUALS THE NUMERICAL VALUE, e.g. 12.0 IN THE FT, FU, FV, FW & FX COLUMN HEADINGS.

SET THE BEGINNING OF THE S-CURVE LAG (BASED ON A SPECIFIC STORM DURATION) IN COLUMNS FT, FU, FV, FW & FX EQUAL TO CELL FS186 BY ENTERING THE FOLLOWING FORMULA, =FS186.

USE COPY & PASTE FORMULAS TO COPY THIS FORMULA UP UNTIL THE END OF EACH COLUMN IN CELL RANGE FT187: FX354.

Unit hydrograph S-curve lag: 0.25 hour:

Only to be used if *cell E55* (Unit hydrograph method worksheet) equals 0.25 hour. Time intervals ranging from zero to 42 hours (1¾ days) can be evaluated.

Cell FS361: Click and hold the mouse cursor in position. The following comment box with the S-curve lagging instructions will appear on screen:

> **THE BEGINNING OF ANY S-CURVE LAG IN COLUMNS FT to FX IS WHERE THE TIME-VALUE (t, hours) IN COLUMN A362: A529 EQUALS THE NUMERICAL VALUE, e.g. 12.0 IN THE FT, FU, FV, FW & FX COLUMN HEADINGS.**
>
> **SET THE BEGINNING OF THE S-CURVE LAG (BASED ON A SPECIFIC STORM DURATION) IN COLUMNS FT, FU, FV, FW & FX EQUAL TO CELL FS361 BY ENTERING THE FOLLOWING FORMULA, =FS361.**
>
> **USE COPY & PASTE FORMULAS TO COPY THIS FORMULA UP UNTIL THE END OF EACH COLUMN IN CELL RANGE FT362: FX529.**

Click on the **UNIT HYDROGRAPH METHOD** button to return to the Unit hydrograph method worksheet. The following applies:

Summary of peak flows:

Cell B54: Comment: "The SUH method can only estimate peak flows for two return periods at a time. After every two return period selections, the results must be entered in the applicable cell within *cell range C54:K54*, before proceeding to the next analysis."

Figure D.24 displays an extract of the S-curve lagging results as obtained by following the above-mentioned instructions.

	B	C	D	E–F	G	H	I	J	K–L
55	Time (t, hours)	t/T_L	T_{SD} =	1.000	UNIT HYDROGRAPHS (hours)				
56			Q/Q_P	S-curve (S_1)	12.0	24.0	38.0	48.0	72.0
57	0	0.000	0.000	0.000	0.000	0.000	0.000	0.000	0.000
58	1	0.027	0.006	0.006	0.000	0.000	0.000	0.000	0.000
59	2	0.053	0.011	0.017	0.001	0.001	0.000	0.000	0.000
60	3	0.080	0.018	0.035	0.003	0.001	0.001	0.001	0.000
61	4	0.106	0.025	0.060	0.005	0.003	0.002	0.001	0.001
62	5	0.133	0.033	0.093	0.008	0.004	0.002	0.002	0.001
63	6	0.159	0.038	0.131	0.011	0.005	0.003	0.003	0.002
64	7	0.186	0.040	0.171	0.014	0.007	0.005	0.004	0.002
65	8	0.212	0.047	0.218	0.018	0.009	0.006	0.005	0.003
66	9	0.239	0.062	0.281	0.023	0.012	0.007	0.006	0.004
67	10	0.265	0.075	0.356	0.030	0.015	0.009	0.007	0.005
68	11	0.292	0.085	0.440	0.037	0.018	0.012	0.009	0.006
69	12	0.319	0.096	0.537	0.045	0.022	0.014	0.011	0.007
70	13	0.345	0.107	0.644	0.053	0.027	0.017	0.013	0.009
71	14	0.372	0.122	0.766	0.062	0.032	0.020	0.016	0.011
72	15	0.398	0.136	0.902	0.072	0.038	0.024	0.019	0.013
73	16	0.425	0.154	1.056	0.083	0.044	0.028	0.022	0.015
74	17	0.451	0.174	1.231	0.095	0.051	0.032	0.026	0.017
75	18	0.478	0.198	1.428	0.108	0.060	0.038	0.030	0.020
76	19	0.504	0.229	1.657	0.124	0.069	0.044	0.035	0.023
77	20	0.531	0.299	1.956	0.145	0.081	0.051	0.041	0.027
78	21	0.558	0.403	2.359	0.173	0.098	0.062	0.049	0.033
79	22	0.584	0.576	2.936	0.215	0.122	0.077	0.061	0.041
80	23	0.611	0.755	3.691	0.271	0.154	0.097	0.077	0.051
81	24	0.637	0.900	4.591	0.338	0.191	0.121	0.096	0.064
82	25	0.664	0.980	5.571	0.411	0.232	0.147	0.116	0.077
83	26	0.690	0.993	6.563	0.483	0.273	0.173	0.137	0.091
84	27	0.717	0.995	7.558	0.555	0.313	0.199	0.157	0.105
85	28	0.743	0.988	8.546	0.624	0.354	0.225	0.178	0.119
86	29	0.770	0.947	9.494	0.689	0.392	0.250	0.198	0.132
87	30	0.796	0.896	10.389	0.747	0.427	0.273	0.216	0.144

Figure D.24: S-curve lagging results

2.10.3 Calculation procedure

Physical characteristics:

$$I_C = \frac{L\,L_C}{\sqrt{S_{Avg}}} \quad (D.34)$$

$$T_L = C_T I_C^{\,0.36} \quad (D.35)$$

$$Q_P = K_U \frac{A}{T_L} \quad (D.36)$$

Where:

A = Catchment area (km²)

C_T = Regional veld-type coefficient, listed in Table D.2

I_C = Catchment-index

K_U = Regional coefficient

L = Hydraulic length of catchment (km)

L_C = Distance to catchment centroid (km)

Q_P = Peak flow of 1 hour unit hydrograph (m^3/s)

S_{Avg} = Average main watercourse slope (m/m)

T_L = Lag time (hours)

Table D.2: Generalised regional veld-type coefficients (HRU, 1972: F.9)

Veld region	Veld-type description	C_T
1	Coastal tropical forest	0.99
2	Schlerophyllous bush	0.62
3	Mountain sourveld	0.35
4	Grassland of interior plateau	0.32
5	Highland sourveld and Dohne sourveld	0.21
5A	Zone 5, soils weakly developed	0.53
6	Karoo	0.19
7	False Karoo	0.19
8	Bushveld	0.19
9	Tall sourveld	0.13

Precipitation data:

Point precipitation ($P_{T\ Alexander}$):

Refer to Section 2.6.3, calculation procedures associated with the RM.

Point precipitation ($P_{T\ Smithers\ \&\ Schulze}$):

Refer to Section 2.6.3, calculation procedures associated with the RM.

Point precipitation intensity (P_{iT}):

Refer to Section 2.6.3, calculation procedures associated with the RM.

ARF:

Refer to Section 2.6.3, calculation procedures associated with the RM.

Average and effective point precipitation:

$$P_{AvgiT} = \frac{ARF}{100} P_T \qquad (D.37)$$

$$P_{eiT} = \frac{f_{iT}}{100} P_{AvgiT} \qquad (D.38)$$

Where:

ARF = Area reduction factor (%)

f_{iT} = Flood run-off factor (%), Figure D.26

P_{AvgiT} = Average point precipitation (mm)

P_{eiT} = Effective point precipitation (mm)

P_T = Point precipitation (mm)

Peak flow and adjusted peak flow:

$$Q_{PiT} = Q_P * UH_{Max\ (n\text{-}hour)} \qquad (D.39)$$

$$Q_{iT} = P_{eiT}\ Q_{PiT} \qquad (D.40)$$

$$Q_T = Q_{iT} \frac{Q_{PiT}}{Q_P} \qquad (D.41)$$

Where:

Q_P = Peak flow of 1-hour unit hydrograph (m^3/s)

Q_{PiT} = Peak flow of *n*-hour unit hydrograph (m^3/s)

Q_T = Adjusted peak flow for *T*-year return period (m^3/s)

P_{eiT} = Effective point precipitation (mm)

The peak flow adjustment calculations contained in the DFET are illustrated in Figure D.25. Figure D.26 shows the average storm losses chart which is representative of the flood run-off factor. However, in the DFET, this chart is included numerically and no user input is required, except for the area distribution (%) associated with the different veld-type regions (Figure D.27) when the catchment under consideration extends over more than one veld-type region.

	A	B	C	D	E	F	G
47	PEAK FLOW ADJUSTMENTS	Return period (T)	100			years	
48		Storm duration (T_{SD}, hours)	12.00	24.00	38.00	48.00	72.00
49		Unit Hydrograph peak (Q_{PiT}, m^3/s)	56.214	44.019	34.845	30.254	22.707
50		Peak flow (Q_T, m^3/s)	1675.822	1667.576	1532.407	1432.641	1219.486
51		$Q_{PiT}/Q_P<1$	0.995	0.995	0.995	0.995	0.995
52		Adjusted peak flow (Q_T, m^3/s)	1667	1659	1524	1425	1213

Figure D.25: Peak flow adjustment calculations

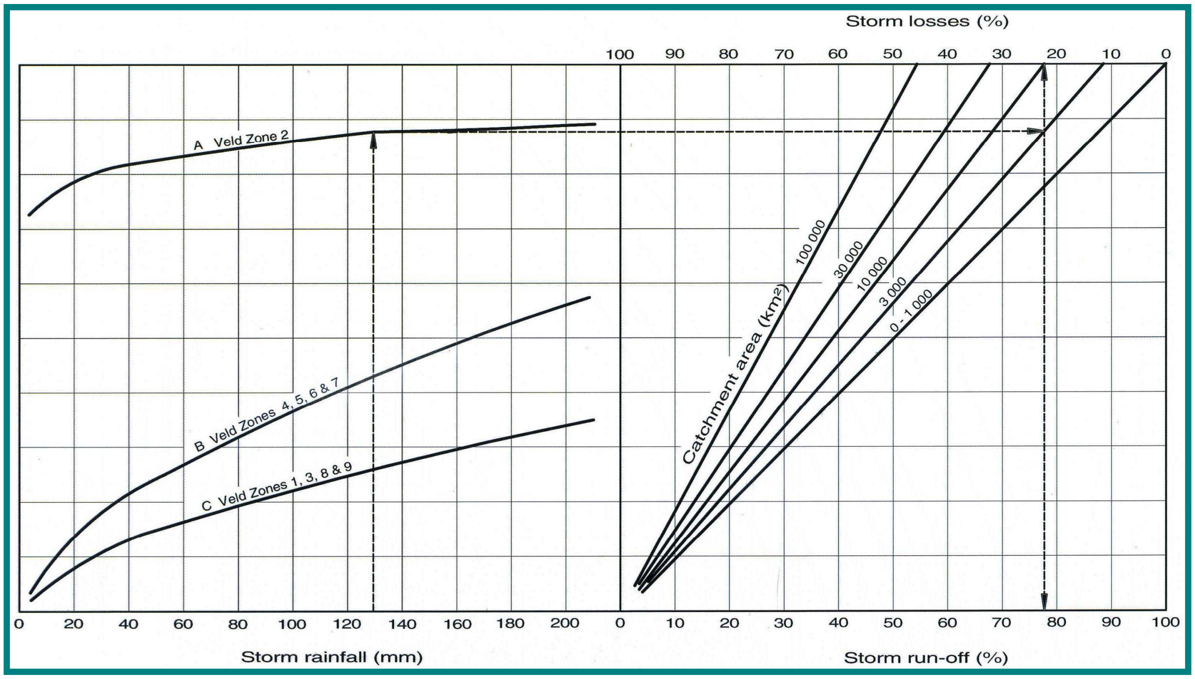

Figure D.26: Average storm losses (SANRAL, 2006: 3.34)

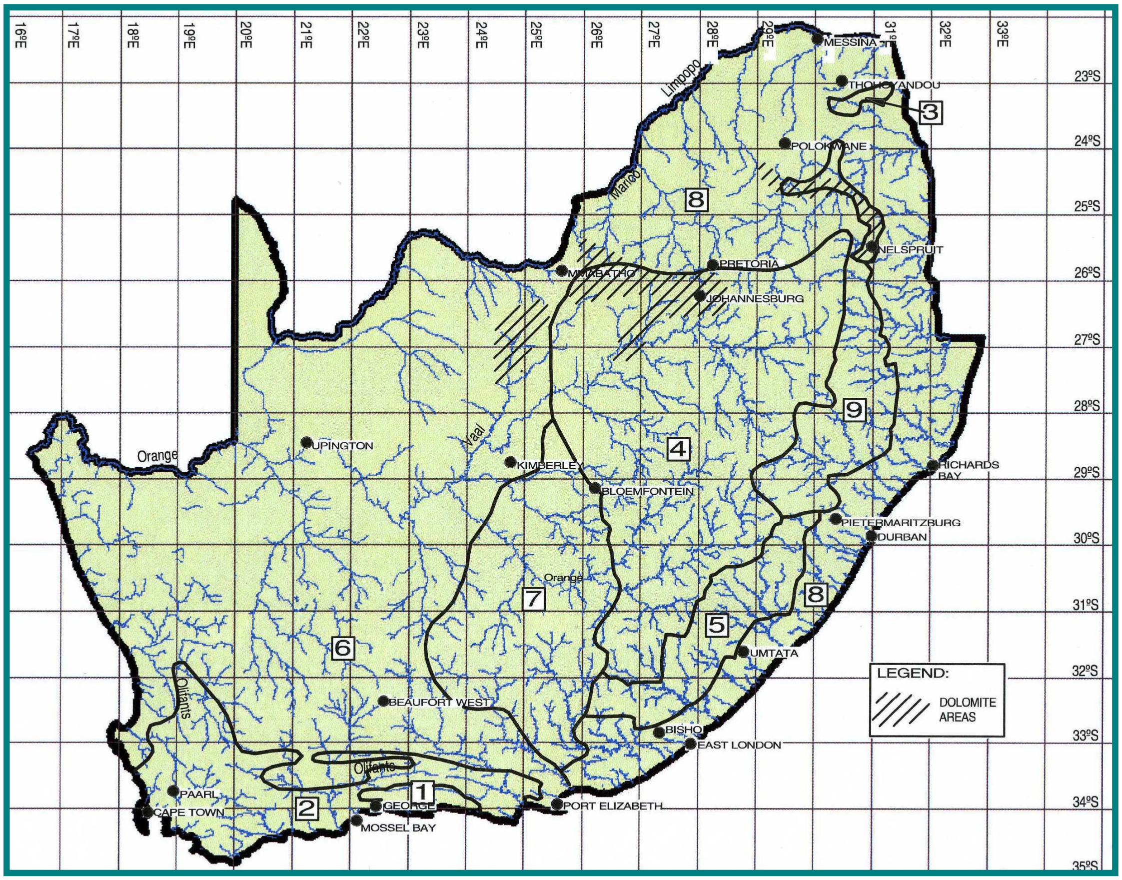

Figure D.27: Regions with generalised veld-types in South Africa (SANRAL, 2006: 3.27)

2.11 LAG-ROUTED HYDROGRAPH (LRH) METHOD

2.11.1 Prerequisite input data and linked worksheets

The Catchment data and Weather data worksheets are prerequisite input data for this worksheet. This worksheet is also linked to the Channel slope, LRH storm run-off and Precipitation distribution worksheets. The Precipitation distribution over time chart can be viewed by clicking on the **PRECIPITATION DISTRIBUTION** button.

2.11.2 Input data ranges and comments

Input data range identifier:

Single cell entries (light-green shaded and unprotected), option buttons and spinner buttons which enable the user to increase or decrease the veld-type number associated with a specific veld-type region. Click and hold the mouse cursor in position to read any comment box (cells with red flags).

Physical characteristics:

Cell range

B9:B11: Enter the area distribution (%) associated with the veld-type region number in *cell range D9:D11*. Use the spinner button to increase or decrease the veld region number in the latter cell range. Click on the **VELD-TYPE MAP** button to view the "*General Veld-type Region*" map to enable the selection of the appropriate region.

<u>*Note:*</u> The sum of *cell range B9:B11* must be equal to 100%.

Cell I12: Select the appropriate option button contained in the Muskingum routing factor group box by indicating either "Veld-type based" or "T_C-based". If "Veld-type based" is selected, the routing factor (K) contained in *cell I11* will be used. By selecting "T_C-based", the routing factor (K) contained in *cell I10* will be used.

Precipitation data:

Cell C21: Only applicable if the 1' x 1'-Grid design precipitation method was selected.

Comment: "Enter a user-defined ARF or an ARF equal to the default ARF in *cell range C20:J20*. To exclude the use of an ARF, enter a value of 100 (recommended)."

2.11.3 Calculation procedure

Physical characteristics:

$$\Delta t = 0.05T_C \quad \text{(D.42)}$$

$$K_1 = 0.6T_C \quad \text{(D.43)}$$

$$K_2 = C_T A^{0.318} \quad \text{(D.44)}$$

$$C_0 = -\frac{K_n}{\Delta t}(1-C_2)+1 \quad \text{(D.45)}$$

$$C_1 = \frac{K_n}{\Delta t}(1-C_2)-C_2 \quad \text{(D.46)}$$

$$C_2 = e^{-\frac{\Delta t}{Kn}} \quad \text{(D.47)}$$

Where:

A = Catchment area (km²)

C_T = Regional veld-type coefficient, listed in Table D.3

C_0 = Muskingum routing coefficient

C_1 = Muskingum routing coefficient

C_2 = Muskingum routing coefficient

K_n = Muskingum routing factor, either T_C-based or Veld-type based

K_1 = Muskingum routing factor, T_C-based

K_2 = Muskingum routing factor, Veld-type based

Δt = Incremental time step (hours)

T_C = Time of concentration (hours)

Table D.3: LRH regional veld-type coefficients (Bauer & Midgley, 1974)

Veld region	Veld-type description	C_T
1	Coastal tropical forest	1.83
2	Schlerophyllous bush	1.30
3	Mountain sourveld	1.10
4	Grassland of interior plateau	0.97
5	Highland sourveld and Dohne sourveld	0.79
6	Karoo	0.86
7	False Karoo	0.48
8	Bushveld	0.45
9	Tall sourveld	0.55

An extract of the LRH method physical characteristics layout screen illustrating above-mentioned instructions and calculation procedures is shown in Figures D.28 and D.29 respectively.

	A	B	C	D
6	PHYSICAL CHARACTERISTICS			
7	Size of catchment (A)	6330.906		km²
8	MAP	518		mm
9	Veld-type region (%) & number	97.29		4
10	Veld-type region (%) & number	2.71	VELD-TYPE MAP	7
11	Veld-type region (%) & number			6
12	Time of concentration (T_C)	47.875		hours
13	Storm duration (T_{SD})	48.000		hours
14	Incremental time step (Δt)	2.400		hours

Figure D.28: Physical characteristics screen (Veld-type regions)

	E	F	G	H	I	J	K
6	PHYSICAL CHARACTERISTICS						
7	Hydraulic length of catchment (L)		CHANNEL SLOPE		186.696		km
8	Average channel slope (S_{avg})				0.00131		m/m
9	Distance to catchment centroid (L_C)				113.015		km
10	Muskingum routing factor (K_1, T_C-based)				28.725		
11	Muskingum routing factor (K_2, Veld type-based)				15.476		
12	Muskingum (C_0)		0.041				
13	Muskingum (C_1)		0.040		○ VELD-TYPE BASED		◉ TC-BASED
14	Muskingum (C_2)		0.920				

Figure D.29: Physical characteristics screen (Muskingum routing)

Precipitation data:

Point precipitation ($P_{T\ Alexander}$):

Refer to Section 2.10.3, calculation procedures associated with the SUH method.

Point precipitation ($P_{T\ Smithers\ \&\ Schulze}$):

Refer to Section 2.10.3, calculation procedures associated with the SUH method.

Point precipitation intensity (P_{iT}):

Refer to Section 2.10.3, calculation procedures associated with the SUH method.

<u>ARF:</u>

Refer to Section 2.10.3, calculation procedures associated with the SUH method.

<u>Average and effective point precipitation</u>:

Refer to Section 2.10.3, calculation procedures associated with the SUH method.

Precipitation distribution over time:

After calculating the effective point precipitation (above-listed steps), the distribution of precipitation over time must be determined. In other words, the percentage of excess precipitation in a certain percentage of the storm duration must be estimated. Figure D.30 shows the precipitation distribution over time curves which are used for this estimation.

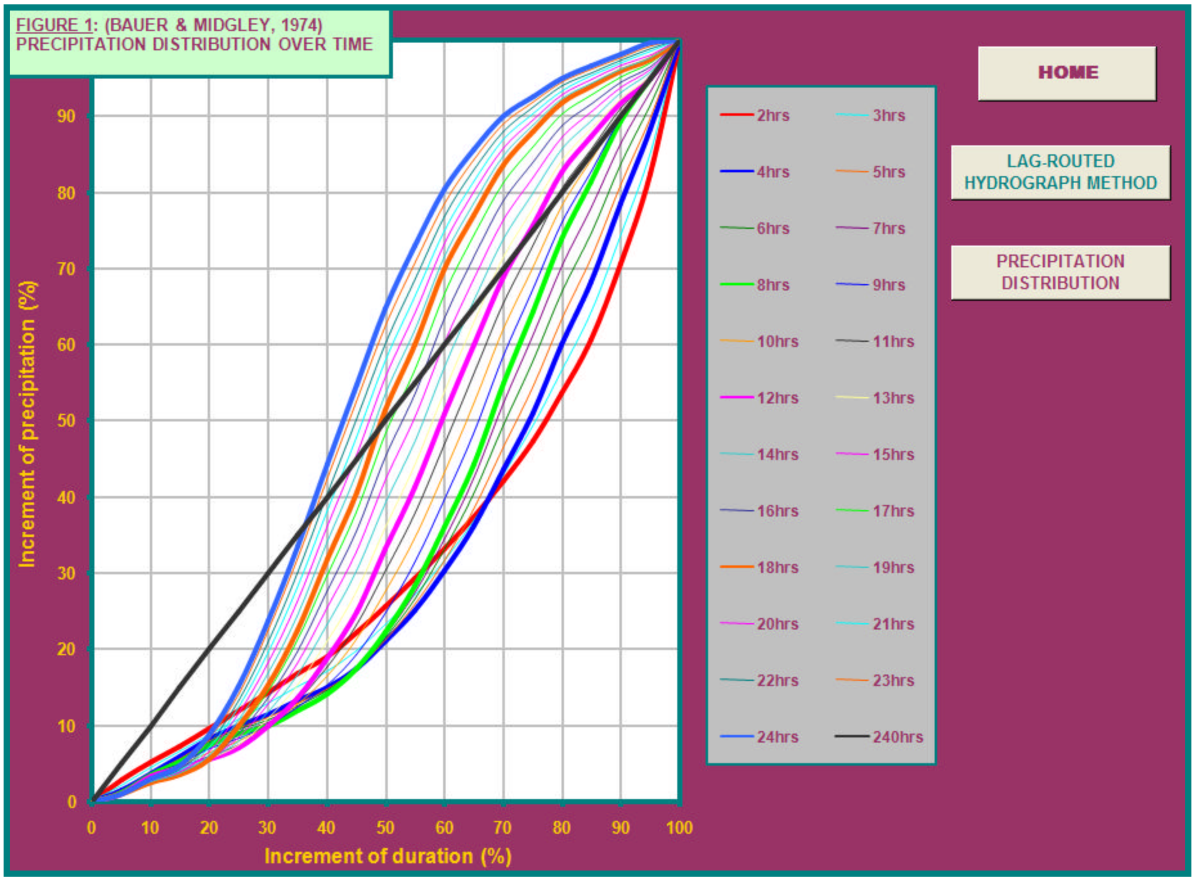

Figure D.30: Precipitation distribution over time curves

In the DFET, these curves are included numerically and no user input is required, thus the hyetographs used to derive the hydrographs are determined automatically.

Muskingum routing:

$$Q_{out(N)} = C_0Q_{in(N)} + C_1Q_{in(N-1)} + C_2Q_{out(N-1)} \quad (D.48)$$

Where:

C_0 = Muskingum routing coefficient

C_1 = Muskingum routing coefficient

C_2 = Muskingum routing coefficient

$Q_{in(N)}$ = Routed peak inflow at current time interval (m^3/s)

$Q_{in(N-1)}$ = Routed peak inflow at previous time interval (m^3/s)

$Q_{out(N)}$ = Routed peak outflow at current time interval (m^3/s)

$Q_{out(N-1)}$ = Routed peak outflow at previous time interval (m^3/s)

Design flows:

$$Q_T = Max\ Q_{out\ (N,T)} \quad (D.49)$$

Where:

Q_T = Peak flow for *T*-year return period (m^3/s)

$Max\ Q_{out\ (N,T)}$ = Maximum routed outflow associated with a specific incremental duration and precipitation distribution for *T*-year return period (m^3/s)

An extract of the LRH method precipitation distribution and Muskingum routing layout screens illustrating above-mentioned instructions and calculation procedures is shown in Figure D.31.

	A	B	C	D	E	F	G	H I	J K
46	PRECIPITATION DISTRIBUTION OVER TIME		MUSKINGUM ROUTING						
47	Duration-increment used	5% PRECIPITATION DISTRIBUTION	1: 2 year	1: 5 year	1: 10 year	1: 20 year	1: 50 year	1: 100 year	1: 200 year
48	Increment of duration (%)	Increment of precipitation (%)	Routed (Out.)	Routed (Out.)	Routed (Out.)	Routed (Out.)	Routed (Out.)	Routed (Out.)	Routed (Out.)
49	0	0.00	0.000	0.000	0.000	0.000	0.000	0.000	0.000
50	5	1.44	2.861	4.678	6.851	9.621	14.531	20.383	24.769
51	10	3.78	10.036	16.408	24.031	33.749	50.972	71.499	86.884
52	15	5.84	17.820	29.134	42.669	59.925	90.506	126.954	154.272
53	20	10.04	28.692	46.908	68.701	96.485	145.724	204.408	248.393
54	25	16.29	46.852	76.597	112.184	157.553	237.955	333.781	405.604
55	30	24.40	71.192	116.390	170.464	239.403	361.574	507.183	616.319
56	35	33.76	99.642	162.903	238.585	335.073	506.067	709.864	862.614
57	40	43.91	129.794	212.197	310.780	436.465	659.202	924.667	1123.638
58	45	53.71	158.365	258.907	379.192	532.544	804.312	1128.214	1370.984
59	50	63.16	183.257	299.603	438.794	616.250	930.735	1305.548	1586.478
60	55	71.00	202.300	330.735	484.390	680.286	1027.449	1441.211	1751.332
61	60	78.13	215.325	352.030	515.579	724.088	1093.604	1534.006	1864.095
62	65	83.40	222.240	363.334	532.134	747.338	1128.719	1583.263	1923.951
63	70	87.78	223.243	364.974	534.536	750.712	1133.815	1590.410	1932.637
64	75	90.64	219.460	358.790	525.479	737.992	1114.603	1563.462	1899.890
65	80	93.33	212.718	347.767	509.335	715.318	1080.359	1515.427	1841.518
66	85	95.40	204.940	335.052	490.713	689.166	1040.860	1460.022	1774.191
67	90	97.20	196.060	320.534	469.449	659.303	995.757	1396.756	1697.312
68	95	99.09	187.554	306.627	449.081	630.698	952.555	1336.156	1623.671
69	100	100.00	177.963	290.948	426.119	598.449	903.849	1267.835	1540.649
70	DESIGN FLOWS		Return period (T, years)						
71			2	5	10	20	50	100	200
72	Peak flow (Q_T, m³/s)		223	365	535	751	1134	1590	1933

Figure D.31: Precipitation distribution and Muskingum routing

2.12 EMPIRICAL METHODS

2.12.1 Prerequisite input data and linked worksheets

The Catchment data and Weather data worksheets are prerequisite input data for this worksheet. This worksheet is also linked to the Catchment slope, Channel slope and Design tables worksheets.

2.12.2 Input data ranges and comments

Input data range identifier:

Single cell entries (light-green shaded and unprotected), group box (drop-down list), option buttons and spinner buttons.

Physical characteristics:

Cell range

A10:A12: Enter the Kovács region %-distribution associated with the Kovács region number selected from the group box (drop-down list, 8 options available). Click on the **KOVÁCS MAP** button to view the "*Kovács Region*" map to enable the selection of the appropriate region.

Note: The sum of *cell range B10:B12* must be equal to 100%.

Cell range

F10:F12: Enter the area distribution (%) associated with the veld-type region number in *cell range G10:G12*. Use the spinner button to increase or decrease the veld region number in the latter cell range. Click on the **VELD-TYPE MAP** button to view the "*General Veld-type Region*" map to enable the selection of the appropriate region.

Note: The sum of *cell range F10:F12* must be equal to 100%.

Cell G13: Select the appropriate option button contained in the veld-type/precipitation group box by indicating either "Winter" or "All year". If "Winter" is selected, the regional distribution coefficient (K_T) used in the MIPI method will be based on the above selected veld-type regions and winter precipitation, whilst "All year" will reflect the chosen veld-type regions and summer/all year precipitation.

Design notes:

Cell range

A79:A86: The user can enter any comments/design notes/recommendations in this cell range.

2.12.3 Calculation procedure

Physical characteristics:

$$C = \frac{A\sqrt{S_{Avg}}}{LL_C} \qquad (D.50)$$

Where:

A = Catchment area (km²)

C = Catchment response time parameter

L = Hydraulic length of catchment (km)

L_C = Distance to catchment centroid (km)

S_{Avg} = Average main watercourse slope (m/m)

An extract of the Empirical methods physical characteristics layout screen illustrating above-mentioned instructions and calculation procedures is shown in Figure D.32.

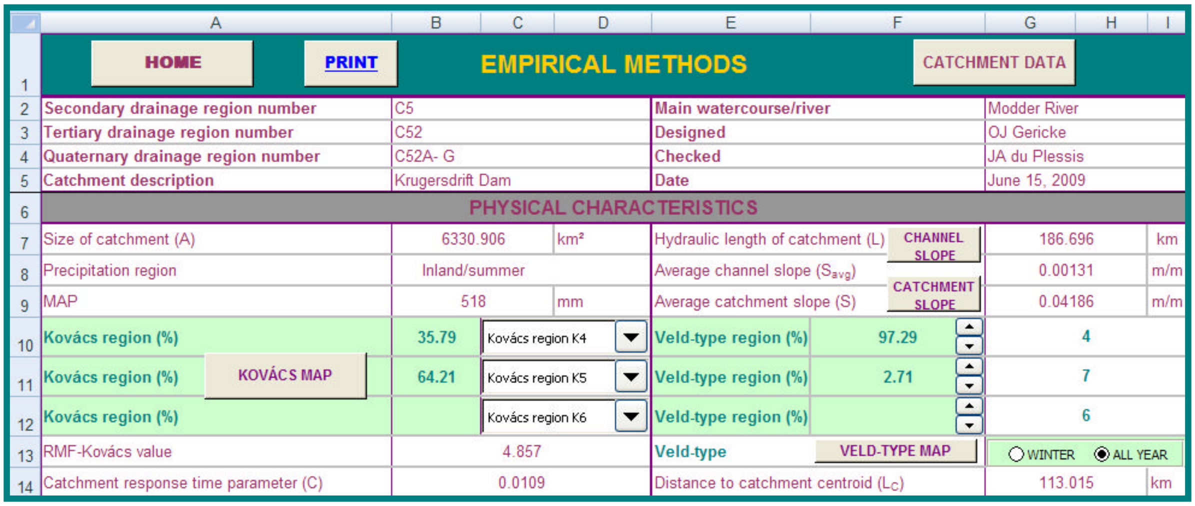

Figure D.32: Empirical methods: Physical characteristics screen

Midgley and Pitman (MIPI) method:

$$Q_T = 0.0377 K_T MAP\, A^{0.6}\, C^{0.2} \qquad (D.51)$$

Where:

A = Catchment area (km²)

C = Catchment response time parameter

K_T = Regional distribution coefficient

MAP = Mean annual precipitation (mm)

Q_T = Peak flow for T-year return period (m^3/s)

Catchment Parameter (CAPA) method:

$$M = MAP\left(\sqrt{\frac{100SA^{0.5}}{L}}\right) \qquad (D.52)$$

$$K_P = x\log(MAP)^y \qquad (D.53)$$

$$MAF = 10^{(a+0.61\log A)} \qquad (D.54)$$

$$Q_T = K_P MAF \qquad (D.55)$$

Where:

A = Catchment area (km²)

K_P = Exceedance probability constant

L = Hydraulic length of catchment (km)

M = Lumped catchment parameter

MAF = Mean annual flood (m^3/s)

MAP = Mean annual precipitation (mm)

Q_T = Peak flow for T-year return period (m^3/s)

S = Average catchment slope (m/m)

T = Return period (years)

$$a = -0.9414 + 1.08073(\log(M) - 2.0163)^{0.7384}$$

$$x = 99.51\log\left(\frac{1}{T}\right)^4 - 5.95\log\left(\frac{1}{T}\right)^2 + 0.722$$

$$y = 0.28\log\left(\frac{1}{T}\right)^4 + 2.22\log\left(\frac{1}{T}\right)^3 + 6.82\log\left(\frac{1}{T}\right)^2 + 10.92\log\left(\frac{1}{T}\right) + 2.73$$

Regional Maximum Flood (RMF) method:

$$Q_{RMF1} = 10^6\left(\frac{A}{10^8}\right)^{1-0.1K} \qquad (D.56)$$

Table D.4 presents all the Q_{RMF2} equations proposed by Kovács for the different Kovács regions.

Table D.4: RMF regional classification in Southern Africa (SANRAL, 2006: 3.46)

Regional constant (K)	Transition zone		Flood zone	
	Q_{RMF2} (m^3/s)	Areal range (km^2)	Q_{RMF2} (m^3/s)	Areal range (km^2)
2.8	$30A^{0.262}$	1 - 500	$1.74A^{0.720}$	500 - 500 000
3.4	$50A^{0.265}$	1 - 300	$5.25A^{0.660}$	300 - 500 000
4	$70A^{0.340}$	1 - 300	$15.9A^{0.600}$	300 - 300 000
4.6	$100A^{0.380}$	1 - 100	$47.9A^{0.540}$	100 - 100 000
5	$100A^{0.500}$	1 - 100	$100A^{0.500}$	100 - 100 000
5.2	$100A^{0.560}$	1 - 100	$145A^{0.480}$	100 - 30 000
5.4	$100A^{0.620}$	1 - 100	$209A^{0.460}$	100 - 20 000
5.6	$100A^{0.680}$	1 - 100	$302A^{0.440}$	100 - 10 000

Where:

A = Catchment area (km²)

K = Kovács regional constant

Q_{RMF1} = RMF based on the Francou-Rodier equation

Q_{RMF2} = RMF based on the Kovács equations

The layout of the Empirical method worksheet containing the flood estimation results is shown in Figure D.33, whilst Figure D.34 is illustrative of the maximum flood peak regions in Southern Africa, in other words, the Kovács regions.

	A	B	C	D	E	F	G	H
15	MIDGLEY AND PITMAN METHOD (MIPI, HRU 1/71)							
16	Return period (T, years)	10			20	50	100	
17	Regional distribution coefficient (K_T)	0.592			0.686	0.958	1.211	
18	Peak flow (Q_T, m³/s)	894			1037	1448	1829	
19	CATCHMENT PARAMETER (CAPA) METHOD							
20	Return period (T, years)	2	5	10	20	50	100	200
21	Lumped catchment parameter (M)	692.499	692.499	692.499	692.499	692.499	692.499	692.499
25	Probability of exceedance constant (K_P)	1.000	2.247	3.449	4.965	7.486	9.511	11.504
26	Mean annual flood (MAF, $Q_{50\%}$, m³/s)	206.241	206.241	206.241	206.241	206.241	206.241	206.241
27	Peak flow (Q_T, m³/s)	206	463	711	1024	1544	1962	2373
28	REGIONAL MAXIMUM FLOOD (RMF) METHOD							
29	Peak flow (Q_{RMF1}, m³/s, Francou-Rodier)	6928						
30	KOVÁCS REGIONALISATION	Transition zone <		100 km²		Flood zone ≤	100000 km²	
31	Peak flow (Q_{RMF2}, m³/s)	6105				7045		
32	MIPI/RMF RATIOS (Q_T/Q_{RMF})							
33	Return period (T, years)	2	5	10	20	50	100	200
34	Weighted $Q_{T/RMF}$-Ratio: ≤ 10km²	DESIGN TABLES						
35	Weighted $Q_{T/RMF}$-Ratio: 10 < x ≤ 3000km²							
36	Weighted $Q_{T/RMF}$-Ratio: 3000 < x ≤ 100000km²					0.492	0.591	0.692
77	Peak flow based on Q_T/Q_{RMF}-ratio (Q_T, m³/s)					3409	4097	4796

Figure D.33: Empirical flood peak estimation results

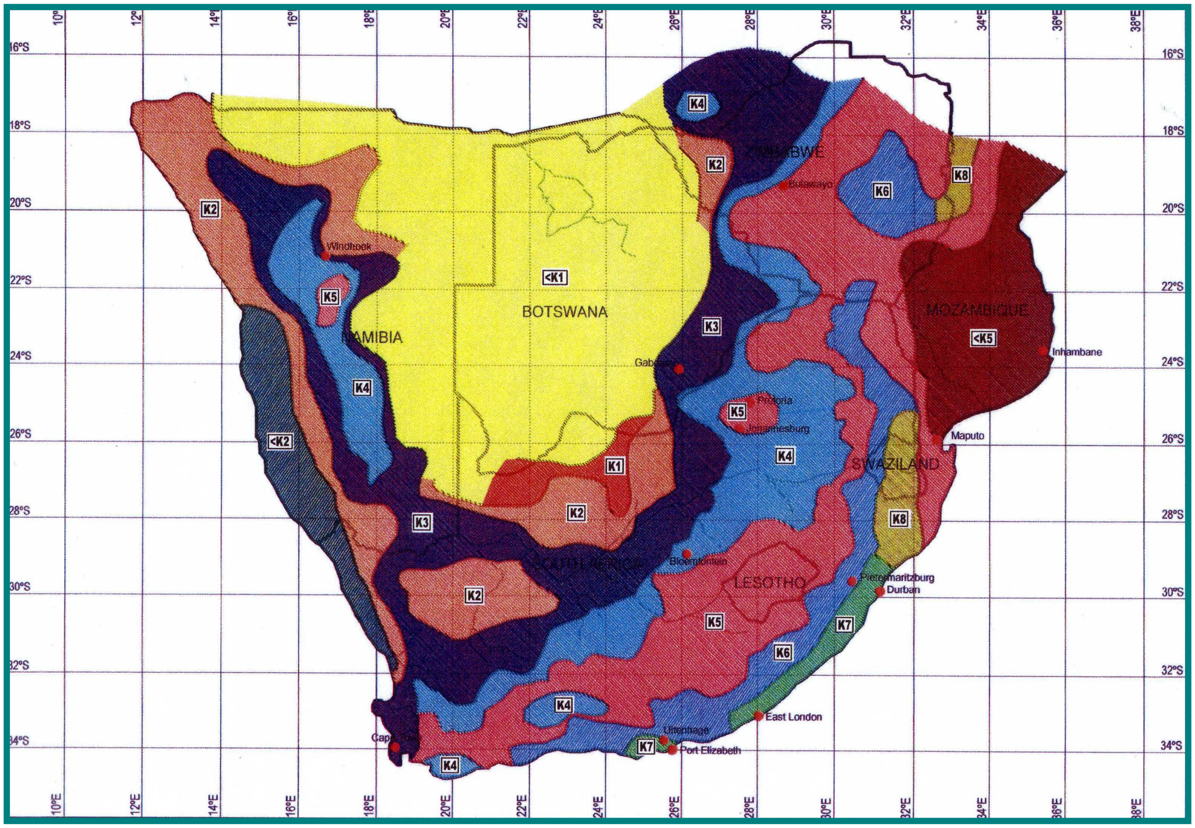

Figure D.34: Maximum flood peak regions in Southern Africa (SANRAL, 2006: 3.48)

3. STATISTICAL METHODS

3.1 ANNUAL MAXIMUM SERIES (AMS)

3.1.1 Prerequisite input data and linked worksheets

The Catchment data worksheet is prerequisite input data for this worksheet. The Annual maximum series worksheet is also linked to the Annual statistics worksheet.

3.1.2 Input data ranges and comments

Input data range identifier:

Single cell and cell range entries (light-green shaded and unprotected). Click and hold the mouse cursor in position to read any comment box (cells with red flags).

Note:

The annual maximum peak flow data as obtained from the Department of Water Affairs (DWA) database must be copied into *cell ranges D14:D213, F14:F213* and *G14:G213*, if applicable. Use *Copy & Paste values* to retain the cell format. A maximum period of 200 years can be used. Enter the start date (year) of the data period in *cell A14*.

Base station:

Cell D7: Compulsory.
Enter the hydrological gauging station name, e.g. Krugersdrift Dam. It can either be a dam or a river flow gauging station.

Cell D8: Compulsory.
Enter the hydrological gauging station number, e.g. C5R004.

Cell D10: Compulsory.
Enter the structural limit (m^3/s) of the hydrological gauging station. If the structural limit is unknown, enter the peak flow as estimated by the RMF method.

Cell A14: Click and hold the mouse cursor in position.
Comment: "Enter the start date (year) of data period."

Cell range D14:D213: Copy the annual maximum peak flow data into this cell range or a part thereof. Use *Copy & Paste values* to retain the cell format.

Additional station 1/2:

Cell F6/G6: Click and hold the mouse cursor in position. The following comment box related to the use of additional stations will appear on screen:

THE ANNUAL MAXIMUM PEAK FLOW DATA (m^3/s) OF THE ADDITIONAL STATIONS ARE USED TO SUPPLEMENT/EXTEND THE RECORD LENGTH OF THE BASE STATION. **COPY THE ANNUAL MAXIMUM PEAK FLOW DATA INTO THE "REQUIRED PART" OF CELL RANGE F14: F213 (STATION 1) or G14: G213 (STATION 2).** **THE "REQUIRED PART" REFERS TO THE BASE STATION DATA PERIOD CHARACTERISED BY MISSING DATA.** **CELL ENTRIES IN THE SAME ROW OF COLUMNS D, F and G ARE NOT ALLOWED.** **IN ALL CASES, USE COPY & PASTE VALUES FOR MULTIPLE ENTRIES.**

Cell F7/G7: Compulsory, if applicable.
Enter the hydrological gauging station name, e.g. Modder River at Stoomhoek. It can either be a dam or a river flow gauging station.

Cell F8/G8: Compulsory, if applicable.
Enter the hydrological gauging station number, e.g. C5H015.

Cell F11/G11: Compulsory, if applicable.
Enter the catchment area (km²) contributing to the specific hydrological gauging station.

Cell range(s) F14:F213 or G14:G213: Refer to above-listed comment box.

3.1.3 Calculation procedure

Square root-area method:

$$Q_{DS} = Q_{US}\left(\frac{\sqrt{A_{DS}}}{\sqrt{A_{US}}}\right) \qquad (D.57)$$

Where:

A_{DS} = Catchment area contributing to downstream gauging station (km²)

A_{US} = Catchment area contributing to upstream gauging station (km²)

Q_{DS} = AMS or PDS at downstream gauging station (m^3/s)

Q_{US} = AMS or PDS at upstream gauging station (m^3/s)

An extract of the AMS data layout screen illustrating above-mentioned instructions and calculation procedure is shown in Figure D.35.

HOME | PRINT | **SINGLE/COMBINED ANNUAL MAXIMUM SERIES** | ANNUAL STATISTICAL ANALYSIS

NOTE:
THE ANNUAL MAXIMUM PEAK FLOW DATA AS OBTAINED FROM THE DEPARTMENT OF WATER AFFAIRS (DWA) DATABASE
MUST BE COPIED INTO CELL RANGES D14:D213, F14:F213 & G14: G213, IF APPLICABLE. USE COPY & PASTE VALUES TO RETAIN THE CELL FORMAT.
A MAXIMUM PERIOD OF 200 YEARS CAN BE USED. ENTER THE START DATE (YEAR) OF THE DATA PERIOD IN CELL A14.

A	B	C	D	E	F	G
BASE STATION					ADDITIONAL STATION 1	ADDITIONAL STATION 2
Station name (Dam/River)			Krugersdrift Dam		Modder River at Stoomhoek	
Station number (R/H)			C5R004		C5H015	
Structural limit (H, m)						
Structural limit (Q, m³/s)			3000			
Catchment area (A, km²)			6330.906		6009.000	
Square-root area factor			1.000		1.026	
Year:Start	/	Year: End	Annual Maximum Q (m³/s)		Annual Maximum Q (m³/s)	Annual Maximum Q (m³/s)
1948	/	1949		137.542	134.000	
1949	/	1950		773.933	754.000	
1950	/	1951		240.186	234.000	
1951	/	1952		339.750	331.000	
1952	/	1953		1090.075	1062.000	
1953	/	1954		187.838	183.000	
1954	/	1955		570.698	556.000	
1955	/	1956		1642.297	1600.000	
1956	/	1957		86.221	84.000	
1957	/	1958		56.454	55.000	
1958	/	1959		362.332	353.000	
1959	/	1960		374.649	365.000	
1960	/	1961		153.965	150.000	
1961	/	1962		60.560	59.000	
1962	/	1963		636.390	620.000	

Figure D.35: AMS data layout screen

3.2 RAW FLOW DATA: PARTIAL DURATION SERIES

3.2.1 Prerequisite input data and linked worksheets

The Annual maximum series worksheet is prerequisite input data for this worksheet. The Raw flow data worksheet is also linked to the Partial duration series and Partial statistics worksheets.

3.2.2 Input data ranges and comments

Input data range identifier:

Single cell entry (light-green shaded and unprotected) and cell range entries (no defined cell format). Click and hold the mouse cursor in position to read any comment box (cells with red flags).

Note:

The maximum monthly peak flow data as obtained from the Department of Water Affairs (DWA) database must be copied into *cell range D9:O208.* A maximum period of 200 years can be used. Use *Copy & Paste values* to retain the cell format. Enter the start date (year) of the data period in *cell A9*.

Cell A9: Click and hold the mouse cursor in position.

Comment: "Enter the start date (year) of data period."

Cell range D9:O208: Copy the maximum monthly peak flow data into this cell range or a part thereof. Use *Copy & Paste values* to retain the cell format.

3.2.3 Calculation procedure

Not applicable, since this worksheet is only used for data management.

3.3 PARTIAL DURATION SERIES (PDS)

3.3.1 Prerequisite input data and linked worksheets

The Catchment data and Raw flow data worksheets are prerequisite input data for this worksheet. The Partial duration series worksheet is also linked to the Annual and Partial statistics worksheets.

3.3.2 Input data ranges and comments

Input data range identifier:

Single cell entry (light-green shaded and unprotected) and a group box (drop-down list). The group box contains the various plotting position methods and associated probability distributions. Click and hold the mouse cursor in position to read any comment box (cells with red flags).

Cell B9: Click and hold the mouse cursor in position. The following comment box related to the use of threshold exceedance values will appear on screen:

IF THE NUMBER OF PEAK YEARS (CELL B9) IS LEFT BLANK, THE NUMBER OF PEAKS EQUAL TO THE NUMBER OF DATA YEARS (CELL B8) WILL BE USED FOR THE CALCULATIONS.

IN ORDER TO MAKE USE OF A THRESHOLD EXCEEDANCE VALUE (EXCLUSION OF PEAKS ABOVE THE STRUCTURAL LIMIT, CELLS B7 or D7), THE USER CAN ENTER A NUMBER OF PEAK YEARS (CELL B9) LESS THAN THE NUMBER OF DATA YEARS (CELL B8).

Cell A10: Select the appropriate plotting position method from the group box (drop-down list, 6 options available) to establish the plotting constants in *cells D8* (a) and *D9* (b) respectively.

3.3.3 Calculation procedure

The calculation procedure used to establish the return period of each ranked peak flow within *N*-years will be discussed in Section 3.5.

An extract of the PDS data layout screen illustrating above-mentioned instructions is shown in Figure D.36.

	A	B	C	D
1	HOME	RAW FLOW DATA	PARTIAL DURATION SERIES	PARTIAL STATISTICAL ANALYSIS
2	Secondary drainage region number	C5	Main watercourse/river	Modder River
3	Tertiary drainage region number	C52	Designed	OJ Gericke
4	Quaternary drainage region number	C52A- G	Checked	JA du Plessis
5	Catchment description	Krugersdrift Dam	Date	June 15, 2009
6	Hydrological gauging station name	Krugersdrift Dam	Hydrological gauging station number	C5R004
7	Structural limit (H, m)		Structural limit (Q, m^3/s)	3000
8	Number of data years (N)	60	Plotting constant (a)	0.200
9	User-input: Number of peak years (N)	35	Plotting constant (b)	0.400
10	Plotting position method	CUNNANE (General purpose)		
11	Rank (m)	Peak flow (m^3/s)	Ranked peak flow (m^3/s) within N-years	Return period (T, years)
12	1	2456.000	2456.000	58.667
13	2	1642.297	1642.297	22.000
14	3	1090.075	1090.075	13.538
15	4	1086.996	1086.996	9.778
16	5	985.378	985.378	7.652
17	6	836.000	836.000	6.286
18	7	792.000	792.000	5.333
19	8	773.933	773.933	4.632
20	9	741.000	741.000	4.093
21	10	687.000	687.000	3.667
22	11	636.390	636.390	3.321
23	12	625.000	625.000	3.034
24	13	616.000	616.000	2.794
25	14	570.698	570.698	2.588
26	15	555.302	555.302	2.411
27	16	537.852	537.852	2.256
28	17	482.425	482.425	2.120
29	18	466.000	466.000	2.000
30	19	456.000	456.000	1.892
31	20	453.685	453.685	1.796

Figure D.36: PDS data layout screen

3.4 ANNUAL STATISTICAL ANALYSIS

3.4.1 Prerequisite input data and linked worksheets

The Catchment data and Annual maximum series worksheets are prerequisite input data for this worksheet. The Annual statistics worksheet is also linked to the Partial statistics and Plot worksheets.

3.4.2 Input data ranges and comments

Input data range identifier:

Not applicable, since this worksheet is only used for calculations.

3.4.3 Calculation procedure

Missing data excluded:

Normal and $\log_{10}$-transformed data:

$$\bar{x} = \frac{\sum x}{N} \quad \text{(D.58a)}$$

$$\overline{\log x} = \frac{\sum \log(x)}{N} \quad \text{(D.58b)}$$

$$s = \left[\frac{\sum (x-\bar{x})^2}{N-1}\right]^{0.5} \quad \text{(D.59a)}$$

$$s_{log} = \left[\frac{\sum \left(\log(x)-\overline{\log(x)}\right)^2}{N-1}\right]^{0.5} \quad \text{(D.59b)}$$

$$c_v = \frac{s}{\bar{x}} \quad \text{(D.60a)}$$

$$c_v = \frac{s_{\log}}{\overline{\log(x)}} \quad \text{(D.60b)}$$

$$g = \left(\frac{N}{(N-1)(N-2)}\right)\left(\frac{\sum (x-\bar{x})^3}{s^3}\right) \quad \text{(D.61a)}$$

$$g_{log} = \left(\frac{N}{(N-1)(N-2)}\right)\left(\frac{\sum \left(\log(x)-\overline{\log(x)}\right)^3}{s_{\log}{}^3}\right) \quad \text{(D.61b)}$$

Where:

c_v = Coefficient of variation

c_{vlog} = Coefficient of variation of the logarithms of the observed values

g = Skewness coefficient

g_{log} = Skewness coefficient of the logarithms of the observed values

N = Total number of observations (sample size)

s = Standard deviation of observed values

s_{log} = Standard deviation of the logarithms of the observed values

x = Observed values

$\overline{x}$ = Mean of observed values

$\overline{\log x}$ = Logarithm of the mean of the observed values

Missing data included (historically weighted variables):

Normal and log$_{10}$-transformed data:

$$\overline{x_h} = \frac{\left((W_T)\sum x_b + \sum x_a\right)}{\left(Y_T - (W_T)(L_W)\right)} \qquad (D.62)$$

$$s_h = \left[\frac{\left((W_T)\sum {d_b}^2 + \sum {d_a}^2\right)}{\left(Y_T - (W_T)(L_W) - 1\right)}\right]^{0.5} \qquad (D.63)$$

$$g_h = \left[\frac{\dfrac{\left(Y_T - (W_T)(L_W)\right)\left((W_T)\sum {d_b}^3 + \sum {d_a}^3\right)}{s^3}}{\left(Y_T - (W_T)(L_W) - 1\right)\left(Y_T - (W_T)(L_W) - 2\right)}\right] \qquad (D.64)$$

Where:

d_a, d_b = Deviations of $x_a + x_b$ from $\overline{x_h}$

g_h = Historically weighted skewness coefficient

L_W = Low outliers including zero flows

N_A = Floods equal to or above high threshold

N_B = Floods between high and low thresholds

N_C = Missing data

s_h = Historically weighted standard deviation

W_T = Weight applied to data, $\dfrac{(Y_T - N_A)}{N_B}$

x_a = Value of peak equal to or above the high threshold

x_b = Value of peak below the high threshold

$\overline{x_h}$ = Historically weighted mean

Y_T = Total time span (years), $N_A+N_B+N_C$

An extract of the Annual statistical analysis worksheet containing the conservation statistics and historically weighted variables is shown in Figure D.37.

	A	B	C	D	E	F	G	H
1	HOME	ANNUAL SERIES	ANNUAL STATISTICAL ANALYSIS				PARTIAL STATISTICAL ANALYSIS	
2	Secondary drainage region number			C5	PRINT	Main watercourse/river		Modder River
3	Tertiary drainage region number			C52		Designed		OJ Gericke
4	Quaternary drainage region number			C52A- G		Checked		JA du Plessis
5	Catchment description			Krugersdrift Dam		Date		June 15, 2009
6	Hydrological gauging station name			Krugersdrift Dam		Hydrological gauging station number		C5R004
7	CONSERVATION STATISTICS						STATISTICAL PLOT DATA	
8	MISSING DATA EXCLUDED					MISSING DATA INCLUDED		
9	Variable		Normal data	Log$_{10}$-transformed data		Variable	Normal data	Log$_{10}$-transformed data
10	Mean (x_{mean})/Log (x_{mean})		398.321	2.351		Mean (x_h)/Log ($x_{h\text{-}mean}$)	398.321	2.351
11	Total time span (Y_T)		60	60		Total time span (Y_T)	60	60
12	Missing data (N_C)		0	0		Missing data (N_C)	0	0
13	Standard deviation (s)/(s_{log})		421.916	0.543		Standard deviation (s_h)/(s_{hlog})	421.916	0.543
14	Coefficient of variation (c_v)/(c_{vlog})		1.059	0.231		Coefficient of variation (c_{vh})/(c_{vhlog})	1.059	0.231
15	Skewness (g)/(g_{log})		2.571	-0.814		Skewness (g_h)/(g_{hlog})	2.571	-0.814
16	HISTORICALLY WEIGHTED VARIABLES							
17	Weight applied to data (W_T)			1.000		Sum of peaks equal to or above the high threshold (Σx_a)		
18	Floods equal to or above the high threshold (N_A)			0		Sum of peaks below the high threshold (Σx_b)		23899.243
19	Floods between high- and low thresholds (N_B)			60		Sum of the deviations of x_a (Σd_a)		
20	Low outliers including zero flows (L_W)			0		Sum of the deviations of x_b (Σd_b)		3240.796

Figure D.37: Annual statistical analysis: Conservation statistics

Probability distributions:

Normal distribution (N/MM):

$$Q_T = \bar{x} - sy \qquad (D.65)$$

Extreme Value Type I (EV1/MM):

$$Q_T = \bar{x} + s(0.781W_T - 0.451) \qquad (D.66)$$

Extreme Value Type II (EV2/MM):

$$Q_T = \bar{x} + \sqrt{\frac{s^2}{\text{var}(y)}}(1 - E(y) - kW_T) \qquad (D.67)$$

Extreme Value Type III (EV3/MM):

$$Q_T = \bar{x} + \sqrt{\frac{s^2}{\text{var}(y)}}(-1 + E(y) + kW_T) \qquad (D.68)$$

Log-Normal distribution (LN/MM):

$$Q_T = anti\log\left[\overline{\log(x)} + s_{\log}W_T\right] \qquad (D.69)$$

<u>Log-Extreme Value Type I (LEV1/MM):</u>

$$Q_T = anti\log\left[\overline{\log(x)} + s_{\log}(0.781W_T - 0.451)\right] \quad (D.70)$$

<u>Log-Pearson Type III (LP3/MM):</u>

$$Q_T = anti\log\left[\overline{\log(x)} + s_{\log}W_T\right] \quad (D.71)$$

Where:

- $E(y)$ = Mean of the standardised variate
- k = Shape parameter
- Q_T = Peak flow for T-year return period (m^3/s)
- s = Standard deviation of observed values
- s_{log} = Standard deviation of the logarithms of the observed values
- $var(y)$ = Variance of the standardised variate
- W_T = Frequency factor for T-year return period or LN standard variate
- $\overline{x}$ = Mean of observed values
- y = Standardised variate

An extract of the Annual statistical analysis worksheet containing the probability distributions is shown in Figure D.38.

	A	B	C	D	E	F	G	H
21		PROBABILITY DISTRIBUTIONS (m^3/s)						
22	Return period	MISSING DATA EXCLUDED						
23	(T, years)	N/MM	EV1/MM		EV2/MM	LN/MM	LEV1/MM	LP3/MM
32	1.25	43	51		88	78	80	84
33	2	398	329		302	225	183	266
34	5	753	702		637	643	553	654
35	10	939	949		893	1114	1149	961
36	20	1092	1187		1168	1755	2321	1266
37	50	1265	1494		1571	2925	5764	1654
38	100	1380	1724		1913	4112	11393	1933
39	200	1485	1953		2293	5617	22476	2195
40	500	1613	2256		2859	8197	55068	2515
41	1000	1702	2484		3343	10685	108318	2736
42	Return period	MISSING DATA INCLUDED						
43	(T, years)	N/MM	EV1/MM		EV2/MM	LN/MM	LEV1/MM	LP3/MM
52	1.25	43	51		88	78	80	84
53	2	398	329		302	225	183	266
54	5	753	702		637	643	553	654
55	10	939	949		893	1114	1149	961
56	20	1092	1187		1168	1755	2321	1266
57	50	1265	1494		1571	2925	5764	1654
58	100	1380	1724		1913	4112	11393	1933
59	200	1485	1953		2293	5617	22476	2195
60	500	1613	2256		2859	8197	55068	2515
61	1000	1702	2484		3343	10685	108318	2736

Figure D.38: Annual statistical analysis: Probability distributions

3.5 PARTIAL STATISTICAL ANALYSIS

3.5.1 Prerequisite input data and linked worksheets

The Catchment data and Partial duration series worksheets are prerequisite input data for this worksheet. The Partial statistics worksheet is also linked to the Annual statistics and Plot worksheets.

3.5.2 Input data ranges and comments

Input data range identifier:

Single cell or cell range entries (light-green shaded and unprotected) in the case of "Design Notes", otherwise not applicable. This worksheet is mainly used for calculations.

Design notes:

Cell range

F9:F14: The user can enter any comments/design notes/recommendations in this cell range.

3.5.3 Calculation procedure

Missing data excluded:

Refer to Section 3.4.3, calculation procedures associated with the Annual statistical analysis.

Probability distributions:

Refer to Section 3.4.3, calculation procedures associated with the Annual statistical analysis.

The layout of the Partial statistical analysis worksheet is shown in Figure D.39.

	A	B	C	D	E	F	G	H
1	HOME		PARTIAL SERIES	PARTIAL STATISTICAL ANALYSIS			ANNUAL STATISTICAL ANALYSIS	
2	Secondary drainage region number			C5	PRINT	Main watercourse/river		Modder River
3	Tertiary drainage region number			C52		Designed		OJ Gericke
4	Quaternary drainage region number			C52A- G		Checked		JA du Plessis
5	Catchment description			Krugersdrift Dam		Date		June 15, 2009
6	Hydrological gauging station name			Krugersdrift Dam		Hydrological gauging station number		C5R004
7	CONSERVATION STATISTICS						STATISTICAL PLOT DATA	
8	MISSING DATA EXCLUDED					DESIGN NOTES		
9	Variable		Normal data	Log$_{10}$-transformed data				
10	Mean (x_{mean})/Log (x_{mean})		613.268	2.717				
11	Total time span (Y_T)		35	35				
12	Standard deviation (s)/(s_{log})		437.606	0.234				
13	Coefficient of variation (c_v)/(c_{vlog})		0.714	0.086				
14	Skewness (g)/(g_{log})		2.698	0.871				
15	PROBABILITY DISTRIBUTIONS (m^3/s)							
16	Return period	MISSING DATA EXCLUDED						
17	(T, years)	N/MM	EV1/MM	EV2/MM		LN/MM	LEV1/MM	LP3/MM
26	1.25	245	253	294		331	334	328
27	2	613	541	512		521	477	482
28	5	982	929	857		820	768	790
29	10	1174	1185	1122		1040	1054	1072
30	20	1333	1431	1408		1265	1427	1415
31	50	1512	1749	1831		1577	2113	1990
32	100	1631	1988	2192		1826	2835	2540
33	200	1740	2226	2595		2089	3800	3215
34	500	1873	2540	3199		2459	5593	4347
35	1000	1966	2777	3719		2757	7489	5427

Figure D.39: Layout of the Partial statistical analysis worksheet

3.6 STATISTICAL PLOT DATA AND PLOTTING POSITIONS

3.6.1 Prerequisite input data and linked worksheets

The Catchment data, Annual statistics and Partial statistics worksheets are prerequisite input data for this worksheet. The Plot worksheet is also linked to the Annual statistical plot and Partial statistical plot charts.

These charts can be viewed by clicking on either the **ANNUAL STATISTICAL PLOT** or **PARTIAL STATISTICAL PLOT** buttons.

3.6.2 Input data ranges and comments

Input data range identifier:

Single cell and cell range entries (light-green shaded and unprotected), check boxes and group boxes (drop-down lists). Each group box (annual and partial statistics) contains the various plotting position methods and associated probability distributions. Click and hold the mouse cursor in position to read any comment box (cells with red flags).

Design notes:

Cell range

G3:G8: The user can enter any comments/design notes/recommendations in this cell range.

Annual statistical analysis:

Cell G11: Select the appropriate plotting position method from the group box (drop-down list, 6 options available) to establish the plotting constants in *cells F7* (a) and *F8* (b) respectively.

Cell C11: Click and hold the mouse cursor in position. The following comment box related to the source data range (flow data series) will appear on screen:

CLICK ON "ANNUAL STATISTICAL PLOT".

RIGHT-CLICK ON THE RELEVANT CHART.

SELECT "SELECT DATA" FROM THE LIST.

SELECT THE "FLOW DATA" SERIES FROM THE LEGEND ENTRIES (SOURCE DATA).

CLICK ON "EDIT".

EDIT THE END X (E) and Y (B) DATA RANGE VALUES ACCORDING TO THE END-VALUE INDICATED IN CELL C11 (e.g. "62").

THE DEFINED DATA RANGE (Ending at e.g. "62") WILL BE AS FOLLOWS:

SERIES X VALUES: E3: E62
SERIES Y VALUES: B3: B62

Figure D.40 is illustrative of the Edit Series window that will appear on screen after the steps contained in the above-listed comment box were followed.

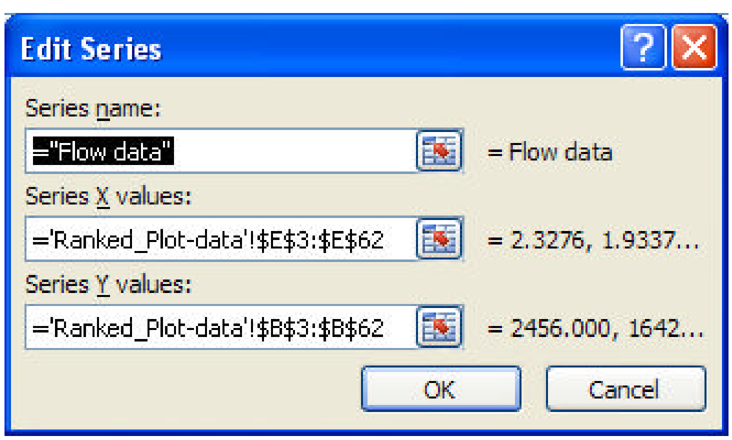

Figure D.40: Annual statistical plot: Edit Series window

Cell range

D12:I12: The check boxes “Included” enable the user to select or exclude single or multiple probability distribution results (*cell range D15:I15*, column headings) from being plotted on the probability graph, the Annual statistical chart.

Cell range

D13:I13: The user must enter the maximum return period in which a particular probability distribution must be taken into consideration. The following applies:

Cell D13: Comment: “Enter the maximum return period (1.25 - 1 000 years) in which the EV1/MM must be taken into consideration.”

Cell E13: Comment: “Enter the maximum return period (1.25 - 1 000 years) in which the EV2/MM or EV3/MM must be taken into consideration.”

Cell F13: Comment: “Enter the maximum return period (1.25 - 1 000 years) in which the LN/MM must be taken into consideration.”

Cell G13: Comment: “Enter the maximum return period (1.25 - 1 000 years) in which the LEV1/MM must be taken into consideration.”

Cell H13: Comment: “Enter the maximum return period (1.25 - 1 000 years) in which the LP3/MM must be taken into consideration.”

Cell I13: Comment: “Enter the maximum return period (1.25 - 1 000 years) in which the LM/PWM must be taken into consideration.”

Cell range

D14:I14: The user must enter the minimum return period in which a particular probability distribution must be taken into consideration. The following applies:

Cell D14: Comment: “Enter the minimum return period (1.25 - 1 000 years) in which the EV1/MM must be taken into consideration.”

Cell E14: Comment: “Enter the minimum return period (1.25 - 1 000 years) in which the EV2/MM or EV3/MM must be taken into consideration.”

Cell F14: Comment: “Enter the minimum return period (1.25 - 1 000 years) in which the LN/MM must be taken into consideration.”

Cell G14: Comment: “Enter the minimum return period (1.25 - 1 000 years) in which the LEV1/MM must be taken into consideration.”

Cell H14: Comment: "Enter the minimum return period (1.25 - 1 000 years) in which the LP3/MM must be taken into consideration."

Cell I14: Comment: "Enter the minimum return period (1.25 - 1 000 years) in which the LM/PWM must be taken into consideration."

Partial statistical analysis:

Cell G29: Select the appropriate plotting position method from the group box (drop-down list, 6 options available) to establish the plotting constants in *cells F7* (a) and *F8* (b) respectively.

Cell C29: Click and hold the mouse cursor in position. The following comment box related to the source data range (flow data series) will appear on screen:

CLICK ON "PARTIAL STATISTICAL PLOT".

RIGHT-CLICK ON THE RELEVANT CHART.

SELECT "SELECT DATA" FROM THE LIST.

SELECT THE "FLOW DATA" SERIES FROM THE LEGEND ENTRIES (SOURCE DATA).

CLICK ON "EDIT".

EDIT THE END X (R) and Y (O) DATA RANGE VALUES ACCORDING TO THE END-VALUE INDICATED IN CELL C29 (e.g. "37").

THE DEFINED DATA RANGE (Ending at e.g. "37") WILL BE AS FOLLOWS:

SERIES X VALUES: R3: R37
SERIES Y VALUES: O3: O37

Figure D.41 is illustrative of the Edit Series window that will appear on screen after the steps contained in the above-listed comment box were followed.

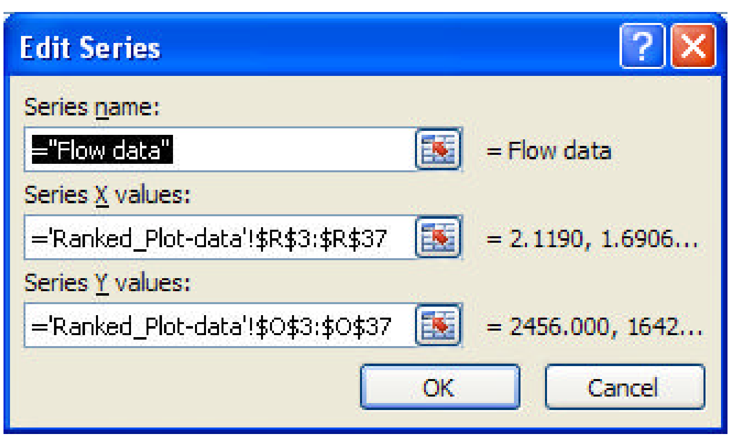

Figure D.41: Partial statistical plot: Edit Series window

Cell range

D30:I30: The check boxes "Included" enable the user to select or exclude single or multiple probability distribution results (*cell range D33:I33*, column headings) from being plotted on the probability graph, the Partial statistical chart.

Cell range

D31:I31: The user must enter the maximum return period in which a particular probability distribution must be taken into consideration. The following applies:

Cell D31: Comment: "Enter the maximum return period (1.25 - 1 000 years) in which the EV1/MM must be taken into consideration."

Cell E31: Comment: "Enter the maximum return period (1.25 - 1 000 years) in which the EV2/MM or EV3/MM must be taken into consideration."

Cell F31: Comment: "Enter the maximum return period (1.25 - 1 000 years) in which the LN/MM must be taken into consideration."

Cell G31: Comment: "Enter the maximum return period (1.25 - 1 000 years) in which the LEV1/MM must be taken into consideration."

Cell H31: Comment: "Enter the maximum return period (1.25 - 1 000 years) in which the LP3/MM must be taken into consideration."

Cell I31: Comment: "Enter the maximum return period (1.25 - 1 000 years) in which the LM/PWM must be taken into consideration."

Cell range

D32:I32: The user must enter the minimum return period in which a particular probability distribution must be taken into consideration. The following applies:

Cell D32: Comment: "Enter the minimum return period (1.25 - 1 000 years) in which the EV1/MM must be taken into consideration."

Cell E32: Comment: "Enter the minimum return period (1.25 - 1 000 years) in which the EV2/MM or EV3/MM must be taken into consideration."

Cell F32: Comment: "Enter the minimum return period (1.25 - 1 000 years) in which the LN/MM must be taken into consideration."

Cell G32: Comment: "Enter the minimum return period (1.25 - 1 000 years) in which the LEV1/MM must be taken into consideration."

Cell H32: Comment: "Enter the minimum return period (1.25 - 1 000 years) in which the LP3/MM must be taken into consideration."

Cell I32: Comment: "Enter the minimum return period (1.25 - 1 000 years) in which the LM/PWM must be taken into consideration."

3.6.3 Calculation procedure

Plotting position:

$$T = \frac{n+a}{m-b} \qquad (D.72)$$

Where:

a = Constant (Table D.5)

b = Constant (Table D.5)

m = Number, in descending order, of the ranked events (peak flows)

n = Number of observations/record length (years)

T = Return period (years)

Table D.5: Common plotting position methods (SANRAL, 2006: 3A.6)

Method		Plotting position	Probability distribution
Beard	(1962)	a = 0.40 and b = 0.30	Pearson 3
Blom	(1958)	a = 0.25 and b = 0.375	Normal
Cunnane	(1978)	a = 0.20 and b = 0.40	General purpose
Greenwood	(1979)	a = 0.00 and b = 0.35	GEV, Wakeby
Gringorten	(1963)	a = 0.12 and b = 0.44	EV1, GEV and Exponential
Weibull	(1939)	a = 1.00 and b = 0.00	Normal and Pearson 3

Annual/Partial statistical analysis:

$$P = \frac{1}{T} \qquad (D.73)$$

$$Q_{Stats} = 10\exp\left[\frac{\log((Q_{EV1MM})(Q_{GEVMM})(Q_{LNMM})(Q_{LEV1MM})(Q_{LP3MM})(Q_{LMPWM}))}{N}\right]$$

(D.74)

Where:

N = Number of probability distributions

Q_{Stats} = Peak flow based on the combined probability distributions (m^3/s)

Q_{EV1MM} = Peak flow based on the EV1/MM probability distribution (m^3/s)

Q_{GEVMM} = Peak flow based on the GEV/MM probability distribution (m^3/s)

Q_{LNMM}	= Peak flow based on the LN/MM probability distribution (m^3/s)
Q_{LEV1MM}	= Peak flow based on the LEV1/MM probability distribution (m^3/s)
Q_{LP3MM}	= Peak flow based on the LP3/MM probability distribution (m^3/s)
Q_{LMPWM}	= Peak flow based on the GLO probability distribution (m^3/s)
P	= Exceedance probability (decimal)
T	= Return period (years)

An extract of the statistical plot data layout screen illustrating the above-mentioned instructions and calculation procedures is shown in Figures D.42 and D.43.

	A	B	C	D	E	F
9	ANNUAL STATISTICAL ANALYSIS					
10	SOURCE DATA RANGE ["Flow Data" series (B3:B202,E3:E202)]			ANNUAL STATISTICAL ANALYSIS		
11	END-VALUE OF DATA PLOT RANGE (B, E):		62	ANNUAL STATISTICAL PLOT		
12	Return period	DISTRIBUTION RESULTS TO BE INCLUDED		☐ INCLUDED	☐ INCLUDED	☐ INCLUDED
13		DISTRIBUTION RANGE (Return period, years)	MAXIMUM	1000	1000	1000
14			MINIMUM	1.25	1.25	1.25
15–16	(T, years)	Exceedance probability (decimal)	Log-Normal Standard variate (W_{TLN})	EV1/MM (m^3/s)	EV2/MM (m^3/s)	LN/MM (m^3/s)
17	1.25	0.800	-0.842	51	104	78
18	2	0.500	0.000	329	302	225
19	5	0.200	0.842	702	637	643
20	10	0.100	1.282	949	893	1114
21	20	0.050	1.645	1187	1168	1755
22	50	0.020	2.054	1494	1571	2925
23	100	0.010	2.326	1724	1913	4112
24	200	0.005	2.576	1953	2293	5617
25	500	0.002	2.878	2256	2859	8197
26	1000	0.001	3.090	2484	3343	10685

	G	H	I	J
9	ANNUAL STATISTICAL ANALYSIS			
10	Plotting position method			
11	CUNNANE (General purpose)			
12	☐ INCLUDED	☑ INCLUDED	☑ INCLUDED	Proposed Q (m^3/s)
13	1000	20	1000	
14	1.25	1.25	1.25	
15–16	LEV1/MM (m^3/s)	LP3/MM (m^3/s)	LM/PWM (m^3/s)	
17	80	84	119	100
18	183	266	317	290
19	553	654	637	646
20	1149	961	910	935
21	2321	1266	1241	1253
22	5764	1654	1807	1807
23	11393	1933	2366	2366
24	22476	2195	3075	3075
25	55068	2515	4317	4317
26	108318	2736	5559	5559

Figure D.42: Annual statistical plot data

	A	B	C	D	E	F
27	PARTIAL STATISTICAL ANALYSIS					
28	SOURCE DATA RANGE ["Flow data" series (O3:O2402,R3:R2402)]			PARTIAL STATISTICAL ANALYSIS		
29	END-VALUE OF DATA PLOT RANGE (O, R):		37	PARTIAL STATISTICAL PLOT		
30	Return period	DISTRIBUTION RESULTS TO BE INCLUDED		☐ INCLUDED	☐ INCLUDED	☐ INCLUDED
31		DISTRIBUTION RANGE (Return period, years)	MAXIMUM	1000	1000	1000
32			MINIMUM	1.25	1.25	1.25
33	(T, years)	Exceedance probability	Log-Normal	EV1/MM	EV2/MM	LN/MM
34		(decimal)	Standard variate (W_{TLN})	(m^3/s)	(m^3/s)	(m^3/s)
35	1.25	0.800	-0.842	253	321	331
36	2	0.500	0.000	541	512	521
37	5	0.200	0.842	929	857	820
38	10	0.100	1.282	1185	1122	1040
39	20	0.050	1.645	1431	1408	1265
40	50	0.020	2.054	1749	1831	1577
41	100	0.010	2.326	1988	2192	1826
42	200	0.005	2.576	2226	2595	2089
43	500	0.002	2.878	2540	3199	2459
44	1000	0.001	3.090	2777	3719	2757

	G	H	I	J
27	PARTIAL STATISTICAL ANALYSIS			
28	Plotting position method			
29	CUNNANE (General purpose)			
30	☐ INCLUDED	☑ INCLUDED	☑ INCLUDED	Proposed Q (m^3/s)
31	1000	20	1000	
32	1.25	1.25	1.25	
33	LEV1/MM	LP3/MM	LM/PWM	
34	(m^3/s)	(m^3/s)	(m^3/s)	
35	334	328	319	**323**
36	477	482	466	**474**
37	768	790	733	**761**
38	1054	1072	981	**1026**
39	1427	1415	1301	**1357**
40	2113	1990	1886	**1886**
41	2835	2540	2504	**2504**
42	3800	3215	3332	**3332**
43	5593	4347	4882	**4882**
44	7489	5427	6533	**6533**

Figure D.43: Partial statistical plot data

The annual and partial statistical plots (charts) are illustrated in Figures D.44 and D.45 respectively.

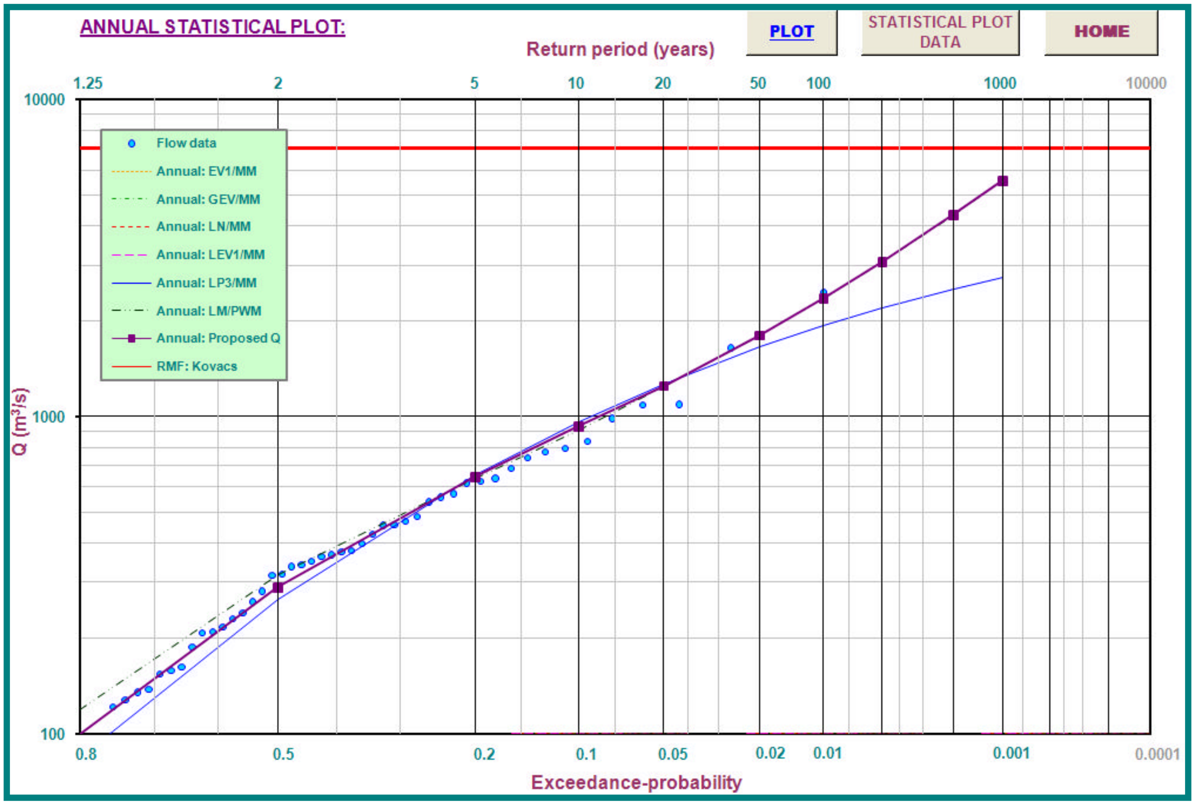

Figure D.44: Annual statistical plot

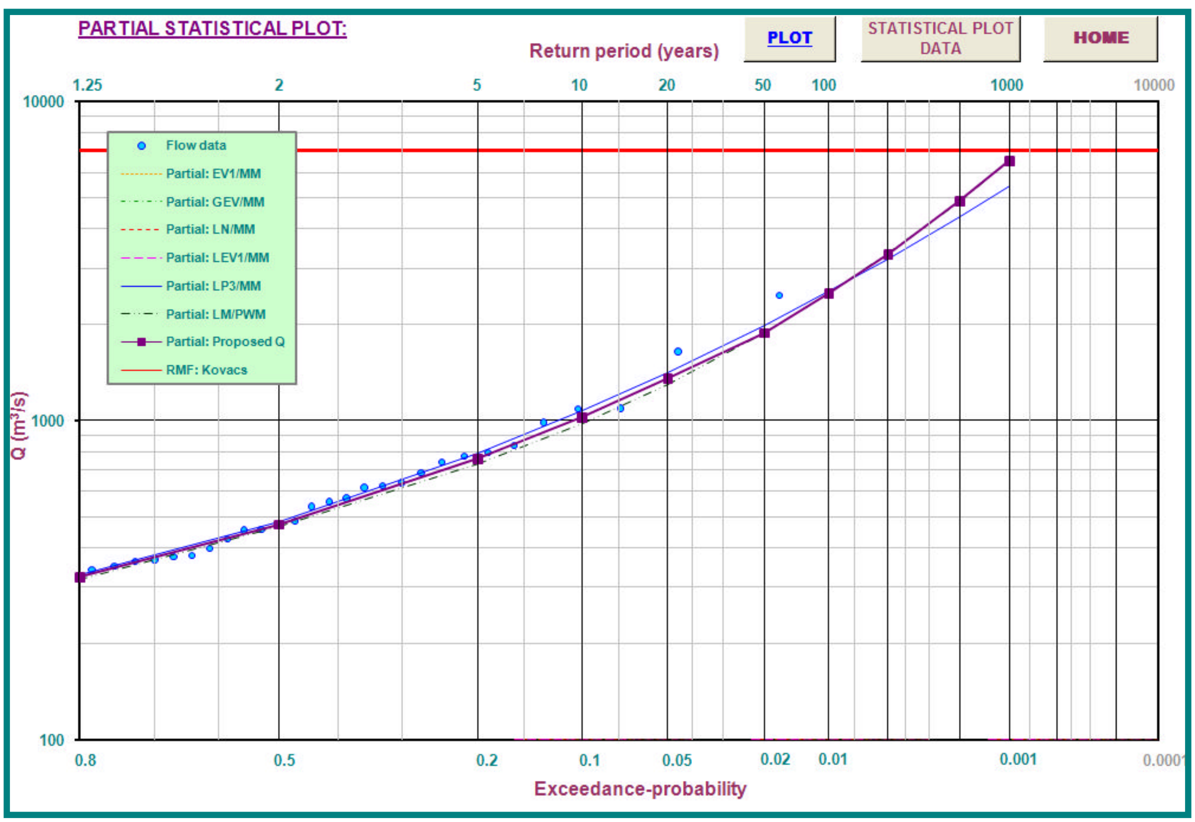

Figure D.45: Partial statistical plot

4. SUMMARY

4.1 SUMMARY REPORT

The SUMMARY and SUMMARY PLOT buttons can be used to view and examine the flood estimation results summarised in both a tabular and graphical format. The summary in tabular format is shown in Figure D.46, whilst the summary plot (chart) is illustrated in Figure D.47.

HOME | SUMMARY PLOT | **SUMMARY OF RESULTS** | PRINT

Catchment description	Krugersdrift Dam	MAP (mm)	518
Catchment classification	Inland/summer precipitation and flat & permeable	Hydrological gauging station	C5R004
Size of catchment (A, km^2)	6330.9	Designed	OJ Gericke
Main watercourse/river	Modder River	Date	JA du Plessis

DESIGN FLOOD ESTIMATION METHODS

DETERMINISTIC METHODS — DESIGN NOTES

Return period (T, years)	Design flow (m^3/s): Rational	Alternative Rational	SCS	SDF	Unit Hydrograph	Lag-routed Hydrograph
2	245	308	324	236	232	223
5	363	451	579	710	386	365
10	497	576	781	1134	562	535
20	678	735	998	1618	790	751
50	1075	1057	1314	2402	1205	1134
100	1576	1409	1573	3129	1667	1590
200	2108	1891	1853	3966	2014	1933

EMPIRICAL METHODS

Return period (T, years)	Design flow (m^3/s): Midgley and Pitman (MIPI)	Catchment parameter (CAPA)	Q_T/Q_{RMF}-ratio	Regional Maximum Flood (RMF): Francou-Rodier	Kovács
2		206		6928	7045
5		463			
10	894	711			
20	1037	1024			
50	1448	1544	3409		
100	1829	1962	4097		
200		2373	4796		

STATISTICAL ANALYSIS: ANNUAL MAXIMUM SERIES

Return period (T, years)	Design flow (m^3/s): N/MM	EV1/MM	EV2/MM	LN/MM	LEV1/MM	LP3/MM	LM/PWM	Proposed $Q_{Statistical}$
2	398	329	302	225	183	266	317	290
5	753	702	637	643	553	654	637	646
10	939	949	893	1114	1149	961	910	935
20	1092	1187	1168	1755	2321	1266	1241	1253
50	1265	1494	1571	2925	5764	1654	1807	1807
100	1380	1724	1913	4112	11393	1933	2366	2366
200	1485	1953	2293	5617	22476	2195	3075	3075

STATISTICAL ANALYSIS: PARTIAL DURATION SERIES

Return period (T, years)	Design flow (m^3/s): N/MM	EV1/MM	EV2/MM	LN/MM	LEV1/MM	LP3/MM	LM/PWM	Proposed $Q_{Statistical}$
2	613	541	512	521	477	482	466	474
5	982	929	857	820	768	790	733	761
10	1174	1185	1122	1040	1054	1072	981	1026
20	1333	1431	1408	1265	1427	1415	1301	1357
50	1512	1749	1831	1577	2113	1990	1886	1886
100	1631	1988	2192	1826	2835	2540	2504	2504
200	1740	2226	2595	2089	3800	3215	3332	3332

Figure D.46: Summary of results (tabular format)

4.2 SUMMARY PLOT

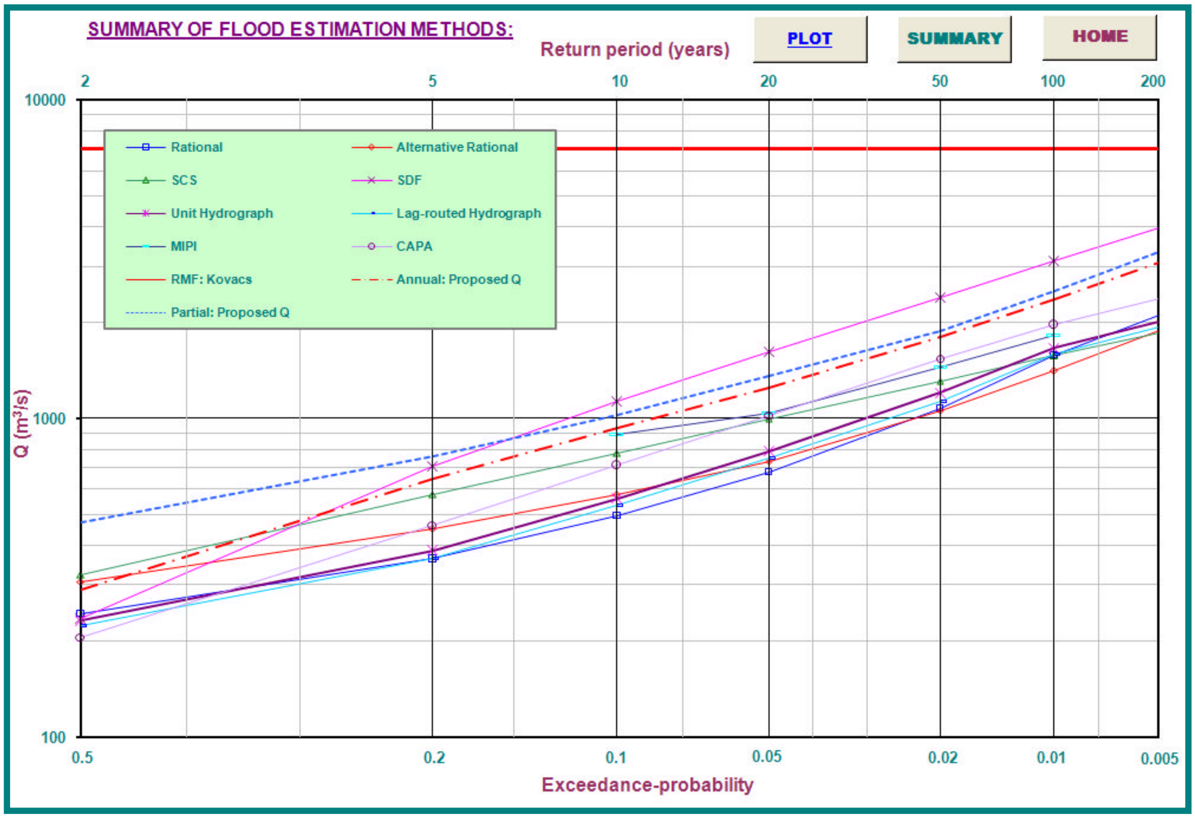

Figure D.47: Summary of results (chart)

5. REFERENCES

The following list of references reflects only the most prominent references used during the development of the DFET:

Adamson, P.T. 1981. *Southern African Storm Rainfall*. Technical Report TR102. Department of Environmental Affairs. Pretoria, South Africa.

Alexander, W.J.R. 1990. *Flood Hydrology for Southern Africa*. SANCOLD. Pretoria, South Africa.

Alexander, W.J.R. 2001. *Flood Risk Reduction Measures: Incorporating Flood Hydrology for Southern Africa*. Department of Civil and Biosystems Engineering, University of Pretoria. Pretoria, South Africa.

Alexander, W.J.R. 2002. *Statistical Analysis of Extreme Floods.* University of Pretoria. Pretoria, South Africa.

Alexander, W.J.R. 2002a. *The Standard Design Flood: Theory and Practice*. University of Pretoria. Pretoria, South Africa.

Alexander, W.J.R. 2003. *The Standard Design Flood: A New Design Philosophy*. University of Pretoria. Pretoria, South Africa.

Bauer, S.W. and Midgley, D.C. 1974. *A Simple Procedure for Synthesizing Direct Run-off Hydrographs*. Hydrological Research Unit. University of Witwatersrand. Johannesburg, South Africa.

Chadwick, A.J. and Morfett, J.C. 2004. *Hydraulics in Civil and Environmental Engineering*. 4^{th} Ed. E & FN Spon, Chapman and Hall. London, United Kingdom.

HRU (Hydrological Research Unit). 1972. *Design Flood Determination in South Africa*. HRU Report 1/72. University of the Witwatersrand. Johannesburg, South Africa.

Kovács, Z.P. 1988. *Regional Maximum Flood Peaks in Southern Africa*. Technical Report TR137. Department of Water Affairs. Pretoria, South Africa.

Midgley, D.C. and Pitman, W.V. 1978. *A Depth-Duration-Frequency Diagram for Point Rainfall in Southern Africa*. HRU Report 2/78. University of Witwatersrand. Johannesburg, South Africa.

Pilgrim, D.H. and Cordery, I. 1993. Flood Run-off. *Handbook of Hydrology*. McGraw-Hill. New York, United States of America.

SANRAL (South African National Roads Agency Limited). 2006. *Drainage Manual*. 5^{th} Ed. South African National Roads Agency Limited. Pretoria, South Africa.

SAWB (South African Weather Bureau). 1992. *Climate Tables of South Africa.* South African Weather Bureau Publication WB42. Pretoria, South Africa.

Smithers, J.C. and Schulze, R.E. 2003. *Design Rainfall and Flood Estimation in South Africa*. Water Research Commission. WRC Report 1060/01/03. Pretoria, South Africa.

Van Bladeren, D. 2005. *Verification of the Proposed Standard Design Flood (SDF).* SRK Consulting Engineers and Scientists. SRK Report 344512/1. Pretoria, South Africa.

Van der Spuy, D. and Rademeyer, P.F. 2008. *Flood Frequency Estimation Methods*. Proceedings of Course: Flood Hydrology. University of Stellenbosch, South Africa.